The background of the cover is a dark red color with a pattern of semi-transparent red circles and arrows. Some arrows point horizontally, some vertically, and some diagonally, creating a sense of movement and flow. The circles vary in size and opacity, some appearing as solid red and others as lighter, semi-transparent washes.

Michele Cini

Topics and Methods in Condensed Matter Theory

From Basic Quantum Mechanics
to the Frontiers of Research

 Springer

Michele Cini

Topics and Methods in Condensed Matter Theory

Michele Cini

Topics and Methods in Condensed Matter Theory

From Basic Quantum Mechanics
to the Frontiers of Research

With 73 Figures and 4 Tables

 Springer

Prof. Michele Cini
University of Rome
Department of Physics
Via della Ricerca Scientifica
00133 Rome
Italy
e-mail: cini@roma2.infn.it

Library of Congress Control Number: 2007925062

ISBN-13 978-3-540-70726-4 Springer Berlin Heidelberg New York

This work is subject to copyright. All rights are reserved, whether the whole or part of the material is concerned, specifically the rights of translation, reprinting, reuse of illustrations, recitation, broadcasting, reproduction on microfilm or in any other way, and storage in data banks. Duplication of this publication or parts thereof is permitted only under the provisions of the German Copyright Law of September 9, 1965, in its current version, and permission for use must always be obtained from Springer. Violations are liable for prosecution under the German Copyright Law.

Springer is a part of Springer Science+Business Media

springer.com

© Springer-Verlag Berlin Heidelberg 2007

The use of general descriptive names, registered names, trademarks, etc. in this publication does not imply, even in the absence of a specific statement, that such names are exempt from the relevant protective laws and regulations and therefore free for general use.

Typesetting: Digital data supplied by Author

Production: LE-TeX Jelonek, Schmidt & Vöckler GbR, Leipzig

Cover Design: eStudio Calamar S.L., F. Steinen-Broo, Girona, Spain

SPIN 11367314 57/3180/YL 5 4 3 2 1 0 Printed on acid-free paper

To my wife Anna and to my son Massimo

Preface

*Quod super est, vacuas auris animumque sagacem
semotum a curis adhibe veram ad rationem,
ne mea dona tibi studio disposta fidei,
intellecta prius quam sint, contempta relinquo.*

Titus Lucretius Carus, De Rerum Natura Liber Primus

This book is structured as a course for students with a good knowledge of basic Quantum Mechanics who want to specialize in Condensed Matter Theory. Indeed it takes the reader to advanced levels in several topics, but there is an obvious trick: no teacher can hope to cover all this material in one semester without facing a serious and rightful student revolt. I am offering alternative advanced topics that I have been developing in different years of teaching and updated to the present time. Yet, I had to remove much important material which is a *condicio sine qua non* for condensed matter theorists; the most serious sacrifice (wisely urged by the Editor) was the removal of all the chapters in Relativistic Quantum Mechanics and QED that I have been teaching for many years in Atomic Physics courses but would have made the size of this work unacceptable as one book. Such topics are covered in excellent Springer books, like the series by Greiner. Even so, there is no encyclopedic attitude, or attempt to cover all the hottest advanced topics, but I privileged those arguments where I did some work and the methods that I used most often or where I gave some contribution in my long research activity. The central part of the book is devoted to the theory and applications of symmetry and Green's functions. In the interest of the class, I present them in such a way that one can easily separate an introductory part, that might be of interest to a broader audience including experimentalists, and a more advanced and demanding part.

Nobody really knows how knowledge grows, particularly in theoretical physics (a rather special environment to study) but my impression is that

it grows by a vivid (if often not very precise initially) understanding of particular problems, that are later combined in more powerful units and made more exact in the process. More complex phenomena require more mathematical ingenuity, new concepts arise, deep unexpected similarities between diverse problems are discovered. By such processes in which mathematics and physics merge into the reasoning process and are a source of inspiration for each other, one can sometimes predict new facts that are later verified experimentally. In condensed matter physics, predicting new experimental features is not reserved to geniuses, and one can really hope to achieve such results, and although the success is not uncommon, it is certainly rewarding. I believe that there is still lot of space for pioneers and while computing is important in a quantitative science like physics most real discoveries will continue to come from intuition and original thought.

Most times it is experiment that brings some unexpected and surprising result. Superconductivity is a typical example: common sense would have predicted that the resistance will unavoidably be present as a part of the imperfection of reality. This is the *magic* of Quantum Mechanics, that continues to make stunning yet tangible reality by the effect of phases. The role of Berry phases, flux quantization and the like is discussed mainly in Chapters 16 and 17. There are many phenomena but if we wish to go from phenomenology to principles progress is conditioned by methods. A large variety of methods have been generated by many theoreticians. Some are time honored, but enlighten new problems in new ways: to make practical predictions in the presence of symmetry we take advantage of abstract Group theory. However, important new methods continue to be invented, and there is no sign that the gold mine of ingenuity is exhausted. On the other hand, while an increasing number of problems are successfully dealt with by the existing codes and computational methods, the ingenuity continues to be required, since new interesting materials and processes are discovered which require fresh modeling.

Some of the subject matter is included because in my career I happened to work in the subject or to make extensive use of the methods; in this way I suppose I can provide in some measure a first-hand presentation of some topics. In particular, Chapters 6, 15, 13, 14 and 17 are the most original in the sense of presenting results from my own research; elsewhere I tried to present mature results in a fresh and attractive way. At least, I hope I will transmit some of the fun I have to work using such results. The discussion of general topics like Group theory or Feynman diagrams, the Keldysh theory, which are discussed in many textbooks, but are traditionally considered rather hard aims to help the reader by many examples and by direct procedures and intuitive arguments. I tend to prove everything and therefore the reader will find sentences like *it can be shown that ...* only seldom and for relatively unimportant side matters. Indeed, in most cases when something is really understood, there is little difficulty in finding a proof; on the other hand, the converse is also true: having no clear justification often means having no

real grasp or lacking mastery of the use of the results. However in several cases, lengthy formal proofs are readily found in the literature and there is no strong reason to reproduce them here: for instance, Wick's theorem and the linked cluster theorem fall in this category. Then I prefer to give my own intuitive arguments, that reflect the way I visualize the result for myself, and reference the literature where the canonical proofs are published.

Finally, I hope the readers will understand that this work costed me a considerable effort and at some point I had to force the writing process to converge. It is always possible to improve the book in many ways, but alas at some point the writing must stop. It was this appeal to the reader's understanding, besides the common interest in the Nature of Things, that prompted to me the above quotation from Titus Lucretius Carus.

It is a pleasure to thank Professor Giancarlo Rossi, Doctor Gianluca Stefanucci and Doctor Yassen Stanev, all at the Physics Department of Rome Tor Vergata University, and Doctor Claudio Verdozzi, currently at Lund, for reading and discussing part of the manuscript and giving useful advice and encouragement.

Rome, May 7, 2007

Michele Cini

Contents

Part I I-Introductory Many-Body Physics

1	Basic Many-Body Quantum Mechanics	1
1.1	Slater Determinants and Matrix Elements	1
1.1.1	Many-electron Matrix Elements	2
1.1.2	Derivation of the Rules	4
1.2	Second Quantization	5
1.2.1	Bosons	5
1.2.2	Field Quantization and Casimir Effect	7
1.2.3	Fermions	9
1.2.4	Basis Change in Second Quantization and Field Operators	11
1.2.5	Hubbard Model for the Hydrogen Molecule	13
1.3	Schrieffer-Wolff Canonical Transformation	15
1.4	Variational Principle	16
1.5	Variational Approximations	18
1.6	Non-degenerate Perturbation Theory	18
2	Adiabatic Switching and Time-Ordered series	19
2.1	Time-dependent is Better: start from the <i>Golden Age</i>	19
2.2	Evolution in Complex Time	21
2.2.1	Heisenberg Picture	21
2.2.2	Thermal Averages	23
2.3	The Interaction Picture and the Viable Expansion	25
	Problems	26
3	Atomic Shells and Multiplets	29
3.1	Shell Structure of Atoms	29
3.2	Hartree-Fock Method	29
3.2.1	Physical Meaning of Exchange: the Cohesion of a Simple Metal	35
3.3	Virial Theorem	37
3.4	Hellmann-Feynman Theorem	38
3.5	Central Field	38
3.5.1	L-S Multiplets ($H'_{rel} \rightarrow 0$ Limit)	40

3.5.2	Hund's First Rule	42
3.6	Atomic Coulomb Integrals	43
3.6.1	Hund's Second Rule	46
3.6.2	J-J Coupling	46
3.6.3	Intermediate Coupling	46
3.7	Meitner-Auger Effect and Spectroscopy	48
3.7.1	Auger Selection Rules and Line Intensities	50
4	Green's Functions as Thought Experiments	55
4.1	Green's Theorem for one-Body Problems	55
4.2	How Many-Body Green's Functions Arise	55
4.2.1	Correlation Functions	55
4.2.2	Quantum Green's Functions	57
4.2.3	Quantum Averages	58
4.2.4	Green's functions at Finite Temperature	59
4.3	Non-interacting Propagators for Solids	61
4.3.1	Green's Functions for Tight-binding Hamiltonians	66
4.3.2	Lippmann-Schwinger Equation	70
4.3.3	t matrix	70
4.3.4	Inglesfield Embedding Method	71
4.4	Kubo Formulae	73
4.5	Vacuum Amplitudes	75
4.6	Lehmann Representation	76
4.6.1	Zero-Temperature Fermi Case	76
4.6.2	Finite Temperatures, Fermi and Bose	78
4.6.3	Fluctuation-Dissipation Theorem	79
5	Hopping Electron Models: an Appetizer	81
5.1	Fano Resonances and Resolvents	81
5.1.1	Resonances	81
5.1.2	Fano Model	82
5.1.3	One-body Treatment	82
5.1.4	Many-Body Treatment	83
5.1.5	The Resolvent	86
5.1.6	Self-Energy Operator	89
5.2	Magnetic Impurities and Chemisorption on Transition Metal Surfaces	90
5.3	Strong Coupling and the Kondo Peak	95
5.3.1	Narrow-Band Anderson Model	95
5.3.2	Anderson Model, s-d Model and Kondo Model	98
5.3.3	Fermi Level Singularity and Kondo Minimum	100
5.4	The $N_f \gg 1$ Expansion	101
5.4.1	Kondo Temperature in the Spin-Fluctuation Case	105
5.4.2	Density of Occupied States	106
	Problems	107

6	Many-body Effects in Electron Spectroscopies	109
6.1	Electron Spectroscopy for Chemical Analysis (ESCA)	109
6.1.1	Chemical Shifts	111
6.1.2	Core-Level Splitting in Paramagnetic Molecules	111
6.1.3	Shake-up, Shake-off, Relaxation	113
6.1.4	Lundqvist Model of Phonon and Plasmon Satellites	115
6.2	Auger CVV Line Shapes: Two-Hole Resonances	118
6.2.1	Desorption	122
6.3	Two Interacting Fermions in a Lattice	123
6.4	Quadratic Response Formalism and Spectroscopies	127
6.4.1	One-Step Theory of Auger Spectra	129
6.4.2	Plasmon Gain	130
	Problems	130

Part II Symmetry in Quantum Physics

7	Group Representations for Physicists	133
7.1	Abstract Groups	133
7.2	Point Symmetry in Molecules and Solids	135
7.2.1	Symmetry operators	135
7.2.2	Dirac characters and Irreducible Representations	140
7.2.3	Schur's lemma	143
7.2.4	Continuous Groups	144
7.3	Accidental degeneracy and hidden symmetries	145
7.4	Great Orthogonality Theorem (GOT)	149
7.5	Little Orthogonality Theorem (LOT)	152
7.6	Projection operators	154
7.7	Regular representation	155
	Problems	156
8	Simpler Uses of Group Theory	157
8.1	Molecular Orbitals	157
8.1.1	Molecular Orbitals of NH_3	157
8.1.2	Molecular Orbitals of CH_4	158
8.1.3	Characters of Angular Momentum Eigenstates	160
8.1.4	Examples: O_h Group, Ligand Group Orbitals, Crystal Field	160
8.2	Normal Modes of vibration	163
8.3	Space-Time Symmetries of Bloch States	169
8.4	Space groups of solids	173
8.4.1	Symmorphic and Nonsymmorphic Groups	174
8.5	Young Diagrams	177
	Problems	179

9 Product of Representations and Further Physical Applications 181

9.1 Irreducible Tensor Operators 181

9.2 Direct Product Representation 183

 9.2.1 Selection Rules 184

9.3 Reduction of the Direct Product Representation 185

9.4 Spin-Orbit Interaction and Double Groups 186

9.5 Static and Dynamical Jahn-Teller Effect 188

 9.5.1 The Born-Oppenheimer (BO) Approximation 188

 9.5.2 The Jahn-Teller Theorem 189

9.6 Non-Adiabatic Operator 193

 9.6.1 Dynamical Jahn-Teller Effect 194

 9.6.2 How the $E \times \epsilon$ Hamiltonian arises 196

 9.6.3 Nuclear Wave Functions Cannot be Taken Real 197

9.7 Wigner-Eckart Theorem with Applications 197

9.8 The Symmetric Group and Many-Electron States 199

9.9 Seniority Numbers in Atomic Physics 201

Problems 204

Part III More on Green Function Techniques

10 Equations of Motion and Further Developments 207

10.1 Equations of motion for the interacting propagator 207

 10.1.1 Equations of Motion and Ground-State Energy 208

10.2 Time-Dependent Problems 208

 10.2.1 Auger Induced Ionic Desorption: Knotek-Feibelman Mechanism 210

10.3 Hierarchy of Greens Functions 212

10.4 Composite Operator Method 213

Problems 216

11 Feynman Diagrams for Condensed Matter Physics 217

11.1 Diagrams for the Vacuum Propagator 217

 11.1.1 Wick's Theorem 219

 11.1.2 Goldstone Diagrams 221

 11.1.3 Diagram Rules for the Thermodynamic Potential 224

11.2 Linked Cluster Theorem 225

 11.2.1 Valence Electron and Core Hole 227

 11.2.2 H_2 Model 229

 11.2.3 The Linked Cluster Expansion and Green's Functions 230

11.3 Diagrams for the Dressed Propagator 231

 11.3.1 Adiabatic Switching and Perturbation Theory 232

 11.3.2 Diagrams for the Propagator in frequency space 235

11.4 Dyson Equation 238

11.4.1	External Potential	241
11.5	Self-Energy from Interactions	242
11.6	Skeleton Diagrams	245
11.7	Two-body Green's Function: the Bethe-Salpeter Equation . . .	245
11.8	Self-Energy and Two-Body Green's Function	247
11.9	Functional Calculus and Diagrams	248
11.9.1	The Self-Energy as a Functional	249
11.9.2	Polarization Bubble	251
11.9.3	The Vertex	253
11.10	Hedin's Equations	254
12	Many-Body Effects and Further Theory	257
12.1	High Density Electron Gas	257
12.1.1	More Physical Insight about the RPA	259
12.2	Low Density Electron gas: Ladder Approximation	263
12.3	Ladder Approximations in Electron Spectroscopies	264
12.3.1	XPS and Auger Spectra from Metals	264
12.3.2	The $U < 0$ Phenomenon	267
12.3.3	Correlation in Early Transition Metals	270
12.4	Conserving Approximations	272
12.4.1	Continuity Equation	272
12.4.2	The Φ Functional	274
12.4.3	Gauge Transformation	275
12.4.4	Ground-State Energy and Grand Potential	276
12.4.5	Luttinger-Ward and ABL Variational Principles	277
12.5	Generalized Ward Identities	278
12.6	Connection of Diagrams to D F T	279
12.6.1	Highlights on Density Functional Theory	279
12.6.2	Sham - Schlüter Equation	282
	Problems	283
13	Non-Equilibrium Theory	285
13.1	Time-Dependent Probes and Nonlinear Response	285
13.2	Kadanoff-Baym and Keldysh Methods	286
13.3	Complex-Time Integrals by Langreth's Technique	288
13.3.1	Finite temperatures	290
13.4	Keldysh-Dyson Equation on the Contour	291
13.5	Evolution on Keldysh Contour	294
13.5.1	Contour Evolution of Bosons	298
13.6	Selected Applications of the Keldysh Formalism	298
13.6.1	Atom-Surface Scattering	299
13.6.2	Quantum Transport	304
	Problems	309

Part IV Non-Perturbative Approaches and Applications

14 Some Recursion Techniques with Applications 313

 14.1 Lanczos-Haydock Recursion 313

 14.1.1 Local Green’s Function for a Chain 313

 14.1.2 Green’s Function of any System 315

 14.1.3 Terminator 316

 14.1.4 Moments 322

 14.2 Spin-Disentangled Diagonalization 323

 14.3 Method of Excitation Amplitudes 326

 14.4 Feenberg Method 329

 14.4.1 Solving Linear Systems 332

 14.4.2 Homogeneous systems 333

 Problems 333

15 Aspects of Nonlinear Optics and Many-Photon Effects . . . 335

 15.1 Diffusion of Radiation in Dipole Approximation 335

 15.1.1 Second-Order Processes 336

 15.2 Sum Frequency and Second-Harmonic Generation (SHG) 342

 15.3 Diffusion of Coherent Light 343

 15.3.1 Effective mode 343

 15.3.2 Dynamical Stark Effect 346

 Problems 351

Part V Selected Exact Results in Many-Body Problems

16 Quantum Phases 355

 16.0.3 Gauge Transformations 355

 16.0.4 Spinor Rotations 356

 16.0.5 Galilean Transformations 356

 16.1 Topologic phases 357

 16.1.1 Parametric Hamiltonians and Berry Phase 358

 16.1.2 Polarization of Solids 362

17 Pairing from repulsive interactions 367

 17.0.3 $W = 0$ Pairing in Cu-O Clusters 369

 17.0.4 Pairing Mechanism 373

 17.0.5 The $W = 0$ theorem 373

 17.0.6 Examples 375

 17.1 Superconducting flux quantization and Josephson effect 378

 Problems 381

18 Algebraic Methods 383

18.1 Lieb Theorems on the Half Filled Hubbard Model 383

18.2 Bethe Ansatz for the Heisenberg Chain 387

18.3 Bethe Ansatz for Interacting Fermions 1 Dimension 392

 18.3.1 δ -Function Interaction 392

 18.3.2 The Hubbard Model in 1d 396

 18.3.3 The Periodic Boundary Conditions 401

 18.3.4 Spin Chain Analogy 403

Problems 406

Part VI Appendices

19 Appendix 1: Zero-point Energy in a Pillbox 409

20 Appendix II-Character Tables 411

21 Proof of the Wigner-Eckart Theorem 413

Solutions 415

References 431

Index 439

Part I

I-Introductory Many-Body Physics

1 Basic Many-Body Quantum Mechanics

1.1 Slater Determinants and Matrix Elements

The solutions of eigenvalue equations like the time-independent one-electron Schrödinger equation $hw_i = \epsilon_i w_i$ form a complete set of spin-orbitals $\{w_i \equiv \varphi_i(x)\chi_i\}$, where $\varphi_i(x)$ are normalized space orbitals and $\chi_i = \uparrow$ or \downarrow . The set can be taken orthogonal and ordered in ascending energy or in any other arbitrary way. Any one-electron state can be expanded as a linear combination of the w_i . Moreover, we can think of a state for N electrons obtained as follows. Choose in any way N spin-orbitals out of the set $\{w_i\}$, keep them in the original order but call them $v_1, v_2 \dots v_N$; now let $|v_1, v_2 \dots v_N\rangle$ be the state with one electron in each. Imagine labeling¹ the indistinguishable electrons with numbers $1, 2, \dots, N$. In this many-body state one has an amplitude $\Psi(1, 2, \dots, N) \equiv \Psi((x_1, \chi_1), (x_2, \chi_2), \dots, (x_N, \chi_N))$ of having electron i in the one-particle state (x_i, χ_i) . How to calculate Ψ ? A product like $v_1 v_2 \dots v_N = \prod_k^N v_k$ is in conflict with the Pauli principle because it fails to be antisymmetric in the exchange of two particles. However, the remedy is easy, because anti-symmetrized products are a basis for the antisymmetric states. To this end, let $\mathcal{P} : \{1, 2, \dots, N\} \rightarrow \{\mathcal{P}_1, \mathcal{P}_2, \dots, \mathcal{P}_N\}$ be one of the $N!$ permutations of N objects. If $N = 3$, the set of 6 permutations comprises the rotations $\{(1, 2, 3), (2, 3, 1), (3, 1, 2)\}$ and $\{(2, 1, 3), (3, 2, 1), (1, 3, 2)\}$.

Anticipating some Group Theory

The last three are just *transpositions*, that is, they are obtained from the *fundamental permutation* $(1, 2, 3)$ by one exchange. One can *multiply* two permutations \mathcal{Q} and \mathcal{P} ; the *product* $\mathcal{Q}\mathcal{P}$ is the permutation obtained by performing \mathcal{P} and then \mathcal{Q} and the result is:

$$\{\mathcal{Q}_1, \mathcal{Q}_2, \dots, \mathcal{Q}_N\} \{\mathcal{P}_1, \mathcal{P}_2, \dots, \mathcal{P}_N\} = \{\mathcal{Q}_{\mathcal{P}_1}, \mathcal{Q}_{\mathcal{P}_2}, \dots, \mathcal{Q}_{\mathcal{P}_N}\}. \quad (1.1)$$

For instance², $(3, 2, 1)(2, 1, 3) = (2, 3, 1)$. *All permutations can be obtained from transpositions by multiplication.* The inverse of a permutation is the one that

¹The electrons are identical, but this does not prevent us from labeling them; rather it imposes that the wave function changes sign for each exchange of labels.

²in words, \mathcal{P} sends $1 \rightarrow 2$ and then \mathcal{Q} sends $2 \rightarrow 1$, and in the same way $2 \rightarrow 1 \rightarrow 3$ and $3 \rightarrow 2 \rightarrow 1$.

upon multiplication restores the standard (ascending) order $(1, 2, \dots, N)$. Any permutation can be shown to be a product of transpositions, usually in more than one way: for example, $(2,3,1)$ is obtained from the standard order by exchanging 1 and 2 and then 1 and 3 but also exchanging 1 and 3 and then 2 and 3. \mathcal{P} has a parity or *signature* $(-)^{\mathcal{P}}$ defined such that an exchange is odd, two are even, and so on, so in the above example $(1,2,3)$, $(2,1,3)$ and $(3,1,2)$ are even and the others odd. In Chapter 7 we shall see that such simple observations have far reaching consequences.

Determinants

The *antisymmetrizer* operator

$$A = \frac{1}{N!} \sum_{\mathcal{P}} (-)^{\mathcal{P}} \mathcal{P} \quad (1.2)$$

converts any product into a normalized Slater determinant, so we may write a physically acceptable solution as

$$\Psi(1, 2, \dots, N) = A \prod_k v_k = \frac{1}{\sqrt{N!}} \sum_{\mathcal{Q}} (-)^{\mathcal{P}} v_{\mathcal{Q}_1}(1) v_{\mathcal{Q}_2}(2) \dots v_{\mathcal{Q}_N}(N), \quad (1.3)$$

or, equivalently,

$$\Psi(1, 2, \dots, N) = \frac{1}{\sqrt{N!}} \begin{pmatrix} v_1(1) & v_2(1) & \dots & v_N(1) \\ v_1(2) & v_2(2) & \dots & v_N(2) \\ \dots & \dots & \dots & \dots \\ v_1(N) & v_2(N) & \dots & v_N(N) \end{pmatrix}. \quad (1.4)$$

Note that the transposed matrix is equivalent since the determinant is the same. Exchanging two rows, that is, two electrons, one gets a - sign. A permutation of the electrons is equivalent to the inverse permutation of the spinorbitals, and $\mathcal{P}\Psi(1, 2, \dots, N) = \Psi(\mathcal{P}_1, \mathcal{P}_2, \dots, \mathcal{P}_N) = (-)^{\mathcal{P}}\Psi(1, 2, \dots, N)$.

The set of all determinants is complete provided an arbitrary order is fixed for the one-electron states (otherwise the set is overcomplete).

Suppose we solve $hw_i = \epsilon_i w_i$ for one electron and then consider the same problem with N electrons and $H = \sum_i^N h(i)$. This problem is no harder than for a single electron, and the N -body Schrödinger equation is solved by (1.4) with energy eigenvalue $\epsilon_1 + \epsilon_2 + \dots + \epsilon_N$.

1.1.1 Many-electron Matrix Elements

The matrix element $\langle \Psi | F | \Phi \rangle$ of operators $F(1, 2, \dots, N)$ between determinantal states, when we expand the determinants, means a sum of $(N!)^2$ terms. This grows disastrously with N ; however there are simple rules to calculate

such matrix elements. Let $\Phi(1, \dots, N)$ be a determinant made by N spinorbitals $u_1, u_2 \dots u_N$; taken out of the orthogonal set $\{w_i\}$ (they may be same as in Ψ , in which case we are dealing with expectation values). One can readily observe these rules by working out a 2×2 example, while the proof requires a trick which is explained in Sect. 1.1.2. The simplest case is $f = 1$, and the rule is: the overlap between determinants is the determinant of the matrix with elements the one-electron overlaps $\langle u_i | v_j \rangle$:

$$\langle \Phi | \Psi \rangle = \text{Det} [\{ \langle u_i | v_j \rangle \}]. \quad (1.5)$$

This useful result holds even if u and v spinorbitals are taken from different sets w and w' . The overlap of a determinant with itself is indeed 1, as it should, which verifies the normalization of determinants. The one-electron matrix elements also imply a spin scalar product.

For one-body operators $F(1, 2, \dots, N) = \sum_i^N f(i)$, where f acts on one electron, the rule is simple: determinants gives the same results as simple product wave functions, and antisymmetry has no consequences. The expectation values are given by

$$\langle \Psi | F | \Psi \rangle = \sum_i^N \langle u_i | f | u_i \rangle. \quad (1.6)$$

For example, if we pick $f(i) = \delta(\mathbf{x} - \mathbf{x}_i)$, $F = \rho(\mathbf{x})$ is the number density and one finds $\langle \rho(\mathbf{x}) \rangle = \sum_i^N |u_i(\mathbf{x})|^2$. Off diagonal elements vanish if Ψ and Φ differ by more than 1 spinorbital; if they differ only by one spinorbital, v_k in Ψ and u_k in Φ ,

$$v_k \neq u_k \Rightarrow \langle \Phi | F | \Psi \rangle = \langle u_k | f | v_k \rangle. \quad (1.7)$$

Two-body operators of the form $F = \sum_{i \neq j}^{pairs} f_{ij} = \frac{1}{2} \sum_{i,j,i \neq j}^N f_{ij}$, like the Coulomb interaction, have vanishing matrix elements when the two determinants differ by more than 2 spin-orbitals. For the rest, the best way to recall the result is by the interaction vertices in Figure 1.1.1 below (embryos of the Feynman diagrams that we introduce later). One must just note carefully which lines enter at 1 and (left and right) and which are outgoing. The order of labels is: the one entering at 1, the one entering at 2, the one outgoing at 1, the one outgoing at 2.

If v_i and v_j in Φ replace u_i and u_j in Ψ , $u_i \neq v_i, u_j \neq v_j$, then

$$\langle \Phi | F | \Psi \rangle = \langle v_i(1)v_j(2) | f(1,2) | u_i(1)u_j(2) \rangle - \langle v_i(1)v_j(2) | f(1,2) | u_i(2)u_j(1) \rangle \quad (1.8)$$

where the second, exchange term comes from the antisymmetry. These correspond to vertices a) and b) below, respectively. If f does not depend on spin the exchange term vanishes for opposite spins.

The two-body operator matrix element describes the collision of a couple of electron, while all the others are spectators. If Φ and Ψ are the same, except

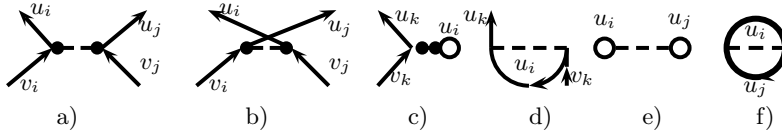


Fig. 1.1. Interaction vertices

for $u_i \neq v_i$, we get the vertex c) and its exchange companion d), representing the two terms in the expression

$$\begin{aligned} \langle \Phi | F | \Psi \rangle &= \sum_{i \neq k}^N [\langle v_k(1)u_i(2) | f(1, 2) | u_k(1)u_i(2) \rangle \\ &\quad - \langle u_i(1)v_k(2) | f(1, 2) | u_k(1)u_i(2) \rangle]. \end{aligned} \quad (1.9)$$

This is similar to (1.8), but there is a summation over all the spinorbitals present in both determinants, which act as background particles while the i -th electrons jumps from $v(i)$ to $u(i)$. Finally, for the expectation value we get the vertices e) and f), that is,

$$\begin{aligned} \langle \Psi | F | \Psi \rangle &= \sum_{j \neq i}^N [\langle u_i(1)u_j(2) | f(1, 2) | u_i(1)u_j(2) \rangle \\ &\quad - \langle u_j(1)u_i(2) | f(1, 2) | u_i(1)u_j(2) \rangle]. \end{aligned} \quad (1.10)$$

1.1.2 Derivation of the Rules

A direct expansion of

$$\begin{aligned} \langle \Psi | F | \Phi \rangle &= \frac{1}{N!} \sum_{\mathcal{P}, \mathcal{Q}} (-)^{\mathcal{P}+\mathcal{Q}} \\ &\langle u_{\mathcal{P}_1}(1)u_{\mathcal{P}_2}(2) \dots u_{\mathcal{P}_N}(N) | f | v_{\mathcal{Q}_1}(1)v_{\mathcal{Q}_2}(2) \dots v_{\mathcal{Q}_N}(N) \rangle \end{aligned} \quad (1.11)$$

involves $N!$ terms and is formidable unless N is small. However, the proof of the above rules is easily obtained by a trick, that I exemplify in the case of one-body operators. The matrix element

$$\langle u_{\mathcal{P}_1}(1)u_{\mathcal{P}_2}(2) \dots u_{\mathcal{P}_N}(N) | f(1, \dots, N) | v_{\mathcal{Q}_1}(1)v_{\mathcal{Q}_2}(2) \dots v_{\mathcal{Q}_N}(N) \rangle$$

is a multiple integral; we permute the names of dummy variables and get $\langle u_{\mathcal{P}_1}(\mathcal{P}_1)u_{\mathcal{P}_2}(\mathcal{P}_2) \dots u_{\mathcal{P}_N}(\mathcal{P}_N) | f | v_{\mathcal{Q}_1}(\mathcal{P}_1)v_{\mathcal{Q}_2}(\mathcal{P}_2) \dots v_{\mathcal{Q}_N}(\mathcal{P}_N) \rangle$; f does not change since it must depend on particles in a symmetric way. The bra is independent of \mathcal{P} , since $\prod_i \langle u_{\mathcal{P}_i} | = \prod_i \langle u_i |$, and we obtain

$$\langle u_1(1)u_2(2)\dots u_N(N)|f|v_{\mathcal{Q}_1}(\mathcal{P}_1)v_{\mathcal{Q}_2}(\mathcal{P}_2)\dots v_{\mathcal{Q}_N}(\mathcal{P}_N)\rangle.$$

Now the \mathcal{Q} summation yields back the Ψ determinant with a permutation \mathcal{P} of the electrons, that is, $\Psi(-)^{\mathcal{P}}$; the $(-)^{\mathcal{P}}$ factor cancels the one already present in (1.11). Hence,

$$\langle \Phi|F|\psi\rangle = \langle u_1(1)u_2(2)\dots u_N(N)|f|\begin{pmatrix} v_1(1) & v_2(1) & \dots & v_N(1) \\ v_1(2) & v_2(2) & \dots & v_N(2) \\ \dots & \dots & \dots & \dots \\ v_1(N) & v_2(N) & \dots & v_N(N) \end{pmatrix}\rangle. \quad (1.12)$$

More explicitly,

$$\langle \Phi|f|\psi\rangle = \frac{1}{\sqrt{N!}}\langle u_1(1)u_2(2)\dots u_N(N)|f|\sum_{\mathcal{Q}}(-)^{\mathcal{Q}}v_{\mathcal{Q}_1}(1)v_{\mathcal{Q}_2}(2)\dots v_{\mathcal{Q}_N}(N)\rangle. \quad (1.13)$$

1.2 Second Quantization

1.2.1 Bosons

Since the time-independent Schrödinger equation for the Harmonic Oscillator,

$$-\frac{\hbar^2}{2m}\frac{d^2\psi}{dx^2} + \frac{m\omega^2 x^2}{2}\psi = E\psi \quad (1.14)$$

has a characteristic length $x_0 = \sqrt{\frac{\hbar}{m\omega}}$, one introduces the *annihilation operator*

$$a = \frac{1}{\sqrt{2}}\left(\frac{x}{x_0} + \frac{ix_0 p}{\hbar}\right). \quad (1.15)$$

this is equivalent to

$$\frac{x}{x_0} = \frac{a + a^\dagger}{\sqrt{2}}, \quad \frac{ix_0 p}{\hbar} = \frac{a - a^\dagger}{\sqrt{2}}, \quad (1.16)$$

with the commutation relation

$$[a, a^\dagger]_- = 1; \quad (1.17)$$

the Hamiltonian can be rewritten

$$H = \left(a^\dagger a + \frac{1}{2}\right)\hbar\omega. \quad (1.18)$$

If ψ is a solution of (1.14) with eigenvalue E , $a\psi$ must be solution with eigenvalue $E - \hbar\omega$. The conclusions are: 1) $a\psi_0 = 0$ if ψ_0 is the ground state

and 2) a^\dagger is a creation operator that in fact creates excitations like a destroys them. One then learns that i) this represents a boson field with one degree of freedom (the x) ii) when dealing with real physical fields one never observes the oscillators but only the excitations, e.g. photons for the electromagnetic field. The noninteracting bosons in a field mode can be created in any number, and each adds the same energy to the field. The oscillator does not exist at all, but the unique property of the oscillator potential which has infinitely many states with uniform spacing $\hbar\omega$ makes it a perfect representation for the field.

Example: Coupled Boson Representation of Angular Momentum

Schwinger [8] has shown how one can build a representation of the angular momentum operators including components J_i , shift J_\pm and more exotic K_\pm operators that conserve m but raise or lower j . All this was obtained using creation and annihilation operators of a couple of modes, and everything comes from a simple observation. For instance let $j = \frac{3}{2}$ in units of \hbar and consider the following scheme: For any j , we can write $j = \frac{n_1+n_2}{2}$ in terms of

n_1	n_2	$j = \frac{n_1+n_2}{2}$	$j_z = \frac{n_1-n_2}{2}$
0	3	3/2	-3/2
1	2	3/2	-1/2
2	1	3/2	1/2
3	0	3/2	3/2

2 integers ≥ 0 in several ways, and each entry corresponds to a choice of j_z ; n_2 increases from 0 in $2j + 1$ steps. So, a J_+ should add 1 to n_1 and remove 1 from n_2 , while K_\pm should add ± 1 to both. Two harmonic oscillators can provide the occupation number operators to represent that. So,

$$j = \frac{\hat{n}_1 + \hat{n}_2}{2}; \quad j_z = \frac{\hat{n}_1 - \hat{n}_2}{2}. \tag{1.19}$$

To extend this idea, one can observe that introducing a spinor operator

$$\psi = \begin{pmatrix} a_1 \\ a_2 \end{pmatrix} \tag{1.20}$$

we may write

$$j = \frac{\hbar}{2} \psi^\dagger \psi; \quad j_z = \frac{\hbar}{2} \psi^\dagger \sigma_z \psi. \tag{1.21}$$

This extends naturally to

$$\vec{j} = \frac{\hbar}{2} \psi^\dagger \vec{\sigma} \psi \tag{1.22}$$

which implies trivially

$$j_x = \frac{\hbar}{2}(a_1^\dagger a_2 + a_2^\dagger a_1); \quad j_y = \frac{i\hbar}{2}(-a_1^\dagger a_2 + a_2^\dagger a_1) \quad (1.23)$$

and hence

$$j_+ = \hbar a_1^\dagger a_2; \quad j_- = \hbar a_2^\dagger a_1. \quad (1.24)$$

Indeed, it is a simple matter to verify that

$$[j_x, j_y] = i\hbar j_z, \quad (1.25)$$

$$j^2 = \hbar^2 j(j+1). \quad (1.26)$$

One can change j by

$$K_+ = \hbar a_1^\dagger a_2^\dagger; \quad K_- = \hbar a_1 a_2. \quad (1.27)$$

Using j and $m = j_z$ in (1.19) one finds n_1 and n_2 , hence

$$|jm\rangle = \frac{(a_1^\dagger)^{j+m}(a_2^\dagger)^{j-m}}{\sqrt{(j+m)!(j-m)!}}|0\rangle. \quad (1.28)$$

This is an alternative way to derive results like Clebsh-Gordan coefficients and the like.

1.2.2 Field Quantization and Casimir Effect

The electromagnetic field fluctuations in vacuo have a macroscopic consequence named Casimir effect. This is of interest for fundamental physics but also for potential applications.

Let two square mirrors of side L be put in front of each other at a distance s . Roughly speaking, this causes boundary conditions $E_{\parallel} = 0$ of vanishing parallel electric field component on both surfaces, at frequencies below the plasma frequency ω_p of the metal. The field between the mirrors is constrained and has a reduced zero point energy; thus, the radiation pressure is lower than in vacuum and a macroscopic attraction between the mirrors appears. The effect was discovered by Casimir [6] theoretically and then verified experimentally [7],[200]. It is important at $m\mu$ distances, so it is longer ranged than Van der Waals forces, which are mainly due to the fluctuating instantaneous dipoles on non-polar systems.

To understand this in more detail consider a metallic pillbox, with reflecting walls, a square basis of side L and height s . How much is the zero-point energy $U(s)$ in the pillbox? Each wave-vector $k = (\frac{\pi a}{s}, \frac{\pi b}{L}, \frac{\pi c}{L})$, (with integer a, b and c) contributes $\hbar ck$ and the sum diverges of course, so we impose an exponential ultraviolet cutoff α , removing the short wavelengths such that $k\alpha \gg 1$. They are not involved anyhow because at ultraviolet frequencies the mirrors are transparent.

$$U(s) = \hbar c \sum_{abc} \sqrt{\left(\frac{a\pi}{s}\right)^2 + \left(\frac{b\pi}{L}\right)^2 + \left(\frac{c\pi}{L}\right)^2} e^{-\alpha \sqrt{\left(\frac{a}{s}\right)^2 + \left(\frac{b}{L}\right)^2 + \left(\frac{c}{L}\right)^2}}. \quad (1.29)$$

We can calculate this exactly for large enough L and the result diverges as $\alpha \rightarrow 0$. One finds (see Appendix 1)

$$U(s) = \frac{\hbar c \pi^2 L^2}{2} \left(\frac{d}{d\alpha}\right)^2 \left(\frac{1}{\alpha} \frac{1}{e^{\frac{\alpha}{s}} - 1}\right) \quad (1.30)$$

Using the expansion

$$\frac{y}{e^y - 1} = 1 - \frac{1}{2}y + \frac{1}{6} \frac{y^2}{2!} - \frac{1}{30} \frac{y^4}{4!} + \dots = \sum_n \frac{B_n y^n}{n!} \quad (1.31)$$

(the B_n are called Bernoulli numbers), one obtains:

$$U(s) = \frac{\hbar c \pi^2 L^2}{2} \left(\frac{d}{d\alpha}\right)^2 \left[\frac{s}{\alpha^2} - \frac{1}{2\alpha} + \frac{1}{12s} - \frac{\alpha^2}{30} \frac{1}{4!s^3} + \dots \right] \quad (1.32)$$

The first two terms lead to the aforementioned divergence: should we try to remove all the radiation from the cavity, including the high frequency modes, that would cost us infinite energy. However, the divergence disappears if we ask: what changes if we shift one side of the cavity by 1 cm? To better answer this question, suppose a cavity of length R is divided in two equal halves by a mirror: evidently the energy of the vacuum is the diverging quantity $2U(R/2)$. If instead the mirror is at distance s from one end and $R - s$ from the other, the vacuum energy must be $U(s) + U(R - s)$, which also diverges. The finite difference

$$\Delta E(s) = \lim_{R \rightarrow \infty} \left\{ U(s) + U(R - s) - 2U\left(\frac{R}{2}\right) \right\} \quad (1.33)$$

has the physical meaning of an energy that must be supplied to the system in order to shift the mirror to the middle of the cavity. If the cavity is large, this can be identified with the interaction energy at distance s . Eventually one can let $\alpha \rightarrow 0$. The zero point energy decrease per unit surface is thus

$$\Delta E = \frac{\pi^2 \hbar c}{720 s^3}, \quad (1.34)$$

and since the radiation pressure is proportional to the energy density one observes an attractive force

$$F = -\frac{\pi^2 \hbar c}{240 s^4}. \quad (1.35)$$

Measuring distances s in μm , one finds

$$F = -\frac{0.013}{s^4} \text{ dyne/cm}^2. \quad (1.36)$$

This force and its dependence on material and surface properties is actively investigated and could be used to operate nano-machines.

1.2.3 Fermions

The second quantization formalism for Fermions was invented in order to deal with phenomena like neutron decay $n \rightarrow p + e + \bar{\nu}$ or pair creation in particle physics, but to create an electron-positron pair one needs about a million eV. In condensed matter physics the typical energy scale is much less than that, yet many important phenomena are naturally described in terms of the creation (or annihilation) of fermion *quasi*-particles. Electron-hole pairs can be created very much like electron-positron ones. In scattering processes, when all the particles are conserved, one can proceed with Slater determinants in first quantization; however, second quantization formalism is much easier to work with.

The change from bosons to fermions replaces permanents with determinants. In place of a N -times excited oscillator representing N bosons in a given mode, we now consider N -fermion determinants $|u_1 u_2 \dots u_N\rangle$, where the spin-orbitals are chosen from a *complete orthonormal* set $\{w_i\}$. The index i can be discrete or continuous but implies a *fixed ordering* of the complete set. In this way, one can convene e.g. that in $|u_1 u_2 \dots u_N\rangle$ the indices $1 \dots N$ are in increasing order thereby avoiding multiple counting of the same state. The zero-particles or *vacuum* state $|\text{vac}\rangle$ replaces the oscillator ground state. For the determinants, it is generally preferable to use a compact notation like $|u_m u_n\rangle$ rather than the explicit $\frac{1}{\sqrt{2}} \text{Det} \begin{pmatrix} u_m(1) & u_m(2) \\ u_n(1) & u_n(2) \end{pmatrix}$ which contains the same information. Consider the following correspondence³ between determinants and states of the Hilbert space with various numbers of electrons:

First Quantization	Second Quantization
No – electrons state(vacuum)	$ \text{vac}\rangle$
1 – body state u_k	$c_k^\dagger \text{vac}\rangle$
2 – body determinant $ u_m u_n\rangle$	$c_m^\dagger c_n^\dagger \text{vac}\rangle$
3 – body determinant $ u_m u_n u_p\rangle$	$c_m^\dagger c_n^\dagger c_p^\dagger \text{vac}\rangle$
...	...

(1.37)

Up to now the second-quantization side looks very similar to the compact notation for determinants: the new idea is using the operator c_m^\dagger , clearly deserving the name of electron creation operator in spin-orbital m , in order to express all other operators. The left column introduces an occupation number representation of the basis of the Hilbert space; second quantization builds such a representation by creation operators c_m^\dagger . Adding a particle to any state cannot lead to the vacuum state,

$$\langle \text{vac} | c_m^\dagger = 0. \quad (1.38)$$

³mathematically, it is an isomorphism; it can be thought of as a change in notation.

Moreover, since a determinant is odd when columns are exchanged, we want an anticommutation rule

$$[c_m^\dagger, c_n^\dagger]_+ \equiv c_m^\dagger c_n^\dagger + c_n^\dagger c_m^\dagger = 0. \quad (1.39)$$

It follows that the square of a creation operator vanishes. By definition,

$$c_m^\dagger \{c_n^\dagger c_r^\dagger |vac\rangle\} = c_m^\dagger c_n^\dagger c_r^\dagger |vac\rangle \quad (1.40)$$

The notation suggests that c_m^\dagger is the Hermitean conjugate of c_m ; this is called annihilation operator. Taking the conjugate of (1.40)

$$\{\langle vac|c_r c_n\rangle\} c_m = \langle vac|c_r c_n c_m \quad (1.41)$$

and taking the scalar product with $c_m^\dagger c_n^\dagger c_r^\dagger |vac\rangle$, we deduce that

$$\{\langle vac|c_r c_n\rangle\} c_m |c_m^\dagger c_n^\dagger c_r^\dagger |vac\rangle = 1. \quad (1.42)$$

If now we consider c_m as acting on the right, we see that it is changing the 3-body state $c_m^\dagger c_n^\dagger c_r^\dagger |vac\rangle$ into the 2-body one $c_n^\dagger c_r^\dagger |vac\rangle$. Thus, annihilation operator is a well deserved name: an annihilation operator c_m for a fermion in the spin-orbital state u_m removes the leftmost state in the determinant leaving a $N - 1$ state determinant:

$$c_1 |u_1 u_2 \dots u_N\rangle = |u_2 \dots u_N\rangle \quad (1.43)$$

and

$$c_m |vac\rangle = 0. \quad (1.44)$$

It obeys the conjugate of the anticommutation rules (1.39), namely,

$$[c_m, c_n]_+ \equiv c_m c_n + c_n c_m = 0, \quad c_m^2 = 0. \quad (1.45)$$

Next consider

$$c_n c_m^\dagger c_n^\dagger c_r^\dagger |vac\rangle, \quad n, m, r \text{ all different.} \quad (1.46)$$

Since the creation operators anticommute, we get

$$-c_n c_n^\dagger c_m^\dagger c_r^\dagger |vac\rangle = c_m^\dagger c_r^\dagger |vac\rangle$$

since the m state is created at the leftmost place in the determinant but is annihilated at once. This shows that creation and annihilation operators also anticommute,

$$[c_n, c_m^\dagger]_+ = 0, \quad n \neq m. \quad (1.47)$$

As long as the indices are different c and c^\dagger all anticommute, so the pairs $c_n c_m, c_n c_m^\dagger, c_n^\dagger c_m$ and $c_n^\dagger c_m^\dagger$ can be carried through any product of creation or annihilation operators where the indices n, m do not occur.

Next we note that $c_p^\dagger |vac\rangle \equiv |p\rangle$ is a one-body wave function; $c_p c_p^\dagger |vac\rangle = |vac\rangle$ and $c_p^\dagger c_p c_p^\dagger |vac\rangle = c_p^\dagger |vac\rangle$. Now one can check that

$$n_p \equiv c_p^\dagger c_p \quad (1.48)$$

is the occupation number operator, having eigenvalue 1 on any determinant where p is occupied and 0 if p is empty. On the other hand, $c_p c_p^\dagger$ having eigenvalue 0 on any determinant where p is occupied and 1 if p is empty. thus in any case $c_p c_p^\dagger + c_p^\dagger c_p = 1$. Since this holds on all the complete set it is an operator identity and we may complete the rules with

$$[c_p, c_q^\dagger]_+ = \delta_{pq}. \quad (1.49)$$

Note that $n_p^\dagger = n_p$ and $n_p^2 = n_p$.

1.2.4 Basis Change in Second Quantization and Field Operators

We can readily go from basis set $\{a_n\}$ to a new set $\{b_n\}$; since

$$|b_n\rangle = \sum_k |a_k\rangle \langle a_k | b_n \rangle \quad (1.50)$$

the rule is

$$b_n^\dagger = \sum_k a_k^\dagger \langle a_k | b_n \rangle, \quad b_n = \sum_k a_k \langle b_n | a_k \rangle. \quad (1.51)$$

It is often useful to go from any set $\{u_n\}$ to the coordinate representation introducing the creation and annihilation field operators

$$\begin{cases} \Psi^\dagger(\mathbf{x}) = \sum_n c_n^\dagger u_n^\dagger(\mathbf{x}) \\ \Psi(\mathbf{x}) = \sum_n c_n u_n(\mathbf{x}), \end{cases} \quad (1.52)$$

(here u_n^\dagger denotes the conjugate spinor). Note that $c_p^\dagger |vac\rangle$ is a one-electron state and corresponds to the first-quantized spinor $u_p(\mathbf{x})$; $\Psi^\dagger(\mathbf{y}) |vac\rangle$ is a one-electron state and corresponds to the first-quantized spinor with spatial wave function $\sum_n u_n^\dagger(\mathbf{y}) u_n(\mathbf{x}) = \delta(\mathbf{x} - \mathbf{y})$; thus it is a perfectly localized electron. The rules are readily seen to be

$$[\Psi(\mathbf{x}), \Psi(\mathbf{y})]_+ = 0, \quad [\Psi^\dagger(\mathbf{x}), \Psi^\dagger(\mathbf{y})]_+ = 0, \quad (1.53)$$

and

$$[\Psi^\dagger(\mathbf{y}), \Psi(\mathbf{x})]_+ = \sum_{p,q} [c_p^\dagger, c_q]_+ u_p^\dagger(\mathbf{x}) u_q(\mathbf{y}) = \sum_{p,q} u_p^\dagger(\mathbf{x}) u_p(\mathbf{y}) = \delta(\mathbf{x} - \mathbf{y}) \quad (1.54)$$

where the δ also imposes the same spin for both spinors.

A one-body operator $V(x)$ in second-quantized form becomes

$$\hat{V} = \int dx \Psi^\dagger(x) V(x) \Psi(x) = \sum_{p,q} V_{p,q} c_p^\dagger c_q. \quad (1.55)$$

This gives the correct matrix elements between determinantal states, as one can verify.

The above expressions imply spin sum along with the space integrals, although this was not shown explicitly; let me write the spin components, for one-body operators:

$$\hat{V} = \sum_{\alpha,\beta} \int dx \Psi_{\alpha}^{\dagger} V_{\alpha,\beta}(x) \Psi_{\beta} \quad (1.56)$$

For the spin operators, setting $\hbar = 1$, and using the Pauli matrices, $S_z = \frac{1}{2}\sigma_z$, $S^+ = \begin{pmatrix} 0 & 1 \\ 0 & 0 \end{pmatrix}$ and the rule (1.55) one finds

$$S_z = \frac{1}{2} \int dx \left(\Psi_{\uparrow}^{\dagger}(x) \Psi_{\uparrow}(x) - \Psi_{\downarrow}^{\dagger}(x) \Psi_{\downarrow}(x) \right), \quad S^+ = \int dx \Psi_{\uparrow}^{\dagger}(x) \Psi_{\downarrow}(x). \quad (1.57)$$

Often we shall use a discrete basis and notation and we shall write

$$S^+ = \sum_k c_{k\uparrow}^{\dagger} c_{k\downarrow} \quad (1.58)$$

which is obtained from (1.57) by taking a Fourier transform in discrete notation. A two-body operator $U(x, y)$ becomes

$$\hat{U} = \int dx \int dy \Psi^{\dagger}(x) \Psi^{\dagger}(y) U(x, y) \Psi(y) \Psi(x) = \sum_{ijkl} U_{ijkl} c_i^{\dagger} c_j^{\dagger} c_l c_k \quad (1.59)$$

(please note the order of indices carefully). The Hamiltonian for N interacting electrons in an external potential $\varphi(x)$ is the *true* many-body Hamiltonian in the non-relativistic limit that we shall often regard as the full many-body problem for which approximations must be sought. It may be written

$$H(r_1, r_2, \dots, r_N) = H_0(r_1, r_2, \dots, r_N) + U(r_1, r_2, \dots, r_N) \quad (1.60)$$

where H_0 is the free part

$$H_0 = T + V_{ext} = \sum_i \left\{ -\frac{1}{2} \nabla_i^2 + V(r_i) \right\} = \sum_i h_0(i) \quad (1.61)$$

with T the kinetic energy and V_{ext} the external potential energy while

$$U = \frac{1}{2} \sum_{i \neq j} u_C(r_i - r_j) \quad (1.62)$$

is the Coulomb interaction. This Hamiltonian may be written in second-quantized form

$$\begin{aligned}
H &= H_0 + U, \\
H_0 &= \sum_{\sigma} \int dr \Psi_{\sigma}^{\dagger}(r) h_0 \Psi_{\sigma}(r), \\
U &= \frac{1}{2} \sum_{\alpha, \beta, \gamma, \delta} \int \int dx dy \psi_{\alpha}^{\dagger}(x) \psi_{\beta}^{\dagger}(y) u_C(x-y)_{\alpha\gamma, \beta\delta} \Psi_{\delta}(y) \Psi_{\gamma}(x). \quad (1.63)
\end{aligned}$$

Often the spin indices are understood as implicit in the integrations. It should be kept in mind that relativistic corrections are needed in most problems with light elements and the relativistic formulation is needed when heavy elements are involved. Fortunately, the ideas that we shall develop lend themselves to a direct generalization to Dirac's framework.

1.2.5 Hubbard Model for the Hydrogen Molecule

The Hubbard Model is a lattice of atoms or sites that can host one electron per spin; there is a hopping term between nearest neighbors like in a tight-binding model and a repulsion U between two electrons on the same atom. The Hubbard Hamiltonian

$$H = K + W = t \sum_{\langle i, j \rangle, \sigma} c_{j\sigma}^{\dagger} c_{i\sigma} + U \sum_i n_{i\uparrow} n_{i\downarrow}, \quad (1.64)$$

where K stands for the kinetic energy while W accounts for the on-site repulsive interaction. The summation on $\langle i, j \rangle$ runs over sites i and j which are nearest neighbors in a cubic lattice. This is often called *trivial* Hubbard Model to distinguish it from its extensions, involving degenerate orbitals and off-site interactions, that have been studied for many purposes.⁴

To model H_2 in the same spirit we represent the 1s orbitals of both atoms by two sites a and b and $\hat{H} = \hat{T} + \hat{W}$ with

$$\hat{T} = t_h \sum_{\sigma} \left[c_{a\sigma}^{\dagger} c_{b\sigma} + c_{b\sigma}^{\dagger} c_{a\sigma} \right] \quad (1.65)$$

the kinetic energy, with $t_h > 0$ the hopping integral;

$$\hat{W} = U (\hat{n}_{a\uparrow} \hat{n}_{a\downarrow} + \hat{n}_{b\uparrow} \hat{n}_{b\downarrow}). \quad (1.66)$$

⁴Some people blame the Hubbard Model and its extensions as too idealized to be realistic. Indeed nobody would use them to refine well-understood properties of Silicon. However, there are lots of problems involving strong correlations and e.g. transport, spectroscopies, time-dependent perturbations, which are far too hard for an *ab-initio* description. Hubbard-like models are primarily conceptual tools aimed at a semi-quantitative understanding. We shall see particularly in Chapters 4, 5 and 10 that often they allow to deal with highly excited states of strongly interacting system very successfully. The Bosonic Hubbard Model is also important, e.g. in the rapidly developing subject of Cold Bosonic Atoms in Optical Lattices (see Ref. [15]).

We wish to solve with two electrons of opposite spin (the $m_s = 0$ sector) so we take

$$\hat{N} = \sum_{\sigma} (\hat{n}_{a\sigma} + \hat{n}_{b\sigma}) = 2.$$

This is conserved. If $U = 0$, one solves the single-electron problem, and finds the orbitals

$$\varphi_{\pm} = \frac{|a\rangle \pm |b\rangle}{\sqrt{2}} \quad (1.67)$$

with energy eigenvalues

$$\varepsilon_{\pm} = \pm t_h \quad (1.68)$$

and the ground state $\Psi = \|\varphi_{-\uparrow}\varphi_{-\downarrow}\|$ has energy $E = -2t_h$. In the interacting case, we choose a basis

$$\begin{aligned} |v_1\rangle &= |a \uparrow a \downarrow\rangle, |v_2\rangle = |a \uparrow b \downarrow\rangle, \\ |v_3\rangle &= |b \uparrow a \downarrow\rangle, |v_4\rangle = |b \uparrow b \downarrow\rangle. \end{aligned}$$

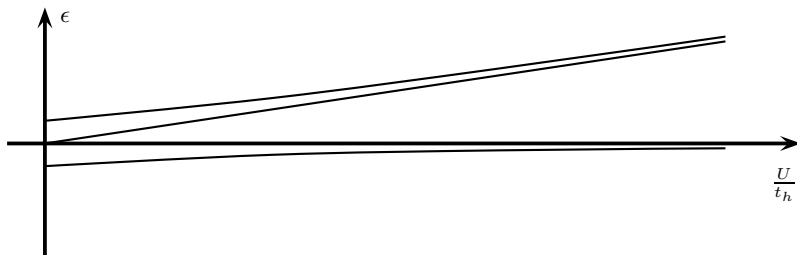


Fig. 1.2. Singlet eigenvalues of the Hydrogen molecule model versus $\frac{U}{t_h}$.

There is a single state in the $m_s = 1$ sector, so out of the 4 states in the $m_s = 0$ sector we expect one triplet and 3 singlets. We form the matrices $W = U \text{Diag}(1, 0, 0, 1)$ and

$$\hat{T} = t_h \begin{pmatrix} 0 & 1 & 1 & 0 \\ 1 & 0 & 0 & 1 \\ 1 & 0 & 0 & 1 \\ 0 & 1 & 1 & 0 \end{pmatrix}. \quad (1.69)$$

One finds the eigenvalues: $E = 0$ for the triplet, and $E_0 = U, E_{\pm} = \frac{1}{2} \left(U \pm \sqrt{16t_h^2 + U^2} \right)$ for the singlets, with E_- the ground state (remarkably) for any $U > 0$. Magnetism never obtains in this model.

1.3 Schrieffer-Wolff Canonical Transformation

One often meets problems with Hamiltonians

$$H = H_0 + \lambda V \quad (1.70)$$

such that the interaction λV takes the system to an enlarged Hilbert space, involving extra degrees of freedom not in action in the simple problem described by H_0 . Let A denote the restricted space and B the enlargement. Typically,

$$H_0 = \begin{pmatrix} H_A & 0 \\ 0 & H_B \end{pmatrix}, \quad (1.71)$$

and

$$V = \begin{pmatrix} 0 & v^\dagger \\ v & 0 \end{pmatrix} \quad (1.72)$$

is the mixing term. A standard way to solve such problems, that we shall meet several times in this book, is by a canonical transformation

$$H \rightarrow \tilde{H} = U H U^{-1} \quad (1.73)$$

where U is designed such that \tilde{H} is block-diagonal:

$$\tilde{H} = \begin{pmatrix} \tilde{H}_A & 0 \\ 0 & \tilde{H}_B \end{pmatrix} \quad (1.74)$$

The transformation must be unitary in order to preserve the norm of states, to this end we want $U^{-1} = U^\dagger$; this is granted if $U = e^S$ with $S = -S^\dagger$. Thus, expanding the exponentials,

$$\tilde{H} = e^S H e^{-S} = H + [S, H] + \frac{1}{2}[S, [S, H]] + \dots \quad (1.75)$$

Now we insert (1.70) with $S = \lambda S_1 + \lambda^2 S_2 + \dots$ and separate orders. Including up to second-order,

$$[S, H]_- = \lambda[S_1, H_0]_- + \lambda^2([S_1, V]_- + [S_2, H_0]_-), \quad (1.76)$$

$$[S, [S, H]_-]_- = \lambda^2[S_1, [S_1, H_0]_-]. \quad (1.77)$$

At order λ , we want to have nothing and we require that S_1 be such that

$$V + [S_1, H_0] = 0, \quad (1.78)$$

that is,

$$\begin{pmatrix} 0 & v^\dagger \\ v & 0 \end{pmatrix} + \left[\begin{pmatrix} 0 & -s^\dagger \\ s & 0 \end{pmatrix}, \begin{pmatrix} H_A & 0 \\ 0 & H_B \end{pmatrix} \right]_- = 0. \quad (1.79)$$

where we tried the solution

$$S_1 = \begin{pmatrix} 0 & -s^\dagger \\ s & 0 \end{pmatrix}. \quad (1.80)$$

We immediately obtain two conditions, $v = -sH_A + H_B s$ and $v^\dagger = -H_A s^\dagger + s^\dagger H_B$. Picking H_0 eigenstates $|m\rangle$ in the A subspace and $|\nu\rangle$ in the B subspace, with eigenvalues $E_m^{(A)}$ and $E_\nu^{(B)}$, we obtain

$$s_{\nu n} = \frac{v_{\nu n}}{E_\nu^{(B)} - E_n^{(A)}}, \quad (s^\dagger)_{m\nu} = \frac{(v^\dagger)_{m\nu}}{E_\nu^{(B)} - E_m^{(A)}}. \quad (1.81)$$

The second-order contribution to (1.75), using (1.76),(1.77) and (1.79), is $\frac{\lambda^2}{2}[S_1, V] + [S_2, H_0]$. We may set $S_2 = 0$ since

$$[S_1, V] = \begin{pmatrix} -(s^\dagger v + v^\dagger s) & 0 \\ 0 & s^\dagger v + v^\dagger s \end{pmatrix} \quad (1.82)$$

already gives a Hermitean, block-diagonal result. Thus, to second order,

$$\tilde{H}_A = H_A + H_{int} \quad (1.83)$$

where

$$H_{int} = \frac{\lambda^2}{2}[S_1, V]. \quad (1.84)$$

The effect of V can be obtained by working within the A subspace with a renormalized Hamiltonian (see (10.48),(1.82)) with elements

$$(H_{int})_{mn} = \frac{1}{2} \sum_{\nu \in B} \left[\frac{v_{m\nu}^\dagger v_{\nu n}}{E_m^{(A)} - E_\nu^{(B)}} + \frac{v_{m\nu}^\dagger v_{\nu n}}{E_n^{(A)} - E_\nu^{(B)}} \right]. \quad (1.85)$$

If the energy separation of A and B is large, the dependence of the energy denominators on m, n is negligible, and we may write

$$H_{int} = - \sum_{\nu \in B} \frac{v^\dagger |\nu\rangle \langle \nu| v}{E_\nu^{(B)} - E^{(A)}}; \quad (1.86)$$

the denominator is a positive excitation energy.

1.4 Variational Principle

The energy of a quantum system is a quadratic functional of the wave function ϕ . Consider a small variation $\phi \rightarrow \phi + \alpha\eta$ where η is an arbitrary function of the same variables on which ϕ depends, while $\alpha \rightarrow 0$ is a complex parameter,

$$E \text{ stationary} \iff \{\delta E = 0, \eta \text{ arbitrary}\}; \quad (1.87)$$

subject to the condition that the norm is conserved, namely,

$$\delta(E - \lambda N) = 0. \tag{1.88}$$

The Lagrange multiplier λ is fixed by the condition $N = \langle \phi(\lambda) | \phi(\lambda) \rangle = 1$.

Applying Lagrange's method, one finds that the following statements are equivalent:

$$\{H\phi = E\phi, \langle \phi | \phi \rangle = 1\} \Leftrightarrow \{\delta(E - \lambda N) = 0, \lambda = E\} \Leftrightarrow \{\delta(E) = 0, N = 1\}. \tag{1.89}$$

This is an exact reformulation of Quantum Mechanics

Example

Given the Hamiltonian

$$H = \begin{pmatrix} -3 & 1 & 1 & 1 & 1 \\ 1 & 0 & 0 & 0 & 0 \\ 1 & 0 & 0 & 0 & 0 \\ 1 & 0 & 0 & 0 & 0 \\ 1 & 0 & 0 & 0 & 0 \end{pmatrix}$$

find variationally the eigenfunctions of the form

$$\psi = \begin{pmatrix} \alpha \\ \beta \\ \beta \\ \beta \\ \beta \end{pmatrix}. \text{ Normalization requires } N = \langle \psi | \psi \rangle = \alpha^2 + 4\beta^2 = 1 \text{ while } E =$$

$$\langle \psi | H | \psi \rangle = 8\alpha\beta - 3\alpha^2, \text{ thus we must look for the extrema of } f(\alpha, \beta) = E - \lambda N.$$

One finds

$$\begin{cases} \frac{\partial f}{\partial \alpha} = 0 \implies 4\beta = (3 + \lambda)\alpha \\ \frac{\partial f}{\partial \beta} = 0 \implies \alpha = \lambda\beta \end{cases}$$

The compatibility condition $\lambda(3 + \lambda) = 4$ yields $\lambda = -4, \lambda = 1$. For $\lambda = -4$

da $\alpha = -4\beta$ one finds $\psi_{-4} = \frac{1}{\sqrt{20}} \begin{pmatrix} -4 \\ 1 \\ 1 \\ 1 \\ 1 \end{pmatrix}$ which is the ground state with

eigenvalue $\epsilon = -4$. For $\lambda = 1$ da $\alpha = \beta$ one finds $\psi_1 = \frac{1}{\sqrt{5}} \begin{pmatrix} 1 \\ 1 \\ 1 \\ 1 \\ 1 \end{pmatrix}$ which is the

exact excited state with eigenvalue $\epsilon = 1$.

1.5 Variational Approximations

One can choose a trial function $\phi(x, \{\lambda_1, \lambda_2, \dots, \lambda_n\})$ depending on parameters $\{\lambda_1, \lambda_2, \dots, \lambda_n\}$ and look for the extremum. If ϕ is not already normalized, the normalization condition can be enforced by Lagrange's method. If the exact ground state ϕ belongs to the class of functions, it corresponds to the minimum energy, otherwise the minimum always overestimates the ground state energy. Some variational approximations, like the Hartree-Fock scheme and the Bardeen-Cooper-Schrieffer theory of superconductivity, have been highly successful.

The excited states also correspond to extrema of the functional, however there are severe limitations to the method.

The trouble is that the true eigenstates are orthogonal, but this cannot be granted in general in a limited class of functions.

We need the orthogonality. For example we cannot give any meaning to an excited state which fails to be orthogonal to the ground state. However, the lowest state of any symmetry can always be found variationally, since it is automatically orthogonal to the ground state.

A symmetry is an operator X , which is unitary (that is $XX^\dagger = 1$), such that $[H, X]_- = 0$. The eigenstates of an unitary operator X belong to different eigenvalues are orthogonal. Indeed, if $X\phi_1 = e^{i\alpha}\phi_1$ and $X\phi_2 = e^{i\beta}\phi_2$,

$$\langle \phi_1, \phi_2 \rangle = \langle \phi_1, X^\dagger X \phi_2 \rangle = e^{i(\beta-\alpha)} \langle \phi_1, \phi_2 \rangle$$

and with $\alpha \neq \beta$, this requires $\langle \phi_1, \phi_2 \rangle = 0$.

1.6 Non-degenerate Perturbation Theory

The standard perturbation series yields [25] the corrected eigenvalues

$$E_m = E_m^{(0)} + \langle m | H' | m \rangle + \sum_n^{\tilde{}} \frac{|\langle m | H' | n \rangle|^2}{E_m^{(0)} - E_n^{(0)}} + \dots \quad (1.90)$$

where $E_m^{(0)}$ are unperturbed eigenvalues and $\langle m | H' | n \rangle$ are perturbation matrix elements; $\sum_n^{\tilde{}}$ excludes the terms with zero denominators. The perturbed wave functions are:

$$\begin{aligned} \psi_n = \psi_n^{(0)} + \sum_k^{\tilde{}} \psi_k^{(0)} & \left[\frac{\langle k | H' | m \rangle}{E_m^{(0)} - E_k^{(0)}} \left(1 - \frac{\langle m | H' | m \rangle}{E_m^{(0)} - E_k^{(0)}} \right) \right. \\ & \left. + \sum_n^{\tilde{}} \frac{\langle k | H' | n \rangle \langle n | H' | m \rangle}{(E_m^{(0)} - E_k^{(0)})(E_m^{(0)} - E_n^{(0)})} \right] + \dots \end{aligned} \quad (1.91)$$

where $\psi_n^{(0)}$ are the unperturbed ones. A much more general form of perturbation theory will be developed starting from Chapter 11.

2 Adiabatic Switching and Time-Ordered series

2.1 Time-dependent is Better: start from the *Golden Age*

If we can solve a problem with a time independent Hamiltonian H_0 , we surely meet many interesting but hard problems with a Hamiltonian

$$H(t) = H_0 + \hat{V}(t) \quad (2.1)$$

where an extra term $\hat{V}(t)$ appears: sometimes the complication $\hat{V}(t)$ depends on time, but in other cases it is static. Here, $H(t)$ is in the Schrödinger picture, the one that comes directly from classical physics with $p^x \rightarrow \frac{\partial}{\partial x}$, and so on, and sometimes we shall write $H_S(t)$ and Ψ_S for extra clarity. So, we have the task of solving

$$i\hbar \frac{\partial}{\partial t} |\Psi_S(t)\rangle = H_S(t) |\Psi_S(t)\rangle \quad (2.2)$$

which is notoriously difficult. We can solve formally by introducing the unitary time evolution operator U_S such that

$$|\Psi_S(t)\rangle = U_S(t, t_0) |\Psi_S(t_0)\rangle. \quad (2.3)$$

The time t_0 is arbitrary, and in time-independent problems one can choose $t_0 = 0$, but this is dull. In general, it is a much better idea taking $H_S(t)$ which depends on time, with the condition that for $t < t_0$, $V \equiv 0$. For static problems this appears lunatic, but it is a useful formal device. Dynamical and static problems are best discussed with the adiabatic switching technique. This is a cool revival of the old tale of the *golden age*, a happy era in the far past. Assume that the interaction is added very slowly, starting from a time $t \rightarrow t_0$, when the Hamiltonian was just H_0 and everything was easy; if we let $t_0 \rightarrow -\infty$ we may reasonably assume that the system does not warm up and evolves adiabatically. Integrating (2.2) over time we find

$$U_S(t, t_0) = 1 - \frac{i}{\hbar} \int_{t_0}^t dt_1 H_S(t_1) U_S(t_1, t_0); \quad (2.4)$$

the advantage is that this may be solved by iteration:

$$U_S(t, t_0) = 1 - \frac{i}{\hbar} \int_{t_0}^t dt_1 H_S(t_1) + \left(\frac{-i}{\hbar}\right)^2 \int_{t_0}^t \int_{t_0}^{t_1} dt_1 dt_2 H_S(t_1) H_S(t_2) + \dots \quad (2.5)$$

Iterating, we face the *nested* integral

$$\mathcal{I}_n(t) = \left(\frac{-i}{\hbar}\right)^n \int_{t_0}^t dt_1 \int_{t_0}^{t_1} dt_2 \dots \int_{t_0}^{t_{n-1}} dt_n H(t_1) \dots H(t_n) \quad (2.6)$$

where the domain is limited to $t > t_1 > \dots > t_n > t_0$. If H does not depend on time, one gets trivially $\mathcal{I}_n(t) = \left(\frac{-i}{\hbar}\right)^n \frac{H^n (t-t_0)^n}{n!}$ and the resulting exponential series is immediately summed. This $n!$ denominator proves useful and we can bring it out in the time dependent case by a trick. Perform any permutation of the time variables $t_1 \dots t_n$ in $\mathcal{I}_n(t)$; in the new ordering the earlier times will remain on the right of the later ones, while the value of the integral remains unaltered. Thus one can sum all the $n!$ identical replicas obtained by permutation and divide by $n!$; accordingly, one defines the time ordering operator P which puts earlier times on the right. For two terms

$$P[H_S(t_1)H_S(t_2)] = H_S(t_1)H_S(t_2)\theta(t_1 - t_2) + H_S(t_2)H_S(t_1)\theta(t_2 - t_1);$$

with more operators,

$$P[H_S(t_1)H_S(t_2) \dots H_S(t_n)] = \sum_Q H_S(t_{Q1})H_S(t_{Q2}) \dots H_S(t_{Qn}) \prod_n \theta(t_{Qn-1} - t_{Qn}). \quad (2.7)$$

Under the action of P the operators can be permuted freely as if they commuted. Actually when dealing with electron operators one uses Wick's time ordering operator T which is defined like P except that any exchange of fermion operators which is needed to go from the given order to the standard *earlier to the right* order brings a $-$ sign. Thus, if A and B are fermion creation or annihilator operators, T is such that

$$T[A(t)B(t')] = A(t)B(t')\theta(t - t') - B(t')A(t)\theta(t' - t).$$

When acting on Hamiltonians where Fermi operators occur in pairs P and T have the same effect, but T permits simplifying the definition of fermion Green's functions. Summing over the permutations, that give identical contributions, and dividing by their number, the integral (2.6) can be rewritten

$$\mathcal{I}_n(t) = \frac{1}{n!} \left(\frac{-i}{\hbar}\right)^n \int_{t_0}^t dt_1 \dots \int_{t_0}^t dt_n T[H(t_1) \dots H(t_n)] \quad (2.8)$$

and we may formally sum the series:

$$\boxed{U_S(t, t_0) = T \exp\left(\frac{-i}{\hbar} \int_{t_0}^t d\tau H_S(\tau)\right);} \quad (2.9)$$

here $T \exp$ is a conventional notation that means nothing but the exponential series of time-ordered products.

2.2 Evolution in Complex Time

2.2.1 Heisenberg Picture

In most cases of interest, the wave function Ψ is a false target and W. Kohn deserved a Nobel price for inventing the Density Functional Method (Section 12.6) that dispenses us from calculating it in important cases. Simply, Ψ is too complicated to be computed or even approximated in really hard problems¹. It depends from a huge number of variables and involves all the information on a system, including 15-electron correlations that nobody cares about. Indeed, our task is another: doing experiments of some kind and interpreting them never gives a complete information, so almost all the information that the Ψ function contains is actually pointless. The interesting information is expressed in the experiment-oriented Heisenberg correlation functions, that we discuss starting from Chapter 10. In this Section we shall pretend that we are still primarily interested in expanding the wave function, but the work is actually oriented towards the Green's functions. In the *Heisenberg picture*,

$$\langle A(t) \rangle = \langle \Psi_H | A_H(t) | \Psi_H \rangle \quad (2.10)$$

where by definition

$$|\Psi_H\rangle \equiv |\Psi_S(t_0)\rangle \quad (2.11)$$

is the t-independent snapshot of the *golden-age* Ψ , while any operator A , including c and c^\dagger , has an extra dynamic time dependence

$$A_H(t) = U_S^\dagger(t, t_0) A_S(t) U_S(t, t_0). \quad (2.12)$$

For a strictly time-independent H (no adiabatic switch) this simplifies to read

$$A(t) = e^{\frac{iHt}{\hbar}} A e^{-\frac{iHt}{\hbar}}, \quad (2.13)$$

but in general, from (2.12) one gets:

$$\begin{aligned} i\hbar \frac{dA_H}{dt} &= i\hbar \frac{dU_S^\dagger(t, t_0)}{dt} A_S U_S(t, t_0) \\ &+ U_S^\dagger(t, t_0) A_S i\hbar \frac{dU_S(t, t_0)}{dt} + U_S^\dagger(t, t_0) i\hbar \frac{dA_S}{dt} U_S(t, t_0); \end{aligned} \quad (2.14)$$

since

$$i\hbar \frac{dU_S(t, t_0)}{dt} = H_S(t) U_S(t, t_0), \quad -i\hbar \frac{dU_S^\dagger(t, t_0)}{dt} = U_S^\dagger(t, t_0) H_S(t) \quad (2.15)$$

the result is

¹In 1 dimension, however, the Bethe Ansatz allows solving exactly some important models, see Chapter 18.

$$\begin{aligned}
 i\hbar \frac{dA_H}{dt} &= -U_S^\dagger(t, t_0) H_S(t) A_S U_S(t, t_0) \\
 &+ U_S^\dagger(t, t_0) A_S H_S(t) U_S(t, t_0) + i\hbar \left(\frac{dA_S}{dt} \right)_H.
 \end{aligned}
 \tag{2.16}$$

It is natural to introduce the Heisenberg picture Hamiltonian and write:

$$i\hbar \frac{dA_H}{dt} = [A_H(t), H_H(t)] + i\hbar \left(\frac{dA_S}{dt} \right)_H.
 \tag{2.17}$$

In the following, unless otherwise stated, we shall normally use the Heisenberg picture, and $\langle A(t) \rangle = \langle \Psi_H | A_H(t) | \Psi_H \rangle$ with $|\Psi_H\rangle$ eigenstate of H_0 (in practice, the ground state in most cases). In terms of the Schrödinger picture, this corresponds to evolving the state from t_0 to time t , applying the operator and then evolving back to t_0 . We can merge the two U_S evolution operators by introducing an oriented path C in complex time from t_0 to t and back (see Figure). This needs a generalized T such that (letting $\hbar = 1$)

$$\begin{aligned}
 A_H(t) &= U_S^\dagger(t, t_0) A_S(t) U_S(t, t_0) = \\
 &\left[T \exp \left(-i \int_t^{t_0} dt' H(t') \right) \right] A_S(t) \left[T \exp \left(-i \int_{t_0}^t dt' H(t') \right) \right] \\
 &= T_C \left[\exp \left(-i \int_t^{t_0} dt' H(t') \right) A_S(t) \right]
 \end{aligned}
 \tag{2.18}$$

where C is an oriented path and T_C is the time ordering operator on C . Note that $A_S(t)$ is under the action of T_C that places it appropriately.

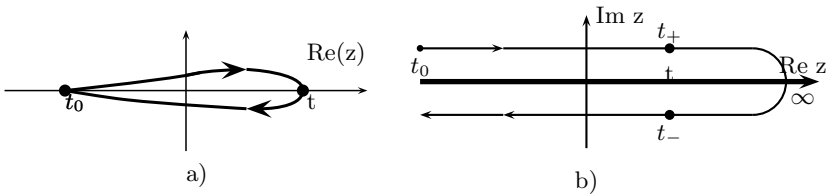


Fig. 2.1. a) A contour on the complex time z plane for obtaining $\langle A(t) \rangle$ from a single Schrödinger-picture evolution. Since along a closed path starting and ending at t^* one collects $U_S(t^*, t^*) = 1$, the path can be deformed freely as long as it starts and ends at t_0 and goes through t . b) The Keldysh contour; its main use will be shown in Chapter (13)

We shall see in Chapter 10 that this is the most natural way to make contact with experiment, and is also important for the connection with thermal physics that follows. The evolution operator satisfies the *group property* $U(t, t_1)U(t_1, t_2) = U(t, t_2)$; hence the path can be deformed freely as long as it starts and ends at t_0 and goes through t . In time-dependent problems, the most common contour is the Keldysh one from t_0 to $-t_0 \rightarrow +\infty$ and back to t_0 ; there are an ascending or positive branch and a descending or negative branch, and a physical time can be taken on any of the two. I shall write t_+ and t_- the times taken on the ascending and descending branch respectively; however $\langle A(t) \rangle = \langle A(t_+) \rangle = \langle A(t_-) \rangle$.

2.2.2 Thermal Averages

The initial state of the experiment on a solid is never an eigenvector of the Hamiltonian; it is described [118] by a Hermitean density matrix that we may denote

$$\rho = \sum_i w_i |i\rangle \langle i|, \quad (2.19)$$

where $|i\rangle$ is a complete orthonormal set, $w_i \geq 0$ is the probability of finding the system in $|i\rangle$ with $\sum_i w_i = 1$. The statistical average of any operator \hat{A} is by definition $\langle A \rangle = \sum_i w_i A_{ii}$ and may be obtained as $\langle A \rangle = \text{Tr} \rho \hat{A}$, where Tr denotes the trace (the sum of all the diagonal elements, which is independent of the basis set.) In temperature-dependent problems, adopting the Grand Canonical ensemble, ρ is the Boltzmann distribution,

$$\rho = \frac{e^{-\beta K}}{Z}, \quad K = H - \mu N, \quad (2.20)$$

where $\beta = \frac{1}{K_B T}$, N the number operator;

$$Z = \text{Tr} e^{-\beta K} \quad (2.21)$$

is the partition function. As detailed e.g. in [117], this ρ yields the maximum entropy $S = K_B \rho \ln(\rho)$ with the constraints that $\text{Tr} \rho = 1$, particle number and energy must be kept fixed. Thus,

Finite T rule: $\langle \hat{A}(t) \rangle = \text{Tr} \rho \hat{A}(t)$.

(2.22)

For an independent-electron system with Hamiltonian $H_0 = \sum_p \epsilon_p c_p^\dagger c_p$, any energy eigenstate is specified by the set of occupation numbers n_p of the one-electron levels, and the trace sums over all possible choices of n_p . Each term of the sum is a product of factors $e^{-\beta(\epsilon_p - \mu)}$ from filled states and factors 1 from empty states. Let us pick a particular level k and let $X(k)$ denote the contribution to Z from all the configurations with $n_k = 0$; then, the contribution to Z from all the configurations with $n_k = 1$ is $e^{-\beta(\epsilon_k - \mu)} X(k)$,

since the other levels give the same contribution regardless the population of level k . We can factor $(1 + e^{-\beta(\epsilon_k - \mu)})$ from the trace. Therefore we may conclude that

$$Z = \prod_k (1 + e^{-\beta(\epsilon_k - \mu)}). \quad (2.23)$$

This is readily worked out for independent Fermions (Problem 2.1.)

The formal similarity between quantum averages and statistical ones stems from the fact that $e^{-\beta K} = e^{-iK(-i\beta)}$ looks like a quantum propagation at imaginary time $t = -i\beta$. The system must be considered in thermal equilibrium at a (real) time t_0 earlier than any time dependence of the Hamiltonian. Then

$$Z = Tr[e^{\beta\mu N} e^{-i \int_{t_0}^{t_0 - i\beta} dt' H}] \equiv Tr[e^{\beta\mu N} T e^{-i \int_{t_0}^{t_0 - i\beta} dt' H}]; \quad (2.24)$$

here T has no effect but was inserted to emphasize that $T e^{-i \int_{t_0}^{t_0 - i\beta} dt' H}$ is an evolution operator along the vertical track in Figure 2.2.2 a). In the complex t plane one draws the so called imaginary-time axis; $\tau = it$ along the axis corresponding to a 90 degrees rotation of the plane is the real variable $\tau = -Imt$. The statistical average of a time-independent operator may be written

$$\langle A \rangle = \frac{1}{Z} Tr[e^{\beta\mu N} T e^{-i \int_{t_0}^{t_0 - i\beta} dt' H_0} A(t_0)]. \quad (2.25)$$

If H is constant and no adiabatic switching is assumed, one can take $t_0 = 0$.

However when using the adiabatic switching we take t_0 as the *golden age* defined above. The switching of the interaction is so slow that no heating of the system is caused, so at *modern* times t we have the full Hamiltonian $H(t)$ with any further explicit time dependence that may be necessary. This allows us to perform the thermal average with the simple, particle-number conserving H_0 , that is,

$$\begin{aligned} \langle \hat{A}(t) \rangle &= Tr \rho_0 A_H(t), \quad \rho = \frac{e^{-\beta K_0}}{Z}, \\ K_0 &= H_0 - \mu N, \quad [H_0, N] = 0. \end{aligned} \quad (2.26)$$

For evolving along the vertical track with a temperature-independent H one can introduce the temperature Heisenberg representation

$$A(\tau) = e^{(H - \mu N)\tau} A e^{-(H - \mu N)\tau}; \quad (2.27)$$

this is obtained from (2.13) by the usual substitution $it \rightarrow \tau$ and by $H \rightarrow H - \mu N$, in order to introduce the grand-canonical ensemble. The statistical average of a time-dependent operator may be written

$$\langle A(t) \rangle = \frac{1}{Z} Tr[e^{\beta\mu N} T e^{-i \int_C dt' H_0} A(t)], \quad (2.28)$$

where C is the contour of Figure 2.2.2 b). The utility of such contours will be more evident in the following, and particularly in Chapter 13.

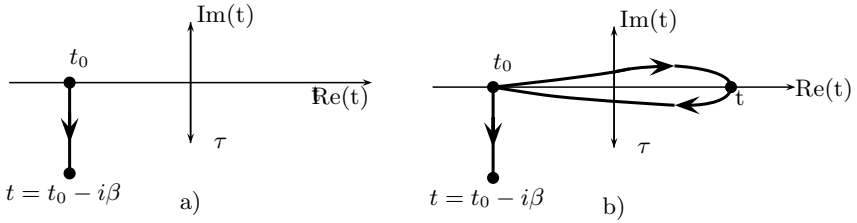


Fig. 2.2. a) Contour for thermal averages at time t_0 . The τ or *imaginary time* axis is shown: $\tau = -\text{Im}(t)$ is actually a real variable. b) Contour for thermal averages at time t . Complex times in the vertical track are latest.

2.3 The Interaction Picture and the Viable Expansion

In the Heisenberg picture, states are fixed while the operators $A_H(t)$ carry the time evolution; however, $A_H(t)$ requires $U_S(t, t_0)$; it is ironic that generally we cannot even write down the Hamiltonian itself

$$H_H(t) = U_S^\dagger(t, t_0)H_S(t)U_S(t, t_0).$$

Life is easy in the only case of stationary problems, when

$$A_H(t) = \exp[iH_S(t - t_0)] A_S \exp[-iH_S(t - t_0)],$$

and in particular $H_H = H_S$. In order to be able to expand in powers of V one introduces the *Interaction Picture* in which the operators evolve only with H_0 :

$$A_I(t) = e^{iH_0 t} A_S e^{-iH_0 t} \quad (2.29)$$

while the wave function is defined by

$$\Psi_I(t) = e^{iH_0 t} \Psi_S(t). \quad (2.30)$$

The physics is unaltered since

$$\begin{aligned} \langle A(t) \rangle &= \langle \Psi_S(t) | A_S(t) | \Psi_S(t) \rangle = \\ &\langle \Psi_S(t) | e^{-iH_0 t} e^{iH_0 t} A_S(t) e^{-iH_0 t} e^{iH_0 t} | \Psi_S(t) \rangle = \langle \Psi_I(t) | A_I(t) | \Psi_I(t) \rangle. \end{aligned} \quad (2.31)$$

Note that $\Psi_H = \Psi_S$ at $t = t_0$ and $\Psi_I = \Psi_S$ at $t = 0$; moreover, during the *golden age* when the system is unperturbed,

$$\Psi_I(t) = e^{iH_0 t} \Psi_S(t) = e^{iE_0 t} \Psi_S(t). \quad (2.32)$$

One finds:

$$i \frac{\bar{\partial}}{\partial t} \Psi_I(t) = e^{iH_0 t} V(t) \Psi_S(t) = V_I(t) \Psi_I(t) \quad (2.33)$$

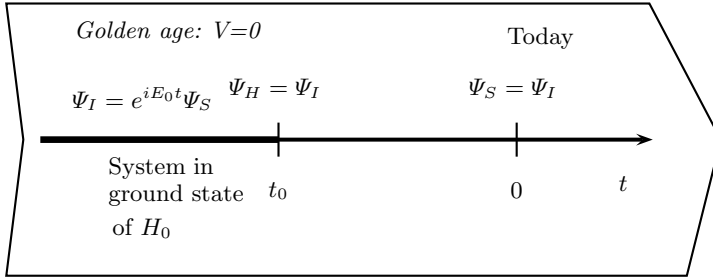


Fig. 2.3. Adiabatic switching and the three quantum pictures.

which is like Schrödinger equation without the obvious part of the dynamics. The evolution operator in the interaction picture from an arbitrary time τ

$$\Psi_I(t) = U_I(t, \tau) \Psi_I(\tau) \quad (2.34)$$

satisfies

$$U_I(t, \tau) = e^{iH_0(t-\tau)} U_S(t, \tau) \quad (2.35)$$

and

$$i \frac{\partial}{\partial t} U_I(t, \tau) = V_I(t) U_I(t, \tau). \quad (2.36)$$

The solution

$$U_I(t, \tau) = T e^{\frac{-i}{\hbar} \int_{\tau}^t dt' V_I(t')} \quad (2.37)$$

is at the basis of all perturbation theory.

One must be able to switch representation. In the Heisenberg picture, $\langle A \rangle = \langle \Psi_H | A_H | \Psi_H \rangle$, where $\Psi_H = \Psi_S(t_0)$; moreover, using (2.32), $\Psi_I(t_0) = e^{iE_0 t_0} \Psi_S(t_0)$ and we may write $\langle A \rangle = \langle \Psi_I(t_0) | A_H | \Psi_I(t_0) \rangle$. In the interaction picture,

$$\langle A(t) \rangle = \langle \Psi_I(t) | A_I(t) | \Psi_I(t) \rangle = \langle \Psi_I(t_0) | U_I^\dagger(t, t_0) A_I(t) U_I(t, t_0) | \Psi_I(t_0) \rangle. \quad (2.38)$$

Therefore,

$$A_H = U_I^\dagger(t, t_0) A_I(t) U_I(t, t_0), \quad (2.39)$$

which is just (2.12) with S replaced by I . Having succeeded in writing Heisenberg operator in terms of interaction ones, we can expand them in series of V_I .

Problems

2.1. For $H_0 = \sum_p \epsilon_p c_p^\dagger c_p$, show that $\langle n_k \rangle$ is given by the Fermi distribution,

$$\langle n_p \rangle = \frac{1}{Z} \text{Tr}(n_p \rho) = \frac{1}{1 + e^{\beta(\epsilon_p - \mu)}}. \quad (2.40)$$

2.2. Let $H = H_0 + H_1$ and $U_{0S}(t, t')$ the evolution operator for H_0 . Write an equation for the evolution operator $U_S(t, t')$ for H .

2.3. Let A_1, A_2 denote fermion creation or annihilation operators and ρ an operator such as a density which commutes with A_1, A_2 under Wick's T ordering. Find $\frac{d}{dt}T\{A_1(t_1)A_2(t_2)\rho(t)\}$. How is the result generalized to several operators A_1, \dots, A_n ?

2.4. Derive the useful identity [205] holding for any Hamiltonian H_λ that depends on a parameter λ

$$\frac{d}{d\lambda}e^{-iH_\lambda(t'-t)} = -i \int_t^{t'} d\tau e^{-iH_\lambda(t'-\tau)} \frac{dH}{d\lambda} e^{-iH_\lambda(\tau-t)}. \quad (2.41)$$

3 Atomic Shells and Multiplets

3.1 Shell Structure of Atoms

X-ray spectroscopy and Photoemission (see Chapter 6) show a correspondence between the electronic levels in many-electron atoms and in Hydrogen. The next Table shows the inner levels of Fe; the first column presents the spectroscopic notation, the second the corresponding Hydrogen quantum numbers and the third the measured binding energy.

Shell	nlj	E_B (eV)
K	$1s_{\frac{1}{2}}$	7112.0
L_I	$2p_{\frac{1}{2}}$	842.0
L_{II}	$2p_{\frac{3}{2}}$	719.9
L_{III}	$3s_{\frac{1}{2}}$	706.8
M_I	$3p_{\frac{1}{2}}$	94.0
M_{II}	$3p_{\frac{3}{2}}$	52.7
M_{III}	$3d_{\frac{3}{2}}$	52.7

It is evident that the shells correspond to the principal quantum numbers and the subshells to the spin-orbit split levels. This Chapter is devoted to the elementary theory of the shell structure and the atomic multiplets, which requires the use of introductory many-body concepts and the inclusion of relativistic effects.

3.2 Hartree-Fock Method

Consider the *true* non-relativistic N-body Hamiltonian for an atom or molecule (1.60,1.61,1.62), namely, $H(r_1, r_2, \dots, r_N) = H_0 + V$, with

$$H_0 = T + H_w = \sum_i h(i) \equiv \sum_i \left\{ -\frac{1}{2} \nabla_i^2 + w(r_i) \right\}, \quad (3.1)$$

$$V = \frac{1}{2} \sum_{i \neq j} v(r_i - r_j) \quad (3.2)$$

(or (1.63) in second quantization). The external potential w is due to the nucleus (or nuclei). Solving the Schrödinger equation is a formidable task; the Hartree-Fock (HF) Method uses as a natural first approximation the determinantal wave function of the form (1.4)

$$\Psi(1, 2, \dots, N) = \frac{1}{\sqrt{N!}} \begin{pmatrix} u_1(1) & u_2(1) & \dots & u_N(1) \\ u_1(2) & u_2(2) & \dots & u_N(2) \\ \dots & \dots & \dots & \dots \\ u_1(N) & u_2(N) & \dots & u_N(N) \end{pmatrix} \quad (3.3)$$

written in terms of spin-orbitals $u_i(i)$ to be determined. This enables us to write the average of the one-body operator according to (1.7)

$$\langle \Psi | F | \Psi \rangle = \sum_i^N \langle u_i | f | u_i \rangle.$$

and the average of the two-body operator according to (1.10)

$$\langle \Psi | F | \Psi \rangle = \sum_{j \neq i}^N [\langle u_i(1) u_j(2) | f(1, 2) | u_i(1) u_j(2) \rangle - \langle u_j(1) u_i(2) | f(1, 2) | u_i(1) u_j(2) \rangle].$$

The average of the N-electron Hamiltonian yields

$$\langle \Psi | H | \Psi \rangle = E_N = \sum_i I_i + \frac{1}{2} \sum_{ij} (C_{ij} - E_{ij}), \quad (3.4)$$

where $I_i = \langle u_i | h(i) | u_i \rangle$, while C_{ij} and E_{ij} are respectively the Coulomb and exchange integrals involving the Coulomb interaction and orbitals i and j .

We are facing two main problems: on one hand, the determinantal wave function is appropriate for independent electrons and on the other we need to specify the orbitals somehow. We find a way out of both problems if we use the determinantal form as a variational *ansatz* and seek for optimal spin-orbitals; we impose normalization by a Lagrange multiplier for each spin-orbital. If we wish, we may use other Lagrange multipliers to enforce orthogonality, but if we forget this requirement, orthogonal spin-orbitals are obtained anyhow.

The main reason why the HF approximation is important is that the equations are written in the same way for all systems; we can illustrate the procedure starting with the ground state of He. Then the two spin-orbitals are $u_{1s\uparrow} = u_{1s}(\mathbf{r})\alpha$ and $u_{1s\downarrow} = u_{1s}(\mathbf{r})\beta$, in obvious notation, and

$$E_2 = \langle u_{1s\uparrow}(1) | h(1) | u_{1s\uparrow}(1) \rangle + \langle u_{1s\downarrow}(2) | h(2) | u_{1s\downarrow}(2) \rangle + \langle u_{1s\uparrow}(1) u_{1s\downarrow}(2) | \frac{1}{r_{12}} | u_{1s\uparrow}(1) u_{1s\downarrow}(2) \rangle \quad (3.5)$$

does not involve exchange terms. We vary the orbital $u_{1s}(\mathbf{r})$ requiring $\delta E_2 = \epsilon \delta N$, where N is the norm of $u_{1s}(\mathbf{r})$ and ϵ is the Lagrange multiplier. We obtain the Hartree equation

$$h(1)u_{1s}(1) + u_{1s}(1) \int d^3r_2 u_{1s}(2)^* \frac{1}{r_{12}} u_{1s}(2) = \varepsilon u_{1s}(1). \quad (3.6)$$

(we speak of Hartree-Fock when exchange terms appear). Thus the optimal orbital is obtained by a Schrödinger-like equation where the electrons feels, along with the nuclear potential contained in h , the Hartree potential

$$V_H(1) = \int d^3r_2 u_{1s}(2)^* \frac{1}{r_{12}} u_{1s}(2); \quad (3.7)$$

V_H is just the electrostatic potential due to the charge cloud of the opposite-spin electron. Having chosen an independent-electron form of Ψ we are trying to compensate the neglect of the Coulomb interaction by including its average as an effective potential or mean field. The Hartree approximation takes into account the quantum nature of the electron and is *self-consistent*, that is, it accounts for electrostatics. Indeed, HF is also called the self-consistent field method. Yet, it is still far from exact. The He ground state energy turns out to be $E_2 = -77.866$ eV, which is more than 1 eV too high compared to the exact result (~ -79 eV). This large discrepancy is the correlation energy and is due exclusively to the determinantal form of Ψ . In other terms, the electron does not see the average cloud of the other one, but a point particle with which it can correlate its motion. The discrepancy may be *small* compared to the binding energy of the system and also compared to core-level binding energies, but since 1eV is the scale of chemical binding energy the accuracy of the HF method is questionable if one wants to predict chemical trends.

The excited state $1s2s^3S$ of He can also be approximated variationally as discussed in Sect. 1.4. Triplet He is called Orthohelium and converts to the singlet Parahelium after a long time (spin-orbit coupling is small). The relevant configurations are $u_{1s\uparrow}u_{2s\uparrow}$, with $m_S = 1$, $u_{1s\downarrow}u_{2s\downarrow}$, with $m_S = -1$. Of course, there is also $m_S = 0$, with the embarrassing non-determinantal configuration $\frac{1}{\sqrt{2}}[u_{1s\uparrow}u_{2s\downarrow} + u_{1s\downarrow}u_{2s\uparrow}]$. This state would be outside the scope of the HF method, but we know that its energy is the same and anyhow it can be reached from the determinantal states by a 90 degrees rotation. Hence we can concentrate on $u_{1s\uparrow}u_{2s\uparrow}$, and repeating the above argument and setting $a = u_{1s\uparrow}$, $b = u_{2s\uparrow}$ we find:

$$E_2 = I_a + I_b + C_{ab} - E_{ab}. \quad (3.8)$$

The extremal condition $\delta E = 0$ is subject to the further conditions $\langle a|a \rangle = \langle b|b \rangle = 1$, and we need two Lagrange multipliers ϵ_a and ϵ_b . So, we get, varying a :

$$h(1)a(1) + a(1) \int d^2 b^*(2) \frac{1}{r_{12}} b(2) - b(1) \int d^2 b^*(2) \frac{1}{r_{12}} a(2) = \varepsilon_a a(1). \quad (3.9)$$

Varying b , we find the same with a and b interchanged. These are the HF equations for the problem. For parallel spins a non-local exchange *potential*

arises. However, this is a non-local potential (the r.h.s does not depend just on the local value of a).

$$V^{ex}(\vec{x})a(\vec{x}) = b(\vec{x}) \int d\vec{y} \frac{b^*(\vec{y})a(\vec{y})}{|\vec{x} - \vec{y}|} \quad (3.10)$$

The physical significance of the exchange term will be further discussed in the next subsection.

It is worth mentioning that had we started with a simple product, without anti-symmetrization, we should have found the direct term but we would have missed the exchange one. The Hartree method, which neglects exchange, has also been widely applied. Its results are not always worse than those of HF. Indeed, since the orbitals are filled according to the *aufbau* method, the shell structure is reproduced and the Pauli principle is not totally ignored; both methods neglect correlation, and this is the most serious limitation for both.

Let us take the scalar product of Equation (3.9) by $|b\rangle$:

$$\langle b|h|a\rangle + \int d1d2 \frac{b^*(1)a(1)|b(2)|^2 - |b(1)|^2b^*(2)a(2)}{r_{12}} = \varepsilon_a \langle b|a\rangle.$$

The formidable-looking integral vanishes and one is left with

$$\langle b|h|a\rangle = \varepsilon_a \langle b|a\rangle. \quad (3.11)$$

Exchanging a and b ,

$$\langle a|h|b\rangle = \varepsilon_b \langle a|b\rangle.$$

Taking the complex conjugate and subtracting from (3.11) we get

$$0 = (\varepsilon_a - \varepsilon_b) \langle b|a\rangle,$$

and non-degenerate orbitals are orthogonal.

The analogy of the HF equations to Schrödinger's suggests that the so called Koopman's eigenvalue ε_a is the energy eigenvalue of the electron moving in spin-orbital a . However, one should not give any physical significance to the individual orbitals. One can introduce unitary linear transformations of orbitals. Then, the determinant Ψ does not change, and nothing changes since Ψ has a physical meaning, the spin-orbitals do not possess any by themselves. No physical observable corresponds to the energy of an orbital. Let us take the scalar product of Equation (3.9) by $|a\rangle$:

$$\langle a(1)|h(1)|a(1)\rangle + \int d1d2 \frac{|a(1)|^2|b(2)|^2}{r_{12}} - \int d1d2 \frac{a(1)^*b(1)a(2)b(2)^*}{r_{12}} = \varepsilon_a,$$

that is,

$$\varepsilon_a = I_a + C_{ab} - E_{ab}. \quad (3.12)$$

Using

$$\varepsilon_b = I_b + C_{ba} - E_{ba}, C_{ba} = C_{ab}, E_{ba} = E_{ab},$$

we may conclude that

$$\varepsilon_a + \varepsilon_b = I_a + I_b + 2(C_{ab} - E_{ab}) \neq E_2 = I_a + I_b + C_{ab} - E_{ab}$$

and the energy of the atom is different from the sum of the Koopman's eigenvalues.

Rather, they can be thought of as approximations to ionization potentials. Suppose the atom is photoionized, and the photo-electron is sent to the threshold of the continuum (also called vacuum level). The ionization potential is the difference between the energy of the initial state He $1s2s^3S$ and the energy of the final state He⁺. The initial energy is $E_2 = I_a + I_b + C_{ab} - E_{ab}$, where a=1s, b=2s; indeed on removing the electron b, we must remove $\varepsilon_b = I_b + C_{ab} - E_{ab}$. This fact is known as *Koopmans theorem*, and shows that the HF calculations do bring some information about the excited states, after all. The main weakness of this approximation is evident from the above He $1s2s^3S$ example, too. The final state He⁺ is hydrogen-like, with Z=2. If we estimate the ionization potential by Koopman's eigenvalue, we pretend that in the final state the electron keeps its unrelaxed orbital a, which is computed including the potential due to the electron in b. Thus, Koopman's eigenvalues imply a frozen-orbital approximation. One can fix this problem by doing separate HF calculations for the initial and final configurations. This is called the Δ -SCF method; the errors due to correlation effects, however, cannot be removed within the HF approach, and require the methods of Chapter 11.

The advantage of the HF approach over more accurate variational methods is that the equations are system-independent. The generalization of Equation (3.8) to the N-electron problem reads

$$E_N = \sum_i^N I_i + \frac{1}{2} \sum_{i \neq j}^N [C_{ij} - E_{ij}]. \quad (3.13)$$

The Koopmans eigenvalues are

$$\varepsilon_i = I_i + \sum_j (C_{ij} - E_{ij}) = E_N - E_{N-1}^{(i)} \quad (3.14)$$

where $E_{N-1}^{(i)}$ refers to the system ionized in spin-orbital i, while the other spin-orbitals remain *frozen*. Looking for the extremum of energy constrained by normalization one finds the HF equations. We introduce the direct potential

$$V^d = \sum_i^N V_i^d(\mathbf{r}), \quad V_i^d(\mathbf{r}) = \int d\mathbf{r}' \frac{|u_i(\mathbf{r}')|^2}{|\mathbf{r} - \mathbf{r}'|}$$

summed over all electrons, and the exchange potential

$$V^{ex} = \sum_i^{\uparrow\uparrow} V_i^{ex}(\mathbf{r}), \quad V_i^{ex}(\mathbf{r})f(\mathbf{r}) = u_i(\mathbf{r}) \int d\mathbf{r}' \frac{u_i(\mathbf{r}')^* f(\mathbf{r}')}{|\mathbf{r} - \mathbf{r}'|} \quad (3.15)$$

where the summation $\sum_i^{\uparrow\uparrow}$ runs over the spin-orbitals with the same spin as i .

For an atom with atomic number Z , the Fock operator

$$f = \frac{p^2}{2m} - \frac{Z}{|\mathbf{r}|} + V^d(\mathbf{r}) - V^{ex}(\mathbf{r}) \quad (3.16)$$

allows to write the HF equations in the deceptively simple form

$$\boxed{f u_i(\mathbf{r}) = \varepsilon_i u_i(\mathbf{r})} \quad (3.17)$$

The HF equations have a complete orthonormal set of solutions. The lowest N allow to build the determinantal wave functions. The rest are called *virtual orbitals*; they are not directly related to any experiment involving excited states, but they are often useful to generate multi-determinantal developments, like the Configuration Interaction expansion.

In open-shell system one does not know a priori which configuration will give the lowest energy, and problems are generally harder than in closed-shell systems. For instance, the u_{1s} and u_{2s} orbitals of Be ($Z=4$) are spin-independent and are determined by a pair of coupled HF equations. The problem is more involved with Li ($Z=3$). We may arbitrarily set the unpaired 2s electron with spin up. This implies that the up-spin 1s electrons has the exchange interaction while the down spin electron does not have such a term, hence there are 2 1s levels and 3 HF equations must be solved. The splitting of the core level is physically correct. This is the HF method in its general form, which is often termed unrestricted HF, or spin-polarized HF. In order to simplify the computations the restricted HF method has been introduced. One then imposes the same orbital for both spins, with half exchange interaction for both spin directions. This approximation, however, leads to incorrect molecular dissociation at large distances and cannot describe magnetism.

The ground state configuration of every atomic species, which is reported in Mendelejeff tables, is the one which yields the minimum energy with the HF method (or its relativistic extension). The Koopmans eigenvalues for the closed-shell Cu^+ ions (658.4 eV for 1s, 82.3 eV for 2s, 71.83 eV for 2p, 10.65 eV for 3s, 7.27 eV for 3p and 1.6 eV for 3d) may be compared with the experimental binding energies (662 eV, 81.3 eV, 61.6 eV, 11.6 eV, 6.1 eV, 0.71 eV, respectively). In this case the relativistic effects are small and there is no doubt that the general trend is correct, however the relative error for the external shell exceeds 100%. The methods of Chapter 11 are needed in order to improve the situation. While the true ground-state energy is always lower than in the HF approximation, there is no such relation between the Koopmans eigenvalues and the true levels of the system; in more advanced theories, actually, they are resonances (see Chapter 5).

The relativistic extension of the HF method is called Dirac-Fock method. One replaces the one-body Hamiltonian h by Dirac's Hamiltonian [203][202]

$$h_D(i) = c\boldsymbol{\alpha}_i \cdot \mathbf{p}_i + \beta mc^2 - \frac{Ze^2}{|\mathbf{r}_i|}, \quad (3.18)$$

where $\boldsymbol{\alpha}_i$ is Dirac's velocity [203] of electron i , $\beta = \gamma_4$ is Dirac's matrix and a four-component wave function is sought. For light atoms, the Coulomb interaction continues to be used, although a better alternative is Breit's interaction [204]

$$W_B(1, 2) = \frac{e^2}{r_{12}} \exp[ikr_{12}](1 - \boldsymbol{\alpha}(1) \cdot \boldsymbol{\alpha}(2)), \quad ck = \omega$$

where $\hbar\omega$ is the absolute value of the energy jump of each electron in the collision. Breit's interaction is particularly needed for the inner shells of heavy elements. With such changes, the self-consistent equations work basically as in the non-relativistic case, and Dirac-Fock atomic codes are available since a long time. GRASP (General Purpose Relativistic Atomic Structure Program[158]) labels Dirac-Fock solutions by J^2 , J_z , parity and seniority number 9.9(See Chapter 9.9) does a partial configuration interaction, keeps into account the finite nuclear dimensions and includes the main corrections due to Quantum Electrodynamics.

3.2.1 Physical Meaning of Exchange: the Cohesion of a Simple Metal

In all metals, the conduction electrons shield the electric field of the Ions. The shielded potential seen by an electron at the Fermi level is considerably attenuated, and in Aluminum and other metals with s and p conduction bands, it is nearly flat. These metals are called simple since many of their properties can be explained with the model of free electrons. The theory of Sommerfeld considers a gas of N electrons confined to volume V , with large N and V such that $\frac{N}{V} = n = \frac{k_F^3}{3\pi^2}$, where n is the number density of conduction electrons, that occupy all the states up to the Fermi level. The Fermi sphere exists indeed and the Sommerfeld theory explains some facts correctly: the contribution of electrons to the specific heat of the metals is correctly predicted to grow linearly with the temperature T . But the energy density of the electron gas $\frac{E}{V} = \frac{3nE_F}{5}$ is positive, and the electrons are prevented from escaping from the metal by a box. The real nature of this box is unexplained. For the metal to be stable, an electron must be attracted by it. The *Jellium* is a hypothetical metal in which a Fermi liquid, that is an interacting electron gas, is neutralized by positive uniform charge. The nuclear charges are smeared out in uniform way and the system have complete translational symmetry; however oversimplified, this model is still hard and nobody knows the exact solution. It is a traditional bench mark of the many-body theory ,

and a constant source of ideas that then are applied to the realistic calculations. The electrostatic effects are included in the theory, and they improve it considerably. We see that what we can learn from SCF approximation. The most fundamental issue is the cohesion of a metal piece. We consider a large cube of Jellium of volume V containing N electrons, with $N/V = n$ and impose periodic boundary conditions. The method of Hartree describes to the state of the Jellium with a product wave function of the form

$$\Phi(1, 2, \dots, N) = u_1(r_1)u_2(r_2) \cdots u_N(r_N) \quad (3.19)$$

where u_i are unknown spin-orbitals; the Hartree potential is $V_b + V_d$, where V_b is the positive background potential and V_d is the direct potential.

We look for a translationally invariant solution¹ as a natural first choice. Then the space function in the u spin-orbitals is a plane-wave; the density is a constant and cancels exactly the background density. Thus, $V_b + V_d = 0$ and the electrons are left with the mere kinetic energy, which is positive; the result (a piece of metal cannot exist) is very unrealistic.

In the Hartree-Fock approximation, we can still find plane-wave orbital solutions, but since the Hartree term just cancels the background, the only potential is the exchange potential $V_k^{(exc)}$. To obtain its expression, one can write down the direct term $V_d u_k(r) = u_k(r) \sum_{k'} \int dr' \frac{e^2}{|r-r'|} u_{k'}^*(r') u_k(r)$ and perform the characteristic exchange

$$V_{ex} u_k = \sum_{k'} \int dr' \frac{e^2}{|r-r'|} u_{k'}(r') u_k(r) = e^{ikr} \frac{1}{\sqrt{V}} \sum_{k'} \frac{4\pi e^2}{|k' - k|^2}. \quad (3.20)$$

The exchange term also goes like e^{ikr} , and the Hartree-Fock equations read

$$\left[\frac{p^2}{2m} - \frac{e^2}{V} \sum_{k'} \frac{4\pi}{|k' - k|^2} \right] \frac{e^{ikr}}{\sqrt{V}} = \epsilon(k) \frac{e^{ikr}}{\sqrt{V}}. \quad (3.21)$$

The Koopmans eigenvalue is

$$\epsilon(k) = \frac{\hbar^2 k^2}{2m} - \frac{4\pi e^2}{(2\pi)^3} \int d^3 k' \theta(k_F - k') \frac{1}{|k' - k|^2}. \quad (3.22)$$

For small k , $\epsilon \sim -\frac{2e^2 k_F}{\pi}$. The electron moves in a potential well in k space; there is a singularity for $k = k_F$. The exchange term is attractive, and this fact has a simple physical interpretation. Every electron travels encircled by a space region (Fermi hole) in which there is deficiency of electrons of its same spin. The electron and the Fermi hole constitute with a quasi-particle, very

¹Spin density wave solution of the Hartree-Fock equations are energetically favored at low n , however the energy difference is far too small to be relevant to the cohesion issue. Cs has low enough n to have a spin density wave in the ground state according to Hartree-Fock equations; the actual metal, however, is not magnetic.

different from that of a free electron. The Jellium is stable if an electron at the Fermi level is bound. This depends on the competition between the negative contribution of the exchange term and that positive one of the kinetic energy. The outcome of the competition depends on k_F , that is on the density n of the Jellium. For sufficiently small density ($k_F a_0 \ll 1$) the attraction prevails, and the metal exists.

The function $\epsilon(k)$ has a logarithmic singularity for $k = k_F$, where its derivative diverges. This is physically wrong, no such behavior is observed, but we have understood the reason for the existence of metals, and if we want to understand more we must go into the many-body problem.

3.3 Virial Theorem

For a classical particle moving in a closed orbit in a potential V , one finds $\frac{d}{dt} \mathbf{r} \cdot \mathbf{p} = \frac{\mathbf{p}^2}{2m} + \mathbf{r} \cdot \mathbf{F}$, where $\mathbf{F} = -\nabla V$ is the force. Averaging over a period, $\langle \frac{d}{dt} \mathbf{r} \cdot \mathbf{p} \rangle = 0$, yields the well known Virial theorem $\langle 2T \rangle = \langle \mathbf{r} \cdot \nabla V \rangle$ where T is the kinetic energy.

For a Schrödinger particle $i\hbar \frac{d}{dt} \mathbf{r} \cdot \mathbf{p} = [\mathbf{r} \cdot \mathbf{p}, H]_-$; averaging over an eigenstate of H , the r.h.s. vanishes; since the quantum commutators give $\frac{d\mathbf{p}}{dt} = -\nabla V$, $\frac{d\mathbf{r}}{dt} = \frac{\mathbf{p}}{m}$ we obtain the same Virial theorem $\langle 2T \rangle = \langle \mathbf{r} \cdot \nabla V \rangle$.

In Dirac's theory[203], if ψ is an eigenspinor of $H = c\boldsymbol{\alpha} \cdot \mathbf{p} + \beta mc^2 + V(\mathbf{r})$, (using standard notation, with $\boldsymbol{\alpha}$ Dirac's velocity) a similar procedure leads to $\langle \psi | c\boldsymbol{\alpha} \cdot \mathbf{p} | \psi \rangle = \langle \psi | c\mathbf{r} \cdot \nabla | \psi \rangle$.

Here we are particularly interested in a system of N non-relativistic particles, including electrons and nuclei, in Coulomb interaction; let e_i and m_i denote charges and masses of the charged particles; the Hamiltonian is of the form

$$H = -\frac{\hbar^2}{2} \sum_{i=1}^N \frac{\nabla_i^2}{m_i} + \sum_{i<j}^N \frac{e_i e_j}{r_{ij}} \equiv T + V. \quad (3.23)$$

The ground state wave function $\Phi(\{\mathbf{r}_i\})$ depends on the set $\{\mathbf{r}_i\}$ of the N position vectors. Consider the rescaled, normalized wave function

$$\Phi_\eta(\{\mathbf{r}_i\}) = \eta^{\frac{3N}{2}} \Phi(\{\eta \mathbf{r}_i\}). \quad (3.24)$$

One checks easily that kinetic and Coulomb energies scale differently, that is,

$$\langle \Phi_\eta | T | \Phi_\eta \rangle = \eta^2 \langle \Phi | T | \Phi \rangle, \quad (3.25)$$

while

$$\langle \Phi_\eta | V | \Phi_\eta \rangle = \eta \langle \Phi | V | \Phi \rangle. \quad (3.26)$$

Hence,

$$\langle \Phi_\eta | H | \Phi_\eta \rangle = \eta^2 \langle \Phi | T | \Phi \rangle + \eta \langle \Phi | V | \Phi \rangle. \quad (3.27)$$

Treating η as a variational parameter, we find the condition

$$2\eta\langle\Phi|T|\Phi\rangle + \langle\Phi|V|\Phi\rangle = 0, \quad (3.28)$$

but since the optimum value is $\eta = 1$ we end up with the Virial theorem

$$\langle 2T + V \rangle = 0. \quad (3.29)$$

This is one of the few known exact statements about interacting many-body problems. The Hartree-Fock ground state satisfies the Virial Theorem, and an approximate self-consistent calculation can be improved by scaling.

3.4 Hellmann-Feynman Theorem

Let $H = H(\lambda)$ denote a Hamiltonian which depends on a parameter λ and $H\Psi = E\Psi$. Then

$$\frac{dE}{d\lambda} = \langle\Psi|\frac{dH}{d\lambda}|\Psi\rangle. \quad (3.30)$$

This follows from $E(\lambda) = \langle\Psi|H(\lambda)|\Psi\rangle$ and from the fact that a small $d\lambda$ produces a first-order variation $d\Psi$ which is orthogonal to Ψ . This is another one of the few exact results for interacting many-body problems.

3.5 Central Field

In this Section we study the ground state and the low excited states of the atom with atomic number Z , including the most important relativistic effects. Using symmetry (exact and approximate) we can tell a lot without heavy computing. The model Hamiltonian is

$$H_{tot} = H_0 + H_C + H'_{rel} \quad (3.31)$$

with

$$H_0 = \sum_i^Z \left[\frac{\mathbf{p}_i^2}{2m} - \frac{Ze^2}{r_i} \right], \quad (3.32)$$

$$H_C = \sum_{i<j}^Z \frac{e^2}{r_{ij}}, \quad (3.33)$$

$$H'_{rel} = \sum_i^Z \xi(r_i) \mathbf{L}_i \cdot \mathbf{S}_i \quad (3.34)$$

where \mathbf{p}_i and \mathbf{r}_i are electron momenta and coordinates, r_{ij} are distances; H'_{rel} contains the spin-orbit coupling between orbital angular momentum L_i and spin S_i of electron i which is the most notable relativistic correction

(other corrections involving the orbital currents are actually larger, but less evident since they fail to split levels). In the central field model, the states of the atom are constructed using 1-electron orbitals computed with a suitable central $V(r)$; the wave functions differ from the Hydrogen-like orbitals only in the radial functions $R_{nL}(r)$. In terms of the one-electron basis states labeled by n, L, m, m_S quantum numbers², one starts assuming a *configuration* of the atom (see Table 3.1).

H	1	1s	Cr	24	$3d^5 4s$	Ag	47	$4d^{10} 5s$	Yb	70	$4f^{14} 6s^2$
He	2	$1s^2$	Mn	25	$3d^5 4s^2$	Cd	48	$4d^{10} 5s^2$	Lu	71	$5d^6 s^2$
Li	3	2s	Fe	26	$3d^6 4s^2$	In	49	$5s^2 5p$	Hf	72	$5d^2 6s^2$
Be	4	$2s^2$	Co	27	$3d^7 4s^2$	Sn	50	$5s^2 5p^2$	Ta	73	$5d^3 6s^2$
B	5	$2s^2 2p$	Ni	28	$3d^8 4s^2$	Sb	51	$5s^2 5p^3$	W	74	$5d^4 6s^2$
C	6	$2s^2 2p^2$	Cu	29	$3d^{10} 4s$	Te	52	$5s^2 5p^4$	Re	75	$5d^5 6s^2$
N	7	$2s^2 2p^3$	Zn	30	$3d^{10} 4s^2$	I	53	$5s^2 5p^5$	Os	76	$5d^6 6s^2$
O	8	$2s^2 2p^4$	Ga	31	$4s^2 4p$	Xe	54	$5p^6$	Ir	77	$5d^7 6s^2$
F	9	$2s^2 2p^5$	Ge	32	$4s^2 4p^2$	Cs	55	6s	Pt	78	$5d^9 6s$
Ne	10	$2p^6$	As	33	$4s^2 4p^3$	Ba	56	$6s^2$	Au	79	$5d^{10} 6s$
Na	11	3s	Se	34	$4s^2 4p^4$	La	57	$5d 6s^2$	Hg	80	$5d^{10} 6s$
Mg	12	$3s^2$	Br	35	$4s^2 4p^5$	Ce	58	$4f 5d 6s^2$	Tl	81	$6s^2 6p$
Al	13	$3s^2 3p$	Kr	36	$4p^6$	Pr	59	$4f^3 6s^2$	Pb	82	$6s^2 6p^2$
Si	14	$3s^2 3p^2$	Rb	37	5s	Nd	60	$4f^4 6s^2$	Bi	83	$6s^2 6p^3$
P	15	$3s^2 3p^3$	Sr	38	$5s^2$	Pm	61	$4f^5 6s^2$	Po	84	$6s^2 6p^4$
S	16	$3s^2 3p^4$	Y	39	$4d 5s^2$	Sm	62	$4f^6 6s^2$	At	85	$6s^2 6p^5$
Cl	17	$3s^2 3p^5$	Zr	40	$4d^2 5s^2$	Eu	63	$4f^7 6s^2$	Rn	86	$6p^6$
Ar	18	$3p^6$	Nb	41	$4d^4 5s$	Gd	64	$4f^7 5d 6s^2$	Fr	87	7s
K	19	4s	Mo	42	$4d^5 5s$	Tb	65	$4f^9 6s^2$	Ra	88	$7s^2$
Ca	20	$4s^2$	Tc	43	$4d^5 5s^2$	Dy	66	$4f^{10} 6s^2$	Ac	89	$6d 7s^2$
Sc	21	$3d 4s^2$	Ru	44	$4d^7 5s$	Ho	67	$4f^{11} 6s^2$	Th	90	$6d^2 7s^2$
Ti	22	$3d^2 4s^2$	Rh	45	$4d^8 5s$	Er	68	$4f^{12} 6s^2$	Pa	91	$5f^2 6d 7s^2$
V	23	$3d^3 4s^2$	Pd	46	$4d^{10}$	Tm	69	$4f^{13} 6s^2$	U	92	$5f^3 6d 7s^2$

Table 3.1. The atomic numbers and the ground state configuration of the elements.

A shell comprises all the orbitals of a given n , and the inner ones, entirely occupied by electrons, are *core* shells. The inner shells contribute most of the binding energy; their charge screens the nuclear potential and contributes in an important way to the $V(r)$, in which the external electrons move. The magnetic quantum number of a closed shell is $M_L = \sum_i M_{L_i} = 0$, the z component of spin is zero and thus all angular momentum quantum numbers

²This is a very convenient basis, but individual electron quantum numbers do not represent observable quantities; any measurement will give the quantum numbers of the atom.

vanish; the parity is +1. Thus, the parity and angular momentum quantum numbers of the atom are determined by the outer (or *valence*) electrons. This suggests that H_{tot} can be simplified. The valence electrons are modeled by

$$H = H_v + H'_C + H'_{rel}, \quad (3.35)$$

where the sums are restricted to incomplete shells. The residual Coulomb interaction H'_C does not contain the core electron contributions and can be dealt with approximately as a perturbation; for light atoms H'_{rel} is also a perturbation. In the limit $H'_C = H'_{rel} = 0$ all the states in a given configuration would be degenerate; for instance, a C atom in the fundamental configuration $1s^2 2s^2 2p^2$ has 2 electrons in the six p spin-orbitals and would have a $\binom{6}{2} = 15$ times degenerate ground state. This degeneracy stems from the invariance of H_v for independent rotations of electrons orbitals in space and of the total spin. The orbital angular momentum of each electron and the total spin are good quantum numbers in this limit. In the presence of interactions, the only conservation laws are

$$[H, \mathbf{J}]_- = 0 \quad (3.36)$$

where $\mathbf{J} = \mathbf{L} + \mathbf{S}$ is the total angular momentum (invariance under rigid rotations) and the parity

$$[H, \Pi]_- = 0 \quad (3.37)$$

(neglecting quite tiny effects of electro-weak mixing).

3.5.1 L-S Multiplets ($H'_{rel} \rightarrow 0$ Limit)

In light atoms, one can neglect H'_{rel} to a good approximation; H'_C breaks the invariance for independent orbital rotations of the electrons, that change r_{ij} . One is left with the invariance under rigid rotations $R(\mathbf{a}) = e^{-\frac{i}{\hbar} \mathbf{a} \cdot \mathbf{L}}$. Hence H commutes with the components of the total orbital angular momentum \mathbf{L} , and the configuration gives raise to a Russell-Saunders multiplet, with different energies for different L . Besides, H commutes with the i -th electron spin \mathbf{S}_i . Is \mathbf{S}_i a good quantum number? Not at all, since individual electrons do not possess observables. What we can measure is the total spin $\mathbf{S} = \sum_i \mathbf{S}_i$ of the atom. Moreover, \mathbf{L} and the total electronic angular momentum

$$\mathbf{J} = \mathbf{L} + \mathbf{S} \quad (3.38)$$

can be measured. But what quantum numbers are compatible? H commutes with $L^2, S^2, J^2, L_z, S_z, J_z$. However, since \mathbf{J}^2 fails to commute with L_i and S_i , these operators are not all compatible and we can label states in two alternative ways: 1) diagonalizing $H, L^2, S^2, L_z, S_z, J_z = L_z + S_z$, defining the $|LSM_L M_S\rangle$ basis with quantum numbers $E, L, S, M_L, M_S, M_J =$

$M_L + M_S$. Since H is invariant for independent rigid rotations in ordinary space and spin space, E is independent of M_L and M_S . 2) diagonalizing $H, \mathbf{L}^2, \mathbf{S}^2, \mathbf{J}^2, J_z$ defining the $|LSJM_J\rangle$ basis with quantum numbers E, L, S, J, M_J . The two bases are connected by a unitary transformation, and both schemes are referred to in literature as L-S or Russell-Saunders scheme. The energy levels of this approximation, or *atomic terms*, are denoted with symbols of the type ^{2S+1}L : as an example, 2P has $L=1, S=1/2$; they are degenerate $(2L+1)(2S+1)$ times.

L-S Terms Inside a Given Configuration

The L-S terms belonging to a given configuration are resolved by H'_C . One can easily find what terms arise. For closed shells there is only 1S . If a single electron *optical* electron moves outside filled shells the entire atom has the quantum numbers L, M_L and $M_S = \frac{1}{2}$ of the electron. If a single electron lacks in order to make filled shells, there is a single hole, this counts like an electron with opposite values of M_L and M_S . If there are two inequivalent electrons (different principal quantum number n) outside filled shells, one must sum their \mathbf{L} and \mathbf{S} . For instance, from two electron labeled $np, n'p$ one builds the atomic terms $^1S, ^3S, ^1P, ^3P, ^1D, ^3D$. With 2 or more equivalent electrons, the possible terms are limited by from the Pauli principle, and the best thing is to proceed by examples.

Example: C atom (configuration $1s^2 2s^2 2p^2$). The closed shells may be ignored, and we must consider the configuration p^2 . The 1-electron states available are (m, σ) with $m \equiv m_L = 1, 0, -1$ and $\sigma = \pm \frac{1}{2}$; there are 6 spin-orbitals involved. Without the Pauli principle we would find $^1S, ^3S, ^1P, ^3P, ^1D, ^3D$, that is $1 + 3 + 3 + 9 + 5 + 15 = 36$ states. Many of those terms are forbidden, since only the 2 electron determinants $(m_1\sigma_1, m_2\sigma_2)$ involving different (m, σ) are allowed. There are $\binom{6}{2} = 15$ pairs of different spin-orbitals; by linear combination one can form 15 allowed 2-electron states with well defined L, S, M_L, M_S . The $(m_1\sigma_1, m_2\sigma_2)$ determinants are labelled by M_L and M_S , and those with parallel spins belong to $S=1$; $M_S = 0$ is compatible with singlet and triplet. Not all determinants have well defined L ; however the determinant with the largest M_L must belong to the maximum L . In this case the largest M_L is 2, and corresponds to $(m_1\sigma_1, m_2\sigma_2) = (1+, 1-)$, having $M_S = 0$. Thus there is a 1D term. 1D has 5 states, $M_L = 2, 1, 0, -1, -2$, and we must find 10 more orthogonal states, with $L < 2$. With $M_L = 1$ we can find the 4 determinants $(1\pm, 0\pm)$ having mixed L . A linear combination, which might be found using the shift operator S^- on the state with $M_L = 2$, belongs to 1D ; 3 $M_L = 1$ states are left, with $L = 1$ and $M_S \leq 1$; these belong to 3P (9 states). we have found $5+9=14$ states out of 15; there is room only for a 1S . Thus the configuration is resolved as follows:

$$p^2 \rightarrow ^1S, ^3P, ^1D. \quad (3.39)$$

(See the Problems section for other examples.)

The parity of the atom is the product of those $(-)^{L_i}$ of the orbitals in the determinant. The ground state configuration of C is even, and all terms including 3P are. The excited configuration $2s^12p^3$ is odd and yields a term denoted by ${}^3P^o$, where o stands for odd.

The L-S wave functions can be obtained by combining the angular momenta with the Clebsh-Gordan coefficients. For two electrons, one forms determinants $|m_1 m_{s_1} m_2 m_{s_2}\rangle$, recalling that in order to avoid double counting the orbitals must be ordered in some way; then,

$$|LSM_L M_S\rangle = \sum_{m_1 m_{s_1} m_2 m_{s_2}} |m_1 m_{s_1} m_2 m_{s_2}\rangle \langle L_1 m_1 L_2 m_2 | LM_L \rangle \langle \frac{1}{2} m_{s_1} \frac{1}{2} m_{s_2} | SM_S \rangle; \quad (3.40)$$

one has to normalize the result again in general (see Problem 3.3, 3.4). A third electron can then be added if needed by multiplying by a spin-orbital with the Clebsh-Gordan coefficients, and antisymmetrizing the result. For many electrons this build-up process becomes very time consuming, but one can make the process faster by using *fractional parentage coefficients* [147] [148]. These tables present the wave functions coded in a special way; this saves labor, but introduces no new physical concepts.

3.5.2 Hund's First Rule

Hund established two empirical rules, that hold with no exception in atomic physics, and are very popular with the students because there is no proof to learn. This is the first.

The lowest L-S level of the atomic configuration has the lowest S and the highest L compatibly with S.

This is no theorem, but is true and reasonable, since high spin implies a very antisymmetrical orbital wave function and therefore a reduced repulsion; increasing L also lowers the energy because higher L wave functions are more diffuse. For $Z=6$ (C atom), the configuration is $2p^2$: the terms are ${}^1S, {}^3P, {}^1D$ and the ground state is 3P . For $Z=74$ (Tungsten) the configuration is $5p^65d^46s^2$; the incomplete shell is $5d^4$. With $M_L = -2, -1, 0, 1, 2$, all spins can be parallel, so the Hund rule wants $S = 2$. The maximum M_L is $2 + 1 + 0 + (-1) = 2$. The ground term is 5D . In the L-S limit (no spin-orbit interaction) the states of a term are all degenerate. Combining the states of a LS term with various M_L and M_S by means of the Clebsh-Gordan coefficients one builds $|L, S, J, M_J\rangle$ states. The allowed values of J are obtained from L with S by the usual angular momentum summation rule, while $M_J \in (-J, J)$. Thus a term 3F , ($L=3, S=1$), gives rise to ${}^3F_4, {}^3F_3$ and 3F_2 , where the index to the right is J. The energy E of the atomic levels is independent of

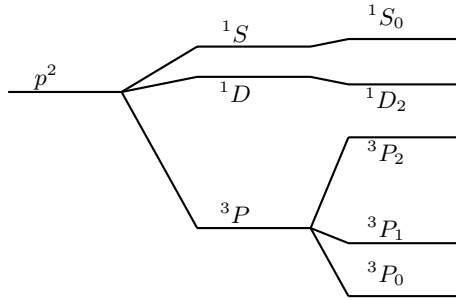


Fig. 3.1. The p^2 configuration splits into the L-S terms $^1S, ^1D$ and 3P , separated by the Coulomb interaction. The relativistic correction then produces the atomic levels as shown.

J and M_J . If we introduce H'_{rel} as a perturbation, the degeneracy is partly removed; E depends on J but not on M_J . Here is the pattern of the levels for the Carbon atom (see Fig. 3.1).

3.6 Atomic Coulomb Integrals

The interaction matrix elements $\langle u_a u_b | \frac{1}{r_{12}} | u_c u_d \rangle$ between spin-orbitals factor into spin scalar products and Coulomb integrals $\langle a(1)b(2) | \frac{1}{r_{12}} | c(1)d(2) \rangle$ involving the central field orbitals $a(\mathbf{r}) = R_{nL}^a(r)Y_{LM}(\theta, \phi)$, and the like. One can expand $\frac{1}{r_{12}} \equiv \frac{1}{|\mathbf{r}_1 - \mathbf{r}_2|}$ in polar coordinates such that $\mathbf{r}_i \rightarrow (r_i, \theta_i, \phi_i)$. Imposing that the result be the Green's function of Poisson's equation one finds, in terms of spherical harmonics and of the shorthand notations

$$\begin{cases} r_{>} = r_1\theta(r_1 - r_2) + r_2\theta(r_2 - r_1), \\ r_{<} = r_2\theta(r_1 - r_2) + r_1\theta(r_2 - r_1), \end{cases} \quad (3.41)$$

$$\frac{1}{r_{12}} = 4\pi \sum_{K=0}^{\infty} \frac{r_{<}^K}{r_{>}^{K+1}} \sum_{m=-K}^K \frac{Y_{Km}^*(\theta_1, \phi_1)Y_{Km}(\theta_2, \phi_2)}{(2K+1)}. \quad (3.42)$$

To carry out this calculation, one needs integrals involving three spherical harmonics; these are easily obtained by codes like Mathematica or Maple; they are tabulated in the literature [144] as c^K tables, where

$$\int d\Omega Y_{L_a m_a}^*(\Omega) Y_{K m}(\Omega) Y_{L_c m_c}(\Omega) \equiv \sqrt{\frac{2K+1}{4\pi}} c^K(L_a m_a, L_c m_c) \delta(m, m_a - m_c). \quad (3.43)$$

One easily finds that

$$\langle ab | \frac{1}{r_{12}} | cd \rangle = \delta(m_a + m_b, m_c + m_d) \times \sum_{K=0}^{\infty} c^K(L_a, m_a, L_c, m_c) c^K(L_d, m_d, L_b, m_b) R^K(ab, cd) \quad (3.44)$$

Actually this summation has in any case a few nonzero terms since they are restricted by the triangular rules

$$\begin{aligned} |L_d - L_b| &\leq K \leq L_d + L_b \\ |L_a - L_c| &\leq K \leq L_a + L_c. \end{aligned} \quad (3.45)$$

The radial integrals contain the specifics of the problem, the rest is geometry. For the diagonal elements (c,d)=(a,b) one uses the Slater integrals

$$\begin{aligned} F^K(n_a L_a, n_b L_b) &\equiv R^K(a, b, a, b) \quad (\text{Coulomb interaction}) \\ G^K(n_a L_a, n_b L_b) &\equiv R^K(a, b, b, a) \quad (\text{Exchange interaction}). \end{aligned} \quad (3.46)$$

Using other widespread notations,

$$\langle ab | \frac{1}{r_{12}} | ab \rangle = \sum_K a_K(L_a m_a, L_b m_b) F^K(n_a L_a, n_b L_b) \quad (3.47)$$

with

$$a_K(L_a m_a, L_b m_b) = c^K(L_a m_a, L_a m_a) c^K(L_b m_b, L_b m_b) \quad (3.48)$$

and

$$\langle ab | \frac{1}{r_{12}} | ba \rangle = \sum_K b_K(L_a m_a, L_b m_b) G^K(n_a L_a, n_b L_b) \quad (3.49)$$

with

$$b_K = |c^K|^2. \quad (3.50)$$

In this way, one can calculate the *multiplet splittings* due to H'_C . The repulsion is invariant for space rotations and (separately) spin rotations of the atom, which are exponentials in \mathbf{L}, \mathbf{S} and the H_C matrix is diagonal in the $|LSM_L M_S\rangle$ basis.

A closed shell contains of angular momentum L contains $2(2L + 1)$ electrons; the configuration with $2(2L + 1) - n$ electrons is said to contain n holes and to be *conjugate* to the one with n electrons. The expressions of the matrices of the Coulomb interactions in terms of the Slater integrals are the same for the conjugate configurations; however the one for n electrons refers to the empty shell as the energy zero, and the one for n holes refers to the filled shell. Thus, if the Slater parameters are the same in both cases, the term separations are the same. The direct diagonalization of the Coulomb matrix by standard methods becomes painstaking with many electrons; efficient methods based on tensor operators are reviewed by Weissbluth [147] who also reports the results for the most common configurations. The multiplet energies for many more configurations are given by Condon and Shortley [144] and by Slater [145].

Relativistic Correction to the L-S Coupling

Hydrogen is a special case, since L remains a good quantum number³ despite the spin-orbit coupling $H'_{rel} = \xi \mathbf{L} \cdot \mathbf{S}$ and the states can be labeled $|LSJM_J\rangle$. Besides, $H'_{rel} = \frac{\xi}{2}(J^2 - L^2 - S^2)$ yields the first-order correction $\Delta E(J) = \frac{\xi}{2}(J(J+1) - L(L+1) - S(S+1))$. Lande's interval rule $\Delta E(J) - \Delta E(J-1) = \xi J$ is obeyed.

In many-electron atoms $H'_{rel} = \sum_i \xi_i \mathbf{L}_i \cdot \mathbf{S}_i$ fails⁴ to commute with L^2 and S^2 ; so, $L - S$ terms sharing the same J are mixed. In the C case, 3P_2 and 1D_2 contaminate each other, and 1S_0 mixes with 3P_0 . Spins and orbits exchange angular momentum; only in the H case this does not happen (the spin of 1 electron is always $1/2$.) For light atoms, H'_{rel} is small, and the mixing of different L-S terms is negligible. So,

$$\Delta E_J = \langle LSJM_J | \sum_i \xi_i \mathbf{L}_i \cdot \mathbf{S}_i | LSJM_J \rangle = K_{LS} \langle LSJM_J | \mathbf{L} \cdot \mathbf{S} | LSJM_J \rangle, \quad (3.51)$$

where we have used the Wigner Eckart theorem. for example, the fine structure of the 3P and 3F terms of the d^2 configuration depends on different K constants. The Lande' rule can again be derived.

The LSJM scheme is unitarily equivalent to the $LSM_L M_S$ scheme:

$$|LSJM\rangle = \sum_{M_L M_S} |LSM_L M_S\rangle \langle LSM_L M_S | LSJM\rangle; \quad (3.52)$$

since the $|LSM_L M_S\rangle$ vectors have the correct normalization and antisymmetry property the result is automatically normalized. For example, let us calculate $|d^2 {}^3P_0\rangle$. The relevant Clebsh-Gordan Table is the one for summing an angular momentum 1 to angular momentum J_1 ;

J	$m_2 = 1$	$m_2 = 0$	$m_2 = -1$
$J_1 + 1$	$\sqrt{\frac{(J_1+m)(J_1+m+1)}{(2J_1+1)(2J_1+2)}}$	$\sqrt{\frac{(J_1-m+1)(J_1+m+1)}{(2J_1+1)(J_1+1)}}$	$\sqrt{\frac{(J_1-m)(J_1-m+1)}{(2J_1+1)(2J_1+2)}}$
J_1	$\sqrt{\frac{(J_1+m)(J_1-m+1)}{2J_1(J_1+1)}}$	$\frac{m}{\sqrt{J_1(J_1+1)}}$	$\sqrt{\frac{(J_1-m)(J_1+m+1)}{2J_1(2J_1+1)}}$
$J_1 - 1$	$\sqrt{\frac{(J_1-m)(J_1-m+1)}{2J_1(2J_1+1)}}$	$\sqrt{\frac{(J_1-m)(J_1+m)}{J_1(2J_1+1)}}$	$\sqrt{\frac{(J_1+m+1)(J_1+m)}{2J_1(2J_1+1)}}$

We identify the momenta as follows: $L \rightarrow J_1, S \rightarrow J_2, M_S \rightarrow m_2$. Since we want $J = 0$ we use the last line, yielding $\frac{1}{\sqrt{3}}, -\frac{1}{\sqrt{3}}, \frac{1}{\sqrt{3}}$. So,

$$\begin{aligned} |d^2 {}^3P_0\rangle &= \frac{1}{\sqrt{3}} \{ |{}^3PM_L = 1, M_S = -1\rangle \\ &\quad - |{}^3PM_L = 0, M_S = 0\rangle + |{}^3PM_L = -1, M_S = 1\rangle \} \end{aligned} \quad (3.53)$$

³Even in the full Dirac theory the L of the large component can be used to label the (4-component) spinor although \mathbf{L} fails to commute with Dirac's Hamiltonian.

⁴developing $L^2 = (\sum_k \mathbf{L}_k)^2$ one obtains squares of angular momenta that commute with the components and cross products that do not; similar considerations apply to the spin operators.

If one substitutes the determinantal expansion derived in Problem 3.4 the result

$$|d^2 \ ^3P_0\rangle = \frac{1}{\sqrt{30}}\{2|1^+, -2^+| - \sqrt{6}|0^+, -1^+| - 2|2^+, -2^-| - 2|2^-, -2^+| + |1^+1^-| + |1^-1^+| + 2|2^-, -1^-| - \sqrt{6}|1^-, 0^-|\} \quad (3.54)$$

is no eigenstate of M_L, M_S but is eigenstate of J, M_J . The interaction H'_C is diagonal in both the LSM_LM_S and the $LSJM_J$ basis, and both fall within the L-S or Russell-Saunders scheme. However, $LSJM_J$ remains a suitable basis even in the presence of the spin-orbit interaction.

3.6.1 Hund's Second Rule

The ground level can be found by the **Second Hund's rule**, also empirical:

The level with the lowest J is lowest if the shell is less than half filled. The level with the highest J is lowest if the shell is more than half filled. There is no spitting (in first order) for half filled shells.

For the C atom the ground state has $J = 0$, as shown in Figure 3.1.

3.6.2 J-J Coupling

The J-J approximation is opposite to L-S coupling: one neglects the Coulomb interaction H_C . This scheme is preferable for large Z and for excited states involving diffuse wave functions. The Hamiltonian reads

$$H_0 = \sum_i \left[\frac{\mathbf{p}_i^2}{2m} + V(r_i) + \xi \mathbf{L}_i \cdot \mathbf{S}_i \right] \quad (3.55)$$

The one-electron eigen-spinors are proportional to the *generalized spherical harmonics* $|L, J, M_J\rangle$. These are obtained combining the spherical harmonics Y_m^L and the spin states α and β with the Clebsch-Gordan coefficients. By the angular momentum rules one can combine the Slater determinants that we can form with these spinors to get total J eigenfunctions.

3.6.3 Intermediate Coupling

In intermediate coupling one treats exactly both H'_C and H'_{rel} . This is necessary e.g. for the valence states of heavy atoms where both interactions are important. With the 1-body eigen-spinors of (3.55) one can form Slater determinants $|u_{j_1 m_1} u_{j_2 m_2} \dots|$ that have M_J quantum number; in general different

J values can be mixed. In the basis of such determinants the $H'_C + H'_{rel}$ matrix is computed and diagonalized; the eigenvectors can be labeled with J and energy eigenvalues are M_J independent. Alternatively, one can start with the determinantal wave functions $|u_{L_1 m_{L_1} m_{S_1}} u_{L_2 m_{L_2} m_{S_2}} \cdots|$ and compute the H'_{rel} , then perform the unitary transformation to the $|LSJM\rangle$ basis where H'_C is already diagonal (its diagonal matrix elements depend only on L and S). We exemplify the latter procedure in the case of the d^2 configuration; $L = 2$ for both electrons and we denote the determinants as $|m_1^\sigma, m_2^\sigma|$; for example, $|1^+, -2^+|$ has two spin-up electrons with $m = 1$ and $m = -2$, respectively. To calculate the matrix of $H'_{rel} = \zeta [\mathbf{L}_1 \cdot \mathbf{S}_1 + \mathbf{L}_2 \cdot \mathbf{S}_2]$, where ζ is the spin-orbit parameter, one uses the expansion $\mathbf{L}_i \cdot \mathbf{S}_i = L_{iz} S_{iz} + \frac{1}{2} \{L_i^+ S_i^- + L_i^- S_i^+\}$; we know how to act on the $|m_1^\sigma, m_2^\sigma|$ determinants, using Equation (6.1.1). So,

$$\sum_i [\mathbf{L}_i \cdot \mathbf{S}_i] |1^+, -2^+| = \left\{ \left(1 \times \frac{1}{2} + (-2) \times \frac{1}{2}\right) |1^+, -2^+| + \frac{1}{2} [2|2^-, -2^+| + 2|1^-, -1^+|] \right\}, \quad (3.56)$$

and so on. We can calculate the effect of the spin-orbit Hamiltonian on the $|LSJM_J\rangle$ basis. Using the results of the problems above,

$$\begin{aligned} H_{SO} |d^2 \ ^3P_0\rangle &= \frac{-\zeta}{\sqrt{30}} [-2|1^+, -2^+| + 8|2^-, -2^+| + \\ &\sqrt{6}|0^+, -1^+| - 7|1^-, -1^+| - 6|0^+, 0^-| - 4|2^+, -2^-| \\ &- 2|2^-, -1^-| + 5|1^+, -1^-| + \sqrt{6}|1^-, 0^-|] \end{aligned} \quad (3.57)$$

Hence,

$$\langle d^2 \ ^3P_0 | H_{SO} | d^2 \ ^3P_0 \rangle = -\zeta. \quad (3.58)$$

Besides, since

$$|d^2 \ ^1S_0\rangle = \frac{-1}{\sqrt{5}} [|2^+, -2^-| - |2^-, -2^+| - |1^+, -1^-| + |1^-, -1^+| + |0^+, 0^-|], \quad (3.59)$$

$$\langle d^2 \ ^1S_0 | H_{SO} | d^2 \ ^3P_0 \rangle = -\zeta\sqrt{6}. \quad (3.60)$$

In this way the full H_{SO} matrix can be built; it is a block matrix since there is no coupling of different J . Letting $\zeta = 2\alpha$, one finds the following Hamiltonians.

For $J=3$ there is only 3F_3 with energy $-\alpha$. For $J=1$ there is only 3P_1 , also with energy $-\alpha$. For $J=4$ there is the basis $^1G_4, ^3F_4$, and $H = \begin{pmatrix} 0 & 2\alpha \\ 2\alpha & 3\alpha \end{pmatrix}$. For

$J=2$, there is the basis $^3F_2, ^1D_2$ and 3P_2 and $H = \alpha \begin{pmatrix} -4 & -4\sqrt{\frac{3}{5}} & 0 \\ -4\sqrt{\frac{3}{5}} & 0 & \sqrt{\frac{42}{5}} \\ 0 & \sqrt{\frac{42}{5}} & 1 \end{pmatrix}$.

Finally, if $J=0$ on the ${}^3P_0, {}^1S_0$ basis, $H = -2\alpha \begin{pmatrix} 1 & \sqrt{6} \\ \sqrt{6} & 0 \end{pmatrix}$. The degeneracy is reduced according to the simple pattern ${}^1S \rightarrow {}^1S_0$, ${}^3P \rightarrow {}^3P_0, {}^3P_1, {}^3P_2$, ${}^1D \rightarrow {}^1D_2$, ${}^3F \rightarrow {}^3F_2, {}^3F_3, {}^3F_4$, ${}^1G \rightarrow {}^1G_0$. More quantum numbers are needed with more than 2 equivalent electrons, as discussed in Chapter 9.9.

3.7 Meitner-Auger Effect and Spectroscopy

An important spectroscopy is based on the Auger Effect. Actually, this effect was first reported in 1923 in *Zeitschrift für Physik* by the Austrian Physicist Lise Meitner (1878-1968), whose great contributions to physics tended to be forgotten on the grounds that she was a lady, was of Jewish origin and lived in the pre-war Germany. In 1925, the great French physicist Pierre Auger (1899-1993) independently discovered the effect while investigating in a bubble chamber the emission of an electron from an atom that absorbs a X-ray photon, that is, photoemission. The photoelectrons have kinetic energy $E_k = h\nu - E_B$, where $E_B(\alpha)$ is one of the binding energies of the atom inner levels. However the Auger electrons have ν -independent energies given approximately by the empirical Auger law

$$E_A(\alpha\beta\gamma) \approx E_B(\alpha) - E_B(\beta) - E_B(\gamma) \quad (3.61)$$

as a combination of 3 binding energies. Thus, $E_A(\alpha\beta\gamma)$ is characteristic of the atomic species and is related to 3 atomic levels. This suggested that X-rays of adequate energy produce a *primary* hole in the state a of binding energy of $E_B(\alpha)$ and a photoelectron; since the ion with a core hole is unstable, the primary holes is filled up by an electron in a less bound level β , and the energy gained in the process is taken by an electron in level γ , than is emitted as the Auger electron.⁵ For particular transition to happen, it is necessary that the primary hole is deep enough (its binding energy must exceed the sum of those of b and c). Of course, energy conservation is compatible with both the processes a) and b) in Figure 3.2. The Auger transitions are denoted by the spectroscopic symbols of the shells (or, more precisely, sub-shells) involved: thus a KL_1M_2 transition is due to a primary hole in the K shell that decays leaving in the final state L_1 and M_2 holes and an Auger electron. One speaks about Core-Core-Core, Core-valence-valence, etc., transitions depending on the levels that are involved.

The Auger effect is caused by the Coulomb interaction: two electrons of the system collide and while one fills up the primary hole, the other is shot out as the Auger electron. Wentzel already in 1927 proposed a theory of the Auger effect based on the independent electron model[204]. In the final state, the atom has two holes in the spin-orbitals β and γ . In the initial state, one

⁵The present two-step description is not completely right, but the one-step one is more involved and is presented in Sect. 6.4.1.

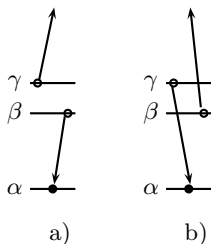


Fig. 3.2. The $\alpha\beta\gamma$ Auger process. The primary hole α is filled by either the β or the γ electron while the other one is emitted as the Auger electron.

hole was in the deep level α ; the other was in the free particle spin-orbital k that will be occupied by the Auger electron in the final state. In this way, the Auger process becomes a collision between two holes. The initial state $|\Phi_i\rangle$ and the final state $|\Phi_f\rangle$ of the atom are represented by 2×2 Slater determinants; they have the same energy and are coupled by the Coulomb interaction. The transition probability is given by the Fermi golden rule

$$P_{if} = \frac{2\pi}{\hbar} \langle \Phi_i | H_C | \Phi_f \rangle^2, \quad (3.62)$$

where H_C is the Coulomb interaction. A deep hole can decay X or Auger. The final-state holes have same the two ways to decay, until a stable ion is formed, in which all the holes are in the most external levels. X decay is faster when the involved levels are distant in energy, because of the ν^3 factor in the transition probability due to the density of photon final states. On the other hand, the Auger decay prevails if the states a, b and c are near in energy, as the Auger matrix element is particularly large when the spin-orbitals have similar sizes. For this reason, the Auger effect is the dominant decay mechanism for inner shell holes of light atoms, while in heavy ones X decay is much more likely.

An alternative mechanism that could take from $|\Phi_i\rangle$ to the final state $|\Phi_f\rangle$ comes to mind. One of electrons in the upper states β, γ could fill up the deep hole via a normal radiative process, emitting a X-ray photon; this photon could then cause the photoemission of the other electron. Would'nt the final state be the same? Indeed, this alternative process does exist, and has the name of internal photoemission; unlike the Auger effect, it obeys to optical selection rules; e.g. it cannot cause a KL_1L_1 transition that instead is observed and is about as probable as any other allowed transition (see Sect. 3.7.1 for the Auger selection rules). The transition probability of the internal photoemission can be calculated by perturbation theory, but since it is a second-order process it turns out to be quite small compared to the Auger effect.

The *Auger spectrum* is plot of the current versus the kinetic energy of electrons. The Auger instruments used to measure the spectra of molecules and solid surfaces keep the sample, the source and the electron detector-analyzer in vacuum. The exciting source can be an electron gun or a X-ray source, like in the ESCA (Electron Spectroscopy for Chemical Analysis) machines. When the sample is a solid surface, in order to limit the problem of the contamination from residual gases one needs the ultra-high vacuum. The mean free path of electrons in a solid depends on their energy, but for the transitions that are observed commonly it is just several Angstroms; the technique is sensitive to the surface. The peaks of the spectrum are characteristic of the atomic species, and the Auger technique lends itself to the surface chemical analysis using a tiny amount of material in a non-destructive way. With scanning techniques, magnified images of the surface can be obtained in which the distribution of elements is visualized .

Actually, the atoms that belong to molecules and solids have transition energies somewhat different from free atoms, and a detailed analysis of these *chemical shifts* supplies further information. This can be done using Core-Core-Core features, but much more can be learned from the study of the shapes of Core-Valence-Valence Auger lines, since the external shells are the most sensitive to the chemical bonds. The analysis of the Auger line shapes is currently an interesting research topic (see also Chapters 6.4,6.2 12.3.).

The original Auger formula yields the transition energies with an error that can be relatively small, but is typically of the order of some tens of eV. Such an error is very large compared to the precision with which routine measurements can be done in a modern apparatus. The main problem is that in the final state there are two holes, and is necessary to account for their repulsion; the hole-hole interaction shifts the peaks of the spectrum to lower kinetic energy and splits them into multiplets. Moreover, every *diagrammatic transition* (that is, a line which is predicted from the previous arguments) has in reality various *satellites*, that correspond to excited states of the final ion. The Wentzel theory is based on a number of assumptions that limit its validity; it neglects the correlation effects and Relativity. The detailed theory of the Auger spectra is necessarily involved, even in the case of free atoms. Nevertheless, the Auger spectroscopy is one of the most important and direct methods for the study of the correlation effects in molecules and solids.

3.7.1 Auger Selection Rules and Line Intensities

Selection rules arise in the two-step model from the conservation of J^2, J_z and parity between the initial, core-hole state $|\Phi_i\rangle$ and the final state $|\Phi_f\rangle$ including the Auger electron. In the L-S approximation, L^2, L_z and S^2, S_z are also conserved, while in the jj scheme, the states are labeled by the j quantum

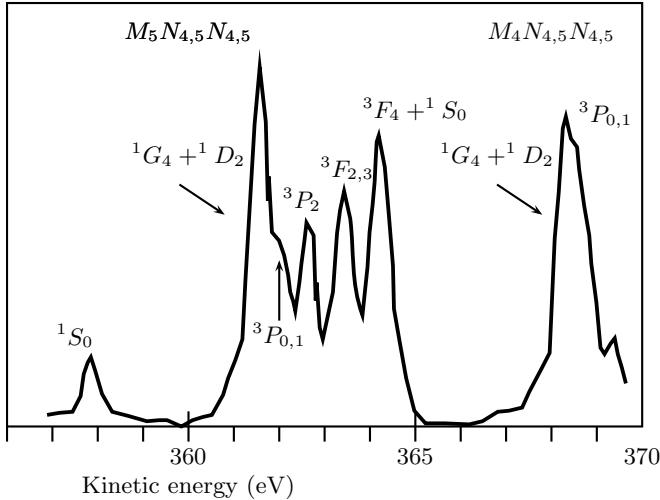


Fig. 3.3. Sketch of the $M_5N_{4,5}N_{4,5}$ and $M_4N_{4,5}N_{4,5}$ spectrum of Cd vapor, in arbitrary units, from measurements by H. Aksela and S. Aksela (Ref. [161]). Many of the multiplet terms are well resolved. The assignments were done by intermediate coupling calculations of line positions and intensities.

numbers of both holes. Remarkably, the predicted number of lines ⁶depends on the scheme used for $|\Phi_f\rangle$: consider for example the KLL transitions. In the pure jj scheme one would predict 6 transitions, namely, $KL_1L_1, KL_1L_2, KL_1L_3, KL_2L_2, KL_2L_3,$ and KL_3L_3 . In the LS scheme, the $2s^02p^6$ configuration yields a 1S term, $2s^12p^5$ gives 1P and 3P ; from $2s^22p^4$ the coupling of angular momenta and the Pauli principle would allow $^1S, ^3P$ and 1D . However, $2s^22p^4 ^3P$ is forbidden by parity conservation; indeed, the primary hole has $L=0$ and is even, $2s^22p^4 ^3P$ has $L=1$ and is even, and by L conservation the Auger electron must be in a p state, which is odd. The transition to the odd $2s^12p^5 ^3P$ final state is allowed, and one predicts 7 lines. When the spin-orbit interaction is introduced, in intermediate coupling the forbidden final-state splits $2s^22p^4 ^3P \rightarrow ^3P_2, ^3P_1, ^3P_0$; then, 3P_2 mixes with 1D_2 and 3P_0 mixes with 1S_0 from the same $2s^22p^4$ configuration. Thus, $2s^22p^4 ^3P_2$ and $2s^22p^4 ^3P_0$ become more and more allowed as Z grows. Instead, 3P_1 remains purely P and forbidden (as long as one can neglect the mixing with higher configurations). Thus, the number of lines grows to 9.

⁶If there are open valence shells, each two-hole final state becomes a multiplet when valence and core-hole angular momenta are recoupled; to a first approximation we can often neglect such complications since usually the splitting is small.

In the non-relativistic limit the Auger intensities are computed by evaluating the matrix elements of H_C with Pauli spinors; as a simple approximation, Coulomb waves are used for the Auger electron states (since the Auger electron leaves a doubly charged ion behind) and Hartree-Fock orbitals for the discrete levels. However, configuration mixing is important. For instance, in computing KLL spectra, the mixing of $2s^2 2p^4 \ ^1S_0$ and $2s^0 2p^6 \ ^1S_0$ has an important effect on the wave functions and hence on the intensities. The calculation simplifies if one can approximate $|\Phi_i\rangle$ and $|\Phi_f\rangle$ as two-hole states, and this is often useful (for instance, in noble gas and in transition metal spectra). One then often uses as a further simplification the *mixed coupling scheme* which consists in treating $|\Phi_i\rangle$ in the jj coupling scheme but $|\Phi_f\rangle$ in the LS one. This is useful for core-valence-valence spectra in a wide range of Z, when the spin-orbit interaction is small for valence holes but is important for deep states. For quantitative work, we need (particularly for intermediate and high Z) the relativistic theory with the Breit interaction

$$W_B(1, 2) = \frac{e^2}{r_{12}} \exp[ikr_{12}][1 - \boldsymbol{\alpha}(1) \cdot \boldsymbol{\alpha}(2)], k = \frac{\omega}{c} \quad (3.63)$$

where $\boldsymbol{\alpha}$ is Dirac's velocity and $\hbar\omega$ is the energy difference between the scattering states (namely, the deep hole and Auger electron states). Codes are now available; GRASP[158] (General-purpose Relativistic Atomic Structure Program) computes Dirac-Fock orbitals, takes linear combinations of determinants with the correct J^2, J_z , parity and seniority number labels; further it takes linear combinations of such states, thus doing a partial configuration mixing, and includes corrections like the effects of nuclear size and the main QED corrections.

Problems

- 3.1.** Find how the ground configuration of N is resolved into L-S terms.
- 3.2.** Find how the ground configuration of Ti is resolved into L-S terms.
- 3.3.** For the configuration d^2 obtain $|^3PM_L = 0, M_S = 0\rangle$ as a combination of determinants $|m_{L_1}^\pm, m_{L_2}^\pm\rangle$ of one-electron wave functions, using the Clebsch-Gordan coefficients.

Note that using $\langle JM_J \pm 1 | J^\pm | JM_J \rangle = \hbar \sqrt{J(J+1) - M_J(M_J \pm 1)}$ one finds for d states

$L^+ 2\rangle = 0$	$L^- 2\rangle = 2 1\rangle$	(3.64)
$L^+ 1\rangle = 2 2\rangle$	$L^- 1\rangle = \sqrt{6} 0\rangle$	
$L^+ 0\rangle = \sqrt{6} 1\rangle$	$L^- 0\rangle = \sqrt{6} -1\rangle$	
$L^+ -1\rangle = \sqrt{6} 0\rangle$	$L^- -1\rangle = 2 -2\rangle$	
$L^+ -2\rangle = 2 -1\rangle$	$L^- -2\rangle = 0$	

3.4. For the configuration d^2 show how to obtain $|^3PM_L, M_S\rangle$ for the other values of M_L, M_S using the results of the previous problem, the shift operators and (6.1.1). Write down all the 9 states.

3.5. Using the results of the previous problem for $|^3PM_L = 0, M_S = 1\rangle$ in the configuration d^2 verify explicitly that it is really 3P with the specified quantum numbers.

4 Green's Functions as Thought Experiments

4.1 Green's Theorem for one-Body Problems

Green's theorem

$$\int_V (\Phi \nabla^2 \Psi - \Psi \nabla^2 \Phi) d^3x = \int_S (\Phi \vec{\nabla} \Psi - \Psi \vec{\nabla} \Phi) \cdot \vec{n} dS \quad (4.1)$$

(where \vec{n} is the outgoing normal to the surface S bounding the volume V) is obtained from the divergence theorem

$$\int_V \text{div} \vec{A} d^3x = \int_S \vec{A} \cdot \vec{n} dS, \quad (4.2)$$

with $\vec{A} = \Phi \vec{\nabla} \Psi - \Psi \vec{\nabla} \Phi$. Consider the one-particle Schrödinger equation

$$\left(-\frac{1}{2} \nabla_{\vec{r}}^2 + V(\vec{r}) - \epsilon\right) \psi(\vec{r}) = 0 \quad (4.3)$$

defined in some volume V with some boundary conditions; it is often convenient to change it into an integral equation by a method which is familiar from classical physics. One introduces a Green's function satisfying

$$\left(-\frac{1}{2} \nabla_{\vec{r}}^2 + V(\vec{r}) - \epsilon\right) G(\vec{r}', \vec{r}) = \delta(\vec{r} - \vec{r}'), \quad (4.4)$$

multiplies (4.3) by $G(\vec{r}', \vec{r})$, (4.4) by $\psi(\vec{r})$ and subtracts; the result is (exchanging \vec{r} with \vec{r}')

$$\psi(\vec{r}) = \frac{1}{2} \int_V d^3\vec{r}' \left[G(\vec{r}, \vec{r}') \nabla_{\vec{r}'}^2 \psi(\vec{r}') - \psi(\vec{r}') \nabla_{\vec{r}}^2 G(\vec{r}, \vec{r}') \right]. \quad (4.5)$$

The V integral can be changed to a surface integral by Equation (4.1).

4.2 How Many-Body Green's Functions Arise

4.2.1 Correlation Functions

In terms of the Schrödinger picture, the Heisenberg representation (Section 2.2.1) corresponds to evolving the state from t_0 to time t , applying the operator and then evolving back to t_0 . This appears insane but it is not so.

Consider for instance a measurement of the light absorption from a system of Hamiltonian $H = H_0 + V$, where H_0 is the kinetic energy and V is the electron-electron interaction which is a large perturbation and makes the problem difficult. However, the transitions are due to the time dependent, further perturbation $H'e^{i\omega t}$ driven by the oscillating field. If H' is weak we can calculate the absorption cross section $\sigma(\omega)$ from an initial state $|i\rangle$ by the Fermi golden rule, introducing a complete set of final states $\{|f\rangle\}$. In obvious notation,

$$\begin{aligned} P &= \sum_f P_{i \rightarrow f} = \sum_f \frac{2\pi}{\hbar} |\langle f|H'|i\rangle|^2 \delta(E_i + \omega - E_f) \\ &= \frac{2\pi}{\hbar} \sum_f \langle i|H'|f\rangle \delta(E_i + \omega - E_f) \langle f|H'|i\rangle \\ &= \frac{2\pi}{\hbar} \sum_f \langle i|H' \delta(E_i + \omega - H)|f\rangle \langle f|H'|i\rangle \\ &= \frac{2\pi}{\hbar} \langle i|H' \delta(E_i + \omega - H)H'|i\rangle \equiv \sigma(\omega). \end{aligned} \quad (4.6)$$

Transforming from frequency to time,

$$\begin{aligned} \sigma(t) &= \int \frac{d\omega}{2\pi} e^{-i\omega t} \sigma(\omega) = \langle i|H'e^{-i(H-E_i)t}H'|i\rangle \\ &= \langle i|e^{iHt}H'e^{-iHt}H'|i\rangle = \langle i|H'_H(t)H'_H(0)|i\rangle. \end{aligned} \quad (4.7)$$

This $\sigma(t)$ is a *correlation function* and is written as an average over $|i\rangle$ of a product of Heisenberg operators. It may appear that there is little to gain in this approach, since $|i\rangle$ is an interacting many-body state that can be quite hard or impossible to calculate. Here is the real breakthrough:

The calculation of many-body states can be completely avoided! There are powerful methods for expanding the correlation functions, or better, their combinations which are called the Green's functions.

In the optical absorption case, the perturbation is a one-body operator, $H' = \sum_{mn} M_{mn} a_m^\dagger a_n$ and the cross section can be expressed in terms of the matrix elements M_{mn} and of a correlation function

$$\gamma_{ph}(t) = \langle i|a_p^\dagger(t)a_q(t)a_r^\dagger(0)a_s(0)|i\rangle. \quad (4.8)$$

$\gamma_{ph}(t)$ is a particle-hole correlation function and tells us about a thought experiment: a particle-hole pair (created in the interacting ground state by the absorption of a photon) is propagated to time t and then destroyed, and we want the amplitude that the system returns in the ground state. We shall discuss photoemission spectra in terms of one-hole correlation functions. In dealing with Auger spectroscopy we shall have to do in Section 6.2 with 2-hole correlation functions like

$$\gamma_{hh}(t) = \langle i|a_p^\dagger(t)a_q^\dagger(t)a_r(0)a_s(0)|i\rangle; \quad (4.9)$$

we shall also need more complicated operator averages, e.g. in Sect. 6.4.1 .

4.2.2 Quantum Green's Functions

It is natural to start assuming for simplicity that the initial state $|i\rangle = |\Psi_0\rangle$ is the ground state of H . Temperature effects are postponed until Section 4.2.4. Thus, the initial state averages are understood to be taken over the ground state $|\Psi_0\rangle$, and summarizing we shall write:

$$\boxed{\text{T}=0 \text{ rule: } \langle \hat{O} \rangle = \langle \Psi_0 | \hat{O} | \Psi_0 \rangle, \text{ with } H | \Psi_0 \rangle = E_0 | \Psi_0 \rangle.} \quad (4.10)$$

Along with $\gamma_{ph}(t) = \langle a_p^\dagger(t) a_q(t) a_r^\dagger(0) a_s(0) \rangle$ and $\gamma_{hh}(t) = \langle a_p^\dagger(t) a_q^\dagger(t) a_r(0) a_s(0) \rangle$ we shall need more complicated objects; however, simpler objects are also extremely useful. Let us start with the one-body ones. Such are the so called lesser and greater Green's functions (ground state averages)

$$g_{i,j}^<(t, t') = \langle \Psi_i^\dagger(t') \Psi_j(t) \rangle \quad (4.11)$$

$$g_{i,j}^>(t, t') = \langle \Psi_j(t) \Psi_i^\dagger(t') \rangle \quad (4.12)$$

One is obtained from the other by exchanging the operators, and in equilibrium $g^<$ informs us about the filled states, while $g^>$ knows about the empty ones. From these, we can build *retarded* and *advanced* Green's functions; now what matters is the order of times:

$$\begin{aligned} ig_{i,j}^r(t, t') &= (g_{i,j}^<(t, t') + g_{i,j}^>(t, t')) \theta(t - t') \\ &= \langle [\Psi_j(t'), \Psi_i^\dagger(t)]_+ \rangle \theta(t - t') \end{aligned} \quad (4.13)$$

while

$$-ig_{i,j}^a(t, t') = (g_{i,j}^<(t, t') + g_{i,j}^>(t, t')) \theta(t' - t). \quad (4.14)$$

The two are related by $g_{i,j}^{(r)}(t, t')^* = g_{j,i}^{(a)}(t', t)$. How do they depend on $|\Psi_0\rangle$? In no way! Averaging on the vacuum, $g^< = 0$ and

$$ig_{i,j}^r(t, t') = \langle \Phi_{vac} | c_j(t) c_i^\dagger(t') | \Phi_{vac} \rangle \theta(t - t') \quad (4.15)$$

and since H acting on the vacuum yields 0, we obtain

$$ig_{i,j}^r(t, t') = \langle \Phi_{vac} | c_j e^{-iH(t-t')} c_i^\dagger | \Phi_{vac} \rangle \theta(t - t'), \quad (4.16)$$

which shows that $g^{(r)}$ is actually a function of $t - t'$; so we can drop t' and write simply

$$ig_{i,j}^{(r)}(t) = \langle \Phi_{vac} | c_j e^{-iHt} c_i^\dagger | \Phi_{vac} \rangle \theta(t).$$

The Fourier transform yields:

$$\begin{aligned} ig_{i,j}^{(r)}(z) &= \langle \Phi_{vac} | c_j \int_0^\infty e^{-iHt + izt} dt c_i^\dagger | \Phi_{vac} \rangle \\ &= \langle \Phi_{vac} | c_j \frac{i}{z - H + i\delta} c_i^\dagger | \Phi_{vac} \rangle. \end{aligned} \quad (4.17)$$

This is a one-body problem, that can be rewritten in first quantization $\langle j | \frac{i}{z-H+i\delta} | i \rangle$. Averaging on a completely filled system, $g^> = 0$ and creation and annihilation operators are interchanged, but the result is the same one-hole amplitude. For a partially filled system, $g^<$ brings information on the occupied states and $g^>$ on the empty ones, but the end result is again a one-body matrix element of $\frac{i}{z-H+i\delta}$ between spin-orbitals irrespective of where the Fermi level is. Thus, $g^{(r)}, g^{(a)}$ can always be computed with the average performed over the vacuum, and are a one-particle property. Both are characterized by the fact that they do not *know* where is the Fermi level (for non-interacting systems at least; in the presence of interactions they may have some smell of a change of occupation numbers through the change in potential it introduces).

$g^{(r)}, g^{(a)}$ are not suited for perturbation theory; the diagrammatic method (Chapter 11) works with the time-ordered ones

$$ig_{k,k'}^{(T)}(t, t') = \langle T a_k(t) a_{k'}^\dagger(t') \rangle \tag{4.18}$$

where T is Wick's time ordering operator such that

$$ig_{kk'}^{(T)}(t, t') \equiv ig^{(T)}(kt, k't') = \theta(t - t') \langle a_k(t) a_{k'}^\dagger(t') | \Psi_0 \rangle - \theta(t' - t) \langle a_{k'}^\dagger(t') a_k(t) \rangle. \tag{4.19}$$

This discontinuity is needed; we shall see (Chapter 10) that it implies a source term in their equation of motion. In field theory every scattering event is represented as the annihilation of the ingoing particle and the creation of the outgoing one: here is where the source is necessary. In real space the time-ordered Green's function is

$$g_{\sigma\sigma'}^{(T)}(\mathbf{x}t, \mathbf{x}'t') = -i \langle T [\psi_\sigma(\mathbf{x}, t) \psi_{\sigma'}^\dagger(\mathbf{x}'t')] \rangle \tag{4.20}$$

with the operators in the Heisenberg picture (the spin indices are often omitted when they are not needed).

4.2.3 Quantum Averages

The average of one-body densities $\hat{f}(x) = \sum_{\sigma\sigma'} f_{\sigma\sigma'}(x) \psi_\sigma^\dagger(x) \psi_{\sigma'}(x)$ is

$$\langle f \rangle = -i \lim_{t' \rightarrow t^+} \lim_{x' \rightarrow x} \sum_{\sigma\sigma'} f_{\sigma\sigma'}(x) g_{\sigma\sigma'}^{(T)}(xt, x't'). \tag{4.21}$$

The number density of spin σ at \vec{x} at time t is given by

$$\rho_\sigma(\vec{x}, t) = -i \lim_{t' \rightarrow t+0} \lim_{\vec{x}' \rightarrow \vec{x}} g_{\sigma\sigma}^{(T)}(\mathbf{x}t, \mathbf{x}'t'); \tag{4.22}$$

the current operator is

$$\hat{\mathbf{j}}(\mathbf{x}) = \frac{e}{2m} [\mathbf{p}_{\mathbf{x}'} \delta(\mathbf{x} - \mathbf{x}') + \delta(\mathbf{x} - \mathbf{x}') \mathbf{p}_{\mathbf{x}'}] \quad (4.23)$$

and its expectation value is given by

$$J_{\sigma}(\vec{x}, t) = -\frac{1}{2m} \lim_{t' \rightarrow t+0} \lim_{\vec{x}' \rightarrow \vec{x}} (\nabla_{\vec{x}} - \nabla_{\vec{x}'}) g_{\sigma\sigma'}^{(T)}(\mathbf{x}t, \mathbf{x}'t'). \quad (4.24)$$

The average of one-body operators $\hat{A} = \sum_{\sigma\sigma'} \int dx a_{\sigma\sigma'}(x) \psi_{\sigma}^{\dagger}(x) \psi_{\sigma'}(x)$ is

$$\langle \hat{A} \rangle = \pm i \lim_{t' \rightarrow t+} \lim_{x' \rightarrow x} \int dx \sum_{\sigma\sigma'} a_{\sigma\sigma'}(x) g_{\sigma\sigma'}^{(T)}(xt, x't'), \quad (4.25)$$

upper sign for Bosons. This may be thought of as a trace over space and spin variables:

$$\langle \hat{A} \rangle = \pm i \lim_{t' \rightarrow t+} \lim_{x' \rightarrow x} Tr [a_{\sigma\sigma'}(x) g_{\sigma\sigma'}^{(T)}(xt, x't')]. \quad (4.26)$$

4.2.4 Green's functions at Finite Temperature

We recall from Section (2.2.2) that

Finite T rule: $\langle \hat{A} \rangle = Tr \rho \hat{A}$.

(4.27)

The ground state average $g_{\sigma\sigma'}^{(T)}(xt, x't')$ of Equation (4.20) must be replaced by a thermal average,

$$\mathbf{g}_{\sigma\sigma'}^{(T)}(xt, x't') = \frac{-i}{Z} Tr \rho T [\psi_{\sigma}(\mathbf{x}, t) \psi_{\sigma'}^{\dagger}(\mathbf{x}', t')], \quad Z = Tr \rho; \quad (4.28)$$

this is the time-ordered finite temperature propagator. When $\mathbf{g}^{(T)}$ is used in (4.26), all temperature effects are included. It is stated in some books that $\mathbf{g}^{(T)}$ does not possess a diagrammatic expansion, but in fact it can be obtained by the methods in Chapter 13 and corresponds to the contour of Figure 2.2 b).

For time-independent problems the temperature Green's function $\mathcal{G}^{(T)}$ defined along the vertical track of the contour of Figure 2.2 a) offers the same information most directly:

$$\begin{aligned} \mathcal{G}^{(T)} \sigma\sigma'(x\tau, x'\tau') &= -\langle T[\psi_{\sigma}(\mathbf{x}, \tau) \psi_{\sigma'}^{\dagger}(\mathbf{x}', \tau')] \rangle \\ &= -Tr \{ \rho T[\psi_{\sigma}(\mathbf{x}, \tau) \psi_{\sigma'}^{\dagger}(\mathbf{x}', \tau')] \} \end{aligned} \quad (4.29)$$

where field operators are in the temperature Heisenberg representation (2.27), T is the Wick operator that orders along the track. The thermal average (4.27) means $\langle \hat{A} \rangle = \int dx Tr a(x) \rho \psi^{\dagger}(x) \psi(x)$ where spin indices are understood and traced over by Tr , and can be rewritten as

$$\langle \hat{A} \rangle = \mp \int dx \lim_{x' \rightarrow x, \tau \rightarrow \tau' + \delta} \text{Tr}[a(x)\mathcal{G}^{(T)}(x\tau, x'\tau')]. \quad (4.30)$$

To see that, one notes that, by the cyclic property of the trace,

$$\text{Tr}[a\rho e^{K\tau}\psi^\dagger(x)\psi(x)e^{-K\tau}] = \sum_{\sigma\sigma'} \int dx a_{\sigma\sigma'}(x) \text{Tr}[e^{-K\tau}\rho e^{K\tau}\psi^\dagger(x)\psi(x)];$$

$e^{-K\tau}$ commutes with $\rho = \frac{e^{-\beta K}}{Z}$ and $\sum_{\sigma\sigma'} \int dx a_{\sigma\sigma'}(x) \text{Tr}[\rho\psi^\dagger(x)\psi(x)] = \text{Tr}\rho\hat{A}$. In this way the common value of τ and τ' disappears from the calculation of the observables and the behavior of \mathcal{G} for τ far from τ' has no physical meaning. $\mathcal{G}^{(T)}\sigma\sigma'(x\tau, x'\tau')$ is periodic:

$$\begin{aligned} \mathcal{G}^{(T)}\sigma\sigma'(x\tau, x'\tau') &= \pm\mathcal{G}^{(T)}\sigma\sigma'(x\tau, x'\tau' + \beta), \tau > \tau' \\ \mathcal{G}^{(T)}\sigma\sigma'(x\tau, x'\tau') &= \pm\mathcal{G}^{(T)}\sigma\sigma'(x\tau + \beta, x'\tau'), \tau < \tau' \end{aligned} \quad (4.31)$$

(upper sign for bosons). Indeed, let $\tau > \tau'$; then $-Z\mathcal{G}^{(T)}\sigma\sigma'(x\tau, x'\tau')$ is given by $\text{Tr}\{e^{-\beta K}\psi_\sigma(\mathbf{x}, \tau)\psi_{\sigma'}^\dagger(\mathbf{x}', \tau')\}$; using the cyclic property of trace this may be transformed to read

$$\text{Tr}\{\psi_{\sigma'}^\dagger(\mathbf{x}', \tau')e^{-\beta K}\psi_\sigma(\mathbf{x}, \tau)\} = \text{Tr}\{e^{-\beta K}e^{+\beta K}\psi_{\sigma'}^\dagger(\mathbf{x}', \tau')e^{-\beta K}\psi_\sigma(\mathbf{x}, \tau)\}.$$

Thus, we got $\psi_{\sigma'}^\dagger(\mathbf{x}', \tau' + \beta)$, standing on the left of ψ , in agreement with the fact that $\tau' + \beta > \tau$, but this implies a sign change for Fermions, a - sign comes from the definition of $\mathcal{G}^{(T)}$ and the first line results; the second follows in a similar way.

$\mathcal{G}^{(T)}$ is useful only in time-independent problems; then it is actually $\mathcal{G}^{(T)}\sigma\sigma'(x, x', \tau - \tau')$. According to the above discussion it is a function of one τ variable defined in $(-\beta, \beta)$ which can be extended to the neighboring intervals like a periodic (antiperiodic) function for Bose (Fermi) systems. For all practical considerations, we may extend $\mathcal{G}^{(T)}$ in this way to the real axis, since this has no physical implications but allows to write the Fourier series

$$\mathcal{G}^{(T)}\sigma\sigma'(x, x', \tau) = \frac{1}{\beta} \sum_{n=-\infty}^{\infty} \mathcal{G}^{(T)}\sigma\sigma'(x, x', \omega_n)e^{-i\omega_n\tau}, \quad (4.32)$$

with the Matsubara frequencies

$$\omega_n = \frac{\pi n}{\beta}, \quad (4.33)$$

and

$$\mathcal{G}^{(T)}\sigma\sigma'(x, x', \omega_n) = \frac{1}{2} \int_{-\beta}^{\beta} d\tau e^{i\omega_n\tau} \mathcal{G}\sigma\sigma'(x, x', \tau). \quad (4.34)$$

For Fermi (Bose) system, $\mathcal{G}^{(T)}$ is odd (even) and $\mathcal{G}^{(T)}\sigma\sigma'(x, x', \omega_n) \neq 0$ for odd (even) n .

4.3 Non-interacting Propagators for Solids

Non-relativistic Electrons

Consider the non-interacting electron system with Hamiltonian $H_0 = -\frac{1}{2}\nabla_{\vec{r}}^2 + V(\vec{r})$, such that $H_0\psi_k(x) = \epsilon_k\psi_k(x)$; in second-quantized form, $H_0 = \sum_k \epsilon_k n_k$; in the Heisenberg picture, setting $\hbar = 1$, the annihilation operator for spin-orbital a evolves with

$$c_a(t) = e^{iH_0t} c_a e^{-iH_0t}.$$

From the *equation of motion* $\dot{c}_a = i[H_0, c_a]_-$, since $[n_k, c_{k'}]_- = -\delta_{kk'} c_k$, one obtains for energy eigenstates $\dot{c}_k = -i\epsilon_k c_k$ and so

$$c_k(t) = c_k e^{-i\epsilon_k t}. \tag{4.35}$$

The propagator is defined by

$$i g_{a,b}(t_2, t_1) \equiv i g_{a,b}(t_2 - t_1) = \langle T[c_a(t_2) c_b^\dagger(t_1)] \rangle, \tag{4.36}$$

where the average is taken over the ground state. For an empty (totally full) system, this reduces to the retarded (advanced) Green's function, but otherwise $g_{a,b}$ propagates both electrons and holes; for $t_1 < t_2$ an electron is added at t_1 , propagates forwards in time and is annihilated at t_2 , for $t_1 > t_2$ a hole is introduced, propagates backwards and is annihilated. Using $b_n^\dagger = \sum_k a_k^\dagger \langle a_k | b_n \rangle$ (Equation 1.51) one readily finds that

$$g_{a,b}(t) = \sum_k \langle a | k \rangle \langle k | b \rangle g_{k,k}(t) \tag{4.37}$$

where $g_{k,k'}(t) = \delta_{kk'} g_k(t)$ and

$$i g_k(t) = e^{-i\epsilon_k t} \{ \theta(t) [1 - n_k] - \theta(-t) n_k \} \tag{4.38}$$

where n_k is the occupation number. The propagator evolves with the same phase factor as the wave functions but has a discontinuity at $t = 0$ and satisfies the *equation of motion*

$$i \frac{\partial}{\partial t} g_{k,k'}(t) = \epsilon_k g_{k,k'}(t) + \delta_{k,k'} \delta(t). \tag{4.39}$$

This useful result is due to the definition of T . The Fourier component at frequency ω is found by the frequently used integrals

$$\int_0^\infty e^{i(\omega+x)t} dt = \frac{i}{\omega+x+i\delta}, \quad \int_{-\infty}^0 e^{i(\omega+x)t} dt = \frac{-i}{\omega+x-i\delta}, \quad \delta \rightarrow +0, \tag{4.40}$$

$$G^0(k, k', \omega) \equiv \delta(k, k') G^0(k, \omega) = \int_{-\infty}^{\infty} dt G^0(k, k', t) e^{i\omega t} = \frac{\delta_{k, k'}}{\omega - \epsilon_k + i\eta_k}, \quad (4.41)$$

with $\eta_k = +\delta$ for empty states and $\eta_k = -\delta$ for filled ones, and δ stands for a positive infinitesimal. Thus one has an electron for $\eta_k > 0$ and a hole otherwise. In the space representation the retarded Green's function (4.17) reads

$$g^{(r)}(\vec{r}', \vec{r}, \omega) = \sum_k \frac{\psi_k(\vec{r}) \psi_k(\vec{r}')^*}{\omega - \epsilon_k + i\delta} = \langle \vec{r} | \frac{1}{\omega - H + i\delta} | \vec{r}' \rangle \quad (4.42)$$

It obeys the same equation of motion as the time-ordered one, the difference arises from the boundary conditions. Indeed, setting $z = \omega + i\delta$, using

$$\begin{aligned} & \langle \vec{r} | \frac{1}{z - H} (z - H) | \vec{r}' \rangle \\ &= \langle \vec{r} | \vec{r}' \rangle = \delta(\vec{r} - \vec{r}') = z \langle \vec{r} | \frac{1}{z - H} | \vec{r}' \rangle - \langle \vec{r} | \frac{1}{z - H} H | \vec{r}' \rangle \end{aligned} \quad (4.43)$$

and exchanging \vec{r}' with \vec{r} one finds

$$(\omega - (-\frac{1}{2} \nabla_{\vec{r}}^2 + V(\vec{r}))) g^{(r)}(\vec{r}', \vec{r}, \omega) = \delta(\vec{r} - \vec{r}') \quad (4.44)$$

which is like (4.39) in another representation. Comparing with (4.4) we see that $g^{(r)} = -G$.

For the temperature Green's function (4.29) we find similar results.

$$\mathcal{G}(k, \tau - \tau') = -\text{Tr} \rho T c_k(\tau) c_k^\dagger(\tau'). \quad (4.45)$$

Using $c_k(t) = e^{-i\epsilon_k t}$ with the substitution $it \rightarrow \tau$ and introducing the chemical potential one gets: $c_k(\tau) = e^{-(\epsilon_k - \mu)\tau} c_k$, $c_k^\dagger(\tau) = e^{(\epsilon_k - \mu)\tau} c_k^\dagger$ and so

$$\mathcal{G}(k, \tau - \tau') = -e^{-(\epsilon_k - \mu)(\tau - \tau')} \{ \theta(\tau - \tau') \text{Tr} \rho c_k c_k^\dagger - \theta(\tau' - \tau) \text{Tr} \rho c_k^\dagger c_k \}. \quad (4.46)$$

Now using (2.40) and setting $\tau' = 0$ for short we obtain

$$\mathcal{G}(k, \tau) = -e^{-(\epsilon_k - \mu)\tau} \{ \theta(\tau)(1 - n(k)) - \theta(-\tau)n(k) \}, \quad (4.47)$$

where $n(k)$ is the Fermi distribution (2.40). This is similar to (4.38); the changes are: i becomes -1 (a mere convention), energies are referenced to the chemical potential, $it \rightarrow \tau$ at the exponent, the energy step functions are smoothed according to the Fermi distribution and the Wick T now acts on the vertical track. Next, we find the thermal Green's function in frequency space by (4.34) and (2.40)

$$\mathcal{G}(k, \omega_n) = \frac{1}{i\omega_n + \mu - \epsilon_k}, \quad (4.48)$$

and in this case the only change (apart from using μ) is $\omega \rightarrow -i\omega_n$.

Non-relativistic Bosons

Consider a Bose field which obeys the harmonic wave equation

$$\frac{\partial^2}{\partial t^2} \phi_{\mathbf{k}}(t) = -\omega_{\mathbf{k}}^2 \phi_{\mathbf{k}}(t). \tag{4.49}$$

If $\omega_{\mathbf{k}} = ck$, this is just

$$\left[\frac{\partial^2}{\partial t^2} + c^2 k^2 \right] \phi_{\mathbf{k}}(t) = 0 \Rightarrow \left[\frac{\partial^2}{\partial t^2} - c^2 \nabla^2 \right] \phi(\mathbf{r}, t) = 0. \tag{4.50}$$

In second quantization ϕ is dealt with like the coordinate of an oscillator of (arbitrary) mass $m=1$, that is

$$\phi_{\mathbf{k}}(t) = \hbar \frac{a_{\mathbf{k}}(t) + a_{\mathbf{k}}^\dagger(t)}{\sqrt{2\varepsilon_{\mathbf{k}}}} = \hbar \frac{a_{\mathbf{k}} \exp[-i\omega_{\mathbf{k}}t] + a_{\mathbf{k}}^\dagger \exp[i\omega_{\mathbf{k}}t]}{\sqrt{2\varepsilon_{\mathbf{k}}}} \tag{4.51}$$

The canonically conjugated momentum is

$$\pi_{\mathbf{k}} = \dot{\phi}_{\mathbf{k}} \tag{4.52}$$

and yields the Hamiltonian

$$H = \sum_{\mathbf{k}} \frac{\pi_{\mathbf{k}}^2 + \omega_{\mathbf{k}}^2 \phi_{\mathbf{k}}^2}{2} = \sum_{\mathbf{k}} \hbar \omega_{\mathbf{k}} \left(a_{\mathbf{k}}^\dagger a_{\mathbf{k}} + \frac{1}{2} \right). \tag{4.53}$$

The propagator is defined as:

$$D_{\mathbf{k}\mathbf{k}'}(t) = \langle 0 | P [\phi_{\mathbf{k}}(t) \phi_{\mathbf{k}'}(0)] | 0 \rangle \tag{4.54}$$

where $a_{\mathbf{k}}|0\rangle = 0$, P is the time ordering operator (earlier times to the right but no sign changes on permuting operators like in T .) Now I show that for $t \neq 0$ the D and ϕ have same wave equation, but at $t = 0$ the source acts. Since $\langle 0 | a_{\mathbf{k}} a_{\mathbf{k}'}^\dagger | 0 \rangle = \delta_{\mathbf{k}\mathbf{k}'}$, obviously $D_{\mathbf{k}\mathbf{k}'}(t) = \delta_{\mathbf{k}\mathbf{k}'} D_{\mathbf{k}}(t)$, where

$$D_{\mathbf{k}}(t) = \frac{\theta(t) \langle 0 | a_{\mathbf{k}} \exp[-i\omega_{\mathbf{k}}t] a_{\mathbf{k}}^\dagger | 0 \rangle + \theta(-t) \langle 0 | a_{\mathbf{k}} a_{\mathbf{k}}^\dagger \exp[i\omega_{\mathbf{k}}t] | 0 \rangle}{2\omega_{\mathbf{k}}}. \tag{4.55}$$

Therefore,

$$D_{\mathbf{k}}(t) = \frac{1}{2\omega_{\mathbf{k}}} \{ \theta(t) \exp[-i\omega_{\mathbf{k}}t] + \theta(-t) \exp[i\omega_{\mathbf{k}}t] \} = \frac{\exp[-i\omega_{\mathbf{k}}|t|]}{2\omega_{\mathbf{k}}}. \tag{4.56}$$

This is continuous, however

$$\begin{aligned} \frac{\partial}{\partial t} D_{\mathbf{k}}(t) &= \frac{1}{2\omega_{\mathbf{k}}} \{ -i\omega_{\mathbf{k}} \theta(t) \exp[-i\omega_{\mathbf{k}}t] + i\omega_{\mathbf{k}} \theta(-t) \exp[i\omega_{\mathbf{k}}t] \} \\ &= \frac{i}{2} \{ \theta(t) \exp[-i\omega_{\mathbf{k}}t] - \theta(-t) \exp[i\omega_{\mathbf{k}}t] \} \end{aligned} \tag{4.57}$$

is not, and

$$\begin{aligned} \frac{\partial^2}{\partial t^2} D_{\mathbf{k}}(t) &= \frac{-i}{2} \{ (-i\omega_{\mathbf{k}}) \theta(t) e^{-i\omega_{\mathbf{k}}t} - i\omega_{\mathbf{k}} \theta(-t) e^{i\omega_{\mathbf{k}}t} \} - \frac{i}{2} \{ \delta(t) + \delta(t) \} \\ &= \frac{-\omega_{\mathbf{k}}}{2} \{ \theta(t) e^{-i\omega_{\mathbf{k}}t} + \theta(-t) e^{i\omega_{\mathbf{k}}t} \} - i \delta(t) \end{aligned}$$

that is,

$$\frac{\partial^2}{\partial t^2} D_{\mathbf{k}}(t) + \omega_{\mathbf{k}}^2 D_{\mathbf{k}}(t) = -i \delta(t) \tag{4.58}$$

Therefore, the propagator is Green's function of the wave equation. Fourier transforming, one finds

$$[-\omega^2 + \omega_{\mathbf{k}}^2] D_{\mathbf{k}}(\omega) = -i. \tag{4.59}$$

However the solution is problematic, because of poles on the real axis, and the transform of (4.56)

$$D_{\mathbf{k}}(\omega) = \int_{-\infty}^{\infty} dt D_{\mathbf{k}}(t) e^{i\omega t} = \frac{1}{2\omega_{\mathbf{k}}} \left[\int_0^{\infty} dt e^{i(\omega - \omega_{\mathbf{k}})t} + \int_{-\infty}^0 dt e^{i(\omega + \omega_{\mathbf{k}})t} \right]$$

does not converge. Therefore one must introduce convergence factors

$$\begin{aligned} D_{\mathbf{k}}(\omega) &= \frac{1}{2\omega_{\mathbf{k}}} \left[\int_0^{\infty} dt e^{i(\omega - \omega_{\mathbf{k}} + i\delta)t} + \int_{-\infty}^0 dt e^{i(\omega + \omega_{\mathbf{k}} - i\delta)t} \right] \\ &= \frac{1}{2\omega_{\mathbf{k}}} \left[\frac{-1}{i(\omega - \omega_{\mathbf{k}} + i\delta)} + \frac{1}{i(\omega + \omega_{\mathbf{k}} - i\delta)} \right] \\ &= \frac{-i}{2\omega_{\mathbf{k}}} \left[\frac{-1}{(\omega - \omega_{\mathbf{k}} + i\delta)} + \frac{1}{(\omega + \omega_{\mathbf{k}} - i\delta)} \right] \end{aligned} \tag{4.60}$$

and finally

$$D_{\mathbf{k}\mathbf{k}'}(\omega) = \frac{-i\delta_{\mathbf{k}\mathbf{k}'}}{-\omega^2 + \omega_{\mathbf{k}}^2 - i\delta}. \tag{4.61}$$

For phonons and other non-relativistic bosons commonly one defines, (understanding the vacuum average)

$$\tilde{D}_{\mathbf{k}}(t) = -i \left\langle P \left[\hat{\phi}_{\mathbf{k}}(t) \hat{\phi}_{\mathbf{k}}(0) \right] \right\rangle \tag{4.62}$$

in terms of

$$\hat{\phi}_{\mathbf{k}}(t) = a_{\mathbf{k}} \exp[-i\varepsilon_{\mathbf{k}}t] + a_{\mathbf{k}}^{\dagger} \exp[i\varepsilon_{\mathbf{k}}t] \tag{4.63}$$

without the normalization factor $\frac{1}{\sqrt{2\varepsilon_{\mathbf{k}}}}$ in (4.51); then

$$iD_{\mathbf{k}}(t) = \exp[-i\omega_{\mathbf{k}}|t|]. \tag{4.64}$$

Relativistic Bosons, Photons

The Klein-Gordon equation

$$\left(\frac{\partial^2}{c^2 \partial t^2} - \nabla^2 + \left(\frac{mc}{\hbar}\right)^2\right) \psi = 0 \tag{4.65}$$

describes a spinless relativistic particle. Introducing the relativistic dispersion

$$\varepsilon_{\mathbf{k}} = \sqrt{(c\hbar\mathbf{k})^2 + m^2c^4} \tag{4.66}$$

one obtains the propagator

$$D_{\mathbf{k}}(\omega) = \frac{-i}{-\omega^2 + (c\hbar\mathbf{k})^2 + m^2c^4 - i\delta}. \tag{4.67}$$

In a 4-dimensional notation with

$$p = \hbar(\mathbf{k}, i\frac{\omega}{c}) \tag{4.68}$$

$$D(p) = \frac{-i}{(cp)^2 + m^2c^4 - i\delta}. \tag{4.69}$$

For a massless scalar particle (if it existed) one would write

$$D(\mathbf{k}, \omega) = D(p) = \frac{-i}{p^2 - i\delta}. \tag{4.70}$$

For a photon, the propagator between two points x, x' in a 4-dimensional notation is naturally given by

$$D_{\mu,\nu}(x, x') = \langle P[A_{\mu}(x)A_{\nu}(x')] \rangle, \tag{4.71}$$

where $A_{\mu} = (\mathbf{A}, i\phi)$ are the four-vector potential components; however a gauge transformation $A_{\mu}(x) \rightarrow A_{\mu} + \frac{\partial\chi(x)}{\partial x_{\mu}}$ with arbitrary $\chi(x)$ will change the potential and the propagator. In the Lorentz gauge such that

$$\partial_{\mu}A_{\mu} = \nabla \cdot \mathbf{A} + \frac{1}{c} \frac{\partial\phi}{\partial t} = 0, \tag{4.72}$$

the wave equation is

$$\partial_{\mu}\partial_{\mu}A_{\nu} = -\frac{4\pi}{c}J_{\nu}. \tag{4.73}$$

thus for the free field the wave equation is

$$\left(\nabla^2 - \frac{1}{c^2} \frac{\partial^2}{\partial t^2}\right) A_{\mu} = 0. \tag{4.74}$$

which suggests writing

$$D_{\mu,\nu}(x, x') = -i\delta_{\mu,\nu} \int \frac{d^4 p}{(2\pi)^4} \frac{e^{ip(x-x')}}{p^2 - i0}; \quad (4.75)$$

this is evidently a Green's function of the wave equation. Actually the Green's function is not unique and the gauge invariance allows to add to the r.h.s. of (4.75) $\frac{\partial^2}{\partial x_\mu \partial x_\nu} f(x-x')$, where f is an arbitrary function. The gauge in which (4.75) holds as it stands is called the Feynman gauge.

4.3.1 Green's Functions for Tight-binding Hamiltonians

The tight-binding model Hamiltonian

$$H = t_h \sum_{\langle i,j \rangle} c_i^\dagger c_j, \quad t_h > 0 \quad (4.76)$$

is defined in terms of a d -dimensional graph or lattice; i and j stand for two sets of d coordinates for two sites or nodes of the lattice and the notation $\sum_{\langle i,j \rangle}$ means that the sum is over all i and overall j that are nearest neighbors of i . Here I consider regular linear, square and cubic lattices. Using continuum normalization, and setting the lattice parameter to 1, the Bloch energy eigenfunctions are

$$|k\rangle = \frac{1}{\sqrt{2\pi}} \sum_i e^{i\mathbf{k}\cdot\mathbf{i}} |i\rangle. \quad (4.77)$$

In d dimensions, the energy eigenvalues are:

$$\epsilon_{\mathbf{k}} = 2t_h \sum_{\alpha}^d \cos k_{\alpha}. \quad (4.78)$$

The local density of states at the site at the origin is

$$\rho_d(\omega) = \sum_k |\langle 0 | k \rangle|^2 \delta(\omega - \epsilon_k) = \frac{1}{(2\pi)^d} \int_{BZ} d^d k \delta\left(\omega - 2t_h \sum_{\alpha}^d \cos(k_{\alpha})\right). \quad (4.79)$$

where the integral extends to the Brillouin Zone. Converting the $\delta(\omega - \epsilon_k)$ -function into a sum of momentum δ functions, a factor $|\nabla_{\mathbf{k}} \epsilon_k|$ appears in the denominator. To better understand the physical meaning, differentiate

$$\left[\frac{(\vec{p} + \vec{k})^2}{2m} + V(\vec{x}) \right] u_{\vec{k}}(\vec{x}) = \epsilon_k u_{\vec{k}}(\vec{x}). \quad (\text{Equation 8.23:})$$

$$\begin{aligned} u_{\vec{k}}(\vec{x})(\nabla_{\mathbf{k}}) \left[\frac{(\vec{p} + \vec{k})^2}{2m} \right] + \left[\frac{(\vec{p} + \vec{k})^2}{2m} + V(\vec{x}) \right] (\nabla_{\mathbf{k}}) u_{\vec{k}}(\vec{x}) \\ = (\nabla_{\mathbf{k}}) \epsilon_k u_{\vec{k}}(\vec{x}) + \epsilon_k \nabla_{\mathbf{k}} u_{\vec{k}}(\vec{x}). \end{aligned} \quad (4.80)$$

Multiplying by $\langle u_{\vec{k}} |$ and recalling (8.22) one obtains

$$\langle \psi_{\vec{k},\lambda}(\vec{x}) | \frac{\mathbf{p}}{m} | \psi_{\vec{k},\lambda}(\vec{x}) \rangle = \frac{1}{\hbar} \nabla_{\mathbf{k}} \epsilon_{\mathbf{k}}. \quad (4.81)$$

1 Dimension

The band edges $\epsilon = \pm 2t_h$ are the extrema of $\epsilon_k = 2t_h \cos k$ at $k = \pm\pi$ and $k = 0$ and $\rho = 0$ if $|\omega| > 2t_h$. The argument of the δ in (4.79) vanishes for $k = k_\omega = \arccos(\frac{\omega}{2t_h})$;

$$\rho_1(\omega) = \frac{1}{\pi} \int_0^\pi dk \frac{\delta(k - k_\omega)}{2t_h \sin(k)} = \frac{1}{2\pi t_h \sin k_\omega}. \quad (4.82)$$

This can be rewritten

$$\rho_1(\omega) = \frac{\theta(4t_h^2 - \omega^2)}{\pi \sqrt{4t_h^2 - \omega^2}}, \quad (4.83)$$

which in fact when integrated over all ω yields 1. The band-edge divergence

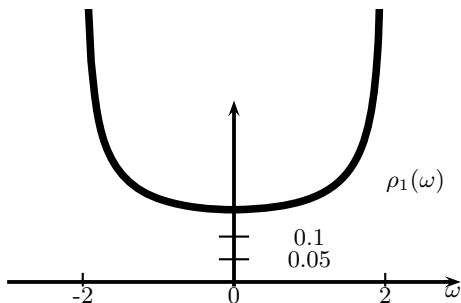


Fig. 4.1. Density of states on the 1d tight-binding lattice. Note the Van Hove singularities at the band edges .

is characteristic: it reflects the fact that at the band edges the group velocity $v_g = \frac{\partial \epsilon}{\partial k}$ vanishes; this, combined with the one-dimensionality, leads to the inverse-square-root singularity. The symmetry around the band centre is typical of **bipartite graphs**. These are lattices with the property that all sites can be painted red or blue in such a way that any red (blue) site has only blue (red) first neighbors; in the linear chain these are odd and even-numbered sites. Changing the sign to all the blue orbitals is just a gauge transformation and cannot change any physical quantity, yet it is equivalent to sending the off-diagonal one-electron matrix element t_h to $-t_h$. However, ϵ_k is proportional to t_h and must change sign as well. This can happen in

just one way: the spectrum is symmetric and the eigenfunctions at ϵ_k and $-\epsilon_k$ get exchanged by the gauge transformation.

The off-diagonal elements $g_{m,n}$ of the resolvent may be found by taking matrix elements of the identity $\omega \frac{1}{\omega-H} = 1 + \frac{1}{\omega-H}H$ between site 0 and $n \neq 0$. One finds

$$\frac{\omega}{t_h}g_{0,n} = g_{0,n+1} + g_{0,n-1} \tag{4.84}$$

which suggests the solution

$$g_{0,n} = g_{0,0}q^{|n|} \tag{4.85}$$

with

$$q^2 - \frac{\omega}{t_h}q + 1 = 0. \tag{4.86}$$

Some care is needed to choose between the roots

$$q_{\pm} = \frac{\omega}{2t_h} \pm \sqrt{\left(\frac{\omega}{2t_h}\right)^2 - 1} \tag{4.87}$$

where $\sqrt{\left(\frac{\omega}{2t_h}\right)^2 - 1}$ is imaginary for ω in the spectrum between $-2t_h$ and $2t_h$. One has to consider the analytic continuation from real ω to complex z , with a branch cut on the real axis; taking $\sqrt{z} = \sqrt{|z|} \exp\left[\frac{i}{2} \arg(z)\right]$ with the cut along the negative $Re(z)$ axis,

$$\sqrt{\left(\frac{z}{2t_h}\right)^2 - 1} = \begin{cases} i\sqrt{\left|\left(\frac{\omega}{2t_h}\right)^2 - 1\right|} & \text{above the axis} \\ -i\sqrt{\left|\left(\frac{\omega}{2t_h}\right)^2 - 1\right|} & \text{below} \end{cases}$$

In the continuum $|q_{\pm}| = 1$, but q_{\pm} is discontinuous across the cut. With $\omega > 2t_h$, we must prefer q_- which is < 1 and implies an exponential attenuation of the amplitude g with distance whereas $q_+ > 1$ would imply that the amplitude grows exponentially.

$\sqrt{\left(\frac{\omega}{2t_h}\right)^2 - 1} > 0, \omega > 2t_h$ becomes negative for $\omega < -2t_h$ and so $|q_-| \leq 1$ everywhere. Therefore, everywhere,

$$g_{0,n}(\omega) = g_{0,0}(\omega)q_-(\omega)^{|n|}. \tag{4.88}$$

2 Dimensions

Using Equations (4.79,4.82), one finds

$$\rho_2(\omega) = \frac{1}{(2\pi)^2} \int_{-\pi}^{\pi} dk_x \int_{-\pi}^{\pi} dk_y \delta(\omega - 2t_h [\cos(k_x) + \cos(k_y)]) \tag{4.89}$$

that is

$$\rho_2(\omega) = \frac{1}{2\pi} \int_{-\pi}^{\pi} dk \rho_1(\omega - 2t_h \cos(k)). \tag{4.90}$$

This integral can be written in terms of the complete elliptic integral [44] of the first kind. The band now extends from $-4t_h$ to $4t_h$, and is symmetric (the graph is bipartite). Singularities become milder when integrated over, however they are still evident (see Figure ??). The worst is the logarithmic *Van Hove* singularity (at $\omega = 0$ the integrand of (4.90) goes like $\frac{1}{|k|}$ for $k \rightarrow 0$. In other terms, this is just the singularity of ρ_1 in integrated form, and is a universal feature of $d=2$ lattices.) In addition, ρ_2 jumps discontinuously to

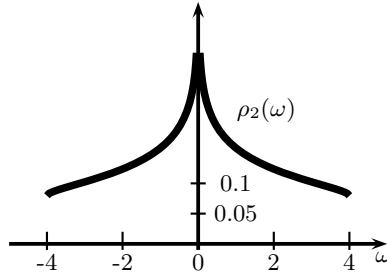


Fig. 4.2. Density of states on the 2d tight-binding square lattice. Note the Van Hove singularities: jumps at the band edges and a diverging cusp at the centre.

0 at the band edges, which represents a milder singularity (in general, this term involves a point where the function is not analytic, not necessarily a divergence). This can again be read off (4.90): $\rho_2 = 0$, for $\omega > 4$, but setting $\omega = (4 - \epsilon)t_h$ the band-edge singularity of ρ_1 enters again since there is an interval near $k = 0$ where $\cos k > 1 - \epsilon/2$; this interval is of order $\sqrt{\epsilon}$ and the integrand there is of order $\frac{1}{\sqrt{\epsilon}}$, so the result is nonzero up to the edge.

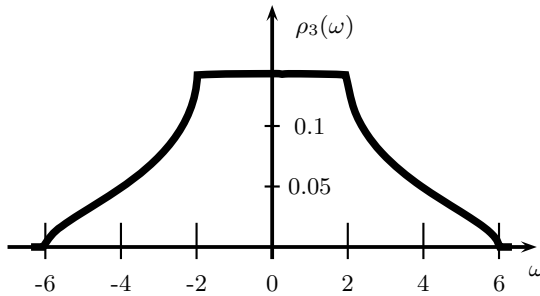


Fig. 4.3. Density of states on the tight-binding cubic lattice.

3 Dimensions

The simple cubic lattice is bipartite, hence the density of states is again symmetric around $\omega = 0$. We can find it by calculating

$$\rho_3(\omega) = \frac{1}{2\pi} \int_{-\pi}^{\pi} dk \rho_2(\omega - 2t_h \cos(k)). \quad (4.91)$$

From this integral representation and from the behavior of ρ_2 it is easy to show the nature of the singularities. The band-edge singularities at $\pm 6t_h$ are of the square-root type, as for free particles. In addition, there are two points where $\frac{d\rho_3}{d\omega}$ is discontinuous. More details may be found in the book by Economou[44].

4.3.2 Lippmann-Schwinger Equation

When the Hamiltonian can be decomposed in a free term and a perturbation, $H = H_0 + H_1$, the perturbed resolvent operator function can be written in terms of the unperturbed one via the often useful identity

$$\frac{1}{z - H} = \frac{1}{z - H_0} + \frac{1}{z - H_0} H_1 \frac{1}{z - H}. \quad (4.92)$$

In one-body problems this translates directly into Green's functions. The usual way of treating impurity problems is via the Lippmann-Schwinger equation,

$$G(\vec{r}, \vec{r}') = G_0(\vec{r}, \vec{r}') - \int d^3\vec{r}'' G_0(\vec{r}, \vec{r}'') \delta V(\vec{r}'') G(\vec{r}'', \vec{r}') \quad (4.93)$$

where δV is the perturbing potential, which is nothing but (4.92) and a special case of the Dyson equation (see Section 11.4 below).

4.3.3 t matrix

Another form of (4.92)

$$\frac{1}{z - H} = \frac{1}{z - H_0} + \frac{1}{z - H} H_1 \frac{1}{z - H_0} \quad (4.94)$$

is also useful; substituting in the r.h.s. of (4.92) one obtains

$$\frac{1}{z - H} = \frac{1}{z - H_0} + \frac{1}{z - H_0} t \frac{1}{z - H_0}, \quad (4.95)$$

where the t matrix obeys

$$t = H_1 + H_1 \frac{1}{z - H_0} t. \quad (4.96)$$

This accounts at once for all the repeated scattering from H_1 .

4.3.4 Inglesfield Embedding Method

The Lippmann-Schwinger equation is less convenient when the perturbation is extended. Typical examples are surface problems, when one wants to treat the effects of surface creation, reconstruction, or contamination. In such cases one can resort to slab models, but there are drawbacks in any attempt to represent a bulk by a few atomic layers, with quantized normal momenta. The only practical alternative is the method of *embedding*. By this term one understands that 1) in an extended system, there is a more or less localized perturbing potential. A surface S (see Figure 4.4 left) divides the perturbed region I from the far region II where the potential is negligible. Over S the potential is also negligible 2) solving the problem in I is easier than in the full system; the region I might be finite, or, in the case of surfaces, it is the finite thickness that helps 3) the extended unperturbed system could be treated easily because it is highly symmetric 4) then one wants to solve the problem in I in such the way that the wave functions match those of the extended system on S .

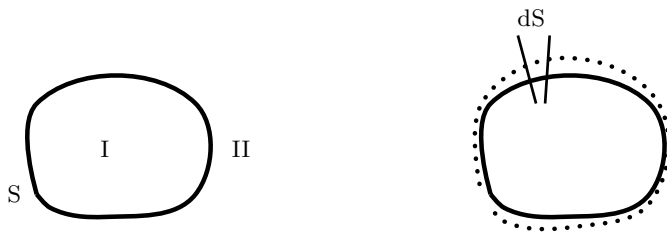


Fig. 4.4. Left: Embedding of region I into II; Right: a pill-box element δV between S and its slightly inflated, dotted version.

Following J.E. Inglesfield [114] we let the wave function

$$\Phi(\vec{r}) = \begin{cases} \phi(\vec{r}) & \vec{r} \in I \\ \psi(\vec{r}) & \vec{r} \in II \\ \psi(\vec{r}) = \phi(\vec{r}) & \vec{r} \in S; \end{cases} \quad (4.97)$$

Φ must make the functional

$$E = \frac{\langle \Phi | H | \Phi \rangle}{\langle \Phi | \Phi \rangle} \quad (4.98)$$

stationary, with

$$H = -\frac{1}{2}\nabla^2 + V(\mathbf{r}). \quad (4.99)$$

We write ψ in II as a functional of ϕ and reformulate the problem such that the latter is the only unknown. Thus, the solution in I yields the solution everywhere. Let us see how this is done in practice.

$$\langle \Phi | H | \Phi \rangle = \int_I d^3 r \phi^*(\vec{r}) H \phi(\vec{r}) + \epsilon \int_{II} d^3 r \psi^*(\vec{r}) \psi(\vec{r}) + \int_S \eta dS \quad (4.100)$$

The surface element dS contributes

$$\eta dS = \int_{\delta V} \delta V \Phi^* H \Phi = -\frac{1}{2} \int_{\delta V} \Phi^* \nabla^2 \Phi \delta V$$

where the integral is over a pill-box of volume δV around dS (Fig. 4.4 right) and we kept only the kinetic contribution since the potential one goes to 0 as $\delta\epsilon \rightarrow 0$; since

$$\int_{\delta V} \Phi^* \nabla^2 \Phi = \phi^* \int_{\delta V} \nabla^2 \Phi = \phi^* (\nabla \psi \cdot \vec{n}_{outer} dS + \nabla \phi \cdot \vec{n}_{inner} dS),$$

we are left with

$$\int_S \eta dS = \frac{1}{2} \int_S \phi^*(\vec{r}) \left(\vec{\nabla}(\phi - \psi) \right) \cdot \vec{n} dS. \quad (4.101)$$

We wish to write everything in terms of ϕ , so we must eliminate $\vec{\nabla} \psi$ from (4.101) and ψ from the normalization condition. The latter is

$$\langle \Phi | \Phi \rangle = \int_I d^3 \vec{r} \phi^*(\vec{r}) \phi(\vec{r}) + \int_{II} d^3 \vec{r} \psi^*(\vec{r}) \psi(\vec{r}). \quad (4.102)$$

To rewrite the normalization integral over II in terms of ϕ only, we vary ϵ , multiply the varied Schrödinger equation $H\delta\psi = \delta\epsilon\psi + \epsilon\delta\psi$ by ψ^* and the complex conjugate Schrödinger equation by $\delta\psi$:

$$\begin{cases} \psi^* H \delta\psi = \delta\epsilon \psi^* \psi + \epsilon \psi^* \delta\psi \\ \delta\psi H \psi^* = \epsilon \psi^* \delta\psi. \end{cases}$$

Dividing by $\delta\epsilon$ and subtracting, one gets:

$$\psi^* \left(-\frac{1}{2} \nabla^2 \right) \frac{\partial \psi}{\partial \epsilon} - \frac{\partial \psi}{\partial \epsilon} \left(-\frac{1}{2} \nabla^2 \right) \psi^* = |\psi|^2.$$

Next, integrating over II and using Green's theorem one finds

$$\int_{II} |\psi|^2 d^3 r = -\frac{1}{2} \int_S \left(\frac{\partial \psi}{\partial \epsilon} \nabla \psi^* - \psi^* \frac{\partial}{\partial \epsilon} \nabla \psi \right) \cdot \vec{n} dS \quad (4.103)$$

Here a - sign comes from the outgoing normal from I which is the opposite of the outgoing normal from II. To simplify matters, we vary ϵ in such a way that $\psi \equiv \phi$ over S; then $\frac{\partial \psi}{\partial \epsilon} \equiv 0$ in S and we dispose the first term on the r.h.s. The presence in (4.101, 4.103) of $\vec{\nabla} \psi \cdot \vec{n}$ is the only difficulty left, that now we proceed to remove. This requires a clever trick: in order to get the gradient on the surface in terms of ψ , we first find ψ in II and on the surface in terms of the gradient, and then invert the relation.

Since the perturbation is localized in I, we know already from Equations (4.5,4.1) how to solve $H\psi = \epsilon\psi$ for ψ in II and for an eigenvalue ϵ if ψ is assigned on S. This can be achieved using Green's functions, and Inglesfield uses the one satisfying

$$(\omega - (-\frac{1}{2}\nabla_{\vec{r}}^2 + V(\vec{r})))g(\vec{r}', \vec{r}, \epsilon) = -\delta(\vec{r} - \vec{r}') \quad (4.104)$$

which is the negative of the retarded Green's function satisfying (4.44). Therefore, he finds for $\vec{r} \in II$

$$\begin{aligned} \psi(\vec{r}) = & -\frac{1}{2} \int_S [g(\vec{r}, \vec{r}') \vec{\nabla}_{\vec{r}'} \psi(\vec{r}') \\ & - \psi(\vec{r}') \vec{\nabla}_{\vec{r}'} g(\vec{r}, \vec{r}')] \cdot \vec{n} d^2 \vec{r}' \end{aligned} \quad (4.105)$$

and ψ in II is a functional of the boundary values of ψ and $\vec{\nabla}\psi$. Now we are in position to write down $\vec{\nabla}\psi \cdot \vec{n}$ as another functional of the surface values of ϕ . In (4.105) we choose g having zero derivative on S , which eliminates the second term, obtaining

$$\psi(\vec{r}) = -\frac{1}{2} \int_S g(\vec{r}, \vec{r}') \vec{\nabla} \psi(\vec{r}') \cdot \vec{n} dS \quad (4.106)$$

then put \vec{r} on S and invert the relation to read

$$\vec{\nabla} \psi(\vec{r}') \cdot \vec{n} = -2 \int_S dS g^{-1}(\vec{r}, \vec{r}') \phi(\vec{r}'), \quad \vec{r}, \vec{r}' \in S \quad (4.107)$$

with g^{-1} a matrix inverse.

At this point ϕ is the only unknown; the numerator and the denominator of the energy functional are written as functionals of ϕ and the problem can be solved in region I. From the variational conditions Inglesfield obtained an effective Schrödinger equation for ϕ . One finds (Problem 4.5) that the particle sees the effective potential

$$V_{eff}(\mathbf{r}) = V(\mathbf{r}) + U(\mathbf{r})\delta(\zeta); \quad (4.108)$$

besides the potential $V(\mathbf{r})$ this comprises an embedding surface potential $U(\mathbf{r})\delta(\zeta)$ where ζ is a curvilinear coordinate such that $\zeta = 0$ on S .

The method was intended first for independent-electron problems but lends itself to iterative self-consistent approaches like density functional theory. The extension of the method to the Dirac equation has been worked out recently by Crampin [115].

4.4 Kubo Formulae

Particle-hole Green's functions also arise through the Kubo formulae[29] of linear response theory. An interacting system with Hamiltonian H_S is probed with a weak time-dependent perturbation

$$H'(t) = -\hat{A}F(t), \quad (4.109)$$

where $F(t)$ is an adiabatically switched time dependence. The total hamiltonian is

$$H = H_S + H'(t). \quad (4.110)$$

We seek the linear response $\Delta B(t) = Tr\rho(t)\hat{B}$ of an observable \hat{B} ; by definition, \hat{B} is a difference from equilibrium and vanishes for $\hat{A} = 0$ (that is, $Tr\rho_{eq}\hat{B} = 0$). Similar to the familiar relation $\mathbf{P} = \chi\mathbf{E}$ of electric field to polarization, the linear response equation is

$$\Delta B(t) = \int_{-\infty}^t dt' \phi_{BA}(t-t')F(t'); \quad (4.111)$$

the role of the polarizability χ is played by the *response function* $\phi_{BA}(t)$. We need the density matrix $\rho(t)$, which deviates a little bit from the equilibrium one ρ_{eq} . The perturbed $\rho(t)$ obeys the Heisenberg equation of motion

$$i\hbar \frac{d}{dt}\rho(t) = [H(t), \rho(t)]_-. \quad (4.112)$$

Setting $\rho(t) \sim \rho_{eq} + \Delta\rho(t)$, one finds a linearized equation

$$i\hbar \frac{d}{dt}\Delta\rho(t) = [H_S, \Delta\rho(t)] + F(t)[- \hat{A}, \rho_{eq}]. \quad (4.113)$$

The solution is

$$-i\hbar\Delta\rho(t) = \int_{-\infty}^t e^{\frac{-i}{\hbar}H_S(t-t')} [\hat{A}, \rho_{eq}] e^{\frac{i}{\hbar}H_S(t-t')} F(t') dt' \quad (4.114)$$

as one can readily check by calculating the derivative. Hence

$$\Delta B(t) = \frac{-1}{i\hbar} Tr \int_{-\infty}^t e^{\frac{-i}{\hbar}H_S(t-t')} [\hat{A}, \rho_{eq}] e^{\frac{i}{\hbar}H_S(t-t')} \hat{B} F(t') dt'. \quad (4.115)$$

Now we move the left exponential to the right (by the cyclic property of the trace) thereby obtaining $\hat{B}(t-t')$ in the Heisenberg picture (with H_S):

$$\Delta B(t) = \frac{-1}{i\hbar} Tr \int_{-\infty}^t [\hat{A}, \rho_{eq}] \hat{B}(t-t') F(t') dt' \quad (4.116)$$

Now for the linear response function $\phi_{BA}(t)$ of (4.111) we obtain

$$-i\hbar\phi_{BA}(t) = Tr\{\rho_{eq}\hat{B}(t) - \rho_{eq}\hat{A}\hat{B}(t)\}; \quad (4.117)$$

using again the cyclic property, we can change this into a more elegant equilibrium thermal average, namely the Kubo formula[29]

$$-i\hbar\phi_{BA}(t) = \text{Tr}\{\rho_{eq}\hat{B}(t)\hat{A} - \rho_{eq}\hat{A}\hat{B}(t)\} = \langle[\hat{B}(t), \hat{A}(0)]\rangle. \quad (4.118)$$

By the identity (Problem 4.1)

$$[\hat{A}, e^{-\beta H}]_- = e^{-\beta H} \int_0^\beta \frac{d\hat{A}(-i\hbar\tau)}{dt} d\tau, \quad (4.119)$$

and Equation (4.114),

$$-i\hbar\phi_{BA}(t) = \text{Tr}\{[\hat{A}(0), e^{-\beta H_S}]_- \hat{B}(t)\},$$

one finds the further Kubo formula

$$\phi_{BA}(t) = \int_0^\beta \left\langle \frac{d\hat{A}(-i\hbar\tau)}{dt} \hat{B}(t) \right\rangle d\tau. \quad (4.120)$$

This formalism has many applications; for example, if the system is exposed to an electric field, \hat{A} is proportional to the position vector components of the electron and the time derivative is proportional to the current, \hat{B} is the current and ϕ the conductivity tensor. For the frequency-dependent conductivity, starting from $\hat{A}(-i\tau) = e^{H\tau}\hat{A}e^{-H\tau}$ and using the cyclic property again, and the fact that it is retarded, one can easily show that, up to a factor,

$$\sigma_{i,j}(\omega, T) = \int_0^\infty dt \int_0^\beta d\tau \langle j_i(0)j_j(t+i\hbar\tau) \rangle e^{i\omega t}. \quad (4.121)$$

4.5 Vacuum Amplitudes

In stationary problems one often uses a zero-body propagator or vacuum amplitude

$$R(t) = \langle U_I(t) \rangle_0, \quad (4.122)$$

where the thermal average of the interacting picture evolution operator $U_I(t) = e^{iH_0 t} e^{-iHt}$ is taken with the *non-interacting* distribution function $\frac{1}{Z_0} \text{Tr} e^{-\beta H_0}$. At zero temperature this becomes

$$R(t) = \langle \Phi | U_I(t) | \Phi \rangle = e^{iW_0 t} \langle \Phi | e^{-iHt} | \Phi \rangle, \quad (4.123)$$

where W_0 is the ground state energy of H_0 . Note that *unlike all the other Green's functions*, here the average is taken on the non-interacting ground state. R is related to the interacting ground state energy E_0 through the following device. Inserting a complete set of H eigenstates,

$$R(t) = \sum_n |\langle \Phi | \psi_n \rangle|^2 e^{-i(E_n - W_0)t}, \quad (4.124)$$

we can isolate the ground state energy from (4.124) by giving the time t an imaginary part: $t \rightarrow t - i\eta$, $\eta > 0$. In this way, the exponent has a real part

$$t \eta (W_0 - E_n)$$

which is largest for $n = 0$. In the long run, the ground state dominates:

$$R(t) = |\langle \Phi | \psi_0 \rangle|^2 e^{-i(E_0 - W_0)t}, \quad t \rightarrow \infty (1 + i\eta).$$

There is a restriction: we need

$$\langle \Phi | \psi_0 \rangle \neq 0;$$

therefore V should not change the ground state symmetry. Special care is needed when Φ is degenerate. When the overlap does not vanish,

$$\dot{R}(t) = -i(E_0 - W_0) |\langle \Phi | \psi_0 \rangle|^2 e^{-i(E_0 - W_0)t},$$

and we get the closed formula

$$E_0 = W_0 + i \lim_{t \rightarrow \infty (1 - i\eta)} \frac{d}{dt} \log(R(t)). \quad (4.125)$$

Since U_I admits the T exp expansion (2.37), the methods of Chapter 11 will provide a practical way to compute R .

4.6 Lehmann Representation

In non-interacting models the poles of the Green's functions close to the real axis correspond to eigenstates of the Hamiltonian where a particle can exist or where one can put a particle. Here we see how to generalize this notion to the interacting case. In this section we let $\hbar = 1$.

4.6.1 Zero-Temperature Fermi Case

Denote the complete set of many-body eigenstates of H by $|M, n\rangle$, where the integer $M = 0, 1, 2, \infty$ runs over the electron numbers and $n = 0, 1, 2, \infty$ runs over the M -body eigenstates, such that

$$H|M, n\rangle = E_{M,n}|M, n\rangle, \quad \hat{N}|M, n\rangle = M|M, n\rangle.$$

Let us write the time-ordered Green's function as

$$G(N; \mathbf{x}t, \mathbf{x}'t') = -i \langle N, 0 | T[\psi(\mathbf{x}, t) \psi^\dagger(\mathbf{x}'t')] | N, 0 \rangle, \quad (4.126)$$

emphasizing that it is the average over the N -body interacting ground state of the Hamiltonian H and that the operators are in the Heisenberg picture. For time-independent H , setting $\hbar = 1$, $\psi(\mathbf{x}, t) = e^{iHt} \psi(\mathbf{x}) e^{-iHt}$, and

$G(\mathbf{x}t, \mathbf{x}'t') \equiv G(\mathbf{x}, \mathbf{x}', t - t')$; inserting the complete set we obtain the very useful Lehmann representation: for $t > t'$,

$$iG(\mathbf{x}, \mathbf{x}', t - t') = \sum_n e^{-i(E_{N+1,n} - E_{N,0})(t-t')} \\ \times \langle N, 0 | \psi(\mathbf{x}) | N + 1, n \rangle \langle N + 1, n | \psi^\dagger(\mathbf{x}') | N, 0 \rangle, \quad (4.127)$$

and the eigenstates with one more particle come into play; for $t < t'$,

$$iG(\mathbf{x}, \mathbf{x}', t - t') = - \sum_n e^{i(E_{N-1,n} - E_{N,0})(t-t')} \\ \times \langle N, 0 | \psi^\dagger(\mathbf{x}) | N - 1, n \rangle \langle N - 1, n | \psi(\mathbf{x}') | N, 0 \rangle, \quad (4.128)$$

the $N-1$ -particle states appear. By the standard integrals (4.40) we obtain

$$G(\mathbf{x}, \mathbf{x}', \omega) = \sum_n \frac{\langle N, 0 | \psi(\mathbf{x}) | N + 1, n \rangle \langle N + 1, n | \psi^\dagger(\mathbf{x}') | N, 0 \rangle}{\omega - (E_{N+1,n} - E_{N,0}) + i\delta} \\ + \sum_n \frac{\langle N, 0 | \psi^\dagger(\mathbf{x}) | N - 1, n \rangle \langle N - 1, n | \psi(\mathbf{x}') | N, 0 \rangle}{\omega - (E_{N,0} - E_{N-1,n}) - i\delta}. \quad (4.129)$$

The poles of G provide information on the excitation spectrum, namely, on the ionization potentials and electron affinities, or in other terms, on quasi-electron and quasi-hole excitations. Now we simplify the notation dropping N and $N \pm 1$. The structure of (4.129) invites us to write

$$G(x, x', \omega) = \int \frac{\rho(x, x', \omega')}{\omega - \omega' + i\delta_{\omega'}} d\omega' \quad (4.130)$$

where δ_w is an infinitesimal quantity, with

$$\rho(\mathbf{x}, \mathbf{x}', \omega) = \sum_n \langle 0 | \psi(\mathbf{x}) | n \rangle \langle n | \psi^\dagger(\mathbf{x}') | 0 \rangle \delta(\omega - (E_{N+1,n} - E_{N,0})) \\ + \sum_n \langle 0 | \psi^\dagger(\mathbf{x}) | n \rangle \langle n | \psi(\mathbf{x}') | 0 \rangle \delta(\omega - (E_{N-1,n} - E_{N,0})). \quad (4.131)$$

The positive spectral function $\rho(\mathbf{x}, \mathbf{x}, \omega)$ generalizes the density of states (5.16): In normal systems the ionization potentials cannot be smaller than the electron affinities and infinitesimal $\delta_w = \delta \operatorname{sgn}(\omega' - \mu)$ where $\mu = \operatorname{Min}_{n,n'} [E(N + 1, n) - E(N, n')]$ is the chemical potential. So,

$$\rho(\omega) = -\frac{1}{\pi} \operatorname{Im} G(\omega) \operatorname{sign}(\omega - \mu). \quad (4.132)$$

The real and imaginary parts of Green's functions are Hilbert transform pairs.

4.6.2 Finite Temperatures, Fermi and Bose

Let us extend the above to finite T , writings $= -1$ for bosons, $s = 1$ for fermions. For the retarded Green's function,

$$g^{(r)}(x, x', t - t') = -iTr\{\rho[\psi(x, t), \psi^\dagger(x', t')]\mathfrak{s}\}, \tag{4.133}$$

one finds, with $K = H - \mu N$ and $\hbar\omega_{nm} = E_n - E_m$,

$$g^{(r)}(x, x', t - t') = \frac{-i}{Z} \sum_{mn} (e^{-\beta K_n} \langle n|\psi(x)|m\rangle \langle m|\psi^\dagger(x')|n\rangle e^{i\omega_{mn}(t-t')} + s e^{-\beta K_n} \langle n|\psi^\dagger(x')|m\rangle \langle m|\psi(x)|n\rangle e^{i\omega_{nm}(t'-t)}) \theta(t - t'). \tag{4.134}$$

Now, let

$$R_{mn}(\mathbf{x}, \mathbf{x}') = \langle n|\psi(\mathbf{x})|m\rangle \langle m|\psi^\dagger(\mathbf{x}')|n\rangle; \tag{4.135}$$

exchanging m with n in the last line and Fourier transforming one readily arrives at

$$g^{(r)}(x, x', \omega) = \frac{1}{Z} \sum_{mn} \frac{R_{mn}(\mathbf{x}, \mathbf{x}')}{\omega + \omega_{mn} + i\delta} (e^{-\beta K_n} + s e^{-\beta K_m}); \tag{4.136}$$

with δ a positive infinitesimal; in the same way the advanced function is

$$g^{(a)}(x, x', \omega) = \frac{1}{Z} \sum_{mn} \frac{R_{mn}(\mathbf{x}, \mathbf{x}')}{\omega + \omega_{mn} - i\delta} (e^{-\beta K_n} + s e^{-\beta K_m}). \tag{4.137}$$

The same manipulations on the time-ordered Green's function yield

$$G(\mathbf{x}, \mathbf{x}', \omega) = \frac{1}{Z} \sum_{mn} R_{mn}(\mathbf{x}, \mathbf{x}') \left(\frac{e^{-\beta K_n}}{\omega + \omega_{mn} + i\delta} - \frac{s e^{-\beta K_m}}{\omega + \omega_{mn} - i\delta} \right). \tag{4.138}$$

Equations (4.130,4.131) can be extended to finite T , introducing the T -dependent spectral function

$$\rho(\mathbf{x}, \mathbf{x}', \omega) = \frac{2\pi}{Z} \sum_{m,n} e^{-\beta K_n} R_{mn}(\mathbf{x}, \mathbf{x}') \delta(\omega + \omega_{mn}) (1 + s e^{\beta\omega}) \tag{4.139}$$

that allows to write down the retarded and advanced functions

$$g^{(r)}(x, x', \omega) = \int \frac{d\omega'}{2\pi} \frac{\rho(x, x', \omega')}{\omega - \omega' + i\delta}, \tag{4.140}$$

$$g^{(a)}(x, x', \omega) = \int \frac{d\omega'}{2\pi} \frac{\rho(x, x', \omega')}{\omega - \omega' - i\delta}; \tag{4.141}$$

the time-ordered one (4.138) may be written

$$G(x, x', \omega) = \int \frac{d\omega'}{2\pi} \left[\frac{n_{\mathbf{S}}(\omega')\rho(x, x', \omega')}{(\omega - \omega' + i\delta)} - s \frac{\rho(x, x', \omega')\bar{n}_{\mathbf{S}}(\omega')}{(\omega - \omega' - i\delta)} \right] \tag{4.142}$$

with $\bar{n}(\omega) = 1 - n_{\mathbf{S}}(\omega)$ and $n_{\mathbf{S}}(\omega) = (1 + se^{\beta\omega})^{-1}$. The knowledge of ρ (also a function of T) determines all the one-body Green's functions. For independent electrons, $g^{(r)}$ and (4.139) are purely one-body properties independent of the Fermi level; therefore the temperature dependence of (4.139) is neglected usually in Density Functional and other self-consistent calculations. This simplification may be wrong when dealing with strongly correlated systems.

4.6.3 Fluctuation-Dissipation Theorem

The above results imply a number of relationships involving ρ and the real and imaginary parts of the various Green's functions. One shows (Problem 4.2) the following. Assuming that $R_{mn}(\mathbf{x}, \mathbf{x}')$ is real (it must be positive for $\mathbf{x} = \mathbf{x}'$ and it can be taken real anyhow in the absence of magnetic fields) show that

$$ReG(\mathbf{x}, \mathbf{x}', \omega) = - \int \frac{d\omega'}{\pi} \frac{ImG(\mathbf{x}, \mathbf{x}', \omega')}{\omega - \omega'} \left(\tanh \left[\frac{\beta\omega'}{2} \right] \right)^{-s}, \quad s = \mp. \tag{4.143}$$

Historically such relations are known as Fluctuation-dissipation theorem.

Problems

4.1. Prove the identity

$$[\hat{A}, e^{-\beta H}]_- = e^{-\beta H} \int_0^\beta e^{\tau H} [H, A]_- e^{-\tau H} d\tau, \tag{4.144}$$

4.2. Show that (4.143) holds.

4.3. In the continuous case of equation (4.44) determine $g(x', x, z)$ in 1 dimension

4.4. In the continuous case of equation (4.44) determine $g(x', x, z)$ in 3 dimensions

4.5. Derive the embedding potential $U(\mathbf{r})$ of Equation (4.108).

5 Hopping Electron Models: an Appetizer

5.1 Fano Resonances and Resolvents

5.1.1 Resonances

Often we treat excited levels as discrete, as they appear in low resolution or in some simple approximation. Sooner or later, however a closer analysis always shows that when all the degrees of freedom are considered they are in a continuum. Thus, the 2p level of H, H(2p), is coupled to a continuum of H(1s) + 1 photon, and thereby gains a width and a structure. The 2p state of H is discrete only if you accept to neglect its interaction with a continuum of photon modes that eventually take the H atom to the ground state while producing photons. In 1952, Fermi discovered a peak in the pion-proton ($\pi^+ - p$) elastic cross section for center-of-mass kinetic energies 1.2 to 1.4 GeV; since the half width at half maximum (~ 100 MeV) implies a lifetime $\tau \sim 10^{-23}$ s, which is very short, the strong interaction was implied in the formation and also in the decay. This was christened the doubly charged Δ^{++} resonance. Such high-energy Physics contents are pertinent to this book: hundreds of resonances are familiar by now to particle physicists, but Fermi's concept of resonances is important in quantum problems at all energy scales. Firing 500 eV electrons on Helium and measuring the loss spectrum, one observes[31] an asymmetric resonance in the ionization continuum at ~ 60 eV which has been identified as the $2s2p^1P$ state of He. Many more are known by now, and they are all due to the neutral, twice excited He atoms in auto-ionizing states. Using soft electrons (with not enough energy to produce ionizations) one sees narrow asymmetric resonances in the elastic cross section, due to temporary He^- ions. In all cases, the transition probability is described by some operator T , like $T \propto \mathbf{A} \cdot \mathbf{p}$ for electromagnetic transitions or, for fast electron scattering, $T \propto \frac{4\pi e^2}{q^2} \sum_j e^{-iq \cdot r_j}$, where r_j sums over the target electron positions. However there are features that do not depend on T ; for instance, the asymmetric He resonances are seen also in optical absorption.

We now develop techniques for dealing with such problems.

5.1.2 Fano Model

Here we consider a system consisting of very unlike parts: let $|k\rangle$ stand for a continuum of states of energy ϵ_k and $|0\rangle, \epsilon_0$ represent a localized state and its energy. Typically, $|0\sigma\rangle$ might represent atomic spin-orbital and $|k\sigma\rangle$ a free-particle states or Bloch states in a solid state problem from which an electron can jump into the continuum of single-particle states $|k\sigma\rangle$ (free-particle states or Bloch states in a solid state problem.) Some perturbation produces hopping matrix elements V_{k0} coupling the continuum to the discrete state. The Fano model is

$$H = H_0 + H_h, H_0 = \sum_{k \in \mathcal{C}, \sigma} \epsilon_{k, \sigma} n_{k, \sigma} + \sum_{\sigma} \epsilon_{0, \sigma} n_{0, \sigma} \quad (5.1)$$

while

$$H_h = \sum_{k, \sigma} \{V_k a_{k\sigma}^\dagger a_{0\sigma} + h.c.\} \quad (5.2)$$

The continuous spectrum of H_0 corresponds to a set \mathcal{C} of the real $\epsilon_{k, \sigma}$ axis; \mathcal{C} can be bound or unbound, and also it can be compact or consist of several pieces; for simplicity I assume that the continuum is not degenerate (only one state corresponds to ϵ_k). This assumption can be removed later by a direct extension of the present treatment[30].

There are no interaction terms (involving 2 creation and 2 annihilation operators) in the Fano model. In first quantization, it would be

$$h = \sum_{k \in \mathcal{C}, \sigma} \epsilon_{k, \sigma} |k\sigma\rangle \langle k, \sigma| + \sum_{\sigma} \epsilon_{0, \sigma} |0\sigma\rangle \langle 0, \sigma| + \sum_{k, \sigma} \{V_k |k\sigma\rangle \langle 0\sigma| + h.c.\} \quad (5.3)$$

and would represent 1 electron instead of representing any number of non-interacting elements. The two problems are closely related, and, for pedagogical reasons, I first present the elementary one-body term and then the many-body equation of motion approach (this is actually a one-body problem but the equation of motion method lends itself to the many-body case.)

5.1.3 One-body Treatment

In the elementary approach one writes:

$$\begin{cases} H |0\rangle = \epsilon_0 |0\rangle + \sum_k V_{0k} |k\rangle \\ H |k\rangle = \epsilon_k |k\rangle + V_{k0} |0\rangle. \end{cases} \quad (5.4)$$

The H eigenstates are expandable on the old basis:

$$|\lambda\rangle = |0\rangle \langle 0 | \lambda\rangle + \sum_k |k\rangle \langle k | \lambda\rangle. \quad (5.5)$$

Taking the scalar product with $\langle \lambda |$ one obtains:

$$(\epsilon_\lambda - \epsilon_0)\langle \lambda | 0 \rangle - \sum_k \langle \lambda | k \rangle V_{0k} = 0 \quad (5.6)$$

$$(\epsilon_\lambda - \epsilon_k)\langle \lambda | k \rangle - \langle \lambda | 0 \rangle V_{k0} = 0. \quad (5.7)$$

We discuss the solution below.

5.1.4 Many-Body Treatment

In the many-body case, we must still diagonalize the Hamiltonian, that is, write it in the form

$$\tilde{H} = \sum_\lambda \epsilon_\lambda n_\lambda; \quad (5.8)$$

the basis change (5.5) entails new creation operators for λ states such that

$$\begin{aligned} a_\lambda^\dagger &= a_0^\dagger \langle 0 | \lambda \rangle + \sum_k a_k^\dagger \langle k | \lambda \rangle \\ a_\lambda &= a_0 \langle \lambda | 0 \rangle + \sum_k a_k \langle \lambda | k \rangle \end{aligned} \quad (5.9)$$

with the inverse

$$\begin{cases} a_k = \sum_\lambda \langle k | \lambda \rangle a_\lambda \\ a_0 = \sum_\lambda \langle 0 | \lambda \rangle a_\lambda \end{cases}$$

We can find the λ states by the equation of motion method. Note that

$$\begin{aligned} [a_\lambda, n_{\lambda'}]_- &= \delta(\lambda, \lambda') [a_\lambda, n_\lambda]_- = \delta(\lambda, \lambda') a_\lambda a_\lambda^\dagger a_\lambda = \\ &= \delta(\lambda, \lambda') \left\{ \left[1 - a_\lambda^\dagger a_\lambda \right] a_\lambda \right\} = \delta(\lambda, \lambda') a_\lambda, \end{aligned}$$

here δ is Kronecker δ if we quantize in a big box, or Dirac's if we normalize on a continuum. In the diagonal basis,

$$[a_\lambda, \tilde{H}]_- = \epsilon_\lambda a_\lambda.$$

This corresponds to the equation of motion

$$i \frac{da_\lambda}{dt} = [a_\lambda, \tilde{H}]_- = \epsilon_\lambda a_\lambda \quad \Rightarrow a_\lambda(t) = a_\lambda(0) e^{-i\epsilon_\lambda t} \quad (5.10)$$

Written in the old basis, using (5.9), this is

$$\begin{aligned} &[\langle \lambda | 0 \rangle a_0 + \sum_k \langle \lambda | k \rangle a_k, H]_- = \\ &\epsilon_\lambda (\langle \lambda | 0 \rangle a_0 + \sum_k \langle \lambda | k \rangle a_k) \end{aligned} \quad (5.11)$$

Now,

$$\left[a_0, a_0^\dagger a_k \right]_- = a_0 a_0^\dagger a_k - a_0^\dagger a_k a_0 = a_0 a_0^\dagger a_k + a_0^\dagger a_0 a_k = a_k$$

and the required commutators read:

$$\begin{aligned} [a_0, H]_- &= \epsilon_0 a_0 + \sum_k V_{k0} a_k, \\ [a_k, H]_- &= \epsilon_k a_k + V_{0k} a_0. \end{aligned} \quad (5.12)$$

The equality holds separately for the coefficients of a_0 and of each a_k , since these are all linearly independent states. So, we find (5.6,5.7) again. Thus, the many-body formulation yields the same system as the one-body one, as it should always happen in non-interacting problems. The system allows to obtain the spin-orbitals and thus build the many-electron Slater determinants.

Now the discrete and continuous solution methods of Equations (5.6,5.7) have quite different characters.

1-Discrete Method of Solution

Placing the system in a box, the continuous spectrum becomes discrete; one can assume $\epsilon_l \neq \epsilon_k$ and write

$$\langle \lambda | k \rangle = - \frac{V_{k0}}{\epsilon_k - \epsilon_\lambda} \langle \lambda | 0 \rangle; \quad (5.13)$$

substituting into the first one gets an algebraic equation for the discrete eigenvalues

$$\epsilon_0 - \epsilon_\lambda - \sum_k \frac{|V_{k0}|^2}{\epsilon_k - \epsilon_\lambda} = 0. \quad (5.14)$$

Note that here only real quantities appear.

The Figure shows a graphical solution. $y = \sum_k \frac{|V_{k0}|^2}{\epsilon_k - \epsilon_\lambda}$ is plotted versus $\epsilon - \epsilon_0$. For illustration, I have taken k -independent V_{0k} coefficients and evenly spaced, positive ϵ_k values. The roots are the ϵ values where the sum crosses $y = \epsilon_0 - \epsilon$. Between two unperturbed ϵ_k eigenvalues there is always one ϵ_λ ; in addition, there is one root below the discretized continuum. Once the roots are found, one normalizes the wave functions by writing $|\langle \lambda | 0 \rangle|^2 \left\{ 1 + \sum_k \left| \frac{V_{k0}}{\epsilon_\lambda - \epsilon_k} \right|^2 \right\} = 1$ and the problem is completely solved. This solution is of little use, however, if we wish to understand what happens in the continuum limit. By increasing the number of k , the degree of the equation grows; a smaller and smaller interval separates a 0 from an ∞ of the sum, and more significant digits must be included to approximate the roots. This large amount of information is not about the system, but its interaction with the

fictitious box. This is not the way to the continuum. A *brute force* approach fails because of the irrelevant complications it produces.

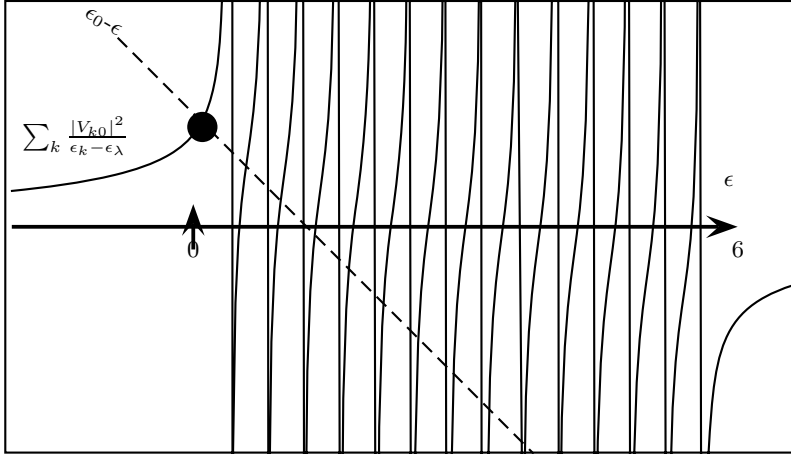


Fig. 5.1. Graphical solution of Equation (5.25). The true continuum \mathcal{C} , before placing the system in the box, extends from $\epsilon = 0$ to $\epsilon = 6$; a dot marks a root below it. Here the continuum is replaced by equally spaced roots.

2- *Solution in the Continuum*

At this stage the discrete and continuous methods of quantization become different, with the latter which is much more suitable. Now the k summations must be read as integrals; now perturbed and unperturbed eigenvalues must coincide, and we want tools to handle the problem, starting with some definitions.

- The density of states of the system is

$$\rho(\omega) = \sum_{\lambda} \delta(\omega - \epsilon_{\lambda}). \tag{5.15}$$

Hence, $\int_{E_1}^{E_2} d\omega \rho(\omega)$ is the number of states in the interval $E_1 < \omega < E_2$; it may diverge in the continuum limit, when $N \rightarrow \infty$, but we can convert the sum to an integral with a suitable measure, like $\sum_k \rightarrow \frac{\Omega}{(2\pi)^3} \int d^3k$, where Ω is the volume of the system. At the end all physical quantities have a finite value when $\Omega \rightarrow \infty$.

- The local (or projected) density of states (LDOS) measures the degree of mixing of the eigenstates at energy ω with the 0 orbital,

$$\rho_0(\omega) = \sum_{\lambda} \delta(\omega - \epsilon_{\lambda}) |\langle 0 | \lambda \rangle|^2. \quad (5.16)$$

The unperturbed quantity is $\rho_0^{(0)}(\omega) = \delta(\omega - \epsilon_0)$. The V coupling changes the discrete delta-like level into a virtual level; this has a width, and can have structure. The λ set is complete, hence $\int_{-\infty}^{\infty} d\omega \rho_0(\omega) = 1$.

- The resolvent, or Green operator

$$G(\omega) = (\omega - H + i\delta)^{-1}, \quad (5.17)$$

where δ stands for a positive infinitesimal, or if you like $\delta = +0$ (*intelligenti pauca*). This is the Fourier transform of causal¹ operator $G(t) = e^{-iHt}\theta(t)$, and is analytical in the upper half plane.

Note that

$$G_{00}(\omega) \equiv \langle 0 | G(\omega) | 0 \rangle = \sum_{\lambda} \frac{|\langle 0 | \lambda \rangle|^2}{\omega - \epsilon_{\lambda} + i\delta}, \quad (5.18)$$

and so

$$\rho_0(\omega) = -\frac{1}{\pi} \text{Im} G_{00}(\omega). \quad (5.19)$$

Here it is understood that $\sum_{\lambda} \equiv \int_{\mathcal{C}} d\epsilon_{\lambda} + \sum_{\lambda \in \mathcal{D}}$, where \mathcal{D} the possible discrete eigenvalues outside \mathcal{C} . If $\langle \lambda | 0 \rangle \neq 0$, a pole exists just below the real axis at $\omega = \epsilon_{\lambda} - i\delta$, and the residue is $|\langle \lambda | 0 \rangle|^2$. In second quantization one defines the Green's function as the vacuum average

$$G_{00} = \langle \text{vac} | a_0 \frac{1}{\omega - H + i\delta} a_0^{\dagger} | \text{vac} \rangle. \quad (5.20)$$

Inserting $a_0^{\dagger} = \sum_{\lambda} a_{\lambda}^{\dagger} \langle \lambda | 0 \rangle$, one finds (5.18) again. However the second quantized formulation lends itself to the many-body treatment when interactions are included.

5.1.5 The Resolvent

We obtain all the elements of G from the identity $(\omega - H + i\delta)\hat{G} = 1$, that is,

$$\begin{aligned} \langle 0 | (\omega - H + i\delta)\hat{G} | 0 \rangle &= \langle 0 | 0 \rangle = 1 \\ \langle k | (\omega - H + i\delta)\hat{G} | 0 \rangle &= \langle k | 0 \rangle = 0 \\ \langle 0 | (\omega - H + i\delta)\hat{G} | k \rangle &= \langle 0 | k \rangle = 0 \\ \langle k | (\omega - H + i\delta)\hat{G} | k' \rangle &= \langle k | k' \rangle = \delta(k - k'). \end{aligned}$$

¹i.e. proportional to $\theta(t)$

Setting $z = \omega - i\delta$, since $H_{kk'} = 0$,

$$\begin{aligned} (\omega - \epsilon_0)G_{00}(\omega) - \sum_k V_{0k}G_{k0}(\omega) &= 1 \\ (\omega - \epsilon_k)G_{k0}(\omega) - V_{k0}G_{00}(\omega) &= 0 \\ (\omega - \epsilon_0)G_{0k}(\omega) - \sum_{k'} V_{0k'}G_{k'k}(\omega) &= 0 \\ -V_{k0}G_{0k'}(\omega) + (\omega - \epsilon_k)G_{kk'}(\omega) &= \delta(k, k'). \end{aligned} \quad (5.21)$$

Now, thanks to δ , nothing diverges, and we obtain

$$G_{00} = \frac{1}{\omega - \epsilon_0 - \Sigma(\omega)}, \quad (5.22)$$

where

$$\Sigma(\omega) = \sum_k \frac{|V_{0k}|^2}{\omega - \epsilon_k + i\delta} \quad (5.23)$$

is the *self-energy*. For the other elements of the resolvent matrix see Problem 5.3.

Unlike the sum in (5.25) this is a smooth complex function of ω , \sum_k stands for an integral;

$$\begin{aligned} \Sigma_1(\omega) &\equiv \text{Re}\Sigma(\omega) = \text{P} \sum_k \frac{|V_{k0}|^2}{\omega - \epsilon_k} \\ \Sigma_2(\omega) &\equiv \text{Im}\Sigma(\omega) = -\pi \sum_k |V_{k0}|^2 \delta(\omega - \epsilon_k). \end{aligned} \quad (5.24)$$

As a function of $z = \omega + i\delta$, Σ is analytic outside the real axis. If $\mathcal{C} = \{a \leq \omega \leq b\}$, then there is a cut just below the axis, with a and b as branch points. Outside \mathcal{C} , $\Sigma_2 = 0$. Σ is a **Herglotz** function, that is, $-\pi^{-1}\text{Im}\Sigma(\omega) \geq 0$; it follows that $G_{00}(\omega)$ is also Herglotz, which is important to ensure $\rho_0 \geq 0$.

We can deduce more analytic properties of G . For $H_h \rightarrow 0$, $G_{00} \rightarrow G_{00}^{(0)} = \frac{1}{\omega - \epsilon_0 + i\delta}$ has a real pole which marks the discrete eigenvalue. For $H_h \neq 0$, $G_{00}(z)$ is analytic except for the cut along \mathcal{C} and possible poles at the roots of

$$z - \epsilon_0 = \Sigma(z). \quad (5.25)$$

Real roots are possible outside the unperturbed continuum where $\Sigma_2 = 0$. If there are roots, equation (5.18) really means

$$G_{00}(\omega) = \int_{\mathcal{C}} d\epsilon_\lambda \rho(\epsilon_\lambda) \frac{|\langle 0|\lambda\rangle|^2}{\omega - \epsilon_\lambda + i\delta} + \sum_{\mu \in \mathcal{D}} \frac{|\langle 0|\mu\rangle|^2}{\omega - \epsilon_\mu + i\delta}; \quad (5.26)$$

the residue at the pole ϵ_μ is the probability that a particle in $|\mu\rangle$ is found in $|0\rangle$.

Complex roots of (5.24) have $\omega \in \mathcal{C}$ and $\text{Im}z < 0$ by causality ($G(t) \propto \theta(t)$); they represent resonances. If Σ were constant, ρ_0 would be Lorentzian; although this can be a poor approximation, qualitatively, Σ_1 is a shift and Σ_2

a broadening; indeed, $\Sigma_2 = -\Gamma = \text{constant}$, for $t > 0$ we obtain $G_{00}(t)$ by closing the integral in the lower half plane:

$$\int_{-\infty}^{\infty} \frac{d\omega}{2\pi} \frac{e^{-i\omega t}}{\omega - \epsilon + i\Gamma} = \oint \frac{dz}{2\pi} \frac{e^{-izt}}{z - \epsilon + i\Gamma} = ie^{-i\epsilon t - \Gamma t}.$$

To calculate the wave functions, we use the assumption of a non-degenerate continuum that allows to make the replacement

$$\sum_{\lambda} \rightarrow \int d\epsilon_l \rho(\epsilon_{\lambda})$$

and write

$$\text{Im}G_{00} = -\pi \int d\epsilon_{\lambda} \rho(\epsilon_{\lambda}) |\langle 0|\lambda\rangle|^2 \delta(\omega - \epsilon_{\lambda}) = -\pi \rho(\omega) |\langle 0|\lambda_{\omega}\rangle|^2, \quad (5.27)$$

where $|\lambda_{\omega}\rangle$ is the eigenstate at energy $\hbar\omega$. Hence,

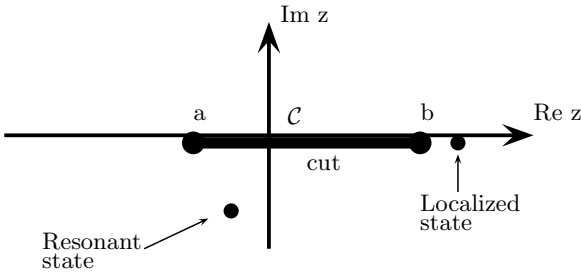


Fig. 5.2. The singularities of $G_{00}(z)$ must be in the lower half of the complex z plane. Outside the continua one can find poles close to the real axis at localized states. Branch cuts correspond to the continua; a and b are branch points; poles below the cuts yield resonant states.

$$|\langle 0|\lambda_{\omega}\rangle|^2 = \frac{-\text{Im}G_{00}(\omega)}{\pi\rho(\omega)} = \frac{\rho_0(\omega)}{\rho(\omega)}, \quad (5.28)$$

and the wave function at site 0 is obtained (the phase is arbitrary). In a similar way, using Fano notations, $V_{k0} \equiv V_{\omega} \equiv V(\omega)$ and one obtains

$$\Sigma_2(\omega) = -\pi \int d\epsilon_k \rho^{(0)}(\epsilon_k) |V_{k0}|^2 \delta(\omega - \epsilon_k) = -\pi \rho^{(0)}(\omega) V^2(\omega) = -\pi \rho(\omega) V^2(\omega) \quad (5.29)$$

where the last equality holds in the thermodynamic limit. Now we can solve (5.7) in the sense of distributions. The most general real solution of $xf(x) = C$ is

$$f(x) = C \left[\text{P} \frac{1}{x} + Z\delta(x) \right],$$

where Z is a constant. Thus we find a family of solutions:

$$\langle \lambda | k \rangle = \langle \lambda_\omega | 0 \rangle V_{k0} \left[\text{P} \frac{1}{\epsilon_\lambda - \epsilon_k} + Z(\epsilon_\lambda) \delta(\epsilon_k - \epsilon_\lambda) \right] \quad (5.30)$$

Putting into (5.6) we find

$$Z(\omega) = -\pi \frac{\omega - \epsilon_0 - \Sigma_1(\omega)}{\Sigma_2(\omega)}, \quad (5.31)$$

and the solution is complete.

5.1.6 Self-Energy Operator

The above Anderson method to calculate the resolvent can be cast in operator form and is very useful in problems when it is convenient to separate the Hilbert space in two subspaces A and B writing

$$H = \begin{pmatrix} H_{AA} & H_{AB} \\ H_{BA} & H_{BB} \end{pmatrix} \quad (5.32)$$

As in Sect. 5.1.2 take the AA matrix element of the identity $(\omega - H)G = 1$:

$$G_{AA} = \frac{1}{\omega - H_{AA}} + \frac{1}{\omega - H_{AA}} H_{AB} G_{BA}. \quad (5.33)$$

Then we take the BA element closing the equations:

$$G_{BA} = \frac{1}{\omega - H_{BB}} H_{BA} G_{AA}. \quad (5.34)$$

Hence,

$$G_{AA} = \frac{1}{\omega - H_{AA} - H_{AB} \frac{1}{\omega - H_{BB}} H_{BA}}. \quad (5.35)$$

Thus we can work within subspace A provided that we work with an energy-dependent effective hamiltonian

$$H_{eff}(\omega) = H_{AA} + \Sigma_{AA}, \quad \Sigma_{AA} = H_{AB} \frac{1}{\omega - H_{BB}} H_{BA}. \quad (5.36)$$

Σ_{AA} is called *self-energy operator*. To get the other matrix elements one simply exchanges A and B in (5.35,5.34). If several subspaces B, C, \dots are coupled to A but not among themselves, they yield additive contributions to Σ_{AA} .

5.2 Magnetic Impurities and Chemisorption on Transition Metal Surfaces

The Anderson model

$$H = \sum_{k\sigma} \varepsilon_{k\sigma} n_{k\sigma} + \sum_{\sigma} \varepsilon_0^0 n_{0\sigma} + \sum_{k\sigma} \{V_{k\sigma} c_{k\sigma}^\dagger c_{0\sigma} + \text{h.c.}\} + U n_{0\uparrow} n_{0\downarrow} \quad (5.37)$$

is just a Fano Hamiltonian with the addition of the innocent-looking but far-reaching U term, which represents an oversimplified electron-electron interaction. It was introduced in a fundamental paper[9] on magnetic impurities in metals. The main question is: in what conditions will the localize state be magnetic? The continuum tends equalize the populations $n_{0\uparrow}, n_{0\downarrow}$ magnetic sub-levels in order to lower the kinetic energy, but there is a price to pay to the local interaction.

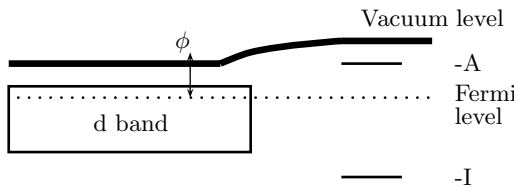


Fig. 5.3. Relative position of energy levels in Newns model (not to scale). ϕ is the work function. The bending of the Vacuum level is due to the surface electric field.

Here I mainly discuss a 1969 paper by D.M. Newns[10] dealing with H chemisorption on Cu and Ni by an Anderson model² because important points were made there. In his scheme, the localized atomic state $|0\rangle$ is the 1s H level with energy $\varepsilon_0^{(0)}$ and the continuum is due to the metal d band states $|k\rangle$, delocalized in the bulk but exponentially damped outside the metal. The chemical bond is due to hopping matrix elements V_{0k} aa in the Fano model. Unlike the Anderson paper, Newns considered the implications of the ω dependence of the self-energy $\Sigma(\omega)$ in detail.

U=0 limit

If U is unimportant, we expect localized states if there are real roots of Equation (5.25). The new feature is the presence of a Fermi level. Instead of local elements of the resolvent we now handle Green's functions. The occupied states are described by the one-hole Green's function

²Chemisorption is the chemical bond between an atom (molecule) and a surface). Now it is studied mainly by *ab-initio* methods, but some key concepts developed from models remain fundamental.

$$G_{00}(\omega) = \langle \Psi | c_0^\dagger \frac{1}{\omega - H} c_0 | \Psi \rangle, \quad (5.38)$$

where $|\Psi\rangle$ is the ground state. For $U = 0$, $|\Psi\rangle$ is a Slater determinant of solutions $|\lambda\rangle$ of the Fano model, and changing the basis with $c_0^\dagger = \sum_\lambda \langle \lambda | 0 \rangle c_\lambda^\dagger$, we find

$$G_{00}(\omega) = \sum_\lambda f_\lambda \frac{|\langle 0 | \lambda \rangle|^2}{\omega - \varepsilon_\lambda + i\delta}; \quad (5.39)$$

this is already familiar except for the appearance of the Fermi function f_λ . For the empty states, one defines the one-electron Green's function

$$G_{00}(\omega) = \langle \Psi | c_0 \frac{1}{\omega - H} c_0^\dagger | \Psi \rangle. \quad (5.40)$$

From the Fano model we can obtain interesting quantities like the level population

$$\langle n_0 \rangle = 2 \int_{-\infty}^{E_F} d\omega \rho_0(\omega) \quad (5.41)$$

where E_F is the Fermi energy and the factor 2 is due to the spin.

Interacting Anderson Model in Mean Field Approximation

For the Hydrogen atom, the ionization potential $I = 13.6eV$ and the electron affinity $A = 0.7eV$, are so different that it is impossible to set up a sensible model without the interaction $U \sim \langle 0 \uparrow 0 \downarrow | \frac{e^2}{r_{12}} | 0 \uparrow 0 \downarrow \rangle \sim |I - A|$. A work function (Typically $\phi \sim 4.5 eV$) separates the Fermi level from the Vacuum Level (minimum energy of a free electron far from the metal); so even ϕ is smaller than $I - A$. We need a simple calculation to orient ourselves. In the Hartree-Fock approximation, one assumes a ground state of the determinantal form

$$|\Psi\rangle = \prod_{\varepsilon_\lambda < E_F, \varepsilon_\mu < E_F} c_{\lambda+}^\dagger c_{\mu-}^\dagger |vac\rangle.$$

Averaging the one-body operator

$$n_{0\uparrow} = \sum_{\lambda, \mu} c_{\lambda\uparrow}^\dagger c_{\mu\uparrow} \langle \lambda | 0 \rangle \langle 0 | \mu \rangle \quad (5.42)$$

on $|\Psi\rangle$, only diagonal terms contribute and one finds

$$\langle n_{0,\sigma} \rangle = \sum_\lambda f_\lambda |\langle \lambda | 0 \rangle|^2. \quad (5.43)$$

Moreover, since the anti-commutation relations allow to lump all the up spin operators on one side, it is readily seen that

$$\langle \Psi | n_{0\uparrow} n_{0\downarrow} | \Psi \rangle = \langle \Psi | n_{0\uparrow} | \Psi \rangle \langle \Psi | n_{0\downarrow} | \Psi \rangle \equiv \langle n_{0\uparrow} \rangle \langle n_{0\downarrow} \rangle. \quad (5.44)$$

Thus,

$$E = \langle \Psi | H | \Psi \rangle = \sum_{\lambda, \sigma} f_{\lambda} \langle \lambda, \sigma | h | \lambda, \sigma \rangle + U \langle n_{0\uparrow} \rangle \langle n_{0\downarrow} \rangle. \quad (5.45)$$

where h is the one-body (Fano) part of H of (5.3). We Set up the variational calculation of λ_{\uparrow} in first quantization, treating bra and ket as independent unknowns. We use (5.43), and vary the bra, for occupied states:

$$\frac{\delta \langle n_{0\uparrow} \rangle}{\delta \lambda_{\uparrow}} = \frac{\delta}{\delta \lambda_{\uparrow}} \langle \lambda_{\uparrow} | 0_{\uparrow} \rangle \langle 0_{\uparrow} | \lambda_{\uparrow} \rangle = |0_{\uparrow}\rangle \langle 0_{\uparrow} | \lambda_{\uparrow} \rangle. \quad (5.46)$$

This contribution multiplied by ϵ_0 appears in the h term and multiplied by $U \langle n_{0\downarrow} \rangle$ in the interaction term. Thus, in the unrestricted³ Hartree-Fock equation $\frac{\delta E}{\delta \lambda_{\uparrow}} = \epsilon_{\lambda_{\uparrow}} | \lambda_{\uparrow} \rangle$, the U term produces a shift

$$\epsilon_{0\sigma}^{(0)} \rightarrow \epsilon_{0\sigma}^{(0)} + U \langle n_{0-\sigma} \rangle. \quad (5.47)$$

Back in second quantization, the spin σ electrons have their Fock Hamiltonian

$$H^{\sigma} = \epsilon_{0\sigma} n_{0\sigma} + \sum_{k\sigma} \epsilon_k n_{k\sigma} + \sum_k \{ V_{k\sigma} c_{k\sigma}^{\dagger} c_{0\sigma} + \text{h.c.} \} \quad (5.48)$$

where $\langle n_{-\sigma} \rangle$ is a parameter; thus the equations for $\pm\sigma$ are coupled. No privileged spin direction exists in this problem, and one could have the impression that $\langle n_{0\sigma} \rangle$ is equal to $\langle n_{0-\sigma} \rangle$ for symmetry reasons: remarkably, this is wrong if U is large, and the level is about half filled, because the symmetry is spontaneously broken (see Fig. 3.3). There is a couple of ground states, namely

$$\langle n_{0,\sigma} \rangle \gg \langle n_{0,-\sigma} \rangle,$$

and another one with $\sigma \rightarrow -\sigma$. The overall symmetry of the problem is not respected by each ground states. The chemisorbed atom has a magnetic moment. The existence of a localized spin requires strong enough U and partial occupation; the Hartree-Fock approximation is known to overestimate somewhat the occurrence of magnetism compared to more refined approaches.

Despite this possibility, Newns found a nonmagnetic solution for H chemisorbed on Cu and Ni; let us consider more closely the case when $\langle n_{0\sigma} \rangle = \langle n_{0-\sigma} \rangle = \frac{1}{2} \langle n_{\sigma} \rangle$ where $\langle n_0 \rangle$ is the total population of the ad-atom. Then, ϵ_0 does not depend on spin but according to (5.47) it depends linearly on $\langle n_0 \rangle$, with $\epsilon_0 \rightarrow -I$ for $\langle n_0 \rangle \rightarrow 0$ and $\epsilon_0 \rightarrow -A$ for $\langle n_0 \rangle \rightarrow 2$. On the other hand, the Fano formalism applied to the Fock Hamiltonian yields another functional dependence through

$$\langle n_0 \rangle = 2 \int_{-\infty}^{E_F} d\omega \rho_0(\omega). \quad (5.49)$$

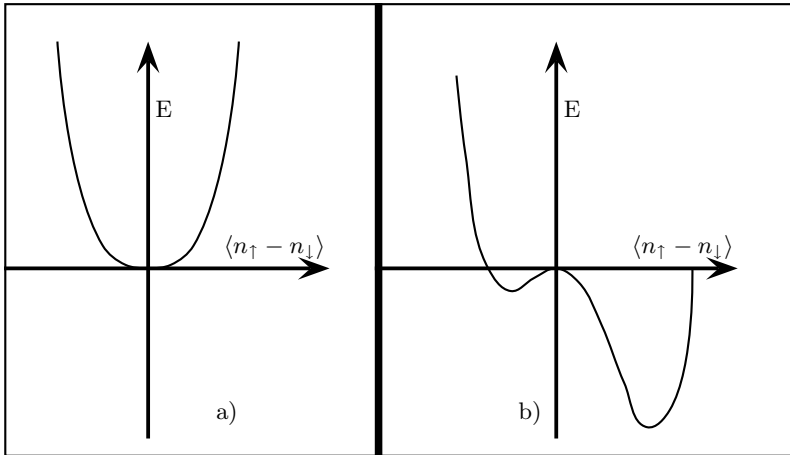


Fig. 5.4. Qualitative dependence of the energy E on local spin when the virtual level is about half filled: a) for U small compared to level width b) strong coupling case.

In this way a self-consistent solution can be obtained. Newns found $\langle n_0 \rangle = 1.06$ for Cu and $\langle n_0 \rangle = 1.16$ for Ni; this small negative charge on the H atom produces an electrostatic dipole at the surface. The result is an increase in the surface dipole due to the spill-over of the conduction electrons past the edge of the positive charge and thus an increase in the work function, which has been observed.

Local View

It is instructive to illustrate this theory by a simple LCAO⁴ model. By expanding the continuum states on a localized basis,

$$|k\rangle = \sum_i |i\rangle \langle i|k\rangle \quad (5.50)$$

one can expand the hopping integrals as well:

$$V_k = \sum_i V_i \langle i|\kappa\rangle. \quad (5.51)$$

The most important V_i are those connecting to nearest neighbors. Various chemisorption geometries can be modeled, including Atop, Bridge (bridging between 2 atoms) and Center (above the center of a triangle) geometries. The

³this is conventional term meaning that we are not assuming that all quantities be spin-independent.

⁴Linear Combination of Atomic Orbitals.

resulting virtual level shapes depend qualitatively on the number of nearest neighbors. Here I consider the Atop case, denoting in this paragraph a the H adatom orbital and 0 the top surface atom;

$$V_k \sim V_{a0} \langle 0|k \rangle, \quad (5.52)$$

is hopping matrix element, and

$$\Sigma_a(\omega) = \sum_k \frac{V_k^2}{\omega - \epsilon_k + i\delta} \sim |V_{a0}|^2 G_S(\omega) \quad (5.53)$$

where $G_S(\omega)$ is the local Green's function of the surface atom, an intrinsic property of the undisturbed surface. For the sake of argument, let us represent the d band by a tight binding $N + 1$ atom chain, with orthogonal site orbitals $\langle i|j \rangle = \delta_{ij}$ and $H_{ij} = \beta$ between nearest neighbor sites, $H_{ij} = 0$ otherwise. Here, the sites of the chain are $0, 1, 2, \dots \infty$ and chemisorption occurs above site 0. In this case, $G_S \equiv G_{00}$. Like a moment ago, the self-energy of the top atom is related to the local Green's function of the chain with the top atom removed, that is the $1, 2, \dots \infty$ atom chain; but removing an atom from a semi-infinite chain makes no difference, and $\Sigma_{00} = \beta^2 G_{00}$. Hence,

$$G_{00}(z) = \frac{1}{z - \beta^2 G_{00}(z)}, \quad z = \omega + i\delta. \quad (5.54)$$

We find the solutions

$$G_{00}(z) = \frac{z \pm \sqrt{z^2 - 4\beta^2}}{2\beta^2}.$$

Taking the cut of \sqrt{z} along the positive real axis, $\sqrt{z} = \sqrt{|\omega|} e^{i \arg \omega / 2}$. For $\sqrt{z^2 - 4\beta^2} = \sqrt{|\omega^2 - 4\beta^2|} \exp \left\{ \frac{i}{2} [\arg(\omega - 2\beta) + \arg(\omega + 2\beta)] \right\}$ the cut is between -2β and 2β along the real axis, and corresponds to the band. Just above the cut, $\sqrt{z^2 - 4\beta^2} = i\sqrt{|\omega^2 - 4\beta^2|}$, just below the cut, $\sqrt{z^2 - 4\beta^2} = -i\sqrt{|\omega^2 - 4\beta^2|}$. The density of states is $\rho(\omega) = -\frac{1}{\pi} \text{Im} G(\omega)$ computed on the real axis, that is, just *above* the cut, and in order to have it positive, we must choose

$$G_{00}(z) = \frac{z - \sqrt{z^2 - 4\beta^2}}{2\beta^2}. \quad (5.55)$$

Thus one obtains the *semi-elliptic density of states*

$$n(\omega) = \frac{\sqrt{4\beta^2 - \omega^2}}{2\pi\beta^2} \theta(4\beta^2 - \omega^2). \quad (5.56)$$

$\text{Re}[G_{00}]$ is the Hilbert transform of $n(\omega)$ and is odd; it is linear in the band and outside

$$\text{Re}[G_{00}] = \frac{\omega - \sqrt{\omega^2 - 4\beta^2}}{2\beta^2}, \quad \omega > 2\beta. \quad (5.57)$$

The chemisorption is weak (strong) when V is small (large) compared to β . For weak chemisorption, the self-energy is small and $\omega - \epsilon_a - \Sigma_1(\omega) = 0$ is solved by $\omega \sim \epsilon_a + \Sigma_1(\epsilon_a)$. So, if ϵ_a is well inside the band, the solution is a resonance having width $\sim \Sigma_2(\epsilon_a)$; if ϵ_a is well outside the band, a discrete state obtains. ϵ_a in the continuum can give a discrete solution only if it is close to the edge. For strong chemisorption, one may have two roots straddling the band. Then,

$$0 = \omega - \epsilon_a - \frac{1}{\pi} \int d\omega' \frac{\Sigma_2(\omega')}{(\omega - \omega')} \sim \omega - \epsilon_a - \frac{1}{\pi} \frac{\int d\omega' \Sigma_2(\omega')}{(\omega - \omega_C)}$$

with ω_C the center of the band. The two roots obtained in this way are the bonding and anti-bonding levels of a localized surface molecule.

5.3 Strong Coupling and the Kondo Peak

J. Kondo [34] in 1964 succeeded in explaining the strong effect of a small amount of magnetic impurities on the resistivity of non-magnetic metals⁵. A magnetic impurity with incomplete d or f shells that at room temperature behaves like a magnetic dipole at very low temperatures appears to lose its spin; lowering the temperature further, the resistivity does not continue to decrease as in pure metals but starts to increase. Even much less than 0.01 atom % Fe in Au suffice to produce the resistivity minimum at the Kondo temperature T_K (several $^{\circ}K$). The Kondo temperature T_K (a few millivolts) is very unlike the characteristic energies (band width, distance of the d or f level from Fermi level, on-site repulsion.) Here I wish to show that idealized models do bring many of the characters of the Kondo physics, that cannot currently be reproduced by the common *ab initio* methods. The Anderson-like models explain how such a small energy scale as T_K arises and how we can monitor the electronic structure by electron spectroscopy. Various regions in parameter space are relevant to different experimental situations. When ϵ_0 is close enough to the Fermi level, like the *f* levels in *SmB₆*, one speaks of mixed valence regime because strong charge fluctuations occur and the different ions can have different, non-integer valence. When $\epsilon_0 + U$ is close enough to the Fermi level similar phenomena occur. By contrast in this Section we investigate the Kondo scenario, when the localized level is deep but multiple occupation is hindered by large U .

5.3.1 Narrow-Band Anderson Model

In the narrow band limit of the Anderson Hamiltonian the continuum is replaced by a single level k at the Fermi energy $\epsilon_F = 0$; we shall have in

⁵For an introduction to the Kondo effect see e.g. [5]; for fine recent reviews see Hewson's book [20] and Ref. [19].

mind applications to d (or f) levels of impurities in metals. Accordingly in this Section we denote the localized state as the d level. A very interesting situation arises in the strongly correlated case $U \gg |\epsilon_d|$ when the d level is deep ($\epsilon_d < 0$ with $V \ll |\epsilon_d|$.) For a single particle, the basis set is $\{|d\rangle, |k\rangle\}$ and the Hamiltonian matrix is

$$H(1) = \begin{pmatrix} \epsilon_d & V \\ V & 0 \end{pmatrix} \quad (5.58)$$

with eigenvalues $\epsilon_{\pm} = \frac{\epsilon_d \pm r}{2}$, $r = \sqrt{\epsilon_d^2 + 4V^2}$. The spin-degenerate ground state $\Psi_{g\sigma}$ has energy $\epsilon_- \sim \epsilon_d - \frac{V^2}{\epsilon_d}$. We are interested in the one-electron Green's function

$$G_{dd}(\omega) = \langle \Psi_{g\uparrow} | c_{d\downarrow} \frac{1}{\omega - H} c_{d\downarrow}^\dagger | \Psi_{g\uparrow} \rangle, \quad (5.59)$$

which brings information in the two-particle states in the $S_z = 0$ sector where U can act. To predict the poles of G_{dd} let us examine the expansion of two-body state $c_{d\downarrow}^\dagger | \Psi_{g\uparrow} \rangle$ into stationary states. With 2 electrons of opposite spin, on the basis

$$\{|1\rangle = |d \uparrow d \downarrow\rangle, |2\rangle = |d \uparrow k \downarrow\rangle, |3\rangle = |k \uparrow d \downarrow\rangle, |4\rangle = |k \uparrow k \downarrow\rangle\}, \quad (5.60)$$

the Hamiltonian matrix is

$$H(2) = \begin{pmatrix} 2\epsilon_d + U & V & V & 0 \\ V & \epsilon_d & 0 & V \\ V & 0 & \epsilon_d & V \\ 0 & V & V & 0 \end{pmatrix}. \quad (5.61)$$

The triplet component brings structure right at ϵ_d . Indeed, the 2-particle triplet states are

$$\{|d \uparrow k \uparrow\rangle, |d \downarrow k \downarrow\rangle\}, \frac{1}{\sqrt{2}}(|d \uparrow k \downarrow\rangle - |k \uparrow d \downarrow\rangle)$$

but only the last one is in the $S_z = 0$ sector; they have eigenvalue ϵ_d .

In the singlet sector, one finds 3 eigenvalues of $H(2)$. Referring to the basis (5.60), the G_{44} singlet is clearly mainly peaked at 0, but does not enter the calculation of G_{dd} . The G_{11} element gives structure mainly at high energies $\epsilon \sim U$. The singlet $|s\rangle = \frac{1}{\sqrt{2}}(|2\rangle + |3\rangle)$ is more interesting, and gives the combination

$$G_{ss} = \frac{G_{22} + G_{33} + G_{32} + G_{23}}{2}.$$

One can readily compute the resolvent matrix $G(\omega) = (\omega - H(2))^{-1}$ and G_{ss} . The density of states derived from G_{ss} has an interesting structure near the Fermi level which persists at high U , as shown in Figure 5.4 This is called the *Abrikosov-Suhl or Kondo peak* and has a striking physical interpretation.

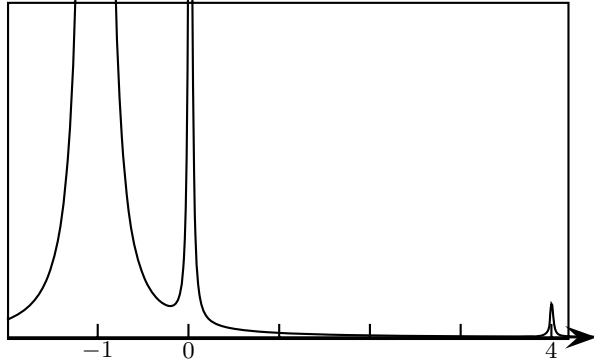


Fig. 5.5. The singlet density of states as obtained from G_{ss} with $\epsilon_0 = -1$, $U = 6$ and $\frac{V}{\epsilon_0} = 0.1$; the eigenvalues of $H(2)$ are at $\omega = -1.023, -1.0, 0.0195, 4.004$ and a triplet at $\omega = -1$. The singlet has little intensity in the *high energy peak* (here at $\omega = 4$); it is practically insensitive to changes in U in the low energy sector as long as U is large. The peak at $\epsilon_0 = 0.0195$ close to the Fermi level is the Kondo peak due to spin flip. The δ lines are broadened into Lorentzians (width $0.02 |\epsilon_0|$).

For $V = 0$ the d level is singly occupied in the ground state and the impurity has a net free spin; the deep level has a $SU(2)$ degree of freedom. For small V , the d level remains essentially singly occupied in the ground state, but the transfer of spectral weight shows that it manages to interact with the Fermi level. The only way this can occur is by an exchange of the conduction electron with the localized one, while the impurity flips its spin.

To simplify the algebra, we can chop from the Hilbert space the uninteresting state with a doubly occupied d level, since it stands alone at high energy, and write

$$H'(2) = \begin{pmatrix} \epsilon_d & 0 & V \\ 0 & \epsilon_d & V \\ V & V & 0 \end{pmatrix} \quad (5.62)$$

on the reduced basis

$$\{|1'\rangle, |2'\rangle, |3'\rangle\} = \{|d \uparrow k \downarrow\rangle, |d \downarrow k \uparrow\rangle, |k \uparrow k \downarrow\rangle\}. \quad (5.63)$$

The triplet noted above, with eigenvalue ϵ_d , is $(r, -r, 0)$, $r = \frac{1}{\sqrt{2}}$. It is easy to find 2 normalized vectors orthogonal to $(r, -r, 0)$ and to each other, for instance $(r, r, 0)$ and $(0, 0, 1)$. Using the orthogonal matrix $c = \begin{pmatrix} r & 0 & r \\ r & 0 & -r \\ 0 & 1 & 0 \end{pmatrix}$,

we find the transformed Hamiltonian $\tilde{h} = c^T h c = \begin{pmatrix} \epsilon_d & V\sqrt{2} & 0 \\ V\sqrt{2} & 0 & 0 \\ 0 & 0 & \epsilon_d \end{pmatrix}$;

hence we obtain two singlets with eigenvalues $\epsilon_{\pm}^{(2)} = \frac{-\epsilon_d \pm \sqrt{\epsilon_d^2 + 8V^2}}{2}$. While

$\epsilon_+^{(2)} \sim 2\frac{V^2}{\epsilon_d}$, the ground state energy $\epsilon_-^{(2)} \sim \epsilon_d - 2\frac{V^2}{-\epsilon_d}$ says that the singlet is slightly lower than the triplet for small V , and a bound state forms in which the spin is screened; the eigenvector (on the basis (5.63) $(-\frac{V}{\sqrt{(\epsilon_+^{(2)})^2+2V^2}}, -\frac{V}{\sqrt{(\epsilon_+^{(2)})^2+2V^2}}, -\frac{\epsilon_+^{(2)}}{\sqrt{(\epsilon_+^{(2)})^2+2V^2}})$) shows that $|d \uparrow k \downarrow\rangle$ and $|d \downarrow k \uparrow\rangle$ components are the important ones. The low energy sector (singlet ground state and triplet excited level) is well represented by an effective Hamiltonian

$$H_{eff} = -2JS_1 \cdot S_2 \quad (5.64)$$

which commutes with the square of the total spin and describes a spin-spin coupling between the two electrons. The small separation $\sim -2\frac{V^2}{\epsilon_F - \epsilon_d}$ between the ground state and the triplet implies that the low-energy excitation is a spin-flip, while charge excitations are frozen. The coupling between the conduction electron and the localized one through spin produces a singlet level in the valence region at $\epsilon_+^{(2)}$.

The narrow-band model is extremely simple, but calculations on larger systems confirm and extend the scenario. Recent exact-diagonalization calculations of Kondo clusters alloyed with mixed-valence impurities in the presence of disorder are of great interest [36] and show T=0 phase diagrams very rich in structure.

5.3.2 Anderson Model, s-d Model and Kondo Model

Consider an Anderson model with $\epsilon_d < 0$ and U chosen such that for $V_k \rightarrow 0$ the d level is singly occupied in the ground state. At small V_k , the low-energy subspace, say, subspace A, corresponds to singly occupied d level; there are two high-energy subspaces, say B and B', with excitation energies $\Delta E(d^1 \rightarrow d^2) = \epsilon_d + U$ and $\Delta E(d^1 \rightarrow d^0) = -\epsilon_d$. Let us use the *Schrieffer-Wolff transformation* (Sect. (1.3)) with the hopping term as v ; Equation (1.86)yields the approximate renormalized interaction

$$H_{int} = - \sum_{k\sigma, k'\sigma'} V_{k'}^* V_k \left[\frac{(c_{k\sigma}^\dagger d_\sigma)(d_{\sigma'}^\dagger c_{k'\sigma'})}{\epsilon_d + U} + \frac{(d_{\sigma'}^\dagger c_{k'\sigma'})(c_{k\sigma}^\dagger d_\sigma)}{-\epsilon_d} \right]. \quad (5.65)$$

Besides a conventional scattering of conduction electrons by an impurity potential, H_{int} produces diffusion with spin flip (of both conduction and impurity spins). The effective Hamiltonian is clearly a particular form of the s-d model proposed long ago by Zener[28], that we now recall.

s-d model

We need a slight generalization of Equation (1.58) in which we write

$$(\sigma_{k \rightarrow k'})_x = \begin{pmatrix} c_{k\uparrow}^\dagger & c_{k\downarrow}^\dagger \\ 1 & 0 \end{pmatrix} \begin{pmatrix} 0 & 1 \\ 1 & 0 \end{pmatrix} \begin{pmatrix} c_{k'\uparrow} \\ c_{k'\downarrow} \end{pmatrix} = \sum_{kk'} (\sigma_{\alpha\beta})_x c_{k\alpha}^\dagger c_{k'\beta}, \quad (5.66)$$

and so on; if k' were equal to k this would be the representation of the spin operator in the k basis, but we are allowing off-diagonal elements. In this way,

$$(\sigma_{k \rightarrow k'})_z = c_{k\uparrow}^\dagger c_{k'\uparrow} - c_{k\downarrow}^\dagger c_{k'\downarrow}, (\sigma_{k \rightarrow k'})^+ = 2c_{k\uparrow}^\dagger c_{k'\downarrow}.$$

The s-d model proposed by Zener[28] for an impurity spin S in a metal reads

$$H = H_F + \sum_{k,k'} J_{k,k'} \left(\frac{1}{2} [S^+(\sigma_{k \rightarrow k'})^- + S^-(\sigma_{k \rightarrow k'})^+] + S_z(\sigma_{k \rightarrow k'})_z \right) \quad (5.67)$$

where H_F is a Fano Hamiltonian[32]. For the impurity we denote the creation operator by d^\dagger and use $\epsilon_d \equiv \epsilon_0$; we set

$$2S_x = d_\uparrow^\dagger d_\downarrow + d_\downarrow^\dagger d_\uparrow, 2S_y = -i(d_\uparrow^\dagger d_\downarrow - d_\downarrow^\dagger d_\uparrow), 2S_z = d_\uparrow^\dagger d_\uparrow - d_\downarrow^\dagger d_\downarrow; \quad (5.68)$$

one can readily verify the angular momentum commutator relations in the subspace with $n_\uparrow n_\downarrow = 0, n_\uparrow + n_\downarrow = 1$.

Spin-flip and the Kondo Model

Now in Equation (5.65) we consider the spin-flip ($\sigma' \neq \sigma$) terms ignoring the dull potential scattering terms; for instance we have a term $c_{k\uparrow}^\dagger d_\uparrow d_\downarrow^\dagger c_{k'\downarrow} = \frac{1}{2}(\sigma_{k \rightarrow k'})^+ S_d^-$ which fits the s-d model. So we arrive at the *Kondo model*[35]

$$H = H_0 + H_K = \sum_{k\sigma} \epsilon_k c_{k\sigma}^\dagger c_{k\sigma} + \sum_{k,k'} J_{k,k'} (\boldsymbol{\sigma}_{\alpha\beta} \cdot \mathbf{S}) c_{k\alpha}^\dagger c_{k'\beta} \quad (5.69)$$

where

$$J_{k,k'} = V_{k'}^* V_k \left[\frac{1}{\epsilon_d + U} + \frac{1}{-\epsilon_d} \right]. \quad (5.70)$$

This describes the net effect of the virtual valence fluctuations; they couple the local spin density of the conduction electrons with the impurity spin. The d electron is reduced to its spin degree of freedom, while the charge is fixed. The k dependence is often neglected. In this case, the Kondo interaction can be written

$$H_{int} = H_K = J \psi_\alpha^\dagger(0) \psi_\beta(0) (\boldsymbol{\sigma}_{\alpha\beta} \cdot \mathbf{S}_d), \quad (5.71)$$

where $\psi_\alpha(0) = \frac{1}{\sqrt{N}} \sum_k c_{k\alpha}$ is the electron field operator at the origin. Since

$$\{\boldsymbol{\sigma}_{\alpha\beta}\} \equiv \begin{pmatrix} (0, 0, 1) & (1, -i, 0) \\ (1, i, 0) & (0, 0, -1) \end{pmatrix} \quad (5.72)$$

we may also write

$$H_K = J \begin{pmatrix} S_z \psi_\uparrow^\dagger(0) \psi_\uparrow(0) & S_- \psi_\uparrow^\dagger(0) \psi_\downarrow(0) \\ S_+ \psi_\downarrow^\dagger(0) \psi_\uparrow(0) & -S_z \psi_\downarrow^\dagger(0) \psi_\downarrow(0) \end{pmatrix}. \quad (5.73)$$

This is the second quantized form of a Hamiltonian $H_K = J(\boldsymbol{\sigma} \cdot \mathbf{S}_d) \delta(x)$.

5.3.3 Fermi Level Singularity and Kondo Minimum

The resistivity of metals decreases with decreasing temperature since the phonon contribution drops; the Kondo minimum at T_K arises because the magnetic impurity contribution increases as $T \rightarrow 0$. The impurity resistivity is due to $\mathbf{k} \rightarrow \mathbf{k}'$ processes where the conduction electrons scatter from one Bloch state to another in the impurity potential and is proportional to the square modulus of the scattering amplitude. The amplitude is an average over the thermal distributions of electrons, and the distribution peaks at the Fermi level as $T \rightarrow 0$. For K or Ca impurities in a metal, nothing special happens with lowering T , but for impurities such as Fe or Co the temperature is very important. This is because the the impurity cross section grows logarithmically when the Fermi energy is approached, and the effect is entirely due to the spin. To see how this is borne out by the Kondo model, let

$$H = H_0 + H_K, \quad H_K = \frac{J}{N} \sum_{k,k'} (\boldsymbol{\sigma}_{\alpha\beta} \cdot \mathbf{S}) c_{k\alpha}^\dagger c_{k'\beta} \quad (5.74)$$

with $\boldsymbol{\sigma}$ the conduction electron spin; let $|\Phi\rangle$ denote a filled Fermi sphere, with the energy origin such that $H_0|\Phi\rangle = 0$, $c_{i\uparrow}^\dagger$ and $c_{f\uparrow}^\dagger$ creation operators for spin-up electrons near the Fermi level,

$$|\Phi_i\rangle = c_{i\uparrow}^\dagger |\Phi\rangle, \quad |\Phi_f\rangle = c_{f\uparrow}^\dagger |\Phi\rangle.$$

One obtains the scattering amplitude $U_{fi} = \langle \Phi_i | U | \Phi_f \rangle$, still an operator in impurity spin space, by the $T \text{ exp}$ formula in the interaction picture (2.36)

$$\begin{aligned} U_{fi} &= \delta_{if} - i \int_0^\infty \langle i | H_K(\tau) | f \rangle d\tau \\ &+ \frac{(-i)^2}{2} \int_0^\infty d\tau_1 \int_0^{\tau_1} d\tau_2 \langle i | H_K(\tau_1) H_K(\tau_2) | f \rangle + \dots \end{aligned} \quad (5.75)$$

The first-order integral gives $2\pi\delta(\omega_{if})(H_K)_{if}$, that is, an energy-independent object. The second-order contribution, introducing a complete set, reads

$$U_{fi}^{(2)} = -\frac{1}{2} \int_0^\infty d\tau_1 \int_0^{\tau_1} d\tau_2 e^{i(\epsilon_f\tau_1 - \epsilon_i\tau_2)} \sum_\nu (H_K)_{f\nu} (H_K)_{\nu i} e^{iE_\nu(\tau_2 - \tau_1)};$$

using a convergence factor at t_0 , $\int_{-\infty}^{\tau_1} d\tau_2 e^{i(E_\nu - \epsilon_i)\tau_2} = \frac{e^{i(E_\nu - \epsilon_i)\tau_1}}{i(E_\nu - \epsilon_i)}$,

$$U_{fi}^{(2)} \propto (-i)^2 2\pi\delta(\omega_{fi}) \frac{1}{i} \sum_\nu \frac{(H_K)_{f\nu} (H_K)_{\nu i}}{E_\nu - \epsilon_i}.$$

Two kinds of matrix elements $\langle \Phi_f | H_K | \nu \rangle \langle \nu | H_K | \Phi_i \rangle$ occur, with the $c_{i\uparrow}$ operator in the right H_K factor or in the left. The terms with $c_{i\uparrow}$ in the right

$$\sum_{\nu} \frac{\langle \Phi_f | (\boldsymbol{\sigma}_{\uparrow\sigma} \cdot \mathbf{S}) c_{f\uparrow}^{\dagger} c_{q\sigma} | \nu \rangle \langle \nu | (\boldsymbol{\sigma}_{\sigma\uparrow} \cdot \mathbf{S}) c_{q\sigma}^{\dagger} c_{i\uparrow} | \Phi_i \rangle}{E_{\nu} - \epsilon_i};$$

where $|\nu\rangle$ has an electron in a state $q\sigma$, yield, using (5.72),

$$\sum_{q,\sigma} \frac{(1-f_q)}{\epsilon_q - \epsilon_i} (\boldsymbol{\sigma}_{\uparrow\sigma} \cdot \mathbf{S}) (\boldsymbol{\sigma}_{\sigma\uparrow} \cdot \mathbf{S}) = \sum_q \frac{(1-f_q)}{\epsilon_q - \epsilon_i} [S_z^2 + S_- S_+]. \quad (5.76)$$

In the terms with $c_{i\uparrow}$ in the left, the operators appear in the order $c_{q\sigma}^{\dagger} c_{i\uparrow} c_{f\uparrow}^{\dagger} c_{q\sigma}$, so $q\sigma$ must refer to a filled state and $|\nu\rangle$ involve two electrons and a hole:

$$\sum_{\nu} \frac{\langle \Phi_f | (\boldsymbol{\sigma}_{\sigma\uparrow} \cdot \mathbf{S}) c_{q\sigma}^{\dagger} c_{i\uparrow} | \nu \rangle \langle \nu | (\boldsymbol{\sigma}_{\uparrow\sigma} \cdot \mathbf{S}) c_{f\uparrow}^{\dagger} c_{q\sigma} | \Phi_i \rangle}{E_{\nu} - \epsilon_i} = \sum_q \frac{f_q}{\epsilon_q - \epsilon_i} [S_z^2 + S_+ S_-].$$

Since $[S_+, S_-]_- = 2S_z$ the second-order amplitude has a contribution proportional to $\sum_q \frac{f_q}{\epsilon_q - \epsilon_i} S_z$. Neglecting the energy dependence of the density of states, the q summation gives $\sum_q \frac{1}{\epsilon_q - \epsilon_i} \sim \int_{\epsilon_F - W}^{\epsilon_F} d\epsilon_q \frac{1}{\epsilon_q - \epsilon_i}$ where W is the band width.

$$U_{if}^{(2)} \propto S_z \log\left(\frac{|\epsilon_i - \epsilon_F|}{W}\right) \quad (5.77)$$

This gives a logarithmic singularity of the scattering amplitude when ϵ_i approaches the the Fermi energy. For the physical meaning of the S_z factor see Problem 5.4.

5.4 The $N_f \gg 1$ Expansion

Spectroscopically, Ce compounds and heavy fermion materials show deep f levels having widths ~ 0.1 eV, while U is several eV. The above discussion indicates that such a special region of parameter space of the Anderson model is particularly intriguing for studies of magnetism: a deep impurity level is weakly coupled to the Fermi level ($V_k \ll \epsilon_F - \epsilon_d$) and is singly occupied in the limit $V_k \rightarrow 0$. This requires ϵ_d well below the bottom of the band and U large; actually there is a mathematically well defined $U \rightarrow \infty$ limit to study. The density of states will contain structure about $\sim \epsilon_d$ and $\sim 2\epsilon_d + U$, but also about ϵ_F . Since U is large one should resort to some expansion in V_k . Here I shall introduce with some changes and simplifications a method proposed by Gunnarsson and Schönhammer (in a comprehensive paper [27]) to calculate the relevant densities of states. Consider an Anderson-like model, with a local *impurity* level which is N_f times degenerate

$$H = \sum_{k,\sigma} \epsilon_k n_{k\sigma} + \epsilon_f \sum_{\nu}^{N_f} n_{f\nu}$$

$$+ \sum_{k\nu}^{N_f} \left[V_{km} c_{0\nu}^\dagger c_{k\sigma} + h.c. \right] + U \sum_{\nu, \nu'} n_{f\nu} n_{f\nu'}, \quad \nu \equiv \{m, \sigma\}. \quad (5.78)$$

The bottom of the band is at $-B$ and the Fermi energy is $\epsilon_F = 0$. In this problem it is expedient to use a discrete formalism as in Section 5.1.4, i.e. with $\{\epsilon_k\} = \epsilon_1, \epsilon_2, \dots$ and Kronecker deltas, and to go to the continuum limit at the end. Let us assume

$$\begin{aligned} \sum_k V_{mk} V_{km'} \delta_{\epsilon, \epsilon_k} &\equiv |\tilde{W}(\epsilon)|^2 \delta_{mm'}, \\ \sum_m V_{mk} V_{k'm} \delta_{\epsilon, \epsilon_k} &\equiv |\tilde{W}(\epsilon)|^2 \delta_{kk'} \end{aligned} \quad (5.79)$$

with the energy \tilde{W} linear in the hopping parameters. The U term fails to account for the multiplet effects, but this has no consequence since the occupation of the impurity is $n_d \leq 2$. Introducing the degeneracy, the model becomes both more realistic *and* more tractable. The reason is that (as expected *a priori* and verified below) each degenerate state gives equal contributions to the ground state energy shift ΔE , so for deep impurity levels

$$\Delta E = N_f \frac{\tilde{W}^2}{\epsilon_f}, \quad (5.80)$$

where \tilde{W}^2 is some average of $\tilde{W}(\epsilon)$. Thus, ΔE is fixed (it corresponds anyhow to a weak chemical interaction), $N_f \rightarrow \infty$ is a weak coupling limit, and we can set up an expansion in inverse powers of N_f . We need the right combinations of conduction states that couple to the impurity, and introduce new conduction operators with the same symmetry as the impurity m orbital⁶:

$$\psi_{\epsilon m \sigma}^\dagger = \frac{1}{\tilde{W}(\epsilon)} \sum_k V_{mk} \delta_{\epsilon, \epsilon_k} c_{k\sigma}^\dagger \quad (5.81)$$

and a combined index $\nu \equiv \{m, \sigma\}$. Equations (5.79) yields

$$[\psi_{\epsilon m \sigma}^\dagger, \psi_{\epsilon' m' \sigma'}]_+ = \delta_{\epsilon, \epsilon'} \delta_{\nu, \nu'}.$$

Then, letting $\int d\epsilon$ stand for the discrete energy summation (that will become continuous at the end)

$$\sum_{m\sigma} \int d\epsilon \epsilon \psi_{\epsilon m \sigma}^\dagger \psi_{\epsilon m \sigma} = \sum_{m\sigma} \sum_{k1k2} \frac{\epsilon_{k1} V_{k1m} \delta(\epsilon_{k2} - \epsilon_{k1}) V_{mk2}}{\tilde{W}^2(\epsilon_{k1})} c_{k1\sigma}^\dagger c_{k2\sigma}; \quad (5.82)$$

now using the second of (5.79), one arrives at the useful form

$$\begin{aligned} H = \sum_{\nu}^{N_f} \left[\int d\epsilon \epsilon \psi_{\epsilon\nu}^\dagger \psi_{\epsilon\nu} + \int d\epsilon \left(\tilde{W}(\epsilon) c_{0\nu}^\dagger \psi_{\epsilon\nu} + h.c. \right) \right. \\ \left. + \epsilon_f c_{0\nu}^\dagger c_{0\nu} \right] + U \sum_{\{\nu, \nu'\}} n_{f\nu} n_{f\nu'} + \text{extra terms} \end{aligned} \quad (5.83)$$

⁶here unlike Ref [27] I use dimensionless the creation operators

where $\sum_{\{\nu, \nu'\}}$ is over distinct pairs and the extra terms describe conduction states that are not coupled to the impurity. We shall see that the ground state can be calculated exactly for $U \rightarrow \infty, N_f \rightarrow \infty$. We start by calling $|\phi_0\rangle$ the ground state of H and $|\Omega\rangle$ the singlet state with a filled shell of k states up to ϵ_F and empty impurity states; let

$$\langle \phi_0 | H | \phi_0 \rangle = E_0, \quad \langle \Omega | H | \Omega \rangle = E_0^0, \quad \Delta E = E_0 - E_0^0. \quad (5.84)$$

Henceforth the many-body energies will be referenced to the constant E_0^0 . By acting on $|\Omega\rangle$ with the hopping term in the hamiltonian we produce electron-hole states $|f, \bar{\epsilon}\rangle$ with one electron on a superposition of the impurity states $|0m\sigma\rangle$ and a hole in the conduction band at some occupied energy ϵ ; denoting holes with bars one writes a particle-hole state as

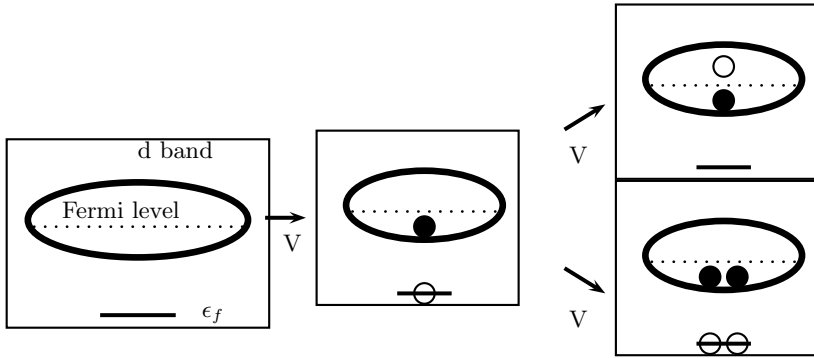


Fig. 5.6. Left: lowest state $|\Omega\rangle$ with no occupation of the f state. Center: hopping leads from $|\Omega\rangle$ to a state with a single occupation of the f state. The full circle represents a hole and the empty one a f electron: this configuration would be the ground state for $V \rightarrow 0$ for the hole at the Fermi level. Right: further hopping may lead to two kind of configurations: 1) a state $|E, \bar{\epsilon}\rangle$ with no electrons in the f state and an electron-hole pair in the valence band (upper panel) 2) a state $|f, f', \bar{\epsilon}, \bar{\epsilon}'\rangle$ with a double f hole (lower panel). For large U , however the latter is excluded, while the coupling to $|E, \bar{\epsilon}\rangle$ is negligible for large N_f . Thus, when both conditions hold, one can solve the problem exactly.

$$|f, \bar{\epsilon}\rangle = \frac{1}{\sqrt{N_f}} \sum_{\nu} c_{0\nu}^{\dagger} \psi_{\epsilon\nu} |\Omega\rangle. \quad (5.85)$$

Note that $\langle f, \bar{\epsilon} | f, \bar{\epsilon} \rangle = 1$, $\langle f, \bar{\epsilon} | H | f, \bar{\epsilon} \rangle = \epsilon_f - \epsilon$. To find the coupling to $|\Omega\rangle$ we insert (5.81) in (5.85), obtain

$$H|\Omega\rangle = E_0^0|\Omega\rangle + \sum_{k\nu} V_{km} c_{0\nu}^{\dagger} c_{k\sigma} |\Omega\rangle \quad (5.86)$$

by the form (5.78) of the Hamiltonian, and take the scalar product. The nonvanishing contributions are those where the creation and annihilation operators match; then, using (5.79) one performs the k summation introducing $|\tilde{W}|^2$; the m summation then introduces a N_f factor yielding

$$\langle \Omega | H | f, \bar{\epsilon} \rangle = \frac{1}{\sqrt{N_f}} \sum_k \sum_\nu^{N_f} \frac{|V_{km}|^2 \delta(\epsilon - \epsilon_k)}{\tilde{W}(\epsilon)} = \tilde{W}^*(\epsilon) \sqrt{N_f}; \quad (5.87)$$

If we act over (5.85) with the hopping term of the hamiltonian we generate new states:

$$H | f, \bar{\epsilon} \rangle \Rightarrow | E, \bar{\epsilon} \rangle, | f, f', \bar{\epsilon}, \bar{\epsilon}' \rangle; \quad (5.88)$$

here,

$$| E, \bar{\epsilon} \rangle = \frac{1}{\sqrt{N_f}} \sum_{m, \sigma} \psi_{E\nu}^\dagger \psi_{\epsilon\nu} | \Omega \rangle \quad (5.89)$$

has a conduction electron with energy $E > E_F$ and keeps the $\bar{\epsilon}$ hole while $| f, f', \bar{\epsilon}, \bar{\epsilon}' \rangle$ has two impurity electrons and two conduction holes and is ruled out as $U \rightarrow \infty$. Since the normalized states $| E, \bar{\epsilon} \rangle$ and $| f, \bar{\epsilon} \rangle$ both bring a $\frac{1}{\sqrt{N_f}}$ factor, their coupling goes like $|\tilde{W}|^2$ and thus vanishes as $N_f \rightarrow \infty$ because of (5.80). Therefore, in that case the problem reduces to the one hole subspace, that is, the ground state may be sought in the form

$$| \phi_0 \rangle = A \left[| \Omega \rangle + \int_{-B}^0 a(\epsilon) | f, \bar{\epsilon} \rangle d\epsilon \right]; \quad (5.90)$$

here $\int_{-B}^0 d\epsilon$ provisionally stands for a discrete summation over the band energies and everything is dimensionless. We write the Schrödinger equation on a basis set

$$\{ | \Omega \rangle, | f, \bar{\epsilon}_1 \rangle, | f, \bar{\epsilon}_2 \rangle, \dots \}$$

with eigenvectors

$$v = (1, a(\epsilon_1), a(\epsilon_2), \dots) \quad (5.91)$$

acted by the Hamiltonian matrix (recalling (5.87))

$$H_M = \begin{pmatrix} 0 & \sqrt{N_f} \tilde{W}^*(\epsilon_1) & \sqrt{N_f} \tilde{W}^*(\epsilon_2) & \dots \\ \sqrt{N_f} \tilde{W}(\epsilon_1) & \epsilon_f - \epsilon_1 & 0 & \dots \\ \sqrt{N_f} \tilde{W}(\epsilon_2) & 0 & \epsilon_f - \epsilon_2 & \dots \\ \dots & \dots & \dots & \dots \end{pmatrix}. \quad (5.92)$$

The first line of $H_M v = \Delta E v$ gives

$$\Delta E = \sqrt{N_f} \int_{-B}^0 d\epsilon \tilde{W}^*(\epsilon) a(\epsilon), \quad (5.93)$$

the second and any other line yield

$$\sqrt{N_f} \tilde{W}(\epsilon) = (\Delta E - \epsilon_f + \epsilon)a(\epsilon). \quad (5.94)$$

Hence,

$$\Delta E = N_f \int_{-B}^0 d\epsilon \frac{|\tilde{W}(\epsilon)|^2}{\Delta E - \epsilon_f + \epsilon} \quad (5.95)$$

is indeed proportional to N_f , as anticipated. Moreover, the normalization condition of (5.91) reads

$$|A|^2 = \frac{1}{1+C}, \quad C = \int_{-B}^0 d\epsilon a^2(\epsilon) = N_f \int_{-B}^0 d\epsilon \left(\frac{\tilde{W}(\epsilon)}{\Delta E - \epsilon_f + \epsilon} \right)^2, \quad (5.96)$$

where again $-B$ is the bottom of the band. The occupation of the impurity is

$$n_f = \frac{C}{1+C}, \quad (5.97)$$

and when $C \gg 1$ (spin fluctuation limit) n_f is close to 1. Equations (5.95,5.96,5.97) remain the same in the continuum limit, when however the Kronecker deltas over energy become Dirac's delta functions and hence

$$\Delta = \pi \tilde{W}^2 \quad (5.98)$$

is the inverse life time due to hopping, a the inverse root of an energy, and so on. Typically, $\Delta \sim 0.1eV$.

5.4.1 Kondo Temperature in the Spin-Fluctuation Case

ΔE is the energy shift with respect to $|\Omega\rangle$, but one is more interested in the Kondo temperature

$$K_B T_K = \delta = \epsilon_f - \Delta E > 0, \quad (5.99)$$

which is the correlation-induced energy gain with respect to the non-interacting lowest eigenvalue of $|f, \bar{\epsilon}\rangle$ levels. In the spin fluctuation case, when $n_f \sim 1$, a reasonable model takes constant \tilde{W}^2 and assumes that $B \gg \delta$; then, setting in (5.95,5.96) $\tilde{W}^2 = \frac{\Delta}{\pi}$, we find

$$\Delta E = \frac{N_f \Delta}{\pi} \ln \left| \frac{\Delta E - \epsilon_f}{B} \right| = \frac{N_f \Delta}{\pi} \ln \left| \frac{\delta}{B} \right| \quad (5.100)$$

and

$$\frac{n_f}{1-n_f} = C = \frac{N_f \Delta}{\pi |\delta|}. \quad (5.101)$$

One obtains from (5.100),

$$\delta = B e^{\frac{\pi \Delta E}{N_f \Delta}};$$

we expect the result to be roughly proportional to $N_f \Delta$ so we introduce this dependence, using (5.99) to eliminate ΔE :

$$\delta = \left(\frac{N_f \Delta}{\pi}\right) \left(\frac{\pi B}{N_f \Delta}\right) e^{\frac{\pi(\epsilon_f - \delta)}{N_f \Delta}} = \left(\frac{N_f \Delta}{\pi}\right) e^{\ln\left[\frac{\pi B}{N_f \Delta}\right] + \frac{\pi(\epsilon_f - \delta)}{N_f \Delta}}.$$

This can be rewritten

$$\delta = \left(\frac{N_f \Delta}{\pi}\right) e^{\frac{\pi}{N_f \Delta} \{(\epsilon_f - \delta) + \frac{N_f \Delta}{\pi} \ln\left[\frac{\pi B}{N_f \Delta}\right]\}} \longrightarrow \delta = \left(\frac{N_f \Delta}{\pi}\right) e^{\frac{\pi(\epsilon_f^* - \delta)}{N_f \Delta}}, \quad (5.102)$$

with the renormalized f level

$$\epsilon_f^* = \epsilon_f + \frac{N_f \Delta}{\pi} \ln\left(\frac{\pi B}{N_f \Delta}\right). \quad (5.103)$$

In the Kondo problem the exponent $\frac{\pi(\epsilon_f^* - \delta)}{N_f \Delta} \sim \frac{\pi \epsilon_f^*}{N_f \Delta}$ is large and negative and the Kondo temperature is given by

$$\delta = \left(\frac{N_f \Delta}{\pi}\right) e^{-\frac{\pi|\epsilon_f^*|}{N_f \Delta}}. \quad (5.104)$$

The population of the f level can be deduced from (5.101), which says that $\frac{n_f}{1-n_f} = \frac{N_f \Delta}{\pi \delta}$. Since n_f is close to 1, the solution is well approximated by

$$1 - n_f = e^{-\frac{\pi|\epsilon_f^*|}{N_f \Delta}}. \quad (5.105)$$

5.4.2 Density of Occupied States

To obtain the density of filled states relevant e.g. for valence photoemission (see next Chapter) we need the $g^<(z)$ Green's function. So, we introduce a (sufficiently) complete set $\{|j\rangle\}$ of many body states and write

$$g^<(z) = \sum_{i,j} \langle \phi_0 | c_{m\sigma}^\dagger | i \rangle \langle i | \frac{1}{z - E_0(N) + H} | j \rangle \langle j | c_{m\sigma} | \phi_0 \rangle. \quad (5.106)$$

One can compute the matrix elements $\langle i | z - H | j \rangle$ without difficulty and then obtain $\langle i | \frac{1}{z - E_0(N) + H} | j \rangle$ by a matrix inversion in analogy with Anderson's procedure used above in Sect. (5.1.2). For large U and N_f one can limit the analysis to the above approximation; the relevant states are the one-hole states

$$|\overline{\epsilon m \sigma}\rangle = \psi_{\epsilon m \sigma} |\Omega\rangle, \quad (5.107)$$

such that $\langle \overline{\epsilon' m' \sigma} | \overline{\epsilon m \sigma} \rangle = \delta(\epsilon - \epsilon')$, and impurity electron -two hole states, namely,

$$|0m'\sigma', \overline{\epsilon_1 m_1 \sigma_1}, \overline{\epsilon_2 m_2 \sigma_2}\rangle = \frac{c_{0m'\sigma'}^\dagger}{\sqrt{N_f - 1}} \sum_{\text{pairs}} \psi_{\epsilon_2 m_2 \sigma_2} \psi_{\epsilon_1 m_1 \sigma_1} |\Omega\rangle. \quad (5.108)$$

Here, \sum_{pairs} sums over different m, σ channels (the normalization is to $N_f - 1$ since the case of $\{m_1, \sigma_1\} = \{m_2, \sigma_2\}$ is excluded, but 1 is negligible compared to N_f). $|\overline{\epsilon m \sigma}\rangle$ is eigenstate of $\sum_{\nu}^{N_f} \int d\epsilon \epsilon \psi_{\epsilon\nu}^{\dagger} \psi_{\epsilon\nu}$ with eigenvalue $E_0^0 - \epsilon$; inspection of (5.83) and (5.84) then shows that

$$\langle \overline{\epsilon' m \sigma} | z - E_0 + H | \overline{\epsilon m \sigma} \rangle = \delta(\epsilon - \epsilon')(z - \Delta E - \epsilon) \quad (5.109)$$

$$\begin{aligned} \langle 0m'\sigma', \overline{\epsilon_1 m_1 \sigma_1}, \overline{\epsilon_2 m_2 \sigma_2} | z - E_0 + H | 0m'\sigma', \overline{\epsilon'_1 m_1 \sigma_1}, \overline{\epsilon'_2 m_2 \sigma_2} \rangle \\ = \delta(\epsilon_1 - \epsilon'_1) \delta(\epsilon_2 - \epsilon'_2) (z - \Delta E - \epsilon_1 - \epsilon_2 + \epsilon_f) \end{aligned} \quad (5.110)$$

The hopping Hamiltonian takes from the one-hole subspace to a two-holes-impurity-electron one; so the matrix inversion is easy, using the method of Sect. 5.1.6 which puts a self-energy in the denominator of the inverse of (5.109); giving

$$\langle \overline{\epsilon' m \sigma} | (z - E_0 + H)^{-1} | \overline{\epsilon m \sigma} \rangle = \frac{\delta(\epsilon - \epsilon')}{z - \Delta E - \epsilon - N_f \int_{-B}^0 \frac{d\xi |\overline{W}(\xi)|^2}{z - \Delta E + \epsilon_f - \epsilon - \xi}}. \quad (5.111)$$

The Kondo peak is borne out by this analysis.

Lacroix [21] using the equation of motion approach computed the density of states of the Anderson model for $U \rightarrow \infty$ by the equation of motion technique, and obtained the Kondo peak and its disappearance above the Kondo temperature.

Problems

5.1. Find by direct matrix inversion $G_{00}(\omega)$ as the 00 element of $(\omega - h)^{-1}$, with the matrix of h from Equation (5.3). This is instructive and very easy!

5.2. Prove Equation (13.136).

5.3. Find the other elements of the resolvent matrix by the method used in the text for G_{00} .

5.4. What does the S_z factor in (5.77) mean?

5.5. Prove Equation (13.136).

6 Many-body Effects in Electron Spectroscopies

6.1 Electron Spectroscopy for Chemical Analysis (ESCA)

Electron spectroscopies and their rich phenomenology convey information on molecules and solids and specifically on their excitations. To describe excited states we shall develop techniques based on modeling the spectra in terms of Green's functions and also more general expectation values. ESCA is a set of spectroscopies, UPS (Ultraviolet Photoemission Spectroscopy), XPS (X-Ray Photoemission Spectroscopy) and AES (Auger Electron Spectroscopy). They can be angular resolved (ARUPS and the like) and time resolved; APECS (Auger Photoelectron Coincidence Spectroscopy) detects the photoelectron and the Auger electron most probably coming from the same atom. ESCA can make a chemical analysis with tiny samples and is able to discriminate the oxidation states and give information about the electronic structure.

In an ESCA apparatus, the sample is excited with monochromatic radiation (X-rays in the case of X-ray Photoemission Spectroscopy or XPS, Ultraviolet light in the case of UPS) and the photoelectrons are analyzed in energy by a spherical or cylindrical analyzer. A photoemission spectrum is a plot of the photoelectron current versus photoelectron kinetic energy. In [94] the XPS spectra of noble gas atoms and of several molecules are reported and discussed. Core levels, with a well resolved spin-orbit separation, and valence levels are observed; they often (but not always) agree qualitatively with the results of Hartree-Fock calculations. However, correlation effects, (that require the methods of Chapter 11 and following Chapters for a microscopic description) are most often clearly seen. Many core and valence levels show a complex structure due to *shake-up* effects (excitations) or *shake-off* effects, if the excitations involve a continuum. The Xe 4p level seen in photoemission (see e.g. [95]) shows a broad continuum with sharp superimposed features in striking contrast with one-particle descriptions, predicting a doublet of lines.

The interaction of the sample with the radiation is

$$H' = \frac{-e}{2mc} \sum_i^N [\mathbf{A}(\mathbf{x}_i) \cdot \mathbf{p}_i + \mathbf{p}_i \cdot \mathbf{A}(\mathbf{x}_i)], \quad (6.1)$$

where N is the number of electrons and \mathbf{A} the vector potential. One also often finds an alternative formulation, that comes directly from the relativistic theory, namely

$$H' = -\frac{1}{c}2mc \sum_i^N \int d^3x \mathbf{A}(\mathbf{x}_i) \cdot \hat{\mathbf{j}}(\mathbf{x}_i) = \sum_{mn} M_{mn} a_m^\dagger a_n \quad (6.2)$$

where the current operator is (4.23); in the second-quantized form, \sum_{mn} runs over an arbitrary complete orthonormal set of one-body states (the set of Hartree-Fock spin-orbitals is a convenient choice). Let $|i\rangle$, E_i denote the initial state of the sample and its energy, $\hbar\omega$ and ϵ_k the photon and photoelectron energies. The cross section σ can be worked out starting from the Fermi golden rule

$$\Delta\sigma = \frac{2\pi}{\hbar} \sum_f |\langle f|H'|i\rangle|^2 \delta(\hbar\omega + E_i - E_f) \quad (6.3)$$

where $|f\rangle$, ϵ_f are the final state of the sample and its energy. For the sake of simplicity we shall consider the case of fast photoelectrons, when we can neglect the *post-collisional interaction* between the photoelectron and the ion left behind. We let \tilde{H} be the N-1-electron Hamiltonian of the sample after photoionization, with $\tilde{H}|\tilde{f}\rangle = \tilde{E}_f|\tilde{f}\rangle$ and write $E_f = \epsilon_k + \tilde{E}_f$. The photoelectron state can be approximately described as a plane-wave of wave vector \mathbf{k} , and $|f\rangle = a_{\mathbf{k}}^\dagger|\tilde{f}\rangle$, where $|\tilde{f}\rangle$ is the N-1-electron final state of the sample¹. Moreover, $\sum_f = \sum_{\tilde{f}} \sum_{\mathbf{k} \in \Delta\Omega}$, where the sum over the wave vectors accepted by the detector in the solid angle $\Delta\Omega$, namely $\sum_{\mathbf{k} \in \Delta\Omega} \propto \rho(\epsilon_{\mathbf{k}})\Delta\Omega$ is the density of final states of the photoelectron $\propto \sqrt{\epsilon_{\mathbf{k}}}$.

Then the cross section reads

$$\frac{\Delta\sigma}{\Delta\Omega} = \frac{2\pi}{\hbar} \rho(\epsilon_{\mathbf{k}}) \sum_{\tilde{f}} \left| \sum_m \langle \tilde{f}|a_m|i\rangle \right|^2 \delta(E_i - E_{\tilde{f}} - \epsilon_{\mathbf{k}} - \hbar\omega). \quad (6.4)$$

The highest kinetic energy features in the photoemission spectrum correspond to events when the system is left at or near the ground state; lower kinetic energy features correspond to excited states of the system left behind, and this occurs by energy conservation, without the need for a post-collisional interaction². Proceeding as in (4.6) one can write this in terms of the hole Green's function

$$G_{mn}(\omega) = \langle i|a_n^\dagger \frac{1}{\omega - \tilde{H} + i0^+} a_m|i\rangle. \quad (6.5)$$

¹Due to the long range of the Coulomb potential, one should use Coulomb waves, but at high kinetic energy one has a good excuse for using plane waves instead.

²The outgoing electron can lose energy by collisions, producing secondary electrons; this is not contained in the above simplified description; the spectrum far from threshold when such effects are important becomes difficult to analyze.

6.1.1 Chemical Shifts

The core level binding energies depend on the charge on the atom and change with the chemical state. For example, the Xenon fluorides XeF_2 , XeF_4 and XeF_6 are colorless solids melting at 140, 114 and 46 °C, respectively; their F and Xe core levels are shifted by some eV along the series. The F 1s level is 5.48 eV less bound in XeF_2 than in F_2 ; this difference reduces to 4.6 eV in XeF_4 and to 3.38 eV, in XeF_6 , while the negative charge on the Fluorine is reduced. The Xe levels shift in the opposite way, even more: the binding energy grows if there is positive charge on the atom. A clear linear correlation exists between the binding energies of the levels and the overall charges of atoms, determined by self-consistent calculations. In a similar way, the 1s levels of C in CH_3Br , CH_2Br_2 , $CHBr_3$, CBr_4 shift compared to CH_4 . Many organic molecules contain in-equivalent C atoms and their core peaks can be resolved .

The chemical shifts are due to a combination of *initial state effects* and *final state effects* . The former are those just mentioned above due to the mean electrostatic potential on the atom in the ground state; depending on the chemical environment, a core level can be more or less tightly bound than in the free atom. The final state effects are due to the polarization of the system around the core hole and are of the same order of magnitude, i.e. several eV. However, they always reduce the binding energy since they stabilize the final state of the sample and the energy is taken off by the photoelectron. From the the chemical shifts it is often possible to deduce the valence of given atom in a compound. This is relevant to elements like transition metals that can have different valence in different compounds.

6.1.2 Core-Level Splitting in Paramagnetic Molecules

The ground electronic configuration of the NO molecule is

$$O1s^2 N1s^2 1\sigma^2 2\sigma^2 1\pi^4 3\sigma^2 2\pi^1;$$

the ground state is a spin doublet and NO^+ has singlet and triplet states. The ground state of O_2 is $^3\Sigma_g$, with a configuration

$$1s^2 \sigma_g(2s)^2 \sigma_u(2s)^2 \sigma_g(2p)^2 \pi_u(2p)^4 [\pi_g(2p)^1]^2$$

with two partially filled π_g states. In both cases this produces a core-level splitting[94]. In N_2 the 1s level has a binding energy ~ 410 eV and is ~ 0.9 eV wide at half maximum; the same level in NO has one component which is less bound than in N_2 by a fraction of eV and is about as wide, but there is also a second component which is more bound by ~ 1.5 eV. The intensity ratio is 3:1. The O level is not resolved in Siegbahn's data but is 0.3 eV broader than in O_2 . To simplify the notation, let us write the degenerate ground determinantal states by

$$\Psi(NO) = \begin{cases} |\pi\alpha s\alpha s\beta\rangle, & s_z = \frac{1}{2} \\ |\pi\beta s\alpha s\beta\rangle, & s_z = \frac{-1}{2} \end{cases} \quad (6.6)$$

omitting filled shells; s denotes the $1s$ level of O or N, according to the process that we wish to describe. For NO^+ we must consider

$$\Psi(NO^+) = \begin{cases} |\pi\alpha s\alpha\rangle, & s_z = 1 \\ |\pi\alpha s\beta\rangle, |\pi\beta s\alpha\rangle, & s_z = 0 \\ |\pi\beta s\beta\rangle, & s_z = -1. \end{cases} \quad (6.7)$$

All these states have $\Lambda = |L_z| = 1$, where z is the internuclear axis, but not all are spin eigenstates. The singlet is

$$\psi(^1\Pi) = \frac{1}{\sqrt{2}}[|\pi\alpha s\beta\rangle - |\pi\beta s\alpha\rangle]; \quad (6.8)$$

the triplet states are:

$$\psi(^3\Pi) = \begin{cases} |\pi\alpha s\alpha\rangle, & s_z = 1 \\ \frac{1}{\sqrt{2}}|\pi\alpha s\beta\rangle + |\pi\beta s\alpha\rangle, & s_z = 0 \\ |\pi\beta s\beta\rangle, & s_z = -1. \end{cases} \quad (6.9)$$

Let us write the total energy of the states with $s_z=0$; since

$$H = \sum_i h_i + \sum_{i<j} \frac{1}{r_{ij}}, \quad (6.10)$$

does not depend on spin and $\langle\alpha\beta|H|\alpha\beta\rangle = \langle\beta\alpha|H|\beta\alpha\rangle$, one finds:

$$\begin{aligned} E(^1\Pi) &= \langle|\pi\alpha s\beta\rangle|H||\pi\alpha s\beta\rangle - \langle|\pi\alpha s\beta\rangle|H||\pi\beta s\alpha\rangle, \\ E(^3\Pi) &= \langle|\pi\alpha s\beta\rangle|H||\pi\alpha s\beta\rangle + \langle|\pi\alpha s\beta\rangle|H||\pi\beta s\alpha\rangle. \end{aligned}$$

In the calculation of $\langle|\pi\alpha s\beta\rangle|H||\pi\beta s\alpha\rangle$, since the two determinants differ by 2 spin-orbitals, there is no contribution from the one-body Hamiltonian; the splitting is $\Delta E = 2J$, where

$$J = \langle|\pi\alpha s\beta\rangle|\frac{1}{r_{12}}||\pi\beta s\alpha\rangle \quad (6.11)$$

is the exchange integral. Hartree-Fock calculations give $\Delta E(N) = 0.88$ eV, $\Delta E(O) = 0.68$ eV. The lowest state is triplet. This agrees with the observation that the peak at lower binding energy is 3 times more intense.

In a similar way, the $1s$ spectrum of O_2 (binding energy ~ 547 eV) has two components separated by 1.1 eV with an intensity ratio 2:1. From the $^3\Sigma_g$ ground state one can go to $^4\Sigma$ and $^2\Sigma$ ions. Let π^\pm represent the π orbitals with $L_z = \pm 1$. From the ground state with components $\psi(^3\Sigma_g) = |\pi^+\alpha\pi^-\alpha\rangle, s_z = 1$

$$\psi(^3\Sigma_g) = \begin{cases} |\pi^+\alpha\pi^-\alpha|, & s_z = 1 \\ \frac{1}{\sqrt{2}}[|\pi^+\alpha\pi^-\beta| + |\pi^+\beta\pi^-\alpha|], & s_z = 0 \\ |\pi^+\beta\pi^-\beta|, & s_z = -1 \end{cases}$$

To write the final state, let us include the unpaired 1s level (that in the initial state was understood with the other closed-shell states). 6 states are found, including the $s_z = \frac{3}{2}$ component of $^4\Sigma$, namely, $\psi(^4\Sigma) = |\pi^+\alpha\pi^-\alpha s\alpha|$. The other components of $^4\Sigma$ are easily obtained by the S^- operator and the doublet $^2\Sigma$ by orthogonality. In this way one explains the splitting, which is again due to an exchange interaction.

6.1.3 Shake-up, Shake-off, Relaxation

In the final state of core-level photoemission, a localized hole exists, producing a field and a polarization of the system. The polarization phenomena are not included in independent particles theory. However, they are commonly observed: they shift the levels towards lower binding energies. The final state effects show up in the spectrum also with the presence of satellite peaks. The electron contribute to the relaxation shift, since the *spectator* electrons actually are involved in some measure in the photoemission process; there is some probability that the ion is left, in the final state, excited. We can adapt the independent particles theory in order to include some correlation effects, by using different orbitals for the initial and final states. Neglecting the energy dependence of the density of states $\rho(\epsilon_k)$ and of the matrix elements, the shape of the photoelectron spectrum from a deep level $|c\rangle$ is given by

$$\sigma(\omega) = -\frac{1}{\pi}\text{Im}G_c(\omega) = \langle i|a_c^\dagger\delta(\omega - H)a_c|i\rangle = \langle i;c|\delta(\omega - H)|i;c\rangle, \quad (6.12)$$

where $|i;c\rangle = a_c|i\rangle$ is the N-1 electrons state that is obtained from the initial state $|i\rangle$ by creating the core hole but holding the orbitals frozen. We calculate $|i\rangle$ in the Hartree-Fock approximation for the neutral sample; under known conditions $|i;c\rangle$ is a single Slater determinant. Introducing the eigenstates $|\nu\rangle$ and eigenvalues ϵ_ν of H with N-1 electrons, we find

$$\sigma(\omega) = \sum_{\nu} |\langle i;c|\nu\rangle|^2 \delta(\omega - \epsilon_\nu). \quad (6.13)$$

However, the $|\nu\rangle$ eigenstates must be calculated in the presence of the core-hole, that is, as determinants formed with relaxed spin-orbitals. We can obtain them too by the Hartree-Fock approximation using an excited N-1 electron configuration with the core electron missing³. Since the overlap of determinants is the determinant of overlaps (Equation 1.5) all the many-body $|\nu\rangle$

³Unfortunately, this approximation has the shortcoming that the excited state is not orthogonal to the ground N-1 electron state or to the lower states of the same symmetry. This is a general drawback of the Hartree-Fock approximation.

states contribute to the summation, each yielding a peak at its eigenvalue. The discrete ones yield narrow shake-up peaks, while those in the continuum contribute broad shake-off structures. Remarkably, the first two moments of the spectrum give

$$\int_{-\infty}^{\infty} d\omega \sum_{\nu} |\langle i; c | \nu \rangle|^2 \delta(\omega - \epsilon_{\nu}) = 1 \quad (6.14)$$

and

$$\int_{-\infty}^{\infty} d\omega \omega \sum_{\nu} |\langle i; c | \nu \rangle|^2 \delta(\omega - \epsilon_{\nu}) = \langle i; c | H | i; c \rangle. \quad (6.15)$$

The excitation of satellites exactly balances the relaxation shift. The 1s spectrum of Ne is rich of satellites (see next Figure).

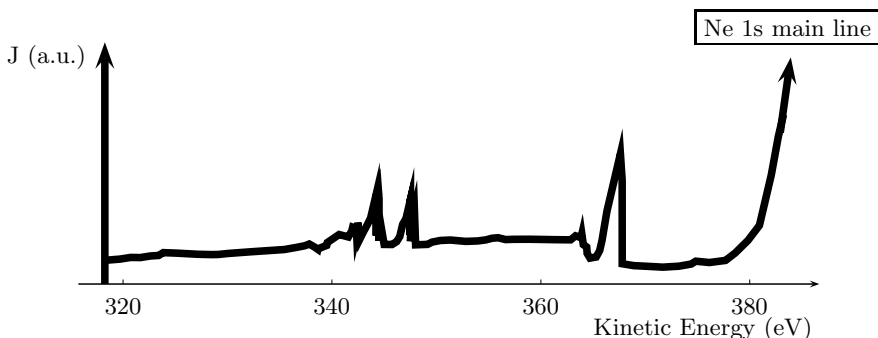


Fig. 6.1. Sketch of the satellite region of the Ne 1s photoemission spectrum (data from Ref. ([94])). The peak in the extreme right at 383 eV kinetic energy is due to 1s holes in the final state; the satellites occur at lower kinetic energy because the Ne^+ ion is left in an excited state. Several satellites are due to states of the $2p^5 np^1 {}^2S$ final configurations, with $n=3, 4, 5, \dots$. The most intense satellites are some 20 times smaller than the main line, since Ne is a filled-shell system with low polarizability.

Besides the single particle excitations, other excitations of the system, like vibrations and plasmons, that can be treated like harmonic oscillators (bosons) contribute to the relaxation energy and to the shake-up spectrum.

The time scale of vibrations is $\sim 10^{-13}s$; typically the dipole-allowed electronic transitions take much shorter than that and according to the Franck-Condon principle the nuclei *do not have time to move during the transition*. Since the equilibrium bond lengths and angles of the ions are different from the initial neutral species, the ion is left in an excited vibrational state. This is easily visualized in the case of bi-atomic molecules by plotting the potential energy surfaces of the neutral molecule and of the ion versus internuclear

distance. The energy of the transition between the vibrational ground states of two electronic states of the neutral species and of the ion is called *adiabatic ionization energy*. The satellites are on the high binding energy side and appear as energy losses; they correspond to vibrationally excited ions in the final state. The energy spacing between satellites is the vibration energy of the ion, which differs from that of the neutral species.

When the equilibrium distances differ slightly compared to the widths of the Gaussian wave functions, there is a high probability to end up in the vibrational ground state of the ion, and this corresponds the most intense peak in the photoemission spectrum. The satellites are small and fast decreasing. On the other hand, if the change in equilibrium distance is large, the intensity of the adiabatic transition is small, the spectrum has many lines of comparable intensities and appears almost continuous, with an intensity maximum at the *vertical ionization energy*, i.e. the energy difference between the two potential energy surfaces at the ground state bond length. To assign the peaks in the photoemission spectrum, an important hint comes from the vibrational structure; this is much more intense for bonding than nonbonding or core levels.

6.1.4 Lundqvist Model of Phonon and Plasmon Satellites

The coupling of a core electron to a vibrational mode affects the Photoemission line shape. To model the vibration, consider a single Boson mode of frequency $\nu_0 = \frac{\omega_0}{2\pi}$ with vibration coordinate x ; in this way we disregard the difference between the initial and final state frequencies, but such details are readily fixed if necessary. Before the photoemission event, the harmonic potential of the vibration of the ion can be written $V(x) = \frac{1}{2}M\omega_0^2x^2$ and has a minimum for $x = 0$. The initial state Hamiltonian of the vibration is

$$H_0 = \omega_0 d^\dagger d, \quad (6.16)$$

with $[d, d^\dagger]_- = 1$; the initial state $|i\rangle$ is the vacuum, $|i\rangle = |0_d\rangle$, and the excited eigenstates are

$$|n_d\rangle = \frac{1}{\sqrt{n!}} d^n |0_d\rangle. \quad (6.17)$$

The photo-ionization produces a sudden change in the Hamiltonian; the potential is still harmonic, but the minimum is shifted. For a harmonic potential, the shift $x \rightarrow x + \Delta$ produces a change $V(x) \rightarrow V(x) + M\omega_0^2x\Delta$ apart from a constant $\propto \Delta^2$. In second quantization, the new interaction term proportional to x , may be written in the form

$$H_1 = g(d + d^\dagger). \quad (6.18)$$

This is the Lundqvist model discussed by Langreth in a very enlightening paper[39]. In the final-state Hamiltonian $H = H_0 + H_1$ we perform a canonical transformation to new bosons

$$s = d - \gamma, \quad s^\dagger = d^\dagger - \gamma^*, \quad (6.19)$$

with γ to be found; since the canonical transformation is time-independent, the transformed Hamiltonian \tilde{H} is just H written in terms of the s operators,

$$\tilde{H} = \omega_0[s^\dagger s + \gamma s^\dagger + \gamma^* s + |\gamma|^2] + g[s + \gamma + s^\dagger + \gamma^*].$$

We require that there be no terms linear in s or s^\dagger , and obtain

$$\gamma = -\frac{g}{\omega_0}; \quad (6.20)$$

the new Hamiltonian is diagonal:

$$\tilde{H} = \omega_0 s^\dagger s - \frac{g^2}{\omega_0}. \quad (6.21)$$

Note the ground state energy is lowered by the relaxation shift $\Delta E = -\frac{g^2}{\omega_0}$ that pushes the threshold of the photoemission spectrum to higher kinetic energy. Remarkably, treating H_1 in second-order perturbation theory one would obtain the exact result for ΔE . Note that the ground state $|0_s\rangle$ of \tilde{H} is the s vacuum while $|i\rangle$ is the d vacuum⁴. Since

$$d|0_s\rangle = \gamma|0_s\rangle \quad (6.22)$$

that is, $|0_s\rangle$ is an eigenstate of the annihilation operator, we say that it is a *coherent state* for the d bosons.

Next I present a very simple way to solve Lundqvist's model for the whole spectrum (see 11.49 for a more sophisticated and general method). The eigenstates of \tilde{H} with eigenvalues $E_n = \Delta E + n\omega_0$ are

$$|n_s\rangle = \frac{1}{\sqrt{n!}}(s^\dagger)^n|0_s\rangle. \quad (6.23)$$

We seek the density of states

$$L(\omega) \equiv \langle i|\delta(\omega - \tilde{H})|i\rangle = \sum_{n=0}^{\infty} |\langle i|n\rangle|^2 \delta(\omega - E_n), \quad (6.24)$$

so we need the *Franck-Condon* factors $|\langle i|n\rangle|^2 \equiv |\langle 0_d|n_s\rangle|^2$. Let $\langle 0_d|0_s\rangle = C$; then, $\langle 0_d|1_s\rangle = \langle 0_d|s^\dagger|0_s\rangle = \langle 0_d|d^\dagger + \frac{g}{\omega_0}|0_s\rangle = \frac{g}{\omega_0}C$, since the d^\dagger contribution is 0. In general,

$$\langle 0_d|n_s\rangle = \frac{1}{\sqrt{n!}}\langle 0_d|(s^\dagger)^n|0_s\rangle = \frac{1}{\sqrt{n!}}\left(\frac{g}{\omega_0}\right)^n C. \quad (6.25)$$

⁴The inflationary cosmology regards the creation of the universe as a transition from a false vacuum. In Physics one often meets amazing connections between very unlike phenomena.

The normalization condition gives

$$C = e^{-\frac{1}{2}a}, \quad a = \frac{g^2}{\omega_0^2} = -\frac{\Delta E}{\omega_0}. \quad (6.26)$$

Hence,

$$L(\omega) = e^{-a} \sum_{n=0}^{\infty} \frac{a^n}{n!} \delta(\omega - \Delta E - n\omega_0). \quad (6.27)$$

The probability of n excited bosons $P_n = \frac{a^n}{n!} e^{-a}$ follows the Poisson statistics, reflecting the statistical independence of the non-interacting bosons, and the average number of excited bosons is

$$\langle \hat{n} \rangle = a = \gamma^2. \quad (6.28)$$

The density of states is normalized to 1 and its first moment is

$$\int_{-\infty}^{\infty} d\omega \omega L(\omega) = e^{-a} \sum_{n=0}^{\infty} \frac{a^n}{n!} (n\omega_0 + \Delta E).$$

Using (6.26) we readily find that this vanishes since

$$\sum_{n=1}^{\infty} \frac{a^n}{n!} n\omega_0 = \sum_{n=1}^{\infty} \frac{a^{n-1}}{(n-1)!} a\omega_0 = -\Delta E e^a.$$

The center-of-mass of the line remains where it would be for $g=0$; the threshold is at lower binding energy, at $a\omega_0$ below the center-of-mass. Fourier transforming $L(\omega)$ one finds the correlation function

$$\begin{aligned} 2\pi L(t) &= \int_{-\infty}^{\infty} d\omega L(\omega) e^{-i\omega t} = \langle i | e^{-iHt} | i \rangle \\ &= e^{-a} \sum_{n=0}^{\infty} \frac{a^n}{n!} e^{ia\omega_0 t - in\omega_0 t}. \end{aligned} \quad (6.29)$$

Thus,

$$\langle i | e^{-iHt} | i \rangle = e^{C(-t)}, \quad (6.30)$$

where

$$C(t) = -ia\omega_0 t + a(e^{i\omega_0 t} - 1). \quad (6.31)$$

Note the characteristic exponential at the exponent. For strongly coupled, slow modes, the $a \gg 1$ case is relevant. Formally, we let $\omega_0 \rightarrow 0$ with $g^2 = a\omega_0^2$ finite. Then, $\langle e^{-iHt} \rangle \rightarrow e^{-\frac{g^2 t^2}{2}}$ and one finds the Gaussian line shape

$$L(\omega) = \frac{1}{g\sqrt{2\pi}} e^{-\frac{\omega^2}{2g^2}}. \quad (6.32)$$

The relaxation energy diverges in the Gaussian limit, which is a serious overestimate; however the Gaussian line shape is often a good approximation for phonon broadened core levels in solids and the width provides a sensible measure of the electron-phonon interaction, although the Gaussian should be convolved with a Lorentzian (producing a so called Voigt profile) to account for the core hole lifetime. The result

$$\lim_{a \rightarrow \infty} e^{-a} \sum_{n=0}^{\infty} \frac{a^n}{n!} \delta(\omega + a\omega_0 - n\omega_0) = \frac{1}{g\sqrt{2\pi}} e^{-\frac{\omega^2}{2g^2}} \quad (6.33)$$

will be useful in Section 15.3.2.

6.2 Auger CVV Line Shapes: Two-Hole Resonances

Electron spectroscopies are a most interesting window over the various and apparently fantastic scenarios of many-body theory including the strong correlation case and the appearing of bound states. This is particularly true for the theory of the Auger effect[107] in solids (for a review of the Auger line shape theory see Ref. [109]). In the core-valence valence transitions, the primary core hole decays into the Auger electrons and a pair of valence holes. In the earliest theory developed by Lander[108] within the band theory of solids, the Auger spectrum is proportional to the self-convolution of the density of occupied states. However, Powell[110] pointed out that while the Al spectrum was qualitatively consistent with the Lander predictions, the Ag spectrum is quasi-atomic (it shows atomic multiplet peaks much narrower than twice the band-width). Other authors [111] proposed a classification of spectra after their atomic-like or band-like shape.

Strong deviations from one-electron theory arose in the first correlated theory[75][76] of Auger CVV line shapes (now known as Cini-Sawatzky theory). Let us consider an atom interacting with a solid, assuming for simplicity that the valence orbitals of the atom and the solid band are completely filled; the model Hamiltonian[76] in the hole representation is

$$H = H_a + H_S + H_{int} + H_f \quad (6.34)$$

where the atomic contribution

$$H_a = \epsilon_{dh} c_{dh\uparrow}^\dagger c_{dh\uparrow} + \epsilon_l \sum_{m,\sigma} c_{m\sigma}^\dagger c_{m\sigma} + H_r \quad (6.35)$$

comprises a spin-up deep hole term for the primary hole, $c_{m\sigma}^\dagger$ creates a valence hole with magnetic quantum number m ; H_r is the hole-hole repulsion Hamiltonian with screened direct and exchange matrix elements $U(m_1, m_2, m_3, m_4)$. The crystal Hamiltonian H_S and the atom-crystal hopping term H_{int} are one-body contributions that can be chosen according to any model deemed appropriate. Finally,

$$H_f = \sum_{k,\sigma} \epsilon_k c_{k\sigma} c_{k\sigma}^\dagger \quad (6.36)$$

describes the free particle continuum above the vacuum level; in the ground state $|\Psi\rangle$ of H only the \vec{k} holes exist and $H|\Psi\rangle = 0$. Our initial state is $|i\rangle = c_{dh\uparrow}^\dagger |\Psi\rangle$. Core-Valence-Valence Auger transitions are produced by the matrix elements

$$A(m, m', \mathbf{k}) = \langle \phi_{dh}(1) \phi_{\mathbf{k}}(2) | \frac{1}{r_{12}} | \phi_m(1) \phi_{m'}(2) \rangle \quad (6.37)$$

of the Coulomb interactions and their exchange counterparts. Inter-atomic Auger transitions, producing holes on nearby atoms, are neglected because their matrix elements are very small. Thus, the transitions lead to a set of states

$$|mn\sigma\rangle = c_{n\sigma}^\dagger c_{m\uparrow}^\dagger |\Psi\rangle \quad (6.38)$$

with two holes localized on the valence orbitals of the same atom that was ionized initially. At this point H_f may be forgotten.

By the Fermi golden rule one finds[76] that the spectrum is proportional to the free-electron density of states and to $S(E_i - E_{\mathbf{k}}, \mathbf{k})$, given by

$$S(\omega, \mathbf{k}) = \sum_{mnpq} A_{mn}^*(\mathbf{k}) A_{pq}(\mathbf{k}) D_{mnpq\sigma}(\omega) \quad (6.39)$$

where the local density of states (LDOS) for the two final-state valence holes is

$$D_{mnpq\sigma}(\omega) = \langle pq\sigma | \delta(\hbar\omega - H_r - H_1) | mn\sigma \rangle; \quad (6.40)$$

here, H_1 is the sum of all the one-body terms of $H - H_f$. The dependence on the angles of \mathbf{k} can be taken care of by multiple scattering techniques, in the spirit of Ref. [86], but here we concentrate on the ω dependence.

The fact that the local density of states appears, rather than the band density of states as in the Lander theory, is one of the main points of Ref.[76] and qualifies Auger spectroscopy as a local probe of valence states. There are two trivial special cases. In the atomic limit $H_{int} = 0$, and $H_S = 0$; then the Hamiltonian is diagonal in the L-S or $|LSMM_S\rangle$ representation; the spectrum consists of unbroadened multiplet terms. The other simple limiting case is the non-interacting ($H_r \rightarrow 0$) case; density of states matrix $D_{mnpq\sigma}^{(0)}(\omega)$ is readily worked out in terms of the one-body local density of states $\rho_{mn}(\omega) = \langle m | \delta(\hbar\omega - H) | n \rangle = \rho_{nm}(\omega)$ using their transforms; here we define the correlation functions $D_{mnpq\sigma}(t) = \langle pq\sigma | e^{-iHt} | mn\sigma \rangle$ and $\rho_{mn}(t) = \langle m | e^{-iHt} | n \rangle$, both with diagonal elements equal to 1 for $t=0$.

Indeed,

$$\begin{aligned} D_{mnpq\downarrow}^{(0)}(t) &= \rho_{mp}(t) \rho_{nq}(t) \\ D_{mnpq\uparrow}^{(0)}(t) &= \rho_{pm}(t) \rho_{qn}(t) - \rho_{pn}(t) \rho_{qm}(t). \end{aligned} \quad (6.41)$$

In frequency space these become convolutions of one-hole densities of states.

To calculate the interacting density of states including the solid one can use the identity (4.92) $\frac{1}{z-H} = \frac{1}{z-H_0} + \frac{1}{z-H_0} H_1 \frac{1}{z-H}$ that holds if $H = H_0 + H_1$. In this case, H_1 is identified with the repulsion H_r and H_0 is the one-body part of $H - H_f$. Taking matrix elements in the basis (6.38) one obtains a matrix equation for the Fourier transform of $D_{mnpq\sigma}(t)\Theta(t)$, using $\int_0^\infty dt \exp[i(\omega - H)t - \delta t] = \frac{i}{\omega - H + i\delta}$. However, if the solid does not significantly perturb the spherical symmetry of the atom, the the D matrices are diagonal in the $|LMSM_S\rangle$ representation, where H_r is diagonal, and obey uncoupled the equations.

Then, we may drop the L,M indices and define

$$\phi^{(0)}(\omega) = i\langle 00 | \frac{1}{\omega - H_0 + i\delta} | 00 \rangle = i[I^{(0)}(\omega) - i\pi D^{(0)}(\omega)], \quad (6.42)$$

with

$$I^{(0)}(\omega) = \int_{-\infty}^{\infty} d\omega' \frac{D^{(0)}(\omega')}{\omega - \omega'}. \quad (6.43)$$

One obtains

$$\phi(\omega) = \frac{\phi^{(0)}(\omega)}{1 + iU\phi^{(0)}(\omega)}, \quad (6.44)$$

and within the bands

$$D(\omega) = \frac{1}{\pi} \text{Re}\phi = \frac{D^{(0)}(\omega)}{(1 - UI^{(0)}(\omega))^2 + \pi^2 U^2 D^{(0)}(\omega)^2}. \quad (6.45)$$

The center-of-mass of D computed from (6.40) is $\int d\omega \omega D(\omega) = \langle H_1 + H_r \rangle$ averaged over the appropriate multiplet L,M component; understanding the term, it is shifted by $U = \langle H_r \rangle$, so correlation must deform the line shape within the continuum. However no line shape can ensure this if U is too large, and something must grow outside. Poles of ϕ outside the bands are *two-hole resonances*.

To better understand the result, let us consider the rectangular local density of states

$$\rho(\omega) = \frac{\theta(\alpha - |\omega|)}{2\alpha}. \quad (6.46)$$

To do self-convolutions of functions that vanish outside an interval, it is expedient to use the identities

$$\begin{cases} i) & \theta(a - |x|) = \theta(a+x)\theta(a-x), \\ ii) & \theta(x+a)\theta(x+b) = \theta(b-a)\theta(x+a) + \theta(a-b)\theta(x+b), \\ iii) & \theta(x+a)\theta(c-x) = \theta(a+c) [\theta(x+a) - \theta(x-c)] \end{cases} \quad (6.47)$$

where iii) comes from ii) and $\theta(-x) = 1 - \theta(x)$. One finds the triangular-shaped result

$$D^0(\omega) = \theta(2\alpha - |\omega|) \left(\frac{1}{2\alpha} - \frac{|\omega|}{4\alpha^2} \right). \quad (6.48)$$

As an alternative route to (6.48) we can use $\rho(t) = \frac{\sin(\alpha t)}{\alpha t}$, $D^0(t) = \left(\frac{\sin(\alpha t)}{\alpha t} \right)^2$, and as this is symmetric we can compute the real Fourier transform by calculating the cosine transform:

$$2\pi D^0(\omega) = \int_{-\infty}^{\infty} dt \cos(\omega t) D^0(t). \quad (6.49)$$

Hence, by direct integration,

$$\begin{aligned} I^0(\omega) &= \int_{-\infty}^{\infty} \frac{dy D^0(y)}{\omega - y} \\ &= \frac{1}{2\alpha} \log \left| \frac{\omega + 2\alpha}{\omega - 2\alpha} \right| + \frac{\omega}{4\alpha^2} \log \left| \frac{\omega^2 - 4\alpha^2}{\omega^2} \right|. \end{aligned} \quad (6.50)$$

This, with (6.45) shows the distortion of band-like line shapes as $\gamma = \frac{U}{\alpha}$ grows. However, for $\gamma > 1.44$, the intensity of the continuous line shape drops. The overall intensity cannot drop, however. The missing intensity is in the split-off the two-hole resonances, that however come into the theory as $\frac{0}{0}$ singularities. To clarify the situation, a trick is in order. One changes the above $I^0(\omega)$ to a complex function by setting $z = \omega + i\delta$, and writing (see 6.42)

$$-i\phi^{(0)}(z) = \frac{1}{2\alpha} \log \left(\frac{z + 2\alpha}{z - 2\alpha} \right) + \frac{z}{4\alpha^2} \log \left(\frac{z^2 - 4\alpha^2}{z^2} \right) = I^0(\omega) - i\pi D^0(\omega). \quad (6.51)$$

This is equivalent to convolving the line shape with a Lorentzian of width δ , which, incidentally, is always appropriate to describe broadenings [124] which are present in reality even if they were not considered in the model. Hence the two-hole singularities show up as Lorentzian peaks.

Two-hole resonances are also observed when core-holes interact with valence holes and the core-valence repulsion is comparable with the valence band width. For example, in Zn, Cu, Fe, Co, Ni metals there is evidence [191] that a L_2 hole can decay in a normal $L_2 M_{45} M_{45}$ process or in a Coster-Kronig $L_2 - L_2 L_3 M_{45} - M_{45} M_{45} M_{45}$ process. It is possible to observe the decay spectrum in coincidence with the L_2 photoelectron in APECS (= Auger-Photoelectron Coincidence spectroscopy) and compare with the $L_3 M_{45} M_{45}$ line shapes. In some of these metals the line shape is much narrower; this suggests that in the $L_2 L_3 M_{45}$ process the final-state M_{45} hole is localized around the L_3 hole and thus can influence the 3-hole final state in the valence band.

The relation between the quasi-atomic states seen in Auger spectroscopy and the Kanamori [67] paper was understood only later, after the Sawatzky paper [112] using the Hubbard model with the Kanamori solution. Indeed a

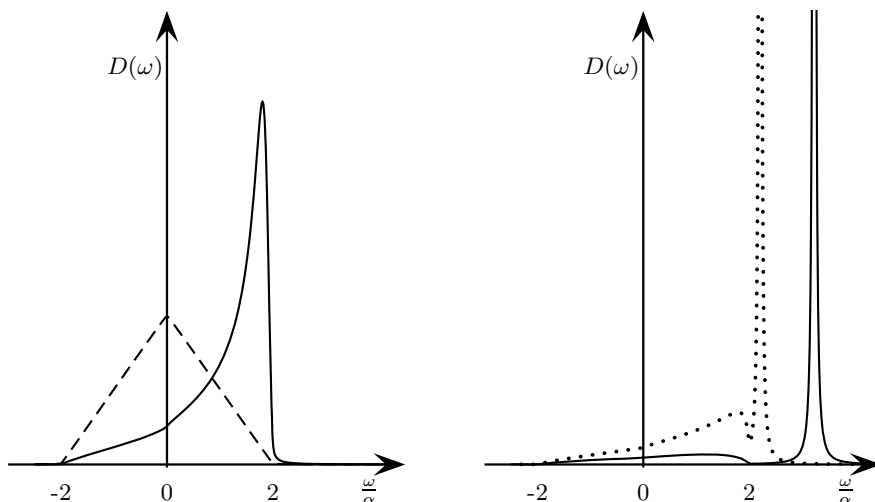


Fig. 6.2. For the rectangular band model, the two-hole line shape is triangular for $U = 0$ (left panel,dotted), and is shown here broadened with $\delta = 0.01\alpha$. With increasing U the maximum becomes sharper and shifts to higher ω , as shown for $U = 1.1\alpha$ (left panel,solid). At $U = 1.8$ a well developed split-off state develops (right panel, dotted). The solid line in the right panel shows the result for $U = 3\alpha$ when most of the intensity is in the two-hole resonance, but a residual band-like continuum can still be seen.

footnote in Kanamori's paper on magnetism pointed out a narrow band of solutions of the Hubbard model outside the band continuum which exist for large enough U . In a periodic solid, the split-off states themselves form a band. However Kanamori's paper was in a different physical context, using a different Hamiltonian than (6.34), and gave no clue about how to observe these solutions.

Further extensions are presented below and in Chapter 12.

To deal with the Auger CVV spectra of covalently bonded semiconductors, one has to include overlap effects[135]; the theory has also been extended to include relativistic effects in intermediate coupling ([201]) and metallic bands (Sections 12.3.1,12.3.2,12.3.3), but is still rather incomplete for strongly correlated nearly half filled bands.

6.2.1 Desorption

Later, Knotek and Feibelman[113] discovered that the two-hole resonances cause ionic desorption⁵, e.g. of O^+ ions from Ti Oxide surfaces. The primary

⁵Desorption is the breaking of an atom-surface chemical bond followed by the emission of a neutral species or an ion; it can be caused e.g. by an increase of the temperature, or by ionizing radiation.

ionization occurs in the Ti 2p level, but the hole has little chance to Auger decay via intra-atomic transitions since the Ti ion (nominally, Ti^{4+}) has no valence electrons left. So, the electrons must come from the surrounding closed-shell O^- ions. One can consider electron transfer to the empty Ti valence shell and/or direct inter-atomic decay. When two electrons come from different O ions no desorption occurs; indeed, desorption takes several phonon periods (of the order of $10^{-13}s$) and bond healing by hole delocalization should be much faster. However, there is some chance of two holes in the same O. In this case, a two-hole resonance forms and lives long enough to allow the O^+ ion to escape. The generalization of the theory to partially filled bands is discussed in Section 12.3.

6.3 Two Interacting Fermions in a Lattice

The so called Cini-Sawatzky theory has been applied[153] to the $N_{6,7}O_{4,5}O_{4,5}$ Auger spectrum of Au metal. The multiplet structure was interpreted in the intermediate coupling scheme using free atom experimental data[154], and using as the only parameter the F_0 Slater integral, that is modified with respect to the free atom by the solid state screening. The top panel (a) in Figure 6.3 shows the experimental data calculated with a value of $U(^1G_4)=3.4$ eV (dashed); the solid line in (a) is obtained by shifting the dashed line to higher binding energy by 1.2 eV. The profile in (a) is in excellent agreement with experiment but its absolute position is wrong by 1.2 eV. On the other hand, the profile calculated with $U(^1G_4)=4.6$ eV is shown in (b). Now it is in agreement with the experimental position of the main features but the shape is in rather poor agreement with experiment. The profile of (c) is obtained from the one in (b) by arbitrarily increasing the width of the Lorentzian lifetime broadening to 2.0 eV. It is clear that this does not fix any problems. So, it appears that the Cini-Sawatzky theory involves a systematic error on the position. A similar shift between the best line shape and the experimental position was found in an accurate analysis of the Ag $M_{4,5}N_{4,5}N_{4,5}$ line[155], where it is possible to get a very good agreement with the experimental profile but the theoretical results must be shifted 2.2 eV to lower binding energy.

In both cases, we traced back the origin of the problem to the extreme on-site repulsion used in the Cini-Sawatzky model. This prompted the following analysis aiming to generalize the calculation to an arbitrary distance dependence of the hole-hole interaction.

Consider two electrons (or holes) in a otherwise empty (full) lattice A of $N \rightarrow \infty$ sites, interacting through an arbitrary potential $V(\rho)$. Let's write $|\mathbf{R}_1\mathbf{R}_2\rangle$ for the determinantal two-body state with a up-spin electron at site 1 and a down-spin one at site 2; the sites belong to a periodic lattice in d dimensions. Here I report exact results by Verdozzi and the writer[66] on the two-hole Green's function,

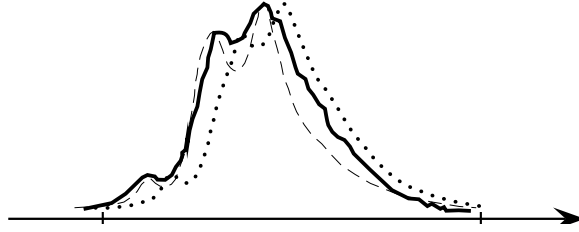


Fig. 6.3. Sketch of the Au $N_{6,7}O_{4,5}O_{4,5}$ Auger spectrum (Ref. ([153])) compared with theoretical profiles (see text). The solid line is a drawing of the experimental profile, on a binding energy scale, where 0 corresponds to both holes from the Fermi level; the theory used the Slater integral F^0 , or equivalently one of the U values, as an adjustable parameter. The dotted line is the best shift to the theoretical line shape obtained with $U(^1G_4) = 3.4eV$, but appears to be shifted compared to experiment. By increasing U one can adjust the line position, but the line shape agreement is lost (dashed line). To fix this problem, one must account for the off-site interactions (see below).

$$G(\mathbf{R}_1, \mathbf{R}_2, \mathbf{R}_3, \mathbf{R}_4, z) = \langle \mathbf{R}_1 \uparrow \mathbf{R}_2 \downarrow | \frac{1}{z - H} | \mathbf{R}_3 \uparrow \mathbf{R}_4 \downarrow \rangle \quad (6.52)$$

with $z = E - i0^+$, as a function of energy E (for two electrons, $z = E + i0^+$, but nothing else changes). The Hamiltonian is:

$$H = H_0 + H_1 = \sum_{\mathbf{k}} \epsilon_{\mathbf{k}} \hat{n}_{\mathbf{k}} + \sum_{\mathbf{R}, \boldsymbol{\rho}} V(\boldsymbol{\rho}) | \mathbf{R} \uparrow, \mathbf{R} + \boldsymbol{\rho} \downarrow \rangle \langle \mathbf{R} \uparrow, \mathbf{R} + \boldsymbol{\rho} \downarrow |. \quad (6.53)$$

Here, $\boldsymbol{\rho}$ belongs to the lattice of relative motion, which we call the $\boldsymbol{\rho}$ lattice, isomorphic to Λ . For $V = 0$, the problem is trivial because $H = H_{\uparrow} + H_{\downarrow}$; then the time evolution operator factors and the non-interacting Green's function that we denote by a small g is given by

$$g(\mathbf{R}_1, \mathbf{R}_2, \mathbf{R}_3, \mathbf{R}_4, z) = g^{(1)}(\mathbf{R}_1, \mathbf{R}_3, z) \otimes g^{(1)}(\mathbf{R}_2, \mathbf{R}_4, z) \quad (6.54)$$

where $g^{(1)}$ is the one-particle Green's function and \otimes denotes a convolution.

Let us deal with the interacting case. The center-of-mass vector

$$\mathbf{R}_{cm} = \mathbf{R} + \frac{1}{2}\boldsymbol{\rho} \quad (6.55)$$

belongs to a $\{\mathbf{R}_{cm}\}$ lattice which besides the sites $\in \Lambda$ also includes the midpoints of all sides.

The translational symmetry allows to take \mathbf{R}_1 as the origin without loss of generality. The key step to exploit the periodicity is a Fourier transformation: the total crystal momentum \mathbf{Q} of the pair is conjugate to \mathbf{R}_{cm} and is conserved, and one is left with an effective one-body problem over the $\boldsymbol{\rho}$ lattice to be solved.

Fourier Transforming the Center-of-mass Motion

Transforming with fixed ρ , and understanding the spin arrows,

$$|\rho; \mathbf{Q}\rangle = \sum_{\mathbf{R}_{cm}} \frac{e^{i\mathbf{Q}\cdot\mathbf{R}_{cm}}}{\sqrt{N}} \left| \mathbf{R}_{cm} - \frac{\rho}{2}, \mathbf{R}_{cm} + \frac{\rho}{2} \right\rangle = \frac{e^{\frac{i}{2}\mathbf{Q}\cdot\rho}}{\sqrt{N}} \sum_{\mathbf{R}} e^{i\mathbf{Q}\cdot\mathbf{R}} |\mathbf{R}, \mathbf{R} + \rho\rangle \quad (6.56)$$

where the integration variable was shifted using (6.55). Moreover,

$$|\mathbf{R}, \mathbf{R} + \rho\rangle = \frac{1}{\sqrt{N}} \sum_{\mathbf{Q}} e^{-i\mathbf{Q}\cdot[\mathbf{R} + \frac{1}{2}\rho]} |\rho; \mathbf{Q}\rangle. \quad (6.57)$$

One can immediately check that this $\{|\rho; \mathbf{Q}\rangle\}$ set is a correctly normalized basis for two particles.

Fourier Transforming the Relative Motion

The trick is

$$\sum_{\mathbf{R}} \frac{e^{i\mathbf{Q}\cdot\mathbf{R}}}{\sqrt{N}} |\mathbf{R}, \mathbf{R} + \rho\rangle = \sum_{\mathbf{R}} \frac{e^{i\mathbf{Q}\cdot\mathbf{R}}}{\sqrt{N}} \sum_{\rho'} \delta(\rho, \rho') |\mathbf{R}, \mathbf{R} + \rho'\rangle \quad (6.58)$$

where we can use $\delta(\rho, \rho') = \sum_{\mathbf{q}} \frac{e^{i\mathbf{q}(\rho' - \rho)}}{N}$. So, this becomes

$$\begin{aligned} & \frac{1}{N^{\frac{3}{2}}} \sum_{\mathbf{q}} e^{-i\mathbf{q}\cdot\rho} \sum_{\mathbf{R}, \rho'} e^{i\mathbf{Q}\cdot\mathbf{R} + i\mathbf{q}\cdot\rho'} |\mathbf{R}, \mathbf{R} + \rho'\rangle = \\ & \frac{1}{N^{\frac{3}{2}}} \sum_{\mathbf{q}} e^{-i\mathbf{q}\cdot\rho} \sum_{\mathbf{R}, \rho'} e^{i[\mathbf{Q} - \mathbf{q}]\cdot\mathbf{R} + i\mathbf{q}\cdot[\mathbf{R} + \rho']} |\mathbf{R}, \mathbf{R} + \rho'\rangle, \end{aligned} \quad (6.59)$$

but $\sum_{\mathbf{R}, \rho'} = \sum_{\mathbf{R}, \mathbf{R} + \rho'}$ and the result is

$$\sum_{\mathbf{R}} \frac{e^{i\mathbf{Q}\cdot\mathbf{R}}}{\sqrt{N}} |\mathbf{R}, \mathbf{R} + \rho\rangle = \frac{1}{\sqrt{N}} \sum_{\mathbf{q}} e^{-i\mathbf{q}\cdot\rho} |\mathbf{Q} - \mathbf{q}, \mathbf{q}\rangle, \quad (6.60)$$

where

$$|\mathbf{Q} - \mathbf{q}, \mathbf{q}\rangle = \frac{1}{N} \sum_{\mathbf{R}, \mathbf{R} + \rho'} e^{i[\mathbf{Q} - \mathbf{q}]\cdot\mathbf{R}} e^{i\mathbf{q}\cdot[\mathbf{R} + \rho']} |\mathbf{R}, \mathbf{R} + \rho'\rangle. \quad (6.61)$$

Substituting (6.60) in (6.56), one obtains

$$|\rho, \mathbf{Q}\rangle = \frac{\exp(\frac{i}{2}\mathbf{Q}\cdot\rho)}{\sqrt{N}} \sum_{\mathbf{q}} e^{-i\mathbf{q}\cdot\rho} |\mathbf{Q} - \mathbf{q}, \mathbf{q}\rangle. \quad (6.62)$$

Projected Hamiltonian

In the $|\boldsymbol{\rho}, \mathbf{Q}\rangle$ basis,

$$H = \sum_{\mathbf{Q}} H^{\mathbf{Q}}, \quad H^{\mathbf{Q}} = H_0^{\mathbf{Q}} + H_1^{\mathbf{Q}}, \quad (6.63)$$

where the interaction is diagonal,

$$H_1^{\mathbf{Q}} = \sum_{\boldsymbol{\rho}} V(\boldsymbol{\rho}) |\boldsymbol{\rho}, \mathbf{Q}\rangle \langle \mathbf{Q}, \boldsymbol{\rho}|, \quad (6.64)$$

while

$$H_0^{\mathbf{Q}} = \sum_{\boldsymbol{\rho}, \boldsymbol{\rho}'} |\boldsymbol{\rho}, \mathbf{Q}\rangle W_{\boldsymbol{\rho}\boldsymbol{\rho}'}^{\mathbf{Q}} \langle \mathbf{Q}, \boldsymbol{\rho}'|; \quad (6.65)$$

we determine $W_{\boldsymbol{\rho}\boldsymbol{\rho}'}^{\mathbf{Q}}$ using (6.62): one finds

$$W_{\boldsymbol{\rho}, \boldsymbol{\rho}'}^{\mathbf{Q}} = e^{-\frac{i}{2}\mathbf{Q}\cdot(\boldsymbol{\rho}-\boldsymbol{\rho}')} \frac{1}{N} \sum_{\mathbf{q}} e^{i\mathbf{q}\cdot(\boldsymbol{\rho}-\boldsymbol{\rho}')} [\epsilon(\mathbf{Q}-\mathbf{q}) + \epsilon(\mathbf{q})]. \quad (6.66)$$

The Green's Function

Due to the translational symmetry, $G(\mathbf{R}_1, \mathbf{R}_2, \mathbf{R}_3, \mathbf{R}_4, z)$ can be computed as $G(\mathbf{0}, \boldsymbol{\rho}, \mathbf{R}, \mathbf{R} + \boldsymbol{\rho}', z)$; we change basis using (6.57) and write

$$\langle \mathbf{0}, \boldsymbol{\rho} | \frac{1}{z-H} | \mathbf{R}, \mathbf{R} + \boldsymbol{\rho}' \rangle = \frac{1}{N} \sum_{\mathbf{Q}} e^{-i\mathbf{Q}\cdot[\mathbf{R}+\frac{1}{2}(\boldsymbol{\rho}'-\boldsymbol{\rho})]} G_{\boldsymbol{\rho}\boldsymbol{\rho}'}^{\mathbf{Q}}(z), \quad (6.67)$$

terms of a \mathbf{Q} -projected Green's function

$$G_{\boldsymbol{\rho}\boldsymbol{\rho}'}^{\mathbf{Q}}(z) = \langle \mathbf{Q}, \boldsymbol{\rho} | \frac{1}{z-H^{\mathbf{Q}}} | \mathbf{Q}, \boldsymbol{\rho}' \rangle. \quad (6.68)$$

The non-interacting two-particle function $g^{\mathbf{Q}}$ has elements

$$g_{\boldsymbol{\rho}, \boldsymbol{\rho}'}^{\mathbf{Q}}(z) = e^{-\frac{i}{2}\mathbf{Q}\cdot[\boldsymbol{\rho}-\boldsymbol{\rho}']} \sum_{\mathbf{q}} \frac{e^{i\mathbf{q}\cdot[\boldsymbol{\rho}-\boldsymbol{\rho}']}}{z - \epsilon(\mathbf{Q}-\mathbf{q}) - \epsilon(\mathbf{q})}. \quad (6.69)$$

The operator identity

$$\frac{1}{z-H^{\mathbf{Q}}} = \frac{1}{z-H_0^{\mathbf{Q}}} + \frac{1}{z-H_0^{\mathbf{Q}}} V \frac{1}{z-H^{\mathbf{Q}}}; \quad (6.70)$$

can be iterated:

$$\begin{aligned} \frac{1}{z-H^{\mathbf{Q}}} &= \frac{1}{z-H_0^{\mathbf{Q}}} + \frac{1}{z-H_0^{\mathbf{Q}}} V \left[\frac{1}{z-H_0^{\mathbf{Q}}} + \frac{1}{z-H_0^{\mathbf{Q}}} V \frac{1}{z-H_0^{\mathbf{Q}}} \right] \\ &= \frac{1}{z-H_0^{\mathbf{Q}}} + \frac{1}{z-H_0^{\mathbf{Q}}} \left\{ V + V \frac{1}{z-H^{\mathbf{Q}}} V \right\} \frac{1}{z-H_0^{\mathbf{Q}}}. \end{aligned} \quad (6.71)$$

Expanding the inverse operator inside the curly brackets and summing the geometric series, we obtain

$$\frac{1}{z - H^{\mathbf{Q}}} = \frac{1}{z - H_0^{\mathbf{Q}}} + \frac{1}{z - H_0^{\mathbf{Q}}} \frac{1}{1 - V \frac{1}{z - H_0^{\mathbf{Q}}}} V \frac{1}{z - H_0^{\mathbf{Q}}}. \quad (6.72)$$

We take matrix elements of (6.72) on the $|\rho; \mathbf{Q}\rangle$ basis and we find, adopting matrix notation on the ρ lattice, with V diagonal,

$$G^{\mathbf{Q}} = g^{\mathbf{Q}} + g^{\mathbf{Q}} [1 - V g^{\mathbf{Q}}]^{-1} V g^{\mathbf{Q}}. \quad (6.73)$$

This is the solution. The size of the matrix that must be inverted depends on the range of the potential. In the zero-range case of the on-site potential (Hubbard Model with local interaction U) we set $\rho = \rho'$, and write

$$g^{\mathbf{Q}}(z) = \sum_{\mathbf{q}} \frac{1}{z - \epsilon(\mathbf{Q} - \mathbf{q}) - \epsilon(\mathbf{q})}. \quad (6.74)$$

Then, Equation (6.73) is scalar and the solution can be simplified to read:

$$G^{\mathbf{Q}} = \frac{g^{\mathbf{Q}}}{1 - U g^{\mathbf{Q}}}. \quad (6.75)$$

This result by Kanamori[67] was proposed by Sawatzky [112] in the present context. In the on-site case, a characteristic feature of the Kanamori theory is the existence of split-off states for each \mathbf{Q} for strong enough interaction U compared to the band width. This single state can develop to a full discrete spectrum for long-range V (see Ref. [66].) The results of the analysis in Ref. [66] showed that the above described shift between the Cini-Sawatzky line shapes and the experimental profile e.g. in Au and Ag could be accounted for by a realistic screened hole-hole interaction. Sect. (12.2) below shows the connection of the Kanamori theory to the Galitzkii self-energy in the low density case and its relation to diagram methods. Some physical applications of this theory to electron spectroscopy are presented in Sect. 6.2

6.4 Quadratic Response Formalism and Spectroscopies

Consider a weak, adiabatically switched periodic perturbation

$$V(t) = f V e^{-i\omega t + \eta t}, \quad (6.76)$$

with η a small positive constant acting on an interacting system with Hamiltonian H ; here f is a parameter and V a time-independent operator. We want the wave function $\Psi(t)$ that reduces to the ground state $e^{-iEt} \phi_g$ for $r \rightarrow -\infty$. In the interaction picture,

$$i \frac{\partial}{\partial t} \Psi_I(t) = V_I(t) \Psi_I(t) \quad (6.77)$$

with the starting condition $\Psi_I(t) \rightarrow \phi_g$ in the remote past. In first approximation, we write (setting $\hbar = 1$)

$$i \frac{\partial}{\partial t} \Psi_I(t) = V_I(t) \Psi_I(t) = f e^{i[H-E-\omega-i\eta]t} V \phi_g. \quad (6.78)$$

Let $z = E + \omega + i\eta$. The solution with the correct initial conditions is

$$\Psi_I(t) = \phi_g + f e^{i[H-z]t} \frac{1}{z-H} V \phi_g. \quad (6.79)$$

In the Schrödinger picture,

$$\Psi(t) = e^{-iEt} \phi_g + f e^{-izt} \frac{1}{z-H} V \phi_g. \quad (6.80)$$

Photoemission

Now let $V = \frac{e}{mc} \sum_i \mathbf{A}(\mathbf{x}_i) \cdot \mathbf{p}_i$ (summed over electrons) the operator which produces photoemission. In second quantization, $V = \sum_{p',d} \tau(p',c) c_{p'}^\dagger c_d$ where deep a electron is annihilated and a photoelectron created, and $\tau(p',c)$ are the matrix elements. We assume that H includes the photoelectron kinetic energy $T_{pe} = \sum_{\mathbf{p}} \epsilon_{\mathbf{p}} n_{\mathbf{p}}$ but no post-collisional interaction with the photoelectrons. The photoelectron current is

$$J_p = \frac{d}{dt} \langle \Psi(t) | n_p | \Psi(t) \rangle. \quad (6.81)$$

in the above approximation, the current is a quadratic response in the perturbation V (which is logical, since it is a d.c. response to an a.c. perturbation.) Since $n_p \phi_g = 0$,

$$\langle n_p \rangle = f^2 e^{2\eta t} \langle \phi_g | V \frac{1}{z^* - H} n_p \frac{1}{z - H} V | \phi_g \rangle. \quad (6.82)$$

Hence,

$$J_p = 2\eta f^2 e^{2\eta t} \langle \phi_g | V \frac{1}{z^* - H} n_p \frac{1}{z - H} V | \phi_g \rangle. \quad (6.83)$$

Now since $[n_p, H]_- = 0$, we develop:

$$J_p = 2\eta f^2 e^{2\eta t} \sum_{dd'} \tau^*(p, d') \tau(p, d) \langle \phi_g | c_{d'}^\dagger \frac{1}{z^* - H} \frac{1}{z - H} c_d | \phi_g \rangle \quad (6.84)$$

letting $\eta \rightarrow 0$,

$$J_p = 2f^2 \sum_{dd'} \tau^*(p, d') \tau(p, d) \langle \phi_g | c_{d'}^\dagger \frac{\eta}{|z - \epsilon_p - H|^2} c_d | \phi_g \rangle \quad (6.85)$$

where the photoelectron energy ϵ_p has appeared (up to now, T_{pe} was part of H , but now we use H for the system Hamiltonian without T_{pe} .) This is actually

$$J_p = 2\pi f^2 \sum_{dd'} \tau^*(p, d') \tau(p, d) \langle \phi_g | c_{d'}^\dagger \delta(E + \omega - \epsilon_p - H) c_d | \phi_g \rangle \quad (6.86)$$

so the result depends on the one-hole density of states matrix $\rho_{dd'}(\omega)$ of the system. This formalism generalizes the elementary theory of photoemission, but offers the possibility of a clear enhancement of the understanding of the Auger effect.

6.4.1 One-Step Theory of Auger Spectra

Let k label the Auger electron; for the current $J_k = \frac{d}{dt} \langle \Psi(t) | n_k | \Psi(t) \rangle$ we find like above

$$J_k = 2\eta f^2 e^{2\eta t} \langle \phi_g | V \frac{1}{z^* - (H + W + T)} n_k \frac{1}{z - (H + W + T)} V | \phi_g \rangle, \quad (6.87)$$

where now, with a slight change in notation, we made explicit the operator

$$W = \sum W_{hh'dk} c_d^\dagger c_k^\dagger c_{h'} c_h + h.c. \quad (6.88)$$

producing the Auger transitions; c_k^\dagger and c_d^\dagger create the Auger electron and the deep electron, respectively, and the annihilation operators create the pair of final-state holes; also, $T = T_{pe} + T_A$ the kinetic energies of photoelectrons and Auger electrons. Using

$$\frac{1}{z - H - W - T} = \frac{1}{z - H - T} + \frac{1}{z - H - T} W \frac{1}{z - H - W - T}$$

and

$$\frac{1}{z - H - W - T} = \frac{1}{z - H - T} + \frac{1}{z - H - W - T} W \frac{1}{z - H - T}$$

since $n_k \frac{1}{z - H - T} V | \phi_g \rangle = 0$ one is left with

$$\begin{aligned} J_k &= 2\eta f^2 e^{2\eta t} \langle \phi_g | V \frac{1}{z^* - H - W - T} W \frac{1}{z^* - H - T} n_k \\ &\quad \times \frac{1}{z - H - T} W \frac{1}{z - H - W - T} V | \phi_g \rangle \end{aligned} \quad (6.89)$$

But n_k commutes with H and T , for $\eta \rightarrow 0$,

$$\eta \frac{1}{z^* - H - T} n_k \frac{1}{z - H - T} = \pi n_k \delta(E + \omega - H - T).$$

So, we reach the general expression of the *one-step description of the Auger effect* by Gunnarsson and Schönhammer [22]:

$$J_k = 2\pi\eta f^2 \langle \phi_g | V \frac{1}{z^* - H - W - T} W n_k \times \delta(E + \omega - H - T) W \frac{1}{z - H - W - T} V | \phi_g \rangle. \quad (6.90)$$

The most important terms are diagonal in the deep hole; writing V explicitly and replacing T by $T_A + \epsilon_p$, where ϵ_p is the photoelectron energy,

$$J_k = 2\pi\eta f^2 \sum_{p,d} |\tau(p,d)|^2 \langle \phi_g | a_d^\dagger \frac{1}{z^* - H - W - \epsilon_p - T_A} W n_k \times \delta(E + \omega - H - T) W \frac{1}{z - H - W - \epsilon_p - T_A} a_d | \phi_g \rangle. \quad (6.91)$$

The W operators in the denominators produce any number of virtual Auger transitions after the deep hole creation and before the real transition takes place; this can mix different decay channels giving interference effects. For filled bands, it is reasonable to neglect interband excitations and deep hole mixing letting (up to a constant)

$$\frac{1}{z - H - W - T} V | \phi_g \rangle \sim V | \phi_g \rangle \langle \phi_g | V \frac{1}{z - H - W - T} V | \phi_g \rangle,$$

recovering the Cini-Sawatzky theory.

Auger CVV spectra of transition metals with incomplete bands and the so-called $U < 0$ phenomenon are discussed in Section 12.3.

6.4.2 Plasmon Gain

Gunnarsson et al. [26] analyzed by their theory the plasmon gain satellites which are observed experimentally in the KL_2L_3 spectra of Na and Mg by a failure of the two-step model.

Problems

6.1. Verify that $\hat{j}(\mathbf{x})$ is the current operator and that (6.2) yields the same matrix elements as (6.1) and so the two formulations are equivalent.

6.2. Prove Equation 13.136.

Part II

Symmetry in Quantum Physics

7 Group Representations for Physicists

7.1 Abstract Groups

Groups are central to Theoretical Physics, not only as mathematical aids to solve problems, but above all as conceptual tools. We shall develop the Group Theory that should be known by Condensed Matter theorists using a physical language and building on what the readers know already about quantum mechanical operators. In this Section, however, we need to introduce some abstract mathematical definitions.

A Group G is a set with an operation or *multiplication* between any two elements satisfying the following conditions:

- G is closed, i.e. $a \in G, b \in G \implies ab \in G$.
- The product is associative : $a(bc) = (ab)c$.
- \exists an identity $e \in G$ such that $ea = ae = a, \forall a \in G$.
- $\forall a \in G, \exists a^{-1}$ that is every element has an inverse, such that $a^{-1}a = aa^{-1} = e$.

It is not necessary that G be commutative and generally $ab \neq ba$. Commutative Groups are called Abelian. Quantum Mechanical operators do not generally commute, and we are mainly interested in non-Abelian Groups. The discrete Groups may have a finite number N_G of elements; N_G is called the order of G .

Many Groups of interest have a finite N_G , like: the Group C_{3v} of symmetry operations of an equilateral triangle, the Group $S(N)$ of permutations of N objects.

Infinite-order Groups are also important. The translations that leave a Bravais lattice are an Abelian Group; the set of symmetry translations and rotations of a crystal are is Space Group, and is not Abelian; both are infinite discrete Groups. Among the continuous Groups, the most useful are the Lie Groups , introduced by Sophus Lie in 1870 to discuss the symmetries of differential equations; by definition, Lie Groups are such that the elements depend smoothly on some parameters. For example, $GL(n)$ (the General Linear Group in n dimensions) is the set of linear operations $x'_i = \sum_j a_{ij}x_j$, where

$A = a_{ij}$ is such that $\text{Det}A \neq 0$. The simplest case is $GL(2)$, the set of 2×2 matrices $\begin{pmatrix} a & b \\ c & d \end{pmatrix}$ with $ad - bc \neq 0$ depends on 4 parameters (such a smooth dependence defines a 4-dimensional *manifold*). The $SL(n)$ Group is a particular case of $GL(n)$, being the Special Linear Group in n dimensions or unimodular Group in n dimensions and is the set of linear operations $x'_i = \sum_j a_{ij}x_j$, where $A = a_{ij}$ is such that $\text{Det}A = 1$. Other frequently used Groups are: the rotation Group $O(n)$ of orthogonal transformations, that leave Euclidean distances invariant¹, and also of the orthogonal matrices such that $A^T = A^{-1}$. We shall also need the Group $U(n)$ of the unitary $n \times n$ matrices such that $A^\dagger = A^{-1}$ and the Group $SU(n)$ of special (determinant equal to +1) unitary transformations.

Let A and B denote two Groups with all the elements different, that is, $a \in A \Rightarrow a \notin B$, (except the identity, of course.) We also assume that all the elements of A commute with those of B . This is what happens if the two Groups have nothing to do with each other, for instance one could do permutations of 7 objects and the other spin rotations. In such cases it is often useful to define a **direct product** $C = A \times B$, which is a Group whose elements are $ab = ba$.

If $H \subset G$ is a Group itself it is a subgroup of the Group G . For instance, $GL(2)$ has a subgroup $O(2)$ which leaves distances invariant; the translations are a subgroup of the Space Group. Another subgroup of $GL(2)$ is defined such that given two points (x, y) and (ξ, η) in the plane, the operations do not change $\text{Det} \begin{pmatrix} x & y \\ \xi & \eta \end{pmatrix} = x\eta - y\xi$. Writing the transformation $\begin{pmatrix} x' \\ y' \end{pmatrix} = \begin{pmatrix} a & b \\ c & d \end{pmatrix} \begin{pmatrix} x \\ y \end{pmatrix}$ and $\begin{pmatrix} \xi' \\ \eta' \end{pmatrix} = \begin{pmatrix} a & b \\ c & d \end{pmatrix} \begin{pmatrix} \xi \\ \eta \end{pmatrix}$, one finds the condition $\text{Det} \begin{pmatrix} a & b \\ c & d \end{pmatrix} = 1$, so one is left with $SL(2)$. Usually one proceeds the other way: one knows a Group H , discovers new operations and so builds G .

Let H be a subgroup of G ; for $A \in G$ consider the set

$$\tilde{H}(a) = \{aha^{-1}, h \in H\}.$$

Since $ah_1a^{-1}ah_2a^{-1} = ah_1h_2a^{-1}$, this is a subgroup of G , the *conjugate subgroup* with respect to a . Occasionally, it may coincide with H itself (as a set, not element by element), in which case we write $aH = Ha$. If $\forall a \in G, aH = Ha$, then H is called *invariant subgroup* of G , or *normal divisor* of G .

¹in 3d, the rotation operators $R(\alpha) = e^{i\frac{\vec{\alpha} \cdot \vec{L}}{\hbar}}$ are familiar; the angular momentum operators are generators of rotations.

7.2 Point Symmetry in Molecules and Solids

In this section I give a brief account of Point Groups with the most frequently used information; for further details, one can use crystallography books, like Ref. [24]. The operations of the 32 point Groups are rotations (proper and improper) and reflections. In the Schönflies notation, which is frequently used in molecular Physics, proper rotations by an angle $\frac{2\pi}{n}$ are denoted C_n and reflections by σ ; improper rotations S_n are products of C_n and σ , the reflection plane being orthogonal to the rotation axis. The molecular axis is one of those with highest n . A symmetry plane can be vertical (i.e. contain the molecular axis) or horizontal (i.e. orthogonal to it), and the reflections are σ_v or σ_h accordingly.

7.2.1 Symmetry operators

Let $G = \{R, S, T, \dots\}$ denote the symmetry Group. Unlike the operators of observables, that must be Hermitean, those of symmetries are unitary:

$$\forall R \in G, R^{-1} = R^\dagger \quad (7.1)$$

in order to preserve normalization: $\langle R\psi | R\psi \rangle = \langle \psi | R^\dagger R \psi \rangle = 1$; this is evident from the familiar rotation operators

$$R_\alpha = \exp \left[-\frac{i}{\hbar} \alpha \cdot \mathbf{L} \right]. \quad (7.2)$$

The same holds for reflections: the $\sigma_z : (x, y, z) \rightarrow (x, y, -z)$ reflection is represented by the unitary matrix $\text{diag}(1, 1, -1)$. Since $R|\psi\rangle = \lambda|\psi\rangle \Rightarrow \langle \psi | R^\dagger = \lambda^* \langle \psi | \Rightarrow |\lambda|^2 = 1$, the eigenvalues are phase factors: $\lambda = e^{i\alpha}$, with real α .

The rule that eigenstates belonging to different eigenvalues are orthogonal holds for unitary operators as well. Let $R|\phi_\alpha\rangle = e^{i\alpha}|\phi_\alpha\rangle$, $R|\phi_\beta\rangle = e^{i\beta}|\phi_\beta\rangle$. Then,

$$R_{\alpha\beta} = \langle \phi_\alpha | R | \phi_\beta \rangle = e^{i\beta} \langle \phi_\alpha | \phi_\beta \rangle; \quad (7.3)$$

on the other hand, taking the complex conjugate

$$R_{\alpha\beta}^* = \langle \phi_\beta | R^\dagger | \phi_\alpha \rangle = \langle \phi_\beta | R^{-1} | \phi_\alpha \rangle = e^{-i\alpha} \langle \phi_\beta | \phi_\alpha \rangle; \quad (7.4)$$

thus if the phases are different the scalar product is 0.

We can represent the operator S by the matrix

$$D_{\mu\nu}(S) = \langle \psi_\mu | S | \psi_\nu \rangle \quad (7.5)$$

on an arbitrary basis; then

$$S|\psi_\nu\rangle = \sum_{\mu} |\psi_\mu\rangle D_{\mu\nu}(S). \quad (7.6)$$

Then, for the symmetry $RS \in G$

$$RS|\psi_\nu\rangle = R \sum_{\mu} |\psi_\mu\rangle D_{\mu\nu}(S) = \sum_{\mu\rho} |\psi_\rho\rangle D_{\rho\mu}(R) D_{\mu\nu}(S) = \sum_{\rho} |\psi_\rho\rangle D_{\rho\nu}(RS) \quad (7.7)$$

with

$$D_{\rho\nu}(RS) = \sum_{\mu} D_{\rho\mu}(R) D_{\mu\nu}(S). \quad (7.8)$$

thus, the matrices are multiplied like the operators and in the same order, providing a *representation of the Group*.

In simple cases, all the symmetry operators commute; then we can diagonalize them simultaneously with the Hamiltonian matrix $\langle\psi_\mu|H|\psi_\nu\rangle$. We can diagonalize R, then with the new basis diagonalize S, and continue until we have a new basis labeled with all the symmetry-related quantum numbers. This breaks up the Hilbert space into several orthogonal subspaces. Then, we can diagonalize H separately in each subspace. In such cases, we get the maximum simplification from symmetry **without** Group Theory. The names of Groups are just nicknames for the symmetry of the problem.

Bloch's Theorem

In band structure calculations one solves

$$\left[\frac{p^2}{2m} + V(\mathbf{x}) \right] \psi(\mathbf{x}) = \epsilon\psi(\mathbf{x}) \quad (7.9)$$

in a periodic $V(\mathbf{x})$. The translation operators $T_i = e^{\frac{i\mathbf{p}\cdot\mathbf{t}_i}{\hbar}}$, $\mathbf{p} = -i\hbar\nabla$ where \mathbf{t}_i primitive translations of the Bravais lattice, define an Abelian Group G_T . The periodic boundary conditions $T_i^N = 1$ for some large integer N allow to use a finite, cyclic G_T . Let \vec{G} be a reciprocal lattice vector; by definition, $e^{i\vec{G}\cdot\vec{t}} = 1$ for any lattice translation \vec{t} . We solve the eigenvalue equation for all the unitary operators T_i

$$T_i\psi(\mathbf{x}) = \psi(\mathbf{x} + \mathbf{t}_i) = e^{i\alpha_i}\psi(\mathbf{x}) \quad (7.10)$$

at a time, by the Bloch Theorem:

Theorem 1. Equation (7.9) is solved by

$$\psi(x) = \psi_k(x) = e^{i\mathbf{k}\cdot\mathbf{x}} u_{\mathbf{k}}(\mathbf{x}) \quad (7.11)$$

with

$$u_{\mathbf{k}}(\mathbf{x}) = u_{\mathbf{k}}(\mathbf{x} + \mathbf{t}_i) \quad (7.12)$$

periodic; $\alpha_i = \mathbf{k}\cdot\mathbf{t}_i$ with the wave vector $\vec{k} = \frac{\vec{G}}{N}$.

Indeed, the conditions $T_i^N = 1$ require that $e^{N\mathbf{k}t_i} = 1$, so $N\mathbf{k}$ must be a reciprocal lattice vector. On the Bloch basis one has a sub-problem for each \mathbf{k} which reduces to seeking periodic solutions of

$$\left[\frac{(\mathbf{p} + \mathbf{k})^2}{2m} + V(x) \right] u_{\mathbf{k}}(\mathbf{x}) = \epsilon_{\mathbf{k}} u_{\mathbf{k}}(\mathbf{x}) \quad (7.13)$$

Water Molecule

Suppose want to calculate the molecular orbitals of H_2O in a LCAO model neglecting overlap. Putting the molecule on the xz plane, with z as the molecular axis, we see that it belongs to the C_{2v} point Group, with the operations $C_2 : (x, y, z) \rightarrow (-x, -y, z)$; $\sigma(xz) : (x, y, z) \rightarrow (x, -y, z)$; $\sigma(yz) : (x, y, z) \rightarrow (-x, y, z)$ We can form the Multiplication Table:

E	C_2	$\sigma(xz)$	$\sigma(yz)$
C_2	E	$\sigma(yz)$	$\sigma(xz)$
$\sigma(xz)$	$\sigma(yz)$	E	C_2
$\sigma(yz)$	$\sigma(xz)$	C_2	E

the Group is Abelian and the square of each operation is the identity E . Therefore the eigenstates of H will be even or odd under any of the operations. From an arbitrary basis $\{|\psi_\nu\rangle\}$ we can generate 2 bases $|C_{2\pm}\rangle = \frac{1 \pm C_2}{\sqrt{2}} |\psi_\nu\rangle$, then 4 bases $|C_2 \pm \sigma(xz)\pm\rangle = \frac{1 \pm \sigma(xz)}{\sqrt{2}} \frac{1 \pm C_2}{\sqrt{2}} |\psi_\nu\rangle$, and 8 bases $|C_2 \pm \sigma(xz) \pm \sigma(yz)\pm\rangle = \frac{1 \pm \sigma_{yz}}{\sqrt{2}} \frac{1 \pm \sigma(xz)}{\sqrt{2}} \frac{1 \pm C_2}{\sqrt{2}} |\psi_\nu\rangle$. One can diagonalize H separately on these bases. Here is a representation of the Group. If we replace every operator by 1, the multiplication Table is trivially verified; -1 choices are also allowed, as follows:

C_{2v}	I	C_2	σ_{xz}	σ_{yz}	$g = 4$
A_1	1	1	1	1	z
A_2	1	1	-1	-1	xy, R_z
B_1	1	-1	1	-1	x, R_y
B_2	1	-1	-1	1	y, R_x

Such are the possible symmetry types of the solutions, that have conventional names shown in the first column.

The C_{3v} Group (NH_3)

The C_{3v} (or $3m$) Group is the symmetry Group of an equilateral triangle (or the Group $S(3)$ of the permutations of 3 objects). Let the vertices be labeled (a,b,c). The operations are a C_3 rotation, its square (or inverse, which is the same) and three vertical planes $\sigma_a, \sigma_b, \sigma_c$ through the center and the vertices. The sense of rotation is arbitrary and we may choose C_3 as the operation $(a, b, c) \rightarrow (c, a, b)$; clearly $\sigma_a (a, b, c) \rightarrow (a, c, b)$. Next, we need a convention

about the multiplication of two operation. $\sigma_a C_3(a, b, c) = \sigma_a(c, a, b)$ The commonly adopted one states that the result is (c, b, a) , that is, σ_a keeps the first entry fixed, although the first operation sent a elsewhere. In other terms, it is the position of symmetry elements that matters, while the label can change.

In this way, one notices that $\sigma_a C_3 = \sigma_b$, but $C_3 \sigma_a = \sigma_c$, thus the Group is not Abelian. All the information about the abstract Group is in the multiplication table.

E	C_3	C_3^2	σ_a	σ_b	σ_c
C_3	C_3^2	E	σ_c	σ_a	σ_b
C_3^2	E	C_3	σ_b	σ_c	σ_a
σ_a	σ_b	σ_c	E	C_3	C_3^2
σ_b	σ_c	σ_a	C_3^2	E	C_3
σ_c	σ_a	σ_b	C_3	C_3^2	E

(7.14)

The *rearrangement theorem* holds:

Theorem 2. *Each line and each column contain all $R \in G$.*

This follows from the definition of Group. In any line or column there are g elements, and all are distinct since for instance $C_3 R = C_3 S \Rightarrow R = S$. Every operation does a permutation of the vertices. In C_{3v} the converse is also true, so C_{3v} is isomorphous to $S(3)$. Already in C_{4v} the 8 operations are fewer than the 24 permutations of 4 objects. The Cayley theorem states that

Theorem 3. *Any group of order N_G is isomorphous to a subgroup of $S(N_G)$.*

$Z_3 = \{E, C_3, C_3^2\} \subset C_{3v}$ is an invariant Abelian subgroup. A Group G is called **simple** if it does not have invariant subgroups. So, Z_3 is simple, but C_{3v} is not. A Group G is called **semi-simple** if it does not have abelian invariant subgroups. So, Z_3 is semi-simple, but C_{3v} is not.

It is interesting to find representations of Z_3 using the multiplication table above. Besides the trivial one, with all the operators represented by 1 (the A_1 representation below in Table 7.1) one can represent C_3 by $\epsilon = e^{\frac{2\pi i}{3}}$ and C_3^2 by the third cubic root of 1, namely ϵ^* ; in a third representation, $C_3 \rightarrow \epsilon^*, C_3^2 \rightarrow \epsilon$. Thus, there are two complex conjugate representations.

The p orbitals of an atom centered at the origin behave differently under Z_3 : the z orbital, that we assume parallel to the rotation axis, is not transformed and belongs to A_1 . The combination $x + iy$ is multiplied by ϵ and $x - iy$ is multiplied by ϵ^* ; thus the (x,y) pair is a basis for the conjugate representations. This is reported in the last column of Table 7.1)

The Quotient Group

Let H be a subgroup of order N_H of G and $g \in G$. the sets

$$Hg = \{hg, h \in H\}, \quad gH = \{gh, h \in H\}$$

are respectively right and left cosets. Both have exactly N_H elements; for instance, $h_1 g = h_2 g$ multiplied on the right by g^{-1} becomes $h_1 = h_2$.

$C_3 = Z_3$	I	C_3	C_3^2	$\varepsilon = e^{\frac{2i\pi}{3}}$
A_1	1	1	1	z
E	$\begin{Bmatrix} 1 \\ 1 \end{Bmatrix}$	$\begin{Bmatrix} \varepsilon \\ \varepsilon^* \end{Bmatrix}$	$\begin{Bmatrix} \varepsilon^* \\ \varepsilon \end{Bmatrix}$	(x, y)

Table 7.1. The Z_3 Group and its representations.

For example, in C_{3v} , using Z_3 and σ_a one forms the right coset

$$\{E, C_3, C_3^2\}\sigma_a = \{\sigma_a, \sigma_b, \sigma_c\}.$$

Using σ_b or σ_c one finds the same coset, while a rotation gives Z_3 . Actually, we have split C_{3v} in two subsets of 3 elements each as follows:

$$C_{3v} = Z_3 + Z_3\sigma_a. \tag{7.15}$$

Let us generalize these findings to any G . If we form a right coset using a subgroup $H \subset G$ of order N_H and $g \in H$ we only get elements $hg \in H$. On the other hand, if $g_1 \notin H$ the coset Hg_1 is totally disjoint from H since for all its N_H elements we conclude $hg_1 \notin H$; otherwise from $hg_1 = h' \in H$ we could deduce $g_1 \in H$. If G is the union of H and Hg , we may conclude that $N_G = 2N_H$. Otherwise, we form the coset Hg_2 with $g_2 \notin H, g_2 \notin Hg$; now Hg_2 is disjoint from H and from Hg_1 (since $hg_2 = h'g_1 \Rightarrow g_2 = h^{-1}h'g_1 \in Hg_1$). We go on until G has been totally partitioned:

$$G = \sum_j Hg_j. \tag{7.16}$$

This proves the famous **Lagrange Theorem**:

Theorem 4. *The order of any subgroup of G is a divisor of N_G .*

Let H be an invariant subgroup of G . All its right cosets are equal to the left cosets, i.e. $aH = Ha, \forall a$. It is useful to define some multiplications of sets. We may say that $aH \times H = aH$, meaning that for any element of the coset $ahh' = ah''$ is again in aH .

For example, Z_3 is an invariant subgroup of C_{3v} and the left coset $\sigma_a Z_3 = \{\sigma_a, \sigma_b, \sigma_c\}$ is the set of reflections; multiplying by the rotations in Z_3 we get nothing more and $\{\sigma_a, \sigma_b, \sigma_c\} \times Z_3 = \{\sigma_a, \sigma_b, \sigma_c\}$. In a similar way, we can define an abstract set multiplication, treating the cosets as elements; for instance $aH \times bH$ is the set of all the elements $ah_1bh_2, h_1 \in H, h_2 \in H$; it is understood that every element may occur more than once and we *remove all duplicates*. Since H is invariant, $h_1b = bh_3$ for some $h_3 \in H$; so, $aH \times bH = abH$ and $aH \times a^{-1}H = H$. Thus, the cosets are elements of the **quotient Group G/H** , where H is the identity. Broadly speaking C_{3v}/Z_3 reduces to two elements, the rotations and the reflections; rotation \times rotation = rotation, rotation \times reflection = reflection, and reflection \times reflection = rotation. This is a powerful synthesis of the multiplication table of C_{3v} .

7.2.2 Dirac characters and Irreducible Representations

When G is not Abelian, the elementary method allows diagonalizing H simultaneously with one or a few $R \in G$. In the C_{3v} example, one can choose C_3 (and C_3^2 , but this adds nothing) or one reflection. In this way, one is neglecting most of the symmetry related information. Although this does not cause errors, the use of Group Theory is much more rewarding.

We must find functions of the operators $R \in G$ such that they commute with all G elements (besides H ; but this we take for granted, by definition of a symmetry Group). We could think about powers or products, but since G is closed the most general function is a linear combination. For any abstract Group, the linear combinations of the elements constitute the Group *algebra*. Intuitively, $\Omega = \sum_{T \in G}^{N_G} T$ should be a symmetric object. This is a good idea, since, by the rearrangement theorem (2) $\sum_{T \in G}^{N_G} TS = \sum_{T \in G}^{N_G} T = S \sum_{T \in G}^{N_G} T$, so Ω commutes with all G .

Actually, we can do much better than that; intuitively, the sum of all rotations of a given angle is already a symmetric object, the sum of all reflections another one. To proceed, we need to introduce the class concept, that allows to classify together operations that do essentially the same thing: such operators are called conjugated². Mathematically, two operators A and B are conjugated

$$A \sim B = \{\exists X \in G : A = X^{-1}BX\} \quad (7.17)$$

which is tantamount to say that X is a change of reference that converts B into A. Thus, C_{3v} has 3 classes $\{E\}, \{C_3, C_3^2\}, \{\sigma_a, \sigma_b, \sigma_c\}$. In Abelian Groups each element is conjugated to itself. The Identity E is trivially a class. For every class C, with n_C elements, we define Dirac's character

$$\Omega_C = \sum_{T \in C}^{n_C} T, \quad (7.18)$$

that commutes with all G , that is $\forall X \in G, \Omega_C = X^{-1}\Omega_C X$. Indeed, $X^{-1}\Omega_C X = \sum_{T \in C}^{n_C} X^{-1}TX$ has n_C terms conjugated with T and such terms are all different because $X^{-1}TX = X^{-1}T'X \Rightarrow T = T'$. So, we have a quantum number for each class.

For C_{3v} , the Dirac characters are

$$\Omega_E = E, \Omega_R = C_3 + C_3^2, \Omega_\sigma = \sigma_a + \sigma_b + \sigma_c.$$

These are simultaneously diagonal and their eigenvalues $\omega_E = 1, \omega_R, \omega_\sigma$ (except the first, which is trivial) are useful wavefunction labels. They are not independent, but occur in combinations. Using the multiplication table,

²this term is rather strange, since an element can be conjugated to any number of elements.

$$\Omega_R^2 = 2 + \Omega_R; \tag{7.19}$$

hence

$$\omega_R^2 = 2 + \omega_R \Rightarrow \omega_R = \begin{cases} 2 \\ -1 \end{cases} \tag{7.20}$$

$$\Omega_\sigma^2 = 3 + 3\Omega_R \Rightarrow \omega_\sigma^2 = 3 + 3\omega_R. \tag{7.21}$$

The allowed combinations correspond to the possible symmetry types allowed by C_{3v} ; they are called **Irreducible Representations** or *Irreps* for short:

Irrep	ω_R	ω_σ
A_1	2	3
A_2	2	-3
E	-1	0

(7.22)

We can label H eigenstates by the irreps; remarkably, they are never mixed by symmetry operations since

$$\forall X \in G, \Omega_C|\psi\rangle = \omega_C|\psi\rangle \Rightarrow \Omega_C X|\psi\rangle = \omega_C X|\psi\rangle. \tag{7.23}$$

A_1 is a trivial representation with all operators represented by 1 and Dirac characters equal to n_C for each class. This totalsymmetric representation exists for any Group, since any multiplication table is satisfied. A_2 is similar but odd for reflections. In all non-Abelian Groups there are irreps that require matrices, rather than numbers, to represent operators, and the irrep E above is an example. Just consider transforming a point (x, y) in the plane ((p_x, p_y)

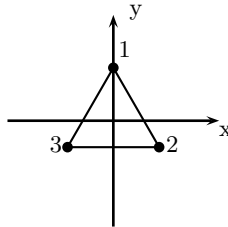


Fig. 7.1. The chosen geometry, with the σ_1 reflection that changes x into $-x$.

orbitals or any pair of functions transforming like (x,y) will do the same):

$$D(E) = \begin{pmatrix} 1 & 0 \\ 0 & 1 \end{pmatrix}; D(C_3) = \begin{pmatrix} c & -s \\ s & c \end{pmatrix}; D(\sigma_a) = \begin{pmatrix} -1 & 0 \\ 0 & 1 \end{pmatrix} \tag{7.24}$$

with $c = \cos(\frac{2\pi}{3}) = -\frac{1}{2}$, $s = \sin(\frac{2\pi}{3}) = \frac{\sqrt{3}}{2}$. These are the generators, i.e., the others can be obtained by multiplication:

$$D(C_3^2) = D(C_3)^2 = \begin{pmatrix} c & s \\ -s & c \end{pmatrix}; D(\sigma_b) = D(\sigma_a)D(C_3) = \begin{pmatrix} -c & s \\ s & c \end{pmatrix};$$

$$D(\sigma_c) = D(\sigma_a)D(C_3^2) = \begin{pmatrix} -c & -s \\ -s & c \end{pmatrix}. \tag{7.25}$$

The multiplication table is obeyed. How can the Dirac characters commute with every D ? One finds $\Omega_R = \begin{pmatrix} -1 & 0 \\ 0 & -1 \end{pmatrix}$, $\Omega_\sigma = \begin{pmatrix} 0 & 0 \\ 0 & 0 \end{pmatrix}$. The size m of the representative matrices of the Irreps ($m=1$ for A_1 and A_2 , $m=2$ for E) grows with the size and complexity of the Group. In the 32 point Groups one finds at most vector or pseudovector representations having $m=3$, but much larger sizes occur in more advanced applications.

The whole Hilbert space is partitioned into subspaces labelled by the irreps; besides the symmetry operators, H does not have matrix elements between states with different good quantum numbers and the diagonalization problem is broken. Diagonalizing H within each subspace one finds eigenstates carrying the Irrep label. Consider a pair of eigenfunctions (ψ_x, ψ_y) belonging to the Irrep E ; $H\psi_x = \epsilon_x\psi_x$, $H\psi_y = \epsilon_y\psi_y$. However, $\epsilon_x = \epsilon_y = \epsilon$, because every operation $S \in G$ maps ψ_x into a linear combination $S\psi_x = \alpha\psi_x + \beta\psi_y$, but since $[S, H]_- = 0$, the transformed function $S\psi_x$ must belong to the same eigenvalue as before. The same reasoning can be repeated for the Ω matrices. To sum up, the matrices of H and those of Dirac characters have the remarkable property of being **constants**, that is, identity matrices $I_{(m \times m)}$ multiplied by numbers:

$$H = \epsilon I_{m \times m}, \Omega_C = \omega_C I_{m \times m} \quad (7.26)$$

By a unitary transformation $\begin{pmatrix} x' \\ y' \end{pmatrix} = U \begin{pmatrix} x \\ y \end{pmatrix}$ we can change basis and matrices within the E irrep. Let U be a rotation: then $\forall R, D(R) \rightarrow UD(R)U^{-1}$ is consistent with the multiplication table and does not modify the Dirac characters. Thus, one of the non-trivial $D(R)$ matrices can always be chosen diagonal. Up to this unitary transformation, the Irreps with the same characters are to be identified. For instance, we may wish to have a new representation \tilde{D} in which $\tilde{D}(C_3)$ is diagonal. Picking $U = \begin{pmatrix} \frac{1}{\sqrt{2}} & \frac{i}{\sqrt{2}} \\ \frac{1}{\sqrt{2}} & \frac{-i}{\sqrt{2}} \end{pmatrix}$, which is unitary ($U^\dagger U = \text{unit matrix}$), $\tilde{D}(C_3) = U \cdot D(C_3) \cdot U^\dagger = \text{diag}(e^{2i\pi/3}, e^{-2i\pi/3})$ is diagonal; $\tilde{D}(C_3^2)$ is also diagonal of course, but $U \cdot D(\sigma_a) \cdot U^\dagger = \begin{pmatrix} 0 & -1 \\ -1 & 0 \end{pmatrix}$ and the other reflections are off-diagonal.

By joining the basis of an Irreps of size m_1 with basis of an Irreps of size m_2 we obtain a basis of size $m_1 + m_2$ with D matrix in block form. By unitary transformations we can generate $m_1 + m_2$ representatives which are no longer in block form. In general, by taking linear combinations of several bases of Irreps, we can form bigger representatives with no simple pattern of vanishing elements. These are called *reducible representations* to imply that the intelligent thing to do is just the reverse of this process. Starting with an arbitrary basis that yield big and useless D matrices one would like to find linear transformations that put the D matrices in block form, and allow separating the basis in symmetry-adapted parts; when the blocks can

no longer be reduced in size, the Irreps are obtained. Therefore we cannot put all the matrices of an irrep in the same block form.

Traces and Characters of an Irrep

Consider a basis and the representative matrices of a m -dimensional irrep i (in this paragraph I omit the index i for short). The trace

$$\chi(C) = \text{Tr}D(R) = \sum_{\mu} D_{\mu\mu}(R), \quad R \in C \quad (7.27)$$

is the same for all D matrices in the given class C , since the Tr operation is invariant under unitary transformations like conjugation. $\chi(C)$ is called **character**, and is related to Dirac's character. The matrices of the Ω_C are constants³, hence, recalling the definition of Ω_C

$$\text{Tr}\Omega_C = m\omega_C = n_C\chi(C). \quad (7.28)$$

Thus,

$$\chi(C) = \frac{m}{n_C}\omega_C. \quad (7.29)$$

The characters $\chi(C)$ are very useful, as we shall see, and are tabulated for the point Groups (See Appendix II; note that these tables are square (the number of irreps is equal to the number of classes)). In particular $\text{Tr}\Omega_E = m$ can be read off the Tables.

Actually, the tables were computed (and can be found for *new* Groups when necessary) from the multiplication Table; one first deduces the classes and ω_c as in the above example. One does not know m *a priori* but shall derive below

$$m^2 = \frac{N_G}{\sum_C \frac{\omega_C^2}{n_C}}. \quad (7.30)$$

With this result, the reader is already able to calculate the character tables.

7.2.3 Schur's lemma

We have shown above that the matrices of Dirac characters and of H within an irrep are multiples of the identity matrix. Due to the importance of this crucial point I'll present a second proof, the traditional one based on Shur's lemma. The two arguments enlighten different facets of the problem; it will be apparent below that this is just a matter of algebra.

Lemma 1. *Any $m \times m$ matrix M commuting with all the representative matrices $D(R_i)$, $1 = 1, \dots, N_G$ of an m -dimensional Irrep must be proportional to the Identity matrix $I_{m \times m}$.*

³ H is also constant and $\text{Tr}H = m\epsilon$.

We first prove the lemma for a 2×2 diagonal matrix, then generalize to any matrix of any size.

Proof for a diagonal matrix

For 2×2 matrices, we let $M = \Delta = \text{diag}(d_1, d_2)$, with $A = \begin{pmatrix} a_{11} & a_{12} \\ a_{21} & a_{22} \end{pmatrix}$, and

$$[A, \Delta]_- = \begin{pmatrix} 0 & a_{12}(d_2 - d_1) \\ -a_{21}(d_2 - d_1) & 0 \end{pmatrix} = \begin{pmatrix} 0 & 0 \\ 0 & 0 \end{pmatrix}.$$

Now, if d_2 were $\neq d_1$, this would require a diagonal A . Since one cannot diagonalize simultaneously all the $D(R_i)$, $1 = 1, \dots, N_G$, we conclude that $d_2 = d_1$.

In the 3×3 case, we let $M = \Delta = \text{diag}(d_1, d_2, d_3)$, and the same reasoning leads to

$$[A, \Delta]_- = \begin{pmatrix} 0 & a_{12}(d_2 - d_1) & a_{13}(d_3 - d_1) \\ a_{21}(d_1 - d_2) & 0 & a_{23}(d_3 - d_2) \\ a_{31}(d_1 - d_3) & a_{32}(d_2 - d_3) & 0 \end{pmatrix}.$$

If all the d_i are different, this vanishes only for diagonal A . If d_1 is different from the other diagonal elements, the a_{11} element must be one block, separated from the rest, which cannot be true for all the representative matrices in an irrep. This is formally generalized formally to matrices of any size with the conclusion that $\Delta = \lambda I_{m \times m}$ for some λ .

Proof for a Hermitian M

Assuming M hermitian we know that by a unitary transformation U it can be diagonalized $U \cdot M \cdot U^\dagger = \Delta = \lambda I_{m \times m}$ and actually this implies that $M = \lambda I_{m \times m}$ in any basis.

Proof for any M

We can do without the assumption that M is Hermitian. Indeed, $H_1 = M + M^\dagger$ and $H_2 = -i(M - M^\dagger)$ are Hermitian at any rate. Now, we show that M^\dagger also commutes, for, by taking the Hermitian conjugate of $D(R_i)M = MD(R_i)$, one finds $M^\dagger D(R_i)^\dagger = D^\dagger(R_i)M^{\text{dag}}$. Now we multiply on the left and on the right by $D(R_i)$ and since it is unitary we find $D(R_i)M^\dagger = M^\dagger D(R_i)$. Then H_1 and H_2 also commute, and are constants. Therefore, $M = \frac{1}{2}(H_1 - iH_2) = \lambda I_{m \times m}$,
q.e.d.

7.2.4 Continuous Groups

Many Groups of fundamental importance in Physics are **Lie Groups**. They are continuous (elements can be labeled by parameters) and continuously

connected (for every pair of elements a continuous path in parameter space can be found that joins them). Moreover, the parameters of the products are C^1 functions of those of the factors.

A **compact** Lie Group has all parameters that vary over a closed interval; the Lorentz Group and the Group of all translations are noncompact Lie Groups, while the rotations are a compact Lie Group.

The phase factors $e^{i\alpha}$ constitute the Group $U(1)$. The $SO(3)$ Group of rotations in 3d is a continuous Group. An element may be represented as a vector $\vec{\phi}$ directed along the axis and with length equal to the angle of (say, counterclockwise) rotation ϕ ; this corresponds to a sphere of radius π where, however, each point of the surface is equivalent to the opposite one. All the rotations with the same $|\phi|$ belong to the same class. the angular momentum operator \vec{L} is the generator of infinitesimal rotations. For integer L one finds $2L+1$ spherical harmonics $Y_{LM}(\theta, \phi)$ that are simultaneous eigenvectors of L^2 and L_z . Only the harmonics of a given L mix under rotations; they are the basis of an irrep.

For angular momentum $J = \frac{1}{2}$, the rotation operators (7.2) build a double valued representation, since $R_{\vec{\phi} + 2\pi} = -R_{\vec{\phi}}$; they make up $SU(2)$, the *covering Group* of $O(3)$ corresponding to a sphere of radius 2π . The Wigner matrices are defined by

$$R_{\alpha}|Jm\rangle = \sum_{m'=-J}^J |Jm'\rangle D_{m'm}^J(\alpha). \tag{7.31}$$

The $SU(3)$ Group is a paradigm of Particle Physics. $SO(4)$ is the rotation group in $4d$; rotations are in the planes ij with i and $j = 1$ to 4. Therefore there are $\binom{4}{2} = 6$ generators $A_1, A_2, A_3, B_1, B_2, B_3$; it can be shown that $[A_i, A_j]_- = i\epsilon_{ijk}A_k, [B_i, B_j]_- = i\epsilon_{ijk}B_k$ and $[A_i, B_j]_- = 0$.

7.3 Accidental degeneracy and hidden symmetries

Let H be a Hamiltonian of C_{3v} symmetry; if one succeeds to separate the Hilbert space according to the irreps, the problem breaks down into independent subproblems of A_1, A_2 and E symmetry; in the E subspace one can decide to have σ_a diagonal; if σ_a is the reflection that sends x to $-x$ one has (ψ_x, ψ_y) pairs that are not mixed by H since they form a $m = 2$ subspace where H is constant. If one diagonalizes H in the x subspace finds all the ψ_x ; from each ψ_x one then finds the corresponding ψ_y without need of further diagonalizations; one could apply any off-diagonal operator like C_3 and then orthogonalize to ψ_x . In general, the knowledge of one eigenfunction is enough to determine all the m degenerate eigenfunctions belonging to the same irrep.

Sometimes one finds unexpected degeneracies. Eigenfunctions belonging to non-degenerate irreps are found to be degenerate; or the actual degeneracy

d is higher than m . The most popular case occurs in the Schrödinger theory of the H atom, when energy depends only on the principal quantum number n and orbitals have a n^2 -fold degeneracy, while the spherical symmetry only allows the energy to be independent on magnetic quantum number. In such cases, one cannot produce the 2p orbitals by rotating the 2s one. In such cases, one speaks of *accidental degeneracy*.

It is possible that by accident two states unrelated by symmetry come so close in energy to appear degenerate in low resolution experiment; however a *mathematically exact* degeneracy with no symmetry reason is miraculous. Simply, one was unaware of using a Subgroup of the actual Group, because some symmetry had still to be discovered, as in the following examples.

Hydrogen Atom

The n^2 -fold degeneracy of the non-relativistic H atom Hamiltonian

$$H = \frac{p^2}{2m} - \frac{k}{r} \quad (7.32)$$

is explained by a *dynamical symmetry*, specific of the $\frac{1}{r}$ potential.

The Classical Runge-Lenz Vector

The fact that the force $\vec{F} = -k\frac{\vec{r}}{r^3}$ is central explains the conservation of angular momentum: $\frac{d\vec{L}}{dt} = \vec{v} \wedge \vec{p} + \vec{r} \wedge \vec{F} = 0$. We take the z axis along \vec{L} , and the motion occurs in the $z = 0$ plane. The special form of the potential entails the conservation of the Runge-Lenz vector

$$\vec{R} = \frac{\vec{p} \wedge \vec{L}}{m} - k\frac{\vec{r}}{r}. \quad (7.33)$$

To see that, using $\frac{d}{dt}\frac{1}{r} = -\frac{\vec{r} \cdot \vec{v}}{r^3}$, one works out

$$\frac{d}{dt}\frac{\vec{r}}{r} = \frac{r^2\vec{v} - \vec{r}(\vec{r} \cdot \vec{v})}{r^3}. \quad (7.34)$$

The x component of the numerator is $(x^2 + y^2)v_x - x(xv_x + yv_y) = -\frac{L}{m}y$. Developing in this way, one finds

$$\frac{d}{dt}\frac{\vec{r}}{r} = \frac{L}{mr^3}(-y, x, 0). \quad (7.35)$$

The conservation of \vec{R} follows comparing this with

$$\frac{d}{dt}\frac{\vec{p} \wedge \vec{L}}{m} = \frac{L}{m}(F_y, -F_x, 0) = \frac{kL}{mr^3}(-y, x, 0). \quad (7.36)$$

During the motion, $\vec{p} \wedge \vec{L}$ is in the xy plane. At perihelion, $\vec{p} \perp \vec{r} \Rightarrow \vec{p} \wedge \vec{L} \parallel \vec{r} \Rightarrow \vec{R} \parallel \vec{r}$. Since it is conserved, \vec{R} is pinned at the aphelion-perihelion direction⁴ and this is why the orbits are closed⁵.

Quantum Runge-Lenz Vector

The quantum Runge-Lenz vector

$$\vec{R} = \frac{\vec{p} \wedge \vec{L} - \vec{L} \wedge \vec{p}}{2m} - k \frac{\vec{r}}{r}. \quad (7.37)$$

commutes with H ; the calculation can be carried out like above, with $\frac{dA}{dt}$ replaced by $\frac{i}{\hbar}[H, A]$. Hence,

$$H\psi_{LM} = E\psi_{LM} \Rightarrow H \vec{R}\psi_{LM} = E \vec{R}\psi_{LM};$$

but one can check that \vec{R} does not commute with L^2 , so $\vec{R}\psi_{LM}$ does not belong to L and the energy must be L independent. More details and the relation to the O(4) Group worked out by Pauli can be found on Schiff's book[25]. In the relativistic case, the Dirac-Coulomb Hamiltonian H_{DC} commutes with the *Biedernharn-Johnson-Lippman (BJL) pseudoscalar operator*

$$B = \frac{i}{mc^2} K \gamma_5 (H_{DC} - \beta mc^2) - \frac{Ze^2}{c} \frac{\vec{\Sigma} \cdot \vec{r}}{r} \quad (7.38)$$

where $K = \beta [\vec{\Sigma} \cdot \vec{L} + \hbar]$, $\vec{\Sigma} = \begin{pmatrix} \vec{\sigma} & 0 \\ 0 & \vec{\sigma} \end{pmatrix}$, $\beta = \gamma_4$, $\gamma_5 = \gamma_1 \gamma_2 \gamma_3 \gamma_4$. This is the reason why the levels do not depend on the sign of K and for instance the pairs $(2s_{1/2}, 2p_{1/2})$, $(3s_{1/2}, 3p_{1/2})$, $(3p_{3/2}, 2d_{3/2})$ are degenerate in Dirac's theory.

Appearance is Deceptive: Simple Example

The square tight-binding cluster described by

$$h = \begin{pmatrix} 0 & 1 & 1 & 0 \\ 1 & 0 & 0 & 1 \\ 1 & 0 & 0 & 1 \\ 0 & 1 & 1 & 0 \end{pmatrix} \quad (7.39)$$

has the following spectrum:

⁴For circular orbits, using $\frac{mv^2}{r} = \frac{k}{r^2}$ one finds that \vec{R} vanishes.

⁵The 2d isotropic harmonic oscillator also does; the energy is conserved along both axes, so there is an extra conserved quantity also in that case.

ϵ	ψ
-2	$\psi_{-2} = (\frac{1}{2}, -\frac{1}{2}, -\frac{1}{2}, \frac{1}{2})$
0	$\psi_{0,1} = (\frac{1}{\sqrt{2}}, 0, 0, -\frac{1}{\sqrt{2}})$
0	$\psi_{0,2} = (0, \frac{1}{\sqrt{2}}, -\frac{1}{\sqrt{2}}, 0)$
2	$\psi_2 = (\frac{1}{2}, \frac{1}{2}, \frac{1}{2}, \frac{1}{2})$

and the degeneracy is expected because the irrep E of C_{4v} has to be represented. The eigenvalues come in pairs $(\pm|\epsilon|)$ since this graph is bipartite.

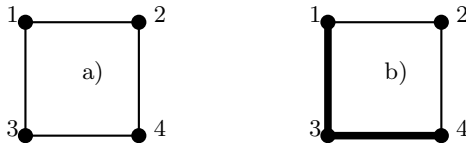


Fig. 7.2. Illustrative example of dynamical symmetry. a) square tight-binding cluster b) deformed cluster with heavy lines denote doubled matrix elements. The symmetry Group of b) is isomorphic to the Group of the square.

Now we *deform* the square, by changing the hopping integrals to and from an atom: let's say, we double those connecting site 3 to 1 and 4. Now, the Hamiltonian reads

$$\check{h} = \begin{pmatrix} 0 & 1 & 2 & 0 \\ 1 & 0 & 0 & 1 \\ 2 & 0 & 0 & 2 \\ 0 & 1 & 2 & 0 \end{pmatrix}. \tag{7.40}$$

The deformed cluster has much less geometrical symmetry but as much dynamical symmetry as before. Was the degeneracy removed? No. The first and last lines are equal and the other two are proportional, thus two zero eigenvalues are still there. Indeed, \check{h} has the following spectrum:

ϵ	ψ
$-\sqrt{10}$	$(\frac{1}{2}, -\frac{1}{\sqrt{10}}, -\sqrt{\frac{2}{5}}, \frac{1}{2})$
0	$(\frac{1}{\sqrt{2}}, 0, 0, -\frac{1}{\sqrt{2}})$
0	$(0, -\frac{2}{\sqrt{5}}, \frac{1}{\sqrt{5}}, 0)$
$\sqrt{10}$	$(\frac{1}{2}, \frac{1}{\sqrt{10}}, \sqrt{\frac{2}{5}}, \frac{1}{2})$

There is accidental degeneracy. One symmetry element is the reflection

$$\sigma = \begin{pmatrix} 0 & 0 & 0 & 1 \\ 0 & 1 & 0 & 0 \\ 0 & 0 & 1 & 0 \\ 1 & 0 & 0 & 0 \end{pmatrix}$$

with $\sigma\psi_{0,1} = -\psi_{0,1}$; $\sigma\psi_{0,2} = \psi_{0,1}$. To explain this degeneracy we want a non-Abelian Group. Indeed, the 90 degree rotation is broken, but we seek a convenient generalization S , with $S^T = S^{-1}$, $S^T \check{h} S = \check{h}$. We seek it such that opposite sites are not coupled ($S_{14} = S_{23} = 0$) and $S_{12} = S_{24}$, $S_{13} = S_{34}$. One solution is the generalized 90⁰ rotation

$$S = \begin{pmatrix} 0 & 0 & 1 & 0 \\ 1 & 0 & 0 & 0 \\ 0 & 0 & 0 & 1 \\ 0 & 1 & 0 & 0 \end{pmatrix} \rightarrow \check{S} = \frac{1}{\sqrt{10}} \begin{pmatrix} 0 & -1 & 3 & 0 \\ 3 & 0 & 0 & -1 \\ 1 & 0 & 0 & 3 \\ 0 & 3 & 1 & 0 \end{pmatrix} \tag{7.41}$$

Note that $S^4 = 1$ and S does not produce a permutation of sites but is a genuine generalization. Moreover S mixes $\psi_{0,1}$ and $\psi_{0,2}$, does not commute with σ and explains the degeneracy. The deformed problem has a lower geometrical symmetry, but actually is still C_{4v} symmetric because of a hidden dynamical symmetry. More dynamical symmetries will be discussed in Sect.17.0.6.

7.4 Great Orthogonality Theorem (GOT)

The theorem states that the D matrices are orthogonal over all their indices.

Theorem 5. (*Great Orthogonality Theorem*)

Let $D_{\mu\nu}^{(i)}(R)$ be the $\mu\nu$ element of the matrix of the irrep i representing the element $R \in G$. Let N_G be the order of the Group and let m_i be the dimension of the irrep i . Then

$$\sum_{R \in G} D_{\mu\nu}^{(i)}(R)^* D_{\alpha\beta}^{(j)}(R) = \frac{N_G}{m_i} \delta_{ij} \delta_{\mu\alpha} \delta_{\nu\beta}. \tag{7.42}$$

The GOT is the central result of Group representation theory, and I prepare the proof by a few remarks.

Remark 1: I am going to present the proof for discrete Groups, however the GOT extends to continuous ones. The following orthogonality holds for the Wigner matrices[23]

$$\int d\Omega D_{ab}^{J*}(\alpha\beta\gamma) D_{a'b'}^{J'}(\alpha\beta\gamma) = \frac{8\pi^2}{2J+1} \delta_{a,a'} \delta_{b,b'} \delta_{J,J'} \tag{7.43}$$

where α, β, γ are Euler angles and $\int d\Omega = \int_0^{2\pi} d\alpha \int_0^\pi \sin \beta d\beta \int_0^{2\pi} d\gamma$.

Remark 2: Let us resume the degenerate ($m = 2$) irrep of C_{3v} and the matrices

E	C_3	C_3^2	σ_a	σ_b	σ_c
$\begin{pmatrix} 1 & 0 \\ 0 & 1 \end{pmatrix}$	$\begin{pmatrix} -\frac{1}{2} & -\frac{\sqrt{3}}{2} \\ \frac{\sqrt{3}}{2} & -\frac{1}{2} \end{pmatrix}$	$\begin{pmatrix} -\frac{1}{2} & \frac{\sqrt{3}}{2} \\ -\frac{\sqrt{3}}{2} & -\frac{1}{2} \end{pmatrix}$	$\begin{pmatrix} -1 & 0 \\ 0 & 1 \end{pmatrix}$	$\begin{pmatrix} \frac{1}{2} & \frac{\sqrt{3}}{2} \\ \frac{\sqrt{3}}{2} & -\frac{1}{2} \end{pmatrix}$	$\begin{pmatrix} \frac{1}{2} & -\frac{\sqrt{3}}{2} \\ -\frac{\sqrt{3}}{2} & -\frac{1}{2} \end{pmatrix}$

(7.44)

Note that C_3^2 is the inverse of C_3 and its matrix is $D(C_3)^T$. More generally, the operators are unitary and

$$D_{\nu\mu}^{(i)}(R)^* = D_{\nu\mu}^{(i)}(R^{-1}). \tag{7.45}$$

Remark 3: Let ψ_μ^i be basis function belonging to the μ -th component of the irrep i and \mathcal{O} represent a total-symmetric operator, that is,

$$[\mathcal{O}, R]_- = 0, \forall R \in G.$$

Theorem 6. *The matrix elements obey the following rule:*

$$\langle \psi_\mu^i | \mathcal{O} | \psi_\nu^j \rangle = \mathcal{O}(i) \delta_{ij} \delta_{\mu\nu}. \tag{7.46}$$

For $i \neq j$, ψ^i and ψ^j are orthogonal because they belong to different eigenvalues of at least some Ω_c . The invariant operator \mathcal{O} commutes with the Dirac characters, so $\mathcal{O}|\psi^j\rangle$ has the same characters as $|\psi^j\rangle$. For $i = j$ the matrix $\{\mathcal{O}_{\mu\nu}\}$ represents an operator that commutes with everything, so it must commute with all the D matrices; so Schur’s lemma applies.

For example, a spherically symmetric potential has vanishing matrix elements between states of different L and within L it has vanishing matrix elements between states of different M_L ; the diagonal matrix elements are independent of M_L and depend on L .

Remark 4:

Theorem 7. *Consider an arbitrary operator Ξ .*

$$\mathcal{O} = \sum_{R \in G} R^{-1} \Xi R \tag{7.47}$$

is an invariant operator.

This follows immediately from the rearrangement theorem: $\forall T \in G, \mathcal{O}T = TT^{-1} \sum_{R \in G} R^{-1} \Xi RT = T \sum_{R \in G} (TR)^{-1} \Xi (TR) = T\mathcal{O}$.

Remark 5:

(example of GOT)

Let us form 6-component lists with the elements of the D matrices; if we treat them like vectors and compute the norms we find 6 for the irreps with $m=1$ and 3 for those with $m=2$.

element	list	\sum of squares
11 of irrep E	$(1, -\frac{1}{2}, -\frac{1}{2}, -1, \frac{1}{2}, \frac{1}{2})$	3
12 of irrep E	$(0, -\frac{\sqrt{3}}{2}, \frac{\sqrt{3}}{2}, 0, \frac{\sqrt{3}}{2}, -\frac{\sqrt{3}}{2})$	3
21 of irrep E	$(0, \frac{\sqrt{3}}{2}, -\frac{\sqrt{3}}{2}, 0, \frac{\sqrt{3}}{2}, -\frac{\sqrt{3}}{2})$	3
22 of irrep E	$(1, -\frac{1}{2}, -\frac{1}{2}, 1, -\frac{1}{2}, -\frac{1}{2})$	3
irrep A_1	$(1, 1, 1, 1, 1, 1)$	6
irrep A_2	$(1, 1, 1, -1, -1, -1)$	6

Moreover these *vectors* are all orthogonal.

Proof of GOT

We insert (7.47) into (7.46) but do not specify yet Ξ :

$$\sum_{R \in G} \langle \psi_\mu^i | R^{-1} \Xi R | \psi_\nu^j \rangle = \mathcal{O}(i) \delta_{ij} \delta_{\mu\nu}. \tag{7.48}$$

Letting R operate with

$$R | \psi_\nu^j \rangle = \sum_\rho | \psi_\rho^j \rangle | D_{\rho\nu}^{(j)}(R),$$

$$\langle \psi_\mu^i | R^\dagger = \sum_\sigma \langle \psi_\sigma^i | D_{\sigma\mu}^{(i)}(R)^*,$$

we find

$$\langle \psi_\mu^i | \Xi | \psi_\nu^j \rangle = \sum_{R \in G} \sum_{\rho\sigma} \langle \psi_\sigma^i | \Xi | \psi_\rho^j \rangle D_{\rho\nu}^{(j)}(R) D_{\sigma\mu}^{(i)}(R)^* = \mathcal{O}(i) \delta_{ij} \delta_{\mu\nu}. \tag{7.49}$$

To prove the GOT we must eliminate $\sum_{\rho\sigma} \langle \psi_\sigma^i | \Xi | \psi_\rho^j \rangle$. Now we take advantage of the total freedom to choose Ξ as we like. If we assume that for some pair of components, α and β , say ,

$$\Xi = | \psi_\alpha^i \rangle \langle \psi_\beta^j |, \tag{7.50}$$

then $\langle \psi_\sigma^i | \Xi | \psi_\rho^j \rangle = \delta_{\alpha\sigma} \delta_{\beta\rho}$, we end up with

$$\sum_{R \in G} D_{\beta\nu}^{(j)}(R) D_{\alpha\mu}^{(i)}(R)^* = O_{\alpha\beta}(i) \delta_{ij} \delta_{\mu\nu}. \tag{7.51}$$

The matrix element $O_{\alpha\beta}(i)$ could in principle have acquired a dependence on the α and β indices, but we have proven the orthogonality on the second indices. The orthogonality on the first indices α and β is obtained by taking the complex conjugate, and noting that this exchanges the indices and $\sum_{R^{-1}} = \sum_R$. Thus,

$$\sum_{R \in G} D_{\beta\nu}^{(j)}(R) D_{\alpha\mu}^{(i)}(R)^* = O(i) \delta_{ij} \delta_{\mu\nu} \delta_{\alpha\beta}. \quad (7.52)$$

To determine $O(i)$ we set $i = j, \mu = \nu$ and $\alpha = \beta$. We get

$$\sum_{R \in G} D_{\alpha\mu}^{(i)}(R)^* D_{\alpha\mu}^{(i)}(R) = O(i) = \sum_{R \in G} D_{\mu\alpha}^{(i)}(R^{-1}) D_{\alpha\mu}^{(i)}(R). \quad (7.53)$$

Summing over α from 1 to m_i ,

$$m_i O(i) = \sum_{R \in G} D_{\mu\mu}^{(i)}(E) = \sum_{R \in G} 1 = N_G. \quad (7.54)$$

This completes the proof.

The GOT is an orthogonality relation between *vectors* having N_G components, one for each component of $D_{\alpha\beta}^{(i)}(R)$; each irrep contributes m_i^2 components, and in order that they be orthogonal

$$\sum_i m_i^2 \leq N_G. \quad (7.55)$$

This is an important restriction on the number and on the dimensions of irreps. We prove below **Burnside's theorem**

$$\sum_i m_i^2 = N_G. \quad (7.56)$$

7.5 Little Orthogonality Theorem (LOT)

From GOT we may obtain an orthogonality theorem between characters which is called LOT. The diagonal elements obey

$$\sum_{R \in G} D_{\mu\mu}^{(i)}(R)^* D_{\alpha\alpha}^{(j)}(R) = \frac{N_G}{m_i} \delta_{ij} \delta_{\mu\alpha}. \quad (7.57)$$

Summing on μ, α one obtains the LOT

$$\boxed{\sum_{R \in G} \chi^{(i)}(R)^* \chi^{(j)}(R) = N_G \delta_{ij}.} \quad (7.58)$$

In particular,

$$\sum_{R \in G} |\chi^{(i)}(R)|^2 = N_G, \tag{7.59}$$

which gives a method to verify that a given representation is indeed irreducible; if we mix two irreps i and j with coefficients n_i and n_j , then $\chi(R) = n_i\chi^{(i)} + n_j\chi^{(j)}$ and the r.h.s. becomes $N_G [n_i^2 + n_j^2 + 2n_in_j\delta_{ij}]$. Rewriting the LOT in terms of classes,

$$\sum_C n_C |\chi^{(i)}(C)|^2 = N_G, \tag{7.60}$$

and inserting $\chi^{(i)}(C) = \frac{m_i \omega_C}{n_C}$ we obtain

$$m_i = \sqrt{\frac{N_G}{\sum_C \frac{\omega_C^2}{n_C}}}. \tag{7.61}$$

A reducible representation can be reduced to block form and the block of the i -th irrep appears n_i times along the diagonal; on any basis, the trace is

$$\chi(R) = \sum_j n_j \chi^{(j)}(R).$$

Now multiply by $\chi^{(i)}(R)^*$ and sum over R :

$$\sum_R \chi^{(i)}(R)^* \chi(R) = \sum_j n_j \sum_R \chi^{(i)}(R)^* \chi^{(j)}(R)$$

which implies

$$n_i = \frac{1}{N_G} \sum_R \chi^{(i)}(R)^* \chi(R). \tag{7.62}$$

Also,

$$n_i = \frac{1}{N_G} \sum_C n_C \chi^{(i)}(C)^* \chi(C). \tag{7.63}$$

The LOT becomes: $\sum_C \chi^{(i)}(C)^* \chi^{(j)}(C) = N_G \delta_{ij}$, so the vectors with components $\sqrt{N_G} \chi^{(i)}(C)$ are also orthogonal. They have component for each class and there is one of them for each irrep. Thus, the number of irreps does not exceed the number of classes. Actually one can prove that they are equal, that is, the character tables must be square [156]. This is related to the second character orthogonality theorem

$$\boxed{\sum_i \chi^{(i)}(C) \chi^{(i)}(C')^* = \frac{N_G}{n_C} \delta_{CC'}}, \tag{7.64}$$

also demonstrated in Ref.[156].

7.6 Projection operators

From any $f(x)$ one can obtain functions of well-defined parity using the inversion operator and its eigenvalues to write $f^{(\pm)}(x) = f(x) \pm f(-x)$. The GOT generalizes this trick converting an arbitrary basis set into symmetry-adapted basis functions without any need to diagonalize any matrix. Multiply (7.42) $\sum_{R \in G} D_{\mu\nu}^{(i)}(R) * D_{\alpha\beta}^{(j)}(R) = \frac{N_G}{m_i} \delta_{ij} \delta_{\mu\alpha} \delta_{\nu\beta}$ by ψ_α^j and sum over α , using the fact that $\sum_\alpha D_{\alpha\beta}^{(j)}(R) \psi_\alpha^j = R\psi_\beta^j$:

$$\sum_\alpha \psi_\alpha^j \sum_{R \in G} D_{\mu\nu}^{(i)}(R) * D_{\alpha\beta}^{(j)}(R) = \sum_R D_{\mu\nu}^{(i)}(R) * R\psi_\beta^j = \sum_\alpha \psi_\alpha^j \frac{N_G}{m_i} \delta_{ij} \delta_{\mu\alpha} \delta_{\nu\beta}$$

that is,

$$\frac{m_i}{N_G} \sum_R D_{\mu\nu}^{(i)}(R) * R\psi_\beta^j = \delta_{ij} \delta_{\nu\beta} \psi_\mu^j. \quad (7.65)$$

Hence

$$P_{\mu\nu}^i = \frac{m_i}{N_G} \sum_R D_{\mu\nu}^{(i)}(R) * R \quad (7.66)$$

is a generalized projection operator⁶ such that $P_{\mu\nu}^i = |\psi_\mu^i\rangle \langle \psi_\nu^i|$. In other terms,

$$P_{\mu\nu}^i \psi_\lambda^j = \delta_{ij} \delta_{\nu\lambda} \psi_\mu^i. \quad (7.67)$$

The diagonal $P_{\mu\mu}^i$ operators are all what we want, and require only the diagonal elements of the $D_{\mu\nu}$ matrices. Let $\psi = \sum_{j\nu} c(j, \nu) \psi_\nu^j$ belong to a reducible representation:

$$P_{\mu\mu}^i \psi = c(i, \mu) \psi_\mu^i \quad (7.68)$$

is projected on ψ_μ^i , unless $c(i, \mu) = 0$ (if the choice was unlucky never mind, we shall succeed with another ψ of the reducible set). To transform the $\{\psi\}$ set to the new $\{\psi_\nu^j\}$ basis we just need to know how every $R \in G$ operates on the old set and the diagonal elements of the $D_{\mu\nu}^{(i)}(R)$ matrices. The $D_{\mu\nu}^{(i)}(R)$ matrices are properties of the abstract Group, and we know them in principle: they are $m_i \times m_i$ matrices and having fixed which operators R we can and wish to have diagonal, we have enough relations from the multiplication table to build them; in the most common problems this is just a matter of geometry to determine how the components of a point or other simple functions transform.

Moreover, the matrices are not really needed to project to the new basis. Indeed,

$$\sum_\mu P_{\mu\mu}^i \psi = \sum_\mu c(i, \mu) \psi_\mu^i. \quad (7.69)$$

In the combination on the r.h.s. all functions belong to the irrep i , so the l.h.s. is the projection operator,

⁶The name is deserved since the diagonal terms are such that $(P_{\mu\mu}^i)^2 = P_{\mu\mu}^i$.

$$P^{(i)} = \sum_{\mu} P_{\mu\mu}^i = \sum_R \chi^i(R)^* R. \tag{7.70}$$

The characters are enough to build $P^{(i)}$ and to obtain $P^{(i)}\psi$ which belongs to irrep i . Repeating this with enough ψ , one builds a basis for the irrep. These bases are typically small sets, where one can easily orthonormalize; usually one readily performs the unitary transformations needed to have as many diagonal operators as possible, in order to increase the number of quantum numbers.

7.7 Regular representation

The next theorem has a very elegant proof:

Theorem 8.

$$\sum_i m_i^2 = N_G. \tag{7.71}$$

Recall the rearrangement theorem: left-multiplying the group elements by one of them produces a permutation. In any Group of order $N_G = g$ with elements $R_1 \cdots R_g$, we associate to each element a vector

$$R_1 \rightarrow (1, 0, 0, 0, 0, 0), R_2 \rightarrow (0, 1, 0, 0, 0, 0), \cdots$$

and a $g \times g$ matrix that does the permutation. Thus, for each $R \in G$ there is a vector and a matrix; what matters is the Multiplication Table, and the vectors are just a way to get the matrices. Let us rewrite the multiplication Table of C_{3v} .

E	C_3	C_3^2	σ_a	σ_b	σ_c
C_3	C_3^2	E	σ_c	σ_a	σ_b
C_3^2	E	C_3	σ_b	σ_c	σ_a
σ_a	σ_b	σ_c	E	C_3	C_3^2
σ_b	σ_c	σ_a	C_3^2	E	C_3
σ_c	σ_a	σ_b	C_3	C_3^2	E

Let us denote the operations $R_1 \cdots R_6$ with $R_1 = E, R_2 = C_3$, and so on; the effect of the left-multiplication by C_3 is $1 \rightarrow 2, 2 \rightarrow 3, 3 \rightarrow 1, 4 \rightarrow 6, 5 \rightarrow 4, 6 \rightarrow 5$; the matrix is

$$D(C_3) = \begin{pmatrix} 0 & 0 & 1 & 0 & 0 & 0 \\ 1 & 0 & 0 & 0 & 0 & 0 \\ 0 & 1 & 0 & 0 & 0 & 0 \\ 0 & 0 & 0 & 0 & 1 & 0 \\ 0 & 0 & 0 & 0 & 0 & 1 \\ 0 & 0 & 0 & 1 & 0 & 0 \end{pmatrix},$$

while $D(E) = \text{Diag}(1, 1, 1, 1, 1)$. This *regular* representation exists for any G ; $\chi(E) = N_G$ while for all the other classes $\chi = 0$ since no other element can have 1 on the diagonal ($RX = X \Leftrightarrow R = E$). Irrep i is contained in the regular representation $n_i = \frac{1}{N_G} \sum_R \chi^i(R)^* \chi(R) = \frac{1}{N_G} \chi^i(E)^* \chi(E) = m_i$ times. Reducing the representation, we shall have on the diagonal m_i times the $m_i \times m_i$ block, and the length of the diagonal is N_G . This proves the Burnside theorem.

Problems

7.1. Prove Equation 13.136.

7.2. Build the character table of C_{4v} .

7.3. Build the projection operator for the irrep E, component y , of C_{4v} .

8 Simpler Uses of Group Theory

8.1 Molecular Orbitals

To exemplify Group theory methods, I present LCAO calculations of molecular orbitals for simple molecules starting with a minimal basis set (only the atomic orbitals which are most directly involved in covalent bonding) neglecting overlap.

8.1.1 Molecular Orbitals of NH_3

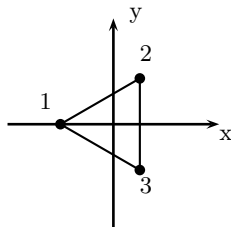


Fig. 8.1. The H atoms of ammonia are at the vertices of an equilateral triangle.

NH_3 belongs to the C_{3v} Group (see the character table in Appendix). A minimal basis set comprises $2s, 2p_x, 2p_y, 2p_z$ for N and the ground state orbitals s_1, s_2, s_3 for the H atoms. The geometry is sketched in Figure 8.1.1; the N atom (not shown) is above the origin and is not shifted by any operations. Therefore $2s$ and $2p_z$ are assigned to A_1 while $(2p_x, 2p_y)$ is a basis for E. Let us write a representation on the basis

$$s_1 \rightarrow \begin{pmatrix} 1 \\ 0 \\ 0 \end{pmatrix}, s_2 \rightarrow \begin{pmatrix} 0 \\ 1 \\ 0 \end{pmatrix}, s_3 \rightarrow \begin{pmatrix} 0 \\ 0 \\ 1 \end{pmatrix}.$$

one finds:

E	C_3	C_3^2	σ_a	σ_b	σ_c
$\begin{pmatrix} 1 & 0 & 0 \\ 0 & 1 & 0 \\ 0 & 0 & 1 \end{pmatrix}$	$\begin{pmatrix} 0 & 0 & 1 \\ 0 & 1 & 0 \\ 0 & 1 & 0 \end{pmatrix}$	$\begin{pmatrix} 0 & 1 & 0 \\ 0 & 0 & 1 \\ 1 & 0 & 0 \end{pmatrix}$	$\begin{pmatrix} 1 & 0 & 0 \\ 0 & 0 & 1 \\ 0 & 1 & 0 \end{pmatrix}$	$\begin{pmatrix} 0 & 0 & 1 \\ 0 & 1 & 0 \\ 1 & 0 & 0 \end{pmatrix}$	$\begin{pmatrix} 0 & 1 & 0 \\ 1 & 0 & 0 \\ 0 & 0 & 1 \end{pmatrix}$

This representation can be reduced by the LOT into $A_1 \oplus E$. The A_1 combination is $\psi_1 = \frac{s_1+s_2+s_3}{\sqrt{3}}$; to find a basis for E one can use projection operators. The operator that projects onto E is

$$P^{(E)} = \sum_R \chi^{(E)}(R)R = \begin{pmatrix} 2 & -1 & -1 \\ -1 & 2 & -1 \\ -1 & -1 & 2 \end{pmatrix}. \quad (8.1)$$

The ψ that one obtains depends on the s orbital; if we start from s_1 , which is $\sigma_v(1)$ invariant, we get (upon normalization) $\psi_2 = \frac{2s_1-s_2-s_3}{\sqrt{6}}$ which is also $\sigma_v(1)$ invariant. This is the x component, which is invariant under the exchange of 2 and 3. The orthogonal function is odd under such an exchange and is $\psi_3 = \frac{s_2-s_3}{\sqrt{2}}$. One can get this result by the projection operator. Starting from s_2 , one obtains $\psi'_3 = \frac{2s_2-s_1-s_3}{\sqrt{6}}$ which is not orthogonal to ψ_2 but has the orthogonal component ψ_3 . Alternatively, one can obtain those results by projecting directly on the x and y components of the irrep E , by

$$P_{xx}^{(E)} = \frac{2}{6} \sum_R D_{xx}^{(E)}(R)^* R. \quad (8.2)$$

In the current geometry, unlike the last Chapter, the reflection 1 leaves x invariant, so we must take $\sigma_1 = \begin{pmatrix} 1 & 0 \\ 0 & -1 \end{pmatrix}$. The other reflections are obtained as $\sigma_2 = \sigma_1 C_3 = \begin{pmatrix} -\frac{1}{2} & -\frac{\sqrt{3}}{2} \\ -\frac{\sqrt{3}}{2} & \frac{1}{2} \end{pmatrix}$ and $\sigma_3 = \sigma_1 C_3^2 = \begin{pmatrix} -\frac{1}{2} & \frac{\sqrt{3}}{2} \\ \frac{\sqrt{3}}{2} & \frac{1}{2} \end{pmatrix}$. Thus, one obtains

$$P_{xx}^{(E)} = \frac{1}{3} \begin{pmatrix} 2 & -1 & -1 \\ -1 & \frac{1}{2} & \frac{1}{2} \\ -1 & \frac{1}{2} & \frac{1}{2} \end{pmatrix}. \quad (8.3)$$

In a similar way,

$$P_{yy}^{(E)} = \begin{pmatrix} 0 & -0 & 0 \\ 0 & \frac{1}{2} & -\frac{1}{2} \\ 0 & -\frac{1}{2} & \frac{1}{2} \end{pmatrix}. \quad (8.4)$$

Thus, we have determined the symmetry orbitals; $2s, 2p_z, \psi_1$ belong to A_1 and the pairs $(2p_x, 2p_y), (\psi_2, \psi_3)$ belong to E . The 7×7 determinant is broken into a 3×3 determinant for the A_1 basis and a pair of 2×2 determinants for the x, y components of E ; moreover, by the Schur lemma, the latter are *identical*.

8.1.2 Molecular Orbitals of CH_4

CH_4 belongs to the tetrahedral symmetry Group T_d ; we may put the C atom at the origin and H atoms at $(-1,1,1), (1,-1,1), (-1,-1,-1), (1,1,-1)$ in appropriate units. There are $N_G=24$ operations. There are C_3 and C_2^2 rotations around

CH bonds, C_2 and S_4 rotations around the x,y,z axes, and 6 σ_d reflexions in the planes that contain two CH bonds. The C orbitals ($2s, 2p_x, 2p_y, 2p_z$) are classified at once under A_1 and T_2 .

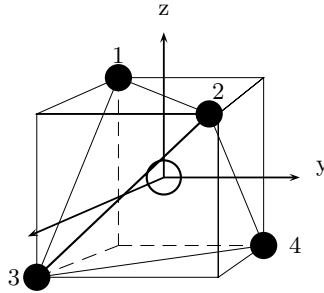


Fig. 8.2. Tetrahedral CH_4 molecule inscribed in a cube; the open circle denotes the C position.

T_d	E	$8C_3$	$3C_2$	$6\sigma_d$	$6S_4$	$g = 24$
A_1	1	1	1	1	1	r^2
A_2	1	1	1	-1	-1	
E	2	-1	2	0	0	$(3z^2 - r^2, x^2 - y^2)$
T_1	3	0	-1	-1	1	(R_x, R_y, R_z)
T_2	3	0	-1	1	-1	(x, y, z)

For the Hydrogens, let $d(i, C)$ denote the list of the destinations of atom 1 under the operations in class C. Here is the situation:

Class	moved	unmoved	χ	$d(1, C)$
E	0	4	4	1
$8C_3$	3	1	1	{1,1,2,2,3,3,4,4}
$3C_2$	4	0	0	{2,3,4}
σ_d	2	2	2	{1,1,1,2,3,4}
$6S_4$	4	0	0	{2,2,3,3,4,4}

Table 8.1. Effects of the operations of T_d on atom 1 and characters of the representation of Hydrogens.

Under each operation, every atom which changes position contributes 0 to the character χ (we are neglecting overlaps), while unmoved atoms contribute 1. Using the LOT with $N_G = 24$ we find that $\Gamma(H_4) = A_1 \oplus T_2$. The A_1 combination is trivially $\Psi_{A_1} = \frac{|1\rangle + |2\rangle + |3\rangle + |4\rangle}{2}$. The destinations in the above

Table 8.1.2 and the Character Table allow to project on T_2 by the operator (7.70):

$$\begin{aligned} P^{(T_2)}|1\rangle &= 3|1\rangle - (|2\rangle + (|3\rangle + |4\rangle) + [3|1\rangle + (|2\rangle + |3\rangle + |4\rangle)]) - 2(|2\rangle + (|3\rangle + |4\rangle)) \\ &= 2[3|1\rangle - (|2\rangle + (|3\rangle + |4\rangle))]. \end{aligned}$$

If we wish to obtain $\bar{\Psi}_z$ the fastest way is probably to symmetrize between 1 and 2. Indeed, if $3|1\rangle - (|2\rangle + (|3\rangle + |4\rangle))$ is in T_2 , $3|2\rangle - (|1\rangle + (|3\rangle + |4\rangle))$ also is; we sum and normalize obtaining

$$|\bar{\Psi}_z\rangle = \frac{|1\rangle + |2\rangle - |3\rangle - |4\rangle}{2}.$$

Also,

$$\begin{aligned} |\bar{\Psi}_x\rangle &= \frac{|1\rangle - |2\rangle - |3\rangle + |4\rangle}{2}, \\ |\bar{\Psi}_y\rangle &= \frac{|1\rangle - |2\rangle + |3\rangle - |4\rangle}{2}. \end{aligned}$$

8.1.3 Characters of Angular Momentum Eigenstates

The set $\{|J, M_J\rangle\}$ is the basis of an irrep of $O(3)$ but reduces in its subgroups. A rotation $R_z(\alpha)$ by an angle α about the z axis multiplies $|J, M_J\rangle$ by $\exp(iM_J\alpha)$, thus the character of $R_z(\alpha)$ is

$$\chi(\alpha) = \sum_{M_J=-J}^J \exp(iM_J\alpha) = \frac{\sin((J + \frac{1}{2})\alpha)}{\sin(\frac{\alpha}{2})}. \quad (8.5)$$

All rotations by an angle α belong to the same class, thus the character is this, independently of the rotation axis.

8.1.4 Examples: O_h Group, Ligand Group Orbitals, Crystal Field

The O_h Group

We consider a cube with a system of cartesian axes through the centers of the faces. The centers of the faces are vertices of an octahedron. The operations of symmetry of the cube and octahedron are the same. We label the vertices of the octahedron as in Figure 8.1.4. There are 48 operations in the cubic Group O_h . The C_4 rotations around the cartesian axes and their inverses form the $6C_4$ class, and the C_2 rotations form the $3C_2$ class. The $\frac{2\pi}{3}$ rotations in both senses around the 4 cube diagonals give a class $8C_3$; these axes are perpendicular to faces of the octahedron. Joining the center of EC with the center of FB we have a C_2 axis. There are 12 edges, so there are 6 axes and the class is $6C_2$. The inversion forms a class; the $3\sigma_h$ class includes reflections like

the one in the BCEF plane. The C_4 rotations followed by a σ_h reflection in the plane perpendicular to the rotation axis form the $6S_4$ improper rotation class. The plane containing A,D and the midpoints of EC and BF is a symmetry plane, and the reflection belongs to a $6\sigma_d$ class. Finally, there are S_6 improper rotations: the axes are those of the C_3 rotations; if we look along a C_3 axis, opposite faces appear as concentric triangles; the figure is invariant under a C_6 rotation followed by a reflection in the orthogonal plane through the center (Figure 6.2). With 4 axes and two senses of rotations one builds a $8S_6$ class.

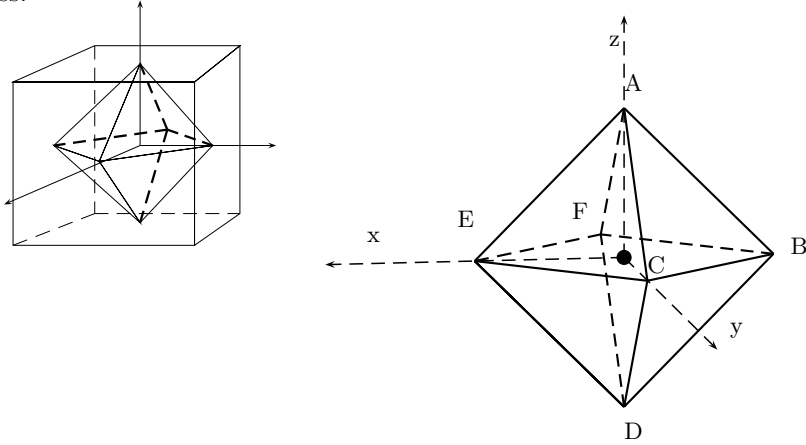


Fig. 8.3. Octahedron

Ligand Group Orbitals

O_h	E	$6C_4$	$3C_2$	$6C_2'$	$8C_3$	i	$6S_4$	$3\sigma_h$	$6\sigma_d$	$8S_6$	$g = 48$
A_{1g}	1	1	1	1	1	1	1	1	1	1	$x^2 + y^2 + z^2$
A_{1u}	1	1	1	1	1	-1	-1	-1	-1	-1	
A_{2g}	1	-1	1	-1	1	1	-1	1	-1	1	
A_{2u}	1	-1	1	-1	1	-1	1	-1	1	-1	
E_g	2	0	2	0	-1	2	0	2	0	-1	$(x^2 - y^2, 2z^2 - x^2 + y^2)$
E_u	2	0	2	0	-1	-2	0	-2	0	1	
T_{1g}	3	1	-1	-1	0	3	1	-1	-1	0	(R_x, R_y, R_z)
T_{1u}	3	1	-1	-1	0	-3	-1	1	1	0	(x, y, z)
T_{2g}	3	-1	-1	1	0	3	-1	-1	1	0	(xy, xz, yz)
T_{2u}	3	-1	-1	1	0	-3	1	1	-1	0	
Γ	6	2	2	0	0	0	0	4	2	0	

The O_h Group is the point Group of many interesting solids, including *complexes* like $\text{CuSO}_4 \cdot 5\text{H}_2\text{O}$ and FeCl_3 where a transition metal ion at the center

of an octahedron; most often the octahedral symmetry is only approximate, as in $\text{CuSO}_4 \cdot 5\text{H}_2\text{O}$ where the central Cu^{++} is bound to 4 H_2O molecules and 2 SO_4^{--} ions. A LCAO model of their properties is often called ligand field theory.

If $A \dots F$ represent 6 s orbitals, they are the basis of a representation Γ with the characters shown above. One finds that $\Gamma = A_{1g} \oplus E_g \oplus T_{1u}$. Let us work out the projection of orbital A into T_{1u} :

Class C	$\sum_{R \in C} RA$	$\chi^{(T_{1u})}$	contribution
E	A	3	3A
6C ₄	2A+B+C+E+F	1	2A+B+C+E+F
3C ₂	A+2D	-1	-(A+2D)
6C ₂ '	2D+B+C+E+F	-1	-(2D+B+C+E+F)
8C ₃	2(B+C+E+F)	0	0
I	D	-3	-3D
6S ₄	2D+B+C+E+F	-1	-(2D+B+C+E+F)
3σ _h	2A+D	1	2A+D
6σ _d	2A+B+C+E+F	1	2A+B+C+E+F
8S ₆	2(B+C+E+F)	0	0

The normalized T_{1u} projection is $\psi_1 = \frac{A-D}{\sqrt{2}}$. Operating in the same way on D we again get ψ_1 . Operating on the other functions, we obtain $\psi_2 = \frac{B-E}{\sqrt{2}}$ and $\psi_3 = \frac{C-F}{\sqrt{2}}$. In this way one easily builds the ligand group orbitals.

Crystal Field

The number of d electrons in transition metal ions is:

	Ti	V	Cr	Mn	Fe	Co	Ni	Cu
M^{++}	2	3	4	5	6	7	8	9
M^{+++}	1	2	3	4	5	6	7	8

Hund's rule allows to find the ground state of partially filled d shells and the corresponding number of unpaired electrons as follows:

	d^1	d^2	d^3	d^4	d^5	d^6	d^7	d^8	d^9
ground state	2D	3F	4F	5D	6S	5D	4F	3F	2D
unpaired	1	2	3	4	5	4	3	2	1

for isolated transition ions one would always predict paramagnetism, but the compounds can be paramagnetic or not. The bivalent Fe ($3d^6$ configuration)

forms the complexes $[Fe(H_2O)_6]^{2+}$, which is green, and paramagnetic, but also $[Fe(CN)_6]^{4-}$, which is yellow and diamagnetic. These facts can already be understood by the *crystal field theory*, in which the ligands behave like point charges, or anyhow they generate a field to octahedral symmetry that resolves the degeneracy of the atomic terms (for the first transition series the spin-orbit interaction is a small perturbation to be introduced subsequently). A more quantitative treatment is obtained then from the *ligand field theory*.

For d (or D) states, from (8.5) and from the even parity we find the characters

$$\frac{O_h}{\Gamma_d} \left| \begin{array}{cccccccccc} E & 6C_4 & 3C_2 & 6C_2' & 8C_3 & i & 6S_4 & 3\sigma_h & 6\sigma_d & 8S_6 \\ 5 & -1 & 1 & 1 & -1 & 5 & -1 & 1 & 1 & -1 \end{array} \right|$$

and conclude $\Gamma_d = E_g \oplus T_{2g}$. This is already clear from the Character Table, reporting (d_{xy}, d_{xz}, d_{yz}) as a basis for T_{2g} and $(d_{x^2-y^2}, z^2)$ for E_g . In transition metal complexes usually $\Delta = E(E_g) - E(T_{2g}) > 0$, since the T_{2g} orbitals stay far from the negative ligands. Thus in the absence of Coulomb interactions one would fill the available levels according to the *aufbau* principle, starting with T_{2g} . In crystal field theory one tries to predict the magnetic properties by diagonalizing a many-electron Hamiltonian which is the sum of the isolated ion Hamiltonian and the one of the crystal field.

There are two simple limiting cases. If $\Delta \ll U$, where U represent the order of magnitude of the multiplet splitting, due mainly to the Coulomb interaction, one treats Δ as a perturbation of the isolated ion multiplet. The atomic Hund rule holds, and paramagnetism obtains. If $\Delta \gg U$, Hund's rule holds (high spin is preferred) within the degenerate T_{2g} and E_g levels, but E_g starts being filled only after T_{2g} is full, and 6 electrons yield a diamagnetic complex.

8.2 Normal Modes of vibration

In the Born-Oppenheimer approximation, the potential that governs the motion of electrons depends parametrically on the positions of the nuclei. The total energy U of the molecule is calculated in function of the nuclear coordinates and the configuration of equilibrium correspond to a minimum energy. The vibrations can then be studied by considering U as the potential energy of the nuclei. The configuration of the molecule is given by a vector \vec{v} that specifies the shift from equilibrium of the coordinates of all the N nuclei,

$$\vec{v} = (\delta x_1, \delta y_1, \delta z_1, \delta x_2, \dots, \delta x_N, \delta y_N, \delta z_N) \equiv (v_1, \dots, v_{3N}) \quad (8.6)$$

where I introduced a notation v_i for the generic cartesian coordinate. All the possible motions of the nuclei are described classically from the equations of Newton,

$$m_i \ddot{v}_i = -\frac{\partial U}{\partial v_i} \quad (8.7)$$

where m_i is the mass associated to v in the obvious way $x_1, y_1, z_1 \rightarrow m_1$ and so on. In the harmonic approximation, expanding around to one configuration of equilibrium,

$$U = \frac{1}{2} \sum_{ij} U_{ij} v_i v_j, \quad (8.8)$$

and the Fourier transform of the equations of the motion is

$$\omega^2 v_i = \frac{1}{m_i} \sum_j U_{ij} v_j. \quad (8.9)$$

We introduce

$$Q_i = v_i \sqrt{m_i} \quad (8.10)$$

and the symmetrized matrix

$$W_{ij} = \frac{U_{ij}}{\sqrt{m_i m_j}} \quad (8.11)$$

then the equations of the motion read:

$$\omega^2 Q_i = \sum_j W_{ij} Q_j. \quad (8.12)$$

The eigenvectors \mathbf{Q}_α of the W matrix are the *normal modes*, and their eigenfrequencies ω_α are obtained from the secular equation. Three modes, of null frequency, correspond to rigid translations of the molecule, and 3 others (or 2, for linear molecules) to rigid rotations. Rotations also have $\omega = 0$, since the energy of the molecule does not depend on its orientation. The remaining $3N-6$ (or $3N-5$) frequencies are vibrational. The Group theory is helpful to simplify the solution of the secular equation. Every R operation of the Group of the molecule sends every nucleus in itself or to another identical nucleus in an equivalent position; meantime, it produces a (proper or improper) rotation the system of cartesian axes that we can imagine fixed at every nucleus. So, R maps each Q_i into a linear combination of the components. In such a way, we associate to every R a matrix $D(R)$, and obtain a representation of the Group in the space of the vectors \mathbf{Q} . Every $D(R)$ commutes with W , since R is a symmetry and W must be invariant under R ; thus if \mathbf{Q}_a is a solution of the secular equation, also $D(R)\mathbf{Q}_a$ must be a solution, and with the same ω . Therefore, we can diagonalize W simultaneously with the maximum number of commuting $D(R)$ matrices. The theory of the Groups adds the Dirac characters; this means that in a new basis whose elements are vibrations pertaining to irreps of the Group, W is block diagonal. Thus, the normal modes can be assigned to irreps of the Group; the reduction of

the \mathcal{Q} , (or equivalently \mathbf{v}) representation, allows to gain in simple way the symmetry and the degeneracy of the normal ways, without having to resolve the secular equation.

The H_2O molecule (C_{2v} Group), and that requires a 9-dimensional \mathbf{v} . We place the molecule on the xz plane. The cartesian components of the shift from the position of equilibrium of each atom transform like its p orbitals and can be thought of as numbered arrows, parallel to the x,y and z axes respectively; th earrows (1,2,3) from one H, (4,5,6) from O and (7,8,9) from the other H, constitute a basis. The operations are C_2 , $\sigma(xz)$, and $\sigma(yz)$. The C_2 operation has the representative

$$D(C_2) = \begin{pmatrix} 0 & 0 & 0 & 0 & 0 & 0 & -1 & 0 & 0 \\ 0 & 0 & 0 & 0 & 0 & 0 & 0 & -1 & 0 \\ 0 & 0 & 0 & 0 & 0 & 0 & 0 & 0 & 1 \\ 0 & 0 & 0 & -1 & 0 & 0 & 0 & 0 & 0 \\ 0 & 0 & 0 & 0 & -1 & 0 & 0 & 0 & 0 \\ 0 & 0 & 0 & 0 & 0 & 1 & 0 & 0 & 0 \\ -1 & 0 & 0 & 0 & 0 & 0 & 0 & 0 & 0 \\ 0 & -1 & 0 & 0 & 0 & 0 & 0 & 0 & 0 \\ 0 & 0 & 1 & 0 & 0 & 0 & 0 & 0 & 0 \end{pmatrix}. \quad (8.13)$$

$D(C_2)$ and $D(\sigma_v(yz))$ have the same block structure

$$D(C_2) = \begin{pmatrix} 0 & 0 & b \\ 0 & b & 0 \\ b & 0 & 0 \end{pmatrix} \quad (8.14)$$

where now 0 is for a null 3×3 block, and

$$b(C_2) = \begin{pmatrix} -1 & 0 & 0 \\ 0 & -1 & 0 \\ 0 & 0 & 1 \end{pmatrix}, \quad b(\sigma(yz)) = \begin{pmatrix} -1 & 0 & 0 \\ 0 & 1 & 0 \\ 0 & 0 & 1 \end{pmatrix}; \quad (8.15)$$

$D(\sigma(xz))$ is block diagonal with $b = \text{diag}(1, -1, 1)$. From the matrices we gain the characters:

$$\Gamma : \chi(E) = 9, \chi(C_2) = -1, \chi(\sigma(yz)) = 1, \chi(\sigma(xz)) = 3. \quad (8.16)$$

We could arrive to this result without writing the D matrices, taking into account that for each operation:

- the atoms that change position contribute 0 to the character; 2)
- each arrow (cartesian movement) that it remains invariant contributes +1, and every arrow that changes sign contributes -1,
- more generally, the cartesian shifts of an atom that does not change position behave like (x, y, z), so if the arrow is rotated by θ the contribution is $\cos(\theta)$.

C_{2v}	I	C_2	σ_v	σ'_v	$g = 4$
A_1	1	1	1	1	z
A_2	1	1	-1	-1	xy, R_z
B_1	1	-1	1	-1	x, R_y
B_2	1	-1	-1	1	y, R_x

The representation Γ is clearly reducible. It includes all the possible movements of atoms, therefore not only the vibrations, but also the rigid rotations and translations of the molecule. In order to classify the vibrations, it is in the first place necessary to separate them from the rigid motions.

The rigid translations along the (x,y,z) axes transform like (x,y,z); they are marked in the character tables and are a basis for the representation of polar vectors (reducible or not, according to the Group).

Adding the characters of x, y and z, we get for the 3 translations the characters:

C_{2v}	E	C_2	$\sigma(xz)$	$\sigma(yz)$
Γ_{trasl}	3	-1	1	1

(8.17)

Having separated 3 coordinated of the center of mass, N-3 remain The motion that they describe is to be decomposed in a rigid rotation and a vibration. So, we can separate to others 3 degrees of freedom (2 for linear molecules) in order to describe the rigid rotation. An infinitesimal rigid rotation transforms the coordinate \mathbf{r}_i of the atom i according to $\delta\mathbf{r}_i = d\phi \times \mathbf{r}_i$; one can expand $d\phi$ as a linear combination of rotations R_x, R_y and R_z around the axes. These are mixed among themselves under the symmetry operations, and are a basis of a representation Γ_{rot} . Since $\delta\phi$ is an axial vectors, Γ_{rot} is the axial vectors representation. The rotation about the x axis transforms like the R_x generator, that is, like yz , and so on; the tables of the characters report the classification of the rotations. In the Abelian Groups, there are only one-dimensional irreps with characters ± 1 ; R is odd (even) if the sense of rotation changes (does not change). For the water molecule, using the character table, we find

C_{2v}	E	C_2	$\sigma(xz)$	$\sigma(yz)$
Γ_{rot}	3	-1	-1	-1

(8.18)

We can proceed to separate the vibrations as it follows:

C_{2v}	E	C_2	$\sigma(xz)$	$\sigma(yz)$
Γ	9	-1	3	1
Γ_{trasl}	3	-1	1	1
Γ_{rot}	3	-1	-1	-1
Γ_{vibr}	3	1	3	1

The reduction of the representation yields

$$\Gamma_{vibr} = 2A_1 \oplus B_1.$$

Finally. The water molecule has two total-symmetric vibrations and one of B_1 symmetry.

A total-symmetric vibration, that all the molecules have, is the *breathing mode*. In the symmetric stretch the angle between the OH bonds varies. In order to discover what kind of vibration is the one labeled B1 that goes like x one can construct the projection operator

$$P(B_1) = E - C_2 + \sigma(xz) - \sigma(yz); \tag{8.19}$$

in terms of block representative matrices,

$$P(B_1) = \begin{pmatrix} 1 + b(\sigma(xz)) & 0 & -b(C_2) - b(\sigma(yz)) \\ 0 & \beta & 0 \\ -b(C_2) - b(\sigma(yz)) & 0 & 1 + b(\sigma(xz)) \end{pmatrix}, \tag{8.20}$$

where $\beta = 1 - b(C_2) + b(\sigma(xz)) - b(\sigma(yz))$. Projecting, one finds a vibration where the only arrows are 3 and 9, and are opposite. One H shifts up along the molecular axis and the other goes down; such a vibration indeed changes sign under C_2 and $\sigma(yz)$.

Vibrations of NH₃

Here the complete table of the characters of the Group.

C_{3v}	I	$2C_3$	$3\sigma_v$	$g = 6$
A_1	1	1	1	z
A_2	1	1	-1	R_z
E	2	-1	0	(x, y)

The Cartesian movements of N are transformed like the coordinates. Therefore for N we have:

C_{3v}	E	$2C_3$	$3\sigma_v$
$\Gamma(N)$	3	0	1

(8.21)

Let's find the characters of $\Gamma(H_3)$. $\chi(E) = 9$ (no arrows move) $\chi(C_3) = 0$ (all the H move and contribute 0) $\chi(\sigma_v) = 1$ (two H reflected one in the other: character 0; for the other H, two arrows in the reflection plane and one orthogonal: character 1) Therefore:

C_{3v}	E	$2C_3$	$3\sigma_v$
$\Gamma(N)$	3	0	1
$\Gamma(H_3)$	9	0	1
$\Gamma(NH_3)$	12	0	2
Γ_{trasl}	3	0	1
Γ_{rot}	3	0	-1
Γ_{vibr}	6	0	2

Finally, $\Gamma_{vibr} = 2A_1 + 2E$.

Vibrations of Methane (CH₄)

Methane is a tetrahedral molecule.

- With 5 atoms $\chi(E) = 15$.
- $8C_3$: all the atoms move except a H and the C: for each an arrow is along the rotation axis (+1), while the others two, on the \perp plane, are transformed as the coordinates (x,y) of this plane and contribute $TrD(R) = 2 \cos(\frac{2\pi}{3}) = -1$. Therefore $\chi(8C_3) = 0$.
- $3C_2$: 2 arrows of the C change sign and the third does not move: $\chi = -1$
- $6\sigma_d$ CH_2 remains in place; each atom has 2 arrows in plane and one reflected and $\chi = 3$.
- S_4 H moved; for the atom of C: 90° rotation around z, $(x, y, z) \rightarrow (y, -x, z)$; then reflection $\rightarrow (y, -x, -z)$. So, $\chi = -1$.

Thus,

T_d	E	$8C_3$	$3C_2$	$6\sigma_d$	$6S_4$	$g = 24$
A_1	1	1	1	1	1	r^2
A_2	1	1	1	-1	-1	
E	2	-1	2	0	0	$(3z^2 - r^2, x^2 - y^2)$
T_1	3	0	-1	-1	1	(R_x, R_y, R_z)
T_1	3	0	-1	1	-1	(x, y, z)
Γ_{tot}	15	0	-1	3	-1	
Γ_{trasl}	3	0	-1	1	-1	$= T_2$
Γ_{rot}	3	0	-1	-1	1	$= T_1$
Γ_{vibr}	9	0	1	3	-1	$A_1 \oplus E \oplus 2T_2$

Vibrations of Benzene (C₆H₆)

There are 12 atoms and 36 coordinates, therefore $\chi(E) = 36$. The rotations C_2, C_3 and C_6 around the vertical axis move all the atoms and have character 0. Rotation C'_2 around to a diagonal of the hexagon leaves 4 atoms in place: for each one arrow is invariant and the others two change sign. Therefore, $\chi(C'_2) = -4$. Rotation C''_2 around an axis \perp to opposite sides and S_3 and S_6 move all the atoms and have character 0. The reflection σ_h in the plane of the hexagon leaves two arrows invariant for every atom and changes sign to the third, therefore $\chi(\sigma_h) = 12$. The reflection for a plane containing the C''_2 axis has character 0. The reflection for a plane containing a axis C'_2 leaves 4 atoms in place, with two arrows invariant and one changed of sign for every atom. Therefore $\chi(\sigma_v) = 4$. The characters of Γ_{trasl} are the sums of those of A_{2u} and E_{1u} ; those of Γ_{rot} adding those of A_{2g} and E_{1g} .

D _{6h}	E	2C ₆	2C ₃	C ₂	3C ₂ '	3C ₂ ''	i	2S ₃	2S ₆	σ _h	3σ _d	3σ _v	g = 24
A _{1g}	1	1	1	1	1	1	1	1	1	1	1	1	R _z
A _{2g}	1	1	1	1	-1	-1	1	1	1	1	-1	-1	
B _{1g}	1	-1	1	-1	1	-1	1	-1	1	-1	1	-1	
B _{2g}	1	-1	1	-1	-1	1	1	-1	1	-1	-1	1	
E _{1g}	2	1	-1	-2	0	0	2	1	-1	-2	0	0	(R _x , R _y) (x ² - y ² , xy)
E _{2g}	2	-1	-1	2	0	0	2	-1	-1	2	0	0	
A _{1u}	1	1	1	1	1	1	-1	-1	-1	-1	-1	-1	z
A _{2u}	1	1	1	1	-1	-1	-1	-1	-1	-1	1	1	
B _{1u}	1	-1	1	-1	1	-1	-1	1	-1	1	-1	1	
B _{2u}	1	-1	1	-1	-1	1	-1	1	-1	1	1	-1	
E _{1u}	2	1	-1	-2	0	0	-2	-1	1	2	0	0	(x, y)
E _{2u}	2	-1	-1	2	0	0	-2	1	1	-2	0	0	
Γ _{tot}	36	0	0	0	-4	0	0	0	0	12	4	0	
Γ _{trasl}	3	2	0	-1	-1	-1	-3	-2	0	1	1	1	
Γ _{rot}	3	2	0	-1	-1	-1	3	2	0	-1	-1	-1	
Γ _{vibr}	30	-4	0	2	-2	2	0	0	0	12	4	0	

The Group has 24 elements, and it is found that $\Gamma_{vibr} = 2A_{1g} \oplus A_{2g} \oplus A_{2u} \oplus 2B_{1u} \oplus 2B_{2g} \oplus 2B_{2u} \oplus E_{1g} \oplus 3E_{1u} \oplus 4E_{2g} \oplus 2E_{2u}$.

8.3 Space-Time Symmetries of Bloch States

Let $\mathbf{t}_1, \mathbf{t}_2, \mathbf{t}_3$ be the primitive translation vectors of a crystal lattice, $\{T_i\}$ the set of lattice translation operators and $V(\vec{x})$ the periodic crystal potential, such that $[T_i, V]_- = 0$. Periodic boundary conditions are assumed, that is, for some $N \gg 1$, $T_i^N = 1$. The simultaneous eigenfunctions $\psi_{\vec{k}}(\vec{x})$ of H and any T_i are such that $T_i \psi_{\vec{k}}(\vec{x}) = \psi_{\vec{k}}(\vec{x} + \vec{t}_i) = C \psi_{\vec{k}}(\vec{x})$ with $C^N = 1$. Now, $T_i^N e^{i\vec{k} \cdot \vec{x}} = e^{i\vec{k} \cdot \vec{x}}$ requires $\vec{k} \cdot \vec{t}_i = \frac{2\pi}{N} * \text{integer}$; therefore,

$$\vec{k} = \frac{pg_1 + qg_2 + rg_3}{N}$$

with $p, q, r \in \mathcal{Z}$, and the reciprocal lattice vectors defined by $\mathbf{t}_i \cdot \mathbf{g}_j = 2\pi\delta_{ij}$. We know from Sect. 7.2.1 that Bloch's functions are

$$\psi_{\vec{k}, \lambda}(\vec{x}) = e^{i\vec{k} \cdot \vec{x}} u_{\vec{k}}(\vec{x}), \quad (8.22)$$

where $u_{\vec{k}}(\vec{x})$ are lattice periodic. Moreover, since (letting $\hbar = 1$)

$$\vec{p} e^{i\vec{k} \cdot \vec{x}} = e^{i\vec{k} \cdot \vec{x}} (\vec{p} + \vec{k}),$$

we may write

$$\left[\frac{(\vec{p} + \vec{k})^2}{2m} + V(\vec{x}) \right] u_{\vec{k}}(\vec{x}) = \epsilon_{\mathbf{k}} u_{\vec{k}}(\vec{x}). \quad (8.23)$$

No degeneracy is predicted, since Abelian Groups have only one-dimensional representations. Each translation T by a vector \mathbf{t} is a class, while each \mathbf{k} vector labels a different irrep. The LOT of Equation(7.58) yields the useful relation

$$\frac{1}{N_C} \sum_{\mathbf{t}} e^{i(\mathbf{k}-\mathbf{k}') \cdot \mathbf{t}} = \delta(\mathbf{k} - \mathbf{k}'), \quad (8.24)$$

where N_C is the number of cells. The second character orthogonality theorem 7.64 gives:

$$\sum_{\mathbf{k} \in BZ} e^{i(\mathbf{t}-\mathbf{t}') \cdot \mathbf{k}} = N_C \delta(\mathbf{t} - \mathbf{t}'), \quad (8.25)$$

with the sum extended to the Brillouin zone.

The trivial spin degeneracy is lifted if the spin-orbit interaction is included,

$$H = \frac{p^2}{2m} + V(\vec{x}) + H'_{SO} \quad (8.26)$$

with

$$H'_{SO} = \frac{1}{4m^2 c^2} \vec{\sigma} \wedge \nabla V \cdot \vec{p}. \quad (8.27)$$

Eigen-spinors can be taken of the Bloch form,

$$\psi_{\vec{k}, \lambda}(\vec{x}) = e^{i \vec{k} \cdot \vec{x}} u_{\vec{k}, \lambda}(\vec{x}) = e^{i \vec{k} \cdot \vec{x}} \begin{cases} u_{\vec{k}, +}(\vec{x}) \\ u_{\vec{k}, -}(\vec{x}) \end{cases} \quad (8.28)$$

One finds spinors with $\lambda = +$ and $-$ that reduce to up and down spin for $c \rightarrow \infty$, but otherwise spin and orbital degrees of freedom mix. The periodic functions are obtained by solving

$$\left[\frac{(\vec{p} + \vec{k})^2}{2m} + V(\vec{x}) + \frac{1}{4m^2 c^2} \vec{\sigma} \wedge \nabla V \cdot (\vec{p} + \vec{k}) \right] u_{\vec{k}, \lambda}(\vec{x}) = \epsilon_{\vec{k}, \lambda} u_{\vec{k}, \lambda}(\vec{x}). \quad (8.29)$$

Space Inversion

The inversion is the operator $P^0 : P^0 \vec{x} = -\vec{x}$. Let $\psi_{\vec{k}, \lambda}(\vec{x})$ solve the Schrödinger equation with a periodic potential $V(\vec{x})$; an inverted crystal poses the same problem with $V^{(i)}(\vec{x}) = P^0 V(\vec{x}) = V(-\vec{x})$ instead. Since $(P^0)^2$ is the identity, from $H\psi_{\mathbf{k}}(\mathbf{x}) = \epsilon_{\mathbf{k}}\psi_{\mathbf{k}}(\mathbf{x})$ one gets

$$P^0 H P^0 P^0 \psi_{\mathbf{k}} = H(-\mathbf{x}) P^0 \psi_{\mathbf{k}} = \epsilon_{\mathbf{k}} P^0 \psi_{\mathbf{k}};$$

thus the solution the inverted crystal is the spinor $\psi_{\vec{k}}(-\vec{x})$ and the energy $\epsilon_{\vec{k}}$ is the same as in the original problem. If $V^{(i)}(\vec{x}) \neq V(\vec{x})$, one cannot speak of degeneracy, since the corresponding problems remain distinct. If however the crystal has inversion symmetry, that is, $[P^0, H]_- = 0$, adding this element to the translations produced a non-Abelian Group which implies degeneracy. Indeed, $\psi_{\mathbf{k}}(\mathbf{x})$ and $\psi_{\mathbf{k}}(-\mathbf{x})$ both belong to the eigenvalue $\epsilon_{\vec{k}}$. However, $P^0\psi_{\mathbf{k}}(\mathbf{x}) \equiv \psi_{\mathbf{k}}(-\mathbf{x}) = e^{-i\mathbf{k}\cdot\mathbf{x}}u_{\mathbf{k}}(-\mathbf{x})$ belongs to $-\mathbf{k}$ since it gets multiplied by $e^{-i\mathbf{k}\cdot\mathbf{t}}$ under a translation by \mathbf{t} . Therefore we must make the identifications

$$P^0\psi_{\mathbf{k}}(\mathbf{x}) = \psi_{-\mathbf{k}}(\mathbf{x}), \quad (8.30)$$

and $u_{\mathbf{k}}(-\mathbf{x}) = u_{-\mathbf{k}}(\mathbf{x})$; so,

$$\epsilon_{-\vec{k}} = \epsilon_{\vec{k}}. \quad (8.31)$$

Time Reversal

The antilinear¹ Kramers operator K takes the complex conjugate, and is useful to discuss time reversal symmetry, as I show in a moment. In the Schrödinger theory, assume one knows how to solve a time-dependent problem

$$i\hbar\frac{\partial\phi(t)}{\partial t} = H(t)\phi(t) \quad (8.32)$$

but wants to solve the Schrödinger equation with a time-reversed Hamiltonian

$$i\hbar\frac{\partial\phi'(t')}{\partial t'} = H(-t')\phi'(t'). \quad (8.33)$$

Applying K to both sides of (8.32) we get $-i\hbar\frac{\partial\phi(t)^*}{\partial t} = H(t)\phi(t)^*$ and setting $t = -t'$ in the operators,

$$i\hbar\frac{\partial\phi(t)^*}{\partial t} = H(-t')\phi(t)^*. \quad (8.34)$$

Comparing with (8.33) we conclude that $\phi'(t') = \phi(t)^*$; introducing a time reversal operator \mathcal{T} this may be interpreted by saying that $\phi'(t') = \mathcal{T}\phi(t)$ is the time reversed wave function with $\mathcal{T} = K$.

Things are more involved with the Pauli equation; I write H_0 the spin-independent part of the Hamiltonian, which I assume real, and separate the spin-field coupling:

$$i\hbar\frac{\partial\psi(t)}{\partial t} = [H_0(t) + \lambda\sigma \cdot B(t)]\psi(t), \quad \lambda = \frac{e\hbar}{2mc}. \quad (8.35)$$

¹An operator \hat{O} is antilinear if $\hat{O}(a\phi + b\psi) = a^*\hat{O}\phi + b^*\hat{O}\psi$.

Taking the complex conjugate and multiplying both sides by $-i\sigma_2 = \begin{pmatrix} 0 & 1 \\ -1 & 0 \end{pmatrix}$, one finds

$$\begin{aligned} i \frac{\partial}{\partial(-t)}(-i\sigma_2)\psi(t)^* &= H_0(t)(-i\sigma_2)\psi(t)^* + \lambda(-i\sigma_2)\sigma^* \cdot B(t)\psi(t)^* \\ &= H_0(t)(-i\sigma_2)\psi(t)^* + (-1)\lambda\{(-i\sigma_2)\sigma^* \cdot B(t)(-i\sigma_2)\}(-i\sigma_2)\psi(t)^*. \end{aligned} \quad (8.36)$$

The familiar anticommutation relations give

$$(-i\sigma_2)\sigma^* \cdot B(t)(-i\sigma_2) = \sigma \cdot B(t).$$

Now let $t' = -t$ in the operators.

$$i \frac{\partial}{\partial t'}(-i\sigma_2)\psi(t)^* = H_0(-t')(-i\sigma_2)\psi(t)^* + (-1)\lambda\sigma \cdot B(-t')(-i\sigma_2)\psi(t)^*. \quad (8.37)$$

which says that now $(-i\sigma_2)\psi(t)^*$ is the time reversed spinor with $B(-t') = -B'(t')$. But this sign is wanted: indeed the currents do change sign under time reversal, hence the vector potential and the magnetic field also change sign. Thus,

$$\mathcal{T} = -i\sigma_y K. \quad (8.38)$$

Note that

$$\langle K\phi, K\psi \rangle = \langle \psi, \phi \rangle, \quad (8.39)$$

and

$$\langle \mathcal{T}\phi, \mathcal{T}\psi \rangle = \langle \psi, \phi \rangle. \quad (8.40)$$

Then

$$\mathcal{T}^2\psi = -\psi,$$

thus

$$\mathcal{T}^{-1} = -\mathcal{T}.$$

\mathcal{T} reverses the sign of \vec{p} (indeed $\mathcal{T}\vec{p}\mathcal{T}^{-1} = -\vec{p}$ because of the complex conjugation) and of the angular momenta \vec{L} and \vec{S} (for instance, $\sigma_2\sigma_1 = -\sigma_1\sigma_2 \Rightarrow \mathcal{T}\sigma_1\mathcal{T}^{-1} = -\sigma_1$). Thus the scalar product $\sigma \cdot L$ is time-reversal invariant.

Kramers' Theorem for one-electron states says that a stationary Hamiltonian like (8.26), without magnetic fields, even in the presence of the spin-orbit interaction, has a twofold degeneracy since ϕ and $\mathcal{T}\phi$ have the same energy and are orthogonal.

Since \mathcal{T} commutes with H , if ϕ is a stationary state of H , $\mathcal{T}\phi$ also is. Moreover $\mathcal{T}\phi \perp \phi$; indeed, if $\phi = \begin{pmatrix} \alpha \\ \beta \end{pmatrix}$,

$$\mathcal{T}\phi = -i\sigma_y K \begin{pmatrix} \alpha \\ \beta \end{pmatrix} = \begin{pmatrix} 0 & -1 \\ 1 & 0 \end{pmatrix} \begin{pmatrix} \alpha^* \\ \beta^* \end{pmatrix} = \begin{pmatrix} -\beta^* \\ \alpha^* \end{pmatrix}$$

then

$$\langle \mathcal{T}\phi | \phi \rangle = (-\beta, \alpha) \begin{pmatrix} \alpha \\ \beta \end{pmatrix} = 0.$$

Since $[\mathcal{T}, H]_- = 0$, the time reversed Bloch eigenspinors

$$\mathcal{T}\psi_{\vec{k}}^{\rightarrow}(\vec{x}) = -ie^{-i\vec{k}\cdot\vec{x}} \sigma_y u_{\vec{k},\lambda}^* (\vec{x}) \quad (8.41)$$

have the same energy and belong to $-\vec{k}$, (they are periodic spinors times $e^{-i\vec{k}\cdot\vec{x}}$). Besides, they belong to $-\lambda$ since time reversal reverses spin. Using (8.40),

$$\langle \psi_{\vec{k}}^{\rightarrow}(\vec{x}), \sigma_z \psi_{\vec{k}}^{\rightarrow}(\vec{x}) \rangle = \langle \mathcal{T}\sigma_z \psi_{\vec{k}}^{\rightarrow}(\vec{x}), \mathcal{T}\psi_{\vec{k}}^{\rightarrow}(\vec{x}) \rangle;$$

the anticommutation rules give

$$= -\langle \sigma_z \mathcal{T}\psi_{\vec{k}}^{\rightarrow}(\vec{x}), \mathcal{T}\psi_{\vec{k}}^{\rightarrow}(\vec{x}) \rangle;$$

since σ_z is Hermitean,

$$\langle \psi_{\vec{k}}^{\rightarrow}(\vec{x}), \sigma_z \psi_{\vec{k}}^{\rightarrow}(\vec{x}) \rangle = -\langle \mathcal{T}\psi_{\vec{k}}^{\rightarrow}(\vec{x}), \sigma_z \mathcal{T}\psi_{\vec{k}}^{\rightarrow}(\vec{x}) \rangle.$$

In summary the time reversal invariance requires

$$\mathcal{T}\psi_{\vec{k},\lambda}^{\rightarrow}(\vec{x}) = \psi_{-\vec{k},-\lambda}^{\rightarrow}(\vec{x}); \quad \epsilon_{\vec{k},\lambda}^{\rightarrow} = \epsilon_{-\vec{k},-\lambda}^{\rightarrow}. \quad (8.42)$$

Conjugation

If P^0 and \mathcal{T} are simultaneous symmetries, the conjugation

$$C = P^0 \mathcal{T} \quad (8.43)$$

also is conserved. Using equations (8.30),(8.42) we see that this is such that

$$C\psi_{\vec{k},\lambda}^{\rightarrow}(\vec{x}) = \psi_{\vec{k},-\lambda}^{\rightarrow}(\vec{x}); \quad \epsilon_{\vec{k},\lambda}^{\rightarrow} = \epsilon_{\vec{k},-\lambda}^{\rightarrow} \quad (8.44)$$

and there is degeneracy at every \vec{k} point.

8.4 Space groups of solids

The Space Group elements are [93]

$$(\alpha|a) : \vec{r}' = \alpha \vec{r} + \vec{a} \quad (8.45)$$

where α denotes an operation of the Point Group while \vec{a} is a translation (as we will see, not always a Bravais one). This is a Group with the multiplication rule

$$(\beta|\vec{b})(\alpha|\vec{a}) = (\beta\alpha|\vec{b} + \beta\vec{a}) \quad (8.46)$$

and it has the Point Group as a subgroup. We can write the faithful representation²

$$\begin{pmatrix} \vec{r}' \\ 1 \end{pmatrix} = \begin{pmatrix} \alpha & \vec{a} \\ 0 & 1 \end{pmatrix} \begin{pmatrix} \vec{r} \\ 1 \end{pmatrix}. \quad (8.47)$$

The inverse operation is

$$(\alpha|\vec{a})^{-1} = (\alpha^{-1}|\alpha^{-1}\vec{a}). \quad (8.48)$$

Since

$$(\alpha|\vec{a})^{-1}(\beta|\vec{b})(\alpha|\vec{a}) = (\alpha^{-1}\beta\alpha|\alpha^{-1}(\vec{b} + \beta\vec{a} - \vec{a})) \quad (8.49)$$

the translations (unlike rotations) are an invariant subgroup.

A Space Group generated from the Bravais translations and from the Point Group is *symmorphic*. The definition (8.46) (8.47) does not correspond to the direct product, that it would give instead $(\beta|\vec{b})(\alpha|\vec{a}) = (\beta\alpha|\vec{b} + \vec{a})$. It is called a *semidirect product*. The translation depends on the choice of the origin: consider the operation

$$\vec{r}' = \alpha\vec{r} + \vec{a}; \quad (8.50)$$

let us rewrite it in a reference with the origin shifted to $-\vec{b}$. The starting point in the new reference is $\vec{s} = \vec{r} + \vec{b}$ and the transformed one is $\vec{s}' = \vec{r}' + \vec{b}$; therefore the transformation is described by

$$\vec{s}' = \alpha\vec{s} - \alpha\vec{b} + \vec{a} + \vec{b}. \quad (8.51)$$

So, the rotation is the same, but $\vec{a} \rightarrow \vec{a}' = \vec{a} - \alpha\vec{b} + \vec{b}$. The operation can be made homogeneous, that is, $\vec{a}' = 0$, if we can find \vec{b} such that

$$\vec{b} = (\alpha - 1)^{-1}\vec{a}. \quad (8.52)$$

8.4.1 Symmorphic and Nonsymmorphic Groups

The symmorphic Groups have the rotations of the point Group and the translations of the Bravais lattice; nonsymmorphic Groups have extra symmetry elements are called *screw axes* and *glide planes*. These new operations depend on special relations between the dimensions of the *basis* (that is, of the unit which is periodically repeated) and of the Bravais translations. For

²different operations have different matrices.

example, CdS (*hexagonal close-packed* structure) has both kinds of extra symmetries. A plane $a - b$ contains alternated Cd and S ions arranged in a regular hexagonal pattern and above this plane at a distance $\frac{c}{2}$ another $a - b$ plane with Cd and S exchanged, and so on. The C_6 rotation about the center of the hexagon exchanges Cd and S; for the same reason, a translation by $\frac{c}{2}$ along the c axis does not belong to the Bravais lattice and is no symmetry; however the combined operation (C_6 and translation by $\frac{c}{2}$) leaves the system invariant. The σ_v reflection of the hexagon is broken since it leads to the exchange of Cd and S; however, the σ_v plane is a glide plane: reflection in this plane becomes a symmetry when accompanied by the $\frac{c}{2}$ translation along the screw axis.

It is natural to ask whether one can eliminate the $\frac{c}{2}$ translation from the screw axis operation by simply shifting the origin to $-\frac{c}{2}\vec{b}$. According to (8.51) the transformation becomes homogeneous, $\vec{s}' = \alpha\vec{s}$, if $0 = (1 - \alpha)\vec{b} + \vec{a}$. This requires satisfying (8.52) but if $\alpha\vec{a} = \vec{a}$, there is no solution, and this is the case since the translation \vec{a} is along the axis of the rotation α . So, the screw axes cannot be eliminated.

Iterating a screw axis operation we must obtain a Bravais translation. Since α belongs to the Point Group, α^n must be the identity for some integer n ; then (8.46) implies $(\alpha|\vec{a})^2 = (\alpha^2|\alpha\vec{a} + \vec{a})$, $(\alpha|\vec{a})^3 = (\alpha^3|\alpha^2\vec{a} + \alpha\vec{a} + \vec{a})$ and iterating we find

$$(\alpha|\vec{a})^n = (\alpha^n | \sum_{k=0}^{n-1} \alpha^k \vec{a}) = (1, \vec{t}). \quad (8.53)$$

where \vec{t} is a pure translation.

Let us write $\vec{a} = \vec{a}_{\parallel} + \vec{a}_{\perp}$ where \vec{a}_{\perp} is normal to the rotation axis. The condition (8.52) can always be solved to eliminate \vec{a}_{\perp} . Setting $\vec{a} = \vec{a}_{\parallel}$, it follows that $\sum_{k=0}^{n-1} \alpha^k \vec{a} = n\vec{a}$ and

$$\vec{a} = \frac{\vec{t}}{n}. \quad (8.54)$$

For instance, a screw-axis with an angle $\alpha = \frac{\pi}{2}$ can have a translation equal to $1/4$, $2/4$ or $3/4$ a Bravais vector. In the case of a glide plane, α is a reflection; the above holds with $n = 2$, and $\alpha\vec{a} + \vec{a} = 2\vec{a} = \vec{t}$; hence a glide plane has a translation of half a Bravais vector.

International Notation

In the international notation³, a screw-axis with an angle $\alpha = \frac{\pi}{2}$ and a translation equal to $1/4$, $2/4$ or $3/4$ a Bravais vector is denoted by 4_1 , 4_2 or 4_3 . The international notation for a Space Group starts with a letter (P

³International Tables for X-Ray Crystallography (1952)

for primitive, I for body-centered, F for face centered, R per rhombohedral) followed by the indication of the Point Group. Thus,

$$F \frac{4}{m} \bar{3} \frac{2}{m}$$

is the face centered Group with the O_h Point Group, with a C_4 axis with an horizontal symmetry plane, a C_3 axis and inversion symmetry; this is symmorphic, while the diamond Group

$$F \frac{4_1}{d} \bar{3} \frac{2}{m}$$

is not; d denotes a glide plane with a translation $1/4$ Bravais vector.

Representations of the Translation Group and of the Space Group

Every \vec{k} labels a representation of the Translation Group, with eigenvalue $e^{i\vec{k}\cdot\vec{t}}$. In general, one defines $Rf(\vec{r}) = f(R^{-1}\vec{r})$; so

$$(\alpha, \vec{a})e^{i\vec{k}\cdot\vec{r}} = e^{i\vec{k}\cdot(\alpha, \vec{a})^{-1}\vec{r}}$$

and using the inverse operation

$$(\alpha, \vec{a})e^{i\vec{k}\cdot\vec{r}} = e^{i\vec{k}\cdot(\alpha^{-1}\vec{r} - \alpha^{-1}\vec{a})}.$$

Rotating two vectors by the same angle the scalar product does not change; so we may write

$$(\alpha, \vec{a})e^{i\vec{k}\cdot\vec{r}} = e^{i(\alpha\vec{k})\cdot(\vec{r} - \vec{a})}. \tag{8.55}$$

In terms of Bloch functions, $(\alpha, \vec{a})\psi_n(\vec{k}, \vec{r})$ yields a linear combination of $\psi_{n'}(\alpha\vec{k}, \vec{r})$, where $n \rightarrow n'$ because in general Point Group operations mix degenerate bands.

One defines *Star of \vec{k}* the set $\{\alpha\vec{k}\}$. Higher symmetry points have stars with fewer elements. For non-degenerate bands, \vec{k} points of low symmetry correspond to a single ψ , but in general there is a subspace associated to a given \vec{k} point.

The *Group of the wave vector \vec{k}* or *little Group* is the Subgroup $G_{\vec{k}} \in G$ which consists of the operations (α, \vec{a}) (with \vec{a} that may be a Bravais vector or not) such that α does not change \vec{k} :

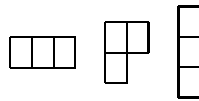
$$\alpha\vec{k} = \vec{k} + \vec{G}$$

with \vec{G} in the reciprocal lattice (k vectors that differ by \vec{G} are equivalent). $G_{\vec{k}}$ has the invariant Subgroup $T_{\vec{k}} \in T \in G$ of the translations \vec{t} such that $e^{i\vec{k}\cdot\vec{t}} = 1$. The set of the basis functions of a representation of $G_{\vec{k}}$ for all the points of a star provide a basis for a representation of the Space Group G . For further reading on this subject see [93].

8.5 Young Diagrams

Young Tableaux for S(3)

Let us consider again the Group C_{3v} . All operators can be expressed as reflections or products of reflections ($C_3 = \sigma_1\sigma_2, C_3^2 = \sigma_1\sigma_3$); moreover since σ_1 exchanges 2 with 3, etc., all operations are permutations and $C_{3v} \equiv S(3)$. In the irrep A_1 all the operators are represented by 1; in A_2 the reflections σ_i are represented by -1. The totally symmetric functions belong to A_1 while those of A_2 are totally antisymmetric under any σ_i . Young diagrams represent the irreps of $S(n)$ by schemes with n boxes. Horizontal lining of boxes is associated with symmetrization, vertical lining with antisymmetrization, and the length of lines does not increase. So the first diagram refers to A_1 , the last to A_2 and the intermediate one to E. Here are the Young diagrams for $S(3)$. Each diagram correspond to an irrep, and this fact is general. E corresponds



to a mixed symmetry; in the geometry of Figure 7.1 with 1 on the y axis, the projector on the x component is

$$P_{xx}^{(E)} = 1 - \frac{1}{2}(C_3 + C_3^2) - \sigma_1 + \frac{1}{2}(\sigma_2 + \sigma_3) = 1 - \frac{1}{2}\sigma_1(\sigma_2 + \sigma_3) - \sigma_1 + \frac{1}{2}(\sigma_2 + \sigma_3), \tag{8.56}$$

that is, introducing the anti-symmetrizer $A(2, 3) = 1 - \sigma_1$ and the symmetrizer $S(2, 3) = 1 + \sigma_1$

$$P_{xx}^{(E)} = A(2, 3)[S(1, 3) + S(1, 2)]. \tag{8.57}$$

$A(2, 3)S(1, 3)$ and $A(2, 3)S(1, 2)$ are mixed symmetries and project on E. These projectors written in terms of symmetrizers and antisymmetrizers are called Young projectors. They may be thought of as projectors on the various irreps based on the regular representation. The three diagrams exhaust the possible partitions of 3 in not increasing integers, that is, $3 = 2+1=1+1+1$.

The Young tables or Young tableaux are obtained from the Young diagrams by inserting numbers from 1 to 3 so that every line and every column grow along. The tableau



represents the projection operator $S(1, 2, 3)$, the *symmetrizer*; the Young

projection operator $A(1, 3)S(12)$ is given by $\begin{array}{|c|c|} \hline 1 & 2 \\ \hline 3 & \\ \hline \end{array}$ but one can also

antisymmetrize with respect to 2, getting $\begin{array}{|c|c|} \hline 1 & 3 \\ \hline 2 & \\ \hline \end{array}$. Finally, $\begin{array}{|c|} \hline 1 \\ \hline 2 \\ \hline 3 \\ \hline \end{array}$

projects on A_2 .

The fact that there are two tables with mixed permutation symmetry is due to degeneracy 2 of the irrep E. In general, in the Young tables for $S(N)$, the m-dimensional irreps occur m times.

Young Tableaux for S(4)

$S(4)$, has 24 elements and the following 5 irreps that may be found by the above stated rules.

$\begin{array}{|c|c|c|c|} \hline 1 & 2 & 3 & 4 \\ \hline \end{array}$ is the 1-dimensional A_1 representation.

$\begin{array}{|c|c|c|} \hline 1 & 2 & 3 \\ \hline 4 & & \\ \hline \end{array}$ $\begin{array}{|c|c|c|} \hline 1 & 2 & 4 \\ \hline 3 & & \\ \hline \end{array}$ $\begin{array}{|c|c|c|} \hline 1 & 3 & 4 \\ \hline 2 & & \\ \hline \end{array}$ are 3 occurrences of a 3-dimensional irrep, while

$\begin{array}{|c|c|} \hline 1 & 2 \\ \hline 3 & 4 \\ \hline \end{array}$ $\begin{array}{|c|c|} \hline 1 & 3 \\ \hline 2 & 4 \\ \hline \end{array}$

is 2-dimensional,

$\begin{array}{|c|c|} \hline 1 & 2 \\ \hline 3 & \\ \hline 4 & \\ \hline \end{array}$ $\begin{array}{|c|c|} \hline 1 & 3 \\ \hline 2 & \\ \hline 4 & \\ \hline \end{array}$ $\begin{array}{|c|c|} \hline 1 & 4 \\ \hline 2 & \\ \hline 3 & \\ \hline \end{array}$ is 3d and finally $\begin{array}{|c|} \hline 1 \\ \hline 2 \\ \hline 3 \\ \hline 4 \\ \hline \end{array}$ is the totally antisymmetric ir-

rep. These correspondences are useful as it extends to all groups $S(N)$ of permutations of N objects. Thus, the irreps of $S(N)$ are known for any N.

Young Tableaux for Spin Eigenfunctions

Consider a system consisting of N spins 1/2 and a set of eigenstates $|S, M_S\rangle$ obtained e.g. by solving the eigenvalue problems for S^2 and S_z . Any permutation of the spins sends an eigenfunction into a linear combination of the eigenfunctions with the same eigenvalues S, M_S ; in other terms, the S, M_S quantum numbers label subspaces of functions that do not mix under permutations. Within each subspace, one can use projection operators to produce S and M_S eigenfunctions that form a basis of irreps of $S(N)$. For each symmetry type (i.e. for each component of each irrep) there exists one solution.

For instance, for $N=3$ a quartet and two doublets exist. With $M_S = \frac{3}{2}$ the only state is $|\uparrow\uparrow\uparrow\rangle$, which is invariant for any permutation of the arrows;

by the shift operators one finds that $|\frac{3}{2}, \frac{1}{2}\rangle = \frac{1}{\sqrt{3}}(|\uparrow\uparrow\downarrow\rangle + |\uparrow\downarrow\uparrow\rangle + |\downarrow\uparrow\uparrow\rangle)$. This is invariant for spin permutations, too, and belongs to the A_1 irrep of $S(3)$. The shift operators preserve the permutation symmetry, and all the $2M_S + 1$ states belong to the same irrep. The orthogonal subspace involving one down spin yields two doublets; one is $|\frac{1}{2}, \frac{1}{2}\rangle = \frac{1}{\sqrt{2}}[|\uparrow\uparrow\downarrow\rangle - |\uparrow\downarrow\uparrow\rangle]$; another one which is not orthogonal is $|\frac{1}{2}, \frac{1}{2}\rangle = \frac{1}{\sqrt{2}}[|\downarrow\uparrow\uparrow\rangle - |\uparrow\downarrow\uparrow\rangle]$; orthonormalizing we obtain $|\frac{1}{2}, \frac{1}{2}\rangle = \frac{1}{\sqrt{6}}[2|\downarrow\uparrow\uparrow\rangle - |\uparrow\downarrow\uparrow\rangle - |\uparrow\uparrow\downarrow\rangle]$. These doublets are not invariant for spin permutations; they are just the two components of the familiar irrep E of the C_{3v} permutation symmetry. Moreover, by the shift operators each yields its $|\frac{1}{2}, -\frac{1}{2}\rangle$ companion. A quartet and 2 doublets exhaust all the 2^3 states available for $N=3$, and there is no space for the A_2 irrep. This is general: since spin 1/2 has two states available, any spin wave function belongs to a Young diagram with 1 or 2 rows.

Thus we realize that rather than solving eigenvalue problems we can be smarter and obtain the eigenfunctions directly by Young projectors. The permutation symmetry of the full many-electron wave function will be discussed in Sect. 9.8.

Problems

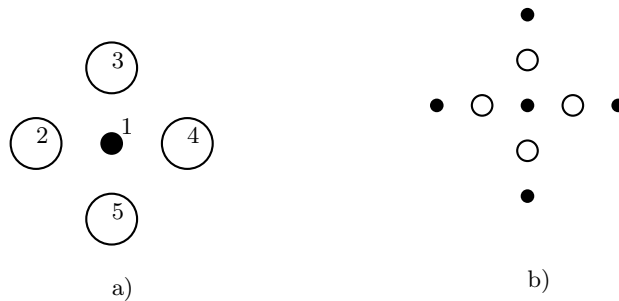


Fig. 8.4. a) The CuO_4 Hubbard model cluster. b) The Cu_5O_4 Hubbard model cluster.

8.1. The CuO_4 Hubbard model cluster

Consider the Hubbard model cluster in Figure (8.5 a)), belonging to C_{4v} symmetry. (1) Find the irreps of the one-electron orbitals.

(2) Consider this cluster with 4 fermions, in the $S_z = 0$ sector. Classify the 4-body states with the irreps of the Group.

8.2. The Cu_5O_4 Hubbard model cluster

For the cluster in Figure (8.5 b)) classify the 4-fermion states in the $S_z = 0$ with the irreps of C_{4v} .

9 Product of Representations and Further Physical Applications

9.1 Irreducible Tensor Operators

Let $\Phi = \hat{A}\Psi$, where Ψ is a wave function and \hat{A} some operator. Then, acting with a unitary operator R , one finds $R\Phi = \hat{A}'R\Psi = R\hat{A}R^\dagger R\Psi$, where the transformed operator is $\hat{A}' = R\hat{A}R^\dagger$. Thus, functions are transformed according to $\Psi \rightarrow R\Psi$ while operators are transformed according to $\hat{A} \rightarrow R\hat{A}R^\dagger$; actually the two rules differ by a matter of notation. R acts on everything on its right, so in the case of operators the last factor $R^\dagger = R^{-1}$ is there just to ensure that the action of R is limited to \hat{A} , while functions are at the extreme right and there is no need for that. We can consider (x_1, x_2, x_3) as a set of functions or as the components of an operator. As functions that transform as a basis of a representation of some symmetry Group, they transform according to the rule

$$(x_1, x_2, x_3) \rightarrow (Rx_1, Rx_2, Rx_3) = (D(R)_{k1}x_k, D(R)_{k2}x_k, D(R)_{k3}x_k);$$

this is the vector representation, which is irreducible in cubic and higher Groups. If we treat them as a set of operators, we write

$$(x, y, z) \rightarrow (RxR^\dagger, RyR^\dagger, RzR^\dagger).$$

This defines a vector operator, but the linear combinations that result are the same. A tensor is a set of operators T_i (the components) that are mapped into linear combinations by every R , that is,

$$T_i \xrightarrow{S} ST_iS^\dagger = \sum_j T_j D_{ji}(S); \quad (9.1)$$

the multiplication Table is followed since

$$T_i \xrightarrow{RS} RST_iS^\dagger R^\dagger = \sum_j T_j D_{ji}(RS). \quad (9.2)$$

If the representation is the irrep α , we can speak of the irreducible tensor operator $T^{(\alpha)}$ and in any representation all its components are mixed by the Group operations. In $GL(n)$ a tensor of rank r is a set of operators T such that

$$T'_{\alpha(1),\alpha(2),\dots,\alpha(r)} = \sum_{\beta(1),\beta(2),\dots,\beta(r)} a_{\alpha(1)\beta(1)} a_{\alpha(2)\beta(2)} \cdots a_{\alpha(r)\beta(r)} T_{\beta(1),\beta(2),\dots,\beta(r)}. \tag{9.3}$$

Given a second-rank tensor T , one can build a symmetric tensor $S_{ij} = T_{ij} + T_{ji}$ and an antisymmetric one $A_{ij} = T_{ij} - T_{ji}$. Obviously a symmetric (antisymmetric) tensor remains symmetric (antisymmetric) under the transformations of $GL(n)$. In general, the tensors of $GL(n)$ are reduced into irreducible parts by taking linear combinations according to the irreps of the permutation Group $S(r)$. Further reduction is possible in subgroups of $GL(n)$.

Tensors in Polar Form

Under the operators of $O^+(3)$ the ITO transform like spherical harmonics. Therefore, the following *polar form* is expedient. For a vector, the polar components are $x_m, m = 0, \pm 1$, where, using a traditional notation,

$$x_{+1} = -\frac{x + iy}{\sqrt{2}}, x_0 = z, x_{-1} = -\frac{x - iy}{\sqrt{2}}, \tag{9.4}$$

and transform according to

$$Rx_m R^{-1} = \sum_n x_n D_{nm}^1(R), \tag{9.5}$$

where $D_{nm}^1(R)$ represents the rotation in the basis of the spherical harmonics with $l = 1$. It is natural to put the basis vectors in polar form too,

$$e_{+1} = -\frac{e_1 + ie_2}{\sqrt{2}}, e_0 = e_3, e_{-1} = -\frac{e_1 - ie_2}{\sqrt{2}}. \tag{9.6}$$

In this way the expansion of a vector in the basis, $\mathbf{V} = \sum_{i=1}^3 V_i \mathbf{e}_i$ is replaced by

$$\mathbf{V} = \sum_{m=-1}^1 (-)^m V_m \mathbf{e}_m. \tag{9.7}$$

The scalar product of two real vectors \mathbf{V} and \mathbf{W} in polar form is

$$\mathbf{V} \cdot \mathbf{W} = \sum_{m=-1}^1 (-)^m V_{-m} W_m, \tag{9.8}$$

as one can readily verify. The advantage of the polar form is that now we can generalize to an ITO of any rank of $O^+(3)$. The definition of such an ITO is

$$RT_p^{(\gamma)} R^{-1} = \sum_q T_q^{(\gamma)} D_{qp}^{(\gamma)}(R). \tag{9.9}$$

For instance if γ denotes the representation with $J = 0$, then $q = 0$ and T is a scalar; if γ denotes the representation with $J = 1$, then $q = 0, \pm 1$ and $T^{(1)}$ is a vector in the polar representation; in general, $T_q^{(l)}$ transforms like $Y_q^{(l)}$.

9.2 Direct Product Representation

Direct Product of Matrices

From the pair of matrices

$$A = \begin{pmatrix} a_{11} & a_{12} \\ a_{21} & a_{22} \end{pmatrix}, \quad B = \begin{pmatrix} b_{11} & b_{12} \\ b_{21} & b_{22} \end{pmatrix},$$

one can build the direct product, that is, the block matrix

$$D = A \otimes B = \begin{pmatrix} a_{11}B & a_{12}B \\ a_{21}B & a_{22}B \end{pmatrix} = \begin{pmatrix} a_{11}b_{11} & a_{11}b_{12} & a_{12}b_{11} & a_{12}b_{12} \\ a_{11}b_{21} & a_{11}b_{22} & a_{12}b_{21} & a_{12}b_{22} \\ a_{21}b_{11} & a_{21}b_{12} & a_{22}b_{11} & a_{22}b_{12} \\ a_{21}b_{21} & a_{21}b_{22} & a_{22}b_{21} & a_{22}b_{22} \end{pmatrix}.$$

Note that $TrD = TrATrB$.

We can number rows and columns as usual and say for instance $D_{24} = a_{12}b_{22}$, but for direct-product matrices a different rule is used. One denotes the matrix element by a pair of row indices and a pair of column indices, so $a_{12}b_{22} = D_{12,22}$. In general, $D_{kp,ij} = a_{ki}b_{pj}$ is the element of a $mn \times mn$ matrix $D = A \otimes B$, where m and n are the sizes of A and B respectively.

Direct Product of Representations

Further important developments of the theory of symmetry are needed for systems that consist of parts (e.g. two electrons, spin and orbit of an electron, one electron and a vibration mode). One starts with two parts 1 and 2. The basis can always be chosen as if they were independent, and any state is a linear combination of products $f^{(\alpha)}(1)g^{(\beta)}(2)$, where $f_1^{(\alpha)}, \dots, f_m^{(\alpha)}$ and $g_1^{(\beta)}, \dots, g_n^{(\beta)}$ are bases for irreps of dimensions m and n respectively:

$$\begin{cases} Rf_i^{(\alpha)} = \sum_{k=1}^m f_k^{(\alpha)}(1)D_{ki}^{(\alpha)}(R), \\ Rg_j^{(\beta)} = \sum_{p=1}^n g_p^{(\beta)}(2)D_{pj}^{(\beta)}(R). \end{cases} \quad (9.10)$$

are a convenient basis; they transform according to

$$\begin{aligned} R|\alpha i \beta j\rangle &= \sum_k^m \sum_p^n |\alpha k \beta p\rangle D_{ki}^{(\alpha)}(R) D_{pj}^{(\beta)}(R) \\ &\equiv \sum_k^m \sum_p^n |\alpha k \beta p\rangle D_{kp,ij}^{(\alpha\beta)}(R). \end{aligned} \quad (9.11)$$

Thus, the direct product matrix $D^{(\alpha\beta)} = D^{(\alpha)} \otimes D^{(\beta)}$ with elements $D_{kp,ij}^{(\alpha\beta)}(R) = D_{ki}^{(\alpha)}(R)D_{pj}^{(\beta)}(R)$ is the representative matrix of R in what is called the *direct product representation*. Its characters are

$$\chi^{(\alpha\beta)}(R) = \sum_{kp} D_{kp, kp}^{(\alpha\beta)}(R) = \chi^{(\alpha)}(R)\chi^{(\beta)}(R). \tag{9.12}$$

It is almost a tongue-twister, but is a far reaching result: the character of the direct product of two representations is the product of the characters of the two representations. Great! We can now perform the usual analysis of the product into irreps by the character orthogonality theorem. Consider for instance the Group of the Square, and suppose that the two parts 1 and 2 belong to known irreps: their products define a representation of G and we wish to reduce it:

C_{4v}	I	C_2	$2C_4$	$2\sigma_v$	$2\sigma_d$	$g = 8$
A_1	1	1	1	1	1	z
A_2	1	1	1	-1	-1	R_z
B_1	1	1	-1	1	-1	$x^2 - y^2$
B_2	1	1	-1	-1	1	xy
E	2	-2	0	0	0	(x, y)
$A_2 \otimes B_1$	1	1	-1	-1	1	B_2
$B_2 \otimes B_1$	1	1	1	-1	-1	A_2
$E \otimes A_2$	2	-2	0	0	0	E
$E \otimes E$	4	4	0	0	0	$A_1 \oplus A_2 \oplus B_1 \oplus B_2$

(9.13)

In this way we can build a multiplication table for the irreps of C_{4v} .

C_{4v}	A_1	A_2	B_1	B_2	E
A_1	A_1	A_2	B_1	B_2	E
A_2	A_2	A_1	B_2	B_1	E
B_1	B_1	B_2	A_1	A_2	E
B_2	B_2	B_1	A_2	A_1	E
E	E	E	E	E	$A_1 + A_2$ $+ B_1 + B_2$

(9.14)

Here A_1 occurs in the diagonal and only there because

$$n^{A_1} = \frac{1}{N_G} \sum_R 1 \cdot \chi^{(\alpha\beta)}(R) = \frac{1}{N_G} \sum_R \chi^{(\alpha)}\chi^{(\beta)}(R) = \delta_{\alpha\beta}. \tag{9.15}$$

9.2.1 Selection Rules

Suppose the amplitude of a physical transition governed by some operator \hat{T} depends on the matrix element $\langle \phi | \hat{T} | \psi \rangle$ which is cumbersome and expensive to compute. It would be disappointing at the end of a computational *tour de force* to discover that the matrix element is 0, or that it is identical to another one that we knew already. Group theory predicts which matrix elements must be equal and which must vanish by establishing selection rules. Indeed, \hat{T} is some tensor component and T generates a representation $\Gamma^{(T)}$; the states also

belong to representations $\Gamma^{(\psi)}$ and $\Gamma^{(\phi)}$ of the Group G . A matrix element $\langle \phi | \hat{T} | \psi \rangle$ is an integral, which is invariant, therefore it vanishes unless the integrand gets some contribution from A_1 . If the reduction of $\Gamma^{(\phi)} \otimes \Gamma^{(T)} \otimes \Gamma^{(\psi)}$ to irreps yields (among others) A_1 , then $\langle \phi | \hat{T} | \psi \rangle \neq 0$, otherwise we can dispense from the calculation of the matrix element since it vanishes by symmetry. In other terms, the condition for a non-vanishing result is that the reductions of $\Gamma^{(T)}$ and of $\Gamma^{(\phi)} \otimes \Gamma^{(\psi)}$ have at least one irrep in common. For example, if one is interested in electromagnetic transitions in C_{4v} symmetry, the dipole operator transforms like a vector (x, y, z) , so one component is in A_1 and two are in E. Thus one finds that a transition from B_1 to B_2 is forbidden, while from the E states all the other states can be reached by the in-plane component of the dipole, while $E \rightarrow E$ is allowed by the z component.

Most molecules with an even number of electrons have filled shells configuration in the ground state, which is total-symmetric¹. Then, the excited states that can be reached by photon absorption are those where one of the components of the dipole is classified. A similar analysis can be done for the infrared transitions between vibrational states that belong to the same electronic level. Clearly, the phonon vacuum belongs to A_1 and the one-phonon states have the symmetry of the normal mode which is excited. On the other hand, the Raman effect is a two-photon process in which the system goes from an initial state $|i\rangle$ to a final state $|f\rangle$ by absorbing a photon of polarization vector ϵ_1 and emitting another one of polarization vector ϵ_2 and different frequency. Emission and absorption are coherent, that is, they are one quantum process, and the amplitude is given by the matrix element of the operator

$$\mathcal{R} = \sum_{pq} R_{pq}(\epsilon_2)_p(\epsilon_1)_q$$

where $R_{pq} \propto x_p x_q$ is the Raman tensor. From the symmetry viewpoint, what matters is that the components of the Raman tensor transform like $x_p x_q$, and this determines the selection rules. In systems with inversion symmetry, the normal modes must be *gerade* or *ungerade* (even or odd). Only ungerade modes are infrared active and gerade ones are Raman active. For instance, infrared and Raman spectra of Benzene have no frequencies in common.

9.3 Reduction of the Direct Product Representation

From the m_α -times degenerate irrep α and the m_β -times degenerate irrep β one forms a direct product representation $\Gamma^{(\alpha)} \otimes \Gamma^{(\beta)}$ of dimension $m_\alpha m_\beta$. We have seen how the direct product representation is reduced; but it remains to be seen how the basis separates in symmetry-adapted bases. By

¹See the Section 9.5.2 on the Jahn-Teller effect for a justification of this statement.

inserting a complete set one can go, with a unitary transformation, from the basis $\{|\alpha i \beta j\rangle\}$ of the direct product $\Gamma^{(\alpha)} \otimes \Gamma^{(\beta)}$ to a basis of functions that transform according to irrep $\Gamma^{(\gamma)}$ of the Group G.

$$|\alpha i \beta j\rangle = \sum_g \sum_r^{irreps\ m_\gamma} |\gamma r\rangle \langle \gamma r | \alpha i \beta j \rangle. \quad (9.16)$$

The coefficients $\langle \gamma r | \alpha i \beta j \rangle$ are the *Clebsh-Gordan (CG) coefficients* of the Group; in the case of the rotation Group O(3) they are the well known coefficients $\langle LM | L_1 M_1 L_2 M_2 \rangle$. For a point group, the CG coefficients are even easier to find than for O(3). One forms a table $R|\alpha i \beta j\rangle, i = 1, \dots, m_\alpha, j = 1, \dots, m_\beta, R \in G$, of the effects of the operations on the direct-product basis, then combines them according to the projectors. In order to decompose the D matrices, we want a basis change, obtained by inserting complete sets:

$$\begin{aligned} D_{ki}^{(\alpha)}(R) D_{pj}^{(\beta)}(R) &= D_{kp,ij}^{(\alpha\beta)}(R) = \langle \alpha k \beta p | R \alpha i \beta j \rangle \\ &= \sum_{\gamma r s} \langle \alpha k \beta p | \gamma s \rangle D_{sr}^{(\gamma)}(R) \langle \gamma r | \alpha i \beta j \rangle. \end{aligned} \quad (9.17)$$

This corresponds to the familiar use of CG coefficients for the sum of angular momenta (for an example, see Problem 9.1).

9.4 Spin-Orbit Interaction and Double Groups

Up to now we have considered only the Group of transformations of the space orbitals, ignoring spin. The spin-orbit interaction makes the problem less symmetrical: as an example, a Hydrogen level of angular $L \neq 0$, $2(2L+1)$ times degenerate, separates in two levels $J_\pm = L \pm 1/2$, degenerate $2J_\pm + 1$ times.

The spin, alone, or in an A_1 orbital, yields a representation of the operators. The rotation around to the z axis by an angle ω is done by

$$R_\omega = e^{-i\frac{\omega}{2}\sigma_z} = \begin{pmatrix} e^{i\frac{\omega}{2}} & 0 \\ 0 & e^{-i\frac{\omega}{2}} \end{pmatrix} = \cos\left(\frac{\omega}{2}\right) - i\sigma_z \sin\left(\frac{\omega}{2}\right) \quad (9.18)$$

and belongs to the SU(2) covering group of SO(3). For $\omega = 2\pi$, $R_\omega = -1$. If we rotate around axis \mathbf{n} , since $(\boldsymbol{\sigma} \cdot \mathbf{n})^2 = 1$,

$$R_\omega = e^{-i\frac{\omega}{2}\boldsymbol{\sigma} \cdot \mathbf{n}} = \cos\left(\frac{\omega}{2}\right) + i(\boldsymbol{\sigma} \cdot \mathbf{n}) \sin\left(\frac{\omega}{2}\right) \quad (9.19)$$

and for $\omega = 2\pi$, $R = -1$ anyway²; this is a rotation that commutes with any other symmetry.

²a closely similar formula with the 4×4 matrices $\boldsymbol{\Sigma}$ in place of $\boldsymbol{\sigma}$ is the starting point of the Group theory using Dirac's equation. In this section we assume that the Pauli theory with the relativistic corrections is adequate.

Following Teller (1929) we indicate with \bar{E} the 2π rotation around an arbitrary axis; $\bar{E} = E$ for a function without spin and $\bar{E} = -E$ and for the spinor representation: in both the cases, \bar{E} commutes with all the $R \in G$. Adding \bar{E} to the generators of the symmetry Group we obtain the so-called *double Group* G' which has, along with every $R \in G$, also $\bar{E}R$.

\bar{E} alone is a class. A rotation by α forms a class with $4\pi - \alpha$ i.e. its inverse in G' , since the two operations are conjugated by a vertical reflection or by another rotation. Reflections times \bar{E} may form a separate class.

Since $\bar{E}^2 = E$ the eigenvalues are ± 1 . By Schur's lemma, $D^{(\alpha)}(\bar{E}) = \pm D^{(\alpha)}(E) \forall \alpha$, so $\chi^{(\alpha)}(\bar{E}R) = \pm \chi^{(\alpha)}(R)$.

Among the new irreps, where the - sign holds, the spinor representation is always there; it is suitable for an electron in a total-symmetric orbital. $\chi(\bar{E}) = -2$; rotation by ω about \mathbf{n} are represented by the SU(2) matrices $D(\omega) = e^{-\frac{i}{2}\boldsymbol{\sigma}\cdot\boldsymbol{\omega}}$. Since the characters are invariant for unitary transformations, we may take \mathbf{n} along the axis z: thus $D(\omega) = \begin{pmatrix} e^{-i\frac{\omega}{2}} & 0 \\ 0 & e^{i\frac{\omega}{2}} \end{pmatrix}$. Thus the character for spin 1/2 is

$$\chi^{(1/2)}(\omega) = 2 \cos\left(\frac{\omega}{2}\right). \quad (9.20)$$

If the inversion \hat{i} is in G , it leaves spin and any angular momentum invariant, so $D(\hat{i}) = D(E)$ and $\chi(i) = 2$. The reflections and all the improper rotations can be written like products $\hat{i}R_\omega$.³ In such a way, we can complete the characters of the spinorial representation⁴. This describes an electron with an orbital A1.

The above information is enough to build easily the character table for G' from that of G , without having to work out everything from the multiplication table. Having listed the classes, one can append the irreps of G , with $\chi^{(\alpha)}(\bar{E}R) = +\chi^{(\alpha)}(R)$. Then one appends the spinor representation, and knows how many irreps are missing to reach the number of classes. The sizes are found by the Burnside theorem, and the LOT allows to find the characters. As an example, we can extend from C_{3v} to C'_{3v} .

C'_{3v}	E	\bar{E}	C_3 $C_3^2\bar{E}$	C_3^2 $C_3\bar{E}$	$3\sigma_v$	$3\sigma_v\bar{E}$
A'_1	1	1	1	1	1	1
A'_2	1	1	1	1	-1	-1
E'	2	2	-1	-1	0	0
$E_{1/2}$	2	-2	1	-1	0	0
Γ^5	1	-1	-1	1	i	$-i$
Γ^6	1	-1	-1	1	$-i$	i

³Example: a reflection in $(xyz) \rightarrow (xy - z)$ in the (x,y) plane can be obtained as a rotation $(xyz) \rightarrow (-x - yz)$ followed by \hat{i} .

⁴The character tables for the most common double Groups are available in the literature, and some are reported in Appendix B

The A'_1, A'_2 and E' irreps have the same characters as in C_{3v} , and $E_{1/2}$ is the spinor representation. Since the classes are 6 two irreps are missing, and since the sum of the squares of the dimensions must be 12, the new ones are one-dimensional. By orthogonality, we find that they are conjugate representations as shown above. At this point the reader could solve Problem 9.4.

In a physical problem, one can begin by classifying the space orbitals according to G and then extend the theory to G' including spin. The direct product of the orbital irrep by the spinor representation will include the spin. In general, the result will be reducible in the double Group applying the LOT. We will be able to thus establish how the spin-orbit interaction reduces the degeneracy in the problem in issue. For example, if the orbital belongs to A_1 or A_2 of C_{3v} , the spinor belongs to $E_{1/2}$, and no level splitting occurs; if the orbital belongs to E the product representation has dimension 4, but one finds that in C'_{3v} , $E \otimes E_{1/2} = E_{1/2} + \Gamma^5 + \Gamma^6$.

9.5 Static and Dynamical Jahn-Teller Effect

9.5.1 The Born-Oppenheimer (BO) Approximation

The total Hamiltonian of a system of electrons and nuclei may be written, with R for set of nuclear and r for the electronic coordinates,

$$H_{tot}(r, R) = T_e(r) + T_N(R) + V(r, R) \quad (9.21)$$

where $T_e(r)$ and $T_N(R)$ are the electronic and nuclear kinetic terms, and

$$V(r, R) = V_{ee} + V_{eN} + V_{NN} \quad (9.22)$$

contains all interactions. The Schrödinger equation

$$H_{tot}(r, R)\Psi_{tot}(r, R) = W\Psi_{tot}(r, R) \quad (9.23)$$

is intractable. In order to separate variables approximately, one keeps the nuclei fixed ($T_N \approx 0$) introducing the *adiabatic electronic Hamiltonian*

$$H_e(r; R) = T_e + V(r, R) \quad (9.24)$$

where the R dependence is only parametric; the Schrödinger equation

$$H_e\Psi_n(r; R) = E_n(R)\Psi_n(r; R) \quad (9.25)$$

yields the *adiabatic eigenstates* $\Psi_n(r; R)$ and the *potential energy surfaces* $E_n(R)$. This is the BO approximation, which further assumes that if nuclei move their evolution is confined to an adiabatic surface, and the harmonic oscillations about equilibrium correspond to the minimum of $E_0(R)$.

Below we adopt a compact notation, writing the nuclear kinetic energy $T_N = \frac{\hbar^2}{2M} \frac{\partial^2}{\partial R^2}$ and understanding indices and summations. The nuclear wave function is then expected to be given by⁵

$$-\frac{\hbar^2}{2M} \frac{\partial^2}{\partial R^2} \chi + E_0(R) \chi(R) = W \chi(R). \quad (9.26)$$

Summarizing the BO approximation:

- the positions of the nuclei are external parameters that determine the Coulomb external potential in which the electrons move, and the Hamiltonian $H(R)$
- the momenta $-i\hbar\nabla_R$ canonically conjugated to the nuclear positions are ignored. This assumes that the nuclear masses are infinitely large
- The equilibrium configuration corresponds to a minimum of the total energy:

$$E_0(R) = \langle \Psi_0 | H | \Psi_0 \rangle \quad (9.27)$$

$$\frac{\delta E_0}{\delta R} = 0. \quad (9.28)$$

($\frac{\delta E_0}{\delta R} = 0$ represents extremum conditions in all the components of the nuclear position vectors)

- the electronic states are calculated at the equilibrium configuration and $E_0(R)$ is the potential energy for the nuclear motion.

9.5.2 The Jahn-Teller Theorem

CH_4 is a tetrahedron (T_d Group), SF_6 an octahedron (O_h Group), and snowflakes have beautiful regular shapes. Why are so many molecules and solids highly symmetric in Nature? Is a *maximum symmetry principle* to be discovered? Although the concept of symmetry is central to quantum physics, from solids down to subnuclear particles, the answer is definitely *no*. Bloch waves that carry crystal momentum and Hydrogen states with angular momentum are less symmetrical than the respective Hamiltonians. Many atoms and nuclei have non-spherical ground states. Yet, the regular shapes of molecules and solids is striking since there would be an infinite number of ways to move the nuclei and seek for a lower energy configuration; we must understand why such molecules cannot gain energy from any distortion. Within the Born-Oppenheimer approximation, the Jahn-Teller Theorem provides an answer, for the 32 point Groups: what matters is degeneracy. The electronic cloud needs to be degenerate, otherwise the electrons do not have enough degrees of freedom to lower the symmetry; on the other hand, if there is degeneracy, a suitable deformation always exists, except for linear molecules.

⁵In Equation (9.41) below we shall see that this statement although reasonable is a bit too simple-minded and actually something is missing.

The CH_4 ground state is non-degenerate in the T_d symmetry; but by removing a bonding t_2 electron the CH_4^+ ion distorts until the symmetry Group becomes Abelian.

Initially proposed as a computational aid which exploits a given symmetry of the Hamiltonian, Group Theory eventually dictates which symmetries are allowed or forbidden at all.

Mathematical Formulation of the Problem

We want a criterion to decide if a given configuration \tilde{R} of the nuclei in the BO approximation can be the equilibrium one, according to (9.28). We must minimize with respect to the shifts of the nuclei from to the reference configuration \tilde{R} ; but first, we eliminate the rigid shifts of the molecule by using the normal modes of vibration of Section (8.2) instead of the nuclear positions. These modes are labeled by the index α of the frequency and by an index i for the degeneracy and multiplicity (the same symmetry can occur several times). The amplitude of the motion according to a normal mode is specified by a normal coordinate q_i^α , and we must minimize $E(q)$, where $q \equiv \{q_i^\alpha\}$ stands for the whole set.

Actually, we do not have any analytic expression of $E(q)$ to differentiate. Therefore, we expand the Hamiltonian H around \tilde{R} in powers of q , letting $H_0 = H(\tilde{R})$; this enables us to find the correction to $E(q)$ by perturbation theory. The correction terms of H yield the interactions between electrons and vibrations, also called the *vibronic couplings*. Including up to the quadratic terms, we find

$$H = H_0 + \sum_{\alpha i} V_{\alpha i} q_i^{(\alpha)} + \sum_{\alpha\beta} \sum_{ik} W_{\alpha i\beta k} q_i^\alpha q_k^\beta. \quad (9.29)$$

The equilibrium condition is that the average first-order corrections to the energy vanish.

In the Born-Oppenheimer approximation, $V_{\alpha i}$ operates on electrons; the true Hamiltonian depends quadratically on the momenta p_i^α canonically conjugated to the q_i^α . If we take into account the momenta, we go beyond the Born-Oppenheimer approximation; one then speaks about the dynamical Jahn-Teller effect, see next Section. Note that V_i^α and q_i^α must transform in the same way, as H must be a scalar and in the table of the direct products A_1 appears only on the diagonal. We do not mind $V_i^{A_1}$ here: such terms do not distort the symmetry.⁶ The equilibrium condition is

$$\langle H' \rangle = \sum_{\alpha i} \langle V_{\alpha i} \rangle q_i^{(\alpha)} = 0. \quad (9.30)$$

Since the $q_i^{(\alpha)}$ are linearly independent we really need

$$\langle \Psi_0 | V_{\alpha i} | \Psi_0 \rangle = 0. \quad (9.31)$$

⁶Actually, they could in principle only increase it: with a A_1 motion the water molecule could be *straightened* and become a $D_{\infty h}$ molecule.

Non-degenerate Case

If the ground state is not degenerate, $\Gamma(\Psi_0\Psi_0) = A_1$ and $\langle\Psi_0|V_{\alpha i}|\Psi_0\rangle = 0$ for $\alpha \neq A_1$. So, all the nuclei move, keeping the symmetry of the molecule, until $\langle\Psi_0|V_i^{(A_1)}|\Psi_0\rangle = 0$. This 0 is not due to the symmetry, but to the existence of a minimum of energy versus breathing mode coordinate: we can vary a bond length or an angle until the condition is satisfied.

Degenerate Case

When $H_0\Psi_\nu^{(0)} = E_0\Psi_\nu^{(0)}$ is solved by several $\Psi_\nu^{(0)}$, we must apply degenerate perturbation theory, diagonalizing the perturbation matrix with elements $\langle\Psi_\nu^{(0)}|H'|\Psi_\nu^{(0)}\rangle$. If the eigenvalues do not vanish all identically, one predicts a splitting linear in the $q_i^{(\alpha)}$ of the degenerate level, a lowering of the symmetry and a distortion of the molecule. The only Hermitean matrix that has all eigenvalues equal to 0 is the null one. Thus, for equilibrium we need to satisfy the strong condition

$$\langle\Psi_\rho^{(0)}|V_{\alpha i}|\Psi_\sigma^{(0)}\rangle = 0 \quad \forall \alpha, \sigma, \rho. \quad (9.32)$$

Now we must examine the normal modes occurring in the assumed geometry in order to see if any generates matrix elements that destroy the symmetry. Let Γ^0 denote the irrep where $\Psi_\sigma^{(0)}$ belongs. The Jahn-Teller effect is caused by a normal mode belonging to an irrep $\alpha \neq A_1$ which is contained in $\Gamma^0 \otimes \Gamma^0$. In such cases there is no reason why the matrix elements vanish, and the molecular configuration is unstable⁷.

In 1937, Jahn and Teller demonstrated that for a non-linear molecule with degenerate ground state irrep Γ^0 , a vibration ω_α always exists such that $\Gamma^\alpha \neq A_1$ is contained in $\Gamma^0 \otimes \Gamma^0$; this implies that the fundamental electronic terms of non-linear molecules are not degenerate (even if not necessarily total-symmetric). The proof is obtained by repeating for all the 32 point Groups⁸ the same analysis that we now exemplify in the case of T_d .

Example

We resume CH_4 (Sections 8.1.2,8.2);

T_d	E	$8C_3$	$3C_2$	$6\sigma_d$	$6S_4$	$g = 24$
A_1	1	1	1	1	1	r^2
A_2	1	1	1	-1	-1	$(3z^2 - r^2, x^2 - y^2)$ (R_x, R_y, R_z) (x, y, z)
E	2	-1	2	0	0	
T_1	3	0	-1	-1	1	
T_2	3	0	-1	1	-1	

⁷One speaks about pseudo-Jahn-Teller effect when the distortion is caused by a vibronic coupling of close energy levels of the same symmetry.

⁸when other Groups are appropriate the situation needs verification.

The degenerate irreps of the T_d Group they are E, T_1 and T_2 , and

$$E \otimes E = A_1 \oplus A_2 \oplus E, T_1 \otimes T_1 = T_2 \otimes T_2 = A_1 \oplus E \oplus T_1 \oplus T_2 \quad (9.33)$$

We saw $\Gamma_{vibr} = A_1 + E + 2T_2$. Therefore at least one *Jahn-Teller active* vibration, able to distort the molecule, exists for any degenerate state. The considerable width of the t_2 level of CH_4 seen in photoemission is due just to the fact that the ionization excites the vibrations of the molecule compelling the nuclei to seek a new equilibrium new position. The distortion must remove the degeneracy completely. The basis of an irrep of a Group G is also a basis of a representation of every subgroup of G , since by eliminating some matrices the remaining ones continue to obey the multiplication Table of the subgroup; but usually the representation is reducible. As an example, from T_d one can go to D_{2d} , e.g. by stretching the tetrahedron along the z axis. This stretching completely resolves the degeneracy of electronic states of symmetry E , but is not enough for T_2 states. Under T_d , the characters are:

T_d	E	$8C_3$	$3C_2$	$6\sigma_d$	$6S_4$	$g = 24$
E	2	-1	2	0	0	$(3z^2 - r^2, x^2 - y^2)$
T_2	3	0	-1	1	-1	(x, y, z)

while the Character Table of the Subgroup is:

D_{2d}	E	C_2	$2C'_2$	$2\sigma_d$	$2S_4$
A_1	1	1	1	1	1
A_2	1	1	-1	-1	1
B_1	1	1	1	-1	-1
B_2	1	1	-1	1	-1
E	2	-2	0	0	0

C_3 is broken; for T_d there is no distinction between C_2 and C'_2 , therefore one of the $3C_2$ one goes under C_2 , and two under C'_2 . We then consider the operations of T_d that survive in the D_{2d} subgroup. The $D(R)$ are the same, even if they are not irreducible any more, and they have the same traces. We place the characters of the surviving operations under the classes of D_{2d} , and analyze the representation. For the degenerate ones one finds

D_{2d}	E	C_2	$2C'_2$	$2\sigma_d$	$2S_4$	<i>analysis</i>
$E(T_d)$	2	2	2	0	0	$A_1 \oplus B_1$
$T_2(T_d)$	1	-1	-1	1	-1	$E \oplus B_2$

therefore the distortion is enough in the first case but not in the second. This analysis cannot determine the type of distortion uniquely.

Linear Molecules

Why is CO_2 straight? For the linear molecules the theorem does not apply. Let A denote the electron angular momentum parallel to the molecular axis.

In molecules with $\Lambda = 0$ degenerate the electronic ground state is unique and there is no problem. In those with $|\Lambda| \geq 1$, the states $\pm\Lambda$ are degenerate. Therefore between the unperturbed states $\Delta\Lambda = 2, 4, 6 \dots$. In order to resolve the degeneracy it would be necessary to fold the molecule; but no fold can occur since the vibronic matrix element vanishes: $\int \Psi_{\Lambda} V \Psi_{-\Lambda} = 0$. In fact, a shift of a nucleus outside of the axis is a vector $(\cos \phi, \sin \phi)$; the matrix elements are subject to the rule of selection rule $\Delta\Lambda = \pm 1$. Therefore the matrix elements vanish and the degeneracy remains.

9.6 Non-Adiabatic Operator

In the BO approximation the evolution is confined to an adiabatic surface⁹ and one could expect to derive Equation (9.26) for the nuclear motion from the ansatz:

$$\Psi_{\text{trial}}(r; R) = \chi(R)\Psi_0(r; R). \quad (9.35)$$

This is not exactly true, as we shall see shortly. Let us look for the best solution of the form (9.35) variationally, with a given $\Psi_0(r; R)$, looking for the $\chi(R)$ that yields the minimum of the energy

$$E = \langle H_{\text{tot}} \rangle = \langle T_N + H_e \rangle. \quad (9.36)$$

Again we adopt a compact notation, writing the nuclear kinetic energy $T_N = \frac{-\hbar^2}{2M} \frac{\partial^2}{\partial R^2}$ and understanding indices and summations. One looks for the unconditional minimum of

$$\begin{aligned} F[\chi] = & \frac{-\hbar^2}{2M} \int dr dR \chi^* \Psi_0^* \frac{\partial^2}{\partial R^2} \chi \Psi_0 + \int dR \chi^*(R) E_0(R) \chi(R) \\ & - W \int dR \chi^*(R) \chi(R) \end{aligned} \quad (9.37)$$

where W is a Lagrange multiplier that ensures normalization. Using

$$\frac{\partial^2}{\partial R^2} |\chi \Psi_0\rangle = |\Psi_0\rangle \frac{\partial^2}{\partial R^2} |\chi\rangle + 2 \frac{\partial |\Psi_0\rangle}{\partial R} \frac{\partial |\chi\rangle}{\partial R} + |\chi\rangle \frac{\partial^2}{\partial R^2} |\Psi_0\rangle$$

⁹If in R_0 one has degenerate wave functions,

$$\Psi_n(r; R_0), \quad n = 1 \dots \nu \quad (9.34)$$

with

$$H_e(r; R_0) \Psi_n(r; R_0) = E(R_0) \Psi_n(r; R_0),$$

the topology of the surfaces is important. For *conical intersections*, when the surfaces cross each other, one speaks of Jahn-Teller effect; when surfaces touch at extremal points one speaks of Renner-Teller effect [5]. However, the JT theorem limits the occurrence of glancing intersections to linear molecules (and to cases when the gradient is accidentally vanishing or particularly small for reasons independent of Group theory).

one finds

$$\begin{aligned}
 F[\chi] = & -\frac{\hbar^2}{2M} \left\{ \int dR \chi^* \frac{\partial^2 \chi}{\partial R^2} + 2 \int dr dR \chi^* \Psi_0^* \frac{\partial \Psi_0}{\partial R} \frac{\partial \chi}{\partial R} \right. \\
 & + \left. \int dR \chi^* \chi \int dr \Psi_0^* \frac{\partial \Psi_0}{\partial R^2} \right\} \\
 & + \int dR \chi^*(R) E_0(R) \chi(R) - W \int dR \chi^*(R) \chi(R).
 \end{aligned} \tag{9.38}$$

We vary the bra (variation of bra and ket produces identical results).

$$\begin{aligned}
 \delta F = & \int dR \delta \chi^*(R) \left\{ -\frac{\hbar^2}{2M} \frac{\partial^2}{\partial R^2} \chi - \frac{\hbar^2}{M} \left(\int dr \Psi_0^* \frac{\partial \Psi_0}{\partial R} \right) \frac{\partial \chi}{\partial R} \right. \\
 & \left. - \frac{\hbar^2}{2M} \left(\int dr \Psi_0^* \frac{\partial^2 \Psi}{\partial R^2} \right) \chi(R) + (E_0(R) - W) \chi(R) \right\} = 0.
 \end{aligned} \tag{9.39}$$

This implies:

$$\begin{aligned}
 -\frac{\hbar^2}{2M} \frac{\partial^2}{\partial R^2} \chi + E_0(R) \chi(R) - \frac{\hbar^2}{M} \left(\int dr \Psi_0^* \frac{\partial \Psi_0}{\partial R} \right) \frac{\partial \chi}{\partial R} \\
 - \frac{\hbar^2}{2M} \left(\int dr \Psi_0^* \frac{\partial^2 \Psi}{\partial R^2} \right) \chi(R) = W \chi(R)
 \end{aligned} \tag{9.40}$$

The minimum condition is

$$-\frac{\hbar^2}{2M} \frac{\partial^2}{\partial R^2} \chi + E_0(R) \chi(R) + \Lambda(R) \chi(R) = W \chi(R) \tag{9.41}$$

where the *non adiabatic operator* appears

$$\Lambda(R) = -\frac{\hbar^2}{M} \left(\int dr \Psi_0^* \frac{\partial \Psi_0}{\partial R} \right) \frac{\partial}{\partial R} - \frac{\hbar^2}{2M} \left(\int dr \Psi_0^* \frac{\partial^2 \Psi_0}{\partial R^2} \right). \tag{9.42}$$

This has been often ignored in the literature; the reasons are that 1) the first contribution, averaged over *real* electronic wave functions vanishes since

$$\int dr \Psi_0(r; R) \frac{\partial}{\partial R} \Psi_0(r; R) = \frac{1}{2} \frac{\partial}{\partial R} \int dr \Psi_0(r; R) \Psi_0(r; R);$$

2) the second contribution is small (of order $\frac{m}{M}$). It will be apparent shortly that such reasons are not generally as safe as they may appear to be.

9.6.1 Dynamical Jahn-Teller Effect

At *strong vibronic coupling*, the energy surfaces have N_{deg} deep and distant minima and the nuclear degrees of freedom can hardly tunnel between them.

Then, the kinetic energy of the nuclei does not play a role, and one can observe a static JT effect with broken symmetry. At *weak coupling*, one speaks about dynamic JT effect and the system oscillates between several minima; the overall symmetry remains unbroken¹⁰. The JT approximation to the solutions of $H_{tot}\Psi^{tot} = W\Psi^{tot}$ (Equation 9.23) uses as a reduced basis set the N_{deg} degenerate adiabatic functions in the symmetric configuration R_0 :

$$\Psi^{tot}(r, R) \sim \sum_n^{N_{deg}} \chi_n(R) \Psi_n(r) \quad (9.43)$$

here $\Psi_n(r)$ are assumed known, and one seeks the nuclear amplitudes $\chi_n(R)$. Substituting into Equation (9.23) and taking the scalar product by $\langle \psi_m |$ leads to

$$\int dr \psi_m^*(r; R_0) [H_{tot} - W] \sum \chi_n(R) \Psi_n(r) = 0, \quad (9.44)$$

that is,

$$\int dr \psi_m^* \left[T_N + \underbrace{T_e(r) + V(r, R)} - W \right] \sum \chi_n(R) \Psi_n(r) = 0,$$

where $T_e(r) + V(r, R) = H_e(r, R)$. By orthogonality,

$$-\frac{\hbar^2}{2M} \frac{\partial^2}{\partial R^2} \chi_m(R) + \sum_n \chi_n(R) \int dr \psi_m^*(r; R_0) H_e(r, R) \Psi_n(r) = W \chi_m(R). \quad (9.45)$$

Defining

$$V_{mn}(R) = \int dr \psi_m^*(r; R_0) H_e(r, R) \Psi_n(r) \quad (9.46)$$

we get the coupled problem

$$-\frac{\hbar^2}{2M} \frac{\partial^2}{\partial R^2} \chi_m(R) + \sum_n V_{mn}(R) \chi_n(R) = W \chi_m(R). \quad (9.47)$$

or in matrix form

¹⁰The distinction between dynamical and static JT effect usually depends only on the time scale of the experiment. For example, $(Cu \cdot 6H_2O)^{++}$ ions look perfectly octahedral when observed at room temperatures in EPR experiments, but below 20 °K or with fast spectroscopies it is seen that this symmetrical configuration is the time average of stretched and compressed ones as the top and bottom H_2O molecules oscillate up and down. On the other hand, X-Ray diffraction at room temperature shows that $(CuBr_6)^{4-}$ ions is a tetragonally distorted, stretched octahedron; the latter is classified as an example of static JT effect. It should be kept in mind, however, that the JT approximation may fail completely, as it does in strongly correlated models with strong electron-phonon coupling [71].

$$H_{JT} = -\frac{\hbar^2}{2M} \frac{\partial^2}{\partial R^2} + \begin{pmatrix} V_{11}(R) & \dots & V_{1\nu}(R) \\ \vdots & \ddots & \vdots \\ V_{\nu 1}(R) & \dots & V_{\nu\nu}(R) \end{pmatrix}. \quad (9.48)$$

9.6.2 How the $E \times \epsilon$ Hamiltonian arises

In the popular $E \times \epsilon$ problem two degenerate potential energy surfaces with electronic wave functions (ψ_x, ψ_y) of E symmetry interact with degenerate vibrations of the same symmetry¹¹; let (q_x, q_y) be the normal coordinates. Neglecting anharmonic terms, (9.29) reads

$$H_e = q_x \hat{V}(x) + q_y \hat{V}(y) + \hat{K} q^2. \quad (9.49)$$

Here, $\hat{V}(x), \hat{V}(y)$ transform according to E and represent the operator potential due to the phonons acting on the electrons; \hat{K} must belong to A_1 and $q^2 = q_x^2 + q_y^2$. Then, (9.48) becomes

$$H_{JT} = -\frac{\hbar^2}{2M} \frac{\partial^2}{\partial q_x^2} - \frac{\hbar^2}{2M} \frac{\partial^2}{\partial q_y^2} + q_x \begin{pmatrix} (V(x))_{xx} & (V(x))_{xy} \\ (V(x))_{yx} & (V(x))_{yy} \end{pmatrix} \\ + q_y \begin{pmatrix} (V(y))_{xx} & (V(y))_{xy} \\ (V(y))_{yx} & (V(y))_{yy} \end{pmatrix} + \langle \hat{K} \rangle q^2. \quad (9.50)$$

Group theory dictates the form of the vibronic interaction; for illustration, we adopt the geometry of Figure 7.1 of Section 7.2.2. (x, y) is a basis for E ; for the present purpose, however, we shall use an alternative basis for E in C_{3v} , with the same D matrices, namely, $(f_x, f_y) = (2xy, x^2 - y^2)$. It is evident that $2xy$ transforms like x and $x^2 - y^2$ like y in the chosen geometry, since $2xy$ is odd and $x^2 - y^2$ even under the σ_1 reflection. For any basis (f_x, f_y) of E , we know from (7.46) that $\langle f_x | y \rangle = \langle f_y | x \rangle = 0$ and that $\langle f_x | x \rangle = \langle f_y | y \rangle$. Therefore, if now (ψ_x, ψ_y) are electronic states and are a basis for E , $\psi_x^2 + \psi_y^2$ belongs to A_1 and for the $V(x)$ elements we find:

$$\begin{cases} \int dr (\psi_x^2 - \psi_y^2) V(y) = 2\lambda = 2 \int dr \psi_x \psi_y V(x), \\ \int dr (\psi_x^2 + \psi_y^2) V(y) = 0 = \int dr (\psi_x^2 + \psi_y^2) V(x), \\ \int dr (\psi_x^2 - \psi_y^2) V(x) = 0 = 2 \int dr \psi_x \psi_y V(y). \end{cases} \quad (9.51)$$

Thus, $V(x)$ has equal off-diagonal matrix elements on (ψ_x, ψ_y) and nothing on the diagonal and $V(y)$ has opposite diagonal elements and 0 off-diagonal; this is clear already when one considers the σ_a parity. Thus, the form of the JT hamiltonian in the $E \times \epsilon$ problem is:

$$H_{JT} = -\frac{\hbar^2}{2M} \frac{\partial^2}{\partial q_x^2} - \frac{\hbar^2}{2M} \frac{\partial^2}{\partial q_y^2} + \lambda [q_x \sigma_x + q_y \sigma_z] + \langle \hat{K} \rangle (q_x^2 + q_y^2). \quad (9.52)$$

¹¹The Na_3 molecule offers a simple example of this situation.

The second-quantized version is:

$$H_{JT} = (a_x^\dagger a_x + 1/2)\hbar\omega + (a_y^\dagger a_y + 1/2)\hbar\omega + \lambda' [(a_x^\dagger + a_x)\sigma_x + (a_y^\dagger + a_y)\sigma_z]; \tag{9.53}$$

(two levels and two-bosons problem) and is among those exactly solved by the method of Excitation Amplitudes (See ([77]) and Section 14.77).

9.6.3 Nuclear Wave Functions Cannot be Taken Real

The BO wave functions are readily found in the $M \rightarrow \infty$ limit, and the result is very interesting. Letting $q_x = q \cos(\theta), q_y = q \sin(\theta)$,

$$H_{JT} \rightarrow +\lambda [q_x \sigma_x + q_y \sigma_z] + \langle \hat{K} \rangle q^2 = \lambda q M + \langle \hat{K} \rangle q^2. \tag{9.54}$$

with

$$M = \begin{pmatrix} \sin(\theta) & \cos(\theta) \\ \cos(\theta) & -\sin(\theta) \end{pmatrix}.$$

$\langle \hat{K} \rangle q^2$ is an additive constant, and H_{JT} is the Hamiltonian ¹² for a spin in a magnetic field $\vec{B} = (q_x, 0, q_y)$. The above matrix M has eigenvalues ± 1 , and the potential energy surfaces are obtained by rotating two intersecting parabolas around the energy axis. The eigenstates corresponding to the eigenvalues ± 1 of M are

$$\chi_-(\theta) = \begin{pmatrix} \cos(\theta/2 + \pi/4) \\ -\sin(\theta/2 + \pi/4) \end{pmatrix}, \quad \chi_+(\theta) = \begin{pmatrix} \sin(\theta/2 + \pi/4) \\ \cos(\theta/2 + \pi/4) \end{pmatrix}. \tag{9.55}$$

These wave functions change sign under a 2π rotation. This is normal in spin-dependent problems (see Section 9.4) but is striking and unacceptable in the present problem; of course, the nuclear wave function must be unique. Indeed, one can have the unique wave function, by inserting a phase factor,

$$\chi_-(\theta) = e^{i\theta/2} \begin{pmatrix} \cos(\theta/2 + \pi/4) \\ -\sin(\theta/2 + \pi/4) \end{pmatrix}, \quad \chi_+(\theta) = e^{-i\theta/2} \begin{pmatrix} \sin(\theta/2 + \pi/4) \\ \cos(\theta/2 + \pi/4) \end{pmatrix}. \tag{9.56}$$

but then the solution is complex. This means that the Berry phase (See Sect. ??) is coming into play. For further information on this and other JT systems one may consult reference [5].

9.7 Wigner-Eckart Theorem with Applications

Let $|\alpha i\rangle$ and $|\beta j\rangle$ denote the components of bases of irreps Γ^α and Γ^β (that could also coincide) and $T_p^{(\gamma)}$ the p component of an irreducible tensor

¹²The Hamiltonian given in Ref. [5] is obtained by a harmless rotation $q_x \rightarrow q_y, q_y \rightarrow -q_x$ in q space.

$$RT_p^{(\gamma)}R^{-1} = \sum_q T_q^{(\gamma)}D_{qp}^{(\gamma)}(R). \tag{9.57}$$

As the components i, p and k vary, one finds a number of matrix elements $\langle \alpha i | T_p^{(\gamma)} | \beta k \rangle$ that are all connected by the Wigner-Eckart theorem

Theorem 9.

$$\langle \alpha i | T_q^{(\gamma)} | \beta k \rangle = \langle \alpha || T^{(\gamma)} || \beta \rangle \langle \alpha i | \gamma p \beta k \rangle, \tag{9.58}$$

where the reduced matrix element $\langle \alpha || T^{(\gamma)} || \beta \rangle$ does not depend on the components; $\langle \alpha i | \gamma p \beta k \rangle$ is the Clebsh-Gordan coefficient.

Since the Clebsh-Gordan coefficients are mere geometry, the dynamics enters through the reduced matrix element. A formal proof is given in Appendix C, but an intuitive argument is also useful. A very crucial point is that the tensor and the function spaces must be irreducible. If you know one basis function of an irrep you can build all of them by the Group operations and orthogonalization; and the same is true of the tensor components; then it is at least very plausible that all the matrix elements can in principle be obtained by symmetry from the knowledge of any non-vanishing one of them. Based on this, the theorem is then most simply understood. *Suppose that by direct computation we obtain a particular element $\langle \alpha i_0 | T_{p_0}^{(\gamma)} | \beta k_0 \rangle = Q \neq 0$. Next, we decide to look at the system from a new transformed reference obtained by some $R \in G$; then, $|\alpha i_0\rangle$, $|\beta k_0\rangle$ and $T_{p_0}^{(\gamma)}$ transform to linear combinations of all the components, still remaining in their irreps; however the matrix element is still Q . Varying R , we can write a system of linear equations linking the components, all with the same right-hand-side. Are all those equations must be compatible, and since there are enough relations to determine $\langle \alpha i | T_q^{(\gamma)} | \beta k \rangle$, one can solve and each matrix element must be proportional to the only r.h.s. Q . Any two tensors T and T' of the same irrep generate the same system, except that the r.h.s. are Q and Q' ; so they must yield proportional results. There is a particularly simple tensor defined by $T_p^\gamma | \beta k \rangle = |\gamma p \beta k \rangle$ which yields the theorem with $\langle \alpha || T^{(\gamma)} || \beta \rangle \equiv 1$. For all the other tensors the theorem holds with some reduced matrix element.*

Simple Applications

The theorem reduces the calculation of a tensor to one of one its components. It implies less that in a symmetry adapted basis all the irreducible tensor operators have the same elements matrix elements, up to a multiplicative constant. We can choose the most comfortable operator (as long as it does not have a null reduced matrix element). As an example, in $O(3)$, $j = 1$ labels the irrep of vectors and $T_q^{(1)}$, $q = 0, \pm 1$ is a vector operator in polar form. Therefore, its matrix elements are proportional them to those of \mathbf{j} , that they are easy to calculate in this basis:

$$\langle jm|\mathbf{T}|j'm'\rangle = C\langle jm|\mathbf{J}|j'm'\rangle. \quad (9.59)$$

To determine the constant C , it is enough to compute explicitly $\langle jm|\mathbf{T}|jm\rangle$. Often it is easier to calculate the matrix elements of the scalar $\mathbf{T} \cdot \mathbf{J}$. Indeed,

$$\langle jm|\mathbf{T} \cdot \mathbf{J}|jm\rangle = \sum_{m'} \langle jm|\mathbf{T}|jm'\rangle \langle jm'|\mathbf{J}|jm\rangle \quad (9.60)$$

but this is simply

$$C \sum_{m'} \langle jm|\mathbf{J}|jm'\rangle \langle jm'|\mathbf{J}|jm\rangle = CJ(J+1). \quad (9.61)$$

For example the nuclear quadrupole moment is the tensor

$$Q_{ik} = \sum_p 3x_{pi}x_{pk} - \delta_{ik}r_p^2, \quad (9.62)$$

where x_{pi} is a Cartesian component of the radius vector \mathbf{r}_p of proton p in the nucleus. It is a traceless symmetric tensor and we can replace it with the tensor with components

$$Q_{ik} = \frac{3Q}{2I(2I-1)} I_i I_k + I_k I_i - \frac{2}{3} \delta_{ik} I^2, \quad (9.63)$$

built with a constant Q (named the quadrupole moment) and with the components of the nuclear spin \mathbf{I} . In a similar way one can build an atomic quadrupole moment tensor from \mathbf{J} .

The spin-orbit interaction is $H_{SO} = \sum_i \zeta(\mathbf{l}(i)) \mathbf{s}(i)$ in many-electron atoms, where $\mathbf{l}(i)$ is the orbital angular momentum of electron i , $\mathbf{s}(i)$ is its spin. Since $\mathbf{l}(i)$ is a vector like the total orbital angular momentum \mathbf{L} and $\mathbf{s}(i)$ is a vector in spin space like the total spin angular momentum \mathbf{S} , the Wigner-Eckart theorem allows to write

$$\langle LML_S M_S | H_{SO} | LML_S M_S \rangle = A \langle LML_S M_S | \mathbf{L} \cdot \mathbf{S} | LML_S M_S \rangle, \quad (9.64)$$

where A is a constant.

9.8 The Symmetric Group and Many-Electron States

For an N -electron system, let $\phi_i^{(\alpha)}(x_1 \dots x_N)$ denote an amplitude depending on the space coordinates only and transforming according the component i of irrep (α) : if \mathcal{P} denote a permutation,

$$\mathcal{P} \phi_i^{(\alpha)} = \sum_j^m \phi_j^{(\alpha)} D_{j,i}^{(\alpha)}(\mathcal{P}). \quad (9.65)$$

Let $\chi_q^{(\beta)}(\sigma_1 \dots \sigma_N)$ denote an amplitude depending on the spin coordinates only and transforming according the component q of irrep (β) , such that

$$\mathcal{P}\chi_q^{(\beta)} = \sum_n^m \chi_n^{(\beta)} D_{n,q}^{(\beta)}(\mathcal{P}). \tag{9.66}$$

When permuting the electrons, i.e. doing the same permutation on spins and coordinates, the wave function Ψ must go into itself up to a sign, therefore components must enter symmetrically, like in

$$\Psi = \sum_k^m \phi_k^{(\alpha)} \chi_k^{(\beta)}. \tag{9.67}$$

Is Ψ a fully antisymmetrized wave function? One preliminary condition is that both irreps must have the same dimension m . Next, we impose

$$\mathcal{P}\Psi = (-)^{\mathcal{P}}\Psi = \sum_k^m [\mathcal{P}\phi_k^{(\alpha)}][\mathcal{P}\chi_k^{(\beta)}]; \tag{9.68}$$

using (9.65,9.66) we find that this requires

$$\sum_k^m D_{j,k}^{(\alpha)}(\mathcal{P})D_{n,k}^{(\beta)}(\mathcal{P}) = (-)^{\mathcal{P}}\delta_{nj}. \tag{9.69}$$

Since the identity permutation is represented by the identity matrix, it is readily seen that this holds if

$$D_{j,k}^{(\alpha)}(\mathcal{P}) = (-)^{\mathcal{P}}D_{k,j}^{(\beta)}(\mathcal{P}^{-1}). \tag{9.70}$$

Two irreps that satisfy the condition (9.70) are *conjugate* or *associate*. We saw in Sect. 8.5 that the spin eigenfunction have a Young tableau consisting of up to two lines. The following $[N - M, M]$ two-line tableau (left) with $N - M$ integers denoted $a_1 \dots a_{N-M}$ on the top line and M integers denoted $b_1 \dots b_M$ on the bottom line is suitable for a spin eigenfunction symmetry of spin $S = \frac{1}{2}(N - 2M)$ (Equation 9.71, left); then, the conjugate tableau is $[2^M, 1^{N-M}]$ as shown below (right).

a_1	a_2	a_{N-M}
b_1	b_2	b_M	

a_1	b_1
a_2	b_2
.	.
.	.
.	.
.	.
.	.
.	b_M
.	
.	
a_{N-M}	

(9.71)

9.9 Seniority Numbers in Atomic Physics

Let $\psi_m(\mathbf{x})$ denote the d orbitals of an atom; under the rotation of an angle α , that we denote $R_\alpha = e^{-\frac{i\alpha \cdot L}{\hbar}} \in O^+(3)$, they transform according to

$$R_\alpha \psi_m(\mathbf{x}) = \sum_n \psi_n(\mathbf{x}) D_{mn}^l(R_\alpha), \tag{9.72}$$

where $l = 2$ and $D_{mn}^l(R_\alpha)$ is the Wigner matrix; therefore $\{\psi_m(\mathbf{x})\}$ is a basis of the irrep $l = 2$ of $O^+(3)$. However, $D_{nm}^l(R_\alpha)$ also play a second role: the transformation

$$\psi_m(\mathbf{x}) \rightarrow R\psi_m(\mathbf{x}) = \sum_n \psi_n(\mathbf{x}) D_{mn}^l(R_\alpha), \tag{9.73}$$

qualifies $\psi_m(\mathbf{x})$ at fixed \mathbf{x} as polar components of a vector under $SU(2l+1) = SU(5)$, and so $D_{nm}^l(R) \in SU(2l+1)$. For the same reason

$$\begin{aligned} T_{mn}(\mathbf{x}_1, \mathbf{x}_1) &= \psi_m(\mathbf{x}_2)\psi_n(\mathbf{x}_2) \\ T_{mnp}(\mathbf{x}_1, \mathbf{x}_2, \mathbf{x}_3) &= \psi_m(\mathbf{x}_1)\psi_n(\mathbf{x}_2)\psi_p(\mathbf{x}_3) \\ &\dots \end{aligned} \tag{9.74}$$

for fixed points x_i , are components of tensors of rank $2, 3, \dots$, respectively. The permutation of two indices of a tensor commutes with the operations of the Group; so the tensors that belong to irrep of S_N of permutation of the indices are the bases of the irreps of $SU(5)$. With 2 indices, the possibilities are

$$\begin{aligned} T_{\boxed{m}\boxed{n}} &= T_{mn} + T_{nm} \\ T_{\boxed{m}\overline{n}} &= T_{mn} - T_{nm} \end{aligned} \tag{9.75}$$

$T_{\boxed{m}\overline{n}}$ is associated with triplet states, while $T_{\boxed{m}\boxed{n}}$ to singlets. Let us see how

we can classify the singlet states of d^2 configuration using the polar T_{mn} of (9.74) projected into $\boxed{\square\square}$. In obvious notation ($m_1 \uparrow, m_2 \downarrow$) for the two-electron determinants, one finds by the shift operators

$$\begin{aligned} {}^1G_{M=4} &= (2, 2) \\ {}^1G_{M=3} &= \frac{(1,2)+(2,1)}{\sqrt{2}} \\ {}^1G_{M=2} &= \frac{\sqrt{6}[(0,2)+(2,0)]+4(1,1)}{\sqrt{28}} \end{aligned} \tag{9.76}$$

and by orthogonality

$${}^1D_{M=2} = \frac{\sqrt{2}[(0, 2) + (2, 0)] - \sqrt{3}(1, 1)}{\sqrt{5}}; \tag{9.77}$$

then

$$\begin{aligned}
 {}^1G_{M=1} &= \frac{[(-1,2)+(2,-1)]+\sqrt{6}[(0,1)+(1,0)]}{\sqrt{14}} \\
 {}^1G_{M=0} &= \frac{[(-2,2)+(2,-2)]+4\frac{\sqrt{14}}{7}[(-1,1)+(1,-1)]+6(0,0)}{\sqrt{14}} \\
 {}^1D_{M=0} &= \frac{2[(-2,2)+(2,-2)]+\frac{\sqrt{70}}{7}[(-1,1)+(1,-1)]-2(0,0)}{\sqrt{14}}
 \end{aligned}
 \tag{9.78}$$

and finally

$${}^1S = \frac{[(-2, 2) + (2, -2)] - [(-1, 1) + (1, -1)] + (0, 0)}{\sqrt{5}}.
 \tag{9.79}$$

The form of 1S is remarkably simple: it is just a scalar product $\psi \cdot \psi$ in the polar form (9.8). Let us see how this calculation extends to the case of more electrons, and higher rank tensors. With 3 indices, the irrep $\begin{bmatrix} \dots & \dots & \dots \end{bmatrix}$ does not take part in the construction of the states to 3 electrons since the function of

spin would have to be $\begin{bmatrix} \dots \\ \dots \\ \dots \end{bmatrix}$ which cannot be antisymmetrized totally on α and

β . Thus one is left with $\begin{bmatrix} \dots \\ \dots \\ \dots \end{bmatrix}$ (for quartets) and $\begin{bmatrix} \dots & \dots \\ \dots & \dots \end{bmatrix}$ (for doublets). Actually

there are two doublets:

$$T_{\begin{bmatrix} m & n \\ p \end{bmatrix}} = A_{13}S_{12}T_{mnp} = T_{mnp} + T_{nmp} - T_{pnm} - T_{npm}
 \tag{9.80}$$

$$T_{\begin{bmatrix} m & p \\ n \end{bmatrix}} = A_{12}S_{13}T_{mnp} = T_{mnp} + T_{pnm} - T_{nmp} - T_{pmn}$$

$SU(5)$ has the subgroup $O^+(5)$ of proper rotations in 5 dimensions; on a cartesian basis its representatives are orthogonal matrices such that $a^T = a^{-1}$ that is $a_{mx}a_{my} = \delta_{xy}$. Transforming any cartesian tensor according to

$$T'_{mn} = a_{mx}a_{ny}T_{xy}$$

and then taking the trace, that is, setting $m=n$ and summing over n , one gets

$$T'_{nn} = a_{nx}a_{ny}T_{xy} = \delta_{xy}T_{xy} = T_{xx};$$

in other terms, the trace T_{mm} is invariant. For a tensor whose cartesian components $T_{mn} = v_m w_n$ are the products of cartesian vector components the trace becomes the scalar product $T_{mm} = v_m w_m$. Thus, in $O^+(5)$ the traces acquire particular meaning. The invariance remains obviously true with any number of components; for instance taking the trace of

$$T'_{mnp} = a_{mx}a_{ny}a_{pz}T_{xyz}$$

one finds

$$T'_{mnp} = a_{mx}a_{my}a_{pz}T_{xyz} = \delta_{xy}a_{pz}T_{xyz} = a_{pz}T_{xxz},$$

thus T_{xxz} is a vector. On the other hand a cartesian tensor of the form $T_{xyz} = \delta_{xy}v_z$ is transformed as follows: $T'_{xyz} = a_{mx}a_{ny}a_{pz}\delta_{xy}v_z = a_{mx}a_{nx}a_{pz}v_z = \delta_{mn}a_{pz}v_z$, and retains its form.

The ψ and the T of Equation (9.74) are tensor components also for the subgroup, except that since they are polar tensors the rule must be slightly modified. In order to agree with the scalar product (9.8), the polar form of the trace reads

$$TrT = \sum_m (-)^m T_{m,-m}. \tag{9.81}$$

For a cartesian tensor T_{mnp} of rank 3, one defines the traces:

$$\begin{aligned} Tr^{(1,2)}T &= T_{mmp} \\ Tr^{(1,3)}T &= T_{mnm} \\ Tr^{(2,3)}T &= T_{mpp}. \end{aligned} \tag{9.82}$$

Since the Tr operation commutes with the operations of the Group $O^+(5)$, many irreps of SU(5) are no longer irreducible. Vectors are sent to vectors and are bases of an irreducible representation of $O^+(5)$. Traceless tensors are sent to traceless tensors and are bases of irreducible representations of $O^+(5)$.

$T_{\begin{smallmatrix} m \\ n \end{smallmatrix}}$ is traceless, while $T_{\begin{smallmatrix} m & n \\ \end{smallmatrix}}$ must be reducible. In fact, all the d^2 states

above belong to $\begin{smallmatrix} \square & \square \\ \end{smallmatrix}$ of SU(5), but in $O^+(5)$ the invariant 1S is classified in the (0,0) irrep (the notation means: no boxes in either the first and the second line). The state with no electrons is already invariant, so this singlet is assigned the seniority number $v = 0$. From $\begin{smallmatrix} \square & \square \\ \end{smallmatrix}$ of SU(5), in $O^+(5)$ one can extract a traceless tensor which is classified in the irrep (2,0). All irreps of $O^+(5)$ are labelled by (μ_1, μ_2) , $\mu_1 \geq \mu_2$; the parentheses denote the space of traceless tensors. Since (2,0) cannot be made with fewer than 2 electrons 1D and 1F receive $v = 2$.

With $\begin{smallmatrix} 1 & 2 \\ 3 \end{smallmatrix}$ the 1-3 trace vanishes and the other two are equal in absolute value; clearly, $v_p = Tr^{(1,2)}T_{\begin{smallmatrix} m & n \\ p \end{smallmatrix}}$ is a 5-component vector, so it deserves

to be classified in (1,0); it is obviously a doublet, so it corresponds to 2_1D . The other doublet states $^2_3P, ^2_3D, ^2_3F, ^2_3G, ^2_3H$ will correspond to the traceless tensor $T_{(2,0)} \equiv T_{\begin{smallmatrix} m & n \\ p \end{smallmatrix}} - \frac{\delta_{mn}v_p}{5}$. This does not occur with less than 3 electrons

nor with orbital angular momentum < 2 . These states deserve the seniority number $v = 3$ along with 4_3P and 4_3F that are classified in (1,1) and are also unprecedented.

Problems

9.1. In a molecule of C_{3v} symmetry, two electrons are in orbitals of the irrep E. Find the space part of the singlet wave function of A_1 symmetry (if any exists) and the relevant CG coefficients.

9.2. In a molecule of C_{3v} symmetry, two electrons are in orbitals of the irrep E. Find the space part of the singlet wave function of A_2 symmetry and the relevant Clebsh-Gordan coefficients.

9.3. In a molecule of C_{3v} symmetry, two electrons are in orbitals of the irrep E. Find the space part of the singlet wave function of E symmetry and the relevant Clebsh-Gordan coefficients.

9.4. Build the character table for C'_{4v} .

9.5. Consider the Cu^{++} ion, with one configuration $3d^9$. How are the $J = 3/2, 5/2$ levels split by a square planar D'_4 environment?

More on Green Function Techniques

10 Equations of Motion and Further Developments

10.1 Equations of motion for the interacting propagator

We used EOM several times (see Sections 4.3,4.4,5.1.2); now we extend the approach used in Equation (4.39) for the free propagator to interacting problems. Using the many-body Hamiltonian (1.63) one readily obtains

$$[\psi_\alpha(\mathbf{x}), H]_- = h_0(\mathbf{x})\psi_\alpha(\mathbf{x}) + \sum_{\beta'\gamma} \int d\mathbf{y} \psi_\gamma^\dagger(\mathbf{y}) v(\mathbf{x}, \mathbf{y})_{\alpha\beta', \gamma\gamma'} \psi_{\gamma'}(\mathbf{y}) \psi_{\beta'}(\mathbf{x}), \quad (10.1)$$

with all the operators in the Heisenberg representation (h_0 is a first-quantized one-body operator), with the notation $x = (\mathbf{x}, t_x)$. We multiply on the left by $\psi_\alpha^\dagger(z)$ and perform an interacting ground state average:

$$\left[i \frac{\partial}{\partial t} - h_0(\mathbf{x}) \right] \langle \psi_\alpha^\dagger(z) \psi_\alpha(x) \rangle = \sum_{\beta'\gamma} \int d\mathbf{y} w(\mathbf{x}, \mathbf{y})_{\alpha\beta', \gamma\gamma'} \langle \psi_\alpha^\dagger(z) \psi_\gamma^\dagger(\mathbf{y}) \psi_{\gamma'}(\mathbf{y}) \psi_{\beta'}(x) \rangle, \quad t_z > t_x. \quad (10.2)$$

The order of operators in the l.h.s. is appropriate for $g^{(T)}$ (Equation (4.20)) if z is later, that is, $t_z > t_x$, and we assume this for the moment. For the r.h.s. we must define the time-ordered two-particle Green's function¹ and understanding the spin indices, we write, still in terms of Heisenberg operators

$$G_2(x_1, x_2, x_3, x_4) = -\langle T[\psi(x_1)\psi(x_2)\psi^\dagger(x_3)\psi^\dagger(x_4)] \rangle. \quad (10.3)$$

Comparison with (10.2) is easier using the fact that Heisenberg operators anticommute under T ordering, hence it holds that $G_2(x_1, x_2, x_3, x_4) = -\langle T[\psi^\dagger(x_4)\psi^\dagger(x_3)\psi(x_2)\psi(x_1)] \rangle$ and

$$\langle \psi_\alpha^\dagger(z) \psi_\gamma^\dagger(\mathbf{y}) \psi_{\gamma'}(\mathbf{y}) \psi_{\beta'}(x) \rangle = (-)G_2(x, \mathbf{y}, \mathbf{y}^+, z) \quad (10.4)$$

where the notation \mathbf{y}^+ means that although $t_y = t_x$ that particular \mathbf{y} is just later.

¹Some authors use different orderings of the arguments.

$$\left[i \frac{\partial}{\partial t} - H_0(\mathbf{x}) \right] ig^{(T)}(\mathbf{x}, z) = \sum_{\beta'\gamma} \int dy w(\mathbf{x}, \mathbf{y})_{\alpha\beta', \gamma\gamma'} (-)G_2(\mathbf{x}, y, y^+, z). \tag{10.5}$$

Extending the calculation to $t_z \leq t_x$ one finds that the Green function obeys

$$\left[i \frac{\partial}{\partial t} - H_0 \right] g^{(T)}(\mathbf{x}t, \mathbf{x}'t') = \delta(\mathbf{x} - \mathbf{x}')\delta(t - t') - i \int d\mathbf{x}_1 v(\mathbf{x} - \mathbf{x}_1) G_2(\mathbf{x}t, \mathbf{x}_1t, \mathbf{x}_1t^+, \mathbf{x}'t') \tag{10.6}$$

which is often written in the literature using lighter notations like

$$\left\{ i \frac{d}{dt_1} - H_0(1) \right\} G(1; 1') = \delta(11') - i \int d2 v(1, 2) G_2(1; 2|2^+; 1') \tag{10.7}$$

One has also the adjoint equation

$$\left\{ -i \frac{d}{dt_2} + \frac{\nabla_2^2}{2m} - U(2) \right\} G(1; 2) = \delta(1 - 2) - i \int G_2(1; \bar{1}^- | \bar{1}^+; 2) V(\bar{1} - 2). \tag{10.8}$$

10.1.1 Equations of Motion and Ground-State Energy

As a byproduct, using (10.4, 10.5) one obtains an expression yielding the ground state energy in terms of the one-body Green's function. Setting $\mathbf{z} = \mathbf{x}$ with $t_z = t_x^+$ and integrating over \mathbf{x} one finds:

$$\begin{aligned} & \int d\mathbf{x} \lim_{t' \rightarrow t^+} \lim_{r' \rightarrow r} \left[i \frac{\partial}{\partial t} - H_0(\mathbf{x}) \right] g^{(T)}(\mathbf{x}, t, \mathbf{x}', t') \\ &= i \int dx dy v(\mathbf{x}, \mathbf{y}) \langle \psi^\dagger(\mathbf{x}) \psi^\dagger(\mathbf{y}) \psi(\mathbf{y}) \psi(\mathbf{x}) \rangle = 2i \langle v \rangle. \end{aligned} \tag{10.9}$$

The average of H_0 can be obtained from Equation (4.26). So, we get the exact ground state energy (lower sign for fermions):

$$E = \langle H_0 + V \rangle = \pm \frac{i}{2} \int d\mathbf{x} \lim_{t' \rightarrow t^+} \lim_{r' \rightarrow r} \left[i \frac{\partial}{\partial t} + h_0(\mathbf{x}) \right] g^{(T)}(\mathbf{x}, t, \mathbf{x}', t') \tag{10.10}$$

10.2 Time-Dependent Problems

The EOM are rewarding when the Hamiltonian depends in time. Let

$$H = H_0 + H_1(t) = \sum_k \varepsilon_k n_k + \sum_{k,k'} V_{k,k'}(t) a_k^\dagger a_k. \quad (10.11)$$

For $ig_{k,k'}^r(t, t') = \theta(t - t') \langle [a_k(t), a_{k'}^\dagger(t')]_+ \rangle$ one finds

$$i \frac{\partial}{\partial t} g_{k,k'}^r(t, t') = \delta(t - t') \delta_{k,k'} + (-i) \theta(t - t') \langle [\frac{\partial}{\partial t} i a_k(t), a_{k'}^\dagger(t')]_+ \rangle. \quad (10.12)$$

Since

$$i \dot{a}_k = [a_k, H]_- = \varepsilon_k a_k + \sum_{k'} V_{k,k'}(t) a_{k'} \quad (10.13)$$

one finds the EOM

$$i \frac{\partial g_{k,k'}^r}{\partial t} = \delta(t - t') \delta_{k,k'} + \varepsilon_k g_{k,k'}^r(t, t') + \sum_p V_{k,p}(t) g_{p,k'}^r(t, t'). \quad (10.14)$$

This must be solved with the initial condition

$$ig_{k,k'}^r(t, t - 0) = \delta_{k,k'}. \quad (10.15)$$

No information about the filling enters the problem, and $g_{k,k'}^r$ is actually a one-body quantity which does not depend on the filling. It is no harder to calculate than a one-body wave function, even in time-dependent problems. The same is true for advanced one, $-ig_{k,k'}^a(t, t') = \theta(t' - t) \langle [a_k(t), a_{k'}^\dagger(t')]_+ \rangle$. For later use, we are interested in the time-ordered Green's function, defined as usual by

$$ig_{k,k'}^{(T)}(t, t') = \langle T a_k(t) a_{k'}^\dagger(t') \rangle. \quad (10.16)$$

Now, the initial conditions

$$g_{k,k'}^{(T)}(0, 0_-) = -i \delta_{kk'} (1 - f_k), \quad g_{k,k'}^{(T)}(0, 0_+) = i \delta_{kk'} f_k \quad (10.17)$$

know where is the Fermi level; note the characteristic discontinuity

$$i [g_{k,k'}^{(T)}(t, t + 0) - g_{k,k'}^{(T)}(t, t - 0)] = -\langle a_k^\dagger a_k + a_k a_k^\dagger \rangle = -\delta_{k,k'}. \quad (10.18)$$

Let us calculate the t derivative of Eq.(4.19), taking into account that the θ functions contribute

$$\delta(t - t') \langle a_k a_{k'}^\dagger + a_{k'}^\dagger a_k \rangle = \delta(t - t') \delta_{k,k'}.$$

Using (10.13), one finds

$$i \frac{\partial g_{k,k'}^{(T)}}{\partial t} = \delta(t - t') \delta_{k,k'} + \varepsilon_k g_{k,k'}^{(T)}(t, t') + \sum_p V_{k,p}(t) g_{p,k'}^{(T)}(t, t'). \quad (10.19)$$

This EOM is the same as (10.14), the difference is in the initial conditions. I stress that $g^{(T)}$ depends on the Fermi level and can describe genuine many-body effects, so it is important to be able to express it in terms of the much simpler $g^{(r)}$. This is achieved as follows:

$$ig_{k,k'}^{(T)}(t, t') = \sum_q g_{k,q}^r(t, \tau) g_{q,k'}^a(\tau, t') \xi_q(t, t'), \quad (10.20)$$

where τ is any time such that $\tau < t, \tau < t'$ and

$$\xi_q(t, t') = (1 - f_q)\theta(t - t') - f_q\theta(t' - t) = \theta(t - t') - f_q. \quad (10.21)$$

This solution was first obtained by Ref. ([48]) by the Keldysh formalism [84]; I found the simple derivation below and used the result to re-formulate the theory of transport[63] (See Chapter 13.6.2). Since retarded and advanced functions do not depend on filling, we may take the system empty, denoting the vacuum by $|0\rangle$, and write

$$g_{k,k'}^r(t, t') = -i\theta(t - t')\langle 0|a_k(t)a_{k'}^\dagger(t')|0\rangle = -i\theta(t - t')\delta_{kk'}e^{-i\epsilon_k(t-t')},$$

$$g_{k,k'}^a(t, t') = i\theta(t' - t)\langle 0|a_k(t)a_{k'}^\dagger(t')|0\rangle = i\theta(t' - t)\delta_{kk'}e^{-i\epsilon_k(t-t')}.$$

Hence,

$$\sum_q g_{k,q}^r(t, \tau) g_{q,k'}^a(\tau, t) = \delta_{k,k'}, \quad (10.22)$$

$$\sum_q f_q g_{k,q}^r(t, \tau) g_{q,k'}^a(\tau, t) = \delta_{k,k'} f_k. \quad (10.23)$$

Thus, the initial conditions are obeyed; the EOM are also satisfied because they are obeyed by $g_{k,q}^r(t, \tau)$: the $\delta(t - \tau)$ term does not arise because $\tau < t$, but the required δ comes in from the ξ derivative. Thus, (10.20) is readily seen to satisfy EOM and initial conditions and is the exact solution.

10.2.1 Auger Induced Ionic Desorption: Knotek-Feibelman Mechanism

Desorption (Section 6.2) is a process of emission of atoms, molecules or ionic species that previously belonged to a surface or were adsorbed (i.e. chemically bound to it). The amount of ions emitted depends on the electronic properties of the species in a striking way. For example, if a Ag surface is bombarded with Ar^+ in the KeV range, some Ag^+ ions can be collected by a mass spectrometer, but the ion yield is often much lower than the K^+ signal arising from traces of K on the surface. This is because Ag^+ has a much lower probability than K^+ of escaping without being neutralized.

When ionic surfaces are irradiated with X-rays one observes the desorption of O^+ or other positive ions that originally were anions[113]. When O^{--}

initially bound by the Madelung potential becomes O^+ by Auger processes, it starts being repelled from the surface; however, the copious ion yield remained quite a puzzle for some time. The reason is that the desorption process occurs on the time scale $\geq 10^{-13}s$ of vibrations; electrons move on the time scale of the inverse band width W and have a lot of time for bond healing.

Knotek and Feibelman pointed out[113] that O^+ remains O^+ due to the same mechanism that localizes the two-hole resonances[76] (Section 6.2). Sometimes it is the easy production of neutrals that needs explanation. For example, F desorbs from fluorides as F and F^- ; in the solid it is basically F^- , but if some process produces neutral F, the Madelung force holding the ion in the solid disappears and desorption starts; however desorption is a slow process and one would expect the ion to quickly resume the electron. The writer proposed[13] to compute the ion yield by a time-dependent Anderson model

$$H(t) = \epsilon(t)(n_{0+} + n_{0-}) + U(t)n_{0+}n_{0-} + \sum_{k,\sigma} \epsilon_k n_{k,\sigma} + \sum_{k,\sigma} [V_k(t)a_{0,\sigma}^\dagger a_{k,\sigma} + h.c.]; \quad (10.24)$$

at time $t=0$ two holes are created in the *adatom* orbital 0 and the consequent desorption causes the time dependence. The band was assumed initially filled and the amplitude for the two holes to be still on-site at time t is

$$N(t) = \langle a_{0-}(t)a_{0+}(t)a_{0+}^\dagger(0)a_{0-}^\dagger(0) \rangle \Theta(t), \quad (10.25)$$

averaged over the hole vacuum. I solved the two-body problem by the EOM method. Consider the correlation functions (averaged over the vacuum)

$$\gamma(t, \tau) = -i \langle a_{0+}(t)a_{0+}^\dagger(\tau) \rangle, \quad (10.26)$$

$$\gamma_k(t, \tau) = -i \langle a_{k+}(t)a_{0+}^\dagger(\tau) \rangle, \quad (10.27)$$

$$\Gamma(t, \tau) = -i \langle a_{0-}(t)a_{0+}(\tau)a_{0+}^\dagger(0)a_{0-}^\dagger(0) \rangle, \quad (10.28)$$

$$\Gamma_k(t, \tau) = -i \langle a_{k-}(t)a_{k+}(\tau)a_{k+}^\dagger(0)a_{0-}^\dagger(0) \rangle, \quad (10.29)$$

where the left hand sides are spin-independent; we want to compute

$$N(t) = i\Gamma(t, t)\theta(t). \quad (10.30)$$

From the equations of motion

$$\begin{aligned} i\dot{a}_{0\sigma} &= \epsilon(t)a_{0\sigma} + \sum_k V_k(t)a_{k\sigma} + U(t)a_{0\sigma}n_{0-\sigma}, \\ i\dot{a}_{k\sigma} &= \epsilon_k a_{k\sigma} + V_k(t)a_{0\sigma}(t), \end{aligned} \quad (10.31)$$

one obtains

$$\begin{aligned} i\frac{\partial}{\partial t}\gamma(t, \tau) &= \epsilon(t)\gamma(t, \tau) + \sum_k V_k(t)\gamma_k(t, \tau), \\ i\frac{\partial}{\partial t}\gamma_k(t, \tau) &= \epsilon_k \gamma_k(t, \tau) + V_k(t)\gamma(t, \tau). \end{aligned} \quad (10.32)$$

The initial conditions are $\gamma(t, t) = -i$, $\gamma_k(t, t) = 0$. It is convenient (although not essential) to set $V_k(t) = V_k(0)u(t)$; then, introducing the self-energy of the local Green's function of $H(0)$,

$$\Sigma(\omega) = \sum_k \frac{|V(0)|^2}{\omega - \epsilon_k + i\delta}, \quad \delta = 0^+ \quad (10.33)$$

we obtain

$$i \frac{\partial}{\partial t} \gamma(t, \tau) = \epsilon(t)\gamma(t, \tau) + u(t) \int_{\tau}^t dt' u(t') \Sigma(t - t') \gamma(t', \tau). \quad (10.34)$$

Moreover,

$$i \frac{\partial}{\partial \tau} \Gamma(t, \tau) = \epsilon(\tau)\Gamma(t, \tau) + \sum_k V_k(\tau) \Gamma_k(t, \tau) + iU(\tau)g(t, \tau)\Gamma(\tau, \tau), \quad (10.35)$$

$$i \frac{\partial}{\partial \tau} \Gamma_k(t, \tau) = \epsilon_k \Gamma_k(t, \tau) + V_k(\tau) \Gamma_k(t, \tau). \quad (10.36)$$

$\Gamma_k(t, \tau = 0) = 0$, and we find the closed equation

$$i \frac{\partial}{\partial \tau} \Gamma(t, \tau) = \epsilon(\tau)\Gamma(t, \tau) + iU(\tau)\gamma(t, \tau)\Gamma(\tau, \tau) + u(\tau) \int_0^{\tau} d\tau' u(\tau') \Sigma(\tau - \tau') \Gamma(t, \tau'). \quad (10.37)$$

This can be integrated[13]:

$$\Gamma(t, \tau)\theta(\tau) = i\gamma(t, 0)\gamma(\tau, 0)\theta(\tau) + i \int_0^{\tau} d\tau' \gamma(t, \tau')\gamma(\tau, \tau')U(\tau')G(\tau', \tau')\theta(\tau'). \quad (10.38)$$

Finally,

$$N(t) = -\gamma^2(t, 0)\theta(t) - iU \int_0^t dt' \gamma^2(t, t')U(t')N(t'). \quad (10.39)$$

The theory accounts for the Knotek-Feibelman mechanism. The theory of desorption and atom-surface scattering with a partially filled band will be discussed in Chapter 13.6.

10.3 Hierarchy of Greens Functions

We can use the EOM to generate approximate non-perturbative solutions of open-shell interacting models. Consider for instance the time-dependent Anderson model obtained by adding an on-site interaction to the time-dependent Fano model of Equation (10.11):

$$H = H_0 + H_1(t) + W = \sum_k \varepsilon_k n_k + \sum_{k,k'} V_{k,k'}(t) a_k^\dagger a_k + \sum_s U_s n_{s,\uparrow} n_{s,\downarrow}. \quad (10.40)$$

Let $\varphi_k(s)$ denote the one-electron wave function labeled by k at site s , such that $a_k = \sum_s a_s \phi_k(s)$. Since

$$i\dot{a}_{k,\uparrow} = [a_{k,\uparrow}, H]_- = \varepsilon_k a_{k,\uparrow} + \sum_{k'} V_{k,k'}(t) a_{k',\uparrow} + \sum_s U_s \varphi_k(s) a_{s,\uparrow} n_{s,\downarrow} \quad (10.41)$$

the EOM read:

$$\begin{aligned} i \frac{\partial g_{k,k'}^{(T)}}{\partial t} &= \delta(t-t') \delta_{k,k'} + \varepsilon_k g_{k,k'}^{(T)}(t, t') \\ &+ \sum_p V_{k,p}(t) g_{p,k'}^{(T)}(t, t') + \sum_s U_s \varphi_k(s) D_{\sigma,s,k'}(t, t') \end{aligned} \quad (10.42)$$

where the two-body propagator

$$D_{\sigma,s,k'}(t, t') = \langle T a_{s,\sigma}(t) n_{s,-\sigma}(t) a_{k',\sigma}^\dagger(t') \rangle. \quad (10.43)$$

appears. The interaction makes the problem hard and the equations do not close any more. If one can be content with a mean-field approximation, then one can try

$$D_{\sigma,s,k'}(t, t') \overset{?}{\approx} \langle T a_{s,\sigma}(t) a_{k',\sigma}^\dagger(t') \rangle \langle n_{s,-\sigma}(t) \rangle \quad (10.44)$$

which closes the equations again. Otherwise, one can generate an equation of motion for $D_{\sigma,s,k}(t, t')$ in order to truncate the hierarchy of Green's functions at an higher level. When we cannot achieve the exact solution, one should compare various approximations.

10.4 Composite Operator Method

For finite systems, one can in principle find the exact solution by the EOM method. As a trivial example, the one-site Hubbard model

$$H_{1site} = E(n_+ + n_-) + U n_+ n_- \quad (10.45)$$

yields the closed set of equations:

$$i \frac{da_+}{dt} = E a_+ + U a_+ n_-, \quad i \frac{da_+ n_-}{dt} = (E + U) a_+ n_-.$$

Without interactions the particles are those annihilated by a_\pm , while in the presence of interactions one has *particles* $\Psi(1) = a_+$, $\Psi(2) = a_+ n_-$ and $\Psi(3) = a_-$, $\Psi(4) = a_- n_+$; the zoological garden Ψ contains no more beasts.

This idea of the hierarchy can be generalized (see Ref.([49],[50][51]) and references therein). These authors call Ψ a *composite operator*, and write

$$\Psi = \begin{pmatrix} a_+ \\ a_+n_- \\ a_- \\ a_-n_+ \end{pmatrix} = \begin{pmatrix} \Psi(1) \\ \Psi(2) \\ \Psi(3) \\ \Psi(4) \end{pmatrix}, \quad J = i \frac{d\Psi}{dt} = \begin{pmatrix} J(1) \\ J(2) \\ J(3) \\ J(4) \end{pmatrix} \quad (10.46)$$

adopting a *spinor* notation (these are not spinors, they are just lists.) Anyhow, since the equation (10.46) is closed in this case, we may write

$$J(\mu, t) = \sum_{\nu} \epsilon(\mu, \nu) \Psi(\nu, t), \quad (10.47)$$

where for the sake of generality I imply a possible time dependence of the operators. For H_{1site} , the 4×4 matrix ϵ is block diagonal, since the first two entries are not connected to the others; each block is

$$\epsilon_{\sigma} = \begin{pmatrix} E & U \\ 0 & E + U \end{pmatrix}.$$

Following Ref.([49],[50][51]), we introduce

$$S_{\mu, \nu}(t, t') = \theta(t - t') \langle \Psi_0 | [\Psi_{\mu}(t), \Psi_{\nu}^{\dagger}(t')]_{\pm} | \Psi_0 \rangle, \quad (10.48)$$

which is just i times the retarded Green's function (4.13), possibly averaged over the Grand-Canonical Ensemble; we are using $[\cdot]_{+}$ for Fermi particles, but it would be $[\cdot]_{-}$ for Bosons. The EOM read

$$i \frac{\partial S(t, t')}{\partial t} \Big|_{t'=t} = \langle [J(t), \Psi^{\dagger}(t)]_{\pm} \rangle. \quad (10.49)$$

We define the m matrix by

$$m = i \frac{\partial S(t, t')}{\partial t} \Big|_{t'=t}, \quad (10.50)$$

use Eq.(10.47) and the so called normalization matrix $I = \{I_{\mu, \nu}\}$ with elements

$$I_{\mu, \nu}(t) = S_{\mu, \nu}(t, t). \quad (10.51)$$

The nonzero diagonal blocks of I are

$$\begin{pmatrix} \langle [a_{\sigma}, a_{\sigma}^{\dagger}]_{\pm} \rangle & \langle [a_{\sigma}, a_{\sigma}^{\dagger} n_{-\sigma}]_{\pm} \rangle \\ \langle [a_{\sigma} n_{-\sigma}, a_{\sigma}^{\dagger}]_{\pm} \rangle & \langle [a_{\sigma} n_{-\sigma}, a_{\sigma}^{\dagger} n_{-\sigma}]_{\pm} \rangle \end{pmatrix} = \begin{pmatrix} 1 & \langle n_{-\sigma} \rangle \\ \langle n_{-\sigma} \rangle & \langle n_{-\sigma} \rangle \end{pmatrix} \text{ for } \sigma = +, -.$$

Finally the EOM become

$$m = \epsilon I. \quad (10.52)$$

Let us extend the treatment to many sites, denoted by latin indices; we start with a N_{op} -component spinor $\Psi_\mu(p, t)$ for each site involving c_p and the operators of nearby sites. We write Green's functions

$$S_{\mu,\nu}(p, t, p, t') = \theta(t - t') \langle [\Psi_\mu(p, t), \Psi_\nu^\dagger(q, t')]_+ \rangle, \quad (10.53)$$

and the initial conditions

$$I_{\mu,\nu}(p, q, t) = S_{\mu,\nu}(p, t, q, t); \quad (10.54)$$

the normalization matrix has site indices as well. From now on spinor indices can be understood; we write the m matrix

$$m(p, q) = \langle [J(p, t), \Psi^\dagger(q, t)]_+ \rangle. \quad (10.55)$$

Formally, the argument proceeds as above: understanding the site indices as well the EOM are still given by Equation (10.52); the eigenvalues of ϵ could be interpreted as the eigen-energies of the system. The trouble is that when one calculates $J = i \frac{d\Psi}{dt}$, new operators arise; Equation (10.47) does not hold, but is replaced by

$$J(p, t) = \sum_q^{N_{op}} \epsilon(p, q) \Psi(q, t) + \delta J(p), \quad (10.56)$$

with δJ is a nonlinear rest. In other terms, the set of operators is not closed, and the spinors have more components than we can afford.

To keep the calculation manageable, one could trivially truncate the spinors at N_{op} operators, throwing away the unwanted ones and δJ ; the ϵ matrix gives a solvable approximation. This is less accurate than the standard EOM method, which prescribes to replace the extra operators by some approximation like (10.44).

However, there is a more clever alternative criterion for sorting out the terms linear in Ψ in the r.h.s. of Equation (10.56). From the N_{op} -component Ψ one can work out the truncated I matrix. The map $\Psi_\mu(p), \Psi_\nu(q) \rightarrow I_{p,q}$ sends two operators into a number like a scalar product in operator space. In this Section I denote this *scalar product* by $\langle\langle \dots, \dots \rangle\rangle$ and write

$$\langle\langle \Psi(p), \Psi(q) \rangle\rangle = I(p, q) = \langle [\Psi(p, t), \Psi^\dagger(q, t)]_+ \rangle.$$

Taking the scalar product of (10.56)

$$\langle\langle J(p), \Psi(s) \rangle\rangle = \sum_q^{N_{op}} \epsilon(p, q) \langle\langle \Psi(q, t), \Psi(s) \rangle\rangle + \langle\langle \delta J(p), \Psi(s) \rangle\rangle. \quad (10.57)$$

Now in order to drop the last term we do not need to assume that δJ is small; we make the milder assumption that it is *orthogonal* to the spinors. Dropping δJ we finally obtain (10.52), that is,

$$\epsilon = mI^{-1} \quad (10.58)$$

and achieve a well defined, solvable approximation. In this way, the new ϵ depends on those complicated operators that we are not considering explicitly. Although this is not a unique way to proceed, it is certainly appealing. Fourier transforming to momentum space, the retarded Green's function is approximated by

$$g^{(\tau)}(\omega, k) = \sum_i^{N_{op}} \frac{\sigma_i(k)}{\omega - E_i(k) + i\delta}, \quad (10.59)$$

where $E_i(k)$ are the eigenvalues of $\epsilon(k)$ and the spectral functions $\sigma_i(k)$ can be derived[199] from $I(k)$.

For a review on the applications to the Hubbard Model, see [198].

Problems

10.1. Verify (10.10) explicitly in the non-interacting limit.

10.2. Prove Equation 13.136.

10.3. Use the tight-binding method to calculate the retarded Green's functions of the tight-binding Hamiltonians in $d=1,2,3$ dimensions.

10.4. Dealing with X-Ray absorption and emission in Metals, Langreth[205] considered the model Hamiltonian

$$H = \sum_q \epsilon_q a_q^\dagger a_q + E_0 b^\dagger b + \sum_{qq'} V_{qq'} a_q^\dagger a_q b b^\dagger \quad (10.60)$$

where b and a_q annihilate core and conduction electrons, respectively; the Green's functions $g(t-t') = \langle T b(t) b^\dagger(t') \rangle$ describes the deep state dynamics and $F_{kk'}(\tau, \tau'; t, t') = \langle T a_k(\tau) a_{k'}(\tau') b(t) b^\dagger(t') \rangle$ the absorption and emission processes. For absorption, the average is a ground-state expectation value in the presence of the core electron. Derive the EOM for $F_{kk'}$ in the absorption case.

11 Feynman Diagrams for Condensed Matter Physics

11.1 Diagrams for the Vacuum Propagator

Consider a many-body system, like a molecule or solid, with Hamiltonian $H = H_0 + V$, where V is the interaction, $H_0 = \sum_j \epsilon_j n_j$ is the kinetic energy with ground state $|\Phi\rangle$ and eigenvalue W_0 . I shall write

$$|\Phi\rangle = \prod_{\epsilon_k < E_F} c_{k\uparrow}^\dagger c_{k\uparrow}^\dagger |0\rangle \tag{11.1}$$

to mean that the product is over occupied spin-orbitals, and produces a Fermi sphere in the thermodynamic limit. How can we find the ground state energy E_0 of H ? Standard perturbation theory fails unless V is small compared to the unperturbed energy difference; in practice, it fails almost always, since in most interesting problems, the spectrum H_0 is continuous.

Continuous spectra can be perturbed in such way that discrete spectra arise. Suppose one wants to find the bound states of the Hydrogen atom by treating the Coulomb interaction as a perturbation: for any Z an infinity of bound levels exists, but there is no hope to get any sensible result with any finite number of terms. The very existence of bound states requires poles of Green's functions to form. The pole of $\frac{1}{1-z} = 1 + z + z^2 + \dots$ can only be found at infinite order. The formula (4.125) for E_0 from the vacuum amplitude (4.123)

$$R(t) = \langle \Phi | U_I(t) | \Phi \rangle = e^{iW_0 t} \langle \Phi | e^{-iHt} | \Phi \rangle \tag{11.2}$$

is useful because we know R at least formally, recalling (2.36)

$$\begin{aligned} U_I(t) &= e^{iH_0 t} e^{-iHt} = T e^{\frac{-i}{\hbar} \int_0^t dt' V_I(t')} \\ &= 1 + \frac{-i}{\hbar} \int_0^t dt_1 V_I(t_1) + \left(\frac{-i}{\hbar}\right)^2 \int_0^t dt_1 \int_0^{t_1} dt_2 V_I(t_2) + \dots, \end{aligned} \tag{11.3}$$

Note that in this section we use the *telescope* form (2.6) of the nested integrals. To illustrate the method, I shall use the simplified interaction

$$V = \sum_{ijkl} U(i, j, k, l) c_{i\uparrow}^\dagger c_{j\downarrow}^\dagger c_{l\downarrow} c_{k\uparrow}. \tag{11.4}$$

In this way, we assume that only opposite-spin electrons interact, and this is the simplification¹. Since $\langle \Phi | V_I(t) | \Phi \rangle = \langle \Phi | V | \Phi \rangle$, the first-order contribution is

$$\begin{aligned}
 R^{(1)}(t) &= -i \int_0^t dt_1 \langle \Phi | V | \Phi \rangle \\
 &= -i t \langle \Phi | V | \Phi \rangle = -i t \sum_{ij} U(i, j, i, j) \langle \Phi | n_{i\uparrow} n_{j\downarrow} | \Phi \rangle
 \end{aligned}
 \tag{11.5}$$

where n is the occupation number. In (11.5) we must average a product of

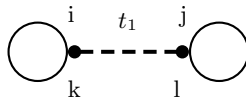


Fig. 11.1. The first-order contribution, with $i=k, j=l$. One says that i is *contracted* with k and j with l . A more explicit definition follows shortly.

occupation numbers, and for each spin-orbital the creation operator is represented by a line leaving a vertex and the annihilation operator by a line entering the vertex. Graphically, if we represent the up-spin operators as the ends of the left line, and the interaction to the dashed line, this corresponds to the pattern of Fig. (15.4). The occupation number product over the non-interacting $|\Phi\rangle$ can be written as a vacuum average and using the anticommutation rules we can separate the two spins: thus it factors:

$$\langle \Phi | n_{i\uparrow} n_{j\downarrow} | \Phi \rangle = \langle \Phi | n_{i\uparrow} | \Phi \rangle \langle \Phi | n_{j\downarrow} | \Phi \rangle = n_i n_j
 \tag{11.6}$$

where the average occupation numbers have been assumed spin-independent for the sake of simplicity. However we did not achieve much, yet: substitution in the energy formula (4.125) yields 0. In second-order,

$$\begin{aligned}
 R^{(2)}(t) &= - \sum_{ijkl} \sum_{i'j'k'l'} U(i, j, k, l) U(i'j'k'l') \int_0^t dt_1 \int_0^{t_1} dt_2 \\
 &\langle \Phi | T [c_{i\uparrow}^\dagger(t_1) c_{j\downarrow}^\dagger(t_1) c_{l\downarrow}(t_1) c_{k\uparrow}(t_1) c_{i'\uparrow}^\dagger(t_2) c_{j'\downarrow}^\dagger(t_2) c_{l'\downarrow}(t_2) c_{k'\uparrow}(t_2)] | \Phi \rangle.
 \end{aligned}
 \tag{11.7}$$

More generally, we need to calculate the ground state average

$$M = \langle \Phi | T [A_1(t_1) A_2(t_2) A_3(t_3) \dots] | \Phi \rangle
 \tag{11.8}$$

where $A_1, A_2, A_3 \dots$ are interaction-picture operators - either creation or annihilation operators - defined on an orthonormal basis in the interaction picture and $|\Phi\rangle$ is the Fermi sphere. This calculation can be worked out by

¹Later we can easily restore the full interaction by adding exchange terms.

writing down all the operators that make up the Fermi sphere according to Equation (11.1); then this becomes an average over the vacuum $|0\rangle$; then, by the anticommutation relations, we can bring the annihilation operators to act on $|0\rangle$ to produce 0; all what remains from the anticommutators is the result. However, we naturally ask if we can do something to reduce all this groundwork. Fortunately, we can, in terms of contractions. A *contraction* of two operators A and B which are either creation or annihilation interaction-picture operators, is defined as

$$\overline{A(t)B(t')} = \langle \Phi | T[A(t)B(t')] | \Phi \rangle. \quad (11.9)$$

For this to be non zero one of the two operators must create and the other annihilate the same one-body state, and the contractions yield (up to a sign) the non-interacting propagators (Equation (4.38))

$$ig_k(t) = \langle T[c_{k,\sigma}(t)c_{k,\sigma}^\dagger(0)] \rangle = e^{-i\epsilon_k t} \{ \theta(t)[1 - n_k] - \theta(-t)n_k \}, \quad (11.10)$$

which propagates a hole for $t < 0$ and an electron for $t > 0$. For equal time contractions one defines:

$$\overline{c^\dagger(t)c(t)} \equiv \langle c^\dagger(t)c(t) \rangle. \quad (11.11)$$

11.1.1 Wick's Theorem

Wick's theorem, basic for all sorts of perturbation expansions, reads:

$$\boxed{M = \langle T[A_1(t_1)A_2(t_2)A_3(t_3)\dots] \rangle = \sum_P (-)^P \overline{A_{P1}A_{P2}} \overline{A_{P3}A_{P4}} \dots;} \quad (11.12)$$

in words, M is the sum of the products $(-)^P \overline{A_{P1}A_{P2}} \overline{A_{P3}A_{P4}} \dots$ of the contractions; P is the permutation that takes from the initial expression $A_1A_2A_3\dots$ to the final one, and $(-)^P$ its signature. I propose an intuitive proof².

As a warm-up, we calculate the ground state expectation value of the product in the second-order term (11.7); for an easy start, we do so without the time ordering T , and for the moment we let

$$M = \langle \Phi | c_{i\uparrow}^\dagger(t_1) c_{j\downarrow}^\dagger(t_1) c_{l\downarrow}(t_1) c_{k\uparrow}(t_1) c_{i'\uparrow}^\dagger(t_2) c_{j'\downarrow}^\dagger(t_2) c_{l'\downarrow}(t_2) c_{k'\uparrow}(t_2) | \Phi \rangle.$$

Also, we assume provisionally that the canonical basis is the one of H_0 eigenstates; then the time dependences are given by c-number phase factors as in Equation (4.35), $c_k(t) = c_k e^{-i\epsilon_k t}$. The \downarrow operators come in pairs at each time and since Fermi operators anticommute, one can lump all the \uparrow spins on the left without changing sign: we obtain

$$M = \langle \Phi | c_{i\uparrow}^\dagger(t_1) c_{k\uparrow}(t_1) c_{i'\uparrow}^\dagger(t_2) c_{k'\uparrow}(t_2) c_{j\downarrow}^\dagger(t_1) c_{l\downarrow}(t_1) c_{j'\downarrow}^\dagger(t_2) c_{l'\downarrow}(t_2) | \Phi \rangle.$$

²the (much longer) standard one by induction may be found in textbooks[2].

Now the \uparrow and \downarrow are different species (mathematically, linearly independent operators); since actually $|\Phi\rangle = |\Phi\uparrow\rangle|\Phi\downarrow\rangle$ the matrix element M factors,

$$M = \langle\Phi|c_{i\uparrow}^\dagger(t_1)c_{k\uparrow}(t_1)c_{i'\uparrow}^\dagger(t_2)c_{k'\uparrow}(t_2)|\Phi\rangle \\ \times \langle\Phi|c_{j\downarrow}^\dagger(t_1)c_{l\downarrow}(t_1)c_{j'\downarrow}^\dagger(t_2)c_{l'\downarrow}(t_2)|\Phi\rangle. \quad (11.13)$$

The assumption that the canonical basis is the one of H_0 eigenstates can be removed, since anyhow $H_0 = H_{0\uparrow} + H_{0\downarrow}$, and since $H_{0\uparrow}$ and $H_{0\downarrow}$ commute, we can write $c_\sigma(t) = e^{iH_{0\sigma}t}c_\sigma e^{-iH_{0\sigma}t}$ and the time-dependent creation and annihilation operators simply anticommute. While using Bloch waves to define the Fermi sphere, we may wish to work with contractions in a site basis. Next, we restore the T operation, and consider

$$M = \langle\Phi|T[c_{i\uparrow}^\dagger(t_1)c_{k\uparrow}(t_1)c_{i'\uparrow}^\dagger(t_2)c_{k'\uparrow}(t_2)c_{j\downarrow}^\dagger(t_1)c_{l\downarrow}(t_1)c_{j'\downarrow}^\dagger(t_2)c_{l'\downarrow}(t_2)]|\Phi\rangle \\ = \theta(t_1 - t_2)M_{12} + \theta(t_2 - t_1)M_{21} \quad (11.14)$$

$$M_{12} = \langle\Phi|c_{i\uparrow}^\dagger(t_1)c_{k\uparrow}(t_1)c_{j\downarrow}^\dagger(t_1)c_{l\downarrow}(t_1)c_{i'\uparrow}^\dagger(t_2)c_{k'\uparrow}(t_2)c_{j'\downarrow}^\dagger(t_2)c_{l'\downarrow}(t_2)|\Phi\rangle,$$

$$M_{21} = \langle\Phi|c_{i'\uparrow}^\dagger(t_2)c_{k'\uparrow}(t_2)c_{j'\downarrow}^\dagger(t_2)c_{l'\downarrow}(t_2)c_{i\uparrow}^\dagger(t_1)c_{k\uparrow}(t_1)c_{j\downarrow}^\dagger(t_1)c_{l\downarrow}(t_1)|\Phi\rangle.$$

Again, the \downarrow operators come in pairs at each time, so *in each term of the sum* (11.14) we can lump the \uparrow spins on the left and factorize like above:

$$M_{12} = \langle\Phi|c_{i\uparrow}^\dagger(t_1)c_{k\uparrow}(t_1)c_{i'\uparrow}^\dagger(t_2)c_{k'\uparrow}(t_2)|\Phi\rangle \\ \times \langle\Phi|c_{j\downarrow}^\dagger(t_1)c_{l\downarrow}(t_1)c_{j'\downarrow}^\dagger(t_2)c_{l'\downarrow}(t_2)|\Phi\rangle \\ M_{21} = \langle\Phi|c_{i'\uparrow}^\dagger(t_2)c_{k'\uparrow}(t_2)c_{i\uparrow}^\dagger(t_1)c_{k\uparrow}(t_1)|\Phi\rangle \\ \times \langle\Phi|c_{j'\downarrow}^\dagger(t_2)c_{l'\downarrow}(t_2)c_{j\downarrow}^\dagger(t_1)c_{l\downarrow}(t_1)|\Phi\rangle$$

and the whole time-ordered matrix element (11.14) breaks down into the time ordered factors:

$$M = \langle\Phi|T[c_{i\uparrow}^\dagger(t_1)c_{k\uparrow}(t_1)c_{i'\uparrow}^\dagger(t_2)c_{k'\uparrow}(t_2)]|\Phi\rangle \\ \times \langle\Phi|T[c_{j\downarrow}^\dagger(t_1)c_{l\downarrow}(t_1)c_{j'\downarrow}^\dagger(t_2)c_{l'\downarrow}(t_2)]|\Phi\rangle. \quad (11.15)$$

Thus, the time-ordering does not prevent the factorization, and the argument works independently of the number of creation and annihilation operators. Now we can breath a little bit, but can we do any better? We can actually use the different spin-orbitals of any canonical basis as the different species, but now we must keep track of the signs. Consider the matrix element for \uparrow spins. Particle i_\uparrow created at time t_1 must be annihilated either by $c_{k\uparrow}(t_1)$ or by

$c_{k'\uparrow}(t_2)$; so, two contractions contribute, but in each case the matrix element breaks as before³. Therefore the ground state average can be obtained as a sum over permutations. However, there is more. In the above discussion, we used no specific property of the ground state $|\Phi\rangle$; we can average the matrix element on any state in the same way (the contractions are then redefined accordingly). We can analytically continue Equation (11.12) from the real axis to the vertical track of Figure 2.2.2 b) (Sect.2.2.2). So, Wick's theorem holds at finite temperatures as well; $\langle \cdot \cdot \cdot \rangle$ then stands for a thermal average.

Comments

This is a very general theorem that is often understated in books. It is obvious that Wick's theorem also holds for averages over the vacuum $|0\rangle$. By the way, Φ is itself a vacuum; for states above the Fermi level we can create electrons like on $|0\rangle$; for occupied states the annihilation of an electron is the creation of a hole. The transformation to hole operators $c = b^\dagger$ is canonical, or if you like it is just a change in notation. So Wick's theorem works in both cases for the same reason.

Wick's theorem for bosons works in the same way, and for the same reasons, except that the Bose operators commute under T and there is no sign nuisance in this case.

11.1.2 Goldstone Diagrams

We represent the second-order terms diagrammatically by drawing two interaction lines, labeled t_1 and t_2 with $t_2 < t_1$ according to the scheme of Fig. (11.1.2). These are time-ordered or *Goldstone* diagrams. Two diagrams must be identified if they are topologically equivalent in the Goldstone sense, that is, if they can be deformed into one another without changing the time ordering. In this example with no interaction for parallel spins the vertices on the left refer to spin up and there are no exchange terms. If we contract only equal-time operators we get the a) diagram of Figure 11.1.2. All the non-propagating lines (those that begin and end at the same time) must refer to occupied orbitals (equal-time Wick's rule).

Diagrams consisting of two separated pieces, like a), are called *unlinked*. Diagrams b),c) and d) are linked and b)and c) have the same value. The contribution of diagram a) is obtained setting $k = i, l = j, k' = i', l' = j'$ in $R^{(2)}(t)$:

³The possibility of contracting 4 or more operators with the same indices can also be included. For averages on either $|0\rangle$ or Φ , $\langle c^\dagger c \rangle$ are either 0 or 1, so the Wick factorization is granted since $0*0=0$ and $1*1=1$. So, these terms do not modify the result. As emphasized in the Landau series[3], in the thermodynamic limit the theorem holds for averages on any state, since taking the same index for two $c^\dagger c$ factors means selecting a set of null measure.

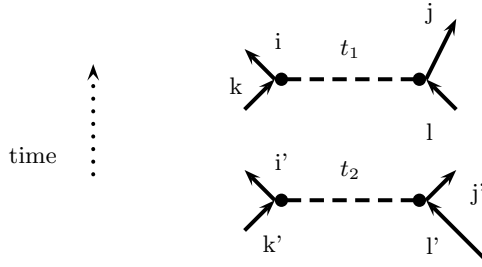


Fig. 11.2. Starting the setup of the second-order contribution.

$$R^{(a)}(t) = - \sum_{ij} \sum_{i'j'} U(i, j, i, j) U(i'j'i'j') \int_0^t dt_1 \int_0^{t_1} dt_2 \langle \Phi | T [c_{i+}^\dagger(t_1) c_{j-}^\dagger(t_1) c_{j-}(t_1) c_{i+}(t_1) c_{i'+}^\dagger(t_2) c_{j'-}^\dagger(t_2) c_{j'-}(t_2) c_{i'+}(t_2)] | \Phi \rangle. \quad (11.16)$$

and contracting one finds

$$R^{(a)}(t) = \frac{-t^2}{2} \left(\sum_{ij} U(i, j, i, j) n_i n_j \right) \left(\sum_{i'j'} U(i'j'i'j') n_{i'} n_{j'} \right). \quad (11.17)$$

Here again we note that a line labeled i closing on itself, or *tadpole*, simply contributes n_i .

Diagram *b*) arises from the identifications $k = i, l' = j, k' = i', l = j'$ and to the contractions

$$\overline{c_{i+}^\dagger(t_1) c_{k+}(t_1) \cdot c_{i'+}^\dagger(t_2) c_{k'+}(t_2) \cdot c_{j-}^\dagger(t_1) c_{l'-}(t_2) \cdot c_{l-}(t_1) c_{j'-}^\dagger(t_2)}. \quad (11.18)$$

The equal-time contractions

$$\overline{c_{i+}^\dagger(t_1) c_{k+}(t_1)} = \delta(i, k) n_i \quad (11.19)$$

and

$$\overline{c_{i'+}^\dagger(t_2) c_{k'+}(t_2)} = \delta(i', k') n_{i'} \quad (11.20)$$

are immediate; let us consider the lines that represent propagators (see (4.37)). The descending line yields

$$\begin{aligned} \overline{c_{j-}^\dagger(t_1) c_{l'-}(t_2)} &= \delta(j, l') e^{i\varepsilon_j(t_1-t_2)} [n_j \theta(t_1-t_2) - (1-n_j) \theta(t_2-t_1)] \\ &= \delta(j, l') (-i) g_j(t_2-t_1) \end{aligned} \quad (11.21)$$

The - sign in front of $(-i)g_j$ comes from the order of operators which is opposite to the convention of (4.36).

The ascending line gives:

$$\begin{aligned} \overline{c_{l-}(t_1) c_{j'-}^\dagger(t_2)} &= \delta(j', l) e^{i\varepsilon_l(t_2-t_1)} [(1-n_l)\theta(t_1-t_2) - n_l\theta(t_2-t_1)] \\ &= \delta(j', l) (i)g_l(t_1-t_2) \end{aligned} \quad (11.22)$$

In both cases, the time argument of g is the final time minus the initial time of the directed line. Since $t_2 < t_1$, the contribution of the descending $l' = j$ line represents a hole in a occupied state, while the for the ascending line is an electron in an empty one. In both cases the directed line brings a factor ig .

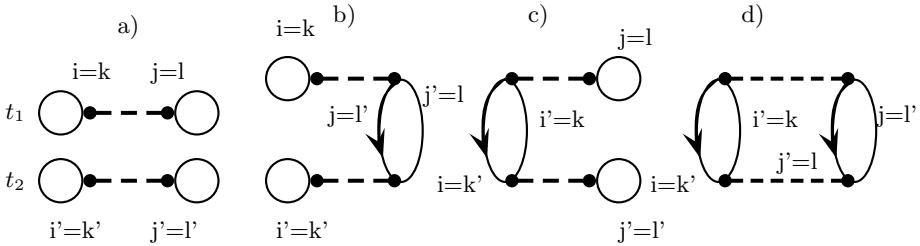


Fig. 11.3. Second-order contributions to $R(t)$.

Thus, diagram $b)$ (like the identical one $c)$) yields the following expression:

$$\begin{aligned} R^{(b)} &= - \sum_{ijkl} \sum_{i'j'k'l'} U(i, j, k, l) U(i', j', k', l') \delta_{ik} \delta_{i'k'} \delta_{l'j} \delta_{j'l} n_i n_{i'} \int_0^t dt_1 \int_0^{t_1} dt_2 \\ &\quad i g_j(t_2 - t_1) i g_l(t_1 - t_2). \end{aligned} \quad (11.23)$$

What is coming from these observations is a convention for representing mathematical expressions graphically; each fermion line labeled j and directed from t to t' yields $ig_j(t' - t)$; each interaction line brings a factor $(-i)U(i, j, k, l)$ (where the arguments refer to the top interaction in Figure 11.1.2 and each closed fermion loop brings a - sign; all internal indices are summed over; the nested time integrals are then evaluated. To evaluate the ground state energy, one takes the $t \rightarrow \infty(1 - i\eta)$ limit and uses the energy formula (4.125). Working out (11.23) one finds

$$\begin{aligned} R^{(b)} &= - \sum_{ijli'} U(i, j, i, l) U(i', l, i', j) n_i n_{i'} \int_0^t dt_1 \int_0^{t_1} dt_2 \\ &\quad e^{-i(\epsilon_l - \epsilon_j)(t_1 - t_2)} (-) n_j (1 - n_l). \end{aligned} \quad (11.24)$$

The integral is elementary:

$$\int_0^t dt_1 \int_0^{t_1} dt_2 e^{-i(\epsilon_l - \epsilon_j)(t_1 - t_2)} = \frac{1 + it(\epsilon_j - \epsilon_l) - e^{it(\epsilon_j - \epsilon_l)}}{(\epsilon_j - \epsilon_l)^2}. \quad (11.25)$$

The term linear in t contributes to the ground state energy. Note however that j is a hole, l is an electron, hence $\epsilon_j - \epsilon_l < 0$ and the exponential in the r.h.s. drops out as $t \rightarrow \infty(1 - i\eta)$. Problem 11.1 deals with diagram d).

Despite the heuristic appeal of cartoons showing the basic scattering events between particles, the diagrammatic expansion does not look promising at all at this stage. The number of different diagrams and their complexity grows catastrophically with the order, and we need to go to order ∞ to get useful results. Worse still, diagrams may defy intuition severely. Their heuristic appeal can become very misleading, since the processes they describe include counter-intuitive ones. Diagrams obtained from d) by appending tadpoles or bubbles freely to each line do belong to the expansion, and must be included, even when the lines at a given time over-number the electrons in the sample and/or violate the Pauli principle. No such principle holds in diagrammatics, and several lines can bear the same quantum numbers. In one-particle problems, diagrams arise that appear to describe several fermions propagating at a time.

11.1.3 Diagram Rules for the Thermodynamic Potential

Using imaginary time, the above results extend directly to the calculation of the thermodynamic potential

$$\Omega = -K_B T \ln Z_G \quad (11.26)$$

where

$$Z_G = \text{Tr} e^{-\beta(H - \mu N)} \quad (11.27)$$

is the grand partition function, μ the chemical potential and N the particle number operator. Ω may be found as the sum of ring diagrams (see Sect. 12.4.5). The mean energy and particle number are related by $\bar{E} = \Omega + \mu \bar{N} + TS$, and since the entropy S goes to 0 at $T=0$ the ground-state energy may be found from the zero-temperature limit. Luttinger and Ward [55] derived and stated the rules for $\beta\Omega$ in frequency space as follows. 1) Draw all possible n-th order diagrams. Put labels on each line (a label like r stands for one-body labels including spin, and the non-interacting Hamiltonian is supposed diagonal with eigenvalues ϵ_r) and associate a Matsubara frequency $\zeta_l = \mu + \frac{(2l+1)\pi i}{\beta}$, with integer l . Conserve frequency at each vertex. 2) For each diagram: insert a factor $\langle rs|v|r's' \rangle$ for each interaction (labeled by one-body states, r' and s' entering and r,s leaving), a factor $\frac{(-)^{n+1}}{2^n n!}$ and a (-) sign for each loop 3) For each line labelled by r write a factor $G_r(\zeta_l) = \frac{1}{\zeta_l - \epsilon_r}$. This

factor is called propagator. Next, sum over all internal labels and all frequencies ζ_l with $\frac{1}{\beta} \sum_l$, including a convergence factor $e^{\zeta_l 0^+}$ for loops. Examples may be found in Ref.[55]. The T=0 version of the expansion is obtained by removing μ , replacing ζ_l by real frequencies ω and $\frac{1}{\beta} \sum_l$ by $\int_{-\infty}^{\infty} d\omega$. Please note that 1) simple diagrams may be easily computed without the diagram rules directly from the T exp formula, 2) nobody ever computes very complex diagrams, which are too many and too complicated to be of any use. The real point is: how to avoid any heavy-duty use of the diagram rules.

11.2 Linked Cluster Theorem

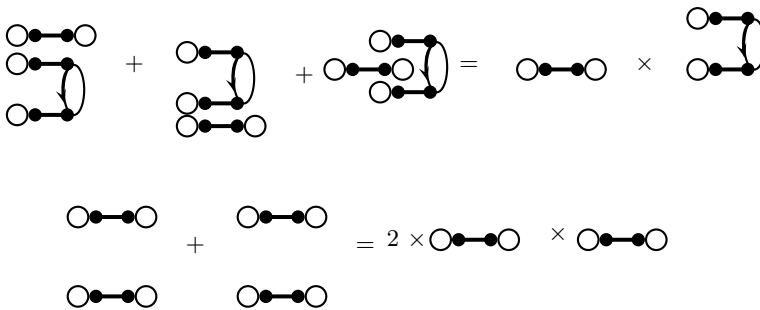


Fig. 11.4. Combining diagrams. Those summed in the first row consist of different subdiagrams, while those of the second row are made up with like subdiagrams.

The only cheap and efficient way to produce and compute lots of high-order diagrams is by combining smaller ones. In a linked diagram one can go from any vertex to any other one by following propagator or interaction lines. The diagram a) of Figure 11.3 is an example of an unlinked diagram made up of two simpler linked ones. Consider doing the same with any pair of different connected diagrams. They give rise to different combined graphs for R as shown in Figure 11.4. The diagrams on the l.h.s., top row, differ by the order of interactions in time and are to be counted as different contributions because the ordering is enforced by different θ functions; their sum is just the product of the original diagrams. If however the same diagram is considered twice, (bottom row and diagram 11.3 a)) the contribution to R comes only once so the result must be divided by 2. Denoting by $\{\tilde{D}_i\}$ the set of linked diagrams, consider a particular unlinked diagram of order n containing, say, 3 linked parts $\tilde{D}_\alpha, \tilde{D}_\beta, \tilde{D}_\gamma$. Each of its n interaction lines labeled by times $t_n < t_{n-1} < \dots < t_1$ belongs to one of the 3 sub-diagrams. Within each sub-diagram, the ordering of the interaction lines is fixed by the fact that it is a

replica of one of the $\tilde{D}_i(t)$, however by varying the relative ordering of two interaction lines belonging to different sub-diagrams we get a diagram which belongs to the series for R . Summing over all such interchanges we simply get rid of the relative orderings; if the three sub-diagrams are different the result is

$$\tilde{D}_\alpha(t)\tilde{D}_\beta(t)\tilde{D}_\gamma(t);$$

however, if there are identical subdiagrams we must pay attention. If, say, $\tilde{D}_\alpha(t) = \tilde{D}_\beta(t)$, then each contribution to R is counted twice (each has a ghost with the two sub-diagrams exchanged, but the series has one of them) and the result is

$$\frac{1}{2!}\tilde{D}_\alpha(t)^2\tilde{D}_\chi(t).$$

These observations extend to any order and to any number of linked sub-diagrams \tilde{D}_i . The sum of all the unlinked diagrams of any order containing p linked parts chosen in any way in $\{\tilde{D}_i\}$ is

$$R_p(t) = \sum_{\{n_i\}} \delta(p, \sum_i n_i) \left[\prod_i \frac{\tilde{D}_i^{n_i}(t)}{n_i!} \right]; \quad (11.28)$$

here $\{n_i\} = n_1, n_2, \dots$ is a list of non-negative integers specifying the number n_i of occurrences of \tilde{D}_i , while the total number of parts is fixed by the Kronecker δ . This is just

$$R_p(t) = \frac{1}{p!} \sum_{\{n_p\}} (n_1, n_2, \dots, n_k, \dots)! \prod_i \tilde{D}_i^{n_i}(t) \quad (11.29)$$

where $(n_1, n_2, \dots, n_k, \dots)! = \frac{(\sum_i n_i)!}{n_1!n_2! \dots}$ is the multinomial coefficient ; thus

$$R_p(t) = \frac{1}{p!} \left(\sum_i \tilde{D}_i(t) \right)^p = \frac{1}{p!} (L(t))^p \quad (11.30)$$

where $L = \sum \tilde{D}_i(t)$ is the sum of all linked diagrams.

Thus we have obtained the simple but far reaching *Linked Cluster Theorem*:

$$R(t) = e^{L(t)} \quad (11.31)$$

Every approximation to $L(t)$ takes us to infinite order in the series for $R(t)$, and a way to achieve real progress is open.

This exact result is the basis of the so called cumulant expansion⁴. Now our task is calculating L and the unlinked second-order diagram 11.3 a) must be discarded, while the first-order generates a partial series:

⁴Note that a Linked Cluster Theorem exists[42] even if the interactions are mediated by bosons; each sub-diagram must then be divided by its order. The combinatorial argument is similar, but is modified by the fact that each line gets two labels instead of one.

$$\ln R^{(1)}(t) = -it \sum_{ij} U(i, j, i, j) n_i n_j,$$

and differentiating with respect to t and multiplying by i we find

$$E^{(1)} = \sum_{i,j} U(i, j, i, j) n_i n_j$$

which is the Hartree-Fock approximation, a marked improvement over the previous null result.

11.2.1 Valence Electron and Core Hole

To see the Linked Cluster Theorem and the diagram rules at work, consider the simplest molecular-orbital model with sites a and b with hopping matrix element V

$$H_0 = \begin{pmatrix} 0 & V \\ V & 0 \end{pmatrix} \quad (11.32)$$

with eigenvalues $\pm V$; now suppose that a core electron sits at site a ; the valence Hamiltonian becomes

$$H = \begin{pmatrix} U & V \\ V & 0 \end{pmatrix}; \quad (11.33)$$

where U is the valence electron-core electron interaction. The new eigenvalues are

$$\epsilon_{\pm} = \frac{U \pm \xi}{2}, \quad (11.34)$$

with $\xi = \sqrt{U^2 + 4V^2}$. The core occupation number is $n_c \equiv 1$ and the core Green's function enters only through n_c . The unperturbed ($U=0$) valence propagator on site a reads

$$ig_{aa}(t) = \frac{-\theta(-t)e^{iVt} + \theta(t)e^{-iVt}}{2}, \quad (11.35)$$

where the first term is the contribution of the filled ground state orbital, and the second comes from the excited state. The unperturbed filling is $n_a^0 = 1/2$. The first-order diagram is $-itUn_a$. There is one second-order diagram (Fig. 11.3 b) or c)). The descending line brings a - sign, another one is due to the ring; one obtains

$$\frac{(-iU)^2}{4} \int_0^t dt_1 \int_0^{t_1} dt_2 e^{2iV(t_2-t_1)} = \left(\frac{U}{V}\right)^2 \left(\frac{-1 + e^{-2iVt} + 2iVt}{16}\right). \quad (11.36)$$

In third order we may add a third tadpole on the electron or on the hole lines; the contributions cancel (since the descending line brings a - sign) and there is no third-order term. In fourth-order one could consider adding two tadpoles to the second-order bubble, but there is a similar cancellation between those attached to electron and hole lines. The contribution comes from the diagram in Figure 11.5 and from a similar diagram with $t_3 < t_4$.

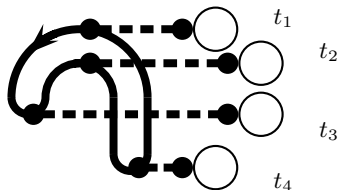


Fig. 11.5. The fourth-order contributions to $R(t)$. Note that two valence electron lines propagate between t_3 and t_2 , although in this problem there is just 1 valence electron. This illustrates that particle-number-violating diagrams must be included.

We get

$$\begin{aligned} & (-) \frac{(-iU)^4}{8} \int_0^t dt_1 \int_0^{t_1} dt_2 \int_0^{t_2} dt_3 \int_0^{t_3} dt_4 e^{2iV(t_4+t_3-t_1-t_2)} \\ &= \left(\frac{U}{V}\right)^4 \left[\frac{5 - e^{-4iVt} - 4e^{-2iVt}}{512} - iVt \frac{1 + 2e^{-2iVt}}{128} \right]. \end{aligned} \tag{11.37}$$

Since the problem is simply solved exactly, we can check these results by calculating $R(t)$ and its expansion. One easily derives the Hamiltonian matrix \tilde{H} on the basis of the $U = 0$ eigenstates and the ground-state-diagonal element its exponential:

$$\tilde{H} = \begin{pmatrix} \frac{U}{2} - V & \frac{U}{2} \\ \frac{U}{2} & \frac{U}{2} + V \end{pmatrix} \Rightarrow R(t) = e^{-\frac{iVt}{2}} \left\{ \cos\left(\frac{\xi t}{2}\right) + \frac{2iV}{\xi} \sin\left(\frac{\xi t}{2}\right) \right\}. \tag{11.38}$$

where we choose $V > 0$ by setting

$$R(t) = e^{-iVt} \left(e^{-i\tilde{H}t} \right)_{11}.$$

Expanding $C(t) = \log(R(t))$ one finds

$$\begin{aligned} C(t) &= -iVt + iVt - \frac{i}{2}Ut + \left(\frac{U}{V}\right)^2 \left(\frac{-1 + e^{-2iVt} + 2iVt}{16} \right) \\ &+ \left(\frac{U}{V}\right)^4 \left[\frac{5 - e^{-4iVt} - 4e^{-2iVt}}{512} - iVt \frac{1 + 2e^{-2iVt}}{128} \right] + O\left(\frac{U}{V}\right)^6. \end{aligned} \tag{11.39}$$

Using (4.125) we compute the time derivative and let the exponential die out as $t \rightarrow \infty(1 - i\eta)$; we obtain, in agreement with the exact solution,

$$W_0 = -V + \frac{U}{2} - \frac{U^2}{8V} + \frac{U^4}{128V^3} + O(U^6) \quad (11.40)$$

11.2.2 H_2 Model

As a further example, we shall use the H_2 model of Sect. 1.2.5.

$$ig_{aa}(t) = \frac{1}{2} \{-\theta(-t)e^{it_h t} + \theta(-t)e^{-it_h t}\} \quad (11.41)$$

From (4.37) one gets

$$ig_{a,a} = ig_{b,b} = \frac{1}{2} [e^{-it_h t} \theta(t) - e^{it_h t} \theta(-t)],$$

$$ig_{a,b} = ig_{b,a} = -\frac{1}{2} [e^{-it_h t} \theta(t) + e^{it_h t} \theta(-t)].$$

The net second-order contribution comes from only 11.3 d). It is

$$4 * (-iu)^2 \int_0^t dt_1 \int_0^{t_1} dt_2 [g_{a,a}(t_2 - t_1)g_{a,a}(t_1 - t_2)]^2$$

$$= u^2 \left[\frac{it}{16t_h} - \frac{1 - e^{-4it_h t}}{64t_h^2} \right] \quad (11.42)$$

where a factor 4 comes from the fact that each interaction line can be labeled a or b indifferently. The diagrams 11.3 b) and c) vanish because the terms with the like interaction lines are canceled by those on interactions on different atoms. In third-order there is no contribution because shifting any vertex from an electron to a hole line changes sign to the diagram. For the same reason, there is considerable cancelation in fourth order, the only surviving terms being the one of Figure (11.2.2) and the one which results from the exchange of t_3 and t_4 . Direct calculation shows that

$$C(t) = 2it_h t - \frac{itu}{2} + u^2 \left[\frac{it}{16t_h} - \frac{1 - e^{-4it_h t}}{64t_h^2} \right]$$

$$+ \frac{u^4}{t_h^4} \left\{ + \frac{5 - e^{-8it_h t}}{8192} - \frac{itt_h}{1024} - \frac{e^{-4it_h t}}{2048} - itt_h \frac{e^{-4it_h t}}{512} \right\}. \quad (11.43)$$

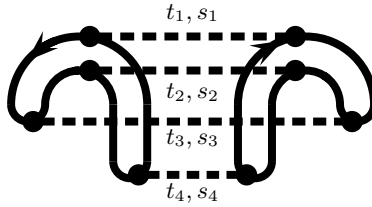


Fig. 11.6. One of the fourth-order diagrams that contribute to $R(t)$ for the Hubbard H_2 model. The interaction lines are labeled with time and site ($s_i = a$ or b) indices.

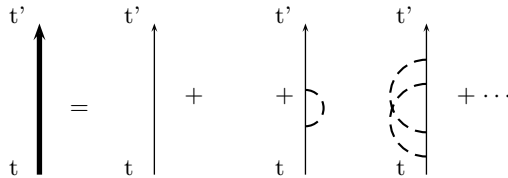


Fig. 11.7. Contributions to the core propagator

11.2.3 The Linked Cluster Expansion and Green’s Functions

The Lundqvist model[38]

$$H = \epsilon c^\dagger c + \sum_q \omega_q a_q^\dagger a_q + cc^\dagger \sum_q g_q (a_q + a_q^\dagger) \tag{11.44}$$

has been used to discuss plasmon effects in core photoelectron spectra. The removal of the core electron shifts the plasmon coordinates and the density of states relevant to the spectrum is obtained from the correlation function

$$N(\omega) = \int_{-\infty}^{\infty} \frac{d\omega}{2\pi} e^{i\omega t} \langle \psi_+ | c^\dagger(0) c(t) | \psi_+ \rangle, \tag{11.45}$$

where ψ_+ is the plasmon vacuum with the core electron present. $N(\omega)$ is obtained from the core propagator

$$g(t) = -i \langle \psi_+ | T c(t) c^\dagger(0) | \psi_+ \rangle. \tag{11.46}$$

By expanding the propagator as above we generate diagrams where the boson propagator (4.64) $iD_{\mathbf{k}}(t) = \exp[-i\omega_{\mathbf{k}}|t|]$ appears; each electron-plasmon vertex contributes a factor ig_q ; plasmon lines ($iD_q(t)$ factors) may be emitted and adsorbed any number of times according to any pattern.

Langreth[39] noted that $g^{(0)}(t-t')$ is a simple phase factor for $t < t'$ while $g^{(0)}(t-t') \equiv 0$ for $t > t'$; thus the ascending time line must be labeled t at the bottom and t' at the top. From each diagram one can collect the same phase factor: $\prod g^{(0)}(t_i - t_j) = g^{(0)}(t - t')$. Hence, $g(t - t') = g^{(0)}(t - t')\gamma(t - t')$. Erasing the deep hole propagator from the diagrams for g we find those for γ , a succession of interaction lines ordered in a particular way; one can classify these diagrams as linked and unlinked. Repeating the above argument one finds that Linked Cluster Theorem applies,

$$g(t - t') = g^{(0)}(t - t')e^{C(t-t')}, \quad (11.47)$$

where C is the only unlinked diagram, namely the second-order one: a boson is emitted at time $t_2 > t$ and later re-adsorbed at $t_1 < t'$. Hence,

$$C(t - t') = \sum_q (ig_q)^2 \int_t^{t'} dt_1 \int_t^{t_1} dt_2 D_q(t_1 - t_2). \quad (11.48)$$

and one achieves the exact solution⁵

$$\begin{aligned} C(-t') &= \sum_q (ig_q)^2 \int_0^{t'} dt_1 \int_0^{t_1} dt_2 e^{-i\omega_q(t_1-t_2)} \\ &= - \sum_q g_q^2 \frac{1 - i\omega_q t' - e^{-i\omega_q t'}}{\omega_q^2}. \end{aligned} \quad (11.49)$$

In addition, the Linked Cluster Theorem has been invoked as an *ansatz* which is useful for special problems[40], [41]. The idea is simple. Start with the ansatz (11.47) and expand both sides in powers of the interaction using the cumulant expansion

$$\exp\left[\sum_1^\infty a_n x^n\right] = 1 + a_1 x + \left(\frac{a_1^2}{2} + a_2\right)x^2 + \left(\frac{a_1^3}{3!} + a_1 a_2 + a_3\right)x^3 + \dots$$

From a few diagrams for g that one can compute directly we can obtain an equal number of a_n coefficients that perform a particular infinite re-summation of the series.

11.3 Diagrams for the Dressed Propagator

The time-ordered propagator (4.20) averaged over the interacting ground state or over the grand-canonical ensemble lends itself to a perturbation expansion. In this section we consider in detail the zero temperature case, using

⁵This agrees with Equations (6.30-6.31) taking into account that there the Fourier transform involved $e^{-i(\omega+H)t}$ and here we are using $e^{i(\omega+H)t}$ instead.

a slightly lighter, discrete notation and the fact that for time-independent problems the dependence is on a single time, namely, $t = t_1 - t_2$. In the non-interacting problem with Hamiltonian H_0 , the propagator is

$$g^0(a, b, t) = -i \langle \Phi | T \left[c_a(t) c_b^\dagger(0) \right] | \Phi \rangle, \quad (11.50)$$

where $|\Phi\rangle$ is the ground state and c_b^\dagger creates an electron in a single-particle state $|b\rangle$. We know that g^0 is diagonal on the basis of the H_0 eigenstates and is Green's function of the Schrödinger equation; moreover,

$$g^0(k, k', \omega) = \frac{\delta_{kk'}}{\omega - \varepsilon_k + i\eta_k} \equiv \delta_{kk'} g^0(k, \omega), \quad (11.51)$$

with $\eta_k = +0$ for empty states, $\eta_k = -0$ for filled ones.

With $H = H_0 + V$, where V is the interaction, the propagator is

$$ig(a, b, t) = \langle \Psi_0 | T \left[c_a(t) c_b^\dagger(0) \right] | \Psi_0 \rangle \quad (11.52)$$

averaged over the unknown **interacting** ground state, and the operators are in the Heisenberg Picture. We use the standard definition (2.12) for the Heisenberg operators but switch to the interaction picture, using (2.39)

$$A_H = U_I^\dagger(t, t_0) A_I(t) U_I(t, t_0),$$

in order to obtain g from an infinite order series expansion of the evolution operator in powers of V :

11.3.1 Adiabatic Switching and Perturbation Theory

To obtain g we do not really need Ψ_0 , as the definition seems to suggest. We can resort to the trick of the adiabatic switching of V . Here we assume⁶ a time-independent H and write

$$U_I(t_1, t_2) = U_I(t_1, 0) U_I(t_2, 0)^\dagger = e^{iH_0 t_1} e^{-iH(t_1 - t_2)} e^{-iH_0 t_2} \quad (11.53)$$

Assume that at time $t = t_0$ in the remote past the system was in the unperturbed ground state $|\Phi\rangle$, with energy eigenvalue W_0 ; then at time 0 the interaction picture state is a wave packet containing $|\Psi_0\rangle$:

$$U_I(0, t_0) |\Phi\rangle = e^{iH t_0} e^{-iH_0 t_0} |\Phi\rangle = e^{-iW_n t_0} \sum_n |\Psi_n\rangle \langle \Psi_n | e^{iE_n t_0} |\Phi\rangle \quad (11.54)$$

For $t_0 \rightarrow -\infty$ we can distil from it the interacting ground state by shifting the path in the complex t plane with a small tilt setting $t \rightarrow t(1 - i\eta)$, $\eta = 0^+$. In this way, among the exponentials

⁶The general case is presented in Chapter 13.

$$e^{iE_n t_0(1-i\eta)} = e^{iE_n t_0} e^{-\eta E_n |t_0|}, \quad (11.55)$$

the one of the ground state dominates, and one is left with

$$U_I(0, t_0) |\Phi\rangle = |\Psi_0\rangle \langle \Psi_0 | e^{iE_0 t_0} |\Phi\rangle e^{-iW_0 t_0} = |\Psi_0\rangle \langle \Psi_0 | U_I(0, t_0) |\Phi\rangle; \quad (11.56)$$

formally, (provided that the denominators do not vanish)

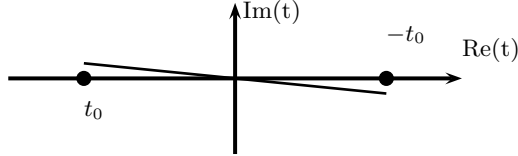


Fig. 11.8. The complex t plane with the tilted Gell-Mann and Low path.

$$|\Psi_0\rangle = \frac{U_I(0, t_0) |\Phi\rangle}{\langle \Psi_0 | U_I(0, t_0) |\Phi\rangle}, \quad \langle \Psi_0 | = \frac{\langle \Phi | U_I(-t_0, 0)}{\langle \Phi | U_I(-t_0, 0) |\Psi_0\rangle}. \quad (11.57)$$

This is the Gell-Mann and Low Theorem [83]⁷. Any expectation value $\langle \Psi_0 | A | \Psi_0 \rangle$ on the interacting ground state can be obtained from non-interacting ground state averages. One obtains:

$$\langle \Psi_0 | A | \Psi_0 \rangle = \frac{\langle \Phi | U_I(-t_0, 0) A U_I(0, t_0) |\Phi\rangle}{\langle \Phi | U_I(-t_0, 0) |\Psi_0\rangle \langle \Psi_0 | U_I(0, t_0) |\Phi\rangle}; \quad (11.58)$$

but along the tilted path, $|\Psi_0\rangle \langle \Psi_0 |$ is equivalent to $\sum_n |\Psi_n\rangle \langle \Psi_n |$; so

$$\langle \Psi_0 | A | \Psi_0 \rangle = \frac{\langle \Phi | U_I(-t_0, 0) A U_I(0, t_0) |\Phi\rangle}{\langle \Phi | U_I(-t_0, 0) U_I(0, t_0) |\Phi\rangle} = \frac{\langle \Phi | U_I(-t_0, 0) A U_I(0, t_0) |\Phi\rangle}{\langle \Phi | U_I(-t_0, t_0) |\Phi\rangle}. \quad (11.59)$$

We take advantage to set the propagator in this form. Consider g for $t > 0$, $\text{ig}(a, b, t) = \langle \Psi_0 | c_a(t) c_b^\dagger(0) | \Psi_0 \rangle$ with Heisenberg operators. In order to use the T exp expansion we must go over to the interaction picture⁸ with $c_{aH}(t) = U_I^\dagger(t, 0) c_a(t) U_I(t, 0)$, hence

⁷The original proof reported by Ref. [2] is based on the perturbation series, so it depends on its validity; also, it shows that numerators and denominators bear a phase factor that diverges in the adiabatic limit.

⁸Recall that with our convention the Schrödinger, Heisenberg and interaction wave functions coincide at $t = 0$ and that at any other time the change of representation is obtained by $\langle A(t) \rangle = \langle \Psi_I(0) | A_H(t) | \Psi_I(0) \rangle = \langle \Psi_I(0) | U_I(0, t) A_I(t) U_I(t, 0) | \Psi_I(0) \rangle$.

$$\begin{aligned}
 ig(a, b, t) &= \langle \Psi_0 | U_I^\dagger(t, 0) c_a(t) U_I(t, 0) c_b^\dagger(0) | \Psi_0 \rangle \\
 &= \frac{\langle \Phi | U_I(-t_0, 0) U_I^\dagger(t, 0) c_a(t) U_I(t, 0) c_b^\dagger(0) U_I(0, t_0) | \Phi \rangle}{\langle \Phi | U_I(-t_0, t_0) | \Phi \rangle}, \quad t > 0. \quad (11.60)
 \end{aligned}$$

Using the Group property of U , the unitarity property $U_I^\dagger(t, 0) = U_I(0, t)$, and the fact that under T the fermion operators anticommute, we shall manoeuvre to obtain a single U in the numerator as well:

$$ig(a, b, t) = \frac{\langle \Phi | U_I(-t_0, 0) U_I(0, t) c_a(t) U_I(t, 0) c_b^\dagger(0) U_I(0, t_0) | \Phi \rangle}{\langle \Phi | U_I(-t_0, t_0) | \Phi \rangle}, \quad t > 0. \quad (11.61)$$

In other terms,

$$ig(a, b, t) = \frac{\langle \Phi | U_I(-t_0, t) c_a(t) U_I(t, 0) c_b^\dagger(0) U_I(0, t_0) | \Phi \rangle}{\langle \Phi | U_I(-t_0, t_0) | \Phi \rangle}, \quad t > 0. \quad (11.62)$$

More generally we can write ⁹, setting $\hat{S} = U_I(\infty, -\infty)$,

$$ig(a, b, t_1, t_2) = \frac{\langle \Phi | T[\hat{S} c_a(t_1) c_b^\dagger(t_2)] | \Phi \rangle}{\langle \Phi | \hat{S} | \Phi \rangle} \quad (11.63)$$

and expand in powers of V using the T exp formula (2.36). At each order one obtains a sum of partial amplitudes, involving V and the bare propagator g^0 ; these expressions are best handled when represented as diagrams. The key point is that different partial amplitudes give topologically inequivalent¹⁰ diagrams; at order n there is a finite set of possible topologies and all correspond to partial amplitudes. In all diagrams, an oriented g^0 line enters at a point b , goes through some *interaction vertices* and then reaches the exit point a . Between two interaction vertices, the propagator line is labeled by a spin-orbital: the one entering from outside will correspond to spin-orbital b and the outgoing one to a . Dotted *interaction lines* start at each vertex; at order n the diagram contains n interaction lines. A properly oriented and labeled propagator line must pass by every vertex; each graph presents a path which takes from b to a , and circuits attached to it (and possibly to other circuits) by interaction lines.

The denominator of Equation (11.63) is like the vacuum amplitude in (11.2) and yields all diagrams not connected to the main line; the only difference is that in (11.2) the interactions are between times 0 and t and here they can take place at any time. In the time representation (11.63), the mathematical expression or amplitude of a disconnected diagram consisting of two parts is the product of the two amplitudes. Therefore, we may

⁹We shall find the result (11.63) more in general in Equation (13.56).

¹⁰Two diagrams are topologically equivalent if they can be deformed with continuity to the same shape; in complex graphs this criterion requires a talent for the fine arts. I shall give a more practical prescription below.

write $\langle \Phi | T[\hat{S}c_a(t_1)c_b^\dagger(t_2)] | \Phi \rangle = \langle \Phi | T[\hat{S}c_a(t_1)c_b^\dagger(t_2)] | \Phi \rangle_L \langle \Phi | \hat{S} | \Phi \rangle$ where the L suffix means that only linked diagrams must be kept (no parts must be disconnected from the $b - a$ line). The denominator cancels with the unlinked diagrams and we are left with

$$ig(a, b, t_1, t_2) = \langle \Phi | T[\hat{S}c_a(t_1)c_b^\dagger(t_2)] | \Phi \rangle_L. \tag{11.64}$$

11.3.2 Diagrams for the Propagator in frequency space

The diagram rules will be derived in the Chapter 13, and can be verified by working out low-order terms from the T exp formula (2.36). I present the Feynman method in frequency space, that is, the expansion of the interacting time-ordered $g_{ab}(\omega)$ in terms of $g_{ab}^{(0)}(\omega)$ and interaction vertices; the interaction is a two-body operator (typically, the Coulomb potential). We must label

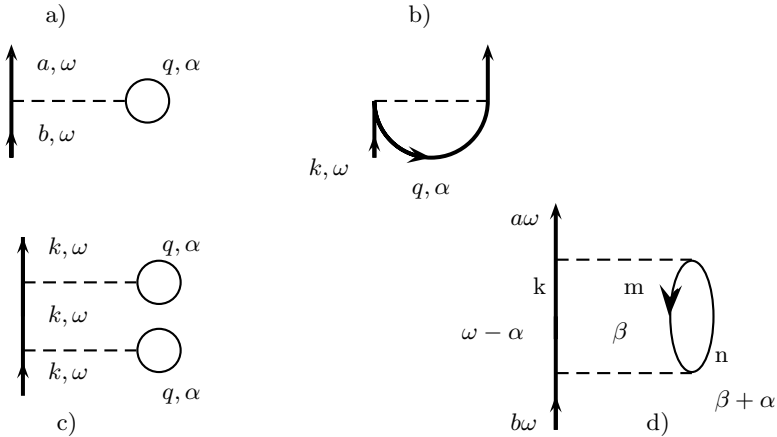


Fig. 11.9. Diagrams for g : a) and b) exhaust the first order, c) and d) are second-order contributions.

the g^0 lines and the interaction lines by frequencies such that a and b have frequency ω and at all vertices the sum of ingoing frequencies equals the sum of outgoing ones. When momentum or crystal momentum are also good quantum numbers (translationally invariant or periodic systems) four-momentum is conserved at each vertex. must pay attention to avoid double counting. To see if two diagrams with an apparent correspondence between the vertices are indeed topologically equivalent, one can start considering a path on one diagram and the corresponding path on the other. If one meets the corresponding points in the same order in both diagrams, and this remains true

$$\sum_{\mathbf{q}} \int_{-\infty}^{\infty} \frac{d\omega}{2\pi} ig^0(\mathbf{q}, \omega) = i \sum_{\mathbf{q}} g^0(\mathbf{q}, t=0). \quad (11.67)$$

Since

$$ig^0(\mathbf{q}, t) = \langle 0 | T [c_{\mathbf{q}}(t) c_{\mathbf{q}}^{\dagger}(0)] | 0 \rangle, \quad (11.68)$$

is discontinuous, we introduce the *equal-times rule*

$$\langle T c_{\mathbf{q}}^{\dagger}(\tau) c_{\mathbf{q}}(\tau) \rangle = \langle c_{\mathbf{q}}^{\dagger}(\tau_+) c_{\mathbf{q}}(\tau_-) \rangle \quad (11.69)$$

where τ_+ is just after τ and τ_- just before. The transform must be taken for $t = 0^-$ (the non-propagating lines simply have no time to propagate). Since

$$ig^0(\mathbf{q}, t = 0^-) = -n_{\mathbf{q}}^{(0)},$$

where $n_{\mathbf{q}}^{(0)}$ is the unperturbed occupation number, the result is $-\sum_{\mathbf{k}} n_{\mathbf{k}}^{(0)}$. Including a $(-)$ for the circuit, the tadpole yields $+\sum_{\mathbf{q}} n_{\mathbf{q}}^{(0)} \dots$, which is ready for inserting the q dependence of the interaction vertex. Let us see the first-order diagram (Figure (11.3.2), a)) and its value $\mathcal{D}[a]$: one obtains

$$\mathcal{D}[a] = ig^0(\mathbf{a}, \omega) ig^0(\mathbf{b}, \omega) \left[(-i) \sum_{\mathbf{k}} V_{\mathbf{a} \mathbf{k} \mathbf{b} \mathbf{k}} n_{\mathbf{k}}^0 \right]. \quad (11.70)$$

If k stands for a one-electron wave-vector which is conserved in the absence of interactions, the matrix element $V_{\mathbf{a}, \mathbf{k}, \mathbf{b}, \mathbf{k}}$ brings a $\delta(\mathbf{a}, \mathbf{b})$ factor (the tadpole cannot exchange energy and momentum). In first-order there is also the exchange diagram (Figure (11.3.2), b)) which is obtained by exchanging the outgoing interaction lines. The $(-)$ sign must not be inserted; the arc is a non-propagating line; one obtains

$$\mathcal{D}[b] = ig^0(\mathbf{a}, \omega) ig^0(\mathbf{b}, \omega) \sum_{\mathbf{k}} \int_{-\infty}^{\infty} \frac{d\alpha}{2\pi} ig^0(\mathbf{k}, \alpha) (-i) V_{\mathbf{k} \mathbf{a} \mathbf{b} \mathbf{k}}. \quad (11.71)$$

(11.3.2), c)) shows a second-order diagram with a couple of tadpoles inserted into a propagating line. In this case,

$$\mathcal{D}[c] = \mathcal{D}[a] ig^0(\mathbf{k}, \omega) \left[(-i) \sum_{\mathbf{k}} V_{\mathbf{a} \mathbf{k} \mathbf{b} \mathbf{k}} n_{\mathbf{k}}^0 \right], \quad (11.72)$$

where the new term in parentheses may be identified with the added tadpole and the new ig^0 represents the new propagator piece.

So, we can calculate a subset of a diagram for later use, knowing that it will appear in many other diagrams and bring some type of process into play. As another example of the diagram rules, we calculate the pair bubble

that appears as an inset in the second-order diagram (11.3.2), d)). This is a prototype *polarization part*, that is, a graph that can be inserted into an interaction line; it will be useful later, and the big bubble unlike the tadpole does exchange energy and momentum.

$$-i\pi_0(\alpha) = (-1) \cdot 2 \cdot \sum_{m,n} \int \frac{d\beta}{2\pi} ig^0(m,\beta)ig^0(n,\beta + \alpha), \tag{11.73}$$

where the (-1) factor is due to the closed circuit and the 2 factor to the sum over the spins of the circuit. We start evaluating the bubble with the β integral

$$\int_{-\infty}^{\infty} \frac{d\beta}{2\pi} g^0(m,\beta)g^0(n,\beta + \alpha) = \int_{-\infty}^{\infty} \frac{d\beta}{2\pi} \frac{1}{\beta - \varepsilon_m + i\eta_m} \frac{1}{\beta + \alpha - \varepsilon_n + i\eta_n} \tag{11.74}$$

by the residue method. When the poles are on the same side of the real axis ($\eta_m\eta_n > 0$,) one closes the path on the other side and gets 0. Otherwise we integrate in the upper half plane, and there are two cases: a) n occupied and m empty b) m occupied and n empty. These represent respectively hole and electron propagation. One finds:

$$\int_{-\infty}^{\infty} \frac{d\beta}{2\pi} \frac{1}{\beta - \varepsilon_m + i\eta_m} \frac{1}{\beta + \alpha - \varepsilon_n + i\eta_n} = \begin{cases} \frac{-if_n[1-f_m]}{\alpha - \varepsilon_n + \varepsilon_m - i0} & \text{case a} \\ \frac{if_m[1-f_n]}{\alpha - \varepsilon_n + \varepsilon_m + i0} & \text{case b} \end{cases} \tag{11.75}$$

So, we end up with

$$-i\pi_0(\alpha) = 2 \cdot \sum_{m,n} \left[-i \frac{f_n(1-f_m)}{\alpha + \varepsilon_m - \varepsilon_n - i0} + i \frac{f_m(1-f_n)}{\alpha + \varepsilon_m - \varepsilon_n + i0} \right]. \tag{11.76}$$

It is already evident at this stage that as the number of interaction lines increases and progressively more complex diagrams arise the labor involved tends to increase in a prohibitive way, except for cases like the one shown in (11.72), when the complex diagrams arise as combinations of simple ones. Now, combining simple things to build structures is something that we may do by using ingenuity, while the most general graph at order n requires computing power. If the crucial physics is hidden in some monster-diagram that first appears at some high order, we have little hope to understand. However, no such cases are known, and ingenuity has been rewarding.

11.4 Dyson Equation

Like the Linked Cluster method, Dyson's leads to a summation to infinite order of selected classes of diagrams. A look to Figure 11.12 , where g with

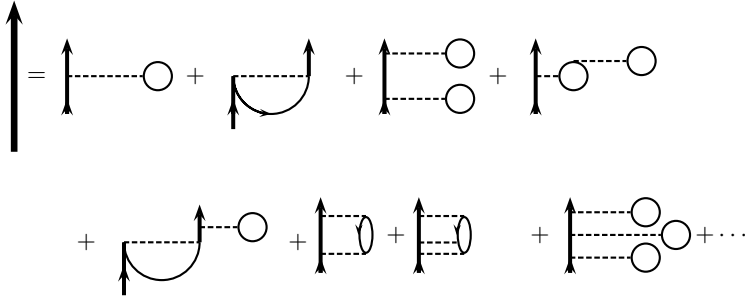


Fig. 11.12. Some of the lowest-order diagrams for g ; there are two kinds in first-order, but the variety grows with order in an impressive way.

the thick line, shows that as we proceed the number and complexity of the diagrams grows in an inordinate way. However, although normally we cannot obtain g exactly, we can use topology to make exact statements about g . All terms except the first have a factor $ig^{(0)}(a, \omega)ig^{(0)}(b, \omega)$, that is, an incoming and an outgoing line. The stuff in between is a *self-energy part*. The latter does not have external lines, but is usually drawn with short ones to show where they belong in the full diagram. Therefore the mathematical expression for the self-energy part is just the one for $ig^{(0)}$ divided by $ig^{(0)}(a, \omega)ig^{(0)}(b, \omega)$. Having computed a simple self-energy part, like the tadpole or the bubble, one can conceive iterating it indefinitely. The diagrammatic series is summed

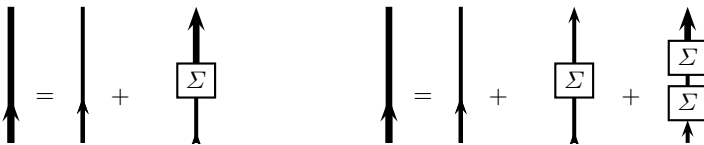


Fig. 11.13. Left: Dyson's equation. Right: iterative solution.

by writing the Dyson equation (Figure 11.13). The simplest approximation to Σ includes in g the repeated scattering of the simplest type any number of times; any approximation is a partial re-summation of the series to infinite order. We can also sum two different self-energy parts, e.g. tadpole + bubble, and the iteration will give all sorts of diagrams in which such insertions occur in any sequence; all such diagrams will occur once. However, if we iterate a diagram showing a bubble followed by a tadpole we miss all the diagrams where two consecutive bubbles (or tadpoles) occur. To avoid missing diagrams in this silly way it is important to use **irreducible self-energy** Σ . A self-

energy part is called **reducible** if it can be split into two diagrams by cutting a single propagator. The left diagram in Figure(11.4) is reducible, the right one is not.

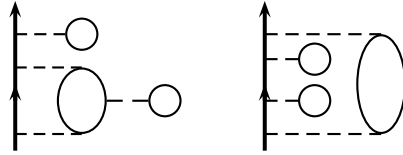


Fig. 11.14. Reducible (left) self-energy part and irreducible (right) self-energy parts.

The Irreducible (or proper) Self-Energy $\boxed{\Sigma}$ is the sum of all the irreducible self-energy parts. The analytic expression of $\boxed{\Sigma}$ is $-i\Sigma(\omega)$, and the function Σ is also called self-energy. The first-order self-energy part reads:

$$(-i)\Sigma^{(1)} = (-i) \left[\sum_k V_{a k b k} n_k^0 - \sum_k V_{k a b k} n_k^0 \right]. \tag{11.77}$$

The Dyson equation yields the exact diagrammatic expansion of the green's function if the exact $\boxed{\Sigma}$ is known. Indeed, each diagram containing whatever insertions in $\boxed{\Sigma}$ any number of times in any order comes out of by the iteration of Figure 11.13 exactly once. Figure 11.13 reads:

$$ig = ig^0 + ig^0(-i\Sigma)ig \Rightarrow g = g^0 + g^0 \Sigma g; \iff g = g^0 + g \Sigma g^0; \tag{11.78}$$

with $x = (\mathbf{r}, t)$ and $\int dx = \int d^3\mathbf{r}dt$, these are

$$g(x, x') = g_0(x, x') + \int dx_1 dx_2 g_0(x, x_1) \Sigma(x_1, x_2) g(x_2, x') \tag{11.79}$$

$$g(x, x') = g_0(x, x') + \int dx_1 dx_2 g(x, x_1) \Sigma(x_1, x_2) g_0(x_2, x').$$

In analogy with (10.7) we can rewrite Dyson's equation in differential form. This analogy will be exploited in Section 11.8. Since the noninteracting $g^{(0)}$ obeys

$$\left\{ i\hbar \frac{d}{dt_1} - H_0(1) \right\} g^{(0)}(1; 1') = \delta(11') \tag{11.80}$$

by applying $\left\{ i \frac{d}{dt_1} - H_0(1) \right\}$ we obtain

$$\left[i \frac{\partial}{\partial t} - H_0(x) \right] g(\mathbf{x}, \mathbf{x}') - \int dx_1 \Sigma(x, x_1) g(x_1, x') = \hbar \delta(x - x'). \tag{11.81}$$

The solution of Dyson's equation is simple when the symmetry is so high that g is diagonal on the basis of H_0 eigenstates. *Jellium* is a theorist's toy

metal; an infinite electron system with a uniform neutralizing background of positive charge. Both g_0 and g are diagonal on a plane-wave basis, and the scalar Dyson's equation yields

$$g(\mathbf{k},\omega) = \frac{1}{\omega - \varepsilon^0(\mathbf{k}) - \Sigma(\mathbf{k},\omega)}; \tag{11.82}$$

thus Σ can be thought of as a complex correction to the energy eigenvalue. The Dyson equation leads to the notion of a *quasi-particle*; as far as g is concerned, the many-body interactions can be summarized in a self-energy correction to the one-body dispersion, leading to a useful picture of an effective, modified or dressed electron moving around. One can produce many-body states that behave like a *quasi-electron* or a *quasi-hole* added to the system, although the imaginary part of Σ eventually damps the single-particle character and redistributes the energy. In this way some of the simplicity of the independent-electron picture is retained; moreover, the independent-electron model is partly validated; thus one understands the fact that band-structure calculations and the Sommerfeld theory are useful in many cases although electrons are far from being independent.

11.4.1 External Potential

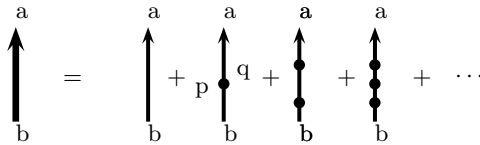


Fig. 11.15. Propagator in external potential (big dot).

For non-interacting electrons in an external potential the diagram rules are similar. The series is shown in Figure 11.15 where the heavy oriented line is $ig(a, b, \omega)$, the light one represents

$$ig^0(a, b, \omega) = \frac{i\delta_{ab}}{\omega - \varepsilon_a + i\eta_a},$$

and the big dot between two lines, one ending with a label p and the second starting with label q stands for $-iV_{pq}$. In the Fano model one has only the V_{0k} matrix elements; to calculate the local Green's function $g_{00}(\omega)$ one can use two ways (see Figure 11.16).

$$g_{00}(\omega) = g_{00}^{(0)}(\omega) + g_{00}^{(0)}(\omega) \Sigma_{00}(\omega) g_{00}(\omega)$$



Fig. 11.16. Two ways to derive Σ for the Fano model: i) the Dyson equation for g_{00} ii) the Dyson equation for the g matrix.

One can write the Dyson equation using the self-energy i) for $g_{00}(\omega)$, which is ready for inserting $g_{00}^{(0)}$ lines; since

$$-i\Sigma(\omega) = \sum_k (-iV_{0k})ig_k^0(\omega)(-iV_{k0}) = -i \sum_k \frac{|V_{0k}|^2}{\omega - \varepsilon_k + i\eta_k} \tag{11.83}$$

we find back the self-energy of Chapter 5, but with the important inclusion of the Fermi level, where $Im\Sigma$ changes sign. The matrix Dyson equation

$$\vec{g} = \vec{g}^0 + \vec{g}^0 \Sigma \vec{g}$$

could be solved by matrix inversion, but it is simpler to write

$$g_{00} = g_{00}^0 + g_{00}^0 \sum_k V_{0k}g_{k0}(\omega),$$

$$g_{k0} = g_{kk}^0 V_{k0}g_{00} = \frac{V_{k0}}{\omega - \varepsilon_k + i\eta_k} g_{00}$$

In the alternative method ii) we are seeking a matrix self-energy, where one should insert not $g_{00}^{(0)}$ lines, but any two lines, which is readily solved.

Another interesting example occurs in the theory of resistivity of metals; the external potential is due to impurities. At second and higher order, the self-energy is complex. One has the problem of calculating the Green's function and then averaging over a random impurity distribution; however, in the dilute case, repeated scattering against the same impurity dominates. The inverse quasi-particle lifetime $\frac{1}{\tau}$ is given by $Im\Sigma$; actually this can be taken as $\frac{1}{\tau}$ in Drude theory and is the dominant contribution to the resistivity at low temperature, while at higher T phonon scattering becomes important.

11.5 Self-Energy from Interactions

First-Order

Suppose we know the spin-orbitals $\{a, b, \dots\}$ that diagonalize the free-particle Hamiltonian H_0 and the Green's function $g^{(0)}$; we wish the Green's function

$g^{(1)}$ including the effects of the direct first-order Coulomb self-energy, i.e. the tadpole (see Fig. 11.5a)). The self-energy is a matrix with elements (from Equation 11.77) $\Sigma_{ab}(\omega) = \sum_k V_{akbk} f_k^{(0)}$, that is,

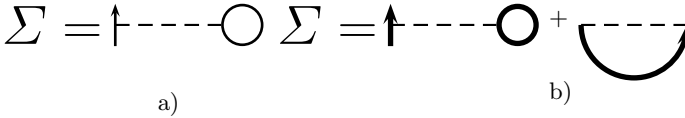


Fig. 11.17. a) Direct Hartree self-energy b) Hartree-Fock self-energy.

$$\Sigma_{ab}(\omega) = \sum_k f_k^{(0)} \int d^3r d^3r' \frac{a(r)^* k(r')^* b(r) k(r')}{|r - r'|}. \quad (11.84)$$

$\Sigma_{ab}(\omega) = W_{ab}^{(0)}$ is just the ab matrix element of an effective potential

$$W^{(0)}(r) = \int dr' \frac{\sum_k f_k^{(0)} |k(r')|^2}{|r - r'|}; \quad (11.85)$$

but this is nothing else than the electrostatic potential produced by the tadpole charge density. Had we considered non-interacting electrons in an effective external potential $W^{(0)}(r)$, we should have obtained the same Σ_{ab} . Note that Σ_{ab} includes the effects of $W^{(0)}(r)$ exactly, as if we had found the eigenstates $\{a^{(1)}, b^{(1)}, \dots\}$ of $H_0 + W^{(0)}(r)$ and computed the new Green's function $g^{(1)}$, taking the matrix elements in the old basis $\{a, b, \dots\}$. We can still improve the approximation using just the tadpole, but this time with $g^{(1)}$. The new correction $\Sigma_{ab}^{(1)}$ can then be interpreted as if the electrons did not interact, but moved in an additional potential $W^{(1)}(r)$. By iterating the argument, one reaches the self-consistency, as shown in Fig. 11.5b) where the exchange term has also been included, and the internal propagators are dressed, renormalized, fully interacting propagators, shown as the thick lines. This corresponds to the Hartree-Fock approximation. Hence, if one starts with the Hartree-Fock basis as $\{a, b, \dots\}$ the series for Σ starts with the second order.

Second-Order

The proper $\Sigma^{(2)}$ has two diagrams (direct and an exchange).

The direct one is shown in Figure 11.18 a). It is convenient to introduce the pair bubble (11.114), and to write:

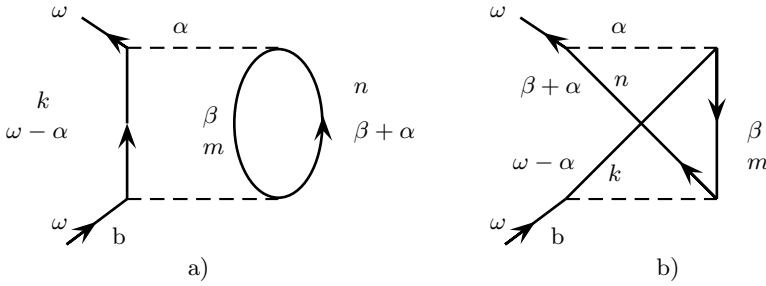


Fig. 11.18. Second-order self-energy: a) direct b) exchange

$$-i\Sigma(\omega) = \int \frac{d\alpha}{2\pi} i g^0(k, \omega - \alpha) (-iV_{knbm}) (-iV_{amkn}) (-i\pi_0(\alpha)) \quad (11.86)$$

The calculation is an exercise in contour integration similar to the calculation of the bubble, and the contribution of Equation (11.76) to (11.86) is

$$-i \sum_{k,m,n} f_n [1 - f_m] V_{knbm} V_{amkn} \int \frac{d\alpha}{2\pi} \frac{1}{\omega - \alpha - \epsilon_k + i\eta_k} \frac{-i}{\alpha - \epsilon_n + \epsilon_m - i0}.$$

Again, we get zero unless the poles $\alpha = \epsilon_n - \epsilon_m + i0$ and $\alpha = \omega - \epsilon_k + i\eta_k$ are on opposite subplanes, which requires $\eta_k < 0$, that is, k must be occupied; the pole in the upper half plane comes from the second factor and yields the contribution $-i \sum_{klm} \frac{f_k f_n (1 - f_m) V_{knbm} V_{amkn}}{\omega + \epsilon_m - \epsilon_n - \epsilon_k - i\eta_m}$. Adding the second contribution with m filled and k, n empty,

$$\Sigma_{ab}(\omega) = \frac{\sum_{m,k,n} [(1 - f_m) f_k f_n + f_m (1 - f_k) (1 - f_n)] V_{knbm} V_{amkn}}{\omega - \epsilon_n + \epsilon_m - \epsilon_k - i\eta_m} \quad (11.87)$$

To get the exchange term from Figure 11.18 a) one cuts the lines raising from the bottom vertices and exchanges their upper ends, labeling in such way that the exchange is done in the upper interaction resulting in $V_{amkn} \rightarrow V_{amnk}$. The value of the diagram is obtained from (11.86) by $V_{amkn} \rightarrow -V_{amnk}$, (no closed circuit any more). Thus, the total second-order self-energy is:

$$\Sigma_{ab}^{(2)}(\omega) = \sum_{m,k,n} [(1 - f_m) f_k f_n + f_m (1 - f_k) (1 - f_n)] \times \frac{V_{knbm} [V_{amkn} - V_{amnk}]}{\omega - \epsilon_n + \epsilon_m - \epsilon_k - i\eta_m}. \quad (11.88)$$

Unlike the first-order result, this correction is beyond Hartree-Fock, complex and ω -dependent. Starting from Hartree-Fock, we now obtain corrections to Koopman ionization potentials and electron affinities and lifetimes without resorting to the often prohibitive Configuration-Interaction computations. This is very useful in atomic and molecular calculations [4]. Typically the corrections are of the order of 1 eV.

11.6 Skeleton Diagrams

We can do better for free (no other diagrams to compute) by considering the self-energy of Figure 11.19. where the heavy lines are dressed propagators. This is *self-consistent perturbation theory*, in analogy with the diagrammatic version of the Hartree-Fock approximation (by the way, no tadpoles and no open-oysters appear, since we assume that the self-consistent potential is our one-body potential). This procedure is equivalent to a summation to infinite

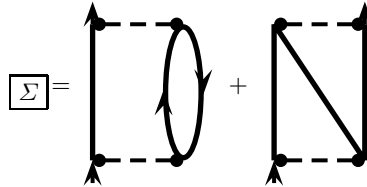


Fig. 11.19. By expanding the right-hand side, one finds an infinite series of self-energy corrections.

order of a series of more and more complex self-energy diagrams, and can simplify enormously the task of summing the most relevant parts of the series for Σ .

Skeleton diagrams are those with no self-energy insertions. Since all the internal propagators are dressed, to avoid double counting only skeleton diagrams are allowed. A few skeleton diagrams can replace an infinity of self-energy ones, if the self-consistency can be carried out by numerical iteration. This can be a very good solution, depending on the choice of skeletons.

11.7 Two-body Green's Function: the Bethe-Salpeter Equation

One can perform a Dyson type analysis on the series for the two-particle Green's function G_2 (10.3). Working in the time representation, we sort out the direct and exchange contributions to G_2 consisting of diagrams with only self-energy insertions. In obvious shorthand notation,

$$G_2(1, 2, 3, 4) = ig(3, 1)g(4, 2) - ig(3, 2)g(4, 1) + \int d5d6d7d8ig(3, 5)ig(7, 1)ig(4, 6)ig(8, 2)\gamma(5, 6, 7, 8), \quad (11.89)$$

where γ is the *scattering amplitude*. The corresponding diagrammatic equation is shown in Figure 11.20. γ is the sum of all two-body diagrams such that each ingoing line starts with an interaction, and each outgoing line leaves an interaction. Internal lines can have all sorts of self-energy insertions.

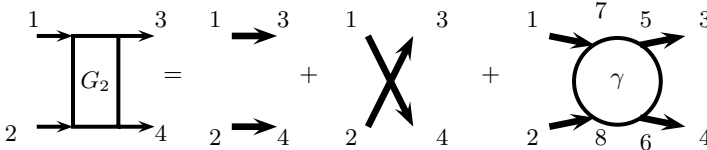


Fig. 11.20. The two-body Green’s function G_2 and the scattering amplitude γ . The dressed incoming and outgoing lines belong to G_2

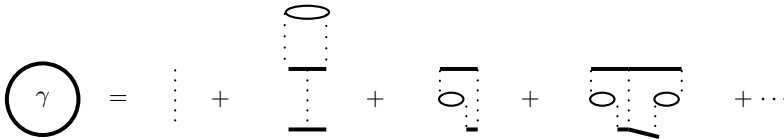


Fig. 11.21. γ is the scattering amplitude; the heavy lines represent dressed propagators, the first two diagrams shown are irreducible, the other two are not; J the irreducible scattering amplitude.

In γ one can separate out the *irreducible interaction* diagrams, that cannot be split in two by cutting only two dressed lines; let J denote their sum. All terms in γ can be obtained by iteration from those of J , and this enables us to write down a Dyson-like equation for γ .

Finally, the whole series is obtained from the Bethe-Salpeter equation

$$G_2(1234) = g(31)g(42) - g(32)g(41) + \int d5d6d7d8J(5678)ig(35)ig(46)G_2(7812) \quad (11.90)$$

which is shown in Figure 11.23.



Fig. 11.22. γ is obtained by iterating J .

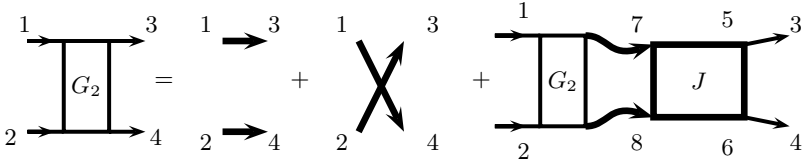


Fig. 11.23. The Bethe-Salpeter equation for the two-body Green's function.

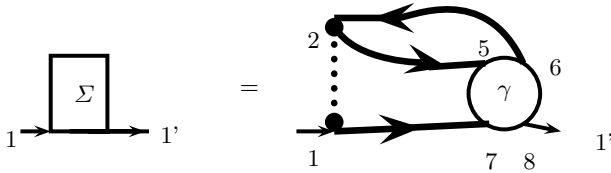


Fig. 11.24. The relation of the self-energy to the scattering amplitude. Replacing γ by its diagrammatic expansion one gets the expansion for Σ . This differs from Ref. [116], Chapter 10.6, since we assume that the Hartree-Fock approximation is embodied in our bare propagator.

11.8 Self-Energy and Two-Body Green's Function

Let us rewrite the equation of motion (10.7),

$$\left\{ i \frac{\partial}{\partial t_1} - H_0(1) \right\} g(1; 1') = \delta(11') - i \int d2v(1, 2)G_2(1; 2|2^+; 1') \quad (11.91)$$

where H_0 is the non-interacting Hamiltonian. We compare with the Dyson equation (11.81)

$$\left[i \frac{\partial}{\partial t_1} - H_0(1) \right] g(1, 1') - \int d2\Sigma(1, 2)g(1, 1') = \hbar\delta(1, 1'). \quad (11.92)$$

Σ is a non-local potential that can have some local contribution (proportional to $\delta(\mathbf{r} - \mathbf{r}')$), so there is some freedom in the definition of Σ . One can decide to include the Hartree potential $V_H(x)$ due to the charge $-ig(x, x^+)$ as a local part of Σ or as a potential in $H_0(x)$. We shall write the one-body term in both the above equations as $H_0(x) + V_H(x)$, where the second term actually comes from the local part of Σ . Thus,

$$\left[i\frac{\partial}{\partial t_1} - H_0(1) - V_H(1)\right]g(1, 1') = \delta(1, 1') + \int d2\Sigma(1, 2)g(2, 1'). \quad (11.93)$$

We find

$$\int d2[V_H(1)\delta(1, 2) + \Sigma(1, 2)]g(2, 1') = -i\hbar \int d2v(1, 2)G_2(1, 2|2^+, 1'). \quad (11.94)$$

We have obtained Σg , not just Σ , since G_2 comprises the incoming and outgoing legs; a formal relation between self-energy and two-body function is obtained by amputating the outgoing one, that is,

$$\Sigma(1; 1') + V_H(1)\delta(1, 1') = -i\hbar \int d2d3v(1, 2)G_2(1, 2|2^+, 3)g^{-1}(3; 1') \quad (11.95)$$

where g^{-1} is the inverse of g in the matrix sense.

It is clear that the approximations for the two-body function and for the self-energy cannot be chosen independently. The relation to the scattering amplitude is given by the figure 11.23.

11.9 Functional Calculus and Diagrams

Given a functional F which depends on a function $\varphi(x)$, one defines the functional derivative¹¹

$$\frac{\delta F[\varphi(x)]}{\delta\phi(y)} = \frac{d}{d\eta}F[\varphi(x) + \eta\delta(x - y)]. \quad (11.96)$$

For instance, if $F[\varphi] = \int d^3x f(\varphi(\mathbf{x}), \nabla\varphi(\mathbf{x}))$, then it turns out that

$$\frac{\delta F}{\delta\varphi(x)} = \frac{\partial f}{\partial\varphi} - \nabla \frac{\partial f}{\partial\nabla\varphi}.$$

If we think of the integrals in discrete form, and the integrand does not depend on derivatives of φ , the functional derivative is just a partial derivative with respect to the value of φ in a particular space-time point. Functional differentiation is a powerful tool that we shall use in parallel with the diagrammatics. Functional derivatives with respect to the propagator g are particularly easy because they undo the integrations which are prescribed by the rules (see Figure 11.25.) This remark will be useful later.

¹¹We shall often use a 4-dimensional notation $x \equiv (\mathbf{x}, t)$ and write

$$\frac{\delta F[\varphi]}{\delta\varphi(x_3, t_3)} = \frac{d}{d\eta}F[\varphi(x, t) + \eta\delta(x - x_3)\delta(t - t_3)].$$

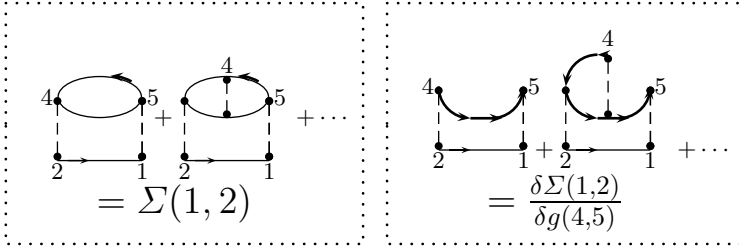


Fig. 11.25. Diagrammatic interpretation of the functional derivative.

11.9.1 The Self-Energy as a Functional

Functional derivatives also naturally arise for another reason. To study an interacting many-body system, one can introduce an external probe potential $\varphi(x, t)$ and look for a one-body response. The response arises from the dependence of the propagator g on small changes in the perturbation

$$H_1 = \int d\mathbf{x} \rho(\mathbf{x}) \varphi(\mathbf{x}, t) \tag{11.97}$$

where $\rho(\mathbf{x}) = \Psi^\dagger(\mathbf{x})\Psi(\mathbf{x})$ is the density operator. The most direct way to study the dependence of g on φ is through the functional derivative $\frac{\delta g(1,2)}{\delta \varphi(3)}$. Rewriting (11.63) in the form

$$ig(1,2) = \frac{\langle \Phi | T[\hat{S}\psi(1)\psi^\dagger(2)] | \Phi \rangle}{\langle \Phi | \hat{S} | \Phi \rangle}, \tag{11.98}$$

since $\langle \Phi | \hat{S} | \Phi \rangle = \lim_{\eta, \epsilon \rightarrow 0} U_I(\infty, t_3 + \epsilon) U_I(t_3 + \epsilon, t_3 - \epsilon) U_I(t_3 - \epsilon, -\infty)$, and $U_I(t_3 + \epsilon, t_3 - \epsilon) = 1 - \frac{i}{\hbar} \int_{t_3 - \epsilon}^{t_3 + \epsilon} H_1(\tau) d\tau + \dots$ one finds

$$\begin{aligned} \frac{\delta}{\delta \varphi(x_3)} \hat{S} &= \lim_{\eta, \epsilon \rightarrow 0} U_I(\infty, t_3 + \epsilon) \\ &\times \frac{\partial}{\partial \eta} \left[1 - \frac{i\eta}{\hbar} \int d\mathbf{x} \int_{t_3 - \epsilon}^{t_3 + \epsilon} dt \rho(x) \delta(x - x_3) \delta(t - t_3) \right] \\ &\times U_I(t_3 - \epsilon, -\infty) = \frac{-i}{\hbar} \hat{S} \rho(3), \end{aligned} \tag{11.99}$$

$$i \frac{\delta}{\delta \varphi(3)} g(1,2) = -\frac{i}{\hbar} \left[\frac{\langle \Phi | T S \rho(3) \psi(1) \psi^\dagger(2) | \Phi \rangle}{\langle \Phi | S | \Phi \rangle} - ig(1,2) \frac{\langle \Phi | T S \rho(3) | \Phi \rangle}{\langle \Phi | S | \Phi \rangle} \right]. \tag{11.100}$$

We may conclude that

$$i\hbar \frac{\delta g(1, 2)}{\delta \varphi(3)} = -iG_2(1, 3|3^+, 2) + ig(1, 2)g(3, 3^+). \quad (11.101)$$

This yields a new, useful link between g and G_2 , but we are interested in involving Σ . We multiply by $v(1, 3)$ and integrate over 3 (that is, over $d\mathbf{x}_3 dt_3$, of course). Since $-ig(3, 3^+) = \rho(3)$ is the density, we may introduce the Hartree potential $V_H(1) = \int d3v(1, 3)n(3)$ and write

$$i\hbar \int d3v(1, 3) \frac{\delta g(1, 2)}{\delta \varphi(3)} = -i \int d3v(1, 3)G_2(1, 3|3^+, 2) - V_H(1)g(1, 2). \quad (11.102)$$

Now replace 2 by 1' and 3 by 2. The result may be used again in (11.91)

$$\left\{ i \frac{\partial}{\partial t_1} - H_0(1) \right\} g(1; 1') = \delta(11') - i \int d2v(1, 2)G_2(1; 2|2^+; 1')$$

with φ added to H_0 , and yields

$$\left(i \frac{\partial}{\partial t_1} - H_0(1) - V_{eff}(1) \right) g(1, 1') = \delta(1, 1') + i\hbar \int d2v(1, 2) \frac{\delta g(1, 1')}{\delta \varphi(2)}; \quad (11.103)$$

here the screened potential $V_{eff}(1) = \varphi(1) + V_H = \varphi(1) + \int d3v(1, 3)\rho(3)$ appears.

Comparison with (11.93),

$$\left[i \frac{\partial}{\partial t_1} - H_0(1) - V_H(1) \right] g(1, 1') = \delta(1, 1') + \int d2\Sigma(1, 2)g(2, 1').$$

again with V_H changed to V_{eff} , yields

$$\int \Sigma(1, 3)g(3, 2)d3 = i\hbar \int v(1, 3) \frac{\delta g(1, 2)}{\delta \varphi(3)} d3 \quad (11.104)$$

where the instantaneous Coulomb potential v fixes $t_3 = t_1$. We can solve this for Σ , introducing the (matrix) inverse g^{-1} of g , such that

$$\int d3g(1, 3)^{-1}g(3, 2) = \int d3g(1, 3)g^{-1}(3, 2) = \delta(1, 2). \quad (11.105)$$

Differentiating (11.105) we obtain

$$\int \frac{\delta g^{-1}(1, 3)}{\delta \varphi(2)} g(3, 2)d3 = - \int g^{-1}(1, 3) \frac{\delta g(3, 2)}{\delta \varphi(2)} d3$$

and substituting in (11.104) we get

$$\frac{\delta g(1, 2)}{\delta \varphi(3)} = - \int d4d5g(1, 4) \frac{\delta g^{-1}(4, 5)}{\delta \varphi(3)} g(5, 2); \quad (11.106)$$

now the rhs has a comfortable g factor on the right. Hence, post-multiplying by g^{-1} we obtain the desired result

$$\Sigma(1, 6) = -i\hbar \int d(3, 4)v(1, 3)g(1, 4)\frac{\delta g^{-1}(4, 6)}{\delta\varphi(3)}. \tag{11.107}$$

11.9.2 Polarization Bubble

The dielectric function $\epsilon(\mathbf{x}, \mathbf{x}')$ is defined by the relation (using a notation with $x \equiv (\mathbf{r}, t)$, $\int dx \equiv \int d^3\mathbf{r}dt$),

$$\mathbf{D}(\mathbf{x}, t) = \int dx' \epsilon(\mathbf{x}, \mathbf{x}', t - t') \mathbf{E}(\mathbf{x}', t')$$

between displacement vector and electric field which holds in linear media. The external charges are the sources of \mathbf{D} ; hence, the effective potential $V_{eff}(\mathbf{r})$ due to an external source having bare potential φ is

$$V_{eff}(\mathbf{r}) = \int d\mathbf{r}' dt' \epsilon^{-1}(\mathbf{r}, t, \mathbf{r}', t') \varphi(\mathbf{r}', t'), \tag{11.108}$$

the inversion implied in the notation ϵ^{-1} is matrix inversion in the $\mathbf{r}, t, \mathbf{r}'$ indices. Hence, adopting a lighter notation,

$$\epsilon^{-1}(1, 2) = \frac{\delta V_{eff}(1)}{\delta\varphi(2)}. \tag{11.109}$$

In the microscopic theory,

$$V_{eff}(1) = \varphi(1) + \int d3 v(1, 3)\rho(3), \quad \rho(3) = -ig(3, 3^+) \tag{11.110}$$

where $v(1, 2)$ is the Coulomb interaction $v(x) = \frac{1}{r}\delta(t)$. When φ is produced by a point charge at $r_1(t)$, $V_{eff}(2)$ is the screened interaction $W(1, 2)$;

$$W(1, 2) = \int d3 \frac{\delta V_{eff}(2)}{\delta\varphi(3)} v(1, 3). \tag{11.111}$$

By a Dyson equation, one can determine the screened interaction W in terms of the bare (Coulomb) one v . In Figure 11.26 the light dotted line stands for $-iV$ and the bold dotted line stands for $-iW$. Therefore, W is



Fig. 11.26. The Dyson equation for the screened interaction W (heavy dashed line) in terms of the Coulomb interaction (light dashed line) and the full polarization propagator π .

determined by the polarization π according to Figure 11.26:

$$W(1, 2) = v(1, 2) - \int v(1, 3)\pi(3, 4)W(4, 2)d(3, 4). \tag{11.112}$$

Here, π is the sum of all the irreducible polarization parts that cannot be split by cutting a single V line. Since the series for $\pi(1, 2)$ is symmetric under a mirror reflection that exchanges 1 and 2, $\pi(2, 1) = \pi(1, 2)$, and also $W(2, 1) = W(2, 1)$; moreover the alternative form exists

$$W(1, 2) = v(1, 2) - \int d(74)W(1, 7)\pi(7, 4)v(4, 2). \tag{11.113}$$

The general structure of the diagrams for π (Figure 11.27) shows that it can be obtained from g and a vertex Γ :

$$\pi(1, 2) = -i\hbar \int g(2, 3)g(4, 2^+)\Gamma(341)d(34) \tag{11.114}$$

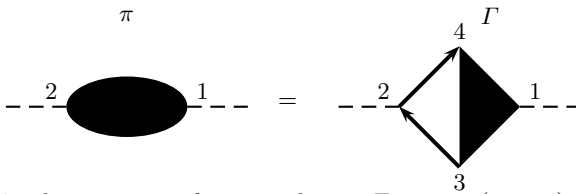


Fig. 11.27. the structure of π , according to Equation (11.114), showing the points where interaction lines can be inserted.

Any approximation for π yields the corresponding approximation to γ , and we shall give an exact expression for this in the next Section. A similar analysis can be done on the diagrams for Σ .

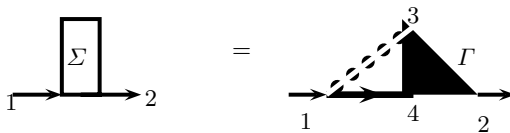


Fig. 11.28. The relation of the self-energy to the vertex function, after Equation (11.115).

A formal expression for Σ is:

$$\Sigma(1, 2) = i\hbar \int g(1, 4)\Gamma(4, 2; 3)W(1^+, 3)d(34) \quad (11.115)$$

in terms of the dressed interaction W and of the vertex Γ . The fact that the same function Γ indeed appears in the expressions for π and Σ will be apparent shortly.

11.9.3 The Vertex

We evaluate (11.111) and obtain a new form of Dyson's equation (11.113) for W , and a new π formula to compare with (11.114). Taking the functional derivative of (11.110) $V_{eff}(1) = \varphi(1) + \int d3v(1, 3)\rho(3)$, one finds

$$\frac{\delta V_{eff}(2)}{\delta \varphi(3)} = \delta(2, 3) - i\hbar \int d4 \frac{\delta g(4, 4^+)}{\delta \varphi(3)} v(2, 4).$$

Since (11.114) says that we want two g factors, we evaluate $\frac{\delta g(4, 4^+)}{\delta \varphi(3)}$ by the trick (11.106),

$$\frac{\delta g(4, 4^+)}{\delta \varphi(3)} = - \int d(56)g(4, 5) \frac{\delta g^{-1}(5, 6)}{\delta \varphi(3)} g(6, 4^+),$$

and then substitute into (11.111): this gives the screened interaction

$$\begin{aligned} W(1, 2) &= v(1, 2) + i\hbar \int v(1, 3)g(4, 5) \\ &\quad \frac{\delta g^{-1}(5, 6)}{\delta \varphi(3)} g(6, 4^+)v(2, 4)d(3456). \end{aligned} \quad (11.116)$$

The integral on the r.h.s. is a functional that begins with a bare interaction $v(1, 3)$ and ends with another bare $v(2, 4)$. If we aim at (11.113) we must convert the first to a screened interaction: we need to screen it by ϵ and we can if we screen φ as well. The correct way to do this is by changing the independent variable from the external to the effective potential via the *functional chain rule*

$$\frac{\delta}{\delta \varphi(3)} = \int d(7) \frac{\delta V_{eff}(7)}{\delta \varphi(3)} \frac{\delta}{\delta V_{eff}(7)} = \int d(7) \epsilon^{-1}(7, 3) \frac{\delta}{\delta V_{eff}(7)}. \quad (11.117)$$

This produces

$$\begin{aligned} W(1, 2) &= v(1, 2) + \int d(47)v(2, 4) \\ &\quad \underbrace{i\hbar \int d(56)g(4, 5)g(6, 4^+) \frac{\delta g^{-1}(5, 6)}{\delta V_{eff}(7)}}_{\int d3v(1, 3)\epsilon^{-1}(7, 3)}. \end{aligned} \quad (11.118)$$

Here the square brackets contain $W(1, 7)$ (see Equation 11.111); the result agrees with Equation (11.113) if the under-braced quantity is $\pi(7, 4)$:

$$\pi(7, 4) = \int d(56)g(4, 5) \frac{\delta g^{-1}(5, 6)}{\delta V_{eff}(7)} g(6, 4^+). \quad (11.119)$$

This yields the following expression for the vertex of Equation (11.114):

$$\Gamma(1, 2, 3) = -\frac{\delta g^{-1}(1, 2)}{\delta V_{eff}(3)}. \quad (11.120)$$

Using the solution to Problem 11.4,

$$g^{-1}(1, 2) = (i\frac{\partial}{\partial t} - H_0 - V_{eff}(1))\delta(1, 2) - \Sigma(1, 2), \quad (11.121)$$

we obtain the exact result

$$\Gamma(1, 2, 3) = \delta(1, 2)\delta(1, 3) + \frac{\delta \Sigma(1, 2)}{\delta V_{eff}(3)}. \quad (11.122)$$

We can re-derive Equation (11.115) for Σ in terms of the dressed interaction W and of the vertex Γ using (11.117) and (11.120) in (11.107).

11.10 Hedin's Equations

Hedin's equations fully determine g , in principle at least. Dyson's equation

$$g(1, 1') = g_0(1, 1') + \int d2d3g_0(1, 2)\Sigma(2, 3)g(3, 1') \quad (11.123)$$

requires the knowledge of Σ ; this is given by Equation (11.115), namely,

$$\Sigma(1, 2) = i\hbar \int g(1, 4)\Gamma(4, 2; 3)W(1^+, 3)d(34), \quad (11.124)$$

in terms of the screened interaction W and the vertex Γ . Equation (11.112)

$$W(1, 2) = v(1, 2) - \int v(1, 3)\pi(3, 4)W(4, 2)d(3, 4) \quad (11.125)$$

allows to calculate W if one knows the polarization π , which by Equation (11.114)

$$\pi(1, 2) = -i\hbar \int g(2, 3)g(4, 2^+)\Gamma(341)d(34) \quad (11.126)$$

again requires the vertex. To close the equations we have to find one for the vertex. To lowest order, $\Gamma(123) \approx \delta(1, 2)\delta(1, 3)$ (this is called the GW

approximation); Migdal proposed plausible arguments to show that the vertex corrections can be neglected to a good approximation in Jellium and weakly correlated solids. This *Migdal theorem* is often violated in strongly correlated systems, but Hedin found a rigorous equation for Γ . The starting point is Equation (11.122)

$$\Gamma(1, 2, 3) = \delta(1, 2)\delta(1, 3) + \frac{\delta\Sigma(1, 2)}{\delta V_{eff}(3)}. \quad (11.127)$$

The functional derivative is done via the chain rule

$$\frac{\delta\Sigma(1, 2)}{\delta V_{eff}(3)} = \int d(4, 5) \frac{\delta\Sigma(1, 2)}{\delta g(4, 5)} \frac{\delta g(4, 5)}{\delta V_{eff}(3)}.$$

By differentiating the identity $g^{-1}g = 1$ and left-multiplying by g one obtains the analogue of (11.106), namely,

$$\frac{\delta g(1, 2)}{\delta V_{eff}(3)} = - \int g(1, 4) \frac{\delta g^{-1}(4, 5)}{\delta V_{eff}(3)} g(5, 2) d(4, 5). \quad (11.128)$$

Thus,

$$\frac{\delta\Sigma(1, 2)}{\delta V_{eff}(3)} = - \int d(4, 5) \frac{\delta\Sigma(1, 2)}{\delta g(4, 5)} g(4, 6) \frac{\delta g^{-1}(6, 7)}{\delta V_{eff}(3)} g(7, 5).$$

Now inserting Equation (11.120) $\Gamma(1, 2, 3) = -\frac{\delta g^{-1}(1, 2)}{\delta V_{eff}(3)}$ we obtain the least obvious of Hedin's equations:

$$\Gamma(123) = \delta(1, 2)\delta(1, 3) + \int \frac{\delta\Sigma(1, 2)}{\delta g(4, 5)} g(46)g(75)\Gamma(673)d(4567). \quad (11.129)$$

Hedin[53] obtained these exact equations that formally determine self-energy, polarization, vertex function and Green's function. Although they were not solved exactly, they lie at the heart of powerful approximate methods for first-principle calculations [54]. This equation lends itself to a diagrammatic interpretation (see Figure 11.10). Indeed, functional differentiation may be understood as removing a propagator line from a self-energy diagram, which then becomes a for-point function with 2 incoming and 2 outgoing lines. By the Hedin equation, all possible combinations and iterations of such scattering diagrams give raise to the most general vertex.

It was pointed out recently[139] that Hedin's equations are helpful in counting Feynman diagrams.

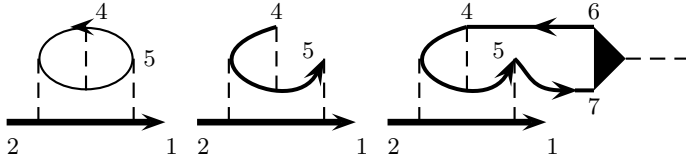


Fig. 11.29. A skeleton Self-energy diagram contributing to $\Sigma(1, 2)$, the corresponding contribution to $\frac{\delta\Sigma(1,2)}{\delta g(4,5)}$, obtained by deleting the $g(4, 5)$ line (Figure 11.9), and the contribution to $\Gamma(2, 1, 3)$ arising from the Hedin equation (11.129).

Problems

11.1. Compute diagram d).

11.2. Express the improper self-energy Σ^* in terms of Σ .

11.3. Are there any skeleton diagrams in the next Figure?

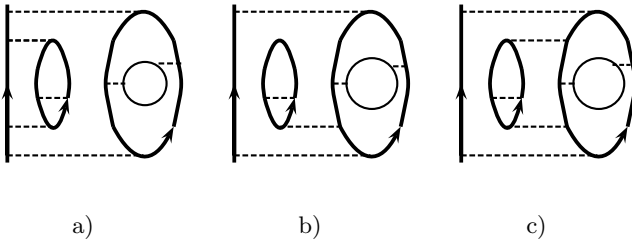


Fig. 11.30. Are there any skeleton diagrams?.

11.4. Evaluate g^{-1} in terms of Σ .

12 Many-Body Effects and Further Theory

12.1 High Density Electron Gas

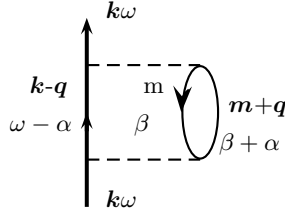


Fig. 12.1. Diagram for g with a self-energy insertion involving π_0 in Jellium.

For Jellium, due to momentum conservation, we re-label the diagram 11.10 d) involving the bubble π_0 as in Figure 12.1 and (11.73) becomes

$$-i\pi_0(\mathbf{q}, \alpha) = -2 \int \frac{d^3 m}{(2\pi)^3} \int \frac{d\beta}{2\pi} i g_0(\mathbf{m}, \beta) i g_0(\mathbf{m} + \mathbf{q}, \beta + \alpha) \quad (12.1)$$

and (11.76) becomes, restoring \hbar ,

$$\pi_0(\mathbf{q}, \alpha) = 2 \int \frac{d^3 m}{(2\pi)^3} \left[\frac{f_{\mathbf{m}}(1 - f_{\mathbf{m}+\mathbf{q}})}{\hbar\alpha + \varepsilon_{\mathbf{m}} - \varepsilon_{\mathbf{m}+\mathbf{q}} + i\eta} - \frac{f_{\mathbf{m}+\mathbf{q}}(1 - f_{\mathbf{m}})}{\hbar\alpha + \varepsilon_{\mathbf{m}} - \varepsilon_{\mathbf{m}+\mathbf{q}} - i\eta} \right] \quad (12.2)$$

with

$$\begin{aligned} \text{Re}\pi_0(\mathbf{q}, \alpha) &= 2 \sum_{\mathbf{m}} \frac{f_{\mathbf{m}} - f_{\mathbf{m}+\mathbf{q}}}{\hbar\alpha + \varepsilon_{\mathbf{m}} - \varepsilon_{\mathbf{m}+\mathbf{q}}}, \\ \text{Im}\pi_0(\mathbf{q}, \alpha) &= -2\pi \sum_{\mathbf{m}} f_{\mathbf{m}}(1 - f_{\mathbf{m}+\mathbf{q}}) \delta(\hbar\alpha + \varepsilon_{\mathbf{m}} - \varepsilon_{\mathbf{m}+\mathbf{q}}). \end{aligned} \quad (12.3)$$

So, the self-energy (11.86) becomes

$$-i\Sigma(\omega) = \int \frac{d^3 \mathbf{q}}{(2\pi)^3} \int \frac{d\alpha}{2\pi} i g^0(\mathbf{k} - \mathbf{q}, \omega - \alpha) (-iV_{\mathbf{q}})^2 (-i)\pi_0(\mathbf{q}, \alpha) \quad (12.4)$$

and since $V_{\mathbf{q}} = \frac{4\pi e^2}{q^2}$, this diverges at small q . The electron gains self-energy by exciting the medium and then re-adsorbing the excitations, but the process runs out of control for the long-wavelength ones. What is going wrong at long distances? It is the Coulomb interaction V , which is causing the divergence by its long range, but should actually be replaced by a shorter ranged screened interaction W .

Equation (11.112) is solved by Fourier transformation thanks to the translational invariance and becomes:

$$W(\mathbf{q}, \omega) = \frac{V_{\mathbf{q}}}{\epsilon(\mathbf{q}, \omega)}, \quad (12.5)$$

where the exact dielectric function is given by

$$\epsilon(\mathbf{q}, \omega) = 1 + V_{\mathbf{q}}\pi(\mathbf{q}, \omega) \quad (12.6)$$

in terms of the exact irreducible polarization part. The cheapest approximation prompts itself: it consists of using instead of the unknown π the lowest polarization part; the resulting approximation is popular as the Random Phase Approximation (RPA) based on

$$\epsilon_{RPA}(\mathbf{q}, \omega) = 1 + V_{\mathbf{q}}\pi_0(\mathbf{q}, \omega). \quad (12.7)$$

As usual, simplicity brings extra benefits; in this case, we can identify the RPA as asymptotically exact in the case of high density (or perfect Fermi gas). Dimensionally $\pi_0 = [E^{-1}]$, that is, it is inverse energy, and any polarization part is clearly the same; to check this, recall that momentum integrals are actually $\sum_{\mathbf{q}}$ summations and carry no dimension, interaction lines V and frequency integrals $\int d\beta$ carry E and Green's functions g bring E^{-1} . Thus, inserting a new V into a polarization part to build a more complicated one brings a dimensionless factor $\sum_{\mathbf{q}} \int d\beta V_{\mathbf{q}} g^2 \equiv \sum_{\mathbf{q}} V_{\mathbf{q}} g = [1]$. However, if we scale the density of the liquid, we are changing the Fermi wave vector k_F ; then for every interaction line $V_{\mathbf{q}}$ scaling like k_F^{-2} there is a q summation (k_F^3) and an energy denominator k_F^{-2} (each energy must be counted k_F^2); thus, $\sum_{\mathbf{q}} \int d\beta V_{\mathbf{q}} g^2 \sim k_F^3 k_F^2 k_F^{-2} k_F^{-4} \sim k_F^{-1}$, and the factor scales like k_F^{-1} , that is, like the Wigner-Seitz radius r_s . Thus π_0 is the dominant polarization part at high density, and the RPA is good in that case. The second fraction in Equation (12.2) may be transformed setting $\mathbf{m} + \mathbf{q} = -\mathbf{n}$, which gives $f_{\mathbf{m}+\mathbf{q}} = f_{\mathbf{n}}$, $f_{\mathbf{m}} = f_{\mathbf{n}+\mathbf{q}}$; now renaming with $\mathbf{n} \rightarrow \mathbf{m}$ one finds

$$\pi_0(q, \omega) = 2 \int \frac{d^3 m}{(2\pi)^3} f_{\mathbf{m}} (1 - f_{\mathbf{m}+\mathbf{q}}) \left[\frac{1}{\hbar\omega + \varepsilon_{\mathbf{m}} - \varepsilon_{\mathbf{m}+\mathbf{q}} + i\eta} - \frac{1}{\hbar\omega + \varepsilon_{\mathbf{m}+\mathbf{q}} - \varepsilon_{\mathbf{m}} - i\eta} \right]. \quad (12.8)$$

This was first evaluated by Lindhard [52]. Writing q for $\frac{q}{k_F}$ and setting: $\nu = \frac{\hbar\omega}{2E_F}$, $a_- = \frac{\nu}{q} - \frac{q}{2}$, $a_+ = \frac{\nu}{q} + \frac{q}{2}$,

$$\begin{aligned}
 \operatorname{Re}(\pi_0) &= \frac{mk_F}{2\pi^2\hbar^2} [-1 \\
 &+ \frac{1}{2q} \{ [1 - a_-^2] \log |\frac{1+a_-}{1-a_-}| - [1 - a_+^2] \log |\frac{1+a_+}{1-a_+}| \}], \\
 \operatorname{Im}(\pi_0) &= \frac{-mk_F}{4\pi q\hbar^2} \times \begin{cases} [1 - a_-^2], & q > 2, \frac{q^2}{2} + q > \nu > \frac{q^2}{2} - q \\ [1 - a_-^2], & q < 2, \frac{q^2}{2} + q > \nu > -\frac{q^2}{2} + q \\ 2\nu, & q < 2, -\frac{q^2}{2} + q > \nu > 0 \\ 0 & \text{otherwise.} \end{cases} \quad (12.9)
 \end{aligned}$$

12.1.1 More Physical Insight about the RPA

It is fairly common that important results are first obtained the hard way by the advances of the general theory and after a while somebody finds that they could have been arrived at by a much simpler, but smart, method. This sort of re-derivation is important as it offers a fuller understanding of the result. H. Ehrenreich and M. H. Cohen [43] have shown that one can derive the Lindhard dielectric function in a purely one-electron formulation. Accordingly, in this Subsection we let H be a one-body Hamiltonian and look for the density response to a *weak* potential $W(\omega)e^{i\omega t}$.

The average of any operator A can be obtained from the density matrix ρ as $\operatorname{Tr}\rho A$. The density operator at \mathbf{x} is $\hat{n}(x) = \delta(\mathbf{x} - \mathbf{x}_e) = \frac{1}{\Omega} \sum_{\mathbf{q}} e^{i\mathbf{q}\cdot(\mathbf{x}_e - \mathbf{x})}$ with \mathbf{x}_e the electron position operator; hence $n(\mathbf{x}) = \frac{1}{\Omega} \sum_{\mathbf{q}} e^{-i\mathbf{q}\cdot\mathbf{x}} \operatorname{Tr}[\rho e^{i\mathbf{q}\cdot\mathbf{x}_e}]$ and the Fourier transform is $n(\mathbf{q}, \omega) = \frac{1}{\Omega} \operatorname{Tr}[\rho e^{i\mathbf{q}\cdot\mathbf{x}_e}]$. Writing the trace on a plane-wave basis,

$$n(\mathbf{q}, \omega) = \frac{2}{\Omega} \sum_{\mathbf{k}} \langle \mathbf{k} | \rho | \mathbf{k} + \mathbf{q} \rangle. \quad (12.10)$$

A factor of 2 is due to the spin trace. For $W = 0$ one is left with a free-particle problem and the zeroth approximation $\rho^{(0)}$ such that its action on the plane waves is $\rho^{(0)}|\mathbf{k}\rangle = f(E_{\mathbf{k}})|\mathbf{k}\rangle$. We consider the equation of motion

$$i\hbar \frac{\partial \rho}{\partial t} = [H, \rho] \quad (12.11)$$

for the one-electron density matrix in the presence of the perturbation W and expand the density matrix $\rho = \rho^{(0)} + \rho^{(1)} + \dots$ in powers of W . Linearizing the equation of motion for the linear response $\rho^{(1)}$ and taking matrix elements between plane-wave states one readily arrives at

$$\begin{aligned}
 i\hbar \frac{\partial}{\partial t} \langle \mathbf{k} | \rho^{(1)} | \mathbf{k} + \mathbf{q} \rangle = \\
 (E_{\mathbf{k}} - E_{\mathbf{k}+\mathbf{q}}) \langle \mathbf{k} | \rho^{(1)} | \mathbf{k} + \mathbf{q} \rangle + [f(E_{\mathbf{k}+\mathbf{q}}) - f(E_{\mathbf{k}})] \langle \mathbf{k} | W | \mathbf{k} + \mathbf{q} \rangle. \quad (12.12)
 \end{aligned}$$

Using $\langle \mathbf{k} | W | \mathbf{k} + \mathbf{q} \rangle = W(\mathbf{q}, \omega)e^{i\omega t}$ and dropping $e^{i\omega t}$ in all terms we obtain:

$$\langle \mathbf{k} | \rho^{(1)} | \mathbf{k} + \mathbf{q} \rangle = W(\mathbf{q}, \omega) \frac{f(E_{\mathbf{k}+\mathbf{q}}) - f(E_{\mathbf{k}})}{E_{\mathbf{k}+\mathbf{q}} - E_{\mathbf{k}} + \hbar\omega} \quad (12.13)$$

Inserting into (12.10),

$$\delta n = W(\mathbf{q}, \omega) \frac{2}{\Omega} \sum_{\mathbf{k}} \frac{f(E_{\mathbf{k}+\mathbf{q}}) - f(E_{\mathbf{k}})}{E_{\mathbf{k}+\mathbf{q}} - E_{\mathbf{k}} + \hbar\omega}. \quad (12.14)$$

$W(\mathbf{q}, \omega)$ is the screened potential induced by introducing external charge with number density $\delta n^{(ext)}(\mathbf{q}, \omega)$:

$$W(\mathbf{q}, \omega) = \frac{4\pi e}{q^2} \left(\delta n^{(ext)}(\mathbf{q}, \omega) + \delta n(\mathbf{q}, \omega) \right) \quad (12.15)$$

where $\delta n(\mathbf{q}, \omega)$ is the induced density. $\delta n^{(ext)}(\mathbf{q}, \omega)$ alone would produce a potential $V_{\mathbf{q}, \omega}$ and with a slight generalization of Equation (12.5) we write

$$\frac{4\pi e}{q^2} \delta n^{(ext)}(\mathbf{q}, \omega) = V_{\mathbf{q}, \omega} = \epsilon(\mathbf{q}, \omega) W(\mathbf{q}, \omega); \quad (12.16)$$

hence,

$$\delta n(\mathbf{q}, \omega) = -\frac{q^2}{4\pi e^2} (\epsilon(\mathbf{q}, \omega) - 1) W(\mathbf{q}, \omega) \quad (12.17)$$

and comparing with (12.12) we obtain the Lindhard dielectric function,

$$\epsilon(\mathbf{q}, \omega) = 1 + \frac{8\pi e^2}{q^2 \Omega} \sum_{\mathbf{k}} \frac{f(\epsilon_{\mathbf{k}}) - f(\epsilon_{\mathbf{k}+\mathbf{q}})}{\epsilon_{\mathbf{k}+\mathbf{q}} - \epsilon_{\mathbf{k}} - \hbar\omega - i\eta}. \quad (12.18)$$

In the static limit, this may be evaluated to read

$$\epsilon(\mathbf{q}, 0) = 1 + \frac{2me^2 k_F}{\pi \hbar^2 q^2} + \frac{2me^2}{\pi \hbar^2 q^3} \left(k_F^2 - \frac{q^2}{4} \right) \ln \left| \frac{2k_F + q}{2k_F - q} \right|. \quad (12.19)$$

It can be shown that for $q \rightarrow 0$,

$$\epsilon(\mathbf{q}, 0) \sim 1 + \frac{K_{TF}^2}{q^2} \quad (12.20)$$

where $K_{TF} = \frac{4k_F}{\pi a_B}$ is the Thomas-Fermi wave vector. Using (12.20), one finds that the screened potential of a point charge becomes a Yukawa potential $\propto \frac{1}{r} \exp(-K_{TF} r)$. Actually, the asymptotic behavior of Fourier transform reflects the singularities [92]; at long distance the behavior of the screening charge is oscillatory (Friedel oscillations):

$$\delta n(r) \propto \frac{\cos(2k_F r)}{r^3}. \quad (12.21)$$

This is due to a divergence in $\frac{d\epsilon(q,0)}{dq}$ at $q = 2k_F$, the largest q that can be transferred to an electron in the Fermi sphere without increasing its energy. Note that for $\omega > 0$ we may write

$$\epsilon_2 \equiv \text{Im}(\epsilon(\mathbf{q}, \omega)) = \frac{8\pi e^2}{q^2 \Omega} \pi \sum_k f(\epsilon_k) [1 - f(\epsilon_{k+q})] \delta(\epsilon_{k+q} - \epsilon_k - \hbar\omega) \quad (12.22)$$

which is positive in the part of the $\omega - q$ plane where $\hbar\omega = \epsilon_{k+q} - \epsilon_k = \frac{\hbar^2}{2m} [2\mathbf{k} \cdot \mathbf{q} + q^2]$ can be satisfied with \mathbf{k} inside the Fermi sphere and $\mathbf{k} + \mathbf{q}$ outside. For a given ω , the shortest q vector is obtained by setting \mathbf{k} right at the Fermi surface and \mathbf{q} parallel to \mathbf{k} , and the longest with \mathbf{q} antiparallel to \mathbf{k} .

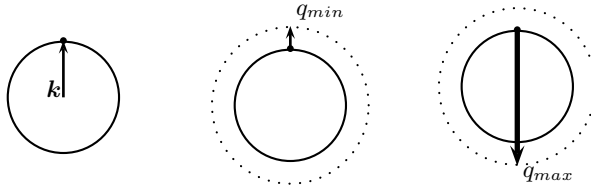


Fig. 12.2. The longest and shortest q vectors for electron-hole excitations with a given excitation energy. One starts with a Fermi wave vector \mathbf{k} and must reach the energy surface at $E_F + \hbar\omega$.

Electron-hole excitations and ϵ_2 are confined to strip between the two parabolas $\hbar\omega = \frac{\hbar^2}{2m}(2k_F q + q^2)$. and $\hbar\omega = \frac{\hbar^2}{2m}(-2k_F q + q^2)$.

The term in $f(\epsilon_{\mathbf{k}+\mathbf{q}})$ in the summation in Equation (12.18) can be rewritten

$$\frac{-f(\epsilon_{\mathbf{k}'})}{\epsilon_{\mathbf{k}'} - \epsilon_{\mathbf{k}+\mathbf{q}} - \hbar\omega - i\eta}$$

by a change of variable $\mathbf{k} + \mathbf{q} \rightarrow -\mathbf{k}'$; then, we can restyle ϵ as

$$\epsilon(q, \omega) = 1 + \frac{16\pi e^2}{q^2 \Omega} \sum_k f(\epsilon_k) \frac{\epsilon_{k+q} - \epsilon_k}{(\epsilon_{k+q} - \epsilon_k)^2 - (\hbar\omega + i\eta)^2}. \quad (12.23)$$

The Drude dielectric function

The classical treatment by Drude also gave raise to a dielectric function. Starting from the electron equation of motion in a periodic field, $m\dot{\mathbf{r}} = -\frac{m}{\tau}\dot{\mathbf{r}} - e\mathbf{E}_0 e^{i(\mathbf{q}\cdot\mathbf{r} - \omega t)}$ where τ is the electron mean free time, one neglects q and solves with $r(t) = Ae^{-i\omega t}$, obtaining $A = \frac{e\tau}{m\omega} \frac{E_0}{\omega\tau + i}$. Then, the current density is $j = -en\dot{r} = \frac{ne^2\tau}{m} \frac{E_0}{1 - i\omega\tau} e^{-i\omega t}$. Thus,

$$\mathbf{J} = \sigma \mathbf{E}, \quad (12.24)$$

with the conductivity $\sigma(\omega) = \frac{\sigma_0}{1-i\omega\tau}$ with $\sigma_0 = \frac{ne^2\tau}{m}$. Assuming that everything depends only on z , Maxwell's equations give:

$$\frac{d^2 E(z)}{dz^2} = -\frac{\omega^2}{c^2} E - \frac{4\pi i\omega}{c^2} J(z).$$

Then (12.24) gives

$$\frac{d^2 E(z)}{dz^2} = -\frac{\omega^2}{c^2} \left[1 + \frac{4\pi i\sigma(\omega)}{\omega} \right] E(z).$$

this is tantamount to say that the medium produces a refractive index n_{ref} and $c \rightarrow \frac{c}{n_{ref}}$ with $n_{ref}^2 = \epsilon = 1 + \frac{4\pi i\sigma(\omega)}{\omega}$. Thus we arrive at

$$\epsilon = 1 - \frac{\omega_p^2}{\omega(\omega + \frac{i}{\tau})} \quad (12.25)$$

where $\omega_p = \sqrt{\frac{4\pi ne^2}{m}}$ is the Plasma frequency. This is qualitatively correct for simple metals, but looks very different from the Lindhard result.

Plasmons and the Lindhard dielectric function

Some resemblance of the Lindhard to the classical calculation is recovered by a long-wavelength ($q \rightarrow 0$) expansion. The $q \rightarrow 0$ limit of Equation (12.23) is obtained by inspection since the $\mathbf{k} \cdot \mathbf{q}$ term in $\epsilon_{k+q} - \epsilon_k$ averages to 0 and $\sum f(\epsilon_k) = \frac{n}{2}$, with the result that $\epsilon(q, \omega) \sim 1 - \frac{\omega_p^2}{(\omega+i\eta)^2}$. A more accurate analysis readily gives:

$$\epsilon(q, \omega) \sim 1 - \frac{\omega_p^2}{(\omega + i\eta)^2} - \frac{3}{5} \left(\frac{\hbar k_F}{m} \right)^2 \frac{\omega_p^2}{(\omega + i\eta)^4} q^2 + \dots \quad (12.26)$$

Plasmon modes are defined by $\epsilon(q, \omega) = 0$, which is the condition for self-sustained oscillations (one can have $W(\mathbf{q}, \omega)$ finite with $V_{\mathbf{q}, \omega} = 0$. They are collective modes of the electron liquid with

$$\omega(q) = \omega_p \left(1 + \frac{3}{10} \left(\frac{\hbar k_F}{m} \right)^2 \frac{q^2}{\omega_p^2} + \dots \right) \quad (12.27)$$

With increasing q , eventually the plasmon branch enters the electron-hole continuum and becomes unstable against converting into a pair. Actually they are sharply defined as $q \rightarrow 0$ but are damped with increasing q ; this *Landau damping* is due to decay in multiple electron-hole pairs. Thus, the plasmons dominate the high-frequency, long wavelength screening, while electron-hole pairs in metals are slower and act as shorter distance (higher q) screening

modes. Plasmon satellites are typically observed in electron spectroscopies of metals in the 10 to 25 eV range (see Chapter 6.4). In semiconductors and insulators plasmons are seen in a similar way, since the gap is often small compared to the ω_P value that can be deduced from the valence electron concentration. The phenomenon of ultraviolet transparency is well known: metals become transparent at frequencies above the plasma frequency because the electrons cannot follow the field.

The Jellium energy in the high density case can be found by summing over the ring diagrams. Gell-Mann and Brueckner found the result

$$\tilde{E} = \int dx [t[n] + \epsilon_x[n] + \epsilon_c[n]]n, \quad (12.28)$$

where I have introduced the following energies *per particle* (small r_s):

$$\begin{aligned} \text{kinetic} \quad t[n] &= \frac{3}{10}(3\pi^2 n)^{\frac{2}{3}} \approx \frac{2.21}{r_s^2} Ry \\ \text{exchange} \quad &\approx -\frac{0.916}{r_s} Ry \\ \text{correlation} \quad &-0.062 \ln(r_s) - 0.096 Ry. \end{aligned} \quad (12.29)$$

12.2 Low Density Electron gas: Ladder Approximation

In the low density case the quantum electron gas is far from perfect, that is, the kinetic energy is dominated by the interaction energy. Yet things again simplify, since many-electron collisions become unlikely and one approaches a two-body problem. So, we start adding two particles to an empty lattice (or holes to a filled one; these two problems can reflect quite different physics, but are related by a canonical particle-hole transformation). The solution for G_2 is very interesting and can be obtained in several ways.

In Sect.(6.3) I show how one can write the two-particle Green's function for two electrons in the empty lattice for any interaction potential; the solution is simplest when the potential is on-site (Hubbard interaction). Let \mathbf{R}_{cm} be the center-of-mass of the pair and $g^{\mathbf{Q}}$ be the Fourier transform of the two-particle Green's function with respect to \mathbf{R}_{cm} , with $g^{\mathbf{Q}}$ the non-interacting limit. The two-particle Green's function is given by the Kanamori [67] result,

$$g^{\mathbf{Q}} = \frac{g^{\mathbf{Q}}}{1 - U g^{\mathbf{Q}}}, \quad (12.30)$$

where, as in (6.74),

$$g^{\mathbf{Q}}(z) = \sum_{\mathbf{q}} \frac{1}{z - \epsilon(\mathbf{Q} - \mathbf{q}) - \epsilon(\mathbf{q})}. \quad (12.31)$$

This formula is readily obtained as the sum of a series of *ladder* diagrams, which in the empty lattice gives the exact solution, and is a useful approximation at low density. Each scattering introduces an interaction and a couple

of propagators; if the pair carries momentum \mathbf{Q} and frequency ω , the propagators may be labeled $\mathbf{Q} - \mathbf{q}, \omega - \eta$ and \mathbf{q}, η . According to the diagram rules, the interaction brings a factor $-iU$ and we must perform the $\sum_{\mathbf{q}} \int \frac{d\eta}{2\pi}$ sum on internal labels. Doing the frequency integral by contour integration, we can show that introducing an interaction and a couple of propagators brings a factor $Ug^{\mathbf{Q}}$ (see Equation 6.69 with $z = \omega + i0$).

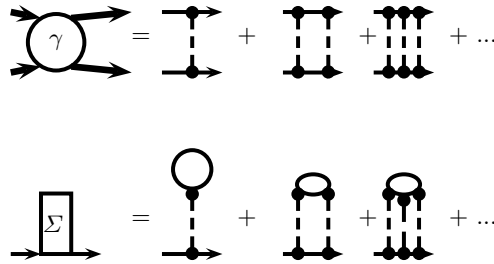


Fig. 12.3. Ladder approximation for the scattering amplitude γ and for the self-energy Σ (the first term is the Hartree contribution). Note that γ and Σ are simply related; there is a general link, as discussed in Section 12.5 below.

Then, the sum of the geometrical series gives the Kanamori result, that we obtained in Sect. 6.3 by quite different means. Then the one-particle self-energy at low density can be gained by Equation of Figure 12.3. This Low Density Approximation (LDA) was first proposed by V. Galitzkii [133].

12.3 Ladder Approximations in Electron Spectroscopies

12.3.1 XPS and Auger Spectra from Metals

The theory of the Auger CVV spectra of closed-band solids outlined in Section (6.2) brings valuable information on the local electronic structure, but needs to be extended to conduction bands. The presence of a Fermi level in the band where the two holes are produced by the transition complicates the problem in several ways. The most evident are: 1) the band can be polarized by the primary hole, so a two-hole Green's function cannot tell the whole story 2) the existence of electron-hole excitations offers an intra-band decay channel for the two-hole resonances. The writer[91] proposed the following model Hamiltonian:

$$H = H_0 + H_1 + H_2. \tag{12.32}$$

The independent-particle part is

$$H_0 = \sum_{ij\sigma} \epsilon_{ij} c_{i\sigma}^\dagger c_{j\sigma} + \epsilon_c b^\dagger b, \quad (12.33)$$

with the first term (in obvious notation) describes the band structure, b^\dagger creates the core electron;

$$H_1 = U n_{0+} n_{0-} \quad (12.34)$$

introduces the local repulsion at site 0, and

$$H_2 = U_{cv} (n_{0+} + n_{0-}) b^\dagger b \quad (12.35)$$

introduces the on-site core-electron valence-electron repulsion.

The theory based on assumption that the band is almost full, that is the number of holes per quantum state in the band satisfies

$$n_h = \langle a_{0\sigma} a_{0\sigma}^\dagger \rangle \ll 1; \quad (12.36)$$

this is satisfied e.g. for the Ni d bands. The $n_h \ll 1$ assumption makes it easier to justify the 2-step model, treating the core-hole decay separately from its creation (by the way, the 1 step approach was not yet available in 1979).

Due to the band polarizability, one needs a 3-body Green's function (the third body is the core electron)

$$\mathbf{g}^{(3)}(t) = \langle T b(t) c_{0+}^\dagger(t) c_{0-}^\dagger(t) c_{0-}(0) c_{0+}(0) b^\dagger(0) \rangle. \quad (12.37)$$

Then, the $n_h \ll 1$ assumption makes it possible to factor the 3-body Green's function as a core-propagator times a two-hole Green's function,

$$\mathbf{g}^{(3)}(t) \sim \langle T b(t) b^\dagger(0) \rangle \langle c_{0+}^\dagger(t) c_{0-}^\dagger(t) c_{0-}(0) c_{0+}(0) \rangle,$$

(see the original paper for details). The core propagator can be expressed a-la Langreth as shown in Section **11.2.3**. Thus, the CVV spectrum from the almost filled band can be modeled as a two-hole spectrum convoluted with an asymmetric core line shape. Finally, the $n_h \ll 1$ assumption justifies the low density approximation (for holes); this is expected to be a good approximation up to $n_h \sim 0.1$ if U is comparable to the band width, but this range shrinks at stronger coupling, while at weak coupling any approximation works. The LDA self-energy was calculated analytically for a band structure having an arbitrary spectral density

$$\begin{aligned} B(\omega), \omega_B < \omega < 0 \\ A(\omega), 0 < \omega < \omega_T \end{aligned} \quad (12.38)$$

where ω_B is the bottom and ω_T the top of the band. Thus, $n_h = \int_0^{\omega_T} d\epsilon A(\epsilon)$ and the non-interacting propagator is given by

$$i g_0(\omega) = \int_0^{\omega_T} d\epsilon \frac{A(\epsilon)}{\omega - \epsilon + i\delta} + \int_0^{-\omega_B} d\epsilon \frac{B(\epsilon)}{\omega + \epsilon - i\delta}. \quad (12.39)$$

The results were displayed numerically for the rectangular band model of Section (6.2). It was necessary to remove the first-order (tadpole) contribution

$$\Sigma^{(1)} = -iU\langle n \rangle : \quad (12.40)$$

it would make the site where the Auger decay takes place more repulsive than the rest of the sites. Thus,

$$\Sigma(\omega) = iU\langle n \rangle + \int_{-\infty}^{\infty} d\omega' g_0(\omega') \mathcal{T}(\omega + \omega'), \quad (12.41)$$

where the \mathcal{T} matrix is given by

$$\mathcal{T}(\omega) = \frac{iU}{1 + iUg_0^{(2)}(\omega)}, g_0^{(2)}(\omega) = \int_{-\infty}^{\infty} \frac{d\omega'}{2\pi} g_0(\omega') g_0(\omega - \omega'). \quad (12.42)$$

The integrals can be done with the help of the Lehmann representation. When U is large enough to produce split-off states in the closed-band theory, there is structure outside the continuum. One finds

$$\text{Re}\Sigma(\omega) \sim \pi U^2 A(-\omega - U)\theta(\omega_T + \omega + U)\theta(-\omega + U), \quad (12.43)$$

that is, a bump between $\omega = -U - \omega_T$ and $\omega = -U$. As a result, there is a bump in the density of states too, due to broadened split-off states. This explained[91] a satellite peak observed in the Ni photoemission spectrum; the physical picture is that the hole produced in the photoemission process has a chance to find another of opposite spin already there; a two-hole resonance forms outside the band continuum, and decays into band holes plus a number of electron-hole pairs. The Auger spectrum was also obtained in this model, in qualitative agreement with the experiments.

The next step appeared to be the self-consistent LDA, obtained as in Section (11.6); it had been applied to the Anderson Model [132] and was expected to have an enhanced range of validity. To our surprise, the writer and Verdozzi in cluster studies found[134] that the self-consistent procedure actually ruins the approximation. Comparing with exact results we found that the non-selfconsistent version, keeping only the diagrams that remain in the closed-band limit, was much superior; we called this the Bare Ladder Approximation (BLA). Actually, the self-consistent LDA puts weight in processes where many electron-hole pairs are virtually excited simultaneously, but the on-site interaction does not allow this, and a vertex correction tends to remove the dressing of the internal lines. The BLA has the further advantage that the *Herglotz* property is granted, that is, the density of states is non-negative. This is of course quite necessary, but most approximations have no built-in device to ensure this.

The property of vertex corrections that tend to undress internal propagators was later observed by people working on the GW approximation (see Section 11.10).

12.3.2 The $U < 0$ Phenomenon

Measurements of Auger spectra of compounds of Sc, Ti and Cr [159] showed that the peak kinetic energy was higher than expected by Lander's theory (Section 6.2); shifts as large as 4 eV were reported. This led the authors to conclude that in such cases the on-site interaction is $U < 0$ and to propose an explanation based on a dynamic bipolaron effect. An alternative, $U > 0$ explanation was put forth by Václav Drchal and the writer [128]. We think that the on-site interaction is always repulsive; the repulsion can indeed produce an effective attraction by a correlation effect (W=0 pairing, see Chapter 17) but this is off-site and the binding energies are expected to be of the order of tens of meV. The probability [22] of measuring a photoelectron of momentum \mathbf{p} and an Auger electron of momentum \mathbf{k} in APECS (Sect. 6.4) is We approximate the probability of emitting by

$$I_{tot}(E, \mathbf{p}, \mathbf{k}) = \int_0^\infty dt \int_0^\infty dt' f(t, t', \mathbf{p}, \mathbf{k}) e^{iE(t-t')}, \quad (12.44)$$

where, introducing complete set summations $\sum_{\mu, \mu'}$ over the states of the neutral system,

$$\begin{aligned} f(t, t', \mathbf{p}, \mathbf{k}) &= \sum_{\mu, \mu'} \sum_{c, c'} \langle \Psi | a_c^\dagger e^{i[H(0)+i\Gamma_{op}]t'} a_{c'} | \mu \rangle \\ &\times \langle \mu | H_A^\dagger(\mathbf{k}) e^{iH(1)(t-t')} H_A(\mathbf{k}) | \mu' \rangle \\ &\times \langle \mu' | a_c^\dagger e^{-i[H(0)-i\Gamma_{op}]t} a_c | \Psi \rangle V(c', \mathbf{p})^* V(c, \mathbf{p}) \end{aligned} \quad (12.45)$$

Here, $V(c, \mathbf{p})$ is the matrix element of the electro-magnetic Hamiltonian between the core-electron state c and the photoelectron state, $H(\nu)$ is the hamiltonian of the system with ν core electrons in the primary-hole state, the operator Γ_{op} describes virtual Auger transitions, but is often replaced by a constant

$$H_A(\mathbf{k}) = \sum_{\alpha\beta} M_{\alpha\beta}(\mathbf{k}) a_{0\alpha} a_{0\beta}$$

is the operator that describes the valence hole creation at site 0 in the local spin-orbitals denoted by greek letters; $M_{\alpha\beta}(\mathbf{k})$ are Auger matrix elements. Moreover, $|\Psi\rangle$ is the *true ground state* with no core-hole ($\nu = 1$), and the sums run over complete sets. *For degenerate core levels a set of relaxed ground states must be included.* We considered a non-degenerate core state and assumed that these sums are saturated by two main contributions, namely $|\mu\rangle = |\Psi\rangle$ and $|\mu\rangle = |\Phi\rangle$, where $|\Phi\rangle$ is the *relaxed ground state* with the core-hole and its screening cloud. In the case it is necessary one could easily extend the theory including plasmon satellites and other excited states. One of the ingredients is the core-hole Green's function $g_c(t) = -i\langle \Psi | a_c^\dagger e^{i[H(0)+i\Gamma_{op}]t'} a_c | \Psi \rangle$. One can observe the core density of states in Photoemission experiments as an asymmetric line shape. We argue that the terms with $\mu \neq \mu'$ are negligible, since the factor

$$\langle \mu | H_A^\dagger e^{iH(0)(t-t')} H_A | \mu' \rangle$$

represents the evolution without the core-hole and it is unlikely that a screening cloud can be created taking from $|\Psi\rangle$ to $|\Phi\rangle$ if there is nothing to screen.

Let δ denote the inverse lifetime of the core hole and Γ denote the inverse characteristic time of the electron-hole pairs screening the core hole and contributing the asymmetry. We assume that both are small compared to the other relevant energies. Thus, we may model the situation with $g_c(t) = -ie^{-i[\epsilon_c - i(\Gamma + \delta)]t}$, where ϵ_c is the core energy level, while

$$\beta_c(t) = -i \langle \Phi | a_c^\dagger e^{i[H(0) + i\Gamma_{op}]t} a_c | \Psi \rangle \approx e^{-i\varepsilon_\beta t - \delta t} \tag{12.46}$$

involves a screened core energy ε_β . Collecting these results,

$$I_{tot} = |V(\mathbf{p})|^2 [I_{\Psi\Psi} + I_{\Phi\Phi}]$$

with the unrelaxed contribution

$$I_{\Psi\Psi} = |M(\mathbf{k})|^2 \int_{-\infty}^{\infty} \frac{d\omega}{2\pi} \frac{D(E - \omega)}{(\omega - \varepsilon_c)^2 + \Gamma^2}$$

written in terms of the two-holes density of states D as in closed-band theory, and an average square matrix element. On the other hand,

$$I_{\Phi\Phi} = \int_{-\infty}^{\infty} \frac{d\omega}{2\pi} \frac{I_{rel}(E - \omega)}{(\omega - E)^2 + \delta^2}$$

where the relaxed line shape requires modeling the screening cloud. We modeled the ground state of the system in the presence of the core hole, using a Hamiltonian of the form

$$H = H_0 + H_{ee} + H_{ch}, \tag{12.47}$$

where H_0 is the usual band term,

$$H_{ee} = U \sum_{i\alpha\beta} n_{i\alpha} n_{i\beta} \tag{12.48}$$

is an approximate electron-electron interaction with i running over the lattice sites and the greek indices over the local atomic valence orbitals, and

$$H_{ch} = -W \sum_{\alpha} n_{0\alpha} \tag{12.49}$$

is the core hole-valence electron interaction at site $i=0$ ($W > 0$). Letting $|\Psi\rangle$ denote the ground state with no core-hole (determinantal state in HF and Local Density approximations) we looked for the ground state $|\Phi\rangle$ with the core-hole in the form

$$|\Phi\rangle + (a + \sum_{q\alpha} b_{q\alpha} a_{0\alpha}^\dagger a_{q\alpha}) |\Psi\rangle$$

with q as the wavevector and $b_{q\alpha}$ variational parameters.

By minimizing the energy one finds a complicated but physically relevant solution until it is clear that the solution must be found in the space of distributions in terms of a wave packet

$$\beta(h, \epsilon) = \sqrt{(1-n)\rho(E_F)hd} \theta(E_F - \epsilon)\theta(-E_F + \epsilon + h)$$

as the following singular limit for $h \rightarrow 0$:

$$|F\alpha\rangle = \sqrt{(1-n)d} \lim_{h \rightarrow 0} \frac{1}{\sqrt{N}} \sum_q \beta(h, E(q)) |q\alpha\rangle. \quad (12.50)$$

The relaxed state turns out to be

$$|\Phi\rangle = \frac{1}{\sqrt{(1-n)d}} \sum_\alpha a_{0\alpha}^\dagger a_{F\alpha} |\Psi\rangle. \quad (12.51)$$

The screening electron comes from the Fermi surface. Now within the two-step model one can obtain the Fermi golden rule expression for the relaxed spectrum

$$I_{rel}(E) = \frac{-1}{\pi} \frac{2|M(\mathbf{k})|^2}{(1-n)d} \text{Im} \left[\int_0^\infty dt e^{-i(E-i0)t} \sum_{\alpha\beta\gamma} g_c^{(hhe)}(\alpha\beta\gamma, t) \right] \quad (12.52)$$

where

$$g_c^{(hhe)}(\alpha\beta\gamma, t) = (-i)^3 \langle \Psi | T [a_{0\gamma}(t) a_{0\beta}^\dagger(t) a_{0\alpha}^\dagger(t) a_{0\alpha} a_{0\beta}(t) a_{0\gamma}^\dagger] | \Psi \rangle \quad (12.53)$$

is a three-body causal Green's function averaged over the unrelaxed ground state. In order to compute $g_c^{(hhe)}$ we proposed the approximation¹ was shown in Figure 12.3.2 for α, β and γ all different.

This means:

$$\begin{aligned} g_c^{(hhe)}(\alpha\beta\gamma, t) &= g_c^{(hh)}(\alpha\beta, t) g_c^{(e)}(\gamma, t) + g_c^{(he)}(\alpha\gamma, t) g_c^{(h)}(\beta, t) \\ &+ g_c^{(he)}(\beta\gamma, t) g_c^{(h)}(\alpha, t) - 2g_c^{(h)}(\alpha, t) g_c^{(h)}(\beta, t) g_c^{(e)}(\gamma, t), \\ &\alpha, \beta, \gamma \text{ all different} \end{aligned}$$

(note the factor 2, which is needed to give the correct $U=0$ limit.) When two indices coincide, we find

$$\begin{aligned} g_c^{(hhe)}(\alpha\gamma\gamma, t) &= (1-n^2) g_c^{(h)}(\alpha, t) + g_c^{(hh)}(\alpha\gamma, t) g_c^{(h)}(\lambda, t) \\ &+ g_c^{(he)}(\alpha\gamma, t) g_c^{(h)}(\alpha, t) - g_c^{(h)}(\alpha, t) g_c^{(h)}(\gamma, t) g_c^{(e)}(\gamma, t), \end{aligned}$$

¹The exact three-body wave function for a system of interacting identical particles can be obtained by a method by Faddeev [206] but here we were looking for a simple approximation for the three-body Green's function.

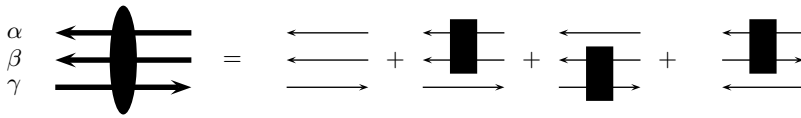


Fig. 12.4. The approximation for $g_c^{(hhe)}$ introduced in ref. [128] for α, β and γ all different. The black box represent ladder interactions involving pairs of Fermions, while all diagrams involving all Fermions are neglected.

and a similar expression if $\alpha = \gamma$. The Auger intensity is

$$I_{rel}(E) = -\frac{1}{\pi} \text{Im}A(E)\Theta(E_F - E) \tag{12.54}$$

where, calling $\Delta g_c^{(he)}$ the correlation part of $g_c^{(he)}$, that is, the difference between $g_c^{(he)}$ and its $U=0$ limit,

$$A(E) = (1 - n)^2 g_c^{(h)}(E) + (d - 1) \int_{-\infty}^{\infty} \frac{d\omega}{2\pi i} \Delta g_c^{(he)}(E - \omega) g_c^h(\omega) + \frac{d}{2} \int_{-\infty}^{\infty} \frac{d\omega}{2\pi i} g_c^{(hh)}(E - \omega) g_c^{(e)}(\omega). \tag{12.55}$$

For partially filled bands, a one-body contribution arises, along with the rest of 3-body contributions and the 2-body ones in the unrelaxed contributions; we called our approach the *1-2-3 theory*. It was shown in Ref. [128] (see Figure 12.5) that this theory qualitatively reproduces the experimental trend for early transition metals.

12.3.3 Correlation in Early Transition Metals

Part of the intensity in Auger CVV and APECS spectra from transition metals comes from the decay of core-holes that are unscreened in the initial state; this is obtained by a two-body Green’s function, as in the filled band case. However, much of the intensity comes from core holes that are screened when the Auger decay occurs.

Some of these spectral features are amenable to the one-body g , but the rest requires[128] a two-hole-one-electron propagator, that is a 3-body function $g^{(3)}$. In the strongly correlated case the approximation of the last Section runs into trouble because the Herglotz property is not granted (the density of states may turn negative.) The Core-Ladder approximation [127]is an extension of the ladder approximation to this problem that has several attractive features. It is based on the idea of formally rewriting the problem in terms of

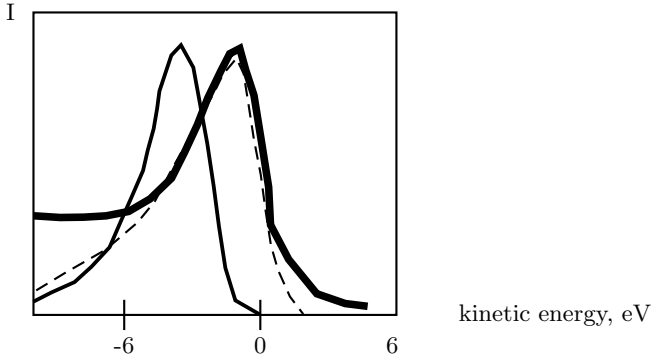


Fig. 12.5. *Thick solid line: schematic drawing of the experimental $Ti L_2M_{45}M_{45}$ line shape (see Ref. [160]) on a kinetic energy scale centered at the maximum. Dashed line: the theory of Ref. [128] (dashed), with $U=1.684$ eV, band width $w=7.14$ eV and $n=0.254$. Thin solid line: the closed-band theory result with the same U and w , which predicts too low kinetic energy and is clearly not applicable in this case.*

a fictitious three-body interaction, where the third body is forward-scattered by an interaction x .

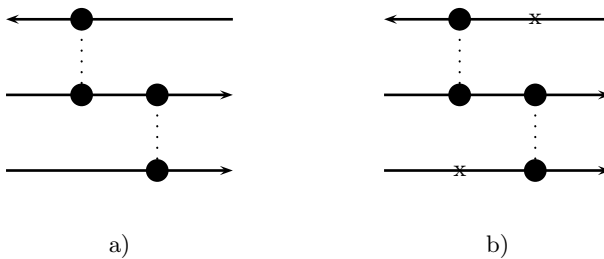


Fig. 12.6. a) typical second-order diagram for the 1 hole- 2-electron function $g^{(3)}(t)$; b) the same diagram with a fictitious 3-body interaction that allows to carry on a partial summation of the 3-line ladder series to infinite order.

The third body is filtered through a $x = \sum_i |i\rangle\langle i|$ -type projector, that is, it is left undisturbed. In core problems, one can exactly dispose of the infinite summation in favour of a local projector. The same applies to localized split-off states that occur at strong coupling. Thus one can base an approximation that can be systematically improved by including more terms if needed. It treats electrons and holes at equal footing, carries on a partial summation of the perturbation series to infinite order, and becomes exact both at weak and at strong coupling (in the sense that it becomes equivalent to a full Ladder approximation). A particularly interesting feature is that our approach grants the *Herglotz* property, that is, the density of states is granted to be non-negative. Indeed it is a common drawback of perturbation approaches that potentially powerful diagram summations become untenable by the failure to guarantee this zero-order requirement of positive probability. In this case we achieve the result by proving that there exists a *model* Hamiltonian for which our Core-Ladder series gives the exact answer. The theory naturally explains the apparent negative-U behaviour of the early transition metal spectra.

12.4 Conserving Approximations

When working with approximate self-energies, we must be ready to get some quantitative details wrong, but we can make no use of approximations that violate the basic conservation laws. The continuity equation must hold; energy and momentum conservation laws, when applicable, must also be obeyed. An approximation that respects these fundamental symmetries is called **conserving**. The Hartree-Fock approximation is, but if we pick a general Σ this is not granted automatically.

12.4.1 Continuity Equation

Let us see how the Green's function formalism embodies current conservation. The Dyson equation has two forms:

$$g(x, x') = g_0(x, x') + \int dx_1 dx_2 g_0(x, x_1) \Sigma(x_1, x_2) g(x_2, x') \quad (12.56)$$

$$g(x, x') = g_0(x, x') + \int dx_1 dx_2 g(x, x_1) \Sigma(x_1, x_2) g_0(x_2, x') \quad (12.57)$$

By applying the g_0^{-1} operator one obtains two equations:²

$$\left\{ i \frac{\partial}{\partial t_1} + \frac{\nabla_1^2}{2m} - U(1) \right\} g(1; 2) = \delta(1 - 2) + \int d\bar{1} \Sigma(1; \bar{1}) g(\bar{1}; 2) \quad (12.58)$$

²recall from (4.20) that $g(1, 2) = -i\langle T[\psi(1)\psi^\dagger(2)] \rangle$.

$$\left\{ -i \frac{\partial}{\partial t_2} + \frac{\nabla_2^2}{2m} - U(2) \right\} g(1; 2) = \delta(1-2) + \int d\bar{1} g(1; \bar{1}) \Sigma(\bar{1}; 2). \quad (12.59)$$

Taking the difference and writing $\nabla_1^2 - \nabla_2^2 = (\nabla_1 + \nabla_2) \cdot (\nabla_1 - \nabla_2)$, we get:

$$(i\partial_{t_1} + i\partial_{t_2})g(1; 2) + (\nabla_1 + \nabla_2) \cdot \frac{\nabla_1 - \nabla_2}{2m} g(1; 2) = [U(1) - U(2)]g(1; 2) + Z(1; 2), \quad (12.60)$$

where

$$Z(1; 2) = \int d\bar{1} \{ \Sigma(1; \bar{1})g(\bar{1}; 2) - g(1; \bar{1})\Sigma(\bar{1}; 2) \}. \quad (12.61)$$

Now we set $2 = 1^+$, which means $t_2 = t_1^+$, $\mathbf{r}_2 = \mathbf{r}_1$. In the left hand side,

$$ig(1; 1^+) = -\langle \Psi^\dagger(1)\Psi(1) \rangle = -\langle \hat{n}(1) \rangle \quad (12.62)$$

is the particle density and

$$\begin{aligned} & \left\{ \frac{\nabla_1 - \nabla_2}{2m} g(1; 2) \right\}_{2=1^+} \\ &= -\frac{1}{2mi} \langle \Psi^\dagger(1)\nabla_1\Psi(1) - \nabla_1\Psi^\dagger(1)\Psi(1) \rangle = -\langle \mathbf{j}(1) \rangle \end{aligned} \quad (12.63)$$

is the current density. Hence we end up with the continuity equation, which is the number conservation law in a differential form, provided that the right hand side vanishes, and this requires

$$Z(1, 1^+) = 0. \quad (12.64)$$

The exact Dyson equations (12.56,12.57) must imply the continuity equation and (12.64). The best way to check this is to use the equations of motion (10.7) involving the two-particle Green's function

$$\left\{ i \frac{d}{dt_1} + \frac{\nabla_1^2}{2m} - U(1) \right\} g(1; 1') = \delta(1, 1') - i \int d\bar{1} V(1, \bar{1}) G_2(1; \bar{1}^- | \bar{1}^+; 1') \quad (12.65)$$

and

$$\left\{ -i \frac{d}{dt_{1'}} + \frac{\nabla_{1'}^2}{2m} - U(1') \right\} g(1; 1') = \delta(1, 1') - i \int d\bar{1} G_2(1; \bar{1}^- | \bar{1}^+; 1') V(\bar{1}, 1'). \quad (12.66)$$

In this way, taking the difference, we get

$$\begin{aligned}
 (i\partial_{t_1} + i\partial_{t_1'})g(1; 1') + \frac{1}{2m}(\nabla_1 + \nabla_2) \cdot (\nabla_1 - \nabla_{1'})g(1; 1') = \\
 = [U(1) - U(1')]g(1; 1') \\
 -i \int d\bar{1}[V(1, \bar{1}) - V(1', \bar{1})]G_2(1; \bar{1}^- | \bar{1}^+; 1'). \quad (12.67)
 \end{aligned}$$

When we set $1' = 1^+$ the r.h.s. vanishes.

This is an obvious statement about the exact Σ and g ; however it is also a condition on approximations, which can only be tenable if they are conserving. *The condition on approximate Σ and g is that both forms (12.56, 12.57) of the Dyson equation be obeyed and (12.64) holds.* Next, we discuss how to build conserving approximations.

12.4.2 The Φ Functional

There is a simple diagrammatic prescription for creating conserving approximations. Let $\delta\Sigma_{skel.}^{(n)}$ denote a skeleton diagram of order n for the self-energy $\Sigma(1, 2)$ and imagine joining the two ends by a propagator $g(2, 1)$. The result is the ring diagram in the next Figure:

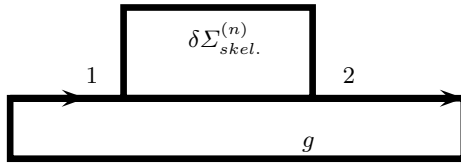


Fig. 12.7. Building a contribution $\delta\Phi^{(n)}$ to the Φ functional (occurring $2n$ times) from a skeleton diagram $\delta\Sigma_{skel.}^{(n)}$ for the self-energy, by closing the ends by an interacting propagator g .

$$\delta\Phi^{(n)} = \int \Sigma(1, 2)g(2, 1)d1d2 \quad (12.68)$$

similar to one of those bubble diagrams that contribute to the no-particle propagator or ground-state energy (Section 11.1), except that the $2n$ internal propagators are dressed g and there are no self-energy insertions. The analytical expression of any diagram is a functional of g . As illustrated in Figure 11.10 the inverse operation (opening the $g(2, 1)$ line to restore the original self-energy) is a functional differentiation. We introduce an interaction strength parameter λ (which is 1 in the fully interacting case). Any graph with $2n$ g lines must be divided by $2n$ to avoid multiple counting of contributions to $\Sigma(1, 2)$ (see Figure 12.8). Let σ_n represent the sum of all the skeleton diagrams with n vertices, and

$$\Phi[g, \lambda] = \sum_n \frac{\lambda^n}{2n} \text{Tr}[g(\omega)\sigma_n(\omega)], \tag{12.69}$$

where the Tr operation now sums over spin and all one-electron labels and integrates in $\frac{d\omega}{\pi}$. This leads to the following result.

Theorem 10. (*Luttinger-Ward theorem*) [55] *The exact self-energy is given by (note the order of arguments!)*

$$\Sigma(1, 2) = \frac{\delta\Phi}{\delta g(2, 1)}. \tag{12.70}$$

A further theorem by Baym and Kadanoff [56] states that the continuity equation and the momentum, angular momentum and energy conservation laws are embodied in the Φ functional;

Theorem 11. *If (and only if) a self-energy is Φ -derivable, that is, comes according to (12.70) from some approximate Φ , the approximation is conserving. In other terms, even for approximate Σ Equation (12.70) is equivalent to the conservation laws.*

The GW approximation is also Φ -derivable and hence conserving.

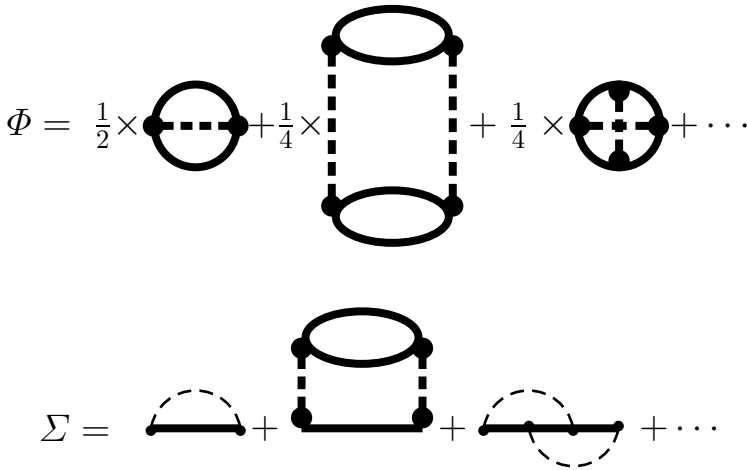


Fig. 12.8. Diagrams for Φ and the corresponding Σ . The first-order example refers to the Hartree-Fock approximation.

12.4.3 Gauge Transformation

We prove Theorem 11 for the continuity equation (the other proofs are somewhat longer but similar). Under a gauge transformation $\Psi(x) \rightarrow \Psi(x)e^{i\Lambda(x)}$ or

$$g(1, 2) \rightarrow e^{i\Lambda(1)}g(1, 2)e^{-i\Lambda(2)}, \tag{12.71}$$

Φ is invariant, since for any line entering a vertex there is another one leaving it. In an infinitesimal gauge transformation $\delta\Lambda$, g changes by the amount $\delta g = [\delta\Lambda(1) - \delta\Lambda(2)]g(1, 2)$. Then to first order Φ as a functional of g will change by the amount

$$\begin{aligned} 0 = \delta\Phi &= \int d1d2 \frac{\delta\Phi}{\delta g(1, 2)} \delta g(1, 2) = \int d1d2 \Sigma(2, 1) \delta g(1, 2) \\ &= i \int d1d2 \Sigma(2, 1) [\delta\Lambda(1) - \delta\Lambda(2)] g(1, 2). \end{aligned} \tag{12.72}$$

Exchanging the dummy variables in the second term, Eq.(12.72) yields

$$0 = \int d1d2 [\Sigma(2, 1)g(1, 2) - g(2, 1)\Sigma(1, 2)]\delta\Lambda(1) \tag{12.73}$$

The coefficient of $\delta\Lambda(1)$ must vanish identically. that is

$$\int d2 \{ \Sigma(1, 2)g(2, 1) - g(1, 2)\Sigma(2, 1) \} = 0. \tag{12.74}$$

and we are back to Equation (12.64): the approximation is conserving.

12.4.4 Ground-State Energy and Grand Potential

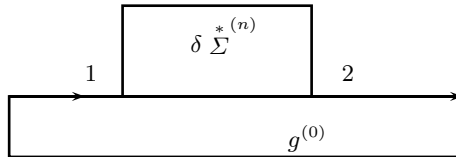


Fig. 12.9. Building a contribution $\delta\Omega^{(n)}$ to the grand potential (occurring $2n$ times) from a diagram $\delta \Sigma^*$ for the self-energy. This looks very much like Fig. 12.7, but please observe the differences: propagators are bare, and the self-energy improper.

The grand potential is the sum of ring diagrams. One may work out the grand-potential and the ground-state energy in parallel; just, in the former case one uses $\frac{1}{\beta} \sum_l$, while in the latter case $\int_{-\infty}^{\infty} d\omega$. We use a short-hand notation valid for both cases ³. Let $\delta\Omega^{(n)}$ denote any such diagram of order n ; it may be thought of as the result of closing a self-energy diagram (improper, in general) with a bare propagator. *Mutatis mutandis*, this is similar to the

³Note however that some expressions are ambiguous if taken literally at $T=0$ and then one should take the $T \rightarrow 0$ limit at the end (see below).

procedure for building Φ from the skeleton diagrams for the self-energy, since there are $2n$ bare lines in $\delta\Omega^{(n)}$. J.M.Luttinger and J.C. Ward [55], derived the diagram rules for the grand-potential in the frequency-momentum representation for Jellium. They wrote the contribution of order n , summed over one-body states r , such that $g^{(0)}$ is diagonal,

$$\Omega_n = \frac{1}{2n} \sum_r \int d\omega g_r^{(0)}(\omega) \Sigma_r^{*(n)} \equiv \frac{1}{2n} Tr g^{(0)} \Sigma^*; \quad (12.75)$$

here $\int d\omega$ stand for $K_B T$ times the summation over Matsubara frequencies in the finite T case, and the Tr operation implies summing over indices and integrating over frequency. To compute $\sum_n \Omega_n$ one can use the fact that

$$a(\lambda) = \sum_n a_n \lambda^n \Rightarrow \sum_n \frac{a_n}{n} \lambda^n = \int_0^\lambda \frac{a(\alpha) d\alpha}{\alpha}. \quad (12.76)$$

Thus, writing $\Sigma_r(\omega, \alpha)$ for Σ at coupling constant α ,

$$\Omega = \Omega_0 + \frac{1}{2} \sum_r \int d\omega \int_0^\lambda \frac{d\alpha}{\alpha} g_r^{(0)}(\omega) \Sigma_r^*(\omega, \alpha), \quad (12.77)$$

where Ω_0 is the non-interacting limit. Recalling (2.23) one finds

$$\Omega_0 = -\frac{1}{\beta} \sum_r \ln(1 + e^{-\beta(\epsilon_r - \mu)}). \quad (12.78)$$

Using the solution to Problem 11.2 and the Dyson equation we end up with

$$\Omega = \Omega_0 + \frac{1}{2} \sum_r \int d\omega \int_0^\lambda \frac{d\alpha}{\alpha} g_r(\omega) \Sigma_r(\omega, \alpha), \quad (12.79)$$

which is a new expression for the ground-state energy in terms of the Green's function, involving a coupling-constant integration. This implies

$$\lambda \frac{d\Omega}{d\lambda} = \frac{1}{2} Tr g(\omega, \lambda) \Sigma(\omega, \lambda). \quad (12.80)$$

12.4.5 Luttinger-Ward and ABL Variational Principles

From Equation (12.70) we know that $\Sigma = \frac{\delta\Phi}{\delta g}$; hence Luttinger and Ward obtained a new functional Ω with the interesting property of being stationary with respect to the correct g , that is,

$$\frac{\delta\Omega}{\delta g} = 0, \quad (12.81)$$

provided that g obeys the Dyson equation $g = (g_0^{-1} - \Sigma)^{-1}$. Indeed, using the same Tr notation as above for the sums of ring diagrams

$$\frac{\delta}{\delta g} Tr [ln(\Sigma - g_0^{-1}) + g\Sigma] = \frac{1}{\Sigma - g_0^{-1}} \frac{\delta \Sigma}{\delta g} + \Sigma + g \frac{\delta \Sigma}{\delta g} = \Sigma, \quad (12.82)$$

and so one finds that (12.81) holds for the functional

$$\Omega = Tr\{ln(\Sigma - g_0^{-1}) + \Sigma g\} - \Phi. \quad (12.83)$$

Luttinger and Ward [55] further proved that, as the notation suggests, Ω verifies (12.80) and coincides with Ω_0 for $\lambda = 0$; so, it is indeed the grand potential (at finite temperatures) or the ground-state energy (at $T=0$). These results have been generalized in the nineties; the Lund Group (C. -O. Almladh and U. von Barth) [136][137] have constructed a functional $\tilde{\Omega}$ which depends on g and on the screened interaction W and is variational in both variables; they tested numerically the performance of $\tilde{\Omega}$ by using simple approximations for g and W and found that the results were competitive. The derivation in Ref.[137] also points out the connection with Kohn-Sham theory (see below).

12.5 Generalized Ward Identities

Still, we have to exploit the continuity equation

$$\frac{\partial \rho}{\partial t} + div J = 0 \quad (12.84)$$

as a source of exact relations between the Green's functions. Here, in obvious notation, $\rho(x) = \psi^\dagger(x)\psi(x)$, $J_i(x) = \frac{-i\hbar}{2m} \left[(\frac{\partial}{\partial x_i} - \frac{\partial}{\partial x'_i})\psi^\dagger(x')\psi(x) \right]_{x'=x}$. Let A_1, A_2 denote Heisenberg operators such as fermion creation or annihilation operators and ρ an operator such as a density which commutes with A_1, A_2 under Wick's T ordering. We know (see Problem 2.3) that

$$\begin{aligned} \frac{d}{dt} T\{A_1(t_1)A_2(t_2)\rho(t)\} &= T\{A_1(t_1)A_2(t_2)\dot{\rho}(t)\} \\ &+ \delta(t-t_1)T\{[\rho(t), A_1(t_1)]_ - A_2(t_2)\} \\ &+ \delta(t-t_2)T\{A_1(t_1)[\rho(t), A_2(t_2)]_ - \}. \end{aligned} \quad (12.85)$$

Following [140] (see also [1]) we set $A_1(t_1) = \psi(x_1), A_2(t_2) = \psi^\dagger(x_2)$, take a (ground-state or thermal) average, use the continuity equation to replace $\dot{\rho}$ and obtain

$$\begin{aligned} \partial_t \langle T\{\psi(x_1)\psi^\dagger(x_2)\psi^\dagger(x)\psi(x)\} \rangle &= T\{\psi(x_1)\psi^\dagger(x_2)\nabla J(x)\} \\ &+ \delta(t-t_1)\langle T\{[\rho(x), \psi(x_1)]_ - \psi^\dagger(x_2)\} \rangle \\ &+ \delta(t-t_2)\langle T\{\psi(x_1)[\rho(x), \psi^\dagger(x_2)]_ - \} \rangle. \end{aligned} \quad (12.86)$$

Since $[\rho(x), \psi(x_1)]_ - = -\delta(x-x_1)\psi(x)$ and $[\rho(x), \psi^\dagger(x_2)]_ - = \delta(x-x_1)\psi^\dagger(x)$, one obtains the Ward identity [141]

$$\begin{aligned} \partial_t G_2(x, x_1, x_2, x) + \frac{\hbar}{2mi} \nabla(\nabla - \nabla') G_2(x, x_1, x_2, x') = \\ = i\delta^{(4)}(x - x_1)g(x, x_2) - i\delta^{(4)}(x - x_2)g(x, x_1) \end{aligned} \quad (12.87)$$

where $\delta^{(4)}(x) = \delta^{(3)}(\mathbf{r})\delta(t)$ is the 4-dimensional δ and the limit $x' \rightarrow x$ is understood. The continuity equation is an expression of charge conservation and is associated by Noether's theorem to the gauge invariance. Ward identities generally arise from invariance Groups of the theory.

12.6 Connection of Diagrams to D F T

12.6.1 Highlights on Density Functional Theory

As W. Kohn emphasized in his Nobel lecture, the many-body problem is rather ill posed in terms of the many-body wave function $\psi_0(x_1, x_2, \dots)$, with $x_i \equiv \{\mathbf{r}_i, \sigma_i\}$, and it of paramount practical and conceptual importance that it can be formulated in terms of the density,

$$n(\mathbf{r}) = \langle \psi_0 | \hat{n} | \psi_0 \rangle = N \sum_{\sigma} \int dx_2 \cdots \int dx_N |\psi(\mathbf{r}, \sigma, x_2, \dots, x_N)|^2. \quad (12.88)$$

Indeed, ψ_0 requires an immense amount of information for large N and a very small change in it gives an orthogonal state, while $n(\mathbf{r})$ is observable. I summarize the topic, starting with the Hohenberg-Kohn theorem [121].

Theorem 12. *For an N -electron liquid in an external potential $V_{ext}(\mathbf{x})$, the ground state energy E_0 is an universal functional of the density $n(\mathbf{r})$.*

This means that n determines E_0 and also the wave function ψ_0 : symbolically,

$$n \Rightarrow E_0, \psi_0.$$

Proof. Suppose we know the ground state wave function $\psi_0(x_1, x_2, \dots)$ and energy E_0 of an interacting electron liquid in an external potential V_{ext} (Equations 1.60, 1.61, 1.62) with Hamiltonian $H = T + U + V_{ext}$. Since $H\psi_0 = (T + U + V_{ext})\psi_0 = E_0\psi_0$, we can infer V_{ext} (apart from an additive constant). Thus, for a different potential energy V'_{ext} , one gets $H'\psi'_0 = (T + U + V'_{ext})\psi'_0 = E'_0\psi'_0$ with $\psi'_0 \neq \psi_0$. Assuming $\psi'_0 = \psi_0$ one should find $(V_{ext} - V'_{ext})\psi_0 = (E_0 - E'_0)\psi_0$ and V_{ext} and V'_{ext} should differ by a constant. If V_{ext} is such that the ground state is degenerate, several wave functions belong to E_0 , but this conclusion is not affected. Thus, ψ'_0 is a wave packet of eigenstates of H involving excited states.

Having shown that ψ_0 determines V_{ext} , that is, $\psi_0 \Rightarrow V_{ext}$; we next show that we can do with much less information, since $n \Rightarrow V_{ext}$, too. Assume the converse is true: then $\exists V'_{ext} \neq V_{ext}$ such that n is the same; the change

$V_{ext} \rightarrow V'_{ext}$ produces a new hamiltonian H' , with a *different* ground state wave function ψ'_0 and eigenvalue E'_0 ; by the variational principle

$$E_0 = \langle \psi_0 | H | \psi_0 \rangle < \langle \psi'_0 | H | \psi'_0 \rangle = \langle \psi'_0 | H' + V_{ext} - V'_{ext} | \psi'_0 \rangle. \quad (12.89)$$

Thus,

$$E_0 < E'_0 + \int d^3x [V_{ext}(x) - V'_{ext}(x)]n(x). \quad (12.90)$$

But this is absurd! If one starts by considering H' one finds

$$E'_0 < E_0 + \int d^3x [V'_{ext}(x) - V_{ext}(x)]n(x), \quad (12.91)$$

and summing the two one finds the contradictory result $E_0 + E'_0 < E_0 + E'_0$. Note that in the case of degeneracy the ground state density is not unique, but this does not change the conclusion that the same n cannot be compatible with two potentials. Thus, $n \Rightarrow V_{ext}$, or (in the DFT parlance) $V_{ext}(\mathbf{r})$ in an unique functional of $n(\mathbf{r})$. So, $n \Rightarrow V_{ext} \Rightarrow H$ and since in principle one can solve the Schrödinger equation, we may conclude that $n \Rightarrow \psi_0, E_0$.

The functional $E_0[n]$ is unknown: it would be the solution of all kinds of ground state problems in a formula. We can think physically, and separate out some obvious contributions. We set

$$E_0[n] = \int dx V_{ext}(x)n(x) + V_H[n] + \tilde{E}[n] \quad (12.92)$$

where

$$V_H[n] = \frac{1}{2} \int dx dx' \frac{n(x)n(x')}{|x-x'|} \quad (12.93)$$

is the Hartree term; this shifts the problem to a new unknown universal functional \tilde{E} . The electrostatic potential is

$$\phi(x) = V_{ext}(x) + \int dx' \frac{n(x')}{|x-x'|} = \frac{\delta}{\delta n} [E_0[n] - \tilde{E}[n]]. \quad (12.94)$$

Since $\frac{\delta E_0}{\delta n} = \mu$ we are left with

$$\phi(x) + \frac{\delta \tilde{E}}{\delta n} = \mu. \quad (12.95)$$

One can try a simple approximation by extrapolating the high-density Jellium result (12.28,12.29) (see also Problem 23). This is not accurate outside the Jellium case. Gradient corrections involving ∇n have been considered but do not take far: the approach remains semi-classical, closely related to the (1927) Thomas-Fermi scheme.

Kohn and Sham [122] invented the fully quantum mechanical version, just in time to take advantage of the computer revolution. To find a quantum kinetic energy functional $T[n]$, first of all one must realize that it exists. As noted above $n \Rightarrow V_{ext} \Rightarrow H$. Now, H determines ψ_0, E_0 and also $T = \langle \psi_0 | \hat{T} | \psi_0 \rangle$. We cannot carry on this program because we cannot solve the Schrödinger equation for the interacting system. However for a non-interacting system S of electrons moving in some external potential V_S we can. Let $T_S[n]$ be the kinetic energy of a fictitious N -electron system S having the same density as the real one; Kohn and Sham wrote

$$E_0[n] = T_S[n] + \int dx V_{ext}(x)n(x) + V_H[n] + E_{xc}[n], \quad (12.96)$$

where $E_{xc}[n]$ is a new unknown exchange-correlation functional. Indeed, we can apply to S the above argument showing that the density yields the external potential: $n \Rightarrow V_S$. Therefore, the required potential ensuring that S has the exact density must exist; having separated out the kinetic energy of S (that will differ from the exact kinetic energy of the interacting system) we can write (12.96) and pretend we know all but $E_{xc}[n]$ potential that must be approximated in some way, usually drawing from the Jellium theory at the density $n(x)$ prevailing at a given point. This is the Local Density Approximation. Among the popular approximations, I mention the interpolation formula

$$E_{xc}[n] = -\frac{3}{10} \left(\frac{3}{\pi} \right)^{\frac{1}{3}} \int n^{\frac{4}{3}} d^3r - 0.056 \int \frac{n^{\frac{4}{3}}}{0.079 + n^{\frac{1}{3}}} d^3r \quad (12.97)$$

and the extensions including gradient corrections

$$E_{xc}[n] = \int d^3r \left\{ \epsilon_{xc}(n)n(\mathbf{r}) + \epsilon_{xc}^{(2)}(n)|\nabla n(\mathbf{r})|^2 + \dots \right\}. \quad (12.98)$$

$E_{xc}[n]$ produces the exchange-correlation potential

$$V_{xc} = \frac{\delta E_{xc}}{\delta n}. \quad (12.99)$$

This contributes to the chemical potential, along with the electrostatic potential ϕ , since

$$\frac{\delta E_0}{\delta n} = \mu = \frac{\delta T_S}{\delta n} + \phi + V_{xc}. \quad (12.100)$$

Thus in the fictitious system the electrons do not interact but feel a potential

$$V_S = \phi(x) + \frac{\delta E_{xc}}{\delta n}, \quad (12.101)$$

which does not coincide with the screened potential but includes V_{xc} . One must solve self-consistently the set of N equations, the Kohn-Sham equations

$$\left(-\frac{1}{2}\nabla^2 + V_S\right)\psi_i(x) = \epsilon_i\psi_i(x), \quad (12.102)$$

and compute T_S and the density

$$n(x) = \sum_{i=1}^N |\psi_i(x)|^2 \quad (12.103)$$

from the determinant of the orbitals $\psi_i(x)$. The exchange-correlation potential can be improved over the jellium estimate (12.29) by including the generalized gradient corrections[138] and the accuracy of the results strongly depends on the system. In metals, typical error may be 0.3 eV per atom but for finite systems they are usually much worse. Bond lengths are usually reproduced to better than 10^{-9} cm.

Further Developments

The density functional perturbation theory is a technique that allows to calculate e.g. phonon dispersion in solids[149]. I quote the following useful result by Janak[146] without reporting the proof.

Theorem 13. *In density functional theory,*

$$\frac{\partial E}{\partial n_i} = \epsilon_i, \quad (12.104)$$

that is, the derivative of the total energy with respect to the occupation number of a Kohn-Sham orbital is equal to the eigenvalue of that orbital.

Vignale and Rasolt [119] formulated the current-density-functional theory, an extension which is needed to include magnetic fields; the current couples to the vector potential \mathbf{A} and a term in A^2 appears. A few pioneers [129],[130] tried time-dependent versions of Kohn-Sham equations in atomic problems; the results were rather encouraging, but a justification was lacking until Runge and Gross[131] found a suitable formalism. This was based on the variational principle $\delta A = 0$, where $A = \int_{t_1}^{t_2} \langle \psi(t) | i \frac{\partial}{\partial t} - H(t) | \psi(t) \rangle$, but for the rest the theory parallels the static one. For further details see[54].

This is the basis of Density Functional method on which most *ab-initio* calculations are performed, [125] and is of paramount importance as a practical calculational scheme when the correlation effects are not too severe. Very good comprehensive reviews on this subject are available [125], [54]; however I wish to discuss less well known consequences.

12.6.2 Sham - Schlüter Equation

There is no diagrammatic expansion for either E_{xc} or v_{xc} , however L.J. Sham and M. Schlüter [123] devised a scheme that in principle allows to deduce v_{xc}

from the self-energy. The exchange-correlation self-energy Σ_{xc} , which is all the self-energy minus the Hartree term, enters the Dyson equation for the Green's function g in terms of the Hartree approximation g_H (which also accounts for the external potential); in a shorthand self-evident matrix notation reads:

$$g = g_H + g_H \Sigma_{xc} g \Rightarrow g^{-1} = g_H^{-1} - \Sigma_{xc}. \quad (12.105)$$

In the fictitious non-interacting system the electrons see an effective potential

$$v_{eff} = V_{ext} + V_H + v_{xc}. \quad (12.106)$$

Thus the Green's function g_{KS} of the fictitious Kohn-Sham system obeys

$$g_{KS} = g_H + g_H V_{xc} g_{KS} \Rightarrow g_{KS}^{-1} = g_H^{-1} - V_{xc}. \quad (12.107)$$

rather than Equation (12.105). Hence,

$$g^{-1} - g_{KS}^{-1} = -(\Sigma_{xc} - V_{xc}) \Rightarrow g = g_{KS} + g_{KS}(\Sigma_{xc} - V_{xc})g. \quad (12.108)$$

Now, we observe that $g_{KS} \neq g$, but both yield the same density; thus, introducing as usual the positive infinitesimal δ ,

$$g(\mathbf{r}, t, \mathbf{r}' = \mathbf{r}, t + \delta) = g_{KS}(\mathbf{r}, t, \mathbf{r}' = \mathbf{r}, t + \delta) = n(\mathbf{r}). \quad (12.109)$$

Hence,

$$[g_{KS}(\Sigma_{xc} - V_{xc})g]_{\mathbf{r}'=\mathbf{r}, t'=t+\delta} = 0; \quad (12.110)$$

more explicitly, letting $x \equiv (\mathbf{r}, t)$, $x^+ \equiv (\mathbf{r}, t + \delta)$, this means

$$\int dx' dx'' g_{KS}(x, x') \{ \Sigma_{xc}(x', x'') - \delta(x' - x'') V_{xc}(x'') \} g(x'', x^+) = 0. \quad (12.111)$$

If an approximation to Σ_{xc} is given, the corresponding g can be obtained from the Dyson equation and this may be considered as an equation for $V_{xc}(x'')$. This Sham - M. Schlüter equation is awkward and highly non-linear (the unknown is also contained in g_{KS}) however it is considered [126] as an important source of information on V_{xc} . Like the density-functional approach, the Sham - M. Schlüter equation also holds generally for time-dependent problems.

Problems

12.1. If as an approximate $E[n]$ one keeps only $t[n]$ (see Equation 12.28), what kind of approximation is obtained?

12.2. Evaluate the diagram of Figure 11.2.2 with all $s_i = a$.

13 Non-Equilibrium Theory

13.1 Time-Dependent Probes and Nonlinear Response

Phenomena like electron transport, electronic transitions in chemisorption, desorption¹, molecule-surface collision processes, and sputtering² are naturally described by time-dependent electronic Hamiltonians. What happens in the Fano-Anderson model (Chapter 5.1.2) if the ϵ and V parameters depend on time? Such a time-dependence occurs because the Hamiltonian of electrons depends on the position of the nuclei, and, through this, from the time³. Such problems are completely outside the scope of the diagram method discussed so far; the equation of motion method (EOM) can work but depends on some approximate truncation procedure. This Chapter is devoted to the quantum theory of such non-equilibrium processes. A powerful generalized perturbation method enables us to deal with time dependent problems and processes that are far from equilibrium, generalizing the Kubo approach [29] to all orders. It is a general and in principle exact technique; the Feynman method is recovered as a particular case. There is no need to assume that the perturbation is small or that the system deviates little from equilibrium; one does not need to make any assumption that the system evolves in a reversible way. As one could expect, the study of the excited states and out-of-equilibrium situations involves special difficulties, however this generalized theoretical framework is also powerful for exploring the equilibrium nonlinear response to strong perturbations, that can be treated to all orders.

¹See Chapters 6.2, 10.2.1.

²This is an important process in industry, and generates a clean surface under vacuum. The surface is bombarded with ions with energies in the KeV range, and can typically disintegrate with the speed of some atomic layers per second.

³In a truly complete theory, the Hamiltonian would be time-independent and there would be no *external* fields, but then one should simultaneously deal with all the degrees of freedom, including light sources, electron beams and all that. Already in the static case this turns out to be difficult and one tries to apply, when possible, the Born-Oppenheimer approximation. The obvious generalization of such approximation to the dynamic case consists in treating the nuclei like classical particles, with a well defined trajectory: the electrons then are subject to a time-dependent potential.

To this end we will develop a formalism introduced many years ago by L.P.Kadanoff and G.Baym[82], above all in the version elaborated little later by L.V.Keldysh[84]. A somewhat generalized formulation in which the initial state is completely arbitrary was provided by Wagner [101]. In the literature, the application of this method is not yet very frequent, although it is gaining ground in recent years e.g. in the field of transport theory; it is still used much less than its potential and importance would deserve; this is due to the relative shortage of examples which constitutes an obstacle to its spread, and surely to its undeniable complexity. The technique generalizes the diagrammatic development of the Green functions to time-dependent problems and systems that are far from the thermodynamic equilibrium. Several kinds of Green functions are indeed needed, each with its place in the theory. Since there are several ways to choose which functions to define and since all possible choices have been made in the literature, the reader of the original articles finds a true zoo of such functions. I'll introduce all the most common species, but having care to specify their relations; I'll try to avoid the notation inconsistencies that frequently transform those exotic beasts into monsters.

13.2 Kadanoff-Baym and Keldysh Methods

Kadanoff and Baym[56] and Keldysh[84] devised different versions of the generalized diagram method; ultimately they are equivalent but the Kadanoff-Baym formalism is more popular in Statistical Mechanics while the Keldysh has been mostly used for dynamics. Here I'll follow the Keldysh scheme.

As in Equation (2.1) we split the Hamiltonian in two parts, $H(t) = H_0 + \hat{V}(t)$, with a free part H_0 , and a *perturbation* $\hat{V}(t)$ which is not necessarily small nor even time-dependent. In Section 2.3 we found how to expand the Interaction Picture evolution operator U_I^\dagger in powers of \hat{V}_I ,

$$U_I(t, t_0) = T \exp \left[-i \int_{t_0}^t dt' V_I(t') \right], \quad U_I^\dagger(t, t_0) = U_I(t_0, t). \quad (13.1)$$

The operators in the Green's functions are in the Heisenberg picture; however for any operator A we can switch representation by starting the evolution from a *golden age* t_0 when Heisenberg and Schrödinger pictures are the same, according to

$$A_H(t) = U_I^\dagger(t, t_0) A_I(t) U_I(t, t_0). \quad (13.2)$$

There are four U_I^\dagger factors to expand in series in

$$g^<(t, t') = \langle \Psi_0(t_0) | \Psi_H^\dagger(t') \Psi_H(t) | \Psi_0(t_0) \rangle = \langle \Psi_0 | U_I^\dagger(t', t_0) \Psi_I^\dagger(t') U_I(t', t_0) U_I^\dagger(t, t_0) \Psi_I(t) U_I(t', t_0) | \Psi_0 \rangle, \quad (13.3)$$

although we can reduce them to 3 since $U_I(t', t_0) U_I^\dagger(t, t_0) = U_I(t', t_0) U_I(t_0, t)$ and this is $U_I(t', t)$ by the group property. It would still be cumbersome to

expand the three U_I factors, but we can do with just one expansion, since for each operator A

$$\begin{aligned}
 A_H(t) &= U_I^\dagger(t, t_0) A_I(t) U_I(t, t_0) = \\
 &= (T e^{-i \int_t^{t_0} dt' V_I(t')}) A_I(t) (T e^{-i \int_{t_0}^t dt' V_I(t')}) = \\
 &= T_C \left[\exp \left(-i \int_{t_0}^t dt' V_I(t') \right) A_I(t) \right]
 \end{aligned}
 \tag{13.4}$$

where C is any oriented path in complex time through t_0 and t , using the generalized time-ordering T_C along C that we met in Section (2.2.1). Note that $A_I(t)$ is under the action of T_C that places it appropriately. In a similar

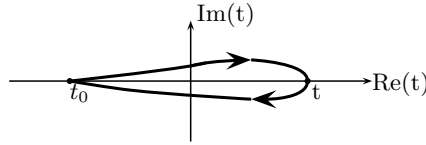


Fig. 13.1. A contour on the complex t plane for inserting $A(t)$ is a single interaction-picture evolution.

way, we can read from left to right $g^<(t, t') = \langle \Psi_0(t_0) | \Psi_H^\dagger(t') \Psi_H(t) | \Psi_0(t_0) \rangle$ as one *story*: the system starts at the golden age $t_0 \rightarrow -\infty$, evolves to t , is acted on by Ψ , then evolves to receive the action of Ψ^\dagger at time t' and eventually it evolves back to the *golden age*. Physically, t' can be before or after t . In this story, we meet Ψ^\dagger *after* Ψ because $g^<$ is defined with Ψ^\dagger on the left of Ψ . Thus along the path $C = C_1 U C_2$, t precedes t' , I write $t <_C t'$, and

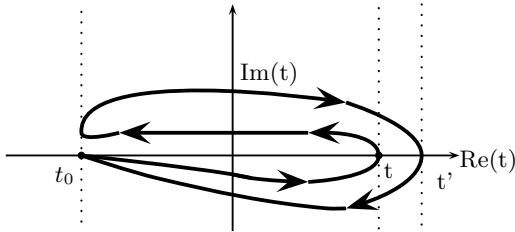


Fig. 13.2. The contour C for $g^<$ on the t plane with $t <_C t'$. Note that C can be analyzed as a two-step path $C = C_1 \cup C_2$, C_1 starts from t_0 and returns there after visiting t , and C_2 starts from t_0 and returns there after visiting t' . The first return and restart from t_0 can be avoided thanks to the group property.

$$\begin{aligned}
 g^<(t, t') &= \left\langle \left\{ T_{C_1} e^{-i \int_{C_1} d\tau V_I(\tau)} \Psi_I^\dagger(t') \right\} \left\{ T_{C_2} e^{-i \int_{C_2} d\tau' V_I(\tau')} \Psi_I^\dagger(t) \right\} \right\rangle \\
 &= \langle T_C e^{-i \int_C d\tau V_I(\tau)} \Psi_I^\dagger(t') \Psi_I^\dagger(t) \rangle \\
 &= -\langle T_C e^{-i \int_C d\tau V_I(\tau)} \Psi_I^\dagger(t) \Psi_I^\dagger(t') \rangle, \quad t <_C t'. \tag{13.5}
 \end{aligned}$$

Because of the group property, the contour C is largely arbitrary. It can go back to t_0 between t and t' any number of times, including 0. The terms arising in the series development of the operators are ordered automatically by T_C with earlier times (on C) to the right. Moreover,

$$\begin{aligned}
 g^>(t, t') &= \langle T_C \exp\{-i \int_C d\tau V_I(\tau)\} \Psi_I(t) \Psi_I^\dagger(t') \rangle \\
 &= -\langle T_C \exp\{-i \int_C d\tau V_I(\tau)\} \Psi_I^\dagger(t') \Psi_I(t) \rangle, \quad t >_C t' \tag{13.6}
 \end{aligned}$$

We can also use the same C in both cases, placing t and t' in opposite orders. As we know, the knowledge of both $g^>$ and $g^<$ gives access to the physically important retarded and advanced Green's functions. We also need to define a time-ordered (on C) Green's function:

$$ig(t, t') = \langle T_C \Psi_H(t) \Psi_H^\dagger(t') \rangle = g^>(t, t') \theta_C(t - t') - g^<(t, t') \theta_C(t' - t), \tag{13.7}$$

where the contour C goes through t and t' and $\theta_C(t - t') = 1$ if C is such that t' is met first and 0 otherwise.

13.3 Complex-Time Integrals by Langreth's Technique

Let A and B denote contour-time-ordered Green's functions analyzed in $>$ and $<$ parts as in Equations (13.5, 13.6)

$$\begin{aligned}
 A(t, t') &= -ia^>(t, t') \theta_C(t - t') + ia^<(t, t') \theta_C(t' - t) \\
 B(t, t') &= -ib^>(t, t') \theta_C(t - t') + ib^<(t, t') \theta_C(t' - t); \tag{13.8}
 \end{aligned}$$

following Langreth we must develop their combinations *in series* and *in parallel* which are needed to calculate diagrams in this theory. The combination in series $D = AB$ is defined by

$$\begin{aligned}
 D(t, t') &= AB(t, t') = \int_C d\tau A(t, \tau) B(\tau, t') \\
 &= -id^>(t, t') \theta_C(t - t') + id^<(t, t') \theta_C(t' - t). \tag{13.9}
 \end{aligned}$$

and must be rewritten as a combination of ordinary real-axis integrals. To calculate $d^<(t, t')$ we want t to be earlier on the contour, so we adopt $C = C_1 \cup C_2$ like in Figure (13.2). C_1 starts from t_0 and returns there after visiting

t , C_1 starts from t_0 and returns there after visiting t' . Along C_1 , $\tau <_C t' \Rightarrow B = ib^<$, while along C_2 , $\tau >_C t \Rightarrow A = ia^<$, hence

$$d^<(t, t') = -iD = d^<[C_1] + d^<[C_2] \quad (13.10)$$

$$\begin{aligned} d^<[C_1] &= -i \int_{C_1} d\tau A(t, \tau) i b^<(\tau, t') \\ d^<[C_2] &= -i \int_{C_2} d\tau i a^<(t, \tau) B(\tau, t'). \end{aligned} \quad (13.11)$$

On C_1 , $A = -ia^>$ on the $t_0 < \tau < t$ branch, $A = ia^<$ on the back trip, so

$$\begin{aligned} d^<[C_1] &= \int_{t_0}^t d\tau (-i) a^>(t, \tau) b^<(\tau, t') + \int_t^{t_0} d\tau i a^<(t, \tau) b^<(\tau, t') = \\ & \int_{t_0}^t d\tau (-i) [a^>(t, \tau) - a^<(t, \tau)] b^<(\tau, t') \end{aligned} \quad (13.12)$$

Now we let $t_0 \rightarrow -\infty$, and formally extend the integration to the full real axis introducing a theta function. The result is

$$\begin{aligned} d^<[C_1] &= \int_{-\infty}^{\infty} d\tau \{(-i) [a^>(t, \tau) - a^<(t, \tau)] \theta(t - \tau)\} b^<(\tau, t') \\ &= \int_{-\infty}^{\infty} d\tau a_r(t, \tau) b^<(\tau, t') = a_r b^< \end{aligned} \quad (13.13)$$

using Langreth's convenient shorthand notation (product of small letters for real axis integrals). One finds $d^<[C_2]$ and $d^>$ in a similar way and gets

$$d^< = a_r b^< + a^< b_a; \quad d^> = a_r b^> + a^> b_a. \quad (13.14)$$

From $d^<, d^>$ one finds d_r, d_a :

$$d_r = -i\theta(t - t') [d^< + d^>] = -i\theta(t - t') [a_r b^< + a^< b_a + a_r b^> + a^> b_a], \quad (13.15)$$

that is, more explicitly,

$$\begin{aligned} d_r(t, t') &= -i\theta(t - t') \int_{-\infty}^{\infty} d\tau \{a_r(t, \tau) [b^>(\tau, t') + b^<(\tau, t')] + \\ & [a^>(\tau, t') + a^<(\tau, t')] b_a(\tau, t')\}. \end{aligned} \quad (13.16)$$

Since $g^< + g^> = i(g_r - g_a)$, we can simplify this to read

$$d_r(t, t') = \theta(t - t') \int_{-\infty}^{\infty} d\tau \{a_r(t, \tau) b_r(\tau, t') - a_a(t, \tau) b_a(\tau, t')\}. \quad (13.17)$$

However, the second integrand vanishes unless $t' > \tau > t$ but then the θ in front of the integral vanishes; therefore, we conclude that

$$d_r = a_r b_r, \quad d_a = a_a b_a. \quad (13.18)$$

The series combination $E = ABC$ is immediately obtained:

$$e^> = (AB)_r c^> + (AB)^> c_a = a_r b_r c^> + (a_r b^> + a^> b_a) c_a, \quad (13.19)$$

$$e^< = (AB)_r c^< + (AB)^< c_a = a_r b_r c^< + (a_r b^< + a^< b_a) c_a, \quad (13.20)$$

and so on. Langreth also introduced the parallel combination

$$F(t, t') = A(t, t') B(t', t), \quad (13.21)$$

where no integration is understood. Recalling (13.8) and splitting F in the same way, one finds

$$\begin{aligned} -i f^>(t, t') &= a^>(t, t') b^<(t', t) \\ i f^<(t, t') &= a^<(t, t') b^>(t', t) \end{aligned} \quad (13.22)$$

where again no integration is understood. Hence,

$$f_r(t, t') = -i\theta(t - t')(f^> + f^<) = \theta(t - t')[a^>b^< - a^<b^>]. \quad (13.23)$$

Other forms are useful. Substituting $a^>\theta(t - t')$ by $(ia_r - a^>)\theta(t - t')$, and using $b^> + b^< = ib_r$, we obtain

$$f_r(t, t') = i\theta(t - t')[a_r b^< - a^< b_r]; \quad (13.24)$$

alternatively one can eliminate $b^<\theta(t - t')$ in favor of $(ib_r - b^>)\theta(t - t')$ to write

$$f_r(t, t') = i\theta(t - t')[a^> b_r - a_r b^>]; \quad (13.25)$$

the advanced part is dealt with in the same way.

13.3.1 Finite temperatures

For the finite temperature extension of this technique we must insert at the end of the contour C the vertical track in Figure 2.2.2 a). Then one can introduce $k^\lceil(\tau, t)$, $k^\lrcorner(t, \tau)$ and the Matsubara function $k^M(\tau, \tau')$ where t is on the real time axis and along C comes before τ, τ' which are imaginary, on the vertical track. Moreover let us denote the integrals on the vertical track

$$f \star g = \int_0^{-i\beta} dz f(z) g(z). \quad (13.26)$$

Equations (13.14) become

$$d^< = a_r b^< + a^< b_a + a^\lceil \star b^\lrcorner, \quad d^> = a_r b^> + a^> b_a + a^\lrcorner \star b^\lceil; \quad (13.27)$$

(13.18) remains as it is. The new functions obey (see [101], [120]):

$$\begin{cases} d^M = a^M \star b^M \\ d^\lceil = a_r b^\lceil + a^\lrcorner \star b^M \\ d^\lrcorner = a^M \star b^\lrcorner + a^\lceil b_a. \end{cases} \quad (13.28)$$

13.4 Keldysh-Dyson Equation on the Contour

The Feynman method of Chapter 11 is generalized by expanding

$$ig(t, t') = \langle T_C [\Psi_H(t) \Psi_H^\dagger(t')] \rangle = \langle T_C \left[e^{-i \int_C d\tau V_I(\tau)} \Psi_I(t) \Psi_I^\dagger(t') \right] \rangle \quad (13.29)$$

where the evolution in the interaction picture is on C and⁴

$$e^{-i \int_C d\tau V_I(\tau)} = \sum_{n=0}^{\infty} \frac{(-i)^n}{n!} \int_C d\tau_1 \cdots \int_C d\tau_n V(\tau_1) \cdots V(\tau_n). \quad (13.30)$$

The diagrams are the same as in the Feynman scheme, but the time integrals must be done on C , e.g. by the Langreth technique.

Example: Independent Particles

In independent-particle problems, V is a one-body operator. Let's write

$$V(t) = v(t) \psi^\dagger \psi, \quad (13.31)$$

where a matrix multiplication on spin-orbital indices such as in

$$V(t) = \sum_{kk'} v(t)_{kk'} \psi_k^\dagger \psi_{k'}$$

is understood. In first-order,

$$\delta g = (-i)^2 \int_C d\tau v(\tau) \langle T_C [\psi^\dagger(\tau) \psi(\tau) \psi(t) \psi^\dagger(t')] \rangle. \quad (13.32)$$

Using Wick's theorem (Section 11.1.1) we may write

$$\langle T_C [\psi^\dagger(\tau) \psi(\tau) \psi(t) \psi^\dagger(t')] \rangle = \langle T_C \psi^\dagger(\tau) \psi(\tau) \rangle \langle T_C \psi(t) \psi^\dagger(t') \rangle + \langle T_C \psi(t) \psi^\dagger(\tau) \rangle \langle T_C \psi(\tau) \psi^\dagger(t') \rangle \quad (13.33)$$

with the equal-times rule (11.69)

$$\langle T_C \psi^\dagger(\tau) \psi(\tau) \rangle = \langle \psi^\dagger(\tau_+) \psi(\tau_-) \rangle \quad (13.34)$$

where τ_+ is just after τ and τ_- just before. Each contraction $\langle T_C \psi^\dagger(t) \psi(t') \rangle = ig^0(t, t')$ brings an unperturbed Green's function; each product of contractions brings a factor $(-)^P$ which is the signature of the permutation of operators implied in doing the contraction. So, 13.32 becomes:

$$\delta g = (-i)^2 \int_C d\tau v(\tau) \{ -ig^0(\tau, \tau) ig^0(t, t') + ig^0(t, \tau) ig^0(\tau, t') \} \quad (13.35)$$

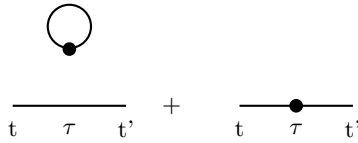


Fig. 13.3. First-order contribution of a one-body perturbation

The first contribution in Figure 13.3 is disconnected. It contains a factor $\int_C d\tau \xi(\tau)$, where ξ is independent of t and t' . The contour C may be taken on the real axis from $-\infty$ to ∞ and then back to $-\infty$; the integral vanishes independently of the positions of t and t' on the contour. This result extends to all orders, the Linked Cluster Theorem of Section 11.9.1 again applies, and the unlinked diagrams yield nothing. So, one obtains the same rules as in Section 11.9.1 with the only difference that the time integrals are on C . Thus, one obtains the Dyson equation,

$$g = g^0 + g^0 \Sigma g \tag{13.36}$$

again with the time integrals on C .

Solving the Dyson equation

If Σ is known, one can develop the Dyson equation where $g^0 \Sigma g$ is a series combination. Indeed, the self-energy, like g , depends on two times, and we write:

$$i\Sigma(t, t') = \sigma^>(t, t')\theta_C(t - t') - \sigma^<(t, t')\theta_C(t' - t). \tag{13.37}$$

Naturally, for $t \neq t'$ one also defines

$$\begin{aligned} i\sigma_r(t, t') &= [\sigma^>(t, t') + \sigma^<(t, t')] \theta(t - t'), \\ -i\sigma_a(t, t') &= [\sigma^>(t, t') + \sigma^<(t, t')] \theta(t' - t). \end{aligned} \tag{13.38}$$

So, from (13.36) one obtains:

$$g_r = g_r^0 + g_r^0 \sigma_r g_r \tag{13.39}$$

$$g_a = g_a^0 + g_a^0 \sigma_a g_a \tag{13.40}$$

$$g^> = g^{0>} + g_r^0 \sigma_r g^> + g_r^0 \sigma^> g_a + g^{0>} \sigma_a g_a \tag{13.41}$$

⁴from now on, all operators are understood to be in the Interaction Picture, and I drop the index I. Moreover I'll often understand \hbar to simplify the writing of the equations.

$$g^< = g^{0<} + g_r^0 \sigma_r g^< + g_r^0 \sigma^< g_a + g^{0<} \sigma_a g_a. \quad (13.42)$$

However all the information is contained in $g^>$ and $g^<$; we need just two equations. The equations for $g^{(r)}$ and $g^{(a)}$ are equivalent and provide $[\sigma^>(t, t') + \sigma^<(t, t')]$, so all we need is

$$f = g^> - g^< \quad (13.43)$$

and to this effect we define

$$\Omega = \sigma^> - \sigma^<. \quad (13.44)$$

The difference of the equations for $g^>$ and $g^<$ gives

$$f = f^0 + g_r^0 \sigma_r f + g_r^0 \Omega g_a + f^0 \sigma_a g_a. \quad (13.45)$$

We can also give a closed solution in terms of the self-energy. This equation is a matrix equation in the indices t, t' with the formal solution

$$f = [1 - g_r^0 \sigma_r]^{-1} (f^0 [1 + \sigma_a g_a] + g_r^0 \Omega g_a). \quad (13.46)$$

The matrix inversion is readily carried out:

$$[1 - g_r^0 \sigma_r]^{-1} = 1 + g_r^0 \sigma_r + g_r^0 \sigma_r g_r^0 \sigma_r + \dots = 1 + [g_r^0 + g_r^0 \sigma_r g_r^0 + \dots] \sigma_r = 1 + g_r \sigma_r;$$

moreover,

$$[1 - g_r^0 \sigma_r]^{-1} g_r^0 = g_r^0 + g_r^0 \sigma_r g_r^0 + \dots = g_r.$$

So,

$$f = [1 + g_r \sigma_r] f^0 [1 + \sigma_a g_a] + g_r \Omega g_a. \quad (13.47)$$

In summary, once Σ is known, a clear cut procedure yields g . One can use σ_a and σ_r to solve for g_a and g_r like in one-electron problems. The results and Ω are then used in Equation 13.47 for f , where the dependence on the Fermi level enters. Eventually, from g_a, g_r and f one also obtains $g^<$ and $g^>$.

Dynamical Independent-Particle Problems

The special case of independent electrons can be solved exactly but is far from trivial due to many-body effects; this case also lends itself to include interactions approximately in a dynamical-Hartree-Fock or time-dependent density-functional scheme. In this case all the self-energy comes from the connected first-order diagram on the right of Figure 13.3, that is,

$$\delta g = \int_C d\tau g^0(t, \tau) v(\tau) g^0(\tau, t'); \quad (13.48)$$

this must be interpreted as

$$\delta g = \int_C d\tau \int_C d\tau' g^0(t, \tau) \Sigma(\tau, \tau') g^0(\tau, t') \tag{13.49}$$

which implies that

$$\Sigma(\tau, \tau') = v(\tau)\delta_C(\tau - \tau') \tag{13.50}$$

that is, the time-dependent self-energy is instantaneous and the propagator line comes out of it at the very same point along the contour where it entered the interaction. This implies that $\sigma^<$, $\sigma^>$ and Ω vanish, so $\sigma_r = \sigma_a = 0$, but at equal times equations (13.38) do not hold, so we may have σ_r and σ_a proportional to $\delta(t - t')$. From $\delta g = g^0 v g^0$ one gets

$$\begin{cases} \delta g_r = g_r^0 v g_r^0 \\ \delta g^< = g_r^0 v g^{0<} + g^{0<} v g_a^0 \end{cases} \tag{13.51}$$

where $g_r^0 v g_r^0 = \int d\tau g_r^0(t, \tau) v(\tau) g_r^0(\tau, t')$, while the Dyson equation is

$$\delta g^< = g_r^0 \sigma_r g^{0<} + g_r^0 \sigma^< g_a^0 + g^{0<} v g_a^0. \tag{13.52}$$

This means that the self-energy is given by

$$\Omega = 0; \sigma_r(t, t') = \sigma_a(t, t') = \delta(t - t')v(t). \tag{13.53}$$

13.5 Evolution on Keldysh Contour

The contour C can be deformed freely as long as it starts and ends at the *golden age* t_0 and goes through t and t' . We have used one with two wings *ad hoc* for series combinations. We could keep introducing new contours to calculate the various combinations arising in the diagrams; however it is more practical to have a standard contour and consider the various position of the times on it. In time-dependent problems, one usually prefers the Keldysh contour of Figure (15.3.2) from t_0 to $-t_0$ and back to t_0 ; there are an ascending or positive branch and a descending or negative branch, and $g(t, t')$ can have each of its arguments on any of the two. Thus, there are 4 different Green's functions defined on the real axis, that as above I shall denote with small letters. Taking both times on the positive branch, one gets

$$g^c(t, t') = -i\langle T_C \psi_H(t_+) \psi_H^\dagger(t'_+) \rangle. \tag{13.54}$$

Note that $g^c(t, t') = -i\langle T \psi_H(t) \psi_H^\dagger(t') \rangle$ is nothing but the time-ordered Green's function of the usual theory

$$i g^c(t, t') = g^>(t, t')\theta(t - t') - g^<(t, t')\theta(t' - t). \tag{13.55}$$

The traditional diagram expansion, that holds for constant V , is a special case of the general one. The time sequence of Figure 13.5 in the interaction picture yields $(-)(-i)\langle U(-\infty, \infty)U(\infty, t')\psi_I^\dagger(t')U(t', t)\psi_I(t)U(t, -\infty) \rangle$ where a

(-) factor arises from the interchange of ψ and ψ^\dagger . Including the other ordering of t and t' , one obtains $-i\langle U(-\infty, \infty)T[\psi_I(t)\psi_I^\dagger(t')U(\infty, -\infty)]\rangle$ with the descending or backwards evolution operator $U(-\infty, \infty)$ relegated on the far left. The expectation value is taken at the golden age t_0 over the non-interacting ground state Φ (Chapter 1).

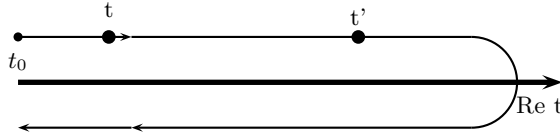


Fig. 13.4. The Keldysh contour with t and t' on the ascending branch.

At finite temperature one completes the contour as follows:

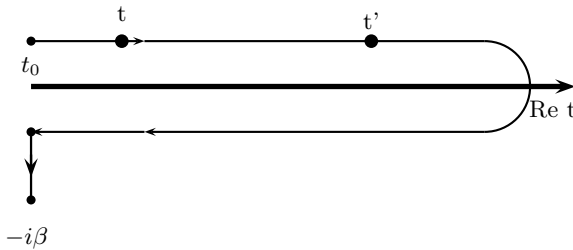


Fig. 13.5. The Keldysh contour with t and t' on the ascending branch. The vertical track is necessary for finite-temperature averages as in Figure 2.2.2.

It is interesting to note that if V is static one can adopt the adiabatic switching on at t_0 and off at $-t_0$; then the adiabatic theorem states that $\langle\Phi|U(-\infty, \infty) = e^{i\alpha}\langle\Phi|$. So,

$$g^c(t, t') = -i \frac{\langle\Phi|T[\psi(t)\psi^\dagger(t')U(\infty, -\infty)]|\Phi\rangle}{\langle\Phi|U(\infty, -\infty)|\Phi\rangle}, \quad (13.56)$$

which is just Equation (11.63), the starting point of the usual expansion. If $V = V(t)$, the adiabatic theorem does not apply, and the new formalism is needed, however even if V is constant there is no need for the adiabatic theorem in the new formalism. So, the general scheme is more powerful and conceptually simpler.

Taking both times on the negative branch one obtains

$$\tilde{g}^c(t, t') = -i\langle T_C\psi_H(t_-)\psi_H^\dagger(t'_-) \rangle = -i\langle \tilde{T}_C\psi_H(t)\psi_H^\dagger(t') \rangle, \quad (13.57)$$

with \tilde{T} that orders times as the reverse of T ; instead of (13.55) we write

$$i\tilde{g}^c(t, t') = g^>(t, t')\theta(t' - t) - g^<(t, t')\theta(t - t') \quad (13.58)$$

The other two combinations, where the order on C is fixed, are

$$\begin{aligned} g^+(t, t') &= -i\langle T_C \psi_H(t_+) \psi_H^\dagger(t_-) \rangle = ig^<(t, t') \\ g^-(t, t') &= -i\langle T_C \psi_H(t_-) \psi_H^\dagger(t_+) \rangle = -ig^>(t, t'). \end{aligned} \quad (13.59)$$

Note that

$$g^+(t, t') + g^-(t, t') = g^c(t, t') + \tilde{g}^c(t, t'), \quad (13.60)$$

$$\begin{aligned} g^c(t, t') - g^+(t, t') &= \\ &= -i [g^>\theta(t - t') - g^<\theta(t' - t)] - ig^< [\theta(t - t') - \theta(t' - t)] \\ &= -i [g^> + g^<] \theta(t - t') = g_r(t, t'), \end{aligned} \quad (13.61)$$

and in a similar way⁵

$$g^c(t, t') - g^-(t, t') = g_a(t, t'). \quad (13.62)$$

On the Keldysh contour, $\int_C d\tau = \int_{-\infty}^{\infty} dt_+ + \int_{\infty}^{-\infty} dt_-$; so one can write all integrals on the real axis by introducing a matrix notation with the pattern $\begin{pmatrix} ++ & +- \\ -+ & -- \end{pmatrix}$ of time labels, that is, by introducing the 2×2 matrix Green's function

$$\underline{\mathcal{G}}(t, t') = \begin{pmatrix} g^c & g^+ \\ g^- & \tilde{g}^c \end{pmatrix}. \quad (13.63)$$

However, since we wish to rewrite $\int_{\infty}^{-\infty} dt_-$ as $-\int_{-\infty}^{\infty} dt_-$ we must insert a - sign for each integration in dt_- . This is conveniently done by inserting a Pauli σ_z matrix factor between any two matrix Green's functions in series combinations. For example, the linked first-order diagram due to a one-body perturbation $V(t)$ given by Equation (13.48) becomes

$$\delta g = \int_C d\tau g^0(t, \tau) v(\tau) g^0(\tau, t') \rightarrow \int_{-\infty}^{\infty} d\tau v(\tau) \underline{\mathcal{G}}^0(t, \tau) \sigma_z \underline{\mathcal{G}}^0(\tau, t'). \quad (13.64)$$

Here

$$\underline{\mathcal{G}}^0(t, \tau) \sigma_z \underline{\mathcal{G}}^0(\tau, t') = \begin{pmatrix} g^c(t, \tau) & -g^+(t, \tau) \\ g^-(t, \tau) & -\tilde{g}^c(t, \tau) \end{pmatrix} \begin{pmatrix} g^c(\tau, t') & g^+(\tau, t') \\ g^-(\tau, t') & \tilde{g}^c(\tau, t') \end{pmatrix} \quad (13.65)$$

⁵These are the correct equations, although in the literature g_r and g_a are often confused.

Check: Dyson's equation from Keldysh matrix formalism

The Keldysh formalism reproduces the results of Sect. 13.3 (although it may be more friendly when performing the diagram expansion). To see that, we define

$$\underline{\mathcal{X}}(t, t', \tau) = \begin{pmatrix} x^c & x^+ \\ x^- & \tilde{x}^c \end{pmatrix} = \underline{\mathcal{G}}^0(t, \tau) \sigma_z \underline{\mathcal{G}}^0(\tau, t') \quad (13.66)$$

and do the matrix multiplications; $\underline{\mathcal{X}}$ is given by

$$\begin{pmatrix} g^c(t, \tau)g^c(\tau, t') - g^+(t, \tau)g^-(\tau, t') & g^c(t, \tau)g^+(\tau, t') - g^+(t, \tau)\tilde{g}^c(\tau, t') \\ g^-(t, \tau)g^c(\tau, t') - \tilde{g}^c(t, \tau)g^-(\tau, t') & g^-(t, \tau)g^+(\tau, t') - \tilde{g}^c(t, \tau)\tilde{g}^c(\tau, t') \end{pmatrix}.$$

Thus for instance $x^- = -ix^> = g^-(t, \tau)g^c(\tau, t') - \tilde{g}^c(t, \tau)g^-(\tau, t')$ that is, $x^> = [g^>(t, \tau)g^c(\tau, t') - \tilde{g}^c(t, \tau)g^>(\tau, t')]$.

Eliminating g^c by Equation (13.62) and \tilde{g}^c by Equation (13.60), one finds $x^> = g^>g_a + g_r g^>$, in agreement with (13.14). The Dyson equation reads

$$\underline{\mathcal{G}}(t, t') = \underline{\mathcal{G}}^0(t, t') + \int_{-\infty}^{\infty} d\tau_1 \int_{-\infty}^{\infty} d\tau_2 \underline{\mathcal{G}}^0(t, \tau_1) \sigma_z \underline{\Sigma}(\tau_1, \tau_2) \sigma_z \underline{\mathcal{G}}(\tau_2, t'), \quad (13.67)$$

where of course

$$\underline{\Sigma} = \begin{pmatrix} \sigma^c & \sigma^+ \\ \sigma^- & \tilde{\sigma}^c \end{pmatrix}. \quad (13.68)$$

Again, this can be cast as in Sect. 13.3 in terms of advanced and retarded functions. To this end, we use the unitary matrix

$$U = \frac{1 + i\sigma_y}{\sqrt{2}} = \begin{pmatrix} \frac{1}{\sqrt{2}} & -\frac{1}{\sqrt{2}} \\ \frac{1}{\sqrt{2}} & \frac{1}{\sqrt{2}} \end{pmatrix}, \quad U^{-1} = \begin{pmatrix} \frac{1}{\sqrt{2}} & \frac{1}{\sqrt{2}} \\ -\frac{1}{\sqrt{2}} & \frac{1}{\sqrt{2}} \end{pmatrix} \quad (13.69)$$

leading to

$$U \cdot \underline{\mathcal{G}} \cdot U^{-1} = \begin{pmatrix} \frac{g^c - g^- - g^+ + \tilde{g}^c}{2} & \frac{g^c - g^- + g^+ - \tilde{g}^c}{2} \\ \frac{g^c + g^- - g^+ - \tilde{g}^c}{2} & \frac{g^c + g^- + g^+ + \tilde{g}^c}{2} \end{pmatrix} = \begin{pmatrix} 0 & g_a \\ g_r & f' \end{pmatrix} \quad (13.70)$$

where $f' = -if = g^+ + g^-$ and

$$U \cdot \underline{\Sigma} \cdot U^{-1} = \begin{pmatrix} 0 & \sigma_a \\ \sigma_r & \Omega' \end{pmatrix} \quad (13.71)$$

where $\Omega' = -i\Omega = \sigma^+ + \sigma^-$. To transform the Dyson equation we also want $U\sigma_z U^{-1} = \sigma_x = \begin{pmatrix} 0 & 1 \\ 1 & 0 \end{pmatrix}$; the self-energy appears in the combination

$$U\sigma_z \underline{\Sigma} \sigma_z U^{-1} = \sigma_x \begin{pmatrix} 0 & \sigma_a \\ \sigma_r & \Omega' \end{pmatrix} \sigma_x = \begin{pmatrix} \Omega' & \sigma_r \\ \sigma_a & 0 \end{pmatrix}, \quad (13.72)$$

and in the literature sometimes Σ is defined as the latter matrix, omitting the problem that leads to introducing the σ_z factors. Using the Langreth shorthand notation of Section 13.3 the Dyson equation becomes (since the (-i) factors in f' and Ω' cancel)

$$\begin{pmatrix} 0 & g_a \\ g_r & f \end{pmatrix} = \begin{pmatrix} 0 & g_a^0 \\ g_r^0 & f^0 \end{pmatrix} + \begin{pmatrix} 0 & g_a^0 \\ g_r^0 & f^0 \end{pmatrix} \begin{pmatrix} \Omega & \sigma_r \\ \sigma_a & 0 \end{pmatrix} \begin{pmatrix} 0 & g_a \\ g_r & f \end{pmatrix}, \quad (13.73)$$

which agrees with the previous result (Equations 13.39 and following ones).

13.5.1 Contour Evolution of Bosons

In the case of bosons, T_C does not imply any sign change when two creation or annihilation operators are exchanged. Green's functions are written in terms of field operators ϕ . For instance, for phonons with field operators $\phi_m = d_m + d_m^\dagger$ one defines[62] the Green's functions

$$D_{mn}(t, t') = -i \langle T_C \phi_m(t) \phi_n(t') \rangle \quad (13.74)$$

with $D_{mn}^>(t, t') = \langle \phi_m(t) \phi_n(t') \rangle$ and so on, such that

$$iD_{mn}(t, t') = D_{mn}^>(t, t')\theta_C(t - t') + D_{mn}^<(t, t')\theta_C(t' - t). \quad (13.75)$$

Moreover, on the Keldysh contour

$$D^+ = -iD^<, \quad D^- = -iD^> \quad (13.76)$$

without the sign change, and so

$$D_{mn}^+(t, t') = -i \langle \phi_n(t') \phi_m(t) \rangle = D_{nm}^-(t', t). \quad (13.77)$$

Moreover, in the definitions of the retarded and advanced functions,

$$D_{mn}^r(t, t') = -i\theta(t - t') \langle [\phi_m(t), \phi_n(t')]_- \rangle, \quad (13.78)$$

$$D_{mn}^a(t, t') = -i\theta(t' - t) \langle [\phi_m(t), \phi_n(t')]_- \rangle, \quad (13.79)$$

commutators rather than anticommutators occur. With these modifications, the Keldysh formalism extends to bosons.

13.6 Selected Applications of the Keldysh Formalism

Being a general theoretical set-up for the many-body problem, this diagram method is virtually unlimited in scope. The examples discussed below were selected among the most instructive known to the writer.

13.6.1 Atom-Surface Scattering

Consider processes like atom-surface scattering, desorption or sputtering, when a moving atom interacts with a surface. As in Section 10.2.1 we model the situation by a Fano model (Chapter 5) with a non-degenerate atomic energy level ϵ_d interacting via time-dependent hopping matrix elements $V_{dk}(t)$ with a solid having a continuum of Bloch eigenvalues ϵ_k ; spin indices are suppressed in this problem. For the sake of definiteness we consider below a problem, where the atom is scattered or is being emitted from the surface, $V_{dk}(t) \rightarrow 0$ for $t \rightarrow \infty$, and we are interested in the probability of detecting a neutral atom or a ion. We want the long-time limit of the mean occupation number $n_d(t) = \langle c_d^\dagger(t)c_d(t) \rangle$. We split the hamiltonian $H = H_0 + H_h$, $H_0 = \sum_{k \in \mathcal{C}, \sigma} \epsilon_k n_{k,\sigma} + \epsilon_d n_{0,\sigma}$ with $H_h = \sum_{k,\sigma} \{V_k a_{k\sigma}^\dagger a_{0\sigma} + h.c.\}$ like in (5.1) but here it is convenient to write

$$H_0 = \sum_{\lambda} \epsilon_{\lambda} c_{\lambda}^{\dagger} c_{\lambda} \quad (13.80)$$

with greek indices running over d and all the k states. Up to time $t_0 \rightarrow -\infty$ the system is in an eigenstate of H_0 specified by occupation numbers n_{λ}^0 ; this sets the initial condition of the problem. In some cases we wish to use adiabatic switching to introduce H_h , as in desorption problems; in scattering problems on the other hand the initial condition does not necessarily coincide with the ground state oh H_0 . The unperturbed Green's functions are readily obtained.

$$g_{\lambda\mu}^{0<}(t, t') = \langle c_{\lambda}^{\dagger}(t')c_{\mu}(t) \rangle = \delta_{\lambda\mu} n_{\lambda}^0 e^{-i\epsilon_{\lambda}(t-t')} \quad (13.81)$$

$$g_{\lambda\mu}^{0>}(t, t') = \langle c_{\mu}(t)c_{\lambda}^{\dagger}(t') \rangle = \delta_{\lambda\mu}(1 - n_{\lambda}^0) e^{-i\epsilon_{\lambda}(t-t')}. \quad (13.82)$$

Hence, the unperturbed retarded and advanced functions are

$$g_{r,\lambda\mu}^0(t, t') = -i\delta_{\lambda\mu} e^{-i\epsilon_{\lambda}(t-t')}, \quad (13.83)$$

$$g_{a,\lambda\mu}^0(t, t') = +i\delta_{\lambda\mu} e^{-i\epsilon_{\lambda}(t'-t)}, \quad (13.84)$$

both independent of occupation numbers. The perturbation is, with a slight change in notation,

$$H_I(t) = \sum_k V_{dk}(t)c_d^{\dagger}c_k + h.c., \quad (13.85)$$

and we want

$$n_d(t) = \langle c_d^{\dagger}(t)c_d(t) \rangle = g_{dd}^<(t, t) = -ig_{dd}^c(t, t+0), \quad t \rightarrow \infty \quad (13.86)$$

where $t+0$ is just more than t .

The self-energy is given by (13.53) where σ_a and σ_r are matrices in the state indices; the Dyson equation may be simplified using the instantaneous character of the self-energy to read

$$g_{r,\lambda\mu}(t, t') = g_{r,\lambda\mu}^0(t, t') + \sum_{\nu\rho} \int_{-\infty}^{\infty} d\tau g_{r,\lambda\nu}(t, \tau) V_{\nu\rho}(\tau) g_{r,\rho\mu}^0(\tau, t'). \quad (13.87)$$

But $g_{r,\rho\mu}^0 \propto \delta_{\rho\mu}$ and we can further simplify ⁶

$$g_{r,\lambda\mu}(t, t') = \delta_{\lambda\mu} g_{r,\lambda\mu}^0(t, t') + \sum_{\nu} \int_{-\infty}^{\infty} d\tau g_{r,\lambda\nu}(t, \tau) V_{\nu\mu}(\tau) g_{r,\mu\mu}^0(\tau, t'). \quad (13.89)$$

The local (dd) component has a closed Dyson equation; indeed, using (in matrix notation)

$$g_{r,dd} = g_{r,dd}^0 + g_{r,dd}^0 \sum_k V_{dk} g_{r,kd} \quad (13.90)$$

and inserting

$$g_{r,kd} = g_{r,kk}^0 V_{kd} g_{r,dd} \quad (13.91)$$

one finds

$$g_{r,dd} = g_{r,dd}^0 + g_{r,dd}^0 \Sigma_r^{(d)} g_{r,dd}, \quad (13.92)$$

with the *dynamical self-energy*

$$\Sigma_r^{(d)}(t, t') = \sum_k V_{dk}(t) g_{r,kk}^0(t, t') V_{kd}(t'). \quad (13.93)$$

These equations solve the problem of an electron in an empty system (and the conjugate problem of a hole in a filled one). Please note carefully that the instantaneous self-energy becomes retarded when a closed (dd) Dyson equation is written; this is similar to what happens in Section 5.1.2 where the proper self-energy of the localized state is ω -dependent.

As an example, we can come back to the desorption model of Section 10.2.1. For instance, if at time $t = 0$, a neutral F atom starts desorbing from a Fluoride surface, where it is F^- , we describe it in the hole picture with $n_d^0 = n_d(0) = 1$, $n_k^0 = n_k(0) = 0$; the problem requires the retarded hole Green's function.

For simplicity one usually introduces the assumption that the time dependence of $V_{dk}(t)$ is the same for all k , that is,

$$V_{dk}(t) = u(t) V_{dk} \quad (13.94)$$

⁶The advanced function parallels the retarded one:

$$g_{a,\lambda\mu}(t, t') = \delta_{\lambda\mu} g_{a,\lambda\mu}^0(t, t') + \sum_{\nu} \int_{-\infty}^{\infty} d\tau g_{a,\lambda\nu}(t, \tau) V_{\nu\mu}(\tau) g_{a,\mu\mu}^0(\tau, t'). \quad (13.88)$$

where $u(t)$ is some time-dependent function. Then,

$$\Sigma_r^{(d)}(t, t') = -i\theta(t, t')u^*(t)u(t') \sum_k |V_{dk}|^2 e^{-i\epsilon_k(t-t')}. \quad (13.95)$$

In static conditions (time-independent H), the virtual level is characterized by a self-energy $\Sigma(\omega)$, that here I'll denote as $\Sigma^S(\omega)$. So, a Fourier transformation gives

$$\Sigma^S(\omega) = \sum_k \frac{|V_{dk}|^2}{\omega - \epsilon_k + i\delta} \Rightarrow \Sigma^S(t) = -i\theta(t) \sum_k |V_{dk}|^2 e^{-i\epsilon_k t}, \quad (13.96)$$

leading to

$$\Sigma_r^{(d)}(t, t') = u^*(t)u(t')\Sigma^S(t - t'). \quad (13.97)$$

The dynamics of the virtual levels is factored from the dynamics due to the time-dependent Hamiltonian. Using (13.83), the Dyson equation for the retarded function reads

$$g_{r,dd}(t, t') = -ie^{-i\epsilon t} \{ e^{i\epsilon t'} \theta(t - t') + \quad (13.98)$$

$$\int_{-\infty}^t d\tau_1 \int_{t'}^{\tau_1} d\tau_2 e^{i\epsilon\tau_1} u(\tau_1)u(\tau_2)\Sigma^S(\tau_1 - \tau_2)g_{r,dd}(\tau_2, t') \}; \quad (13.99)$$

the limits of integration are the effect of the θ functions. By differentiation one can check that⁷

$$i\frac{\partial}{\partial t}g_{r,dd}(t, t') = \epsilon g_{r,dd}(t, t') + u^*(t) \int_{t'}^t d\tau u(\tau)\Sigma^S(t - \tau)g_{r,dd}(\tau, t'). \quad (13.100)$$

In the theory of desorption from an ionic crystal, $g_{r,dd}(t, t')$ is the probability amplitude that a hole created on the desorbing species at time t' is found there at time t . Let us calculate the probability

$$P = |g_{r,dd}(\infty, 0)|^2 \quad (13.101)$$

in a simple model with

$$u(t) = e^{-\lambda t}; \quad (13.102)$$

this may be reasonable if the hopping integrals decrease exponentially with the atom-surface distance and the normal component v of the speed is about constant. The frequency associated with bond-breaking is $\lambda \sim \frac{v}{d}$, where $d \sim 1 \text{ \AA}$ is the bond length. For any atom desorbing with a kinetic energy of some eV one finds that $\hbar\lambda \ll 1 \text{ eV}$ is much less than a typical band width.

⁷this integro-differential equation remains valid even if ϵ depends on time (see Ref. [99])

For a Lorentzian virtual level, $\Sigma^S = A - 2i\Delta$ is a complex constant, with the real part A a mere shift of the level that we can re-adsorb in the definition of ϵ_d . The lifetime width Δ is significant. Then one can assume⁸

$$\Sigma^S(t) = -2i\Delta\theta(t)\delta(t). \quad (13.103)$$

Thanks to the δ equation (13.100) become differential,

$$i\frac{\partial}{\partial t}g_{r,dd}(t, t') = [\epsilon - 2i\Delta e^{-2\lambda t}] g_{r,dd}(t, t'), \quad (13.104)$$

and its solution is straightforward:

$$g_{r,dd}(t, 0) = -i\theta(t)e^{-i\epsilon t - \frac{\Delta}{\lambda}(1 - e^{-2\lambda t})}. \quad (13.105)$$

Thus, the probability P that a neutral F is detected at infinity is

$$P = e^{-\frac{2\Delta}{\lambda}}. \quad (13.106)$$

The Lorentzian model predicts a velocity dependence $P(v) \propto e^{-\frac{v_0}{v}}$, where v_0 is a constant; for $v \ll v_0$, P is close to 0. However, $P(v)$ is not analytic as $v \rightarrow 0$, and any development in powers of λ fails despite the fact that $\frac{\Delta}{\lambda} \ll 1$.

An evident weakness of the Lorentzian approximation is that P in (13.106) is independent of the position of ϵ_d with respect to the band continuum, while the shape of the virtual level depends on it. The solutions of Equation (13.100) (Ref. [47]) show that P may be enhanced by orders of magnitude if the level is near the band edges.

Including the Fermi Level

The general formalism is necessary when the band is partly occupied. f is the quantity that depends explicitly on the occupation numbers, and the Dyson equation for $\Omega = 0$ is solved by

$$f = [1 + g_r\sigma_r] f^0 [1 + \sigma_a g_a] \quad (13.107)$$

where it is understood that

$$f_{\mu\nu}^0(t, t') = g_{\mu\nu}^{0>}(t, t') - g_{\mu\nu}^{0<}(t, t') = \delta_{\mu\nu}(1 - 2n_{\mu}^0)e^{-i\epsilon_{\mu}(t-t')}. \quad (13.108)$$

The equation for f is a matrix equation in the time indices (t, t' and intermediate times) and in those denoting spin-orbital states (d, k and intermediate states). Let me make such dependence explicit by the notation change $f \rightarrow [f]_{\lambda\rho}(t, t')$, and the like, when necessary; then, Equation (13.107) reads

⁸The self-energy must have a factor $\theta(t)$ because it is retarded. However, the product $\theta(t)\delta(t)$ is ambiguous; here it is understood that $\theta(0) = 1$ and therefore the transform is $\Sigma^S(\omega) = -2i\Delta$.

$$\begin{aligned}
 f_{\lambda\rho}(t, t') &= \sum_{\mu\nu} \int_{-\infty}^{\infty} d\tau_1 [1 + g_r \sigma_r]_{\lambda\mu}(t, \tau_1) \\
 &\times \int_{-\infty}^{\infty} d\tau_2 f_{\mu\nu}^0(\tau_1, \tau_2) [1 + \sigma_a g_a]_{\nu\rho}(\tau_2, t'). \quad (13.109)
 \end{aligned}$$

The following device is very useful. Introducing $t_0 \rightarrow -\infty$ and the trivial factorization

$$e^{-i\epsilon_\lambda(t-t')} = (-i)e^{-i\epsilon_\lambda(t-t_0)}\theta(t-t_0)(i)e^{-i\epsilon_\lambda(t-t')}\theta(t'-t_0),$$

one can write

$$f_{\lambda\mu}^0(t, t') = \delta_{\lambda\mu}(1 - 2n_\lambda^0)g_{r,\lambda\lambda}^0(t, t_0)g_{a,\lambda\lambda}^0(t_0, t'). \quad (13.110)$$

When this is inserted into (13.109) the result is

$$\begin{aligned}
 f_{\lambda\rho}(t, t') &= \sum_{\nu} (1 - 2n_\lambda^0) \int_{-\infty}^{\infty} d\tau_1 [1 + g_r \sigma_r]_{\lambda\nu}(t, \tau_1) g_{r,\nu\nu}^0(\tau_1, t_0) \\
 &\times \int_{-\infty}^{\infty} d\tau_2 g_{a,\nu\nu}^0(t_0, \tau_2) [1 + \sigma_a g_a]_{\nu\rho}(\tau_2, t'). \quad (13.111)
 \end{aligned}$$

Now we recall the Dyson equations $[1 + g_r \sigma_r]g_r^0 = g_r, [1 + g_a \sigma_a]g_a^0 = g_a$, and simplify to

$$f_{\lambda\rho}(t, t') = \sum_{\nu} (1 - 2n_\lambda^0) g_{r,\lambda\nu}(t, t_0) g_{a,\nu\rho}(t_0, t'). \quad (13.112)$$

This compact result completes the general solution of the many-electron problem with time-dependent Hamiltonian which is exact in the absence of interactions. The advanced and retarded are merely single-electron problems, while the many body effects are accounted for by the equation for f .

Once we know g_r, g_a and f , since

$$2g^< = g^< + g^> + g^< - g^> = i(g_r - g_a) - f, \quad (13.113)$$

we readily gain $n_d(t) = g_{dd}^<(t)$. Applying Equation(13.113) to the vacuum, $g^< \equiv 0$ and $i(g_{r\lambda\rho} - g_{a\lambda\rho}) - f_{\lambda\rho} = 0$, hence (13.112) yields the rather unusual expression of a matrix difference as a matrix product

$$i(g_{r\lambda\rho} - g_{a\lambda\rho}) = \sum_{\nu} g_{r,\lambda\nu}(t, t_0) g_{a,\nu\rho}(t_0, t'). \quad (13.114)$$

Remarkably, for a noninteracting system g_r and g_a and do not depend on the filling, so this expression must hold for any⁹ n_λ^0 . Inserting (13.114) into (13.113) one gets

⁹It is easy to check this for the totally filled system, writing $2g^> = i(g_r - g_a) + f = 0$ and using (13.112) again.

$$2g_{\lambda\rho}^< = \sum_{\nu} g_{r,\lambda\nu}(t, t_0)g_{a,\nu\rho}(t_0, t') - f_{\lambda\rho},$$

that is,

$$g_{\lambda\rho}^<(t, t') = \sum_{\nu} n_{\nu}^0 g_{r,\lambda\nu}(t, t_0)g_{a,\nu\rho}(t_0, t'). \quad (13.115)$$

To solve the atom-surface scattering problem we set $\lambda = \rho = d$,

$$n_d(t) = \sum_{\nu} n_{\nu}^0 g_{r,d\nu}(t, t_0)g_{a,\nu d}(t_0, t) = \sum_{\nu} n_{\nu}^0 |g_{r,d\nu}(t, t_0)|^2. \quad (13.116)$$

If an atom with an occupied d level scatters against the surface and the k states of interest are empty, we shall consider $n_d^0 = 1, n_k^0 = 0$; then this is essentially a one-particle problem and the result says $n_d(t) = |g_{r,dd}(t, t_0)|^2$. In the case of F desorption from an alkali fluoride, approximately $n_d^0 = 1, n_k^0 = 0$ in the hole picture. the many-body complications arise in the study of the ionization probability of a positive ion hitting a metal surface. In this case, $n_d^0 = 0$ and

$$n_d(t) = \sum_k n_k^0 |g_{r,dk}(t, t_0)|^2, \quad (13.117)$$

where n_k^0 is the Fermi distribution. We can write the result in terms of the local component $g_{r,dd}$ by using the appropriate component of the Dyson equation, namely,

$$\begin{aligned} g_{r,dk}(t, t_0) &= \int_{-\infty}^{\infty} d\tau g_{r,dd}(t, \tau) V_{dk}(\tau) g_{r,dk}^0(\tau, t_0) \\ &= -ie^{i\epsilon_k t} \int_{t_0}^{\infty} d\tau g_{r,dd}(t, \tau) V_{dk}(\tau) e^{-i\epsilon_k \tau}; \end{aligned} \quad (13.118)$$

this is convenient as $g_{r,dd}$ can be determined by a closed equation in terms of $\Sigma_r^{(d)}$.

A.Blandin, A.Nourtier and D.W.Hone[48] developed the theory for an atom which is initially in equilibrium with a metal surface with Fermi energy E_F and is suddenly sputtered away with speed v ; they assumed a Lorentzian virtual level. The deviation from the adiabatic ($v \rightarrow 0$) result $n_d(\infty) = \theta(E_F - \epsilon)$ is still of the singular form $e^{-\frac{v_0}{v}}$, with v_0 a characteristic speed. This looks like the one-body result (13.106), but should change when including a less pathological virtual level shape.

13.6.2 Quantum Transport

Partitioned Static Transport Theories

The earliest quantum theory of transport through a junction which is still used today after 50 years is the pioneering one due to Landauer [61]. It deals

with non-interacting electrons and allows to calculate the current-voltage characteristics, that is, $J(V)$, where J is the stationary (d.c.) current due to a static potential difference V . Consider a system \mathcal{S} between two electrodes; we let the L and R subscripts or superscripts refer to left and right leads, e.g. $\rho^{(L)}(\epsilon)$, $\rho^{(R)}(\epsilon)$ are the respective densities of states, and V_m^R , V_m^L the hopping matrix elements between the lead states at energy ϵ and the eigenstate m of \mathcal{S} . (We shall omit these labels when unnecessary). In the presence of a bias, the chemical potentials μ_L, μ_R differ, and therefore there are two Fermi distributions f_L, f_R . The Landauer formula for the current is

$$J = \frac{e}{h} \int d\epsilon [f_L(\epsilon) - f_R(\epsilon)] \sum_{m,n} t_{m,n} t_{n,m}^* \quad (13.119)$$

where m, n label eigenstates of the isolated S and the transmission coefficients are

$$t_{m,n} = 2\pi \sqrt{\rho^{(L)}(\epsilon)\rho^{(R)}(\epsilon)} V_m^R V_n^{L*} g_{m,n}^{(r)}(\epsilon).$$

Phenomenological approaches, like the one due to Beenakker, [69] based on a master equation, are very useful, particularly when dealing with strongly correlated systems, like for instance single-electron transistors and related devices. For an application to superconducting systems see for example [70] where the main issue is the Coulomb blockade pattern of two-electron tunneling in the framework of $W=0$ pairing (Chapter 17).

The application of the Keldysh formalism to the calculation of stationary tunneling currents was pioneered by C. Caroli, R. Combescot, P. Nozieres and D. Saint-James in a series of fundamental joint papers [62]. They considered a 1d tight-binding model for a metal-insulator-metal (MIM) junction. The main feature of their approach is the use of an ideal partition which enables them to reach the stationary state adiabatically: to zeroth order, the applied bias is already there, but $J = 0$ since left and right subsystems are disconnected. The perturbation to be accounted for to all orders is a static pseudo-Hamiltonian that establishes the connection. In principle, the pseudo-Hamiltonian can be calculated *ab initio*. It is switched on adiabatically in the presence of the bias and a stationary state is obtained in which a time-independent current flows. The theory was originally formulated in a tight-binding model and the expression for the current was established from the continuity equation and written in terms of Green's functions:

$$J = \frac{eT}{i\hbar} \langle (c_a^\dagger c_a - c_a^\dagger c_\alpha) \rangle = \frac{eT}{\hbar} \int_{-\infty}^{\infty} \frac{d\omega}{2\pi} \{g_{a\alpha}^<(\omega) - g_{\alpha a}^<(\omega)\}, \quad (13.120)$$

where a, α stand for the sites connected by the hopping T . The theory was then extended to a continuous formulation. In both cases, the current-voltage characteristics were obtained in terms of local densities of states calculated on both sides of the partition. However, the left and right unperturbed subsystems cannot exist in insulation because the zero-order wave functions obey

special boundary conditions at the idealized partition. The partitioned theory of transport through junctions was put on a more general foundation by Feuchtwang[85], who obtained the current-voltage characteristics of one-dimensional model systems, rigorous within the Schrödinger theory in the non-interacting limit; he also used the Keldysh formalism but questioned some technical aspects of the previous formulations.

The partitioned approaches manage to work out the theory without introducing the time by an artifice. One considers that the left and right halves of the system are already biased while an ideal partition prevents the electrical continuity. The adiabatic removal of the partition eventually allows a stationary current to flow. Thus, the partitioned approach describes a situation that is quite different from the experimental one, when the connection is there when the bias is applied. The static treatments were based on a crucial assumption of equivalence with the physical situation; this assumption can fail as we know today (see below).

Partition-free Dynamical Transport Theory

A time-dependent, partition-free framework was proposed in 1980 by the writer[63]; the new scheme was found to be powerful to calculate the current-voltage characteristics, but above all for the first time allowed to obtain transient responses as well. The dynamical theory using the Keldysh formalism and the equation of motion method is no harder than the static one and yields much more information; it has not received much attention in the past but it is gaining ground in recent years for its clear advantages. One crucial point in favour of my approach is that it is partition-free: the whole system including the leads is in thermal equilibrium at some temperature until the bias is applied. This is physically much more appealing, and reflects the experimental situation. I worked out the theory in parallel for discrete and continuous models using time-ordered Green's functions and Equation (4.24) for the current. In the discrete one-dimensional case, when the unperturbed Hamiltonian is of the form

$$H_0 = \sum_{s=-\infty}^{\infty} c_s^\dagger (c_{s+1} + c_{s-1}) \quad (13.121)$$

the perturbation, which is dealt with exactly, is

$$H_1 = \Theta(t) \sum_{s=-\infty}^{\infty} V_s(t) c_s^\dagger c_s \quad (13.122)$$

and the current flowing through site s in the 1d electrodes is

$$J_s = \frac{eT_s}{\hbar} \lim_{t' \rightarrow t+0} [g_{s,s+1}^T(t, t') - g_{s,s-1}^T(t, t')]; \quad (13.123)$$

this is physically equivalent if not identical to (13.120). where T_s is the hopping matrix element between site s and its neighbors. For the continuous model, in obvious notation,

$$H_0 = \sum_k \epsilon_k c_k^\dagger c_k, \quad (13.124)$$

$$H_1(t) = \sum_{k,k'} \Theta(t) V_{k,k'}(t) c_k^\dagger c_{k'}, \quad (13.125)$$

and the current density was obtained by Equation (4.24). As we saw below Equation (10.16), the equation of motion

$$i \frac{\partial}{\partial t} g_{kk'}^T(t, t') = \delta_{kk'} \delta(t - t') + \epsilon_k g_{kk'}^T(t, t') + \sum_p V_{kp}(t) g_{pk'}^T(t, t'), \quad (13.126)$$

with the initial conditions $g_{kk'}^T(0, 0_-) = -i\delta_{kk'}(1 - f_k)$, $g_{kk'}^T(0, 0_+) = i\delta_{kk'} f_k$ (f_k is the Fermi function) and $g_{kk'}^T(t, t + 0_+) - g_{kk'}^T(t, t + 0_-) = i\delta_{kk'}$, are satisfied by

$$\begin{aligned} g_{kk'}^T(t, t') &= i\Theta(t' - t) \sum_q f_q g_{kq}^{(r)}(t, \tau) g_{qk'}^{(a)}(\tau, t') \\ &\quad - i\Theta(t - t') \sum_q (1 - f_q) g_{kq}^{(r)}(t, \tau) g_{qk'}^{(a)}(\tau, t') \end{aligned} \quad (13.127)$$

provided that τ is earlier than t and t' . This is essentially the Blandin et al. solution[48] with a much simpler derivation. Here we need $g^T(t, t')$ with $t > 0$, and t' just large than t , so we may set $\tau = 0$. Writing $g_{kk'}^{r,a}(t) = g_{kk'}^{r,a}(t, 0)$, one finds

$$\mathbf{J}(\mathbf{x}, t) = \frac{e\hbar}{m} \text{Im} \sum_{\mathbf{q}} g_{\mathbf{x},\mathbf{q}}^{(r)}(t) \nabla g_{\mathbf{x},\mathbf{q}}^{(r)}(t). \quad (13.128)$$

The corresponding solution for the current flowing at site $\{i, j, k\}$ in a lead oriented along the x axis in a 3d discrete model is

$$J_{ijk} = \frac{2eT}{\hbar} \Im \sum_q f_q g_{ijk,q}^{(r)}(t) g_{i-1jk,q}^{r*}(t). \quad (13.129)$$

The solution is valid for any time dependence of V , but in order to make the results more explicitly in Reference [63] I assumed $H_1(t) = \Theta(t)V(x)$, with $V(x) \rightarrow 0$ deep in the left electrode and $V(x) \rightarrow \text{constant}$ deep in the right one. Now the retarded and advanced Green's functions can be computed simply using a constant final-state Hamiltonian.

In the non-interacting case, the current-voltage characteristics are obtained by taking the $t \rightarrow \infty$ limit by asymptotic methods[63] [92] and agree with the results by Feuchtwang[85]. It turns out that the current response is

very indirectly related to the local Green's functions and is much more naturally written in terms of the asymptotic behavior of the wave function at long distance in the free-electron wires. For small enough V , both the continuous and the discrete models become ohmic and

$$J = -\frac{eV}{\pi\hbar}. \quad (13.130)$$

It was shown in Ref. [63] and proved formally by Stefanucci and Ambladh [103] that for the non-interacting system the current-voltage characteristics obtained by the partitioned approach must coincide generally with those of the partition-free approach; moreover, these Authors considered including correlation effects within the Time Dependent Density Functional Theory (TDLDA) scheme. In strongly correlated systems and in the presence of bound states the proof does not apply and the current can oscillate for long times, as in the Josephson effect. Examples are discussed in Ref. [192] where Hubbard clusters produce Josephson supercurrents by the $W=0$ mechanism (Chapter 17). A new implementation of the time-dependent quantum transport theory within the TDLDA scheme has proposed quite recently ([102]).

Meir-WinGreen Weak-Coupling Formula

In 1992, Yigal Meir and Ned S. WinGreen [64] proposed a Landauer formula for the current through an interacting electron region. The system S is placed between two non-interacting electrodes characterized by

$$g_{k,k}^<(\omega) = 2\pi i f(\omega) \delta(\omega - \varepsilon_k), \quad g_{k,k}^>(\omega) = -2\pi i [1 - f(\omega)] \delta(\omega - \varepsilon_k). \quad (13.131)$$

They started from

$$J = \frac{e}{\hbar} \sum_{k_L, n_{-\infty}} \int_{-\infty}^{\infty} \frac{d\omega}{2\pi} \left[V_{k_L, n}^L g_{n, k_L}^<(\omega) - V_{k, n}^{L*} g_{k_L, n}^<(\omega) \right]. \quad (13.132)$$

Here, $g_{k_L, n}^<$ links the k state in the left electrode to the S state annihilated by d_n , and once integrated in ω yields $\langle c_{k_L}^\dagger d_n \rangle$. Let us calculate the current which enters from L . One can write down these mixed Green's functions in terms of those based in S through

$$\begin{aligned} g_{k, n}^< &= \sum_m V_{k, m} \left[g_{k, k}^T(\omega) g_{m, n}^<(\omega) - g_{k, k}^<(\omega) \tilde{g}_{m, n}^T(\omega) \right], \\ g_{n, k}^< &= \sum_m V_{k, m}^* \left[g_{k, k}^<(\omega) g_{n, m}^T(\omega) - \tilde{g}_{k, k}^T(\omega) g_{n, m}^<(\omega) \right]. \end{aligned} \quad (13.133)$$

Substituting in (13.132), we are free to exchange m and n in the second term; in this way, we can collect terms and get a summand proportional to

$$V_{k,n} V_{k,m}^* \left\{ g_{k,k}^< (g_{n,m}^T + \tilde{g}_{n,m}^T) - g_{n,m}^< (\tilde{g}_{k,k}^T + g_{k,k}^T) \right\};$$

now we replace $g_{n,m}^T + \tilde{g}_{n,m}^T$ by $g_{n,m}^< + \tilde{g}_{n,m}^>$, simplify according to

$$g^< (g^> + g^<) - g^< (g^> + g^<) = g^< g^> - g^> g^<,$$

and use $g^> = g^< + g^{(r)} - g^{(a)}$. Next, we perform the sum with $\sum_k = \int d\epsilon \rho(\epsilon)$ and introduce

$$\gamma_{m,n} = 2\pi \sum_a d\epsilon \rho(\epsilon) V_{a,n} V_{a,m}^*, \quad (13.134)$$

where \sum_a adds some generality by summing over possible independent channels in the L electrode, like for instance angular momentum or spin.

$$J = \frac{ie}{\hbar} \int d\epsilon \sum_{m,n} \gamma_{m,n}^{(L)}(\epsilon) \left\{ f^{(L)}(\epsilon) [g_{n,m}^r - g_{n,m}^a] + g_{n,m}^< \right\}. \quad (13.135)$$

The same formula with R in place of L will give the current entering from the right electrode, which is the opposite in stationary conditions; thus one can symmetrize the expression with

$$\gamma^{(L)} \rightarrow \frac{\gamma^{(L)} - \gamma^{(R)}}{2}, \quad \gamma^{(L)} f^{(L)} \rightarrow \frac{\gamma^{(L)} f^{(L)} - \gamma^{(R)} f^{(R)}}{2}.$$

In the special case $\gamma_{m,n}^{(L)}(E) = \lambda \gamma_{m,n}^{(R)}(E)$, that is when the couplings are the same apart from a constant, the formula simplifies to (see Problem 15.1)

$$J = \frac{ie}{\hbar} \int d\epsilon [f^{(L)}(\epsilon) - f^{(R)}(\epsilon)] \sum_{m,n} \gamma_{m,n} [g_{m,n}^{(r)} - g_{m,n}^{(a)}]. \quad (13.136)$$

where

$$\gamma = \frac{\gamma^{(L)} \gamma^{(R)}}{\gamma^{(L)} + \gamma^{(R)}}. \quad (13.137)$$

Since

$$\sum_{m,n} \gamma_{m,n} [g_{m,n}^{(r)} - g_{m,n}^{(a)}] = 2iIm \sum_{m,n} \gamma_{m,n} g_{m,n}^{(r)},$$

this expression has a strong intuitive appeal if $\gamma_{m,n}$ can be taken real: contributions to the current arise from that slice of the density of states which is occupied at the μ one side of the junction and empty at μ of the other side. The density of states must be computed in the presence of the connections; however, the theory of [64] is particularly suited for small γ , when the coupling to the leads is so weak that one can approximate g as the Green's function of the isolated S .

Problems

13.1. Prove Equation (13.137).

Part IV

**Non-Perturbative Approaches and
Applications**

14 Some Recursion Techniques with Applications

14.1 Lanczos-Haydock Recursion

14.1.1 Local Green's Function for a Chain

Any stationary quantum problem, with any number of degrees of freedom, can be mapped into a solvable linear chain one-body tight-binding model *exactly*. From an abstract mathematical viewpoint, the method for putting a symmetric matrix in three-diagonal form which is readily diagonalized was invented by Lanczos[58] in 1950. This is enough to calculate the Green's function of systems with a finite number of states, and the algorithm is powerful and convenient even for large matrices provided that they are sparse, that is, most elements vanish. Haydock and coworkers[59] extended the method and developed applications to physical systems with many degrees of freedom. Let $u_n, n = 0, 1, 2 \dots$ be the site orbitals of a semi-infinite chain, with local levels a_n . The Hamiltonian is defined by

$$Hu_n = a_n u_n + b_{n+1} u_{n+1} + b_n u_{n-1}, \tag{14.1}$$

where b 's are hopping integrals, and its matrix is three-diagonal:

$$H = \begin{pmatrix} a_0 & b_1 & 0 & 0 & \dots \\ b_1 & a_1 & b_2 & 0 & \dots \\ 0 & b_2 & a_2 & b_3 & 0 \\ 0 & 0 & b_3 & a_3 & b_4 \\ \dots & \dots & \dots & \dots & \dots \end{pmatrix}. \tag{14.2}$$

For this model, we want the local retarded Green's function is

$$G_0(E) = \langle u_0 | \frac{1}{E - H} | u_0 \rangle, \tag{14.3}$$

which is the 00 element of

$$(E - H)^{-1} = \begin{pmatrix} E - a_0 & -b_1 & 0 & 0 & \dots \\ -b_1 & E - a_1 & -b_2 & 0 & \dots \\ 0 & -b_2 & E - a_2 & -b_3 & 0 \\ 0 & 0 & -b_3 & E - a_3 & -b_4 \\ \dots & \dots & \dots & \dots & \dots \end{pmatrix}^{-1}. \tag{14.4}$$

Now, $\frac{1}{z-H}$ with $z = E + i\delta$, $\delta = +0$ is the Fourier transform of $e^{iHt}\Theta(t)$, hence $G_0(z)$ is causal; moreover it vanishes for $z \rightarrow \infty$ in all directions, $G_0(z)^* = G_0(z^*)$ and is a Herglotz function, i.e. yields a non-negative density of states $n(E) = -\frac{1}{\pi} \text{Im}G_0(z = E) \geq 0$. According to the standard rule, the 00 element is given by

$$G_0(E) = \frac{D_1(E)}{D_0(E)}, \tag{14.5}$$

where the denominator is $\det(E - H)$ and the numerator is obtained from it by cropping the first row and column,

$$D_0 = \text{Det} \begin{pmatrix} E - a_0 & -b_1 & 0 & 0 & \dots \\ -b_1 & E - a_1 & -b_2 & 0 & \dots \\ 0 & -b_2 & E - a_2 & -b_3 & 0 \\ 0 & 0 & -b_3 & E - a_3 & -b_4 \\ \dots & \dots & \dots & \dots & \dots \end{pmatrix},$$

$$D_1 = \text{Det} \begin{pmatrix} E - a_1 & -b_2 & 0 & 0 & \dots \\ -b_2 & E - a_2 & -b_3 & 0 & \dots \\ 0 & -b_3 & E - a_3 & -b_4 & 0 \\ 0 & 0 & -b_4 & E - a_4 & -b_5 \\ \dots & \dots & \dots & \dots & \dots \end{pmatrix}. \tag{14.6}$$

Both are secular determinants of matrices representing chain Hamiltonians. Similarly, we define D_n as obtained by a crop of the first n rows and columns; it refers to a shortened chain with the first n sites removed. Later, we shall also consider shortening the chain the other way, defining $\Delta_N = D_0$ and Δ_n , $n < N$ the shortened chain with the first n sites left. Now expand D_0 by Laplace's rule along the first line:

$$D_0 = (E - a_0)D_1 - (-b_1)\text{Det} \begin{pmatrix} -b_1 & -b_2 & 0 & 0 & \dots \\ 0 & E - a_2 & -b_3 & 0 & \dots \\ 0 & -b_3 & E - a_3 & -b_4 & \dots \\ \dots & \dots & \dots & \dots & \dots \end{pmatrix}. \tag{14.7}$$

The $-b_2$ term in the first line does not contribute, and

$$D_0(E) = (E - a_0)D_1(E) - b_1^2 D_2(E)$$

which inserted into Eq.(14.5) yields

$$G_0(E) = \frac{D_1}{D_0} = \frac{D_1}{(E - a_0)D_1 - b_1^2 D_2} = \frac{1}{(E - a_0) - b_1^2 \frac{D_2}{D_1}}.$$

Then,

$$\frac{D_2}{D_1} = \frac{1}{(E - a_1) - b_2^2 \frac{D_3}{D_2}}$$

and iterating,

$$G_0(E) = \frac{1}{E - a_0 - \frac{b_1^2}{E - a_1 - \frac{b_2^2}{E - a_2 - \frac{b_3^2}{E - a_3 - \dots}}}}. \tag{14.8}$$

For the uniform chain, with $a_n \equiv 0$ and $b_n \equiv b$, one gets

$$G_0(E) = \frac{1}{E - b^2 G_0(E)}. \tag{14.9}$$

This yields the semi-elliptic density of states

$$n(E) = \frac{\Theta(4b^2 - E^2)\sqrt{4b^2 - E^2}}{2\pi b^2}.$$

14.1.2 Green’s Function of any System

Consider an arbitrary Hamiltonian H , possibly representing a complicated many-body system, and any normalized state u_0 ; if this is an eigenstate we are finished, otherwise we may always write :

$$H|u_0\rangle = a_0|u_0\rangle + b_1|u_1\rangle, \quad \langle u_0|u_1\rangle = 0, \quad \langle u_1|u_1\rangle = 1. \tag{14.10}$$

This is tantamount to call $b_1|u_1\rangle$ the part of $H|u_0\rangle$ which is orthogonal to $|u_0\rangle$, and implies that $a_0 = \langle u_0|H|u_0\rangle$, and $b_1 = \langle u_1|H|u_0\rangle$; since

$$u_1 = \frac{1}{b_1}(H - a_0)|u_0\rangle \tag{14.11}$$

is normalized, we get (up to an arbitrary phase factor)

$$b_1 = \|(H - a_0)|u_0\rangle\|, \tag{14.12}$$

where $\|v\|$ denotes the norm of v . This can be computed from the given H and u_0 ; now we also know u_1 and we can proceed with

$$H|u_1\rangle = a_1|u_1\rangle + b_1|u_0\rangle + b_2|u_2\rangle, \quad \langle u_0|u_2\rangle = 0, \quad \langle u_1|u_2\rangle = 0. \tag{14.13}$$

Here, b_1 is the same as above since H is Hermitean and u_2 is taken to be normalized. Thus, $a_1 = \langle u_1|H|u_1\rangle$, and $b_2|u_2\rangle = (H - a_1)|u_1\rangle - b_1|u_0\rangle$. Imposing that u_2 is indeed normalized, we obtain, since the phase of b_2 can be chosen at will,

$$b_2 = \|(H - a_1)|u_1\rangle - b_1|u_0\rangle\|; \tag{14.14}$$

again, we can compute that, write

$$u_2 = \frac{1}{b_2} [(H - a_1)|u_1\rangle - b_1|u_0\rangle] \tag{14.15}$$

and expect the next step

$$H|u_2\rangle = a_2|u_2\rangle + c|u_0\rangle + b_2|u_1\rangle + b_3|u_3\rangle$$

This might appear a boring way to get equations of increasing complexity, but here the clever idea first comes into play, since $H|u_2\rangle$ does not contain anything like $c|u_0\rangle$. This is because $c = \langle u_0|H|u_2\rangle$, but Eq. (14.10) shows that $H|u_0\rangle$ is orthogonal to all u_n with $n > 1$. Hence, continuing to introduce orthogonal u_n states, we always get three-term recursion relations

$$H|u_n\rangle = a_n|u_n\rangle + b_n|u_{n-1}\rangle + b_{n+1}|u_{n+1}\rangle \quad (14.16)$$

with

$$a_n = \langle u_n|H|u_n\rangle \quad (14.17)$$

$$b_{n+1} = \| (H - a_n)|u_n\rangle - b_n|u_{n-1}\rangle \| \quad (14.18)$$

$$|u_{n+1}\rangle = \frac{1}{b_{n+1}} [(H - a_n)|u_n\rangle - b_n|u_{n-1}\rangle]. \quad (14.19)$$

Hence, we have a general algorithm to find the local Green's function of any state u_0 , mapping it to site 0 of a chain of u_n that can be generated stepwise, with their levels a_n and hoppings to their nearest neighbors. The chain is semi-infinite, that is does not end, unless the system has a finite Hilbert space or the choice of u_0 was extremely clever.

14.1.3 Terminator

Let N be the number of sites that we can afford to compute; the N -th denominator of the continued fraction (14.8) reads $E - a_{N-1} - b_N^2/\dots$ and one gets an approximation by setting $b_N = 0$. By truncating the continued fraction in this way we get a discrete spectrum; this can then be broadened by shifting the poles a bit below the real axis with $E \rightarrow z = E + i\delta$, which converts the δ functions into Lorentzians. As an illustration, consider the rectangular level with band width $W = 2\alpha$, $n(E) = \Theta(\alpha^2 - E^2)/2\alpha$, which we met in Section 6.2 and arises from

$$G(z) = \frac{1}{2\alpha} \log \left(\frac{z + \alpha}{z - \alpha} \right). \quad (14.20)$$

We shall see in Sect. (14.1.4) how to calculate the a and b coefficients from G . The comparison with the $N = 5, 10$ and 40 continued fractions (Figure 14.1) shows that such an artificial procedure, while allowing a comparison of some qualitative kind, is too rough for many purposes; it is mathematically pathological, e.g. the second and all the even moments of the approximate $n(E)$ diverge.

As an alternative to the Lorentzian broadening, one can compute the integrated local dos

$$\mathcal{N}(E) = \int_{-\infty}^E n(E) dE,$$

which is a bar diagram but converges to the exact result in norm. One can smooth it by fitting with a continuous function and then differentiate to find an approximate $n(E)$; the results are much better than before, and at least for one-electron problems converge quickly *almost everywhere*. Interestingly, for regular solids there are always special intervals centered at E values where the approximation fails badly; these singular values, where n is a bad function, are band-edge singularities or Van Hove singularities, where $\frac{dn}{dE}$ is discontinuous. If one is interested in the overall line shape of some spectroscopy, this may be of minor importance, since such singularities tend to be masked somewhat by the experimental broadenings. However there is a message there: the long-time behavior of the Fourier transform of any function of frequency depends [92] precisely on such *details*, and the transform is a correlation function, which can be observed in appropriate experiments. We know from Section

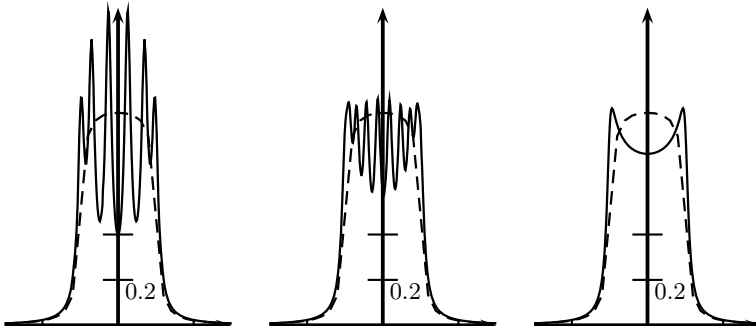


Fig. 14.1. The rectangular $n(E)$ with $W = 0.5$ and a broadening $\delta = 0.05$ (dashed) compared with the continued fraction approximations using $N=5$ denominators (left), $N=10$ denominators (centre), $N=40$ (right). The continued fraction coefficient are discussed in the next Sections.

4.3.1 that the band-edge singularities depend only on dimensionality; some weaker singularities inside the band depend on the lattice symmetry, too. The Van-Hove singularities are *universal* features, independent of the details of the Hamiltonian. Stubborn computing fails, but one can gain them directly from a simpler model in the same universality class. We do not need the model to be realistic, but to have the correct singularities at the correct places. Such a model is called *terminator*. The local Green's function of the terminator is exactly known and we can calculate, say, N denominators of the continued fraction expansion, using Greek letters for the coefficients we write

$$\Gamma_0(E) = \frac{1}{E - \alpha_0 - \frac{\beta_1^2}{E - \alpha_1 - \frac{\beta_2^2}{E - \alpha_2 - \frac{\beta_3^2}{\dots}}}} \tag{14.21}$$

At level N the full continued fraction truncated ends with

$$E - \alpha_{N-1} - \frac{\beta_{N-1}^2}{E - \alpha_{N-1} - \beta_N^2 t_N(E)}.$$

Here, $t_N(E)$ defines the *tail* of the continued fraction. The idea is: pick the tail and attach it to G . Doing this by brute force is not rewarding, while deepening the mathematics is a far better idea.

Pade' Representation

Orthogonal Polynomials

It is evident that the continued fraction truncated at level N is the ratio of two polynomials. To find them, consider the linear chain eigenstates,

$$|\alpha\rangle = \sum_{n=0}^N f_n^{(\alpha)} |n\rangle \tag{14.22}$$

that satisfy

$$\sum_{n=0}^N f_n^{\alpha*} f_n^\beta = \delta_{\alpha,\beta}, \tag{14.23}$$

and the Schrödinger equation

$$\begin{aligned} \sum_{n=0}^N f_n^{(\alpha)} [a_n |n\rangle + b_{n+1} |n+1\rangle + b_n |n-1\rangle] \\ = E^{(\alpha)} \sum_{n=0}^\infty f_n^{(\alpha)} |n\rangle, \quad b_0 = 0. \end{aligned} \tag{14.24}$$

Since $\sum_{n=0}^N f_n b_{n+1} |n+1\rangle = \sum_{n=0}^N f_{n-1} b_n |n\rangle$, and $\sum_{n=0}^N f_n b_n |n-1\rangle = \sum_{n=0}^N f_{n+1} b_{n+1} |n\rangle$, ($f_{N+1} = 0$), one finds

$$\sum_{n=0}^\infty [(a_n - E^{(\alpha)}) f_n^{(\alpha)} + b_{n+1} f_{n+1}^{(\alpha)} + b_n f_{n-1}^{(\alpha)}] |n\rangle = 0. \tag{14.25}$$

This implies the recurrence relations (r.r.)

$$(a_n - E^{(\alpha)}) f_n^{(\alpha)} + b_{n+1} f_{n+1}^{(\alpha)} + b_n f_{n-1}^{(\alpha)} = 0, \quad f_{-1}^{(\alpha)} = 0. \tag{14.26}$$

$f_0^\alpha \equiv \langle 0|\alpha \rangle$ does not vanish (otherwise $f_n \equiv 0$) and we may define N independent functions

$$P_n(E^{(\alpha)}) = \frac{f_n^\alpha}{f_0^\alpha}, \tag{14.27}$$

having the same r.r.

$$(a_n - E^{(\alpha)})P_n + b_{n+1}P_{n+1} + b_nP_{n-1} = 0, \quad P_{-1}=0. \tag{14.28}$$

but $P_0(E) = 1$; all the others are determined by the r.r. and depend on the a, b coefficients of the previous sites. Evidently, they are just polynomials in E . Changing the sum

$$\sum_\alpha^N f_m^{\alpha*} f_n^\alpha = \delta_{m,n} \tag{14.29}$$

to an energy integral,

$$\delta_{m,n} = \sum_\alpha^N \int_{-\infty}^\infty dE \delta(E - E^{(\alpha)}) f_m^{\alpha*} f_n^\alpha \tag{14.30}$$

and using (14.27) we find

$$\delta_{m,n} = \int_{-\infty}^\infty dE \sum_\alpha^N \langle 0|\alpha \rangle \langle \alpha|0 \rangle \delta(E - E^{(\alpha)}) P_m^*(E) P_n(E) \tag{14.31}$$

that is, the P are orthogonal polynomials

$$\delta_{m,n} = \int_{-\infty}^\infty dE n(E) P_m^*(E) P_n(E) \tag{14.32}$$

with a weight $n(E)$, the local density of states at $|0\rangle$ (compare with Section 5.1.4).

Polynomials, Secular Determinants and G

The secular determinant $\Delta_N(E)$ consists of the first N rows and columns of D_0 (Equation 14.6)

$$\Delta_N = Det \begin{pmatrix} E - a_0 & -b_1 & 0 & 0 & \dots \\ -b_1 & E - a_1 & -b_2 & 0 & \dots \\ 0 & -b_2 & E - a_2 & -b_3 & 0 \\ 0 & 0 & -b_3 & E - a_3 & -b_4 \\ \dots & \dots & \dots & \dots & \dots \end{pmatrix}_{N \times N} ; \tag{14.33}$$

let us consider then the succession of determinants $\Delta_n(E)$ and expand $\Delta_{n+1}(E)$ using the last row:

$$\begin{aligned} \Delta_{n+1} &= Det \begin{pmatrix} \dots & \dots & \dots & \dots & \dots \\ \dots & E - a_3 & -b_{n-2} & 0 & 0 \\ \dots & -b_{n-2} & E - a_{n-2} & -b_{n-1} & 0 \\ \dots & 0 & -b_{n-1} & E - a_{n-1} & -b_n \\ \dots & 0 & 0 & -b_n & E - a_n \end{pmatrix}_{n+1 \times n+1} \\ &= (E - a_n)\Delta_n + b_n Det \begin{pmatrix} \dots & \dots & \dots & \dots \\ \dots & E - a_3 & -b_{n-2} & 0 \\ \dots & -b_{n-2} & E - a_{n-2} & 0 \\ \dots & 0 & -b_{n-1} & -b_n \end{pmatrix}_{n \times n} \end{aligned} \quad (14.34)$$

and we are left with

$$\Delta_{n+1}(E) = (E - a_n)\Delta_n(E) - b_n^2\Delta_{n-1}(E). \quad (14.35)$$

Multiplying (14.28) by $\prod_{i=1}^n b_n$ we find (14.35) with

$$\Delta_n(E) = P_n(E) \prod_{i=1}^n b_n. \quad (14.36)$$

Thus, we have got $D_0 = \Delta_N(E)$ for the N -site chain in terms of the P_n and in view of (14.5) a new expression for G_0 is within reach if we can also express $D_1(E)$. However, $D_1(E)$ is the counterpart of $D_0(E)$ in a chain where site 0 has been cut off. The polynomials of that chain satisfy the same r.r.(14.28) but they vanish on site 0. We can specify them as follows:

$$Q_0 = 0, \quad Q_1(E) = 1, \quad (a_n - E)Q_n + b_{n+1}Q_{n+1} + b_nQ_{n-1} = 0. \quad (14.37)$$

P_n and Q_n are the independent solutions for the N site chain that correspond to different initial conditions. Therefore,

$$D_1(E) = Q_N(E) \prod_{i=2}^N b_n. \quad (14.38)$$

Finally, we get for the N site chain

$$G_0^{(N)}(E) = \frac{Q_N(E)}{b_1 P_N(E)}. \quad (14.39)$$

Such a representation as a ratio of polynomials is exact here, but is popular as a way to approximate functions and is called *Pade' approximant*.

How to Append the Terminator 's Tail to G.

We compute G up to the N -th denominator, and continue the continued fraction with $t_N(E)$ taken from the terminator. That will be much better than nothing, and will bring much of the missing information. We need to

pick up $t_N(E)$ from the terminator continued fraction, but we are not so silly to use it directly. For the truncated terminator, we write, in place of (14.39,14.28,14.37)

$$\Gamma_0^{(N)}(E) = \frac{\Theta_N(E)}{\beta_1 \Pi_N(E)}. \tag{14.40}$$

where Θ 's are the counterparts of the Q 's in the terminator's chain; the polynomials,

$$(\alpha_n - E^{(\alpha)})\Pi_n + \beta_{n+1}\Pi_{n+1} + \beta_n\Pi_{n-1} = 0, \quad \Pi_{-1}=0. \tag{14.41}$$

$$\Theta_0 = 0, \Theta_1(E) = 1, (\alpha_n - E)\Theta_n + \beta_{n+1}\Theta_{n+1} + \beta_n\Theta_{n-1} = 0. \tag{14.42}$$

The rule for inserting the tail is:

$$\alpha_{N-1} \rightarrow \alpha_{N-1} + \beta_N^2 t_N(E) \tag{14.43}$$

In order to use (14.43) in (14.40,) we need to show up α_{N-1} , so we obtain Π_{n+1} and Θ_{n+1} from (14.41,14.42), then set $n + 1 = N$ and obtain:

$$\Gamma_0^{(N)} = \frac{1}{\beta_1} \frac{E - \alpha_{N-1}\Theta_{N-1}(E) - \beta_{N-1}\Theta_{N-2}(E)}{E - \alpha_{N-1}\Pi_{N-1}(E) - \beta_{N-1}\Pi_{N-2}(E)}. \tag{14.44}$$

Now, using (14.43), the full terminator reads:

$$\Gamma_0(E) = \frac{1}{\beta_1} \frac{E - [\alpha_{N-1} + \beta_N^2 t_N(E)]\Theta_{N-1}(E) - \beta_{N-1}\Theta_{N-2}(E)}{E - [\alpha_{N-1} + \beta_N^2 t_N(E)]\Pi_{N-1}(E) - \beta_{N-1}\Pi_{N-2}(E)}. \tag{14.45}$$

We can clean it up using (14.41,14.42) again to eliminate the $N - 2$ items:

$$\Gamma_0 = \frac{1}{\beta_1} \frac{\Theta_N - \beta_N t_N(E)\Theta_{N-1}}{\Pi_N - \beta_N t_N(E)\Pi_{N-1}}. \tag{14.46}$$

Finally, this is a compact tail indeed:

$$t_N(E) = \frac{1}{\beta_N} \frac{\Pi_N \beta_1 \Gamma_0 - \Theta_N}{\beta_1 \Pi_{N-1} \Gamma_0 - \Theta_{N-1}}. \tag{14.47}$$

The transplantation is obtained by replacing Greek by Latin letters in (14.46):

$$G_0(E) = \frac{1}{b_1} \frac{Q_N - b_N t_N(E)Q_{N-1}}{P_N - b_N t_N(E)P_{N-1}}. \tag{14.48}$$

This method can give excellent results already with $N \approx$ a few tens if the terminator has the correct edges of the continua with the right edge and Van Hove singularities.

14.1.4 Moments

The above method is in a way a refined version of the moments method [60], which is itself worth considering for its conceptual and practical importance. Let $|0\rangle$ be any state of the system, and

$$n(\omega) = \langle 0|\delta(\omega - H)|0\rangle = -\frac{1}{\pi} \text{Im}G(\omega) \tag{14.49}$$

the local density of states. Even for complicated H we can obtain useful results by computing the moments

$$\mu_n = \langle 0|H^n|0\rangle = \int_{-\infty}^{\infty} d\omega \omega^n n(\omega); \tag{14.50}$$

if we could obtain them all and sum an exponential series we would build the Fourier transform of (14.49). Now, $\mu_0 = 1$, μ_1 is the center-of-mass of the virtual level, μ_2 informs us about its width, μ_3 characterizes its skewness, and with increasing n finer details are revealed. The moments allow computing the Green's function: if $\text{Re } z$ is larger than the eigenvalues of H , $G(z) = \sum_{k=0}^{\infty} \frac{\mu_k}{z^{k+1}}$. The short time behavior of $n(t)$ depends on the first moments, that we can compute; the long-time $n(t)$ is often needed and even the asymptotic trend is of interest, but that information must be sought elsewhere. Letting N denote the number of moments that we can compute, we face the problem of using them in the best way. One possibility would be choosing a functional form which depends on N parameters and imposing the values of N moments. For instance, if the edges of the continuum are known one can pick a polynomial or an expansion in Tchebychev polynomials. However, the Van Hove singularities will prevent the uniform convergence of the procedure. A more powerful method exists. By the $M + 1$ -site chain Hamiltonian¹ H_M of the form (14.2) one computes the moments $\mu_p = (H_M^p)_{00}$ by matrix multiplication; from $\mu_p, p = 1, \dots, N$ one can deduce the a_k and b_k coefficients for $k \leq N - 1$. In fact, $\mu_1 = a_0$; inserting into $\mu_2 = a_0^2 + b_1^2$ we have one unknown and solve immediately obtaining $b_1^2 = \mu_2 - \mu_1^2$. The third moment is

$$\mu_3 = a_0^3 + (2a_0 + a_1)b_1^2;$$

inserting the previous results we obtain

$$a_1 = \frac{-\mu_1^3 + 2\mu_1\mu_2 - \mu_3}{\mu_1^2 - \mu_2}.$$

We can continue in this way as long as we please:

$$\mu_4 = (a_0 + a_1)^2 b_1^2 + (a_0^2 + b_1^2)^2 + b_1^2 b_2^2;$$

¹The N moments obtained by matrix multiplication using H_M are obviously exact if M is large enough.

again we have only one unknown and find

$$b_2^2 = \frac{-\mu_2^3 + 2\mu_1\mu_2\mu_3 - \mu_3^2 - \mu_1^2\mu_4 + \mu_2\mu_4}{(\mu_1^2 - \mu_2)^2}.$$

General explicit formulas are also available from the theory of Pade' approximants [157].

In this way we solve the inverse of Haydock's problem: given a normalized Herglotz function $n(\omega)$, to determine a semi-infinite chain Hamiltonian such that $n(\omega)$ is its density of states. For a symmetric $n(\omega)$, like those arising from bipartite lattices (Section 4.3.1) we may take $a_k \equiv 0$. For the rectangular band model (14.20) one readily determines the coefficients (Problem 14.2); in this way I performed the comparison between the truncated fraction and the exact density of states following Equation(14.20).

14.2 Spin-Disentangled Diagonalization

If the Hamiltonian matrix H is too large to store, and is not assumed to be sparse², we may still be able to find eigenvalues and eigenvectors by the recently introduced *Spin-Disentangled technique* [18]. I find that it is fast and easy to use and works very well with the Lanczos-Haydock algorithm discussed above. Let M_σ be the number of electrons of spin σ , and $M_\uparrow + M_\downarrow = N$ their total number. Consider a real orthonormal basis $\{|\phi_{\alpha\sigma}\rangle\}$, $\alpha = 1 \cdots m_\sigma$, of dimension m_σ , for the M_σ electrons of spin σ . The dimension of the Hilbert space is $N_H = m_\uparrow m_\downarrow$ and H is a $N_H \times N_H$ matrix; now I show how to solve by matrices no larger than the largest between $m_\uparrow \times m_\uparrow$ and $m_\downarrow \times m_\downarrow$. For $m_\uparrow = m_\downarrow$, a 1,000,000 \times 1,000,000 problem is solved by 1,000 \times 1,000 matrices. One can write the ground state wave function in the interesting form

$$|\Psi\rangle = \sum_{\alpha\beta} L_{\alpha\beta} |\phi_{\alpha\uparrow}\rangle \otimes |\phi_{\beta\downarrow}\rangle \quad (14.51)$$

which shows how the \uparrow and \downarrow configurations are entangled. The particles of one spin are treated as the *bath* for those of the opposite spin: this form also enters the proof of a famous theorem by Lieb[37] discussed in Section 18.6. In Equation (14.51) $L_{\alpha\beta}$ is a $m_\uparrow \times m_\downarrow$ rectangular matrix.

Schrödinger Equation

Let K_σ denote the kinetic energy $m_\sigma \times m_\sigma$ square matrix in the basis $\{|\phi_{\alpha\sigma}\rangle\}$, and $n_s^{(\sigma)}$ the spin- σ occupation number matrix at site s in the same basis ($n_s^{(\sigma)}$

²If it is sparse, one can store and manipulate the nonzero elements H_{ij} together with i and j ; this procedure is annoying and leads to a slowing down of the computations. Moreover, in many problems of interest H is *not sparse*.

is a symmetric matrix since the $|\phi_{\alpha\sigma}\rangle$'s are real). The Hamiltonian (in a lattice model, or the *realistic* Hamiltonian on a discrete grid) is $H = H_0 + U$, with $H_0 = K_{\uparrow} + K_{\downarrow}$, while $U = \sum_{s,s'} U(s, s') n_{s\uparrow} n_{s'\downarrow}$. Using $(K_{\uparrow})\phi_{\alpha\uparrow} = \sum_{\gamma} (K_{\uparrow})_{\gamma\alpha} \phi_{\gamma\uparrow}$ and the like, one finds that

$$\begin{aligned} H_0|\Psi\rangle &= \sum_{\alpha\beta\gamma} L_{\alpha\beta} [|\phi_{\gamma\uparrow}\rangle|\phi_{\beta\downarrow}\rangle(K_{\uparrow})_{\gamma\alpha} + |\phi_{\alpha\uparrow}\rangle|\phi_{\gamma\downarrow}\rangle(K_{\downarrow})_{\gamma\beta}] \\ &= \sum_{\beta\gamma} (K_{\uparrow}L)_{\gamma\beta} |\phi_{\gamma\uparrow}\rangle|\phi_{\beta\downarrow}\rangle + \sum_{\alpha\gamma} (LK_{\downarrow}^T)_{\alpha\gamma} |\phi_{\alpha\uparrow}\rangle|\phi_{\gamma\downarrow}\rangle \\ &= \sum_{\alpha\beta} [K_{\uparrow}L + LK_{\downarrow}^T]_{\alpha\beta} |\phi_{\alpha\uparrow}\rangle|\phi_{\beta\downarrow}\rangle \end{aligned} \quad (14.52)$$

where T stands for Transpose. Since $n_{s\sigma}|\phi_{\alpha\sigma}\rangle = \sum_{\gamma} |\phi_{\gamma\sigma}\rangle\langle\phi_{\gamma\sigma}|n_{s\sigma}|\phi_{\alpha\sigma}\rangle$,

$$U|\Psi\rangle = \sum_{s,s'} U(s, s') \sum_{\alpha,\beta} \sum_{\gamma,\delta} L_{\alpha,\beta} |\phi_{\gamma\uparrow}\rangle|\phi_{\delta\downarrow}\rangle (n_{s\uparrow})_{\gamma\alpha} (n_{s'\downarrow})_{\delta\beta}; \quad (14.53)$$

but $(n_{s\downarrow})_{\delta\beta} = (n_{s\downarrow})_{\beta\delta}$ and one can write

$$\begin{aligned} U|\Psi\rangle &= \sum_{s,s'} U(s, s') \sum_{\gamma,\delta} (n_{s\uparrow}Ln_{s'\downarrow})_{\gamma,\delta} |\phi_{\gamma\uparrow}\rangle|\phi_{\delta\downarrow}\rangle \\ &\equiv \sum_{s,s'} \sum_{\alpha,\beta} (n_{s\uparrow}Ln_{s'\downarrow})_{\alpha,\beta} |\phi_{\alpha\uparrow}\rangle|\phi_{\beta\downarrow}\rangle. \end{aligned} \quad (14.54)$$

Recalling Equation (14.51) we see how H acts:

$$H : L \rightarrow K_{\uparrow}L + LK_{\downarrow}^T + \sum_{s,s'} U(s, s') n_{s\uparrow}Ln_{s'\downarrow}. \quad (14.55)$$

For illustration, below I adopt the on-site Hubbard interaction, when this reduces to Lieb's rule [37]

$$H[L] = [K_{\uparrow}L + LK_{\downarrow}^T] + U \sum_s n_s^{(\uparrow)} Ln_s^{(\downarrow)}. \quad (14.56)$$

In the absence of magnetic fields, K_{\uparrow}^T can be taken real and symmetric, hence we drop the transposition sign. In particular in the $S_z = 0$ sector ($M_{\uparrow} = M_{\downarrow}$) and $K_{\uparrow} = K_{\downarrow}$, $n_s^{(\uparrow)} = n_s^{(\downarrow)}$. The action of H is obtained in a spin-disentangled way, in terms of operators acting in the spin subspaces. The generality of the method is not spoiled by the fact that it is fastest in the $S_z = 0$ sector, because it is useful provided that the spins are not totally lined up; on the other hand, $S_z = 0$ can always be assumed, as long as the hamiltonian is $SU(2)$ invariant. For example, consider the Hubbard Model with 2 sites a and b and 2 electrons (H_2 molecule, Section 1.2.5). The intersite hopping

is t and the on-site repulsion U . In the standard method, one sets up basis vectors for the $S_z = 0$ sector

$$\begin{aligned} |v_1\rangle &= |a \uparrow a \downarrow\rangle, |v_2\rangle = |a \uparrow b \downarrow\rangle, \\ |v_3\rangle &= |b \uparrow a \downarrow\rangle, |v_4\rangle = |b \uparrow b \downarrow\rangle. \end{aligned}$$

One then looks for eigenstates (three singlets and one triplet)

$$|\Psi\rangle = \sum_{i=1}^4 \psi_i |v_i\rangle \quad (14.57)$$

using the Hamiltonian

$$H = \begin{pmatrix} U & t & t & 0 \\ t & 0 & 0 & t \\ t & 0 & 0 & t \\ 0 & t & t & U \end{pmatrix}. \quad (14.58)$$

We can do with 2×2 (rather than 4×4) matrices by the spin-disentangled method with $L = \begin{pmatrix} \psi_1 & \psi_2 \\ \psi_3 & \psi_4 \end{pmatrix}$, $K = \begin{pmatrix} 0 & t \\ t & 0 \end{pmatrix}$, $n_a = \begin{pmatrix} 1 & 0 \\ 0 & 0 \end{pmatrix}$, $n_b = \begin{pmatrix} 0 & 0 \\ 0 & 1 \end{pmatrix}$.

By (14.56),

$$H|\Psi\rangle = \sum_{\alpha}^{a,b} \sum_{\beta}^{a,b} (H[L])_{\alpha\beta} |\phi_{\alpha\uparrow}\rangle \otimes |\phi_{\beta\downarrow}\rangle \quad (14.59)$$

with $(H[L]) = \begin{pmatrix} U\psi_1 + t(\psi_2 + \psi_3) & t(\psi_1 + \psi_4) \\ t(\psi_1 + \psi_4) & U\psi_4 + t(\psi_2 + \psi_3) \end{pmatrix}$.

The reader can readily verify that this is the same as applying H in the form (14.58) to the standard wave function (14.57) and then casting the result in the form (14.51). Since we can apply H we can also diagonalize it. By this device, we can work with matrices whose dimensions is the square root of those of the Hilbert space: $\sqrt{N_H} \times \sqrt{N_H}$ matrices solve the $N_H \times N_H$ problem.

The Practical Numerical Recipe

Starting from a trial wave function of the form (14.51), preferably having the proper symmetry, one can avoid computing the Hamiltonian matrix, since its operation is given by Eq. (14.56). Each new application of the Hamiltonian takes us to a new Lanczos *site* and we can proceed by generating a Lanczos *chain*. To this end we need to orthogonalize to the previous *sites* by the scalar product

$$\langle \Psi_1 | \Psi_2 \rangle = \text{Tr}(L_1^\dagger L_2). \quad (14.60)$$

In this way one can put the Hamiltonian matrix in a tri-diagonal form. This method is better suited if one is mainly interested in the low-lying part of the spectrum. A severe numerical instability sets in when the chain is longer than a few tens of *sites*, i.e. well before the Lanczos method converges. On several occasions, I found it preferable to use repeated two-site chains alternated with moderate-size ones.

14.3 Method of Excitation Amplitudes

In 1977 I found the exact solution [77] of a model introduced by Hewson and Newns [79] to discuss photoemission spectroscopy from valence states³; the same idea can solve exactly a class of models and later I published many extensions and applications to photoemission and Auger spectroscopy[124] and non-linear optics⁴. The simplest Hewson-Newns model is a Fano model interacting with a boson degree of freedom. Consider a spin-less Fano model, (Chapter 5),

$$h_F = \varepsilon_r n_r + \sum_k \varepsilon_k n_k + \sum_k \{V_{kr} c_k^\dagger c_r + h.c.\},$$

where as usual n_r is the occupation number operator of some *resonant* orbital, while the index k runs over the electron continuum; let

$$H_v = \omega_0 d^\dagger d, \quad (14.61)$$

be some harmonic oscillator (vibration or or plasmon). The Hewson-Newns [79] model Hamiltonian reads

$$H = h_F + H_v + H_{ev}, \quad (14.62)$$

where a linear coupling is assumed between the oscillator and the resonant state:

$$H_{ev} = g(d + d^\dagger)n_r. \quad (14.63)$$

The electron can be captured by the resonance and excite the plasmons, but if eventually the resonance decays, the interaction with the plasmons is turned off, otherwise a permanent shift of the oscillator coordinate may result. The interaction can be very strong if the boson frequency resonates with dressed electronic excitations. The purpose of the method is to calculate exactly the the excitation amplitudes

$$\psi_v(E) = \langle 0 | d^v c_r \frac{1}{E - H + i\delta} c_r^\dagger | 0 \rangle \quad (14.64)$$

where $|0\rangle$ is the electron and plasmon vacuum. The amplitude of exciting v plasmons is $A_v(E) = \frac{1}{\sqrt{v!}} \psi_v(E)$. The identity (4.92)

³This approach should not be confused with other useful recursion methods, which are completely different, despite the fact that they lead to continued fraction solutions. Among the most important examples, I recall the Mori generalized Langevin Equation Method [208] and the Lee solution technique [209]; for a review see Ref. [210]. However, quite recently, I became aware of a related solution of a boson-boson model had been put forth previously by Sumi[100] developing a theory of exciton polaritons.

⁴For applications to many-photon effects, see Reference [78] and next Chapter.

$$\frac{1}{E-H+i\delta} = \frac{1}{E-h+i\delta} + \frac{1}{E-h+i\delta} H_{ev} \frac{1}{E-H+i\delta}$$

yields

$$\begin{aligned} \psi_v(E) &= \langle 0 | d^v c_r \frac{1}{E-h+i\delta} c_r^\dagger | 0 \rangle + \\ &\langle 0 | d^v c_r \frac{1}{E-h+i\delta} H_{ev} \frac{1}{E-H+i\delta} c_r^\dagger | 0 \rangle = \\ \delta_{v0} G_{rr}^0(E) &+ \langle 0 | d^v c_r \frac{1}{E-h+i\delta} H_{ev} \frac{1}{E-H+i\delta} c_r^\dagger | 0 \rangle \end{aligned} \quad (14.65)$$

where $G_{rr}^0(E)$ is the retarded Green's function for $g=0$. In other terms, this is the solution of the Fano problem,

$$G_{rr}^0(E) = \langle 0 | c_r \frac{1}{E-h+i\delta} c_r^\dagger | 0 \rangle. \quad (14.66)$$

One verifies by induction that

$$d^v h^n = (h + v\omega_0)^n d^v \quad (14.67)$$

with the consequence that

$$d^v \frac{1}{E-h+i\delta} = \frac{1}{E-h-v\omega_0+i\delta} d^v. \quad (14.68)$$

Thus,

$$\psi_v(E) = \delta_{v0} G_{rr}^0(E) + \langle 0 | c_r \frac{1}{E-h-v\omega_0+i\delta} d^v H_{ev} \frac{1}{E-H+i\delta} c_r^\dagger | 0 \rangle \quad (14.69)$$

$$= \delta_{v0} G_{rr}^0(E) + \langle 0 | c_r \frac{1}{E-h-v\omega_0+i\delta} c_r^\dagger g d^v (d + d^\dagger) c_r \frac{1}{E-H+i\delta} c_r^\dagger | 0 \rangle. \quad (14.70)$$

Now note that, by reading the matrix element from right to left, the electron is created, annihilated, created and annihilated again, thus the first annihilation produces the electron vacuum; moreover, on the left of d^v the only boson operators are those contained in h . Therefore, the matrix element gets factored.

$$\begin{aligned} \psi_v(E) &= \delta_{v0} G_{rr}^0(E) + g \langle 0 | c_r \frac{1}{E-h-v\omega_0+i\delta} c_r^\dagger | 0 \rangle \\ &\times \langle 0 | d^v (d + d^\dagger) c_r \frac{1}{E-H+i\delta} c_r^\dagger | 0 \rangle. \end{aligned} \quad (14.71)$$

Since

$$d (d^+)^n = n (d^+)^{n-1} + (d^+)^n d, \tag{14.72}$$

one gets

$$\langle 0|d^\nu d^\dagger = \nu \langle 0|d^{\nu-1} \tag{14.73}$$

and finds the recursion relations

$$\psi_\nu (E) = \delta_{\nu 0} G_{\text{Tr}}^0 (E) + gG (E - \nu\omega_0) \{ \psi_{\nu+1} (E) + \nu\psi_{\nu-1} (E) \}. \tag{14.74}$$

To solve this system, it is convenient to define

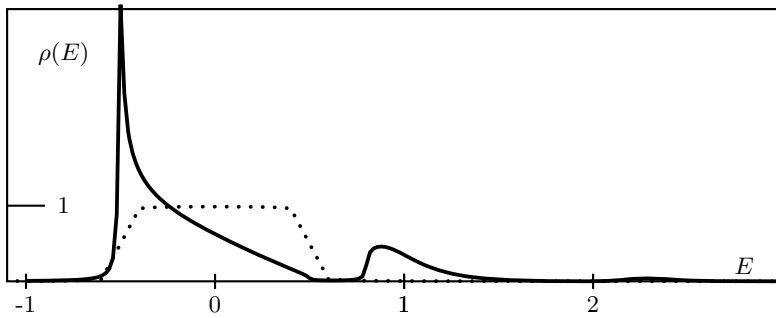


Fig. 14.2. The interaction of a slightly broadened ($\delta = 0.01$) rectangular level of Equation (14.20)(dotted line, width=1, arbitrary units) with a plasmon mode of frequency $\omega_p = 1.3$ with coupling $g=0.5$, according to Equation(14.77). Note that the local density of states is deformed by interaction with the plasmon mode, while the plasmon satellites are not identical in shape to the main line. At strong coupling (stronger g) localized resonances also arise.

$$\phi_\nu (E) = g^\nu \psi_\nu (E) \tag{14.75}$$

casting the r.r. in the form

$$\phi_\nu (E) = \delta_{\nu 0} G_{\text{Tr}}^0 (E) + G^0 (E - \nu\omega_0) \{ \phi_{\nu+1} (E) + \nu g^2 \phi_{\nu-1} (E) \}. \tag{14.76}$$

For $\nu = 0$, the solution is given by the continued fraction

$$\phi_0 (E) = G(E) \equiv \frac{G^0(E)}{1 - \frac{g^2 G^0(E)G^0(E-\omega_0)}{1 - \frac{2g^2 G^0(E-\omega_0)G^0(E-2\omega_0)}{1 - \frac{3g^2 G^0(E-2\omega_0)G^0(E-3\omega_0)}{\dots}}}} \tag{14.77}$$

from which, using the r.r. again, the other amplitudes with are easily derived. The interacting density of states $\rho(E) = -\frac{Im(\phi)}{\pi}$ gets satellites and

is deformed in a characteristic way (see Fig. 14.2). Note that $G_{rr}^0(E)$ is not a simple energy denominator as in Haydock's method and contains the full band-theory information. This method has already been applied to a variety of problems involving few electrons interacting with bosons, leading to exact solutions in many cases. The present is a simple example, and more generally the solution([124])[46]) is not given by a continued fraction.

14.4 Feenberg Method

Feenberg[97] long ago introduced a very general method for solving linear problems, later reviewed by Swain[98] who aimed at applications in the field of Nonlinear Optics. Let A denote a square matrix of order N and a_{ij} its elements. By definition,

$$Det A = \sum_Q (-)^Q a_{q(1)1} a_{q(2)2} \dots a_{q(N)N} \tag{14.78}$$

is the sum of all the products of N elements in the matrix, one for each line and column; each product is multiplied by the sign of the permutation Q of the first indices, when the product is ordered with the second indices in ascending order 1 to N . Below I'll write simply A for $Det A$. Everybody knows the Laplace development; choosing an arbitrary row index i ,

$$A = \sum_j (-)^{(i+j)} a_{ij} A^{ij}, \tag{14.79}$$

where A^{rc} is obtained from A by removing row r and column c . This is not the only useful expansion, however. It often happens that the diagonal elements are finite, that is, $O(1)$, while the off-diagonal ones are $O(V)$, where V is some small parameter. In such cases, the Feenberg development is specially suited, since besides being exact, it can serve as an expansion in powers of V .

Let A_i be the determinant obtained from A by removing the i -th row and column; A_{ij} the determinant of the matrix that one obtains from A by removing rows and columns i and j ; and so on. Chosen at will a diagonal element a_{ii} , in each term of A it is multiplied by elements coming from rows and columns $\neq i$; thus $\frac{\partial A}{\partial a_{ii}}$ is an antisymmetrized product of all the elements from other rows and columns, and this is just $\frac{\partial A}{\partial a_{ii}} = A_i$. Given a pair of indices i and j and the product $p_{ij} = a_{ij} a_{ji}$, $\frac{\partial A}{\partial p_{ij}}$ is an antisymmetrized product of the elements from other rows and columns, so $\frac{\partial A}{\partial p_{ij}} = -A_{ij}$; one can continue in this way, ending with $A_{123\dots N} \equiv 1$. Thus, one obtains a closed development:

$$A = a_{ii} A_i - \sum_{j \neq i} a_{ij} a_{ji} A_{ij} + \sum_{k \neq j, i} \sum_{j \neq i} a_{ij} a_{jk} a_{ki} A_{ijk} - \sum_{l \neq k, j, i} \sum_{k \neq j, i} \sum_{j \neq i} a_{ij} a_{jk} a_{kl} a_{li} A_{ijkl} + \dots \tag{14.80}$$

A convenient notation is

$$\begin{aligned}
 A = a_{ii}A_i - \sum_j^* a_{ij}a_{ji}A_{ij} + \sum_j^* \sum_k^* a_{ij}a_{jk}a_{ki}A_{ijk} \\
 - \sum_l^* \sum_k^* \sum_j^* a_{ij}a_{jk}a_{kl}a_{li}A_{ijkl} + \dots \tag{14.81}
 \end{aligned}$$

where \sum_j^* means that the index j must be different from any other index in the summand. Equating the Feenberg and the Laplace developments one finds for $i \neq j$; summarizing,

$$\begin{aligned}
 A^{ij} &= A_i, \quad i = j \\
 &= -(-)^{(i+j)}[a_{ji}A_{ij} - \sum_k^* a_{jk}a_{ki}A_{ijk} + \\
 &\quad \sum_l^* \sum_k^* a_{jk}a_{kl}a_{li}A_{ijkl} - \dots], \quad i \neq j. \tag{14.82}
 \end{aligned}$$

The sequences of different indices like those in $a_{jk}a_{kl}a_{li}$ are called by Swain[98] *irreducible processes*. To write down a general term of such an expansion one can start from enumerating all the irreducible processes that occur at a given order. The elements of the inverse matrix are:

$$(A^{-1})_{ij} = (-)^{(i+j)} \frac{A^{ji}}{A} \tag{14.83}$$

and the diagonal ones read⁵

$$G_i \equiv (A^{-1})_{ii} = \frac{A_i}{A}. \tag{14.84}$$

Let us introduce:

$$\begin{aligned}
 D_i = \frac{A}{A_i}, \quad D_{ij} = \frac{A}{A_{ij}}, \quad D_{ijk} = \frac{A}{A_{ijk}}, \dots \\
 D_j^i = \frac{A_i}{A_{ij}}, \quad D_{jk}^i = \frac{A_i}{A_{ijk}}, \quad D_{jkl}^{il} = \frac{A_{il}}{A_{ijkl}}, \dots \tag{14.85}
 \end{aligned}$$

where where each D brings lower and possibly upper indices; the upper ones are those of the A above, while the A below bears the upper and the lower indices. Directly from the Feenberg development,

$$\begin{aligned}
 D_i = \frac{A}{A_i} &= a_{ii} - \sum_j^* \frac{a_{ij}a_{ji}A_{ij}}{A_i} + \sum_j^* \sum_k^* a_{ij}a_{jk}a_{ki} \frac{A_{ijk}}{A_i} \\
 &- \sum_l^* \sum_k^* \sum_j^* a_{ij}a_{jk}a_{kl}a_{li} \frac{A_{ijkl}}{A_i} + \dots \\
 &= a_{ii} - \sum_j^* \frac{a_{ij}a_{ji}}{D_j^i} + \sum_j^* \sum_k^* \frac{a_{ij}a_{jk}a_{ki}}{D_{jk}^i} \\
 &- \sum_l^* \sum_k^* \sum_j^* \frac{a_{ij}a_{jk}a_{kl}a_{li}}{D_{jkl}^i} + \dots \tag{14.86}
 \end{aligned}$$

and similarly

⁵one uses the notation G_i since if $A = z - H$ these are resolvent matrix elements.

$$D_k^i = \frac{A_i}{A_{ik}} = a_{kk} - \sum_j^* \frac{a_{kj}a_{jk}}{D_j^{ik}} + \sum_{jm}^* \frac{a_{kj}a_{jm}a_{mk}}{D_{jm}^{ik}} + \dots \quad (14.87)$$

where the summation indices cannot be equal to i .

We can expand the D ratios: from the formula for A one obtains for instance

$$A_{uv} = a_{ii}A_{iuv} - \sum_j^* a_{ij}a_{ji}A_{ijuv} + \sum_j^* \sum_k^* a_{ij}a_{jk}a_{ki}A_{ijkuv} - \sum_l^* \sum_k^* \sum_j^* a_{ij}a_{jk}a_{kl}a_{li}A_{ijkluv} + \dots \quad (14.88)$$

hence we obtain a D with a single low index:

$$D_i^{uv} = \frac{A_{uv}}{A_{uvi}} = a_{ii} - \sum_j^* a_{ij}a_{ji} \frac{A_{ijuv}}{A_{uvi}} + \sum_j^* \sum_k^* a_{ij}a_{jk}a_{ki} \frac{A_{ijkuv}}{A_{uvi}} - \sum_l^* \sum_k^* \sum_j^* a_{ij}a_{jk}a_{kl}a_{li} \frac{A_{ijkluv}}{A_{uvi}} + \dots \quad (14.89)$$

that is,

$$D_i^{uv} = a_{ii} - \sum_j^* \frac{a_{ij}a_{ji}}{D_j^{\mu\nu i}} + \sum_j^* \sum_k^* \frac{a_{ij}a_{jk}a_{ki}}{D_{jk}^{\mu\nu i}} - \sum_l^* \sum_k^* \sum_j^* \frac{a_{ij}a_{jk}a_{kl}a_{li}}{D_{jkl}^{\mu\nu i}} + \dots \quad (14.90)$$

D objects with several low indices can be written down as products of D objects having fewer low indices:

$$D_{ij} = \frac{A}{A_{ij}} = \frac{A}{A_i} \frac{A_i}{A_{ij}} = D_i D_j^i = D_j D_i^j \quad (14.91)$$

By raising indices one generates a recursive solution.

Example: $(A^{-1})_{11}$ for a Three-Diagonal Matrix A .

$$(A^{-1})_{11} = \frac{A_1}{A} = G_1 = \frac{1}{D_1} \quad (14.92)$$

where

$$D_1 = a_{11} - \sum_j^* \frac{a_{1j}a_{j1}}{D_j^1} + \sum_j^* \sum_k^* \frac{a_{1j}a_{jk}a_{k1}}{D_{jk}^1} - \dots$$

we realize that $a_{1j} = 0$ unless $j = 2$; then, in the second summation we must read $a_{12}a_{2k}a_{k1}$, where $k \neq 1, k \neq 2$. Then since $a_{k1} = 0$, only the first sum remains, and

$$D_1 = a_{11} - \frac{a_{12}a_{21}}{D_2^1}. \quad (14.93)$$

$$D_2^1 = \frac{A_1}{A_{12}} = a_{22} - \sum_j^* \frac{a_{2j}a_{j2}}{D_j^{12}} + \sum_{jk}^* \frac{a_{2j}a_{jk}a_{k2}}{D_{jk}^{12}} - \dots \quad (14.94)$$

where $j=1$ is forbidden, and so $j=3$; then, no k is acceptable and we are left with

$$D_2^1 = a_{22} - \frac{a_{23}a_{32}}{D_3^{12}}. \tag{14.95}$$

So,

$$G_1 = \frac{1}{a_{11} - \frac{a_{12}a_{21}}{a_{22} - \frac{a_{23}a_{32}}{D_3^{12}}}} \tag{14.96}$$

In this way, one finds the recurrence relations

$$C_i = a_{ii} - \frac{a_{i,i+1}a_{i+1,i}}{C_{i+1}}, \tag{14.97}$$

$$C_i = D_i^{1,2,\dots,i-1} \tag{14.98}$$

and the result is a continued fraction.

14.4.1 Solving Linear Systems

Given the linear non-homogeneous system

$$\sum_j a_{ij}x_j = b_i \tag{14.99}$$

Cramer’s formula yields the well-known solution

$$x_i = \sum_j \frac{(-)^{(i+j)}A^{ji}}{A} b_j \tag{14.100}$$

and we can expand the numerator by (14.82)

$$\begin{aligned} x_i &= \frac{A_i b_i}{A} + \sum_j^* \frac{b_j (-)^{(i+j)}}{A} (-)^{(i+j)} \\ &\times [a_{ji}A_{ij} - \sum_k^* a_{jk}a_{ki}A_{ijk} + \sum_l^* \sum_k^* a_{jk}a_{kl}a_{li}A_{ijkl} - \dots] \end{aligned}$$

that is, since $A_{ijl\dots}$ are symmetric in the exchange of indices,

$$\begin{aligned} x_i &= \frac{A_i b_i}{A} - \sum_j^* \frac{a_{ij}A_{ij}b_j}{A} + \\ &\sum_{jk}^* \frac{a_{ik}a_{kj}A_{ijk}b_j}{A} - \sum_{jkl}^* \frac{a_{ik}a_{kl}a_{lj}A_{ijkl}b_j}{A} - \dots \end{aligned}$$

or

$$x_i = \frac{b_i}{D_i} - \sum_j^* \frac{a_{ij}b_j}{D_{ij}} + \sum_{jk}^* \frac{a_{ij}a_{jk}b_k}{D_{ijk}} - \sum_{jkl}^* \frac{a_{ij}a_{jk}a_{kl}b_l}{D_{ijkl}} - \dots \tag{14.101}$$

14.4.2 Homogeneous systems

Homogeneous linear systems are also of interest, for instance to find the eigenvectors of a matrix H :

$$\sum_j a_{ij}x_j = 0, i = 1, \dots, N. \tag{14.102}$$

This case reduces to the previous one: provided r is such that the determinant A_r does not vanish, one can assign an arbitrary value to x_r and the reduced system

$$\sum_{j \neq r} a_{ij}x_j = -a_{ir}x_r, \quad i = 1, \dots, N, \quad i \neq r \tag{14.103}$$

with $b_i = -a_{ir}x_r$ (excluding row and column r from all determinants) has a unique solution

$$\frac{x_i}{x_r} = -\frac{a_{ir}}{D_i^r} + \sum_j^* \frac{a_{ij}a_{jr}}{D_{ij}^r} - \sum_{jk}^* \frac{a_{ij}a_{jk}a_{kr}}{D_{ijk}^r} + \dots \tag{14.104}$$

Problems

14.1. Show that if we can calculate the local Green's function, we can also obtain any matrix element $G_{mn}(E)$.

14.2. For the rectangular band model (14.20) $n(\omega) = \frac{\theta(W^2 - \omega^2)}{2W}$, find the continued fraction coefficients.

14.3. For the semielliptic band model, find the continued fraction coefficients.

14.4. The 3×3 linear system $A\mathbf{x} = \mathbf{b}$ with a non-singular matrix

$$A = \begin{pmatrix} a_{11} & a_{12} & a_{13} \\ a_{21} & a_{22} & a_{23} \\ a_{31} & a_{32} & a_{33} \end{pmatrix}$$

is notoriously solved by $\mathbf{x} = A^{-1}\mathbf{b}$, where

$$A^{-1} = \frac{1}{\det A} \begin{pmatrix} \left| \begin{array}{cc|cc} a_{22} & a_{23} & a_{13} & a_{12} \\ a_{32} & a_{33} & a_{33} & a_{32} \end{array} \right| & \left| \begin{array}{cc|cc} a_{13} & a_{12} & a_{12} & a_{13} \\ a_{22} & a_{23} & a_{22} & a_{23} \end{array} \right| & \left| \begin{array}{cc|cc} a_{12} & a_{13} & a_{13} & a_{11} \\ a_{23} & a_{21} & a_{23} & a_{21} \end{array} \right| \\ \left| \begin{array}{cc|cc} a_{23} & a_{21} & a_{11} & a_{13} \\ a_{33} & a_{31} & a_{31} & a_{33} \end{array} \right| & \left| \begin{array}{cc|cc} a_{13} & a_{11} & a_{13} & a_{11} \\ a_{23} & a_{21} & a_{23} & a_{21} \end{array} \right| & \left| \begin{array}{cc|cc} a_{13} & a_{11} & a_{13} & a_{11} \\ a_{23} & a_{21} & a_{23} & a_{21} \end{array} \right| \\ \left| \begin{array}{cc|cc} a_{21} & a_{22} & a_{12} & a_{11} \\ a_{31} & a_{32} & a_{32} & a_{31} \end{array} \right| & \left| \begin{array}{cc|cc} a_{12} & a_{11} & a_{11} & a_{12} \\ a_{21} & a_{22} & a_{21} & a_{22} \end{array} \right| & \left| \begin{array}{cc|cc} a_{11} & a_{12} & a_{11} & a_{12} \\ a_{21} & a_{22} & a_{21} & a_{22} \end{array} \right| \end{pmatrix}.$$

But how does the solution work by Feenberg's method? Try to find x_1 .

15 Aspects of Nonlinear Optics and Many-Photon Effects

15.1 Diffusion of Radiation in Dipole Approximation

For strong electromagnetic fields, like those produced by a laser, the linear response theory fails. Interesting processes leading to color changes become important, and this has implications and applications. In this Chapter we shall study the Raman effect, Second Harmonic Generation, the diffusion of Coherent light and the Dynamical Stark effect.

By diffusion or scattering we mean those 2-photon processes where one photon is annihilated and one is created. In the elastic (Rayleigh) diffusion the frequency of the two photons is the same, in the inelastic (Raman) scattering a shift of frequency brings further information about the scatterer. The Quadratic Response formalism of Section 6.4 is well suited to describe two-photon processes (not only the scattering processes, but also others, like the decay of the H 2s level).

Classical Model of Diffusion by a Molecule

Classically, the elastic diffusion is caused by the induced currents. The inelastic diffusion is due to the following mechanism. An oscillating dipole of frequency ω_0 radiates a power

$$I = \frac{2}{3} \frac{\omega_0^4}{c^3} \langle \vec{d}^2 \rangle. \quad (15.1)$$

Now let an electromagnetic wave of pulsation ω induce in the molecule a dipole

$$\vec{d} = \hat{\alpha} \vec{E} \cos(\omega t); \quad (15.2)$$

the polarizability $\hat{\alpha}$ is a second-rank tensor. If ω_m is the pulsation of the molecular vibrations,

$$\hat{\alpha} = \hat{\alpha}_0 + \hat{\alpha}_1 \cos(\omega_m t + \beta) \quad (15.3)$$

where β is an arbitrary phase. Thus, one expects elastic radiation at ω and inelastic components at $\omega \pm \omega_m$. The one at $\omega - \omega_m$ and $\omega + \omega_m$ are called Stokes and anti-Stokes radiation, respectively. Classically, their intensity should be the same, actually the Stokes light is more intense, but this requires Quantum Theory to explain.

Photon

We use the trasverse gauge, without scalar potential ϕ and vector potential

$$\vec{A} = N\vec{\epsilon} e^{i\vec{k}\cdot\vec{r} - i\omega t}, \quad (15.4)$$

for the normalization we ask that a unit volume V contains a photon energy, that is,

$$\frac{1}{4\pi} \int_V [\vec{E}\vec{E}^* + \vec{B}\vec{B}^*] d^3r = \hbar\omega. \quad (15.5)$$

From $\vec{E} = -\frac{\partial\vec{A}}{\partial t}$, $\vec{B} = \text{rot}\vec{A}$, one finds $\vec{E}\vec{E}^* = \vec{B}\vec{B}^* = N^2\omega^2$; putting into (15.5), $\frac{2N^2}{4\pi}\omega^2V = \hbar\omega$ and

$$\vec{A} = \sqrt{\frac{2\pi\hbar}{\omega V}} \vec{\epsilon} e^{i\vec{k}\cdot\vec{r} - i\omega t}, \quad (15.6)$$

We shall often work with $V = 1$ and $\hbar = 1$.

Dipole Approximation

In the semiclassical theory, the dipole moment $e\vec{r} = \vec{d}$ is a time-independent operator, while $\vec{E}(t)$ is an external field. The radiation-matter interaction is introduced by adding to the Lagrangian $-e\phi - e\vec{A}\cdot\vec{v}$, where v is the velocity. Here, $\phi = 0$ and we are considering long wavelengths $k \rightarrow 0$, when $\vec{A} \rightarrow \sqrt{\frac{2\pi\hbar}{\omega V}} \vec{\epsilon} e^{-i\omega t}$. Then, using $\frac{-e}{c}\vec{A}\cdot\frac{d}{dt}\vec{r} = \frac{-e}{c} \left[\frac{d(\vec{A}\cdot\vec{r})}{dt} - \vec{r}\cdot\frac{d\vec{A}}{dt} \right]$ we drop the total derivative ending up with the Hamiltonian

$$H'(t) = -\vec{E}\cdot\vec{d} = V_A e^{-i\omega t} + V_E e^{i\omega t}. \quad (15.7)$$

Here,

$$V_A = -i\sqrt{\frac{2\pi\hbar\omega}{V}} \vec{\epsilon}\cdot\vec{d}, V_E = V_A^\dagger, \quad (15.8)$$

where V_A and V_E describe photon absorption and emission, respectively.

15.1.1 Second-Order Processes

Let $|i\rangle$ and $|f\rangle$ denote two stationary states of the unperturbed molecule. An incident photon of pulsation ω_1 can induce a $|i\rangle \rightarrow |f\rangle$ transition ending up as a photon of pulsation ω_2 in the solid angle $d\Omega_2$ leading to a detector. We wish to obtain the differential cross section of this two-photon process. The answer is contained in the second-order term of Equation (2.36) or in the more intuitive, but equivalent argument below.

As a preliminary, simpler calculation we seek the probability amplitude $A_{if}(t) = \langle f|t\rangle$ that the molecule makes the transition to $\langle f|$ assuming 1) that

both photons belong to sharply specified modes 2) that photon ω_1 is absorbed at time t_1 and photon ω_2 is emitted at time t_2 . There are two time orderings and two contributions, represented by a) and b) in Figure 15.1. Quantum theory also yields diagram b), contrary to the classical intuition, because the effect (photon emission) precedes the cause. The quantum uncertainty also affects time.

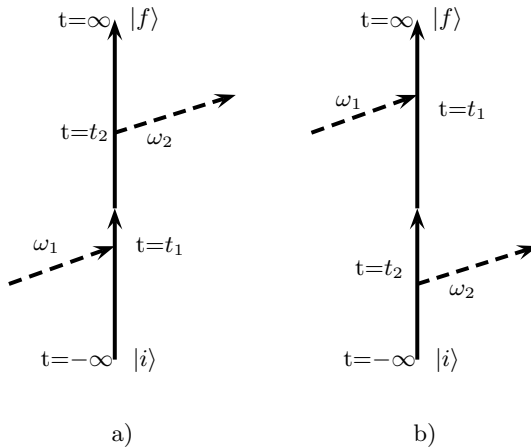


Fig. 15.1. A photon scattering second order process: in a) the photon is absorbed and then re-emitted, in b) it is re-emitted and then absorbed.

The interaction picture state at time t corresponding to diagram a) is

$$|t\rangle = [-iV_E(\omega_2, t_2)]_I e^{i\omega_2 t_2} [-iV_A(\omega_1, t_1)]_I e^{i\omega_1 t_1} |i\rangle. \quad (15.9)$$

This would be the correct result if the times t_1 and t_2 were assigned by the experiment. Since this is not the case, we must allow for the interference of different values, by integrating over the intermediate times. A part ΔA_{if} of the amplitude comes from events in which $t_2 > t_1$: the contribution to the process is $\langle f|t\rangle$ where

$$|t\rangle = - \int_{-\infty}^t dt_2 \int_{-\infty}^{t_2} dt_1 [V_E(\omega_2, t_2)]_I [V_A(\omega_1, t_1)]_I e^{i(\omega_2 t_2 - \omega_1 t_1)}, \quad (15.10)$$

thus

$$\Delta A_{if}^a(t) = - \int_{-\infty}^t dt_2 \int_{-\infty}^{t_2} dt_1 \langle f| [V_E(\omega_2, t_2)]_I [V_A(\omega_1, t_1)]_I |i\rangle e^{i(\omega_2 t_2 - \omega_1 t_1)}. \quad (15.11)$$

Expanding the interaction picture operators

$$\Delta A_{if}^a(t) = - \int_{-\infty}^t dt_2 \int_{-\infty}^{t_2} dt_1 \langle f | e^{iHt_2} V_E(\omega_2) e^{-i(H-\omega_2)t_2} e^{iHt_1} V_A(\omega_1) e^{-i(H-\omega_1)t_1} | i \rangle \quad (15.12)$$

and working out the calculations, one finds

$$A_{if}(t) = - \int_{-\infty}^t dt_2 \int_{-\infty}^{t_2} dt_1 \langle f | V_E(\omega_2) e^{-i(H-E_f-\omega_2)t_2} e^{i(H-E_i-\omega_1)t_1} V_A(\omega_1) | i \rangle. \quad (15.13)$$

We do the t_1 integral giving the integrand the usual adiabatic switch:

$$\int_{-\infty}^{t_2} dt_1 e^{ixt_1} = \frac{e^{ixt_2}}{ix}. \quad (15.14)$$

Thus,

$$\begin{aligned} A_{if}^a(t) &= - \int_{-\infty}^t dt_2 \langle f | V_E(\omega_2) e^{-i(H-E_f-\omega_2)t_2} e^{i(H-E_i-\omega_1)t_2} \times \\ &\quad \frac{-i}{H-E_i-\omega_1-i0} V_A(\omega_1) | i \rangle \\ &= - \int_{-\infty}^t dt_2 e^{-i(-E_f-\omega_2)t_2+i(-E_i-\omega_1)t_2} \times \\ &\quad \langle f | V_E(\omega_2) \frac{-i}{H-E_i-\omega_1-i0} V_A(\omega_1) | i \rangle \end{aligned} \quad (15.15)$$

and finally

$$\begin{aligned} A_{if}^a(t) &= -e^{i(E_f+\omega_2-E_i-\omega_1)t} \frac{-i}{E_f-E_i+\omega_2-\omega_1-i0} \times \\ &\quad \langle f | V_E(\omega_2) \frac{-i}{H-E_i-\omega_1-i0} V_A(\omega_1) | i \rangle. \end{aligned} \quad (15.16)$$

The contribution of diagram b) is

$$\begin{aligned} A_{if}^b(t) &= -e^{i(E_f+\omega_2-E_i-\omega_1)t} \frac{-i}{E_f-E_i+\omega_2-\omega_1-i0} \times \\ &\quad \langle f | V_A(\omega_1) \frac{-i}{H-E_i-\omega_2-i0} V_E(\omega_2) | i \rangle, \end{aligned} \quad (15.17)$$

and the total amplitude is

$$A_{if}(t) = A_{if}^a(t) + A_{if}^b(t). \quad (15.18)$$

Energy Conservation

The ω_1 photon is incoming, and must be switched on adiabatically; therefore $A_{if}(t)$ must have an infinitesimal exponential growth. Letting $x = E_f - E_i + \omega_2 - \omega_1$,

$$A_{if} \propto \frac{e^{\eta t}}{x - i\eta} \Rightarrow |A_{if}|^2 \propto \frac{e^{2\eta t}}{x^2 + \eta^2}, \quad \eta \rightarrow 0.$$

The transition probability per unit time is

$$\frac{dP_{if}}{dt} \propto \frac{2\eta e^{2\eta t}}{x^2 + \eta^2} \rightarrow 2\pi\delta(x), \quad \eta \rightarrow 0. \quad (15.19)$$

In this way, the energy conserving $\delta(E_f - E_i + \omega_2 - \omega_1)$ factor arises much more elegantly than in more elementary treatments.

Density of States for the Outgoing Photon

The experiment measures the energy $\hbar\omega_2$ of the outgoing photon and its direction within a solid angle $d\Omega_2$: instead, P_{if} refers to a well determined photon mode with given four-momentum $\hbar(\vec{k}, \omega)$. Therefore, we must sum $\frac{dP_{if}}{dt}$ on the modes with $\omega_2 = \omega_1 + E_i - E_f$ having \vec{k} within $d\Omega_2$. The sum is the density of states $d\rho(\omega_2) \equiv \sum_{\vec{k} \in d\Omega_2} \delta(\omega_2 - |k|)$, that is,

$$d\rho(\omega_2) = \frac{V d\Omega_2}{(2\pi)^3} \int d^3k \delta(\omega_2 - |k|) = \frac{V d\Omega_2}{(2\pi)^3} \omega_2^2. \quad (15.20)$$

The incident photon is normalized to 1 in volume V ; the probability per unit time to observe the outgoing photon is the differential cross section

$$d\sigma_{if} = 2\pi \left| \langle f | V_E(\omega_2) \frac{-i}{H - E_i - \omega_1 - i0} V_A(\omega_1) | i \rangle + \langle f | V_A(\omega_1) \frac{-i}{H - E_i - \omega_2 - i0} V_E(\omega_2) | i \rangle \right|^2 d\rho(\omega_2). \quad (15.21)$$

Recalling (15.8),

$$d\sigma_{if} = |M|^2 \frac{\omega_1 \omega_2^3 d\Omega_2}{\hbar^2 c^4}, \quad (15.22)$$

where

$$M = \langle f | \vec{\epsilon}_2 \cdot \vec{d} \frac{-i}{H - E_i - \omega_1 - i0} \vec{\epsilon}_1 \cdot \vec{d} | i \rangle + \langle f | \vec{\epsilon}_1 \cdot \vec{d} \frac{-i}{H - E_i - \omega_2 - i0} \vec{\epsilon}_2 \cdot \vec{d} | i \rangle. \quad (15.23)$$

In the second denominator, we introduce a complete set and since $\omega_2 = \omega_1 + E_i - E_f$ we obtain

$$M = \sum_n \left[\frac{(\vec{\epsilon}_2 \cdot \vec{d}_{fn}) (\vec{\epsilon}_1 \cdot \vec{d}_{ni})}{\omega_{ni} - \omega_1} + \frac{(\vec{\epsilon}_1 \cdot \vec{d}_{fn}) (\vec{\epsilon}_2 \cdot \vec{d}_{ni})}{\omega_{nf} + \omega_1} \right] \quad (15.24)$$

provided that no denominator vanishes (otherwise one speaks of resonant Raman scattering which requires a separate treatment). Following Kramers and Heisenberg, we may write

$$M = \sum_{pq} R_{pq}(\epsilon_2)_p(\epsilon_1)_q, \quad (15.25)$$

in terms of the Raman tensor

$$R_{pq} = \sum_n \left[\frac{\langle f | \vec{d}_p | n \rangle \langle n | \vec{d}_q | i \rangle}{\omega_{ni} - \omega_1} + \frac{\langle f | \vec{d}_q | n \rangle \langle n | \vec{d}_p | i \rangle}{\omega_{nf} - \omega_1} \right]. \quad (15.26)$$

In the elastic $f = i$ case, the tensor describes the Rayleigh scattering. Otherwise if $\omega_1 > \omega_2$ then $E_f > E_i$ (Stokes transition); in the opposite case the system gives energy to the photon (anti-Stokes transition).

Inversion Symmetry

We saw in Chapter 8 that in systems like the Benzene molecule possessing inversion symmetry, $R_{pq} = 0$ unless $|i\rangle$ and $|f\rangle$ are of the same parity. Thus, Raman-active modes are not seen in infrared absorption, and conversely infrared active modes yield no Raman scattering. infrared.

Low-frequency Scattering

For $\omega_1 \rightarrow 0$, the Raman tensor has a finite limit. Hence, the cross-section (15.22) goes like $\omega_1 \omega_2^3$. The elastic scattering goes with ω_1^4 . This explains why the sky is blue and the advantage of radio-astronomy over infrared or optical observations of objects that are beyond interstellar clouds.

High-frequency Scattering

When ω_1 is large compared to the main absorption frequencies, we insert into (15.26) the expansions

$$\begin{aligned} \frac{1}{\omega_{ni} - \omega_1} &\sim -\frac{1}{\omega_1} - \frac{\omega_{ni}}{\omega_1^2} + \dots, \\ \frac{1}{\omega_{nf} + \omega_1} &\sim \frac{1}{\omega_1} - \frac{\omega_{nf}}{\omega_1^2} + \dots, \end{aligned}$$

and find

$$R_{pq} = R_{pq}^{(1)} + R_{pq}^{(2)} + \dots \quad (15.27)$$

with

$$R_{pq}^{(1)} = \frac{1}{\omega_1} \sum_n \left[-\langle f | \vec{d}_p | n \rangle \langle n | \vec{d}_q | i \rangle + \langle f | \vec{d}_q | n \rangle \langle n | \vec{d}_p | i \rangle \right] = 0 \quad (15.28)$$

and

$$R_{pq}^{(2)} = \frac{-1}{\omega_1^2} \sum_n \left[\omega_{ni} \langle f | \vec{d}_p | n \rangle \langle n | \vec{d}_q | i \rangle + \omega_{nf} \langle f | \vec{d}_q | n \rangle \langle n | \vec{d}_p | i \rangle \right]. \quad (15.29)$$

Since

$$\begin{aligned} \omega_{ni} \langle n | \vec{d}_q | i \rangle &= \langle n | [H, \vec{d}_q]_- | i \rangle = -i \langle n | \frac{d}{dt} \vec{d}_q | i \rangle, \\ \omega_{nf} \langle f | \vec{d}_q | n \rangle &= i \langle f | \frac{d}{dt} \vec{d}_q | n \rangle, \end{aligned} \quad (15.30)$$

keeping up to second-order terms,

$$\begin{aligned} R_{pq} &= \frac{i}{\omega_1^2} \sum_n \left[\langle f | \vec{d}_p | n \rangle \langle n | \frac{d}{dt} \vec{d}_q | i \rangle - \langle f | \frac{d}{dt} \vec{d}_q | n \rangle \langle n | \vec{d}_p | i \rangle \right] \\ &= \frac{i}{\omega_1^2} \left[\langle f | \vec{d}_p \frac{d}{dt} \vec{d}_q - \left(\frac{d}{dt} \vec{d}_q \right) \vec{d}_p | i \rangle \right]. \end{aligned} \quad (15.31)$$

For one electron, $[\vec{d}_p, \left(\frac{d}{dt} \vec{d}_q\right)]_- = \frac{ie^2}{m} \delta_{pq}$. With N electrons, $\vec{d} = e \sum_{k=1}^N \vec{r}_k$ and

$$[\vec{d}_p, \left(\frac{d}{dt} \vec{d}_q\right)]_- = \frac{Nie^2}{m} \delta_{pq}. \quad (15.32)$$

Thus, for large ω_1 ,

$$R_{pq} = -\frac{Ne^2}{m\omega_1^2} \delta_{if} \delta_{pq}. \quad (15.33)$$

No Raman scattering occurs. For the elastic scattering, remarkably the cross-section (15.22) becomes frequency independent:

$$\begin{aligned} d\sigma &= \left| \frac{Ne^2}{m\omega_1^2} \delta_{pq} (\vec{\epsilon}_2)_p (\vec{\epsilon}_1)_q \right|^2 \frac{\omega_1^4 d\Omega_2}{c^4} = N^2 \left[\frac{e^2}{mc^2} \right]^2 |\vec{\epsilon}_2 \cdot \vec{\epsilon}_1|^2 d\Omega_2 \\ &= N^2 r_e^2 |\vec{\epsilon}_2 \cdot \vec{\epsilon}_1|^2 d\Omega_2, \end{aligned} \quad (15.34)$$

where $r_e = \frac{e^2}{mc^2}$ is the classical radius of the electron. If α is the angle between $\vec{\epsilon}_1$ and $\vec{\epsilon}_2$,

$$|\vec{\epsilon}_2 \cdot \vec{\epsilon}_1|^2 = \cos^2(\alpha).$$

The outgoing photon polarization $\vec{\epsilon}_2$ must be orthogonal to \vec{k}_2 but according to (15.34), cannot be orthogonal to the incoming photon polarization $\vec{\epsilon}_1$. Therefore $\vec{\epsilon}_2$ is in the $\vec{k}_2 - \vec{\epsilon}_1$ plane. Let θ be the $\vec{\epsilon}_1 - \vec{k}_2$ angle; we obtain the classical Thomson formula

$$d\sigma = N^2 r_e^2 \sin^2(\theta) d\Omega_2. \quad (15.35)$$

15.2 Sum Frequency and Second-Harmonic Generation (SHG)

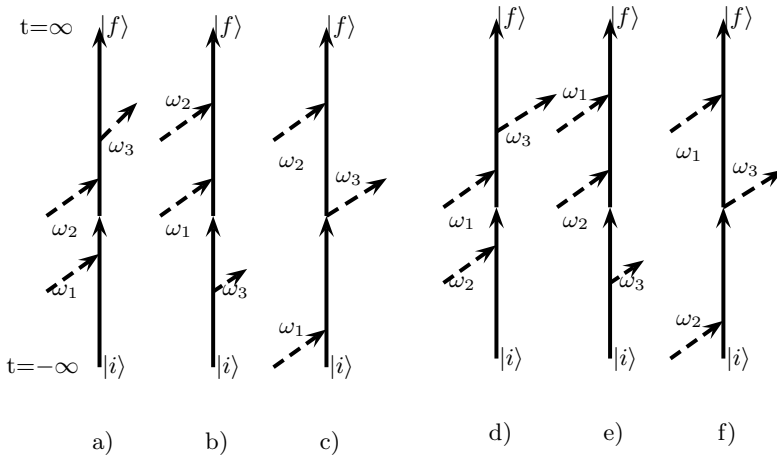


Fig. 15.2. The lowest-order second-harmonic generation diagrams.

As discussed in the last Section, the inelastic emission of radiation can be treated by perturbation theory, unless of course the incident radiation fields are comparable to those that exist in the unperturbed crystal and can reach $\sim 10^9$ Volt/cm. Such fields can alter and even destroy the specimen¹. So, the method used above for the Raman scattering is useful again and yields the probability of absorbing ω_1 and ω_2 photons and emitting ω_3 . Since there are $3!$ orderings, 6 diagrams contribute in lowest order (figure 15.2) . The amplitude is

$$B = X(\omega_1, \omega_2) + X(\omega_2, \omega_1) \tag{15.36}$$

where in obvious notation, with $f_n \equiv f(\epsilon_n)$ the Fermi distribution, and $\bar{f} = 1 - f$,

$$X(\omega_1, \omega_2) = \sum_i^6 \sum_{snr} f_s \bar{f}_n \xi(s, n, r, i, \omega_1, \omega_2), \tag{15.37}$$

$$\xi(s, n, r, 1, \omega_1, \omega_2) = \bar{f}_r \frac{[V_E(\omega_3)]_{sn} [V_A(\omega_2)]_{nr} [V_A(\omega_1)]_{rs}}{(\omega_{rs} - \omega_1 - i0) (\omega_{ns} - \omega_1 - \omega_2 - i0)}, \tag{15.38}$$

¹Blowing up the sample is not the best way to study it; however the next Section deals with interesting cases that cannot be treated at low order because the field is so strong that all the degrees of freedom are dressed and deeply affected by photons.

$$\xi(s, n, r, 2, \omega_1, \omega_2) = \bar{f}_r \frac{[V_A(\omega_2)]_{sn} [V_E(\omega_3)]_{nr} [V_A(\omega_1)]_{rs}}{(\omega_{rs} - \omega_1 - i0)(\omega_3 - \omega_1 + \omega_{ns} - i0)}, \quad (15.39)$$

$$\xi(s, n, r, 3, \omega_1, \omega_2) = \bar{f}_r \frac{[V_A(\omega_2)]_{sn} [V_A(\omega_1)]_{nr} [V_E(\omega_3)]_{rs}}{(\omega_3 + \omega_{rs} - i0)(\omega_3 - \omega_1 + \omega_{ns} - i0)}, \quad (15.40)$$

$$\xi(s, n, r, 4, \omega_1, \omega_2) = -f_r \frac{[V_E(\omega_3)]_{rn} [V_A(\omega_2)]_{sr} [V_A(\omega_1)]_{ns}}{(\omega_{ns} - \omega_1 - i0)(\omega_{nr} - \omega_1 - \omega_2 - i0)}, \quad (15.41)$$

$$\xi(s, n, r, 5, \omega_1, \omega_2) = -f_r \frac{[V_A(\omega_2)]_{rn} [V_E(\omega_3)]_{sr} [V_A(\omega_1)]_{ns}}{(\omega_{ns} - \omega_1 - i0)(\omega_3 - \omega_1 - \omega_{rn} - i0)}, \quad (15.42)$$

and

$$\xi(s, n, r, 6, \omega_1, \omega_2) = -f_r \frac{[V_A(\omega_2)]_{rn} [V_A(\omega_1)]_{sr} [V_E(\omega_3)]_{ns}}{(\omega_3 + \omega_{ns} - i0)(\omega_3 - \omega_1 + \omega_{rn} - i0)}. \quad (15.43)$$

The transition probability is proportional to

$$\sigma = \delta(\omega_3 - \omega_1 - \omega_2) |B(V_E; V_A)|^2. \quad (15.44)$$

This was my starting point for a calculation² of SHG spectra from interfaces [104], an unexplored subject at the time, in the European Esprit Project EPIOPTICS. Experiments were planned to observe the SHG signal from Si surfaces and interfaces. EPIOPTICS had the main motivation that SHG may carry information from buried interfaces, without exposing them, which is important for materials characterization. A photon is odd under inversion, and it can be shown that to second order no SHG occurs from systems with inversion symmetry such as Si. The surface breaks the inversion symmetry, and with the available radiation sources a tiny fraction (even 10^{-15} or less) of the incident power was predicted and observed to go into the SHG signal ????

With a similar formalism one can study other nonlinear effects like the two-photon decay of the 2s level of the H atom. In the following, we shall deal with many photon effects that occur when the fields are so strong that low order diagrams cannot work.

15.3 Diffusion of Coherent Light

15.3.1 Effective mode

When polarized monochromatic radiation (e.g. a laser beam) is shed over the sample, one can often formulate the scattering problem to a good approximation as if the photons belonged to one effective mode. Suppose there are

²In atomic and molecular problems, when no medium affects the field propagation, my formulation is an alternative to a more traditional one for bulk materials[105], which was based on the second-order susceptibility $\chi^{(2)}$.

M modes of frequency ω and polarization $\vec{\epsilon}$ in the beam; let H_e denote the many-electron Hamiltonian and $N \rightarrow \infty$ the dimensionality of the Hilbert space. For each mode k with vector potential $\vec{A}^{(k)}$ and creation operator b_k^\dagger , treating the vector potential as a constant in the interaction region in the spirit of the dipole approximation, the radiation-matter coupling reads

$$H'_k = \sum_{m,n,\sigma} M_{mn}^{(k)} a_{m\sigma}^\dagger a_{n\sigma} (b_k + b_k^\dagger) \tag{15.45}$$

with

$$M_{mn}^{(k)} = \frac{e}{mc} \langle m | \vec{A} \cdot \vec{p} | n \rangle = \frac{e}{mc} A^{(k)} \langle m | \vec{\epsilon} \cdot \vec{p} | n \rangle \tag{15.46}$$

where \vec{p} is the momentum operator. Therefore,

$$H'_k = A^{(k)} \hat{L}(b_k + b_k^\dagger), \tag{15.47}$$

where \hat{L} operates on the electrons but not on the photons. The part of the Hamiltonian that describes the field and its interaction is

$$H = \sum_k^M \left\{ \omega b_k^\dagger b_k + A^{(k)} \hat{L}(b_k + b_k^\dagger) \right\}. \tag{15.48}$$

By a real rotation α_{mk} in the mode space, such that $\alpha_{mk}\alpha_{nk} = \delta_{mn}$, I introduce new operators d :

$$\sum_k A^{(k)} b_k = \sum_k A^{(k)} \sum_m \alpha_{mk} d_m, \tag{15.49}$$

the rotated vector with components $\sum_k A^{(k)} \alpha_{mk}$ has the same length as the original one,

$$\|A\| = \sqrt{\sum_k (A^{(k)})^2}.$$

We need not specify the rotation further provided that

$$\sum_k A^{(k)} \alpha_{mk} = \|A\| \delta_{m1}; \tag{15.50}$$

then,

$$H = \hbar\omega \sum_m d_m^\dagger d_m + \|A\| \hat{L}(d_1 + d_1^\dagger). \tag{15.51}$$

Thus we can use a single mode with effective coupling $\|A\|$.

Mode Normalization

For a single mode, with $\vec{A} = c\sqrt{\frac{2\pi\hbar}{V\omega}}\vec{\epsilon}e^{i\vec{k}\cdot\vec{r}}e^{-i\omega t}$, that is, $A^{(k)} = c\sqrt{\frac{2\pi\hbar}{V\omega}}$,

$$\|A\|^2 = \frac{2\pi\hbar c^2}{V\omega} \sum_k = \frac{2\pi\hbar c^2}{V\omega} \frac{V}{(2\pi)^3} \Delta^{(3)}\mathbf{k}, \quad (15.52)$$

where $\Delta^{(3)}\mathbf{k}$ is the spread of the laser beam in \mathbf{k} space. Actually, $\frac{\Delta^{(3)}\mathbf{k}}{(2\pi)^3}$ is comparable to the inverse of the volume where the laser beam is coherent; hence we can safely work with one effective mode if V is the coherence volume.

Coherent Light Scattering

The diffusion of laser radiation from a sample can be studied by a model Hamiltonian of the form

$$H = H_e + H_{ph} + H_I + H'_I, \quad (15.53)$$

where H_e represents the electronic system, H_{ph} the free photons, H_I and H'_I the interactions of the electrons with the laser and scattered photons, respectively. The free field may be described by the Hamiltonian

$$H_{ph} = \omega_0 d^\dagger d + \omega'_0 d'_{scatt}{}^\dagger d'_{scatt}, \quad (15.54)$$

where d annihilates photons ω_0 from the laser while d'_{scatt} destroys scattered photons. The interaction terms are:

$$H_I = \hat{M}(d + d^\dagger) \quad (15.55)$$

$$H'_I = \hat{M}'(d'_{scatt} + d'_{scatt}{}^\dagger), \quad (15.56)$$

where \hat{M} and \hat{M}' are operators acting on the electronic degrees of freedom. The laser photons belong to one mode and are in a *coherent* state such that

$$d|c\rangle = \gamma|c\rangle \quad (15.57)$$

that is, $s|c\rangle = 0$ with

$$s = d - \gamma. \quad (15.58)$$

We take γ real for simplicity. We met a coherent state already in Section 6.1.4; in that case the shift was produced by the g coupling and γ could be found by Equation (6.20), while now γ is a property of the laser. Equation (6.28) $\bar{n} = \gamma^2$, still holds, however. In the case of laser radiation, γ can vary in a wide range: it can reach $\sim 10^4$ in continuously operated lasers and largely exceed $\sim 10^8$ in pulsed lasers (pulses last a few tens of a nanosecond).

It is often convenient to perform a canonical transformation to the s representation,

$$\tilde{H} = \tilde{H}_e + \tilde{H}_{ph} + \tilde{H}_I + H'_I, \tag{15.59}$$

where

$$\tilde{H}_e = H_e + \omega_0 \gamma^2 + 2\gamma \hat{M} \tag{15.60}$$

$$\tilde{H}_{ph} = \omega_0 s^\dagger s + \omega'_0 d^\dagger_{scatt} d_{scatt}, \tag{15.61}$$

$$\tilde{H}_I = \left[\omega_0 \gamma + \hat{M} \right] (s + s^\dagger) = \tilde{M} (s + s^\dagger) \tag{15.62}$$

The initial state of the system is $|g; 0\rangle \equiv |g\rangle|0\rangle$, where $|g\rangle$ stands for the electronic ground state and $|0\rangle$ for the photon vacuum.

The scattered spectrum $S(\omega_0)$ is proportional to the d_{scatt} photon emission rate. Instead of deriving a general formal expression for the rate (see Ref. [46]), here I consider a special case by a simple, physically motivated treatment.

15.3.2 Dynamical Stark Effect

A photon impinging on a molecule or a solid can give rise to lots of processes, but one can choose the symmetry of the system and the photon such that just one transition is possible. Then the system-radiation interaction can be understood by a two-level model. F Schuda, C R Stroud Jr and M Hercher [106] using a dye laser and a beam of Na atoms realized this situation: the laser was tuned at $\nu_0 \sim 5890 \text{ \AA}$ in resonance with a dipole allowed transition; this connects the F=2 hyperfine level arising from the $^2S_{\frac{1}{2}}$ ground state and the F=3 hyperfine level arising from the $^2P_{\frac{3}{2}}$ state³. These two levels form an ideal two-level system because by the $\Delta F = 0, \pm 1$ selection rules no other levels can be reached by the exciting radiation. They discovered that if a

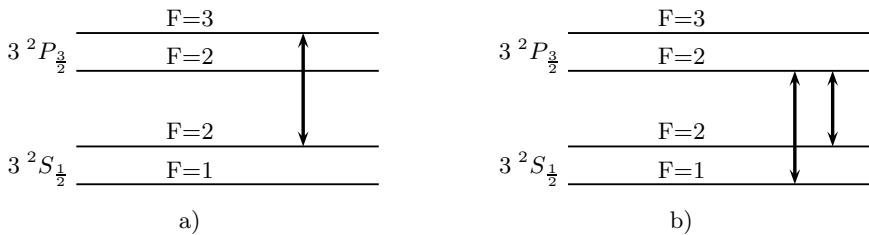


Fig. 15.3. Hyperfine levels of Na with a) the two-level system b) a three-level system.

³Here, F is the total angular momentum resulting from the nuclear spin $I = \frac{3}{2}$ of $^{23}_{11}\text{Na}$ and the electronic $\vec{J} = \vec{L} + \vec{S}$ angular momentum.

coherent field is in resonance with a two-level system, the scattered radiation consists of a central quasi-elastic radiations with two symmetric satellites at higher and lower frequencies, like in the Stark effect. The separation of the side bands from the central lines is $\Delta\nu \sim 100$ MHz, thus $\frac{\Delta\nu}{\nu_0} \sim 2 \times 10^{-10}$, a very small effect which however is clearly seen (a typical situation in atomic physics). The Hamiltonian⁴ which describes the two-level system interacting with the laser field is:

$$\begin{aligned} H_0 &= H_e + H_{ph} + H_I \\ H_e &= \epsilon_1 n_1 + \epsilon_2 n_2, H_{ph} = \omega_0 d^\dagger d \\ H_I &= (a_1^\dagger a_2 + a_2^\dagger a_1) g (d + d^\dagger). \end{aligned} \quad (15.63)$$

Here, ϵ_m, a_m denote the unperturbed atomic levels and annihilation operators, $n_m = a_m^\dagger a_m$, g the electron-photon matrix elements, ω_0 the laser frequency. The scattered photons and their emission

$$\begin{aligned} H' &= \omega' d_{scatt}^\dagger d_{scatt} + H'_I \\ H'_I &= (a_1^\dagger a_2 + a_2^\dagger a_1) g (d_{scatt} + d_{scatt}^\dagger) \end{aligned} \quad (15.64)$$

will be introduced later and treated perturbatively.

Shifted Representation

We now shift the laser photon operators by $d \rightarrow s + \gamma$, with $\gamma = \frac{g}{\omega_0}$ obtaining the following effects:

$$\begin{aligned} H_{ph} &\rightarrow \omega_0 s^\dagger s + \gamma \omega_0 (s + s^\dagger) + \omega_0 \gamma^2, \\ H_I &\rightarrow (a_1^\dagger a_2 + a_2^\dagger a_1) g (s + s^\dagger) + 2g\gamma (a_1^\dagger a_2 + a_2^\dagger a_1). \end{aligned}$$

We rearrange the terms of the transformed H_0 as follows:

$$\tilde{H}_0 = \tilde{H}_e + \tilde{H}_I + \omega_0 s^\dagger s, \quad (15.65)$$

with

$$\tilde{H}_e = \epsilon_1 n_1 + \epsilon_2 n_2 + \omega_0 \gamma^2 + 2G \left(a_1^\dagger a_2 + a_2^\dagger a_1 \right), G = g\gamma \quad (15.66)$$

$$\tilde{H}_I = \left[\omega_0 \gamma + g \left(a_1^\dagger a_2 + a_2^\dagger a_1 \right) \right] (s + s^\dagger) = \tilde{M} (s + s^\dagger). \quad (15.67)$$

the initial state of the system is $a_1^\dagger |0\rangle$, where $|0\rangle$ is the vacuum for s and d_{scatt} photons. Note that g enters as $G = g\gamma$ in Equation(15.66) and as g in equation (15.67). The two entries have quite different consequences.

⁴For simplicity, we ignore the M_F multiplicity and model this as a two-level system for a spin-less effective particle.

Without the g term in equation (15.67) there would be no dynamical Stark effect. However, to understand the situation, we need to evaluate the relative importance of the various couplings.

The atomic target has the characteristic length $a_0 = 1$ Bohr radius, with a characteristic energy $\frac{e^2}{a_0} = 1$ Hartree. We can get reasonable estimates of the coupling energy g and the number γ by the following arguments: 1) g must be proportional to the fluctuating atomic dipole ea_0 2) $\gamma^2 = \bar{n}$ is proportional to the beam energy density $\frac{\bar{n}\hbar\omega}{V}$ in the coherence volume $V \sim 1\text{cm}^3$. This reasoning leads to

$$(g\gamma)^2 \sim g^2\bar{n} \sim \bar{n}\hbar\omega \frac{e^2}{a_0} \times \frac{a_0^3}{V}. \quad (15.68)$$

At optical or near ultraviolet frequencies such that $\hbar\omega \sim \frac{e^2}{a_0}$, for $\bar{n} = 10^8$ ($\gamma = 10^4$) we may have $g\gamma \sim 10^{-9}\hbar\omega$ or even less. Then in Equation (15.67) the g term is quite tiny compared to the one in $\gamma\omega_0$ and we can expand around the limiting case⁵ $g \rightarrow 0, \gamma \rightarrow \infty$ with constant $G = g\gamma$. For $g = 0$ we diagonalize \tilde{H}_e , that becomes

$$\tilde{H}_e = \tilde{\epsilon}_1\tilde{n}_1 + \tilde{\epsilon}_2\tilde{n}_2 + \omega_0\gamma^2; \quad (15.69)$$

the unperturbed ($g \rightarrow 0$) Hamiltonian is:

$$\tilde{H}_{g \rightarrow 0} = \tilde{\epsilon}_1\tilde{n}_1 + \tilde{\epsilon}_2\tilde{n}_2 + \omega_0\gamma^2 + \omega_0(s + s^\dagger). \quad (15.70)$$

Back to the Unshifted Representation

Here \tilde{n}_1 and \tilde{n}_2 are conserved; there are eigenstates with $\tilde{n}_1 = 1, \tilde{n}_2 = 0$ and with $\tilde{n}_1 = 0, \tilde{n}_2 = 1$. At this point it is simplest to work in the old representation setting $d = s + \gamma$ and getting in the two cases the unperturbed Hamiltonians

$$h_{0,i} = \tilde{\epsilon}_i\tilde{n}_i + \omega_0d^\dagger d, i = 1, 2. \quad (15.71)$$

In this round trip among the representations we did not simply take the $g \rightarrow 0$ limit, since we are keeping the corrections of order G that renormalize the levels. The $|\tilde{i}, n\rangle$ eigenstates have eigenvalues $\tilde{\epsilon}_i + n\omega_0$. In the resonant case $\hbar\omega_0 = \epsilon_2 - \epsilon_1$, $|\tilde{1}, n + 1\rangle$ is almost degenerate with $|\tilde{2}, n\rangle$.

The perturbation is the term that we had neglected,

$$g(a_1^\dagger a_2 + a_2^\dagger a_1)(s + s^\dagger) = g(a_1^\dagger a_2 + a_2^\dagger a_1)(d + d^\dagger - 2\gamma). \quad (15.72)$$

Since $G \ll \epsilon_2 - \epsilon_1$, states are little affected by the tildes, and the matrix element between almost degenerate states is⁶

$$\langle \tilde{1}, n + 1 | g(a_1^\dagger a_2 + a_2^\dagger a_1)(d + d^\dagger - 2\gamma) | \tilde{2}, n \rangle \sim g\langle n + 1 | d^\dagger | n \rangle = g\sqrt{n + 1}. \quad (15.73)$$

⁵Note that the limit $\gamma \rightarrow \infty$ alone would correspond to classical fields.

⁶Note that the most important n values are $\sim \gamma^2$, and in this sense a high degree of coherence leads to stronger radiation-matter coupling.

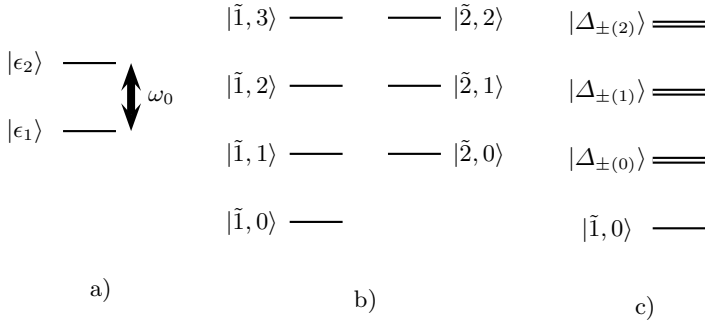


Fig. 15.4. Resonant radiation interacting with a two-level system. The energy spectrum is represented a) according to a simple one-photon view b) in the many-photon description, involving an infinite ladder of states, neglecting the $g(a_1^\dagger a_2 + a_2^\dagger a_1)(s + s^\dagger)$ term c) with the $g(a_1^\dagger a_2 + a_2^\dagger a_1)(s + s^\dagger)$ term included.

First-order perturbation theory yields a very accurate description of the effect of the tiny perturbation (15.72). The perturbed spectrum consists of the $|\tilde{1}, 0\rangle$ ground state and an infinity of close doublets; the doublet $\frac{|\tilde{1}, n+1\rangle + |\tilde{2}, n\rangle}{\sqrt{2}}$ arises from $|\tilde{1}, n+1\rangle$ $|\tilde{2}, n\rangle$ and the splitting is $2g\sqrt{n+1}$.

Scattered Light

Up to now we have dressed the atomic levels with photons from the laser obtaining an infinite double ladder of states, but the scattered photons still have to be considered. The scattered light arises from the spontaneous emission between the dressed states, according to A. Einstein's A coefficient

$$A_{m \rightarrow n} = \frac{4\omega_{mn}^3}{3\hbar c^3} \mathbf{d}_{mn}^2, \quad (15.74)$$

where \mathbf{d} is the dipole operator.

\mathbf{d} connects $|\tilde{2}, n\rangle$ with $|\tilde{1}, n\rangle$ with the same n , hence there are transitions only between consecutive doublets, with $\omega \sim \omega_0$. The frequencies of the transitions in Figure 15.5 a) are given by the scheme:

transition	ω	
$\Delta_+(n) \rightarrow \Delta_-(n-1)$	$\omega_0 + g(\sqrt{n+1} + \sqrt{n}) \sim \omega_0 + 2g\sqrt{n}$	(15.75)
$\Delta_+(n) \rightarrow \Delta_+(n-1)$	$\omega_0 + g(\sqrt{n+1} - \sqrt{n}) \sim \omega_0$	
$\Delta_-(n) \rightarrow \Delta_-(n-1)$	$\omega_0 + g(-\sqrt{n+1} + \sqrt{n}) \sim \omega_0$	
$\Delta_-(n) \rightarrow \Delta_+(n-1)$	$\omega_0 + -g(\sqrt{n+1} + \sqrt{n}) \sim \omega_0 - 2g\sqrt{n}$	

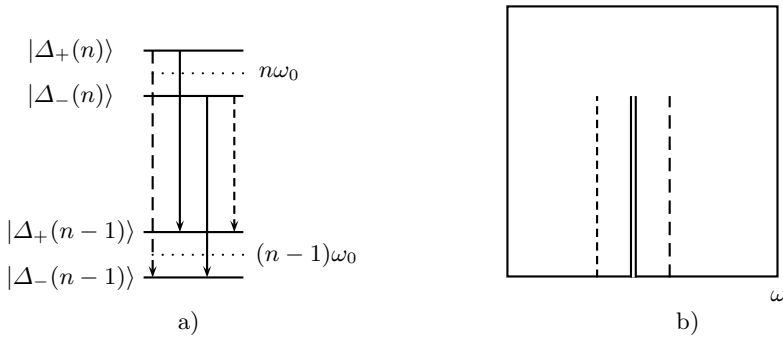


Fig. 15.5. The contribution of two consecutive doublets to the scattered radiation. a) the spontaneous emission lines b) the resulting spectral intensity versus ω .

Simple Explanation of the Dynamic Stark Triplet Spectrum

We wish to plot the spectral intensity $S(x)$ versus $x = \frac{\omega - \omega_0}{2g}$. Since the matrix elements are equal, and the frequencies are so close that the variation of the ω^3 factor is negligible, the 4 transitions in (15.75) have practically the same intensity. The width Δ of the central peak is of the order of the inverse lifetime $\sim g\gamma$ of the excited state, and we represent it by a Lorentzian. The system is prepared in a state that for $g \rightarrow 0$ corresponds to the atom in ϵ_1 and a coherent state of d photons. The doublet of states corresponding to $|1, n\rangle$ is occupied with probability $P_n = \frac{1}{2n!} a^n e^{-a}$, where $a = \gamma^2$. The most important contributions arise from $n \sim \sqrt{\gamma}$. Now note that

$$\begin{aligned} & \frac{e^{-a}}{4} \sum_{n=0}^{\infty} \frac{a^n}{n!} [\delta(\omega - \omega_0 - 2g\sqrt{n}) + \delta(\omega - \omega_0 + 2g\sqrt{n})] \\ & \sim \frac{|\omega - \omega_0| e^{-a}}{2} \sum_{n=0}^{\infty} \frac{a^n}{n!} \delta((\omega - \omega_0)^2 - 4g^2 n). \end{aligned} \quad (15.76)$$

To obtain the shape of the side peaks, one can rewrite Equation (6.33) in the form:

$$e^{-a} \sum_n \frac{a^n}{n!} \delta(z - nz_0) \sim \frac{e^{-\frac{(z - az_0)^2}{2g^2}}}{z_0 \sqrt{2\pi a}}, \quad a \gg 1, \quad (15.77)$$

with $z = (\omega - \omega_0)^2$ and $z_0 = 4g^2$. Finally, the spectrum may be approximated by

$$S(x) = \frac{|x|}{4g\sqrt{2\pi a}} \exp\left[-\frac{(x^2 - a)^2}{2a}\right] + \frac{\Delta}{2\pi} \frac{1}{\Delta^2 + (2x)^2}. \quad (15.78)$$

The spectral maximum at $\omega = \omega_0$ is due to the unresolved central transitions, while half of the intensity belongs to the two satellites at $\omega = \omega_0 \pm 2g\gamma$. This pattern agrees with experiments.

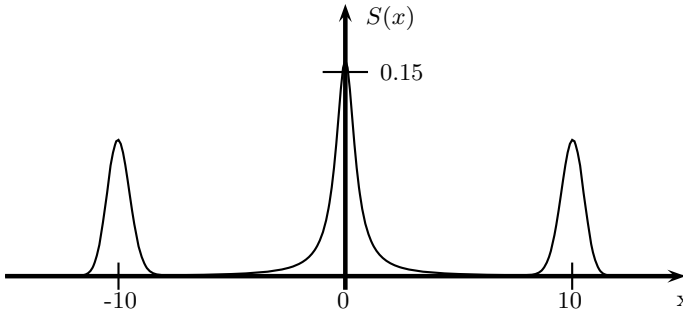


Fig. 15.6. *The characteristic shape of $S(x)$ versus x for $a = 100$ and $\Delta = g$.*

Problems

15.1. Prove Equation (13.136).

Part V

**Selected Exact Results in Many-Body
Problems**

16 Quantum Phases

16.0.3 Gauge Transformations

Without the gauge invariance, any theory is untenable. In classical theory, the Hamiltonian of a charged particle is

$$H = \frac{(\mathbf{p} - \frac{e\mathbf{A}}{c})^2}{2m} + eV(x) \quad (16.1)$$

where \mathbf{p} is the kinetic momentum and \mathbf{A} the vector potential. Both are unobservable; one could have started with new potentials \mathbf{A}' , V' such that

$$\mathbf{A}' = \mathbf{A} + \nabla\chi, \quad V' = V - \frac{1}{c} \frac{\partial\chi}{\partial t} \quad (16.2)$$

where $\chi(x, t)$ is a completely arbitrary function. Only fields appear in the classical equations of motion; quite the other way, the gauge transformed Schrödinger equation in terms of the old potentials reads

$$\left[\frac{1}{2m} (\mathbf{p} - \frac{e}{c} \{\mathbf{A} + \nabla\chi\})^2 + e \left\{ V - \frac{1}{c} \frac{\partial\chi}{\partial t} \right\} \right] \Psi' = i\hbar \frac{\partial\Psi'}{\partial t}. \quad (16.3)$$

Thus, the changes are:

$$\mathbf{p}\Psi \rightarrow (\mathbf{p} - \frac{e}{c} \nabla\chi)\Psi', \quad i\frac{\partial\Psi}{\partial t} \rightarrow (i\hbar \frac{\partial}{\partial t} + \frac{e}{c} \frac{\partial\chi}{\partial t})\Psi'. \quad (16.4)$$

One finds that the new wave function is related to the old by

$$\Psi'(\mathbf{x}, t) = \Psi(\mathbf{x}, t) \exp\left[\frac{ie\chi(\mathbf{x}, t)}{\hbar c}\right], \quad (16.5)$$

that is, substitution into (16.3) gives the correct equation for Ψ . The gauge changes the phase at any point and at any time in an arbitrary way. The matrix elements of the coordinates are trivially invariant, while those of the canonical momentum are shifted by $\mathbf{p}_{mn} \rightarrow (\mathbf{p} + \frac{e}{c} \nabla)_{mn}$; the Schrödinger theory is invariant because what matters is the mechanical momentum $\mathbf{p} - \frac{e}{c} \mathbf{A}$ which remains unshifted. Thus, the theory is gauge invariant. Equation (16.5) also holds in Klein-Gordon and Dirac theories.

16.0.4 Spinor Rotations

Consider the Pauli equation

$$(\boldsymbol{\sigma} \cdot \mathbf{B})\psi = \eta\psi \tag{16.6}$$

for a spin in a magnetic field in a Cartesian reference K . Rotating by an angle α *counterclockwise* about any axis one obtains a reference K' . Choosing the $z = z'$ axis parallel to the rotation axis, $x'_{ik} = a_{ik}x_k$ with

$$\{a_{ik}\} = \begin{pmatrix} \cos(\alpha) & \sin(\alpha) & 0 \\ -\sin(\alpha) & \cos(\alpha) & 0 \\ 0 & 0 & 1 \end{pmatrix} \tag{16.7}$$

and \mathbf{x}' appears like \mathbf{x} rotated clockwise. How does (16.6) transform to K' ? Since the Pauli equations must hold in the rotated system,

$$(\boldsymbol{\sigma} \cdot \mathbf{B}')\psi' = \eta\psi', \tag{16.8}$$

with the same Pauli matrices as before. Let $\psi' = R^\dagger\psi$ where R^\dagger rotates ψ *clockwise*; $\psi' \neq \psi$ and $(\boldsymbol{\sigma} \cdot \mathbf{B})$ is not a scalar. Writing (16.8) in K one obtains

$$(R\boldsymbol{\sigma}R^\dagger \cdot \mathbf{B}')\psi = \eta\psi;$$

this agrees with (16.6) if

$$R\sigma_iR^\dagger = a_{ik}\sigma_k \tag{16.9}$$

since then $(R\boldsymbol{\sigma}R^\dagger \cdot \mathbf{B}') = (\boldsymbol{\sigma} \cdot \mathbf{B})$. This is satisfied by $R = e^{\frac{-i\alpha\sigma_z}{2}}$. Thus, R can be considered as an operator phase, that imparts vector-like transformations on the Pauli matrices, although they are not the components of any vector. The same reasoning applies to Dirac's γ matrices under rotations and boosts: they are not four-vector components, yet Dirac's equation is covariant.

16.0.5 Galilean Transformations

In order to simplify the writing, let us consider a one-dimensional problem for a spinless particle in a potential U ,

$$-\frac{\hbar^2}{2m} \frac{\partial^2}{\partial x^2} \Psi(x, t) + U(x, t)\Psi(x, t) = i\hbar \frac{\partial}{\partial t} \Psi(x, t). \tag{16.10}$$

We go from the reference K of coordinates (x, t) to a reference K' of coordinates (x', t) moving with speed v , via the Galilei transformation $x' = x - vt, t' = t$. Galilean covariance requires that the problem in K' becomes

$$-\frac{\hbar^2}{2m} \frac{\partial^2}{\partial (x')^2} \Psi'(x', t) + U'(x', t)\Psi'(x', t) = i\hbar \frac{\partial}{\partial t} \Psi'(x', t). \tag{16.11}$$

We need to specify how U transforms and we assume that it is a scalar, that is,

$$U'(x', t) = U'(x - vt, t) = U(x, t). \quad (16.12)$$

We need to write (16.11) in K and in order to change variables we note that for any $f(x, t)$ it holds that

$$\frac{\partial}{\partial t'} f(x, t) = \frac{\partial}{\partial t'} f(x' + vt', t') = \frac{\partial}{\partial t} f(x, t) + v \frac{\partial}{\partial x} f(x, t).$$

Hence, the rule is:

$$\begin{cases} \frac{\partial}{\partial t'} = \frac{\partial}{\partial t} = v \frac{\partial}{\partial x} \\ \frac{\partial}{\partial x'} = \frac{\partial}{\partial x} \end{cases} \quad (16.13)$$

and (16.11) becomes

$$\left[-\frac{\hbar^2}{2m} \frac{\partial^2}{\partial x^2} + U(x, t) \right] \Psi'(x - vt, t) = \left[i\hbar \frac{\partial}{\partial t} + i\hbar v \frac{\partial}{\partial x} \right] \Psi'(x - vt, t). \quad (16.14)$$

We get back (16.10) by introducing a phase factor:

$$\Psi'(x', t) = \Psi(x, t) e^{-i\phi(x, t)}. \quad (16.15)$$

$\phi(x, t) = 0$ would mean that the wave function is a scalar, as in fact it is in the relativistic Klein Gordon-theory¹; in the present case, instead, the invariance is obtained by

$$\phi(x, t) = \frac{mvx}{\hbar} - \frac{mv^2 t}{2\hbar}. \quad (16.16)$$

The probability density is scalar although the wave function is not.

16.1 Topologic phases

Pancharatnam phase

The Indian physicist S. Pancharatnam in 1956 introduced[14] the concept of a geometrical phase. Let $H(\vec{\xi})$ be an Hamiltonian which depends from some parameters, represented by $\vec{\xi}$; let $|\psi(\vec{\xi})\rangle$ be the ground state. We can define the phase difference $\Delta\varphi_{12}$ between two ground states $|\psi(\vec{\xi}_1)\rangle$ and $|\psi(\vec{\xi}_2)\rangle$ (provided that they are not orthogonal):

¹Klein-Gordon particles may be pseudoscalar (change sign under parity) as pions do. In Dirac's theory a Lorentz transformation (boost) corresponds to a rotation by an imaginary angle in 4-dimensional space-time, and the 4-component spinor undergoes such a rotation. Thus, the transformation law depends on the kind of particle.

$$\langle \psi(\vec{\xi}_1) | \psi(\vec{\xi}_2) \rangle = |\langle \psi(\vec{\xi}_1) | \psi(\vec{\xi}_2) \rangle| e^{i\Delta\varphi_{12}}.$$

However, this is gauge dependent and cannot have any physical meaning. Now consider 3 points ξ and compute the total phase γ in a closed circuit $\xi_1 \rightarrow \xi_2 \rightarrow \xi_3 \rightarrow \xi_1$; remarkably,

$$\gamma = \Delta\varphi_{12} + \Delta\varphi_{23} + \Delta\varphi_{31} \quad (16.17)$$

is gauge independent! Indeed, the phase of any ψ can be changed at will by a gauge transformation, but such arbitrary changes cancel out in computing γ . This clearly holds for any closed circuit with any number of ξ . Therefore γ is entitled to have physical meaning. **This revealed that there may be observables that are not given by Hermitean operators.** For instance, consider a Linear Combination of Atomic Orbitals (LCAO) model for a molecule or cluster (or a Hubbard Model[17]). Thus, t_h is the matrix element of the one-body Hamiltonian between site orbitals. We want a rough estimate, because in order to understand the essentials we are ready to neglect details. Thus we neglect overlaps between different orbitals ; phase differences are implied from (16.2). Therefore, the inter-atomic hopping terms are modified by the vector potential according to the Peierls prescription

$$t_h \rightarrow t_h e^{\frac{2\pi i}{\phi_0} \int_a^b \vec{A} \cdot d\vec{r}}, \quad (16.18)$$

where

$$\phi_0 = \frac{hc}{e} = 4 \times 10^{-7} \text{Gauss cm}^2 \quad (16.19)$$

is the flux quantum or *fluxon*. In the case of H_2 this can be gauged away, but with three or more atoms the physical meaning is that a magnetic flux ϕ is concatenated with the molecule; changing ϕ by a fluxon has no physical meaning, however.

16.1.1 Parametric Hamiltonians and Berry Phase

Let $H[R]$ be an Hamiltonian which depends on a set R of 3 parameters, as for example the components of a vector ². A basis of stationary eigenstates is defined (up to the phases, which are arbitrary) by:

$$H[R]a_n[R] = E_n[R]a_n[R] \quad (16.20)$$

Now suppose the system is prepared in an energy eigenstate of the Hamiltonian at time $t = 0$ but $\vec{R} = \vec{R}(t)$ depends on the time. It is assumed that $H[R]$ has a discrete spectrum with no degeneracy and the evolution of the Hamiltonian $H[\vec{R}(t)]$ adiabatic, i.e. it is very slow; the involved frequencies are small compared to the resonance frequencies that a stationary copy of

²With more parameters the problem requires more complicated mathematics.

the system at any time would have³. To be specific, let the motion start at time 0 and end at time T ; therefore the duration T must be long enough to meet the adiabatic assumptions. We wish to solve

$$i\hbar \frac{\partial}{\partial t} \psi_n = H[R(t)]\psi_n \quad (16.21)$$

with the initial condition

$$\psi(t=0) \equiv \psi_n(t=0) = a_n[R(0)]. \quad (16.22)$$

We shall find that the integral of (16.21) bears a real Berry phase [65] $\gamma_n(t)$, which turns out to be due to the topology of H in parameter space. This phase can then be dropped or altered by a gauge transformation at any t , but a net phase acquired in a closed path cannot be gauged away. To calculate the phase, let's expand on the instantaneous basis:

$$\psi_n(t) = a_n[R(t)]c_n(t) + \sum_{m \neq n} c_m a_m[R(t)], \quad c_n(0) = 1. \quad (16.23)$$

By the *Kato adiabatic theorem*⁴ under our assumptions (nondegenerate discrete spectrum and slow enough evolution) only the first term remains: the system does not move from the n -th eigenstate. The adiabatic solution has $|c_n(t)| \equiv 1$, and the only effect of the evolution is on the phase, namely,

$$c_n(t) = e^{i(\theta_n(t) + \gamma_n(t))}; \quad (16.24)$$

here

$$\hbar\theta_n(t) = - \int_0^t dt' E_n[R(t')] \quad (16.25)$$

is the familiar dynamic phase, which exists in stationary problems as well. To compute $i\hbar \frac{\partial}{\partial t} \psi_n(t)$ using (16.23,16.24) we need to keep in mind that $\frac{\partial}{\partial t} a_n = \vec{R} \cdot \nabla_R a_n$ where $\vec{R} \cdot \nabla_R$ is a scalar product in parameter space; hence

$$\begin{aligned} \frac{\partial}{\partial t} \psi_n(t) &= \left(\frac{-i}{\hbar} E_n + i\dot{\gamma}_n + \vec{R} \cdot \nabla_R \right) a_n e^{\frac{-i}{\hbar} \int_0^t dt' [E_n[R(t')] + i\gamma_n(t)]} \\ &+ \sum_{m \neq n} \dot{c}_m a_m + \sum_{m \neq n} c_m \dot{a}_m. \end{aligned} \quad (16.26)$$

We drop the last term which is negligible, because the coefficients of the $m \neq n$ terms are small and the derivative is also small: these are second-order terms. Using (16.24), $0 = (i\hbar \frac{\partial}{\partial t} - H)\psi_n$ becomes

³The original paper by Berry is based on the adiabatic hypothesis which makes the analysis easier, however the existence of the Berry phase does not depend on this assumption.

⁴The proof is clearly discussed in Ref.[194].

$$0 = \left(-\hbar\dot{\gamma}_n + i\hbar\dot{\vec{R}} \cdot \nabla_R \right) a_n e^{\frac{-i}{\hbar} \int_0^t dt' [E_n[R(t')] + i\gamma_n(t)]} + \sum_{m \neq n} [\dot{c}_m - E_m] a_m$$

Now, a scalar product by a_n removes completely all states with $m \neq n$ and leaves us with an equation for the Berry phase:

$$\dot{\gamma}_n = i\dot{\vec{R}} \cdot \langle a_n[R(t)] | \nabla_R | a_n[R(t)] \rangle. \quad (16.27)$$

The matrix element looks similar to a momentum average, but the gradient is in parameter space. The overall phase change is a line integral

$$\Delta\gamma_n = i \int_0^T dt \langle a_n | \nabla_R | a_n \rangle \cdot \dot{\vec{R}} = i \int \langle a_n | \nabla_R | a_n \rangle dR.$$

The phase difference between two $a_n[R]$ at different R points is arbitrary; so the integrand is undefined and this result is quite un-physical, except that in a closed circuit C, the Berry phase, given by

$$\gamma_n(C) = i \int_C \langle a_n | \nabla_R | a_n \rangle \cdot d\vec{R} \quad (16.28)$$

is a property of H. In trivial topologies when C can be contracted to a point the phase vanishes. In multiply connected problems the phase does not vanish in general and is a geometric property which characterizes the Hamiltonian as a function of the parameter space. Discretizing a continuous path in parameter space, the Pancharatnam phase $\Delta\varphi$ picks contributions

$$e^{i\Delta\varphi} = \frac{\langle \psi(\xi) | \psi(\xi + \Delta\xi) \rangle}{|\langle \psi(\xi) | \psi(\xi + \Delta\xi) \rangle|} \quad (16.29)$$

at each step and we arrive at Berry's phase as a limit.

Open-path Berry Phase

Let a (discrete or continuous) path in parameter space go from ξ_1 to an equivalent point ξ_N connected to ξ_1 by a symmetry: $H(\xi_N) = U^\dagger H(\xi_1)U$, with unitary U ; adopting the natural choice $\psi(\xi_N) = U^\dagger \psi(\xi_1)$ one makes the phase difference along the path

$$\gamma = \sum_{i=1}^N \Delta\phi_{i,i+1}$$

gauge invariant. This is an open path Berry phase; $|\langle \psi(\xi_1) | U | \psi(\xi_1) \rangle| = 1$ because the spectrum is not degenerate. In the case of a symmetry connecting ξ_1 to itself, we speak of a single-point Berry phase; by (16.29),

$$e^{i\gamma} = \langle \psi | U | \psi \rangle \Leftrightarrow \gamma = \arg(\langle \psi | U | \psi \rangle). \quad (16.30)$$

Vector Potential Analogy

One naturally writes

$$\gamma_n(C) = \int_C \vec{A}_n \cdot d\vec{R} \tag{16.31}$$

introducing a sort of *vector potential* (which depends on n , however) $\vec{A}_n = i\langle a_n | \nabla_R | a_n \rangle$. The gauge invariance arises in the familiar way, that is, if we modify the basis with

$$a_n[R] \rightarrow e^{i\chi(R)} a_n[R],$$

then $\vec{A}_n \rightarrow \vec{A}_n - \nabla_R \chi$, and the extra term, being a gradient, does not contribute to $\gamma_n(C)$. The Berry phase is gauge independent and real since

$$\langle a_n | a_n \rangle = 1 \implies \nabla_R \langle a_n | a_n \rangle = 0$$

that is $\langle \nabla_R a_n | a_n \rangle + \langle a_n | \nabla_R a_n \rangle = 0$, or $\langle a_n | \nabla_R a_n \rangle + c.c. = 0$; this implies that $\langle a_n | \nabla_R a_n \rangle$ is imaginary. We can also grant the reality of

$$\vec{A}_n = i\langle a_n[R] | \nabla_R a_n[R] \rangle = \text{Im} \langle a_n[R] | \nabla_R a_n[R] \rangle.$$

We prefer to work with a manifestly real and gauge independent integrand; going on with the electromagnetic analogy, we introduce the *field* as well:

$$\gamma_n(C) = \int_S \text{rot} \vec{A}_n \cdot \vec{n} dS \equiv \int_S \vec{B}_n \cdot \vec{n} dS. \tag{16.32}$$

Let us derive an explicit formula for \mathbf{B} . We start by computing $[\nabla \wedge (a|\nabla a)]_i = \varepsilon_{ijk} \partial_j (a|\partial_k a)$. When performing the derivative, the term in $\partial_j \partial_k a$ is symmetric in j and k and therefore vanishes when antisymmetrized. Hence, $[\nabla \wedge (a|\nabla a)]_i = \varepsilon_{ijk} (\partial_j a|\partial_k a) = [(\nabla a| \wedge |\nabla a)]_i$. Next we insert a complete set $|a_m\rangle\langle a_m|$ and obtain

$$\vec{B}_n = -\text{Im} \langle \nabla_R a_n | \wedge | \nabla a_R a_n \rangle = -\text{Im} \sum_m \langle \nabla_R a_n | a_m \rangle \wedge \langle a_m | \nabla a_R a_n \rangle.$$

Note that

$$\langle a_n | \nabla_R a_n [R] \rangle$$

is imaginary, (the terms with $m \neq n$ have arbitrary phases). Thus under the Im operator we may remove the real $m=n$ term. If you think that saving one term is not an achievement, wait a moment. We get:

$$\vec{B}_n = -\text{Im} \sum_{m \neq n} \langle \nabla_R a_n | a_m \rangle \wedge \langle a_m | \nabla a_R a_n \rangle. \tag{16.33}$$

To simplify (16.33), we apply ∇_R to $H[R]a_n[R] = E_n[R]a_n[R]$:

$$(\nabla_R H[R])a_n[R] + H[R]\nabla_R a_n[R] = (\nabla_R E_n[R])a_n[R] + E_n[R]\nabla_R a_n[R];$$

next we multiply by $a_m[R]$, with $m \neq n$. We obtain:

$$\langle a_m | \nabla_R | a_n \rangle = \frac{\langle a_m | \nabla_R H | a_n \rangle}{E_m - E_n}. \quad (16.34)$$

There are severe divergence problems if there are degeneracies along C , and we wisely limited ourselves to discrete non-degenerate spectra.

Example

For example, consider a particle with any spin s in a magnetic field B (a physical one, this time) with $H = k\hbar \vec{B} \cdot \vec{s}$, with k a constant. The energy eigenvalues are

$$E_n(B) = n\hbar k B, \quad n \in (-s, s).$$

Initially the particle is in a stationary state. Let us shift the direction of \vec{B} adiabatically, sweeping a solid angle $\Omega(C)$. Berry has shown that the geometric phase is $\gamma_n(C) = -n\Omega(C)$.

16.1.2 Polarization of Solids

The modern theory of polarization in solids is based on these ideas; for a review, see [16]. Consider a periodic solid with Hamiltonian

$$H = \frac{1}{2m} \sum_{i=1}^N p_i^2 + V. \quad (16.35)$$

The usual definition of the dipole moment of a system in terms of the density $\rho(r)$, which applies to molecules, is:

$$\vec{d} = e \int d\vec{r} \vec{r} \rho(\vec{r}) = e \langle \Psi_0 | \vec{R} | \Psi_0 \rangle \quad (16.36)$$

where $|\Psi_0\rangle$ is the ground state and

$$e\vec{R} = e \sum_{i=1}^N \vec{r}_i, \quad (16.37)$$

summed over the N electrons, is the dipole operator. There are problems in applying this to solids because: 1) in solids we should like to use periodic boundary conditions, and the dipole operator is forbidden, since it takes outside the Hilbert space of periodic functions 2) we should like to deal with a bulk property, while (16.36) depends crucially on the surfaces 3) one never measures anything like (16.36). What one can do is rather to measure the current (which is proportional to $\frac{d}{dt}(e\vec{R})$) coming out from the crystal under some time-dependent probe, like a mechanical stress; we suppose that the experiment is done adiabatically.

Adiabatic Current

One can define the current density $\langle j \rangle = \text{Tr} \hat{\rho} j$,

$$j = \frac{\vec{P}}{mL^3}, \quad \vec{P} = \sum_{i=1}^N \vec{p}_i \quad (16.38)$$

in terms of the total momentum \vec{P} , the electron mass m and the super-cell size L ; the polarization change in the experiment is

$$\Delta P = \int dt \langle j(t) \rangle. \quad (16.39)$$

The density matrix $\rho(t)$ in the adiabatic limit was given by Niu and Thouless [80] in terms of the eigenstates $|n, t\rangle$; the instantaneous density matrix

$$\rho_i = |0, t\rangle \langle 0, t| \quad (16.40)$$

commutes with $H(t)$; we write

$$\rho(t) = \rho_i(t) + \Delta\rho(t). \quad (16.41)$$

By the adiabatic theorem, the correction is small, and to a good approximation,

$$\rho = |0, t\rangle \langle 0, t| + \sum_{n>0} (\Delta\rho_{0n} |0, t\rangle \langle n, t| + \Delta\rho_{n0} |n, t\rangle \langle 0, t|). \quad (16.42)$$

Since ρ does not depend on time explicitly,

$$i \frac{d}{dt} [\rho_i + \Delta\rho] = [H, \Delta\rho]; \quad (16.43)$$

in the adiabatic case $\frac{d}{dt} \Delta\rho$ is negligible (time derivatives are small, the correction is small). Hence, we are left with

$$i \frac{d}{dt} \rho_i = [H, \Delta\rho]. \quad (16.44)$$

For $n > 0$, since (16.40) implies $\langle 0, t | \rho_i | n, t \rangle \equiv 0$,

$$0 = \frac{d}{dt} \langle 0, t | \rho_i | n, t \rangle = \langle 0, t | \frac{d}{dt} \rho_i | n, t \rangle + \langle \frac{d}{dt} 0, t | \rho_i | n, t \rangle + \langle 0, t | \rho_i | \frac{d}{dt} n, t \rangle; \quad (16.45)$$

but $\langle \frac{d}{dt} 0, t | \rho_i | n, t \rangle = 0$ also vanishes (since $\langle \frac{d}{dt} 0, t | 0, t \rangle = 0$) and

$$\langle 0, t | \frac{d}{dt} \rho_i | n, t \rangle = -\langle 0, t | \rho_i | \frac{d}{dt} n, t \rangle = -\langle 0, t | \frac{d}{dt} n, t \rangle = \langle \frac{d}{dt} 0, t | n, t \rangle, \quad (16.46)$$

where the last equality follows from $\langle 0, t | n, t \rangle = 0$. Taking matrix elements of (16.44) we obtain the desired correction

$$\Delta\rho_{0n} = i \frac{\langle \dot{0}, t | n, t \rangle}{E_0 - E_n}. \quad (16.47)$$

Taking into account Equations (16.38) and (16.42) the average current is

$$\langle \mathbf{j} \rangle = -\frac{ie\hbar}{mL^3} \sum_{n>0} \frac{\langle \dot{\Psi}_0 | \Psi_n \rangle \langle \Psi_n | \mathbf{P} | \Psi_0 \rangle}{E_n - E_0} + c.c. \quad (16.48)$$

Idealized Experiment

Rather than a mechanical stress, we can more simply (from the theorist's point of view) use ingenuity to introduce a tiny electric field without disturbing the periodicity of the solid. Consider modifying the Hamiltonian (16.35) to read

$$H = \frac{1}{2m} \sum_{i=1}^N (\mathbf{p}_i - \hbar \mathbf{k})^2 + V. \quad (16.49)$$

This device [81] corresponds to a constant vector potential (that will vary slowly in time) and would represent a gauge change, were it not for the periodic boundary conditions; running through the supercell of length L an electron collects a magnetic flux. Indeed, this is called Hamiltonian with a flux. In order to make this compatible with the periodicity, we must choose \mathbf{k} appropriately; we introduce vectors $\vec{k}^{(\alpha)}$ with components

$$k_{\beta}^{(\alpha)} = \frac{2\pi}{L} \delta_{\alpha\beta}; \quad (16.50)$$

now if \vec{k} is a combination with integer coefficients of $\vec{k}^{(\alpha)}$, the Resta operator

$$U(\mathbf{k}) = e^{i \vec{k} \cdot \vec{R}}, \quad (16.51)$$

is allowed by the periodic boundary conditions. The vector potential requires a phase factor which is the many-body version of (16.5); in this case this is just $U(\vec{k})$: picking $\vec{k} = \vec{k}^{(\alpha)}$, which makes U allowed, we satisfy the modified Schrödinger equation and the periodic boundary conditions by writing the ground state of (16.49)

$$|\Phi_0(\vec{k}^{(\alpha)})\rangle = U(\vec{k}^{(\alpha)})|\Psi_0\rangle \quad (16.52)$$

Relation to Berry Phase

To see how this has to do with the Berry phase, the relevant quantity is

$$z^{(\alpha)} = \langle \Psi_0 | U(\vec{k}^{(\alpha)}) | \Psi_0 \rangle = |z^{(\alpha)}| e^{i\gamma} \quad (16.53)$$

where γ , that may depend on α , is a single-point Berry phase. Note that U is unitary and replacing the ground state by a sum over the complete set,

$$|z^{(\alpha)}|^2 \leq \sum_k \langle \Psi_0 | U(\vec{k}^{(\alpha)})^\dagger | \Psi_k \rangle \langle \Psi_k | U(\vec{k}^{(\alpha)}) | \Psi_0 \rangle;$$

however the r.h.s. is unity and we may conclude $|z^{(\alpha)}|^2 \leq 1$. We may note that $z^{(\alpha)}$ is a true and highly correlated many-body quantity, that unlike the dipole (16.36) cannot be expressed in terms of the density.

We need to deal with this problem by perturbation theory, since then the expressions of the current and of $\dot{\gamma}$ turn out to be closely related. Using (16.49) with the periodic boundary conditions we have \mathbf{k} -dependent eigenvalues and to first-order the modified ground state $U|\Psi_0\rangle$ reads

$$|\Phi_0(k)^{(1)}\rangle \sim |\Psi_0\rangle + \sum_{n>0} \frac{|\Psi_n\rangle \langle \Psi_n | \frac{\hbar k \cdot P}{m} | \Psi_0 \rangle}{E_n - E_0}. \quad (16.54)$$

Normally in writing this first-order expansion one does not care about the phase, but here we must keep track of (16.53); so we write using (16.50)

$$|\Phi_0(k)\rangle = e^{i\gamma} \left\{ |\Psi_0\rangle + \frac{2\pi\hbar}{mL} \sum_{n>0} \frac{|\Psi_n\rangle \langle \Psi_n | P_\alpha | \Psi_0 \rangle}{E_n - E_0} \right\}. \quad (16.55)$$

Multiplying by $\langle \Psi_0 |$ one finds

$$z^\alpha = e^{i\gamma}, \quad (16.56)$$

and multiplying by $\langle \dot{\Psi}_0 |$, since $\langle \dot{\Psi}_0 | \Psi_0 \rangle = 0$,

$$\langle \dot{\Psi}_0 | U(k^{(\alpha)}) | \Psi_0 \rangle = e^{i\gamma} \left\{ \frac{2\pi\hbar}{mL} \sum_{n>0} \frac{\langle \dot{\Psi}_0 | \Psi_n \rangle \langle \Psi_n | P_\alpha | \Psi_0 \rangle}{E_n - E_0} \right\}. \quad (16.57)$$

From (16.56) one finds $\gamma = \text{Im} \log(z^\alpha)$; hence

$$\dot{\gamma} = \text{Im} \left[\frac{\langle \dot{\Psi}_0 | U | \Psi_0 \rangle + \langle \Psi_0 | U | \dot{\Psi}_0 \rangle}{\langle \Psi_0 | U | \Psi_0 \rangle} \right]$$

and then (16.57,16.53) yield

$$\frac{d\gamma}{dt} = -i \frac{\langle \dot{\Psi}_0 | U(k^{(\alpha)}) | \Psi_0 \rangle}{\langle \Psi_0 | U(k^{(\alpha)}) | \Psi_0 \rangle} + c.c. \quad (16.58)$$

and eventually, comparing with (16.48),

$$\langle j \rangle = \frac{e}{2\pi L^2} \dot{\gamma}. \quad (16.59)$$

The connection with the Berry phase is established, and the polarization change ΔP is proportional to γ .

The actual calculation can be accomplished by expanding in determinants. Indeed, if $|\Psi_0\rangle = \text{Det}|\psi_1 \cdots \psi_N|$ is a determinant,

$$U(k^{(\alpha)}) |\Psi_0\rangle = \exp \left[i\mathbf{k}^\alpha \cdot \sum_i \mathbf{r}_i \right] \text{Det}|\psi_1 \cdots \psi_N|$$

also is, with spin-orbital i multiplied by $\exp [i\mathbf{k}^\alpha \cdot \mathbf{r}_i]$. The overlap (16.53) is computed as a determinant of one-body overlaps.

Problems

16.1. Given the two reference systems of Section 16.0.5, if in K

$$\psi(x, t) = e^{ikx - i\hbar \frac{k^2 t}{2m}}$$

what does the transformed state look like in K' ?

17 Pairing from repulsive interactions

Long ago, Kohn and Luttinger [174] proposed that a superconducting instability should occur in Jellium. They focussed on pairs of parallel spin electrons of large relative angular momentum L . The large L and the triplet state keep the electrons apart, so the Coulomb repulsion is particularly mild in such pairs. At long distances, the screened interaction undergoes Friedel oscillations due to the singularity of the dielectric function at $2k_F$ (See Section 12.1.1). This means a slight over-screening of the repulsion in some distance ranges: one gets an effective attraction from the repulsion via a quantum mechanical correlation effect. Attraction in some distance ranges does not necessarily imply binding, but Kohn and Luttinger suggested that this effect could indeed produce pairing. While no such superconducting instability appears to be relevant to ordinary metals, the paradoxical theoretical idea that attraction could result from repulsion is fascinating and the discovery of high- T_c superconductivity [175] has stimulated a **hot** discussion on the possibility that something similar is realized in the Cuprates (although the pairs are singlets with $L=2$, so some important modification is needed). The fact that T_C can be above liquid N_2 (rather than liquid He) temperatures, and the evidence that this occurs in strongly correlated materials suggests to part of the community that the mechanism must be different from the conventional phonon-assisted BCS one[181]. Other Authors prefer a conventional, or an enhanced[182] phonon-assisted mechanism. New superconductors including doped Fullerenes and Carbon nanotubes[197] complicate the riddle.

Anyhow, strong correlations *and* phonons are there, so they are likely to be involved, with a complex trade between the various degrees of freedom; some modeling is in order. Then, it looks natural to *start* by the repulsive *trivial* Hubbard model (1.64), or some of its variants, in 2 dimensions, while keeping in mind the claims that such a model cannot superconduct at all [168] [169] or at least cannot have superconducting long-range order [170]. An effective attractive force comes from second-order effects, e.g., the exchange of spin fluctuations, but it must overcome the strong direct Hubbard repulsion to give pairing. Bickers and co-workers[162] explored the consequences of a spin density wave instability within the RPA approximation using the *trivial* Hubbard Hamiltonian. They found a spin density wave phase and a superconducting phase with pair-wavefunctions of $d_{x^2-y^2}$ symmetry. These findings

were confirmed by using the FLEX approximation[163] which treats the fluctuations in the magnetic, density and pairing channels in a self-consistent and conserving way. Renormalization Group (RG) methods[164] are a well controlled alternative approach to deal with Fermi systems having competing singularities. The RG has been used by several authors[165],[166],[167] to study the coupling flows at different particle densities. In agreement with the previous findings, RG calculations show a *d*-wave superconducting instability away from half filling driven by the exchange of spin- or charge-density fluctuations.

States of different symmetry may be separated by tiny energies per electron, so it is very desirable to have exact data to rely on and *observe* pairing or get clear-cut results. The 1d Hubbard model is solved[73] by Bethe Ansatz techniques (Chapter 18) but does not show pairing. In 2d one can compute the exact ground state of small clusters by Lanczos techniques (Section 14.1). A pairing criterion that we shall discuss below was given by Richardson in the context of nuclear physics[176]. Defining

$$\tilde{\Delta}(N + 2) = E(N + 2) + E(N) - 2E(N + 1) \tag{17.1}$$

where $E(N)$ is the N -body ground state energy,

$$\tilde{\Delta}(N + 2) < 0 \tag{17.2}$$

signals a bound pair in the ground state with $N + 2$ particles and $|\tilde{\Delta}|$ is interpreted as the binding energy of the pair.

The writer and Balzarotti[171][172] discovered how one can systematically

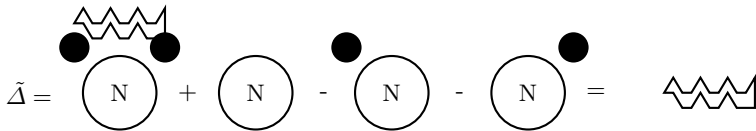


Fig. 17.1. Pictorial representation of Equation (17.1);the large circles stand for the interacting N-body system, the black circles represents the added particle, and the wiggly line is the interaction, which remains after the *simplification*.

build repulsive models that yield pairing and superconducting flux quantization, and that the two properties have a strong mathematical connection to each other. Both require special symmetric clusters (it was known that pairing occurs in the 4×4 system[177] but the simpler examples like CuO_4 and the general case had not been discovered yet) and derived an analytic theory of pairing interactions ($W=0$ pairing). We reported several detailed case studies where the formulas are validated by comparison with the numerical data. The results support general qualitative criteria for pairing induced by the on-site repulsion only. Our approach successfully predicts the formation of bound pairs, and explains why other ingredients like strong off-site interactions are needed to force pairing in other geometries. The analytic approach

is also needed to predict what happens for large systems and in the thermodynamic limit. Understanding the implications of the small cluster results is not trivial since the computed pair binding energies show a rapid decrease with increasing the cluster size; so several authors on the basis of the numerical data on 4×4 or even 6×6 clusters wrongly concluded that pairing in the Hubbard model as a size effect. However, much larger cells (at least 30×30) are needed to estimate the asymptotic behaviour and the analytic treatment suggests that pairing with a reduced but substantial binding energy persists in the full plane. Details may be found in a recent review paper [173].

17.0.3 $W = 0$ Pairing in Cu-O Clusters

In this Section, we illustrate the concept of $W = 0$ pairs and the way they become bound states, by using examples with a geometry relevant for the Cuprates. Nevertheless, the simple square Hubbard plane and its symmetric clusters like the 4×4 cluster with periodic boundary conditions also present $W=0$ pairing [189]. Moreover, Hubbard models with the geometry of Carbon

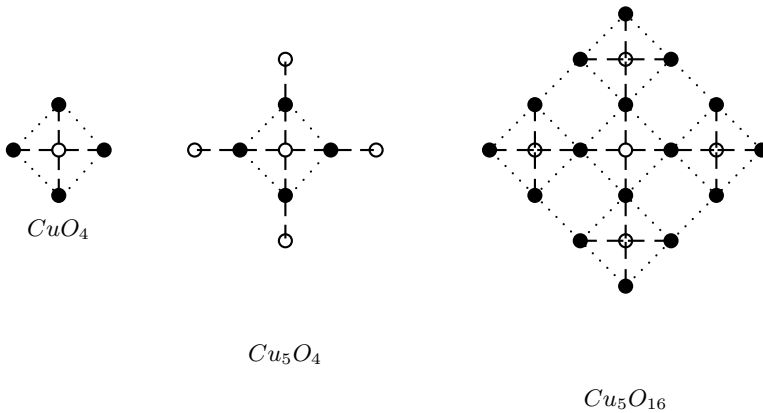


Fig. 17.2. Allowed clusters that were used to show pairing and superconducting flux quantization by exact diagonalization methods in Ref. [172]; the holes were 4, and the number of configurations involved in the case of Cu_5O_{16} is 44,100.

Nanotubes (CNT) [188] allow $W=0$ pairing away from half filling, opening the possibility that even there the mechanism of superconductivity is basically electronic [207]. Here we focus on the three-band Hubbard Hamiltonian

$$H = K + W + W_{\text{off-site}} \quad (17.3)$$

where introducing the site energies ε_p and ε_d referring to Oxygen and Copper, the kinetic term is

$$K = t \sum_{\langle ij \rangle, \sigma} (p_{j\sigma}^\dagger d_{i\sigma} + \text{h.c.}) + t_{pp} \sum_{\langle jj' \rangle, \sigma} p_{j\sigma}^\dagger p_{j'\sigma} + \varepsilon_d \sum_{i, \sigma} n_{i\sigma} + \varepsilon_p \sum_{j, \sigma} n_{j\sigma}; \quad (17.4)$$

here t 's are hopping parameters; p_j (d_i) destroy holes at the Oxygen (Copper) ions labeled j (i) and n are the number operators; $\langle ij \rangle$ refers to pairs of nearest neighbors. The interaction terms are

$$W = U_d \sum_i n_{i\uparrow} n_{i\downarrow} + U_p \sum_j n_{j\uparrow} n_{j\downarrow}, \quad W_{\text{off-site}} = U_{pd} \sum_{\langle ij \rangle, \sigma\sigma'} n_{i\sigma} n_{j\sigma'}. \quad (17.5)$$

the positive U parameters represent repulsion, U_d and U_p on-site and U_{pd} off-site on adjacent Cu and O sites. In line with literature estimates[183] we assume the following values (in eV): $\varepsilon_p - \varepsilon_d = 3.5$, $t = 1.3$, $t_{pp} = -0.65$, $U_d = 5.3$, $U_p = 6$ and, most probably, $U_{pd} < 1.2$. Note that we are using the same t for all Cu-O bonds, while some authors use more complicated conventions. For instance, F. C. Zhang and T. M. Rice[184] use an alternating sign prescription for t , which may be obtained by changing the sign of all the O orbitals in the horizontal lines containing Cu ions. The two pictures are related by a gauge transformation, under which the orbital symmetry labels A_1 and B_1 are interchanged. Some of the symmetry related information is gauge dependent and unobservable, while some is physical (e.g. degeneracies are).

As Balzarotti and the writer[171][172] pointed out, highly symmetric clusters possess 2-holes singlet eigenstates of H which do not feel the on-site repulsion W ; such eigenstates were called $W = 0$ pairs and play a crucial role for pairing. In order to have $W = 0$ solutions, the clusters must possess the full C_{4v} (square) symmetry, and must be centered around a Cu site¹. In particular, the geometries, examined by Hirsch *et al.*[179], and Balseiro *et al.*[178] are *forbidden* from our viewpoint. The Cu_4O_4 geometry considered by Ogata and Shiba[180] has the C_{4v} symmetry, but lacks the central Cu, and therefore it is *forbidden*, too [171].

The *aufbau* principle is strictly valid for non-interacting electrons, yet here it is useful in a wide range of parameters to predict the symmetry of the ground state in the allowed clusters. Concerning the many-body ground state, an interesting situation arises when the ground state can be thought of as consisting in $W=0$ pairs moving on a closed-shell background. $W=0$ pairs can arise when there are degenerate one-body levels, and a preliminary analysis can be done assuming that the symmetry Group is C_{4v} (below we shall discuss more general groups). In the Character Table of the C_{4v} Group (Appendix 20) we see that there are 4 one-dimensional irreducible representations (irreps) A_1 , A_2 , B_1 , B_2 and 1 two-dimensional irrep E . The smallest

¹For large enough clusters, the local physics is well described by an infinite plane, and the cluster shape is no longer important, but such large systems are outside the scope of diagonalization methods. Yet, our approach emphasizes the importance of the symmetry in the mechanism and predicts that any important distortion of the lattice readily destroys pairing.

square Cu-O cluster, CuO_4 , see Fig. 17.2, is also the simplest² where $W = 0$ pairing occurs, and we shall use it as a prototype. The one-body levels and their symmetry labels are reported in Table 17.1. Let us build a 4-hole state

ε_{A_1}	ε_{E_x}	ε_{E_y}	ε_{B_1}	$\varepsilon_{A'_1}$
$\tau - \sqrt{4 + \tau^2}$	0	0	-2τ	$\tau + \sqrt{4 + \tau^2}$

Table 17.1. One-body levels of the CuO_4 cluster in units of t as a function of the dimensionless parameter $\tau \equiv t_{pp}/t$.

in CuO_4 (see Fig. 17.3 b)). The first two holes go into a bonding level of A_1 symmetry; this is a totally symmetric (1A_1) pair. For negative τ , the other two holes go into a non-bonding level of $E(x, y)$ symmetry, which contains 4 spin-orbital states. Labelling sites as in Figure 17.3 a), the creation operators for the degenerate orbitals are $E_{y\sigma}^\dagger = \frac{1}{\sqrt{2}}(p_{2\sigma}^\dagger - p_{4\sigma}^\dagger)$ $E_{x\sigma}^\dagger = \frac{1}{\sqrt{2}}(p_{1\sigma}^\dagger - p_{3\sigma}^\dagger)$

Using the E orbitals according to the Pauli principle one obtains $\binom{4}{2} = 6$ different pair-states. The irrep multiplication table allows for labeling them according with their space symmetry: $E \otimes E = A_1 \oplus A_2 \oplus B_1 \oplus B_2$. Projecting according to usual rules we see that A_2 is a spin-triplet, 3A_2 , while the remaining irreps are spin-singlets, 1A_1 , 1B_1 and 1B_2 . One can readily verify that the B_2 singlet operator

$$b_{B_2}^\dagger = \frac{1}{\sqrt{2}} \left(E_{x,\uparrow}^\dagger E_{y,\downarrow}^\dagger + E_{y,\uparrow}^\dagger E_{x,\downarrow}^\dagger \right) \quad (17.6)$$

is a $W = 0$ pair (no double occupation)³. To first order in perturbation theory, the 4-body singlet state of B_2 symmetry is degenerate with the A_2 triplet; Hund's rule would have predicted a 3A_2 ground state. However, the true ground state turns out to be singlet. The numerical results on the CuO_4 cluster show that $\tilde{\Delta}(4)$ is negative for $0 > \tau > -0.5$ and that its minimum value occurs at $\tau = 0$, when the non-bonding orbitals B_1 and E become degenerate: the paired interacting ground state is also degenerate in this particular case. This accidental degeneracy is due to the fact that any permutation of the oxygens is a symmetry and the symmetry Group becomes $S_4 \supset C_{4v}$; the existence of two different $W=0$ pairs has a deep influence on the magnetic properties (Section 17.1 below). In Fig.17.3 c) we plot $\tilde{\Delta}(4)$ for $\tau = 0$, $\varepsilon_p - \varepsilon_d = 0$, $U_{pd} = 0$ and $U_p = U_d = U$.

$\tilde{\Delta}(4)$ has a minimum at $U \approx 5t$ and it is negative when $0 < U < 34.77t$.

²One can obtain $\tilde{\Delta} < 0$ at half filling with 4 fermions in a 4-site cluster, omitting the Cu site; we regard this as a limiting case with a strongly repulsive central site.

³Note that 1B_2 is the symmetry label of the pair wave function in the gauge we are using, and must not be confused with the symmetry of the order parameter.

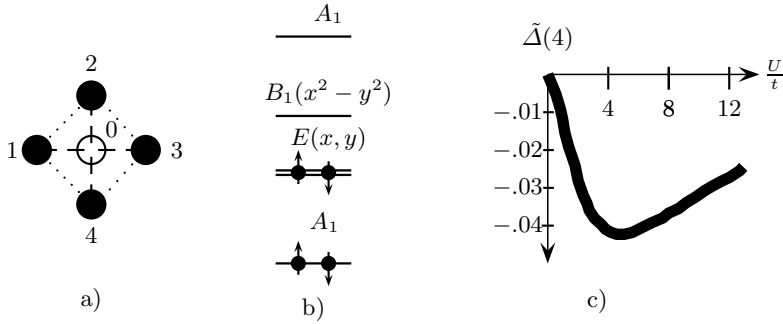


Fig. 17.3. a) The CuO_4 unit. b) One-particle energy levels for $\tau < 0$ with their symmetry labels and their fillings in the 4-particle ground state according to the *aufbau* principle. Two fermions belong to the doubly degenerate $E(x, y)$ representation. For $\tau \rightarrow 0$, the Group becomes $S_4 \supset C_{4v}$ and the $B_1(x^2 - y^2)$ level merges with $E(x, y)$ giving raise to triple degeneracy. Note that among the irreps of C_{4v} (see the Character Table in Appendix II) A_2 and B_2 are not represented in this scheme. Below we shall see that this observation is crucial for $W=0$ pairing theory. c) $\tilde{\Delta}(4)$ versus $\frac{U}{t}$ for this cluster is negative in a wide range (it becomes positive for $\frac{U}{t} > 34.77$) and the maximum pairing occurs at $U \sim 5t$; this is not a weak coupling phenomenon.

I emphasize that $\tilde{\Delta}(4)$ becomes positive for large values of U/t and hence pairing disappears in the strong coupling regime. In the present problem U must exceed several tens of times t before the asymptotic *strong coupling regime* sets in. A perturbation theory will strictly apply at *weak coupling* where the second derivative of the curve is negative. However, qualitatively a weak coupling approach is rewarding in all the physically interesting range of parameters. The sign of $\tilde{\Delta}$ depends on U and τ and its magnitude is unlike any of the input parameters. Since the opening Chapters of this book, dealing with Kondo physics, two-hole resonances, and plasmon effects, we have appreciated that the occurrence of bound states giving raise to new energy scales is the most intriguing signature of strong correlation; actually, it could be its definition.

On the other hand, at positive τ 's the B_1 non-bonding level is pushed below the degenerate one and $\tilde{\Delta}(4)$ becomes large and positive (at $\tau = +0.65$, $\tilde{\Delta}(4) = 0.53$ eV). The dependence of $\tilde{\Delta}(4)$ on the input parameters has been studied in detail; also, we have found that any lowering of the symmetry is reflected by a corresponding increase of $\tilde{\Delta}(4)$ [171]. We have performed numerical explorations in other fully symmetric clusters like Cu_5O_4 and Cu_5O_{16} and we have found negative values of $\tilde{\Delta}(4)$, of the order of few meV, using physical parameter values.

17.0.4 Pairing Mechanism

In all the allowed clusters up to 21 atoms, the lowest one-hole level belongs to A_1 symmetry, and the next E level yields the $W = 0$ pair. The interactions produce a non-degenerate 1B_2 4-hole ground state *having the same symmetry as the $W = 0$ pair*. The interested reader may see Refs.[186],[187] for the details.

In symmetric clusters as well as in the full plane, $\tilde{\Delta}(4) < 0$ arises[172] from an effective attractive interaction between the holes of the $W = 0$ pair; the same interaction is repulsive for triplet pairs. In the lowest approximation, the attraction stems from the second-order exchange diagram. The effective

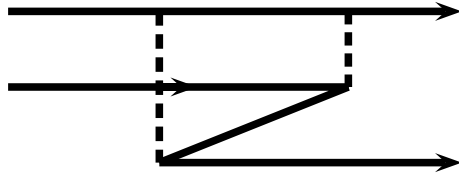


Fig. 17.4. The second-order exchange interaction that at weak coupling can be the leading contribution to the effective attraction, depending on the lattice and on the parameters (see Ref. [172]).

interaction can be found by a canonical transformation (basically a Schrieffer-Wolff-type argument) which is long and not easily summarized, so I defer the reader to the original paper [196]. The results reduce to those of perturbation theory in the weak coupling case. Moreover, the analytical results compared semi-quantitatively with those from exact diagonalization of several clusters at various fillings including the 4×4 Hubbard cluster[190]. Being predictive in strongly correlated problems is the exception, rather than the rule, but in this case simplicity has emerged from symmetry. Applying the formulas to supercells of increasing size, it was possible to extrapolate the results to the thermodynamic limit, showing that $\tilde{\Delta} < 0$ is not a size effect and could well contribute a pair binding energy in the 10 meV range. The inclusion of phonon effects in the $W=0$ scheme was envisaged in Ref. [70].

17.0.5 The $W = 0$ theorem

A general theorem puts useful restrictions on the many-body ground state symmetry. Consider a Hubbard model⁴ $H = H_0 + W$ on a lattice Λ , where

$$H_0 = \sum_{\langle ij \rangle, \sigma} t_{ij} c_{j\sigma}^\dagger c_{i\sigma} \quad (17.7)$$

⁴that is, a model with on-site, possibly site-dependent, interactions U_i .

is the free part and

$$W = \sum_{i \in \Lambda} U_i n_{i\uparrow} n_{i\downarrow}, \tag{17.8}$$

with an irrep of \mathcal{G}_0 . Let \mathcal{G}_0 be the *optimal symmetry Group* of H_0 , that is, a Group containing enough symmetry operations that no degeneracy between one-body eigenstates is accidental. In other terms, \mathcal{G}_0 must contain enough operations to justify all such degeneracies by mixing all the degenerate subspaces.

We can construct[185] all the $W = 0$ pair eigenstates by using projection operators of \mathcal{G}_0 . We start by using the irreps of \mathcal{G}_0 to label all the one-body eigenstate of H_0 . In this way, we are splitting the irreps of \mathcal{G}_0 according to the following definition.

Definition. An irrep η is represented in the one-body spectrum of H if at least one of the one-body levels belongs to η .

Let \mathcal{E} be the set of the irreps of \mathcal{G}_0 which are represented in the one-body spectrum of H . Let $|\psi\rangle$ be a two-body eigenstate of the non-interacting Hamiltonian with spin $S^z = 0$ and $P^{(\eta)}$ the projection operator on the irrep η . We wish to prove the $W = 0$ Theorem:

$$\eta \notin \mathcal{E} \Leftrightarrow WP^{(\eta)}|\psi\rangle = 0. \tag{17.9}$$

Let us first translate this into words:

- Any nonvanishing projection of $|\psi\rangle$ on an irrep not contained in \mathcal{E} , is an eigenstate of H with no double occupancy. The singlet component of this state is a $W = 0$ pair. Conversely, any pair belonging to an irrep represented in the spectrum must have non-vanishing W expectation value:

Proof: Let us consider a two-body state of opposite spins belonging to the irrep η of \mathcal{G}_0 :

$$|\psi^{(\eta)}\rangle = \sum_{ij \in \Lambda} \psi^{(\eta)}(i, j) c_{i\uparrow}^\dagger c_{j\downarrow}^\dagger |0\rangle.$$

Then we have

$$n_{i\uparrow} n_{i\downarrow} |\psi^{(\eta)}\rangle = \psi^{(\eta)}(i, i) c_{i\uparrow}^\dagger c_{i\downarrow}^\dagger |0\rangle \equiv \psi^{(\eta)}(i, i) |i\uparrow, i\downarrow\rangle.$$

Consider the projection operator $P^{(\eta)}$ on the irrep η : since

$$P^{(\eta)} \sum_{i \in \Lambda} \psi^{(\eta)}(i, i) |i\uparrow, i\downarrow\rangle = \sum_{i \in \Lambda} \psi^{(\eta)}(i, i) |i\uparrow, i\downarrow\rangle,$$

if $P^{(\eta)}|i \uparrow, i \downarrow\rangle = 0 \forall i \in \Lambda$, then $\psi^{(\eta)}(i, i) = 0 \forall i \in \Lambda$. It is worth to note that this condition is satisfied if and only if $P^{(\eta)}|i\sigma\rangle = 0 \forall i \in \Lambda$, where $|i\sigma\rangle = c_{i\sigma}^\dagger|0\rangle$. Now it is always possible to write $|i\sigma\rangle$ in the form $|i\sigma\rangle = \sum_{\eta \in \mathcal{E}} c^{(\eta)}(i)|\eta_\sigma\rangle$ where $|\eta_\sigma\rangle$ is the one-body eigenstate of H with spin σ belonging to the irrep η . Hence, if $\eta' \notin \mathcal{E}$, $P^{(\eta')}|i\sigma\rangle = 0$ and so $P^{(\eta')}|i \uparrow, i \downarrow\rangle = 0$. Therefore, if $|\psi^{(\eta)}\rangle$ is a two-hole singlet eigenstate of the kinetic term and $\eta \notin \mathcal{E}$, then it is also an eigenstate of W with vanishing eigenvalue, that means a $W = 0$ pair.

Q.E.D.

Remark: Suppose we perform a gauge change in H such that \mathcal{G}_0 is preserved; clearly, a $W = 0$ pair goes to another $W = 0$ pair. Thus, the theorem implies a distinction between symmetry types which is gauge-independent.

Remark: The complete characterization of the symmetry of $W = 0$ pairs requires the knowledge of \mathcal{G}_0 . A partial use of the theorem is possible if one does not know \mathcal{G}_0 but knows a Subgroup $\mathcal{G}_0^<$. It is then still granted that any pair belonging to an irrep of $\mathcal{G}_0^<$ not represented in the spectrum has the $W = 0$ property. On the other hand, accidental degeneracies occur with a Subgroup of \mathcal{G}_0 , and by mixing degenerate pairs belonging to irreps represented in the spectrum one can find $W = 0$ pairs also there.

17.0.6 Examples

CuO_4

The CuO_4 cluster is a simple example of the $W=0$ theorem. If $\tau \neq 0, \mathcal{G}_0 = C_{4v}$; of the $W = 0$ pair belongs to the irrep B_2 which is not represented in the spectrum (see Table 17.1). A_2 is also not represented, but projecting any two-body state one finds nothing. If $\tau = 0$, a three-times degenerate one-body level exists due to an *accidental* degeneracy between $E(x, y)$ and B_1 orbitals; with 4 interacting fermions, pairing occurs in two ways, as A_1 and B_2 are both degenerate ground states. The extra degeneracy cannot be explained in terms of C_{4v} , whose irreps have dimension 2 at most. For $\tau = 0$ any permutation of the four Oxygen sites is actually a symmetry and therefore \mathcal{G}_0 is enlarged to S_4 (the group of permutations of four objects). S_4 has the irreducible representations \mathcal{A}_1 (total-symmetric), \mathcal{B}_2 (total-antisymmetric), \mathcal{E} (self-dual), \mathcal{T}_1 and its dual \mathcal{T}_2 , of dimensions 1, 1, 2, 3 and 3, respectively. These irreps break in C_{4v} as follows

$$\mathcal{A}_1 = A_1, \quad \mathcal{T}_1 = B_1 \oplus E, \quad \mathcal{T}_2 = A_2 \oplus E, \quad \mathcal{B}_2 = B_2, \quad \mathcal{E} = A_1 \oplus B_2.$$

Labelling the one-body levels with the irreps of S_4 , one finds that \mathcal{E} is not contained in the spectrum and thus yields $W = 0$ pairs:

$${}^1\mathcal{E} = {}^1A_1 \oplus {}^1B_2. \quad (17.10)$$

The corresponding pair-creation operators reads:

$$b_{A_1}^\dagger = \frac{2}{\sqrt{3}}B_{1\uparrow}^\dagger B_{1\downarrow}^\dagger + \frac{1}{\sqrt{3}}\left(E_{x\uparrow}^\dagger E_{x\downarrow}^\dagger + E_{y\uparrow}^\dagger E_{y\downarrow}^\dagger\right) \tag{17.11}$$

for the total-symmetric pair and Eq. (17.6) for the B_2 component.

The 4×4 Hubbard cluster with periodic boundary conditions

Energy	Irrep of \mathcal{G}	Degeneracy
4	B_2	1
2	Λ_4	4
0	Ω_4	6
-2	A_1	4
-4	A_1	1

Table 17.2. *One-body spectrum for $t = -1$. The irrep symbols will be explained shortly.*

The one-body spectrum of the model (see Table (17.0.6)) involves a 6 times degenerate shell, whereas the Space Group \mathbf{G} does not have irreps with dimensions bigger than 4 (see Ref.[156]). The optimal Group \mathcal{G}_0 is larger than the Space Group and includes symmetries which are not isometries[190].

Consider the transformation d of the 4×4 lattice shown in Equation (17.12):

$$d : \begin{array}{|c|c|c|c|} \hline 1 & 2 & 3 & 4 \\ \hline 5 & 6 & 7 & 8 \\ \hline 9 & 10 & 11 & 12 \\ \hline 13 & 14 & 15 & 16 \\ \hline \end{array} \longrightarrow \begin{array}{|c|c|c|c|} \hline 5 & 1 & 4 & 8 \\ \hline 6 & 2 & 3 & 7 \\ \hline 10 & 14 & 15 & 11 \\ \hline 9 & 13 & 16 & 12 \\ \hline \end{array} \tag{17.12}$$

Because of the periodic boundary conditions, the nearest neighbours of 1 are 2, 5, 4 and 13. The dynamical symmetry operation d can be obtained by rotating the plaquettes 1,2,5,6 and 11,12,15,16 clockwise and the other two counterclockwise by 90 degrees. This preserves nearest neighbours (and so, each order of neighbours) but is no isometry (for example, the distance between 1 and 3 changes). Thus, this symmetry operation d is a new, dynamical symmetry. Including d and closing the multiplication table one obtains the required Optimal Group \mathcal{G} with 384 elements in 20 classes (like \mathbf{G}) as shown in Table .

\mathcal{C}_1	\mathcal{C}_2	\mathcal{C}_3	\mathcal{C}_4	\mathcal{C}_5	\mathcal{C}_6	\mathcal{C}_7	\mathcal{C}_8	\mathcal{C}_9	\mathcal{C}_{10}
I	t_{22}	$C_4\sigma'[2]$	σ_x	C_2	σ'	C_2d	$C_2t_{22}d$	$C_2\sigma'[1]$	$C_4^3t_{02}d$
\mathcal{C}_{11}	\mathcal{C}_{12}	\mathcal{C}_{13}	\mathcal{C}_{14}	\mathcal{C}_{15}	\mathcal{C}_{16}	\mathcal{C}_{17}	\mathcal{C}_{18}	\mathcal{C}_{19}	\mathcal{C}_{20}
$C_4^3t_{20}d$	C_2t_{01}	$C_2\sigma_x[1]$	C_4	$C_2t_{01}d$	$C_2t_{12}d$	$C_2\sigma_x[1]d$	$C_4[1]d$	$C_2[1]d$	$C_4[1]$

Table . Here, we report one operation for each of the 20 classes \mathcal{C}_i ; the others can be obtained by conjugation. The operations are: the identity I , the translation t_{mn} of m steps along x and n along y axis; the other operations $C_2, C_4, \sigma, \sigma'$ are those of the Group of the square and are referenced to the centre; however, $C_2[i], C_4[i], \sigma[i]$, and $\sigma'[i]$ are centered on site i .

The complete Character Table of \mathcal{G} is shown below.

\mathcal{G}	\mathcal{C}_1	\mathcal{C}_2	\mathcal{C}_3	\mathcal{C}_4	\mathcal{C}_5	\mathcal{C}_6	\mathcal{C}_7	\mathcal{C}_8	\mathcal{C}_9	\mathcal{C}_{10}	\mathcal{C}_{11}	\mathcal{C}_{12}	\mathcal{C}_{13}	\mathcal{C}_{14}	\mathcal{C}_{15}	\mathcal{C}_{16}	\mathcal{C}_{17}	\mathcal{C}_{18}	\mathcal{C}_{19}	\mathcal{C}_{20}
A_1	1	1	1	1	1	1	1	1	1	1	1	1	1	1	1	1	1	1	1	1
\tilde{A}_1	1	1	1	1	1	1	-1	-1	1	-1	-1	-1	-1	1	1	1	1	1	-1	-1
B_2	1	1	-1	-1	1	1	1	1	1	-1	-1	1	-1	-1	1	1	-1	-1	1	-1
\tilde{B}_2	1	1	-1	-1	1	1	-1	-1	1	1	1	-1	1	-1	1	1	-1	-1	-1	1
Γ_1	2	2	-2	-2	2	2	0	0	2	0	0	0	0	-2	-1	-1	1	1	0	0
Γ_2	2	2	2	2	2	2	0	0	2	0	0	0	0	2	-1	-1	-1	-1	0	0
Σ_1	3	3	3	3	3	-1	-1	-1	-1	-1	-1	-1	-1	-1	0	0	0	0	1	1
Σ_2	3	3	3	3	3	-1	1	1	-1	1	1	1	1	-1	0	0	0	0	-1	-1
Σ_3	3	3	-3	-3	3	-1	-1	-1	-1	1	1	-1	1	1	0	0	0	0	1	-1
Σ_4	3	3	-3	-3	3	-1	1	1	-1	-1	1	-1	1	1	0	0	0	0	-1	1
Λ_1	4	-4	-2	2	0	0	-2	2	0	-2	2	0	0	0	-1	1	-1	1	0	0
Λ_2	4	-4	-2	2	0	0	2	-2	0	2	-2	0	0	0	-1	1	-1	1	0	0
Λ_3	4	-4	2	-2	0	0	-2	2	0	2	-2	0	0	0	-1	1	1	-1	0	0
Λ_4	4	-4	2	-2	0	0	2	-2	0	-2	2	0	0	0	-1	1	1	-1	0	0
Ω_1	6	6	0	0	-2	-2	-2	-2	2	0	0	2	0	0	0	0	0	0	0	0
Ω_2	6	6	0	0	-2	-2	2	2	2	0	0	-2	0	0	0	0	0	0	0	0
Ω_3	6	6	0	0	-2	2	0	0	-2	-2	-2	0	2	0	0	0	0	0	0	0
Ω_4	6	6	0	0	-2	2	0	0	-2	2	2	0	-2	0	0	0	0	0	0	0
Π_1	8	-8	-4	4	0	0	0	0	0	0	0	0	0	0	1	-1	1	-1	0	0
Π_2	8	-8	4	-4	0	0	0	0	0	0	0	0	0	0	1	-1	-1	1	0	0

Character Table of the Optimal Group \mathcal{G} of the 4×4 model.

As the notation suggests, the irreps A_1 and \tilde{A}_1 both reduce to A_1 , in C_{4v} , while B_2 and \tilde{B}_2 both reduce to B_2 . One can easily determine how the irreps of \mathcal{G} split in C_{4v} (see problem17.1). We rightly called \mathcal{G} the Optimal Group

because no accidental degeneracy of orbitals occurs using \mathcal{G} . All the $W = 0$ pairs can be found by projecting on the appropriate irreps, determined using the $W = 0$ *Theorem*(see Problem 17.2).

17.1 Superconducting flux quantization and Josephson effect

Magnetic flux can be trapped in the hole of a hollow superconducting cylinder with thick walls compared to the penetration depth and persist in the absence of an applied field. As explained by Schrieffer[181] the flux quantum is $\frac{hc}{e} = 4 \times 10^{-7} \text{gausscm}^2$, (see 16.19) but the flux quantum in superconductors is actually $\frac{hc}{2e}$. The Superconducting Flux Quantization (SFQ) is a signature of superconductivity, since it clearly implies that the external magnetic field excites diamagnetic currents in a system where the carriers have charge $2e$. The perturbation due to the field must be gentle enough, otherwise the superconductor becomes normal; the field is screened by supercurrents at the surface of the superconductor and its perturbation on the system cannot be too strong otherwise the supercurrent exceeds the critical current.

The above models with on-site repulsive interactions and $W=0$ pairing give this signature. The vector potential \mathbf{A} enters through the Peierls prescription (16.18)

$$t_{ab} \rightarrow t_{ab} e^{\frac{2\pi i}{\phi_0} \int_a^b \mathbf{A} \cdot d\mathbf{r}}$$

In small clusters, $W=0$ pairing requires full C_{4v} symmetry; moreover, the flux tubes must be inserted in such a way that the symmetry is not distorted. We must arrange the thought experiment in such a way that the perturbation due to the field is gentle, and does not destroy the pairing. In small clusters, that we may study more easily, the current carrying bonds must be so weak that the current screening the field is not excessive and the change in the ground state energy due to the field is of the order $\bar{\Delta}$ or less. When this is done, the SFQ already obtains with a few pairs and even one pair yields a well defined double-minimum pattern. This means that although in textbooks SFQ is explained in terms of the order parameter, it is basically a single-pair symmetry property. Going to the thermodynamic limit is necessary to achieve macroscopically large barriers that localize the system in one of the minima.

The simplest case is CuO_4 and the insertion of flux tubes is shown in Figure 17.4 a). In order to preserve the symmetry, a flux ϕ is inserted in each of the four Cu-O-O triangles or *plaquettes* of the cluster. The dotted bonds must represent negative hopping integrals t_{pp} of the order of 50 meV or less, otherwise the pairing mechanism breaks down and paramagnetism prevails. Figure 17.4 b) shows the ground state energy of the cluster versus ϕ . The flux dependence was computed with $\epsilon_p - \epsilon_d = 3.5$, $t = 1.3$, $U_d = 5.3$, $U_p = 6$. This pattern is characteristic of SFQ. The system is diamagnetic at small ϕ

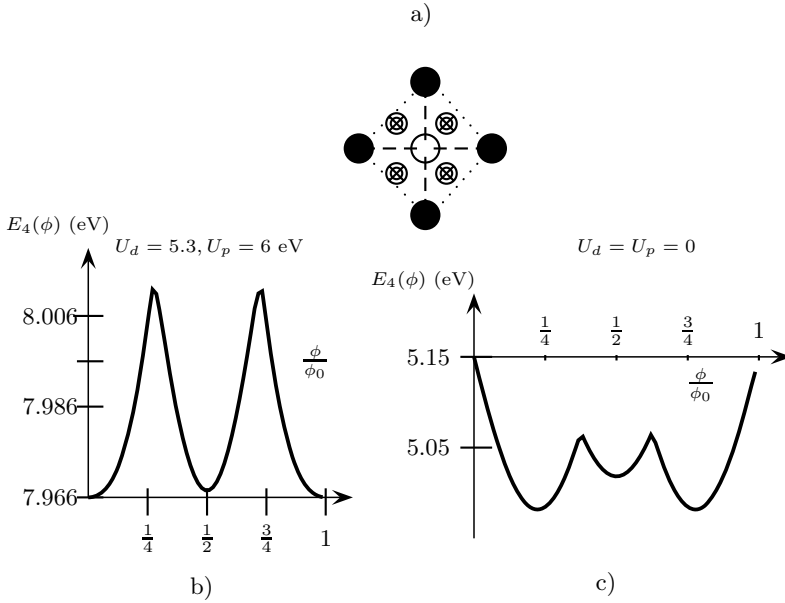


Fig. 17.5. Correlation-induced flux quantization in the CuO_4 cluster. a) The CuO_4 unit with 4 inserted flux tubes ϕ . A flux ϕ is inserted in each of the four Cu-O-O triangles or *plaquettes* of the cluster. b) Flux dependence of the ground state energy of the cluster with the standard parameter values $\epsilon_p - \epsilon_d = 3.5, t = 1.3, U_d = 5.3, U_p = 6$ but $t_{pp} = -0.05$ eV. Note that the system is diamagnetic at small flux and exhibits the characteristic minimum at half fluxon. c) Ground state energy of the cluster with $U_d = U_p = 0$. without correlation the cluster shows a normal, paramagnetic behaviour. Similar phenomena have been observed in exact diagonalization work with larger clusters (up to 21 atoms) in Ref. [172] and with rings of clusters.

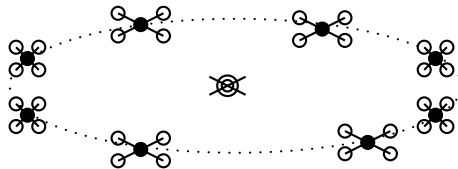


Fig. 17.6. Rings of clusters threaded by flux tubes allow to study the propagation of bound $W=0$ pairs. The dotted line represents hopping between two consecutive clusters that must be designed in such a way that the square symmetry of each cluster is preserved.

(its energy increases with flux) but reaches a maximum due to a level crossing and goes through a second minimum at $\phi = \frac{\phi_0}{2}$; $\phi = \phi_0$ is equivalent to $\phi = 0$. The two ground states at $\phi = 0$ and $\phi = \frac{\phi_0}{2}$ are of comparable depth and are due to $W=0$ pairs of different symmetry.

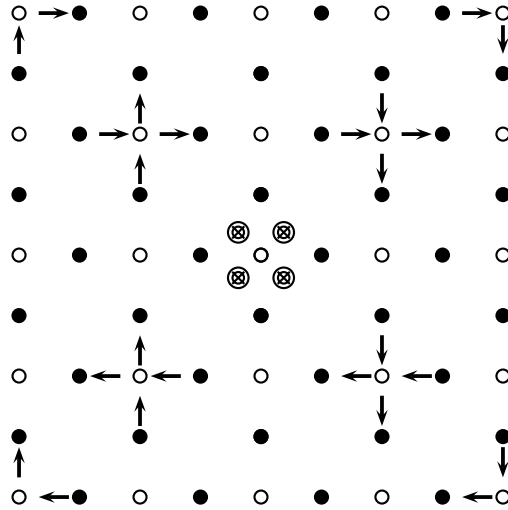


Fig. 17.7. Inserting 4 flux tubes, each carrying a flux ϕ in a CuO_4 unit in the plane, the magnetic flux through any path in the plane must equal ϕ times the number of tubes encircled by the path. This is achieved by choosing the vector potential according to the above pattern, with $\int \mathbf{A} \cdot d\mathbf{r} = 0$ along each bond without arrow, $\int_{\rightarrow} \mathbf{A} \cdot d\mathbf{r} = \frac{\phi}{2}$ along each oriented bond with the integration path parallel to the arrow. For a generic flux ϕ in each tube any reflection σ of C_{4v} reverses the arrows ($\phi \rightarrow -\phi$) and thus C_{4v} is broken and only the commutative Z_4 Group of the rotations survives. $W=0$ pairs are forbidden in the field and pairing is destroyed. However, at $\phi = \frac{\phi_0}{2}$, one finds $\int_{\rightarrow} \mathbf{A} \cdot d\mathbf{r} = \frac{\phi_0}{4}$ and the Peierls prescription is $t \rightarrow it$ on any bond with arrow; now any reflection σ implies $\phi \rightarrow -\phi$ which is just a gauge change, replacing it by $-it$. This is equivalent to a unitary transformation S that changes the signs to all the Cu orbitals along the diagonals except the central one. Since S reverses the arrows, $\sigma \times S$ is a symmetry.

Indeed, as we saw earlier, two $W=0$ irreps exist for $t_{pp} = 0$. SFQ is a correlation effect and disappears for $U_d = U_p = 0$; without correlation the cluster shows a normal, paramagnetic behaviour, shown in Figure 17.4 c) Similar phenomena have been observed in exact diagonalization work with larger clusters (up to 21 atoms) in Ref. [172] and with rings of clusters. Larger systems can be obtained by joining several clusters in such a way that bound pairs can propagate. Rings of clusters threaded by flux tubes also show SFQ, and Figure 17.5) illustrates the general idea of how such systems can be

built, in such a way that the square symmetry of each cluster is preserved. The SFQ pattern is quite similar [18], [?] to the one discussed above; this time the inter-cluster hopping must be a weak link in order to make the magnetic perturbation gentle enough. By projecting on the low energy sector, we can solve very large clusters in an essentially analytic way and show that the superconducting behavior remains independent of size.

This suggests that the SFQ pattern must be a property of the Hubbard model which extends to the thermodynamic limit and is essentially related to the symmetry. The minimum at $\phi = 0$ is clearly due to the $W=0$ pair, yielding a nondegenerate ground state (when there is degeneracy, the ground state must be paramagnetic, since the system interacts with the field by a Zeeman mixing of the degenerate components and gains energy). The field tends to destroy the pairs and does so by lowering the symmetry; indeed the reflections are broken. The second minimum at $\phi = \frac{\phi_0}{2}$ is due to the lattice which for this particular flux recovers the flux symmetry. This is actually a theorem, and the proof was obtained by a construction shown in figure 17.6. One can see how one can choose the gauge for the vector potential when the 4 flux tubes are inserted like in figure 17.4 in a CuO_4 unit belonging to a full plane. From the construction in the Figure one sees that a general flux ϕ in the flux tubes destroys the $W=0$ pairing by breaking the symmetry ($C_{4v} \rightarrow Z_4$) but at $\phi = \frac{\phi_0}{2}$ the full symmetry is restored, because the reflections are equivalent to a gauge transformation. The flux quantization pattern arises from a level crossing between the ground states at $\phi = 0$ and $\phi = \frac{\phi_0}{2}$.

Models systems capable of superconducting flux quantization such as rings of CuO_4 clusters can also be operated [192] as Josephson junctions. One needs to include a barrier and introduce a mild violation of the symmetry to produce avoided crossings; Josephson and inverse-Josephson (Shapiro) effects then appear as adiabatic responses to slowly changing flux $\phi(t)$.

Recently, exact studies on small Hubbard clusters at finite temperatures by Fernando et al. [193] have given useful insight on phase separation and pairing.

Problems

17.1. Find how the irreps of the optimal Group \mathcal{G} split in C_{4v} .

17.2. Using the $W=0$ theorem and the Optimal Group, find the irreps with no double occupation in the 4×4 lattice.

18 Algebraic Methods

18.1 Lieb Theorems on the Half Filled Hubbard Model

Consider a repulsive Hubbard model, defined on a d -dimensional lattice or graph Λ of $|\Lambda|$ sites, with nearest-neighbor hopping. No symmetry is assumed; however we can use as an example a $\sqrt{|\Lambda|} \times \sqrt{|\Lambda|}$ simple square Hubbard Model with periodic boundary conditions and hopping between nearest neighbors (n.n.):

$$H = T + W = t \sum_{\sigma} \sum_{x,y \in \Lambda}^{n.n.} c_{x\sigma}^{\dagger} c_{y\sigma} + U \sum_{x \in \Lambda} n_{x\uparrow} n_{x\downarrow}; \quad U > 0. \quad (18.1)$$

Let us specialize at half filling with $n \equiv N_{\uparrow} = N_{\downarrow} = \frac{|\Lambda|}{2}$ electrons for each spin. For each spin, there are $m = \binom{|\Lambda|}{n}$ configurations, and the dimensionality of the problem is m^2 . Here I present a simplified proof that the Hubbard Model at half filling has a unique ground state; this could serve as an introduction to Lieb's paper [37] which contains the proofs of more general exact statements.

For the total spin, which is conserved, the second quantization operators (1.57,1.58) become in the lattice case

$$S_z = \frac{1}{2} \sum_x (n_{\uparrow}(x) - n_{\downarrow}(x)), \quad S^+ = \sum_x c_{\downarrow}^{\dagger}(x) c_{\uparrow}(x), \quad (18.2)$$

and one can work out

$$S^2 = S_z^2 + \frac{1}{2}(S^+ S^- + S^- S^+).$$

A symmetric determinantal configuration like

$$|\psi_{\text{sites}}\rangle = |i \uparrow, j \uparrow, k \uparrow, \dots, i \downarrow, j \downarrow, k \downarrow, \dots\rangle \quad (18.3)$$

in the site representation has $S=0$ and is singlet. A two-site system is the most trivial bipartite lattice; with two electrons it becomes the model system that we met in Sect. 14.2; there, I used it for illustrating the form (14.51),

$$|\phi\rangle = \sum_{\alpha\beta} L_{\alpha\beta} |\psi_{\alpha\uparrow}\rangle \otimes |\psi_{\beta\downarrow}\rangle \quad (18.4)$$

of the many-electron the wave function. The eigenvector given by the matrix $L = i\frac{\sigma_y}{\sqrt{2}}$ represents the only triplet, and has nothing on the diagonal. Out of the $\binom{4}{2} = 6$ states of the model, three are singlets. At half filling L is a square $m \times m$ matrix. A glance to (18.4) suggests that there would be much to gain in complex problems if L were diagonal, because fewer numbers would represent $|\phi\rangle$, and one knows that L can be diagonalized if it is Hermitean. If L can be taken Hermitean, it remains Hermitean when changing the basis. Thus it is natural to ask if this advantage is free or we must pay for it.

Hermitean L

There is no magnetic field, the Hamiltonian is real and we take the basis functions ψ_α real as well. Then, if $\phi = \sum_{\alpha,\beta} L_{\alpha,\beta} \psi_\alpha \psi_\beta$ is an eigenstate of H with eigenvalue ϵ , L^* also belongs to ϵ ; the transposed matrix L^T has the up and down spin amplitudes interchanged, and since this is a symmetry operation it leaves the subspace of ϵ invariant. Hence, if L belongs to ϵ , this applies to L^\dagger and for the Hermitean combinations $L + L^\dagger, i(L - L^\dagger)$. So we shall take L Hermitean¹. Hermiticity implies that we may impose the normalization condition (14.60) $\langle\phi|\phi\rangle = 1$ by writing $\text{Tr}L^2 = 1$. If all the eigenvalues of L are non-negative, we write $L \geq 0$. Then, we must have $\text{Tr}L > 0$ strictly, because otherwise $L = 0$ and the state vanishes. One can infer about the spin of the many-body state² if $L \geq 0$. In fact, some diagonal elements must be positive, and this holds true on the site basis like in (18.3); therefore, ϕ is singlet, or has some mixture with a singlet. In the two-site two-electron example one can see that for large negative U the eigenvalues of L are of the same sign, while for large positive U they are of opposite signs: attraction favors singlets.

In his proof, Lieb used the Schrödinger Equation in the form (14.56):

$$H : L \rightarrow K_\uparrow L + L K_\downarrow^T + U \sum_s n_{s\uparrow} L n_{s\downarrow}. \quad (18.6)$$

He had obtained (14.54)(for the real Hamiltonian case) from the variational principle starting from the energy

¹As a two-electron example, writing x, y for sites or orbitals, we may use the singlet

$$\phi = \frac{|x_\uparrow y_\downarrow| + |y_\uparrow x_\downarrow|}{\sqrt{2}} \Leftrightarrow L = \frac{\sigma_x}{2}; \quad (18.5)$$

incidentally, this shows that the vanishing of the diagonal elements does not prevent L from representing a singlet. However a singlet can give a non-zero contribution to $\text{Tr}L$ while triplets and higher spins cannot.

²It is not the sign of the wave function that brings information, of course, but a non-vanishing $\text{Tr}L$.

$$E = 2Tr(KLL) + U \sum_x Tr(Ln_xLn_x). \quad (18.7)$$

Canonical Transformation and Pseudospin

Electron-electron repulsion is the same as electron-hole attraction; by a canonical transformation starting from the model (18.1) we now get a Hamiltonian with electron-electron attraction. We need to change the up spin operators only, according to

$$d_{x\uparrow} = c_{\uparrow}^\dagger, \quad (18.8)$$

whereby the transformed kinetic energy for up-spin electrons reads

$$K_{\uparrow} \rightarrow \tilde{K}_{\uparrow} = t \sum_{x,y \in \Lambda}^{n.n.} d_x d_y^\dagger = -t \sum_{x,y \in \Lambda}^{n.n.} d_y^\dagger d_x.$$

Having t for down spins and $-t$ for up spins is definitely ugly; so we change signs to the \uparrow orbitals in a sublattice (here the bipartite hypothesis enters) replacing (18.8) by

$$d_{x\uparrow} = \text{sign}(x)c_{x\uparrow}^\dagger. \quad (18.9)$$

Now, the transformed Hamiltonian reads

$$\tilde{H} = t \sum_{\sigma} \sum_{x,y \in \Lambda}^{n.n.} \left[d_{x\uparrow}^\dagger d_{y\uparrow} + c_{x\downarrow}^\dagger c_{y\downarrow} \right] - U \sum_{x \in \Lambda} d_{x\uparrow}^\dagger d_{x\uparrow} n_{x\downarrow} + U N_{\downarrow}; \quad U > 0, \quad (18.10)$$

where $N_{\downarrow} = \sum_x n_{x\downarrow}$ is conserved. At half filling, we keep dealing with $N_{\uparrow} = N_{\downarrow} = \frac{|A|}{2}$ Fermions for each spin, and the amplitudes $L_{\alpha\beta}$ in a site picture are the same, except that α is replaced by the configuration with the sites not in α . For example, the repulsive H_2 molecule model $H(t, U)$ (14.58) has the energy eigenvalues $\epsilon(U) = \frac{U-r}{2}, 0, U, \frac{U+r}{2}$, $r = \sqrt{16t^2 + U^2}$; the eigenvalues of

$$\tilde{H} = H(t, -U) + U = \begin{pmatrix} 0 & t & t & 0 \\ t & U & 0 & t \\ t & 0 & U & t \\ 0 & t & t & 0 \end{pmatrix}, \quad U > 0 \quad (18.11)$$

are the same as those of $H(t, U)$.

With the above substitution of d for c , S_z of Equation (18.2) becomes

$$\tilde{S}_z = \frac{1}{2} \sum_x ([1 - d_{x\uparrow}^\dagger d_{x\uparrow} - n_{x\downarrow}]) = \frac{1}{2} [A - N_{\uparrow} - N_{\downarrow}] \quad (18.12)$$

and S^+ reads

$$\tilde{S}^+ = \sum_x \epsilon(x) d_{x\uparrow} c_{x\downarrow}. \quad (18.13)$$

Both are still conserved of course although they do not mean spin any more in the transformed problem and are therefore called pseudo-spin.

Unique Ground State: Attractive Case

Let us assume H as in (18.1) but $U < 0$. If the Hermitian L matrix is a ground state, then we can diagonalize L and write $C^\dagger LC = \text{diag}(\lambda_i)$, where C is an eigenvector matrix, and λ_i are the eigenvalues. Thus we can form a positive semi-definite matrix $|L| = \text{diag}(|\lambda_i|)$, which is granted to be singlet or a linear combination including a singlet.

Now it is easy to show that $|L|$ is also a ground state. To this end, we calculate the energy according to (18.7) on a basis of eigenvectors of L . For the kinetic energy $\text{Tr}KL^2 = \sum_i K_{ii}\lambda_i^2$ the result is the same for L and $|L|$. For the potential energy the result for L is $U \sum_{x,i} \lambda_i \lambda_j (n_x)_{i,j}^2$ and for $|L|$ $U \sum_{x,i} |\lambda_i \lambda_j| (n_x)_{i,j}^2$; since $U < 0$ the latter result cannot be larger than the former, thus $|L|$ is a ground state. In the two-electron case (18.5) one finds $C = \frac{1}{\sqrt{2}} \begin{pmatrix} -1 & 1 \\ 1 & 1 \end{pmatrix}$ and gets $C^\dagger LC = \frac{1}{\sqrt{2}} \begin{pmatrix} -1 & 0 \\ 0 & 1 \end{pmatrix}$, hence $|L| = C \frac{1}{\sqrt{2}} \begin{pmatrix} 1 & 0 \\ 0 & 1 \end{pmatrix} = C^\dagger = \frac{1}{\sqrt{2}} \begin{pmatrix} 1 & 0 \\ 0 & 1 \end{pmatrix}$; this yields the ground state

$$\phi = \frac{|x_\uparrow x_\downarrow| + |y_\uparrow y_\downarrow|}{\sqrt{2}}, \tag{18.14}$$

which is degenerate with (18.5) for $U = 0$ but is actually better for $U < 0$.

The question arises: is $|L|$ really different from L ? If it is, we get a new ground state, namely the difference, which we write in terms of the eigenvectors:

$$R = |L| - L = \sum_i |\lambda_i\rangle [|\lambda_i| - \lambda_i] \langle \lambda_i|. \tag{18.15}$$

Being a ground state, $R > 0$, unless $R = 0$. We now show that this is the case, that is, $|\lambda_i| = \lambda_i \forall i$. The latter equality must be true for some i , otherwise $L = -|L|$ and we obtain the same ground state with a uninteresting (-) sign in front; thus, the kernel of R is not empty, that is, $RV = 0$ for some m -component vector V . The Schrödinger equation (18.6) for R

$$K_\uparrow R + RK_\downarrow^T + U \sum_s n_{s\uparrow} R n_{s\downarrow} = \epsilon R. \tag{18.16}$$

averaged over V has no kinetic terms because $RV = 0$; it follows that

$$\sum_x \langle V | n_x R n_x | V \rangle = 0.$$

This implies that either $n_x |V\rangle = 0$ or $n_x |V\rangle$ is also in the kernel of R . Since V does not vanish, $n_x |V\rangle \neq 0$ for some x , then the kernel extends to $n_x |V\rangle$. The proliferation of the kernel never stops; applying the Schrödinger equation to V ,

$$\left[KR + RK + U \sum_x n_x R n_x \right] V = \epsilon RV. \tag{18.17}$$

Now since $RV = 0$ and $Rn_xV = 0$ we find $RKV = 0$, that is, every configuration connected to V by K is in the kernel; but any two configuration can be reached from each other in a finite number of steps, that is K^p has matrix elements between them for some p . Finally the kernel has swallowed all the Hilbert space! Thus, $L = |L|$ (although, of course, we remain free to choose $L = -|L|$). Thus there is a singlet component in the ground state and $L \geq 0$.

This implies that the ground state is unique. If L_1 and L_2 were different ground states any combination $L_\xi = L_1 + \xi L_2$ would be a ground state, but we would be free to choose ξ such that $TrL_\xi = 0$; this is impossible since any ground state must be positive semidefinite.

Repulsive Case

Now we assume H as in (18.1) with $U > 0$. The ground state is the transform of the one with $U < 0$. (See Problem 18.1 for an example). This implies that the eigenvalue is the same; the eigenvector is also the same, albeit it is written in a reshuffled basis, and is therefore a unique singlet.

More generally, one can study bipartite lattices with sublattices A and B with $|A|$ and $|B|$ sites per cell. Lieb showed that the ground state has spin $S = |B| - |A|$ per cell; thus, the trivial Hubbard model has a singlet ground state, while the three-band Hubbard model has $S = \frac{1}{2}$ per cell.

18.2 Bethe Ansatz for the Heisenberg Chain

For an electron in magnetic field in classical canonical ensemble,

$$Z = \int d^3x \int d^3p \exp\left[-\frac{(p_x - eHy/c)^2 + p_y^2 + p_z^2}{2mK_B T}\right] = V(2\pi mK_B T)^{3/2} \quad (18.18)$$

is actually independent of the field H , since the field dependence can be eliminated by a change of variable; this extends to any system. Thus the very existence of magnetism cannot be understood classically. The Heisenberg model was one of the first quantum mechanical theories aimed at describing ferromagnetism. Consider N spins $s = 1/2$ arranged on a ring ($\mathbf{S}_{N+1} = \mathbf{S}_1$); $\sigma_n = \uparrow$ and $\sigma_n = \downarrow$ are the two possible states at site n , and a configuration may be specified by assigning $|\sigma_1, \sigma_2, \dots, \sigma_N\rangle$; the Hilbert space has 2^N dimensions. The Heisenberg Hamiltonian is

$$H_H = -J \sum_{n=1}^N \mathbf{S}_n \cdot \mathbf{S}_{n+1} = H_0 + H_{XY}, \quad (18.19)$$

$$H_0 = -J \sum_{n=1}^N S_n^z S_{n+1}^z \quad (18.20)$$

while the so-called XY model hamiltonian, which has been studied by its own sake, reads

$$H_{XY} = -\frac{J}{2} \sum_{n=1}^N (S_n^+ S_{n+1}^- + S_n^- S_{n+1}^+). \quad (18.21)$$

Let $N_{\downarrow} \equiv r$ be the number of \downarrow spins; H_H is invariant for translations along the chain (which implies conservation of a momentum K) and for rotation in spin space (conservation of the total spin S and of its z component, $S_z = \frac{N_{\uparrow} - N_{\downarrow}}{2}$, $N_{\uparrow} = N - N_{\downarrow}$). For $r = 0$ the problem is trivial because

$$H_H |\uparrow \uparrow \dots \uparrow\rangle = E^{(N_{\downarrow}=0)} |\uparrow \uparrow \dots \uparrow\rangle, \quad E^{(N_{\downarrow}=0)} = -J \frac{N}{4} \quad (18.22)$$

and this is the only state. Here I assume ferromagnetic coupling, i.e. $J > 0$ for definiteness. Note that

$$H_0 |\sigma_1, \sigma_2, \dots, \sigma_N\rangle = \{E^{(N_{\downarrow}=0)} + \frac{(-J)}{4} (-2) N_{\uparrow\downarrow}\} |\sigma_1, \sigma_2, \dots, \sigma_N\rangle \quad (18.23)$$

where $N_{\uparrow\downarrow}$ is the number of reversed scalar products (number of times $\uparrow\downarrow$ or $\downarrow\uparrow$ nearest neighbors are encountered instead of $\uparrow\uparrow$ or $\downarrow\downarrow$); the (-2) factor enters because the scalar products are counted as positive in $E^{(N_{\downarrow}=0)}$ and must be reversed. We may think of H_{XY} as moving \downarrow spins to the left or to the right *provided that the neighboring spins are \uparrow* ; this important limitation causes the interaction between excitations and makes the problem interesting. The method invented by Bethe in 1931 [68] to solve the Schrödinger equation for this model for any N and r has been later applied with great success to several many-body problems. Excellent reviews of recent work are available[72]; here I show its principle.

One Magnon

For $r \equiv N_{\downarrow} = 1$ a configuration can be written $|n\rangle$, where n is the only \downarrow spin; since $N_{\uparrow\downarrow} = 2$, $\langle n | H_0 - E^{(N_{\downarrow}=0)} | n \rangle = J$, $\langle n | H_{XY} | n \pm 1 \rangle = \frac{J}{2}$ and

$$(H_H - E^{(N_{\downarrow}=0)}) | n \rangle = J | n \rangle - \frac{J}{2} (| n + 1 \rangle + | n - 1 \rangle). \quad (18.24)$$

Taking the scalar product $f(n) = \langle \psi_E | n \rangle$ with the solution of $H |\psi_E\rangle = E |\psi_E\rangle$, one finds the recurrence relation

$$(E - E^{(N_{\downarrow}=0)}) f(n) = -J \left[\frac{f(n+1) + f(n-1)}{2} - f(n) \right] \quad (18.25)$$

which is readily solved to give the *magnon* solution

$$\psi_E \equiv \psi_j = \frac{1}{\sqrt{N}} \sum_{n=1}^N e^{ik_j n} | n \rangle, \quad E = E^{(N_{\downarrow}=0)} + J [1 - \cos(k_j)] \quad (18.26)$$

with the wave vector

$$k_j = \frac{2\pi j}{N}, \quad j \text{ integer} \quad (18.27)$$

reflecting the translation invariance of the problem. This represents a spin wave excitation of a ferromagnet.

Two Magnons

For $N_\downarrow = r = 2$ it is natural to write a basis $\{|n_1, n_2\rangle\}$, $n_2 > n_1$ specifying the positions of \downarrow spins. If $n_2 > n_1 + 1$, $N_{\uparrow\downarrow} = 4$ and one finds:

$$\frac{(H_H - E^{(N_\downarrow=0)})|n_1, n_2\rangle}{-J} = -2|n_1, n_2\rangle + \frac{|n_1+1, n_2\rangle + |n_1-1, n_2\rangle + |n_1, n_2+1\rangle + |n_1, n_2-1\rangle}{2}; \quad (18.28)$$

let us take the scalar product $f(n_1, n_2) = \langle \psi_E | n_1, n_2 \rangle$ with the solution of $H|\psi_E\rangle = E|\psi_E\rangle$, and write the recurrence formula:

$$\frac{(E - E^{(N_\downarrow=0)})f(n_1, n_2)}{-J} = -2f(n_1, n_2) + \frac{f(n_1+1, n_2) + f(n_1-1, n_2) + f(n_1, n_2+1) + f(n_1, n_2-1)}{2} \quad (18.29)$$

This is satisfied by $f(n_1, n_2) = e^{i(k_1 n_1 + k_2 n_2)}$ with energy eigenvalue

$$E = E^{(N_\downarrow=0)} + J(1 - \cos(k_1) + 1 - \cos(k_2)) \quad (18.30)$$

that would be the same as the sum of two magnon energies and would represent the superposition of two magnons if the momenta k_i were given by (18.27). However, the periodic boundary conditions do not apply separately to the two momenta. Instead, we must have

$$e^{i(k_1+k_2)N} = 1, \quad (18.31)$$

or also

$$e^{ik_1 N} = e^{i\theta}, \quad e^{ik_2 N} = e^{-i\theta}. \quad (18.32)$$

The *interaction* of the two magnons produces a relative phase shift, which also changes the energy although the eigenvalue (18.30) is formally the sum of two magnon energies. In terms of this (yet unknown) phase, we may write

$$Nk_1 = \theta + 2\pi\lambda_1, \quad Nk_2 = -\theta + 2\pi\lambda_2. \quad (18.33)$$

The *Bethe quantum numbers* λ_i are integers and range from 0 to $N - 1$.

However, one must pay more attention. First, there is a degenerate solution with the k_1 and k_2 exchanged and must be included for generality and also to satisfy the boundary conditions, as I show in a moment; so one should write

$$f(n_1, n_2) = Ae^{i(k_1 n_1 + k_2 n_2)} + Be^{i(k_2 n_1 + k_1 n_2)}, \quad 0 < n_1 < n_2 < N. \quad (18.34)$$

Note that:

- the ordering $0 < n_1 < n_2 < N$ is needed otherwise the basis would be over-complete.
- The two contributions must enter with the same probability, A and B differ by a phase θ (I have the right to use the same symbol, as I show shortly) and we rewrite (18.34) as

$$f(n_1, n_2) = e^{i(k_1 n_1 + k_2 n_2 + \frac{\theta}{2})} + e^{i(k_2 n_1 + k_1 n_2 - \frac{\theta}{2})}, \quad 0 < n_1 < n_2 < N \quad (18.35)$$

This is not normalized but we do not care.

- θ may be identified with the same real phase θ as in (18.32) above. Indeed, we must be free to decide that the numbering of spins runs in the range $(n_2, \dots, n_2 + N - 1)$ rather than $(1, \dots, N)$; now $n_2 < n_1 + N$; therefore

$$\begin{aligned} f(n_1, n_2) &= f(n_2, n_1 + N) \\ &= e^{i\{k_1 n_2 + k_2 (n_1 + N) + \frac{\theta}{2}\}} + e^{i\{k_2 n_2 + k_1 (n_1 + N) - \frac{\theta}{2}\}}, \\ & \qquad \qquad \qquad n_2 < n_1 + N. \end{aligned} \quad (18.36)$$

This shift of the origin exchanges n_1 and n_2 , and the two terms in (18.35) are therefore exchanged; the second term of (18.35) becomes the first of (18.36), but the phase $-\theta/2$ changes sign and an extra Nk_2 term appears in the exponent. These differences must cancel because the boundary condition holds. Comparing with (18.35) we find the conditions $e^{i\frac{\theta}{2}} e^{ik_2 N} = e^{-i\frac{\theta}{2}}$, $e^{-i\frac{\theta}{2}} e^{ik_1 N} = e^{i\frac{\theta}{2}}$, which are satisfied, according to (18.32); θ is indeed the same.

It is time worry about configurations like $\dots \uparrow \uparrow \downarrow \downarrow \uparrow \uparrow \dots$, when $n_2 = n_1 + 1$ and the down spin in n_1 cannot jump to the right and the one in n_2 cannot jump to the left; Equation (18.29) must change because $N_{\uparrow\downarrow} = 2$ and $f(n, n)$ does not occur in the equation since $|n, n\rangle$ has no meaning, therefore

$$\begin{aligned} & \frac{(E - E^{(N_1=0)})f(n_1, n_1 + 1)}{-J} = \\ & = -f(n_1, n_1 + 1) + \frac{f(n_1 - 1, n_2) + f(n_1, n_1 + 2)}{2}. \end{aligned} \quad (18.37)$$

However the *ansatz* is still (18.35); the *ansatz* allows $f(n, n) \neq 0$ and grants that (18.29) continues to hold formally for $n_2 = n_1 + 1$ as well,

$$\begin{aligned} & \frac{(E - E^{(N_1=0)})f(n_1, n_1 + 1)}{-J} = -2f(n_1, n_1 + 1) + \frac{f(n_1 + 1, n_1 + 1)}{2} \\ & + \frac{f(n_1 - 1, n_1 + 1) + f(n_1, n_1 + 2) + f(n_1, n_1)}{2}. \end{aligned} \quad (18.38)$$

Comparing the last two equations we get the condition

$$f(n_1, n_1 + 1) = \frac{1}{2}[f(n_1, n_1) + f(n_1 + 1, n_1 + 1)]. \quad (18.39)$$

When we substitute the ansatz (18.35), we are free to set $n_1 = 0$ to obtain more readily the n_1 -independent condition

$$e^{i\theta} = -\frac{e^{i(k_1+k_2)} + 1 - 2e^{ik_1}}{e^{i(k_1+k_2)} + 1 - 2e^{ik_2}} \equiv \frac{N}{D}. \quad (18.40)$$

One moment, is this really a phase factor? To check that, one observes that $|N|^2 = 6 + 2\cos(k_1 + k_2) - 6[\cos(k_1) + \cos(k_2)]$ is symmetric in k_1 and k_2 , hence $|N| = |D|$. Now the identity

$$\cot\left(\frac{\theta}{2}\right) = i\frac{e^{i\theta} + 1}{e^{i\theta} - 1} \quad (18.41)$$

is very useful to cast (18.40) in real form:

$$2\cot\left(\frac{\theta}{2}\right) = \cot\left(\frac{k_1}{2}\right) + \cot\left(\frac{k_2}{2}\right). \quad (18.42)$$

The Bethe Ansatz equations (18.33, 18.42), can be solved for k_1, k_2 and θ by combined analytic and numerical techniques for $N \sim$ some tens [72]. Most solutions are scattering states with real momenta and a finite θ ; however when one of the Bethe quantum numbers λ vanishes, the corresponding k and θ also vanish, and there is no interaction. Other solutions with λ_1 and λ_2 close to each other have complex momenta with $k_1 = k_2^*$ and represent magnon bound states in which the two flipped spins propagate at a close distance.

Many Magnons

It is stunning that the Bethe ansatz works for any system size, and is generalized for any r . Again one chooses the origin and orders the spins with $n_i < n_{i+1}$; a basis is $\{|n_1, n_2 \dots n_r\}$, specifying the positions of \downarrow spins. We first seek a possible H eigenstate as a product of r magnon wave functions of momenta k_j . As the natural extension of (18.32) we allow each k to pick up a phase from each of the others;

$$e^{ik_i N} = e^{i\sum_{j \neq i} \theta_{ij}}, \quad \theta_{ij} = -\theta_{ji}. \quad (18.43)$$

Equation (18.33) becomes

$$Nk_i = \sum_{j \neq i} \theta_{ij} + 2\pi\lambda_i \quad (18.44)$$

and the integers λ_i ranging from 0 to $N-1$ are Bethe quantum numbers. The $r!$ permutations \mathcal{P} of the momenta yield degenerate r -magnon plane waves that must be summed, so the Bethe Ansatz reads

$$f(n_1, \dots, n_r) = \sum_{\mathcal{P}} e^{i\left(\sum_{j=1}^r k_{\mathcal{P}j} n_j + \frac{1}{2} \sum_{i < j} \theta_{\mathcal{P}i \mathcal{P}j}\right)} \quad (18.45)$$

Again, we must consider two cases: 1) the reversed spins are all far away 2) there are neighboring reversed spins. In case 1) Schrödinger equation is satisfied identically and yields the direct extension of (18.30) for the energy eigenvalue:

$$E - E_0 = J \sum_{j=1}^r (1 - \cos k_j). \quad (18.46)$$

We can count our spins starting anywhere without changing the amplitude, so we impose

$$f(n_1, \dots, n_r) = f(n_2, \dots, n_r, n_1 + N).$$

This causes a permutation of the terms of the sum, and in each exponent the θ term changes sign and an extra contribution proportional to N appears. Exactly as in the two-magnon case, these changes are fixed by (18.44) and we may conclude that the θ phases are the same in (18.44) and (18.45).

Some changes occur in the Schrödinger equation when there are neighboring reversed spins because $N_{\uparrow\downarrow}$ is reduced and some hoppings do not exist; the same reasoning that took us to (18.40) can be extended directly and yields

$$e^{i\theta_{ij}} = - \frac{e^{i(k_i+k_j)} + 1 - 2e^{ik_i}}{e^{i(k_i+k_j)} + 1 - 2e^{ik_j}}. \quad (18.47)$$

which in real form can be written, as above,

$$2 \cot \frac{\theta_{ij}}{2} = \cot \frac{k_i}{2} - \cot \frac{k_j}{2}, \quad i, j = 1, \dots, r. \quad (18.48)$$

The Bethe equations (18.44,18.48) are hard to solve for many flipped spins in large systems. In recent years solutions have been obtained which are far from trivial; among others, bound states of several magnons have been reported.

The Bethe Ansatz is a rare example of exact solution of an interacting many-body problem; it keeps the same form independent of the size of the system. The root of the (relative) simplicity that allows this solution is one-dimensionality: the evolution does not allow overtakings, and spins always keep a fixed order. However, without the ingenuity of Hans Bethe, the solution could have remained undetected; who knows how many important model problems are solvable, but still unsolved.

18.3 Bethe Ansatz for Interacting Fermions 1 Dimension

18.3.1 δ -Function Interaction

Let N electrons in 1 dimension on a line of length L whose ends are identified interact with short-range repulsion. We seek the space wave function belonging to a given irrep of S_N , having separated the spin variables according to

Sect. 9.8. The Hamiltonian, which can be shown [142] to be related to the Kondo Hamiltonian, is:

$$H = - \sum_{i=1}^N \frac{\partial^2}{\partial x_i^2} + 2c \sum_{i < j} \delta(x_i - x_j), \quad c > 0. \tag{18.49}$$

Here $x_1 \dots x_i \dots x_N$ are the electron coordinates, in short $\{x_i\}$. Indeed, as in Section 1.1, one pretends that first of all the electrons receive *a priori* labels $1, 2, \dots, N$; one runs though the line and notes down where one meets electrons and in what order. The order defines a permutation $Q \in S_N$; the i -th electron along the line is the one bearing the *a priori* label Q_i , we label its position x_{Q_i} , and say that we are in in *sector* Q . The *Bethe ansatz* solution[74] yields the many-electron wave function in the *sector*, which is just the ordering

$$\text{sector } Q : 0 < x_{Q_1} < \dots < x_{Q_N} \tag{18.50}$$

It is:

$$\begin{aligned} \psi(x_1 \dots x_i \dots x_N) &= \psi_Q(x_1 \dots x_i \dots x_N), \quad 0 < x_{Q_1} < \dots < x_{Q_N}, \\ \psi_Q(x_1 \dots x_i \dots x_N) &= \sum_P \psi_{Q,P}(x_1 \dots x_i \dots x_N), \\ \psi_{Q,P}(x_1 \dots x_i \dots x_N) &= [Q, P] e^{i \sum_i k_{P_i} x_{Q_i}}. \end{aligned} \tag{18.51}$$

Here, $P \in S_N$ while $k_1 \dots k_N$ denote different numbers, and $[Q, P]$ are amplitudes to be determined.

Thus each electron has 2 labels, the physical one is i , which is the order along the line, while Q_i depends on a fictitious (for indistinguishable particles) and unobservable order, that is on the sector. However, if we remain in a sector Q , we cannot describe any overtaking: when an electron i overtakes the one on its right, the description automatically switches to a new sector.



Fig. 18.1. If a classical electron (triangle) overtakes another one they exchange their physical labels and keep their sector labels. Since actual electrons are indistinguishable, one ends up in a neighbor sector $Q' = \mathcal{P}^{(i \leftrightarrow i+1)} Q$, where \mathcal{P} is a transposition.

Now we study under what conditions

$$H\psi = \sum_{i=1}^N k_i^2 \psi \tag{18.52}$$

and how one can determine the *momenta* k_i .

Thus, $\psi_Q = \sum_P \psi_{Q,P}$, where ψ_{QP} is $[Q, P]$ times a plane-wave state where the ordering of electrons sector labels Q and the ordering of momenta are fixed. We are in a given sector Q as long as x_{Q_i} increases as i increases, but if two electrons with consecutive physical labels sit at the same x , we are also in the sector $Q' = \mathcal{P}^{(i \leftrightarrow i+1)}Q$, in which the images of i and $i+1$ are exchanged. This fact allows to impose sector boundary conditions: at the boundary each plane wave must have the same amplitude in both neighboring sectors. For example, in the Q sector the contribution to ψ_Q proportional to $[Q, P]$ when $x_{Q_3} = x_{Q_4}$ is

$$\psi_{Q,P} = [Q, P] e^{i(k_{P_3} + k_{P_4})x_{Q_3} + i \sum_{i \neq 3,4} p_{P_i} x_{Q_i}}, \tag{18.53}$$

both in ψ_Q and in $\psi_{Q'}$ the contribution of P is summed to the contribution of the permutation $P' = \mathcal{P}^{(3 \leftrightarrow 4)}P$ bringing the same exponential:

$$\psi_{Q,P} + \psi_{Q,P'} = ([Q, P] + [Q, P']) e^{i(k_{P_3} + k_{P_4})x_{Q_3} + i \sum_{i \neq 3,4} p_{P_i} x_{Q_i}}. \tag{18.54}$$

This amplitude must be the same as

$$\psi_{Q',P} + \psi_{Q',P'} = ([Q', P] + [Q', P']) e^{i(k_{P_3} + k_{P_4})x_{Q_3} + i \sum_{i \neq 3,4} p_{P_i} x_{Q_i}}$$

and the continuity condition is

$$\boxed{[Q, P] + [Q, P'] = [Q', P] + [Q', P']}. \tag{18.55}$$

Next, we integrate the Schrödinger equation for ψ over x_{Q_3} at the sector boundary, recalling that $x_{Q_3} \leq x_{Q_4}$ by definition:

$$\int_{x_{Q_4} - \epsilon}^{x_{Q_4}} dx_{Q_3} H\psi(\{x_{Q_i}\}) = E \int_{x_{Q_4} - \epsilon}^{x_{Q_4}} dx_{Q_3} \psi. \tag{18.56}$$

Since this is $O(\epsilon)$ and goes to 0,

$$\int_{x_{Q_4} - \epsilon}^{x_{Q_4}} dx_{Q_3} \left(-\frac{\partial^2}{\partial x_{Q_3}^2} + 2c\delta(x_{Q_3} - x_{Q_4}) \right) \psi(\{x_{Q_i}\}) = 0,$$

and using

$$\int_{-\infty}^0 dx \delta(x) = \frac{1}{2}$$

one finds a discontinuity in the derivative of the full amplitude ψ of (18.51):

$$\left[\frac{\partial}{\partial x_{Q_3}} \psi \right]_{x_{Q_3}=x_{Q_4}} - \left[\frac{\partial}{\partial x_{Q_3}} \psi \right]_{x_{Q_3}=x_{Q_4} - \epsilon} = c\psi(\{x_{Q_i}, x_{Q_3} = x_{Q_4}\}). \tag{18.57}$$

Identifying the solution in each sector with ψ_Q we can specify

$$\left[\frac{\partial}{\partial x_{Q_3}}\psi_{Q'}\right]_{x_{Q_3}=x_{Q_4}} - \left[\frac{\partial}{\partial x_{Q_3}}\psi_Q\right]_{x_{Q_3}=x_{Q_4}-\epsilon} = c\psi_Q(\{x_{Q_i}, x_{Q_{Q_3}} = x_{Q_4}\}). \quad (18.58)$$

We need to write this in terms of the $[P, Q]$ unknowns. In sector Q , $x_{Q_3} \leq x_{Q_4}$, from (18.54)

$$c\psi(\{x_i, x_3 = x_4\}) = c([Q, P] + [Q, P'])e^{i(k_{P_3}+k_{P_4})x_{Q_3}+i\sum_{i\neq 3,4}P_{P_i}x_{Q_i}}, \quad (18.59)$$

the contribution to $[\frac{\partial}{\partial x_{Q_3}}\psi]_{x_{Q_3}=x_{Q_4}-\epsilon}$ proportional to $[Q, P]$ is

$$\psi'_{Q,P} = ik_{P_3}[Q, P]e^{ik_{P_3}x_{Q_3}+i\sum_{i\neq 3,4}k_{P_i}x_{Q_i}}, \quad (18.60)$$

still in sector Q we must include the contribution of the permutation $P' = \mathcal{P}^{(3\leftrightarrow 4)}P$ bringing the same plane wave:

$$\begin{aligned} \psi'_{QP} + \psi'_{QP'} &= i(k_{P_3}[Q, P] + k_{P'_3}[Q, P'])e^{i(k_{P_3}+k_{P_4})x_{Q_3}+i\sum_{i\neq 3,4}k_{P_i}x_{Q_i}} \\ &= i(k_{P_3}[Q, P] + k_{P_4}[Q, P'])e^{i(k_{P_3}+k_{P_4})x_{Q_3}+i\sum_{i\neq 3,4}P_{P_i}x_{Q_i}} \end{aligned} \quad (18.61)$$

On the other hand, in the neighboring sector $Q' = \mathcal{P}^{(3\leftrightarrow 4)}Q$, we have

$$\begin{aligned} \psi'_{Q',P} + \psi'_{Q',P'} &= [Q', P]e^{ik_{P_3}x_{Q'_3}+ik_{P_4}x_{Q'_4}+i\sum_{i\neq 3,4}k_{P_i}x_{Q_i}} \\ &\quad + [Q', P']e^{ik_{P'_3}x_{Q'_3}+ik_{P'_4}x_{Q'_4}+i\sum_{i\neq 3,4}k_{P_i}x_{Q_i}}. \end{aligned} \quad (18.62)$$

We need to write this in the x_{Q_i} variables,

$$\begin{aligned} \psi'_{Q',P} + \psi'_{Q',P'} &= [Q', P]e^{ik_{P_3}x_{Q_4}+ik_{P_4}x_{Q_3}+i\sum_{i\neq 3,4}k_{P_i}x_{Q_i}} \\ &\quad + [Q', P']e^{ik_{P_4}x_{Q_4}+ik_{P_3}x_{Q_3}+i\sum_{i\neq 3,4}k_{P_i}x_{Q_i}}. \end{aligned} \quad (18.63)$$

Evaluating $[\frac{\partial}{\partial x_{Q_3}}\psi]_{x_{Q_3}=x_{Q_4}}$ one finds

$$\psi'_{Q',P} + \psi'_{Q',P'} = i(k_{P_4}[Q', P] + k_{P_3}[Q', P'])e^{i(k_{P_3}+k_{P_4})x_{Q_3}+i\sum_{i\neq 3,4}k_{P_i}x_{Q_i}}. \quad (18.64)$$

Thus (18.58) gives

$$\begin{aligned} k_{P_4}[Q', P] + k_{P_3}[Q', P'] - k_{P_3}[Q, P] - k_{P_4}[Q, P'] \\ = -ic([Q, P] + [Q, P']). \end{aligned} \quad (18.65)$$

We eliminate $[Q', P']$ from (18.65, 18.55) and get:

$$\boxed{[Q, P'] = \frac{(k_{P_4}-k_{P_3})[Q'P] + ic[QP]}{k_{P_4}-k_{P_3}-ic}}. \quad (18.66)$$

Besides, we must add periodic boundary conditions,

$$\psi(x_1 \dots x_i \dots x_N) = \psi(x_1 \dots x_i + L \dots x_N), \quad i = 1, 2, \dots, N \quad (18.67)$$

which, like in the $c = 0$ case, determine the spectrum. However, unlike the non-interacting problem, the N momenta are not independent. Before tackling this problem I show that the 1d Hubbard Model leads to similar equations.

18.3.2 The Hubbard Model in 1d

Consider N Fermions moving on a linear Hubbard chain of N_s sites

$$H = T \sum_{\langle ij \rangle} \sum_{\sigma} c_{i\sigma}^{\dagger} c_{j\sigma} + U \sum_i n_{i\uparrow} n_{i\downarrow}, \quad (18.68)$$

with nearest-neighbor hopping $T = -1$ and periodic boundary conditions. This problem was solved by Lieb and Wu [73] by a Bethe Ansatz and is a discrete variant of the one of the previous Section. For $N = 1$,

$$\begin{aligned} \langle y | \sum_i c_{i+1}^{\dagger} c_i \sum_x f(x) | x \rangle &= \langle y | \sum_i f(i) | i + 1 \rangle \\ &= \sum_i f(i) \langle y | i + 1 \rangle = \sum_i f(i) \delta(i, y - 1) = f(y - 1); \end{aligned} \quad (18.69)$$

then the elementary Schrödinger equation

$$-[f(x + 1) - f(x - 1)] = Ef(x) \quad (18.70)$$

is solved by $f(x) = e^{ikx}$, $e^{ikN_s} = 1$, $E = -2 \cos(x)$. For N Fermions, let us denote an eigenfunction of H explicitly by

$$|M \downarrow, M' \uparrow \rangle = \sum_{x_1=1}^{N_s} \dots \sum_{x_i=1}^{N_s} \dots \sum_{x_N=1}^{N_s} f(x_1 \dots x_N) | \underbrace{x_1 \dots x_M}_{\downarrow} \underbrace{x_{M+1} \dots x_N}_{\uparrow} \rangle, \quad (18.71)$$

where x_i is the site of electron i ; more simply, we shall also write

$$|x_1 \dots x_M x_{M+1} \dots x_N \rangle \equiv | \underbrace{x_1 \dots x_M}_{\downarrow} \underbrace{x_{M+1} \dots x_N}_{\uparrow} \rangle.$$

The first-quantized schrödinger equation reads:

$$\begin{aligned} - \sum_{i=1}^N [f(x_1, \dots, x_i + 1, \dots, x_N) + f(x_1, \dots, x_i - 1, \dots, x_N)] \\ + U \sum_{\substack{i \in (1, M), j \in (M+1, N) \\ (x_i, x_j)}} \delta(x_i, x_j) f(x_1, \dots, x_i, \dots, x_j \dots x_N) \\ = Ef(x_1, \dots, x_i, \dots, x_N). \end{aligned} \quad (18.72)$$

where the spin in $x_i \pm 1$ is the same as in x_i . In configuration space there are sectors

$$R_Q = \{X : 1 \leq x_{Q_1} \leq x_{Q_2} \dots \leq x_{Q_N} \dots \leq N_s\} \tag{18.73}$$

where Q is a permutation. The \leq inequalities imply a partial superposition: for instance both R_Q and $\mathcal{P}^{(1 \leftrightarrow 2)}R_Q = \{X' : 1 \leq x_{Q_2} \leq x_{Q_1} \dots \leq x_{Q_N} \dots \leq N_s\}$ include the configurations with $\{1 \leq x_{Q_1} = x_{Q_2} \dots \leq x_{Q_N} \dots \leq N_s\}$. Each electron carries two labels; label i marks the electron position along the chain, while Q_i keeps track of its place in the fundamental sequence $1 \dots N$ and of its spin, which is \uparrow for $n \geq M + 1$.

For $U = 0$ momenta would arise because of the need of each one-body orbital to be periodic. In the interacting case things are less simple, but in the *Bethe Ansatz* we consider the electron momenta

$$k_1 < k_2 < \dots < k_N,$$

with their permutations

$$P : \{k_1, k_2 \dots k_N\} \rightarrow \{k_{P_1}, k_{P_2} \dots k_{P_N}\}.$$

The *Bethe Ansatz* for the wave function is the same as in Equation (18.51):

$$f_Q(x_1 \dots x_N) = \sum_P [QP] e^{i \sum_i k_{P_i} x_{Q_i}}. \tag{18.74}$$

f_Q is the amplitude in the sector R_Q in terms of $N!$ coefficients $[QP]$. The k_i and f_Q are unknown, but we know that if Q and Q' differ by the exchange of two electrons of the same spin, $f_Q = -f_{Q'}$.

For example, in the 2-body case, let $k_1 < k_2$; the possible permutations are $Q = P = (1, 2)$ and $Q' = P' = (2, 1)$, the only sectors are $R_Q = \{X : 1 \leq x_1 \leq x_2 \leq N_s\}$, $R_{Q'} = \{X' : 1 \leq x_2 \leq x_1 \leq N_s\}$, and the Bethe ansatz reads

amplitude	sector	
$f_Q(x_1, x_2) = [QP]e^{i(k_1x_1+k_2x_2)} + [QP']e^{i(k_2x_1+k_1x_2)}$	$Q : x_1 \leq x_2$	(18.75)
$f_{Q'}(x_1, x_2) = [Q'P]e^{i(k_1x_2+k_2x_1)} + [Q'P']e^{i(k_2x_2+k_1x_1)}$	$Q' : x_1 \geq x_2$	

If the spins are parallel, U does not act, and the two sectors are disjoint.

The Schrödinger equation Equation (18.72) links the amplitude $f(X)$ of a given configuration $X = (x_1, \dots, x_i, \dots, x_j, \dots, x_N)$ to those that can be reached from X in one step, that is, applying H once. If $X \in R_Q$, applying H we remain in R_Q , if X is an interior point, that is $|x_i - x_j| > 1, \forall i \neq j$; otherwise X is a frontier point. We get different conditions from in the two cases.

X is an Interior Point

Let $f_Q(x_1 \dots x_N) = \sum_P [QP] e^{i \sum_n k_{P_n} x_{Q_n}}$; consider the contribution from a particular P to the $i = r$ term in the i sum of Equation (18.72): we obtain the kinetic term

$$\begin{aligned}
 & - [f_Q(x_1 \dots x_r + 1, \dots x_N) + f_Q(x_1 \dots x_r - 1, \dots x_N)] \\
 & = -(e^{ik_{P_r}} + e^{-ik_{P_r}})[QP] e^{i \sum_n k_{P_n} x_{Q_n}}; \tag{18.76}
 \end{aligned}$$

summing over i we get, independently of P ,

$$E = -2 \sum_{j=1}^N \cos(k_j). \tag{18.77}$$

Note that U enters indirectly, by modifying the k values. There are no interior points if the filling is too high, because then double occupations are unavoidable; however (18.77) holds in general.

X is a Frontier Point

Consider any configuration in (18.74) with at least a double occupation on a site that must be among the first M and among the last M' . For a given Q , in (18.73) for some i , $x_{Q_i} = x_{Q_{i+1}}$; then, in Equation (18.74) for given Q, P one finds at the exponent a contribution $(k_{P_i} + k_{P_{i+1}})x_{Q_i}$. However, if P' is the permutation obtained from P by exchanging i and $i + 1$, the resulting exponential is the same. For $X \in Q$, the permutations P and P' both contribute to f_Q with the same exponential factor,

$$([Q, P] + [Q, P']) e^{i(k_{P_i} + k_{P_{i+1}})x_{Q_i}} e^{i \sum_{m \neq i, i+1} k_{P_m} x_{Q_m}}.$$

The same exponential also arises from the permutation Q' obtained from Q by exchanging $i, i + 1$. Indeed, the contribution to $f_{Q'}$ from P and P' is

$$([Q', P] + [Q', P']) e^{i(k_{P_i} + k_{P_{i+1}})x_{Q_i}} e^{i \sum_{m \neq i, i+1} k_{P_m} x_{Q_m}}.$$

We must ensure that f is single-valued, that is, $\{X \in R_Q, X \in R_{Q'}\} \implies f_Q(X) = f_{Q'}(X)$. This reproduces the condition (18.55)

$$\boxed{[QP] + [QP'] = [Q'P] + [Q'P']}. \tag{18.78}$$

Nesting of a Two-Body Problem in the Many-Body One

From the above, we may conclude that 1) any double occupancy arises as an equality $x_i = x_{i+1}$ 2) configurations with double occupancies are at the border between sectors and belong to neighboring ones, defined by $x_{Q_i} \leq x_{Q_{i+1}}$, and

by $x_{Q_i} \geq x_{Q_{i+1}}$. 3) (18.77) must hold in both sectors. Let site i be the same as $i + 1$ (double occupation). In sector Q defined by $x_{Q_i} \leq x_{Q_{i+1}}$, the two electrons are those labelled Q_i, Q_{i+1} ; there is superposition with the sector $Q' = \mathcal{P}^{(i \leftrightarrow i+1)}Q$ where the permutations differ by $Q_i \leftrightarrow Q_{i+1}$ (\mathcal{P} is a transposition). The contribution to the Bethe function arising from a permutation P of momenta is

$$[QP]e^{i(k_{P_i}x_{Q_i} + k_{P_{i+1}}x_{Q_{i+1}})}e^{i\sum_{m \neq i, i+1} k_{P_m}x_{Q_m}},$$

however in the case $x_{Q_i} = x_{Q_{i+1}}$, also belonging to the sector there is mixing of the permutations P, P' that differ by $i \leftrightarrow i + 1$; the exponential is the same, $e^{i\sum_{m \neq i, i+1} k_{P_m}x_{Q_m}}$. To proceed, we introduce the amplitude

$$\begin{aligned} \varphi_Q^{PP'}(x_{Q_i}, x_{Q_{i+1}}) &\equiv [QP]e^{i(k_{P_i}x_{Q_i} + k_{P_{i+1}}x_{Q_{i+1}})} \\ &+ [QP']e^{i(k_{P'_i}x_{Q_i} + k_{P'_{i+1}}x_{Q_{i+1}})} \\ &= [QP]e^{i(k_{P_i}x_{Q_i} + k_{P_{i+1}}x_{Q_{i+1}})} + [QP']e^{i(k_{P_{i+1}}x_{Q_i} + k_{P_i}x_{Q_{i+1}})}, \end{aligned} \quad (18.79)$$

such that the contribution to f_Q arising from P and P' is:

$$\psi_Q^{PP'} = \varphi_Q^{PP'} e^{i\sum_{m \neq i, i+1} k_{P_m}x_{Q_m}}, \quad x_{Q_i} \leq x_{Q_{i+1}}. \quad (18.80)$$

The sector Q' defined by $x_{Q'_i} \leq x_{Q'_{i+1}}$, gets from permutations P, P' the amplitude

$$\psi_{Q'}^{PP'} = \varphi_{Q'}^{PP'} e^{i\sum_{m \neq i, i+1} k_{P_m}x_{Q_m}}, \quad x_{Q_i} \geq x_{Q_{i+1}} \quad (18.81)$$

(same exponential as in (18.80)) and

$$\begin{aligned} \varphi_{Q'}^{PP'} &= [Q'P]e^{i(k_{P_i}x_{Q'_i} + k_{P_{i+1}}x_{Q'_{i+1}})} + [Q'P']e^{i(k_{P'_i}x_{Q'_i} + k_{P'_{i+1}}x_{Q'_{i+1}})} \\ &= [Q'P]e^{i(k_{P_i}x_{Q_{i+1}} + k_{P_{i+1}}x_{Q_i})} + [Q'P']e^{i(k_{P_{i+1}}x_{Q_{i+1}} + k_{P_i}x_{Q_i})} \end{aligned} \quad (18.82)$$

There is superposition of sectors, so in order to write (18.72) and obtain relations among the coefficients we must consider

$$\psi_{QQ'}^{PP'} = \varphi_{QQ'}^{PP'} e^{i\sum_{m \neq i, i+1} k_{P_m}x_{Q_m}}, \quad (18.83)$$

where one understands that

$$\varphi_{QQ'}^{PP'} = \begin{cases} \varphi_Q^{PP'} & x_{Q_i} \leq x_{Q_{i+1}} \\ \varphi_{Q'}^{PP'} & x_{Q_i} > x_{Q_{i+1}}. \end{cases} \quad (18.84)$$

We define the set of the indices that in a given sector correspond to electrons that do not participate to double occupations: $\mathcal{S}_Q := \{i : x_{Q_i} \neq$

$x_{Q_{r_i-1}}, x_{Q_{r_i+1}}$ } Now, the first member of (18.72) involves one sum on electrons; the contribution of those that do not participate to double occupations is the correspondent piece of the energy eigenvalue (18.77):

$$\begin{aligned} & \sum_{r,r \in \mathcal{S}_Q}^N \left[\psi_{QQ'}^{PP'}(x_1, \dots, x_{Q_r} + 1, \dots, x_N) + \psi_{QQ'}^{PP'}(x_1, \dots, x_{Q_r} - 1, \dots, x_N) \right] \\ &= -2 \sum_{r,r \in \mathcal{S}_Q}^N \cos(k_{P_r}) \psi_{QQ'}^{PP'}. \end{aligned} \tag{18.85}$$

Since the eigenvalue is (18.77), the two-body function $\varphi_{QQ'}^{PP'}$ must contribute, and obeys in $x_{Q_i} = x_{Q_{i+1}} = x$ to (18.72) with eigenvalue $-2 \cos(k_{P_i}) - 2 \cos(k_{P_{i+1}})$. Equation (18.72) grants that

$$\begin{aligned} & -[\varphi_{QQ'}^{PP'}(x + 1, x) + \varphi_{QQ'}^{PP'}(x - 1, x) + \varphi_{QQ'}^{PP'}(x, x + 1) \\ & \quad + \varphi_{QQ'}^{PP'}(x, x - 1)] + U \varphi_{QQ'}^{PP'}(x, x) \\ &= -2(\cos(k_{P_i}) + \cos(k_{P_{i+1}})) \varphi_{QQ'}^{PP'}(x, x). \end{aligned} \tag{18.86}$$

The 2 body problem is nested into the N body one in such the way that everything generalizes. In view of (18.84), Equation (18.86) means

$$\begin{aligned} & -[\varphi_Q^{PP'}(x + 1, x) + \varphi_Q^{PP'}(x - 1, x) \\ & \quad + \varphi_Q^{PP'}(x, x + 1) + \varphi_Q^{PP'}(x, x - 1)] + U \varphi_Q^{PP'}(x, x) \\ &= -2(\cos(k_{P_i}) + \cos(k_{P_{i+1}})) \varphi_Q^{PP'}(x, x). \end{aligned} \tag{18.87}$$

Substituting (18.79,18.82), eliminating the common factor $e^{i(k_{P_i} + k_{P_{i+1}})x}$ and making the substitutions:

$\varphi_Q^{PP'}(x + 1, x) \rightarrow$	$[Q'P]e^{ik_{P_{i+1}}} + [Q'P']e^{ik_{P_i}}$	(18.88)
$\varphi_Q^{PP'}(x - 1, x) \rightarrow$	$[QP]e^{-ik_{P_i}} + [QP']e^{-ik_{P_{i+1}}}$	
$\varphi_Q^{PP'}(x, x + 1) \rightarrow$	$[QP]e^{ik_{P_{i+1}}} + [QP']e^{ik_{P_i}}$	
$\varphi_Q^{PP'}(x, x - 1) \rightarrow$	$[Q'P]e^{-ik_{P_i}} + [Q'P']e^{-ik_{P_{i+1}}}$	
$\varphi_Q^{PP'}(x, x) \rightarrow$	$[QP] + [QP']$	

we obtain

$$\begin{aligned} & [QP](e^{ik_{P_i}} + e^{-ik_{P_{i+1}}} + U) + [QP'](e^{-ik_{P_i}} + e^{ik_{P_{i+1}}} + U) \\ &= [Q'P](e^{ik_{P_{i+1}}} + e^{-ik_{P_i}}) + [Q'P'](e^{ik_{P_i}} + e^{-ik_{P_{i+1}}}). \end{aligned} \tag{18.89}$$

We eliminate $[Q'P]$ using (18.78), and find

$$[QP] = \frac{-\frac{U}{2i}[QP'] + (\sin(k_{P_i}) - \sin(k_{P_{i+1}}))[Q'P']}{\sin(k_{P_i}) - \sin(k_{P_{i+1}}) + \frac{U}{2i}}. \quad (18.90)$$

This looks like a slightly modified version of Equation (18.66). It is instructive to work out the explicit solution of the problem with 2 electrons, see Problem 18.2; it is somewhat harder than one could expect.

18.3.3 The Periodic Boundary Conditions

The problems of the last two Subsections are closely related and can be carried out by similar means; we choose to refer to the continuous case in the following. We need to find efficient ways to impose the periodic boundary conditions (18.67). Following Yang[74], we arrange the $[Q, P]$ amplitudes as a $N! \times N!$ matrix and consider the column with some particular P :

$$\xi_P = \begin{pmatrix} [1, 2, 3, \dots, N, P] \\ [Q_2, P] \\ \dots \\ [Q_{N!}, P] \end{pmatrix} \quad (18.91)$$

Let ξ_0 denote the column corresponding to the fundamental (or identity) permutation $I = \{1, 2, 3, \dots, N\}$. We cast the equations (18.66) in a more convenient form,

$$[QP'] = \frac{[Q'P] - \lambda_{ij}[QP]}{1 + \lambda_{ij}}, \quad \lambda_{ij} = \frac{ic}{k_i - k_j}. \quad (18.92)$$

This is a relation involving two columns, in shorthand³:

$$\xi_{P'} = Y_{ij}^{i,j} \xi_P, \quad P' = \mathcal{P}^{(i \leftrightarrow j)} P, \quad ; j = i + 1. \quad (18.93)$$

To write down the column-switching operator $Y_{ij}^{a,b}$ which performs a transposition of consecutive indices, we also need to introduce a row-switching operator $\tilde{\mathcal{P}}_{Q \rightarrow Q'}^{b \leftrightarrow a}$ which acts on the Q_i and exchanges a and b . Indeed,

$$Y_{ij}^{a,b} = \frac{-\lambda_{ij} + \tilde{\mathcal{P}}_{Q \rightarrow Q'}^{b \leftrightarrow a}}{1 + \lambda_{ij}} \equiv a_{ij} + b_{ij} P^{ab}, \quad b = a + 1. \quad (18.94)$$

The upper indices of $Y_{ij}^{a,b}$ give the position of the consecutive electron pair in the list, the lower indices the *identity* of the elements; for example, for $N=4$, $Y_{24}^{3,4}$ exchanges the third and fourth elements in the list, provided that they

³When it is clear from the context which are the i and j indices we are referring to, we shall also continue to use the shorthand notation P' for the permutation of momenta obtained from P by exchanging k_i and k_j , and shall use $\xi_{P'}$ for the column corresponding to it.

are 2 and 4, giving $Y_{24}^{3,4} \xi_{3124} = \xi_{3142}$; moreover, $Y_{14}^{2,3} Y_{24}^{3,4} \xi_{3124} = \xi_{3412}$, and so on; any ξ_P can be obtained from ξ_0 by applying products of Y operators.

The action of $Y_{ij}^{a,b}$ is the same as the action of P_{ij} on any permutation P . From this very fact one that can prove some identities, that can of course be checked starting from the definition of Y . Since $P_{ij} P_{ji} = 1$,

$$Y_{ij}^{a,b} Y_{ji}^{a,b} = 1 \tag{18.95}$$

and since $P_{ij} P_{kl} = P_{kl} P_{ij}$,

$$Y_{ij}^{ab} Y_{kl}^{cd} = Y_{kl}^{cd} Y_{ij}^{ab}. \tag{18.96}$$

Moreover, one can check that $P_{12} P_{13} P_{23} = P_{23} P_{13} P_{12}$; in this way one finds that

$$Y_{jk}^{a,b} Y_{ik}^{b,c} Y_{ij}^{a,b} = Y_{ij}^{b,c} Y_{ik}^{a,b} Y_{jk}^{b,c}. \tag{18.97}$$

Here is the operator that exchanges both rows and columns:

$$X_{ij} = \tilde{P}_{Q \rightarrow Q'}^{i \leftrightarrow j} Y_{ij}^{i,j} = \frac{1 - \tilde{P}_{Q \rightarrow Q'}^{i \leftrightarrow j} \lambda_{ij}}{1 + \lambda_{ij}}, \quad j = i + 1. \tag{18.98}$$

This operator lets the electron i to overtake the electron $j=i+1$ (recall that the phase factors have already been dealt with). For example if $N = 3$,

$$\xi_0 = \begin{pmatrix} \{ \{1, 2, 3\}, \{1, 2, 3\} \} \\ \{ \{2, 1, 3\}, \{1, 2, 3\} \} \\ \{ \{1, 3, 2\}, \{1, 2, 3\} \} \\ \{ \{3, 2, 1\}, \{1, 2, 3\} \} \\ \{ \{2, 3, 1\}, \{1, 2, 3\} \} \\ \{ \{3, 1, 2\}, \{1, 2, 3\} \} \end{pmatrix} \tag{18.99}$$

and one finds

$$X_{1,3} \xi_0 = \begin{pmatrix} \{ \{3, 2, 1\}, \{3, 2, 1\} \} \\ \{ \{2, 3, 1\}, \{3, 2, 1\} \} \\ \{ \{3, 1, 2\}, \{3, 2, 1\} \} \\ \{ \{1, 2, 3\}, \{3, 2, 1\} \} \\ \{ \{2, 1, 3\}, \{3, 2, 1\} \} \\ \{ \{1, 3, 2\}, \{3, 2, 1\} \} \end{pmatrix}, \quad X_{2,1} X_{1,3} \xi_0 = \begin{pmatrix} \{ \{3, 1, 2\}, \{3, 1, 2\} \} \\ \{ \{1, 3, 2\}, \{3, 1, 2\} \} \\ \{ \{3, 2, 1\}, \{3, 1, 2\} \} \\ \{ \{2, 1, 3\}, \{3, 1, 2\} \} \\ \{ \{1, 2, 3\}, \{3, 1, 2\} \} \\ \{ \{2, 3, 1\}, \{3, 1, 2\} \} \end{pmatrix} \tag{18.100}$$

Now if we consider the amplitude

$$[Q, P] e^{i \sum_i k_{P_i} x_{Q_i}}$$

in sector Q ($x_{Q_i} \leq x_{Q_{i+1}}$) and consider the transformation

$$x_{Q_1} \rightarrow x_{Q_1} + L,$$

we land in the sector $\tilde{Q} : x_{Q_2} \leq x_{Q_3} \leq \dots x_{Q_1}$ with $\tilde{P} : k_{P_2}, k_{P_3}, \dots k_{P_1}$ with an amplitude

$$e^{ik_{P_1}L} [\tilde{Q}, \tilde{P}] e^{i \sum_i k_{P_i} x_{Q_i}}.$$

Since the wave function must be single valued, this implies

$$[Q, P] = e^{ik_{P_1}L} [\tilde{Q}, \tilde{P}]. \quad (18.101)$$

Consider for instance the last but one component $[\{2, 3, 1\}, \{1, 2, 3\}]$ of ξ_0 in (18.99) and its evolution in (18.100): the boundary condition is

$$[\{1, 2, 3\}, \{3, 1, 2\}] = e^{ik_1L} [\{2, 3, 1\}, \{1, 2, 3\}]. \quad (18.102)$$

In general, by the same reasoning,

$$e^{ik_jL} \xi_0 = X_{j+1,j} X_{j+2,j} \cdots X_{N,j} X_{1,j} X_{2,j} \cdots X_{j-1,j} \xi_0. \quad (18.103)$$

Thus, ξ_0 is a simultaneous eigenfunction of N operators; these however may be shown to commute, so we can limit ourselves to consider one of them, e.g. letting $j = N$.

18.3.4 Spin Chain Analogy

Usually a problem is practically solved when reduced to a linear system, but this is not the case here. Since there are $N!^2$ amplitudes $[P, Q]$ and for each amplitude there are $N-1$ consecutive $i, i+1$ pairs, this is a large homogeneous system and cannot practically be solved by the usual methods, unless N is rather small. Yang achieved a solution by the use of the symmetry, a very smart and profound one.

If all the electrons have parallel spins, $\tilde{\mathcal{P}}_{Q \rightarrow Q'}^{i \leftrightarrow j} = -1, \Rightarrow X_{ij} \equiv 1$ and (18.103) yields $e^{ik_jL} = 1$. This is nothing but the condition of the non-interacting theory, as one should expect, since parallel spin electrons cannot be at the same position. Recalling Sect.(9.8), more generally ξ_0 is associated with a Yang diagram with one or two columns, and the spin function Φ then belongs to the conjugate representation. We go to the conjugate representation by change $\tilde{\mathcal{P}}_{Q \rightarrow Q'}^{b \leftrightarrow a} \rightarrow -\tilde{\mathcal{P}}_{Q \rightarrow Q'}^{b \leftrightarrow a}$, and to this end we introduce

$$X'_{ij} = \frac{1 + \tilde{\mathcal{P}}_{Q \rightarrow Q'}^{i \leftrightarrow j} \lambda_{ij}}{1 + \lambda_{ij}} \quad (18.104)$$

where $\tilde{\mathcal{P}}$ now operates on the spin variables. The eigenvalue equation is

$$Z_j \Phi \equiv X'_{j+1,j} X'_{j+2,j} \cdots X'_{N,j} X'_{1,j} X'_{2,j} \cdots X'_{j-1,j} \Phi = \mu_j \Phi, \quad (18.105)$$

but, since since we are looking for the spin part of the same wave function,

$$\mu_j = e^{ik_j L}. \tag{18.106}$$

These are N equations, but each yields all the eigenvalues since they can be shown to commute; so we can limit ourselves to solve

$$Z_N \Phi = \mu_N \Phi, \quad Z_N = X'_{1N} X'_{2N} \cdots X'_{N-1,N}. \tag{18.107}$$

One can interpret Φ as the wave function of N spins on a ring, $\Phi = \Phi(y_1, y_2, \dots, y_m; z_1, z_2, \dots, z_{N-M})$ where the integers y_1, y_2, \dots, y_m denote the positions along the chain of the M reversed spins, and the z 's those of the $N-M$ up spins. This may be taken to be symmetric in the interchange of y 's and separately in the interchange of z 's while any attempt to symmetrize simultaneously in variables belonging to the two sets must give 0. The same information is contained in a *reduced wave function* that we denote by $\Phi \equiv \Phi(y_1, y_2, \dots, y_M)$, with the y 's in increasing order, which depends on M variables only; for $N - M$ spins up and M spins down the components are just $\binom{N}{M}$, that is, the size of the problem is substantially reduced.

Three Spins, $\uparrow, \uparrow, \downarrow$

Since for parallel spins the problem is trivial, let us start considering $M = 1$ reversed spin. For example if $N = 3$, we may replace the unknown 6-component amplitude (18.99) by the 3-component reduced wave function

$$\Phi = \begin{pmatrix} \Phi(1) \\ \Phi(2) \\ \Phi(3) \end{pmatrix}, \tag{18.108}$$

where the components can be interpreted as the amplitude that the overturned spin comes first, second and third, respectively. In terms of the full wave function for the three spins, $\Phi(1)$ stands for $[\{\downarrow, 2, 3\}, \{1, 2, 3\}] = [\{\downarrow, 3, 2\}, \{1, 2, 3\}]$; $\Phi(2)$ is the amplitude that spin 2 is down and is symmetric in 1 and 3, and so on. The full ξ_0 can be obtained from the reduced Φ . Let us work out⁴ the eigenvalue equation (18.107)

$$Z_3 \Phi = \mu_3 \Phi, \quad Z_3 = X'_{13} X'_{23}. \tag{18.109}$$

Recalling (18.104), and setting

$$a_{ij} = \frac{1}{1 + \lambda_{23}} \quad b_{ij} = \frac{\lambda_{23}}{1 + \lambda_{23}} \tag{18.110}$$

we see that $a_{ij} + b_{ij} = 1$ and $X'_{ij} = a_{ij} + b_{ij} \tilde{\mathcal{P}}_{Q \rightarrow Q'}^{i \leftrightarrow j}$; $X'_{23} \Phi(1) = \Phi(1)$, but X'_{23} mixes the other components:

⁴Here and below this section involves some algebra which is quite elementary but somewhat tedious; using a computer code is a good idea.

$$\begin{pmatrix} a_{23} & b_{23} \\ b_{23} & a_{23} \end{pmatrix} \begin{pmatrix} \Phi(2) \\ \Phi(3) \end{pmatrix} = \begin{pmatrix} \Phi(2)[a_{23} + b_{23} \frac{\Phi(3)}{\Phi(2)}] \\ \Phi(3)[a_{23} + b_{23} \frac{\Phi(2)}{\Phi(3)}] \end{pmatrix}. \quad (18.111)$$

The solution is gained by the following inspired *ansatz*, with some real Λ :

$$\frac{\Phi(3)}{\Phi(2)} = \frac{k_2 - \Lambda + \frac{ic}{2}}{k_3 - \Lambda - \frac{ic}{2}}$$

which means, the ratio of two consecutive components is obtained as the ratio of two linear functions. Indeed, now we show that we can solve the boundary condition eigenvalue problem by writing

$$\Phi = \begin{pmatrix} 1 \\ \frac{k_1 - \Lambda + ic/2}{k_2 - \Lambda - ic/2} \\ \frac{k_1 - \Lambda + ic/2}{k_2 - \Lambda - ic/2} \frac{k_2 - \Lambda + ic/2}{k_3 - \Lambda - ic/2} \end{pmatrix}. \quad (18.112)$$

It holds:

$$\begin{pmatrix} a_{23} & b_{23} \\ b_{23} & a_{23} \end{pmatrix} \begin{pmatrix} \Phi(2) \\ \Phi(3) \end{pmatrix} = \begin{pmatrix} \mu'_3 \Phi(2) \\ \frac{\Phi(3)}{\mu'_2} \end{pmatrix}, \quad (18.113)$$

where I have introduced

$$\mu'_j = \frac{k_j - \Lambda + ic/2}{k_j - \Lambda - ic/2}, \quad (18.114)$$

a simplify command yields immediately

$$\frac{\mu'_j - a_{ij}}{b_{ij}} = \frac{k_i - \Lambda + ic/2}{k_j - \Lambda - ic/2}. \quad (18.115)$$

Next, to apply X'_{13} to the result, we compute

$$\begin{pmatrix} a_{13} & b_{13} \\ b_{13} & a_{13} \end{pmatrix} \begin{pmatrix} \Phi(1) \\ \frac{\Phi(3)}{\mu'_2} \end{pmatrix} = \begin{pmatrix} \mu'_3 \Phi(1) \\ \frac{\Phi(3)}{\mu'_2 \mu'_1} \end{pmatrix}. \quad (18.116)$$

Thus,

$$Z_3 \Phi = \mu'_3 \begin{pmatrix} 1 \\ \frac{\Phi(2)}{\mu'_3 \mu'_2 \mu'_1} \\ \frac{\Phi(3)}{\mu'_3 \mu'_2 \mu'_1} \end{pmatrix}. \quad (18.117)$$

Now we can solve the eigenvalue equation by requiring that $\mu'_j = \mu_j$ and that

$$\mu_1 \mu_2 \mu_3 = 1; \quad (18.118)$$

this means that a translation by L of the whole system has no effect. Putting together (18.106) and (18.114) one gets

$$e^{ik_j L} = \frac{k_j - \Lambda + ic/2}{k_j - \Lambda - ic/2} \quad (18.119)$$

and with (18.118) one can determine Λ and the momenta. The beauty of this approach is that it can be fully extended.

N Spins, 1 Overturned

The above results extend immediately to arbitrary N ; thus,

$$\Phi(\Lambda, y) = \prod_{j=1}^{y-1} \left(\frac{k_j - \Lambda + ic/2}{k_{j+1} - \Lambda - ic/2} \right), \quad (18.120)$$

where the integer y specifies the position of the overturned spin along the chain.

General Case

The above solution extends to any N and M via the following generalized Bethe ansatz involving M different Λ parameters:

$$\Phi = \prod_{P \in S_M} a(P) \Phi(\Lambda_{P_1}, y_1) \Phi(\Lambda_{P_2}, y_2) \cdots \Phi(\Lambda_{P_M}, y_M), \quad (18.121)$$

with the same Φ as before; here given two permutations P and P' that differ by the exchange of elements γ and $\gamma + 1$ the coefficients obey [142]

$$a(P') = a(P) \frac{\Lambda_{P\gamma} - \Lambda_{P(\gamma+1)} + ic}{\Lambda_{P\gamma} - \Lambda_{P(\gamma+1)} - ic}. \quad (18.122)$$

The extension of (18.119) is

$$e^{ik_j L} = \prod_{\beta} \frac{k_j - \Lambda_{\beta} + ic/2}{k_j - \Lambda_{\beta} - ic/2}. \quad (18.123)$$

The general proof that the solution has the $[N - M, M]$ permutation symmetry may be found in [142]. Note that the ansatz (18.121) describes one kind of particles, the down-spin electrons, while the up-spin electrons are reduced to sites in an effective chain; Yang's procedure reduced by 1 the number of particle species.

Problems

18.1. Work out the L matrix (Section 18.6) for the ground state of the repulsive H_2 molecular model $H(t, U)$ (14.58) and for the canonically transformed, attractive model (21.32) and compare the results for $\frac{U}{t} = 7$.

18.2. Work out the detailed solution for the Hubbard chain with $N = 2$ electrons. Verify the solution by writing down explicit energy eigenvalues for $N_s = 3$.

Part VI

Appendices

19 Appendix 1: Zero-point Energy in a Pillbox

Setting $\frac{b}{L} = q_x$, $\frac{c}{L} = q_y$, $d^2q = \left(\frac{a}{s}\right)^2 d^2k$, (1.29) yields:

$$U(s) = \hbar c \pi L^2 \sum_a \left(\frac{a}{s}\right)^3 \int_{k_x, k_y > 0} d^2k \sqrt{1+k^2} e^{-\alpha\left(\frac{a}{s}\right)\sqrt{1+k^2}}. \quad (19.1)$$

The angle integral from 0 to $\frac{\pi}{2}$ yields

$$\begin{aligned} U(s) &= \frac{\hbar c \pi^2 L^2}{4s^3} \sum_a a^3 \int_0^\infty dz \sqrt{1+z} e^{-\alpha\left(\frac{a}{s}\right)\sqrt{1+z}} \\ &= -\frac{\hbar c \pi^2 L^2}{4s^3} \left(\frac{d}{d\alpha}\right)^3 \sum_a \int_0^\infty \frac{dz}{1+z} e^{-\alpha\left(\frac{a}{s}\right)\sqrt{1+z}}; \end{aligned} \quad (19.2)$$

the summation is performed by $\sum_1^\infty e^{-n\gamma} = \frac{1}{1-e^{-\gamma}} - 1 = \frac{1}{e^\gamma - 1}$; thus

$$U(s) = -\frac{\hbar c \pi^2 L^2}{4} \left(\frac{d}{d\alpha}\right)^3 \int_0^\infty \frac{dz}{1+z} \frac{1}{e^{\frac{\alpha}{s}\sqrt{1+z}} - 1}. \quad (19.3)$$

By the substitution $u = \sqrt{1+z}$, and doing one of the derivatives one gets

$$U(s) = -\frac{\hbar c \pi^2 L^2}{2} \left(\frac{d}{d\alpha}\right)^2 \left[-\frac{1}{s} \int_1^\infty du \frac{e^{\frac{\alpha}{s}u}}{\left(e^{\frac{\alpha}{s}u} - 1\right)^2} \right]; \quad (19.4)$$

and putting

$$\int_1^\infty du \frac{e^{\frac{\alpha}{s}u}}{\left(e^{\frac{\alpha}{s}u} - 1\right)^2} = \frac{1}{\alpha} \int_{\frac{\alpha}{s}}^\infty dx \frac{1}{(x-1)^2} = \frac{1}{\alpha} \frac{1}{e^{\frac{\alpha}{s}} - 1}. \quad (19.5)$$

Finally,

$$U(s) = \frac{\hbar c \pi^2 L^2}{2} \left(\frac{d}{d\alpha}\right)^2 \left(\frac{1}{\alpha} \frac{1}{e^{\frac{\alpha}{s}} - 1} \right). \quad (19.6)$$

20 Appendix II-Character Tables

$C_3 = Z_3$	I	C_3	C_3^2	$\varepsilon = e^{\frac{2i\pi}{3}}$
A_1	1	1	1	z
E	$\begin{Bmatrix} 1 \\ 1 \end{Bmatrix}$	$\begin{Bmatrix} \varepsilon \\ \varepsilon^* \end{Bmatrix}$	$\begin{Bmatrix} \varepsilon^* \\ \varepsilon \end{Bmatrix}$	(x, y)

C_{2v}	I	C_2	σ_v	σ'_v	$g = 4$
A_1	1	1	1	1	z
A_2	1	1	-1	-1	xy, R_z
B_1	1	-1	1	-1	x, R_y
B_2	1	-1	-1	1	y, R_x

C_{3v}	I	$2C_3$	$3\sigma_v$	$g = 6$
A_1	1	1	1	z
A_2	1	1	-1	R_z
E	2	-1	0	(x, y)

C_{4v}	I	C_2	$2C_4$	$2\sigma_v$	$2\sigma_d$	$g = 8$
A_1	1	1	1	1	1	z
A_2	1	1	1	-1	-1	R_z
B_1	1	1	-1	1	-1	$x^2 - y^2$
B_2	1	1	-1	-1	1	xy
E	2	-2	0	0	0	(x, y)

C_{5v}	I	$2C_5$	$2C_5^2$	$5\sigma_v$	$g = 10, \theta = \frac{2\pi}{5}$
A_1	1	1	1	1	z
A_2	1	1	1	-1	R_z
E_1	2	$2 \cos \theta$	$2 \cos 2\theta$	0	(x, y)
E_2	2	$2 \cos 2\theta$	$2 \cos \theta$	0	$(xy, x^2 - y^2)$

C_{6v}	I	C_2	$2C_3$	$2C_6$	$3\sigma_d$	$3\sigma_v$	$g = 12$
A_1	1	1	1	1	1	1	z
A_2	1	1	1	1	-1	-1	R_z
B_1	1	-1	1	-1	-1	1	
B_2	1	-1	1	-1	1	-1	
E_1	2	-2	-1	1	0	0	$(x, y), (R_x, R_y)$
E_2	2	2	-1	-1	0	0	$(xy, x^2 - y^2)$

$C_{\infty v}$	I	C_2	$2C_\omega$	σ_v	$g = \infty$
$A_1 (\Sigma^+)$	1	1	1	1	z
$A_2 (\Sigma^-)$	1	1	1	-1	R_z
$E_1 (\Pi)$	2	-2	$2 \cos \omega$	0	(x, y)
$E_2 (\Delta)$	2	2	$2 \cos 2\omega$	0	$(xy, x^2 - y^2)$

D_2	I	C_2^z	C_2^y	C_2^x	$g = 4$
A_1	1	1	1	1	x^2, y^2, z^2
B_1	1	1	-1	-1	z, xy, R_z
B_2	1	-1	1	-1	y, xz, R_y
B_3	1	-1	-1	1	x, yz, R_x

D_3	I	$2C_3$	$2C_2'$	$g = 6$			D_4	I	C_2	$2C_4$	C_2'	$2C_2''$	$g = 8$	
A_1	1	1	1	$z^2, x^2 + y^2$			A_1	1	1	1	1	1	$z^2, x^2 + y^2$	
A_2	1	1	-1	z, R_z			A_2	1	1	1	-1	-1	z	
E	2	-1	0	$(x, y), (R_x, R_y)$			B_1	1	1	-1	1	-1	$x^2 - y^2$	
							B_2	1	1	-1	-1	1	xy	
							E	2	-2	0	0	0	$(x, y), (R_x, R_y)$	

D_{3h}	I	σ_h	$2C_3$	$2S_3$	$3C_2'$	$3\sigma_v$	$g = 12$	
A_1	1	1	1	1	1	1	z^2	
A_2	1	1	1	1	-1	-1	R_z	
A_1'	1	-1	1	-1	1	-1		
A_2'	1	-1	1	-1	-1	1	z	
E	2	2	-1	-1	0	0	$(x, y), (xy, x^2 - y^2)$	
E'	2	-2	-1	1	0	0	$(xz, yz), (R_x, R_y)$	

D_{6h}	E	$2C_6$	$2C_3$	C_2	$3C_2'$	$3C_2''$	i	$2S_3$	$2S_6$	σ_h	$3\sigma_d$	$3\sigma_v$	$g = 24$	
A_{1g}	1	1	1	1	1	1	1	1	1	1	1	1		
A_{2g}	1	1	1	1	-1	-1	1	1	1	1	-1	-1	R_z	
B_{1g}	1	-1	1	-1	1	-1	1	-1	1	-1	1	-1		
B_{2g}	1	-1	1	-1	-1	1	1	-1	1	-1	-1	1		
E_{1g}	2	1	-1	-2	0	0	2	1	-1	-2	0	0	(R_x, R_y)	
E_{2g}	2	-1	-1	2	0	0	2	-1	-1	2	0	0	$(x^2 - y^2, xy)$	
A_{1u}	1	1	1	1	1	-1	-1	-1	-1	-1	-1	-1		
A_{2u}	1	1	1	1	-1	-1	-1	-1	-1	-1	1	1	z	
B_{1u}	1	-1	1	-1	1	-1	-1	1	-1	1	-1	1		
B_{2u}	1	-1	1	-1	-1	1	-1	1	-1	1	1	-1		
E_{1u}	2	1	-1	-2	0	0	-2	-1	1	2	0	0	(x, y)	
E_{2u}	2	-1	-1	2	0	0	-2	1	1	-2	0	0		

Double Groups

C'_{3v}	E	\bar{E}	C_3	C_3^2	$3\sigma_v$	$3\sigma_v \bar{E}$
			$C_3^3 \bar{E}$	$C_3 \bar{E}$		
A_1	1	1	1	1	1	1
A_2	1	1	1	1	-1	-1
E	2	2	-1	-1	0	0
$E_{1/2}$	2	-2	1	-1	0	0
Γ^5	1	-1	-1	1	i	$-i$
Γ^6	1	-1	-1	1	$-i$	i

C'_{4v}	E	\bar{E}	C_4	C_4^3	C_2	$2C_2'$	$2C_2''$
			$C_4^3 \bar{E}$	$C_4 \bar{E}$	$C_2 \bar{E}$	$2C_2' \bar{E}$	$2C_2'' \bar{E}$
A_1'	1	1	1	1	1	1	1
A_2'	1	1	1	1	1	-1	-1
B_1'	1	1	-1	-1	1	1	-1
B_2'	1	1	-1	-1	1	-1	1
E_1'	2	2	0	0	-2	0	0
E_2'	2	-2	$\sqrt{2}$	$-\sqrt{2}$	0	0	0
E_3'	2	-2	$-\sqrt{2}$	$\sqrt{2}$	0	0	0

21 Proof of the Wigner-Eckart Theorem

Here I reinforce the intuitive discussion given in Chapter 9 by a proof of the Wigner-Eckart theorem :

$$\langle \alpha i | T_q^{(\gamma)} | \beta k \rangle = \langle \alpha || T^{(\gamma)} || \beta \rangle \langle \alpha i | \gamma p \beta k \rangle,$$

where the *reduced matrix element* $\langle \alpha || T^{(\gamma)} || \beta \rangle$ does not depend on the components; $\langle \alpha i | \gamma p \beta k \rangle$ is the Clebsch-Gordan coefficient.

Here, $|\alpha i \rangle$ and $|\beta j \rangle$ denote the components of bases of irreps Γ^α and Γ^β (that could also coincide) and $T_p^{(\gamma)}$ the p component of an irreducible tensor

$$R T_p^{(\gamma)} R^{-1} = \sum_q T_q^{(\gamma)} D_{qp}^{(\gamma)}(R). \quad (21.1)$$

As the components i, p and k vary, one finds a number of matrix elements $\langle \alpha i | T_p^{(\gamma)} | \beta k \rangle$ that are all connected by the theorem.

Proof

$\forall R \in G, R^\dagger = R^{-1}$ implies

$$\begin{aligned} \langle \alpha i | T_q^{(\gamma)} | \beta k \rangle &= \langle \alpha i | R^\dagger R T_q^{(\gamma)} R^\dagger R | \beta k \rangle = \\ &= \langle \alpha i | R^\dagger \sum_q T_q^{(\gamma)} D_{qp}^{(\gamma)}(R) R | \beta k \rangle = \\ &= \sum_{qj r} \langle \alpha j | T_q^{(\gamma)} | \beta r \rangle D_{ji}^{(\alpha)}(R)^* D_{qp}^{(\gamma)}(R) D_{rk}^{(\beta)}(R). \end{aligned} \quad (21.2)$$

In order to use the GOT, we write the product of two D matrices as one D. Actually, $D_{qp}^{(\gamma)}(R) D_{rk}^{(\beta)}(R)$ is the direct product of two irreps,

$$D_{qp}^{(\gamma)}(R) D_{rk}^{(\beta)}(R) = \sum_{\delta st} \langle \gamma q \beta r | \delta s \rangle D_{st}^{(\delta)} \langle \delta t | \gamma p \beta k \rangle,$$

where we have used Clebsch-Gordan coefficients, and inserting in (21.2),

$$\langle \alpha i | T_p^{(\gamma)} | \beta k \rangle = \sum_{qj r} \langle \alpha j | T_q^{(\gamma)} | \beta r \rangle D_{ji}^{(\alpha)}(R)^* \sum_{\delta st} \langle \gamma q \beta r | \delta s \rangle D_{st}^{(\delta)} \langle \delta t | \gamma p \beta k \rangle. \quad (21.3)$$

Here R is arbitrary; summing over R , in the l.h.s. we get a factor N_G (=Group order); in the r.h.s. the GOT yields

$$\sum_R D_{ji}^{(\alpha)}(R)^* D_{st}^{(\delta)}(R) = \frac{N_g}{m_\alpha} \delta_{\alpha\delta} \delta_{js} \delta_{it},$$

and finally we obtain

$$N_G \langle \alpha i | T_p^{(\gamma)} | \beta k \rangle = \sum_{qjr} \langle \alpha j | T_q^{(\gamma)} | \beta r \rangle \sum_{\delta st} \langle \gamma q \beta r | \delta s \rangle \langle \delta t | \gamma p \beta k \rangle \frac{N_G}{m_\alpha} \delta_{\alpha\delta} \delta_{js} \delta_{it},$$

that is

$$\langle \alpha i | T_q^{(\gamma)} | \beta k \rangle = \langle \alpha || T^{(\gamma)} || \beta \rangle \langle \alpha i | \gamma p \beta k \rangle, \tag{21.4}$$

where the *reduced matrix element*

$$\langle \alpha || T^{(\gamma)} || \beta \rangle = \frac{1}{m_\alpha} \sum_{qjr} \langle \alpha j | T_q^{(\gamma)} | \beta r \rangle \langle \gamma q \beta r | \alpha j \rangle$$

does not depend on the components.

q.e.d.

Solutions

Problems of Chapter 2

2.1 $\langle n_p \rangle = \frac{1}{Z} Tr(n_p \rho)$ has a denominator $Z = \prod_k (1 + e^{-\beta(\epsilon_k - \mu)})$ and a numerator $\prod_{k \neq p} (1 + e^{-\beta(\epsilon_k - \mu)}) e^{-\beta(\epsilon_p - \mu)}$, since p is filled in all states that contribute.

2.2 One readily verifies by computing the time derivative that

$$U(t, t') = U_0(t, t') - \frac{i}{\hbar} \int_{t'}^t U(t, \tau) H_1(\tau) U(\tau, t')$$

is equivalent to the Schrödinger equation.

2.3 From the definition one can easily verify that

$$\begin{aligned} \frac{d}{dt} T\{A_1(t_1) A_2(t_2) \rho(t)\} &= T\{A_1(t_1) A_2(t_2) \dot{\rho}(t)\} + \\ &\delta(t - t_1) T\{[\rho(t), A_1(t_1)]_- A_2(t_2)\} \\ &+ \delta(t - t_2) T\{A_1(t_1) [\rho(t), A_2(t_2)]_-\} \end{aligned} \quad (21.5)$$

where the δ functions arise from $\theta(t - t_i)$ factors (for $\rho(t)$ standing on the left of $A_i(t_i)$) and from $\theta(t_i - t)$ factors (for $\rho(t)$ standing on the right of $A_i(t_i)$); hence one gets the commutators. The argument extends immediately to any n yielding the term in $\dot{\rho}$ and an extra term

$$\sum_{q=1}^n \delta(t - t_q) T\{A_1(t_1) \cdots [\rho(t), A_q(t_q)]_- \cdots A_n(t_n)\}. \quad (21.6)$$

2.4 One can think of the (t, t') interval divided into $N \gg 1$ intervals and write $e^{-iH_\lambda(t'-t)} = \prod_n e^{-iH_\lambda(t_n - t_{n-1})}$; after differentiating, one lets $N \rightarrow \infty$.

Problems of Chapter 3

3.1 The ground configuration $1s^2 2s^2 2p^3$ has $\binom{6}{3} = 20$ states. The largest M_L is reached by $(1+, 1-, 0\pm)$ thus $M_L = 2, M_S = \pm \frac{1}{2}$. The resulting

2D occupies 10 states. There are 4 determinants with $M_L = 1$, namely, $(1, 1-, -1), (1, 0+, 0, -)$.

$$p^3 \rightarrow {}^4S, {}^2P, {}^2D.$$

3.2 The ground configuration of Ti is $1s^2 2s^2 2p^6 3d^2$. There are $\binom{10}{2} = 45$ states. The largest M_L is 4. One finds:

$$d^2 \rightarrow {}^1S, {}^3P, {}^1D, {}^3F, {}^1G.$$

3.3 The tables of Clebsh-Gordan coefficients yield

$$\langle \frac{1}{2}m_{s_1} \frac{1}{2}m_{s_2} | S = 1, M_S = 0 \rangle = \frac{\delta(m_{s_1}, -m_{s_2})}{\sqrt{2}}$$

and for $\langle l_1 = 2m_1 l_2 = 2m_2 | L = 1, M_L = 0 \rangle$ the following values:

$m_2 = 2$	$-\sqrt{\frac{2}{5}}$
$m_2 = 1$	$\sqrt{\frac{1}{10}}$
$m_2 = 0$	0
$m_2 = -1$	$-\sqrt{\frac{1}{10}}$
$m_2 = -2$	$\sqrt{\frac{2}{5}}$

hence normalizing again (which is generally necessary when using Clebsh-Gordan coefficients)

$$|{}^3PM_L = 0, M_S = 0\rangle = \frac{1}{\sqrt{10}}\{2|2^+, -2^-| + 2|2^-, -2^+| - |1^+, -1^-| - |1^-, -1^+|\}.$$

3.4 For two-electron states, $L^\pm = L_1^\pm + L_2^\pm$. For $L=1$ one learns from (6.1.1) that $L^+|0\rangle = \sqrt{2}|1\rangle, L^-|0\rangle = \sqrt{2}|-1\rangle$.

So,

$$\begin{aligned} |{}^3PM_L = 1, M_S = 0\rangle &= \frac{1}{\sqrt{2}}L^+|{}^3PM_L = 0, M_S = 0\rangle = \\ &= \frac{L_1^+ + L_2^+}{\sqrt{2}} \frac{1}{\sqrt{10}}\{2|2^+, -2^-| + 2|2^-, -2^+| - |1^+, -1^-| - |1^-, -1^+|\}. \end{aligned}$$

Bringing the one-body operators to act on the respective states, using (6.1.1) and the spin shift operators one finds

$$|{}^3PM_L = 0, M_S = 1\rangle = \frac{1}{\sqrt{5}}\{2|2^+, -2^+| - |1^+, -1^+|\}.$$

Moreover,

$$|{}^3PM_L = 1, M_S = 1\rangle = \frac{1}{\sqrt{10}}\{2|2^+, -1^+| - \sqrt{6}|1^+, 0^+|\},$$

$$|^3PM_L = 1, M_S = -1\rangle = \frac{1}{\sqrt{10}}\{2|2^-, -1^-| - \sqrt{6}|1^-, 0^-\},$$

$$|^3PM_L = 0, M_S = 0\rangle = \frac{1}{\sqrt{10}}\{2|2^+, -2^-| + 2|2^-, -2^+| - |1^+, -1^-| - |1^-, -1^+|\},$$

$$|^3PM_L = 0, M_S = -1\rangle = \frac{1}{\sqrt{5}}\{2|2^-, -2^-| - |1^-, -1^-|\},$$

$$|^3PM_L = -1, M_S = 1\rangle = \frac{1}{\sqrt{10}}\{2|1^+, -2^+| - \sqrt{6}|0^+, -1^+|\},$$

$$|^3PM_L = -1, M_S = -1\rangle = \frac{1}{\sqrt{10}}\{2|1^-, -2^-| - \sqrt{6}|0^-, -1^-|\},$$

3.5 We found

$$|^3PM_L = 0, M_S = 1\rangle = \frac{1}{\sqrt{5}}\{2|2^+, -2^+| - |1^+, -1^+|\}.$$

It is clearly a triplet since the spin configuration is $\alpha\alpha$, and $M_L = m_1 + m_2 = 0$. In order to verify that it is a P state, we use

$$L^2 = L_1^2 + L_2^2 + 2L_{1z}L_{2z} + L_1^+L_2^- + L_1^-L_2^+$$

where $L_1^2 = L_2^2 = 2 \times 3$. Now, $2L_{1z}L_{2z}\{2|2^+, -2^+| - |1^+, -1^+|\} = 2 \times 2 \times 2 \times (-2)|2^+, -2^+| - 2 \times 1 \times (-1)|1^+, -1^+|$; $L_1^+L_2^-|2^+, -2^+| = 0$, $L_1^+L_2^-|1^+, -1^+| = (-2) \times 2|1^+, -1^+|$, and in this way the check is readily completed.

Problems of Chapter 4

4.1 Integrate $\frac{d}{d\beta}(e^{\beta H}[A, e^{-\beta H}]_-) = e^{\beta H}[H, A]_-e^{-\beta H}$.

4.2 Let

$$f_{mn}(\mathbf{x}, \mathbf{x}', \omega) = \sum_{mn} e^{-\beta K_n} R_{mn}(\mathbf{x}, \mathbf{x}') \delta(\omega - \omega_{mn}),$$

which incidentally is just the spectral density (4.139) without the $1 - s e^{-\beta\omega}$ factor. Equation (4.138) implies

$$\begin{aligned} Z \operatorname{Re} G(\mathbf{x}, \mathbf{x}', \omega) &= P \int \frac{d\omega'}{\omega - \omega'} (1 + s e^{-\beta\omega'}) f_{mn}(\mathbf{x}, \mathbf{x}', \omega'), \\ -Z \operatorname{Im} G(\mathbf{x}, \mathbf{x}', \omega) &= \pi(1 - s e^{-\beta\omega}) f_{mn}(\mathbf{x}, \mathbf{x}', \omega), \end{aligned} \quad (21.7)$$

and the results follows by substitution.

4.3 In the continuous case, equation (4.44) reads

$$(z + \frac{\hbar^2}{2m} \frac{d^2}{dx^2})g(x', x, z) = \delta(x - x') \quad (21.8)$$

and is solved by

$$g(x', x, z) = \sqrt{\frac{2m}{\hbar^2}} \frac{e^{i\sqrt{\frac{2mz}{\hbar^2}}|x-x'|}}{i\sqrt{z}}; \quad (21.9)$$

[note that $\frac{d|x-x'|}{dx} = \text{sign}(x-x')$] and the band-edge singularity is similar to the discrete case (with one band edge, however).

4.4 In the continuous case, for 3d, the solution of (4.44), namely,

$$(z + \frac{\hbar^2}{2m} \nabla^2)g(\mathbf{r}', \mathbf{r}, z) = \delta(\mathbf{r} - \mathbf{r}') \quad (21.10)$$

is readily verified to be

$$g(\mathbf{r}', \mathbf{r}, z) = -\frac{m}{2\pi\hbar^2} \frac{e^{i\sqrt{\frac{2mz}{\hbar^2}}|\mathbf{r}-\mathbf{r}'|}}{|\mathbf{r} - \mathbf{r}'|}. \quad (21.11)$$

Therefore, $\frac{-1}{\pi} Im \lim_{r' \rightarrow r} g(\mathbf{r}, \mathbf{r}', z)$ yields the well known \sqrt{z} singularity.

4.5 $U(\mathbf{r}) = \frac{1}{2} \nabla \phi \cdot \mathbf{n} + \int_S d^2 r' (g^{-1}(r, r', \epsilon) + (\epsilon - E) \frac{\partial}{\partial \epsilon} g^{-1}(r, r', \epsilon)) \phi(\mathbf{r}')$, where ϵ and E are the unperturbed and perturbed energy eigenvalues, respectively.

Problems of Chapter 5

5.3 We found already that

$$G_{k0}(\omega) = \frac{V_{k0}}{\omega - \epsilon_k} G_{00}(\omega). \quad (21.12)$$

The off-diagonal element of the last of 5.21 yields

$$G_{kk'}(\omega) = \frac{V_{k0}}{\omega - \epsilon_k} G_{0k'}(\omega), \quad k \neq k', \quad (21.13)$$

and by substituting into the third of (5.21) we obtain

$$G_{0k}(\omega) = \frac{V_{0k} G_{kk}}{\omega - \epsilon_0 - \Sigma(\omega)}. \quad (21.14)$$

Combining with the -diagonal element of the last of (5.21) we obtain

$$G_{kk}(\omega) = \frac{1}{\omega - \epsilon_k - \frac{|V_{0k}|^2}{\omega - \epsilon_0 - \Sigma(\omega)}}, \quad (21.15)$$

$$G_{0k}(\omega) = \frac{V_{0k}}{(\omega - \epsilon_k)(\omega - \epsilon_0 - \Sigma(\omega)) - |V_{0k}|^2}, \quad (21.16)$$

and finally

$$G_{kk'}(\omega) = \frac{V_{k0}}{\omega - \epsilon_k} \frac{V_{0k'}}{(\omega - \epsilon_{k'}) (\omega - \epsilon_0 - \Sigma(\omega)) - |V_{0k'}|^2}. \quad (21.17)$$

5.4 The S_z factor implies that 1) the scattering conduction spin direction is the quantization axis for the impurity spin, 2) the singular scattering does not flip the impurity spin 3) for $S > \frac{1}{2}$ the scattering probability grows with the square of the spin component m_S 4) opposite m_S gives opposite amplitude 5) The resistivity goes with $Tr U_{if}^{(2)\dagger} U_{if}^{(2)}$.

Problems of Chapter 6

6.1 Averaging over a one-electron wave function,

$$\langle \hat{\mathbf{j}}(\mathbf{x}) \rangle = \frac{e}{2m} \int d^3x' \psi(\mathbf{x}')^* [\mathbf{p}_{\mathbf{x}'} \delta(\mathbf{x} - \mathbf{x}') + \delta(\mathbf{x} - \mathbf{x}') \mathbf{p}_{\mathbf{x}'}] \psi(\mathbf{x}'),$$

but the first term in the integrand can be rewritten $(\mathbf{p}_{\mathbf{x}'} \psi(\mathbf{x}'))^* \delta(\mathbf{x} - \mathbf{x}') \psi(\mathbf{x}') = i\hbar \nabla_{\mathbf{x}'} \psi(\mathbf{x}')^* \delta(\mathbf{x} - \mathbf{x}') \psi(\mathbf{x}')$ and the expectation value is the current. Then

$$\begin{aligned} H' &= -\frac{1}{c} 2mc \sum_i^N \int d^3x \mathbf{A}(\mathbf{x}_i) \cdot \hat{\mathbf{j}}(\mathbf{x}_i) \\ &= \frac{-e}{2mc} \int d^3x [\mathbf{A}(\mathbf{x}) \cdot \mathbf{p}_{\mathbf{x}'} \delta(\mathbf{x} - \mathbf{x}') + \mathbf{A}(\mathbf{x}) \delta(\mathbf{x} - \mathbf{x}') \mathbf{p}_{\mathbf{x}'}] \end{aligned} \quad (21.18)$$

where $\mathbf{A}(\mathbf{x})$ and $\mathbf{p}_{\mathbf{x}'}$ commute. Let us take the matrix element H'_{mn} . The first term contributes

$$\frac{-e}{2mc} \int d^3x' \psi_m^*(x') \int d^3x p_{x'} A(x) \delta(x - x') \psi_n(x').$$

Caution is needed when integrating with the δ functions if there are operators. $\int d^3x \delta(\mathbf{x} - \mathbf{x}') \phi(\mathbf{x}') = \phi(\mathbf{x})$ holds even if ϕ contains operators, but δ must stand on the left. So we cannot integrate over d^3x' directly, but we can over d^3x and we find

$$\frac{-e}{2mc} \int d^3x' \psi_m^*(x') p_{x'} A(x') \psi_n(x').$$

The second contribution

$$\frac{-e}{2mc} \int d^3x' \psi_m^*(x') \int d^3x A(x) \delta(x - x') p_{x'} \psi_n(x')$$

is (integrating in either way)

$$\frac{-e}{2mc} \int d^3x \psi_m^*(x') A(x) p_x \psi_n(x).$$

Therefore the two formulations are equivalent.

Problems of Chapter 8

8.1

1) The characters of the representation $\Gamma(1)$ with one electron are $\chi(E) = 5, \chi(C_2) = 1, \chi(2C_4) = 1, \chi(2\sigma_v) = 3, \chi(2\sigma_d) = 1$. Applying the LOT one finds $\Gamma(1) = 2A_1 \oplus E \oplus B_1$.

2) We choose a basis whose elements are determinants $(i, j, k, m) \equiv |i \uparrow j \uparrow k \downarrow m \downarrow|$ with, say, $i > j, k > m$, numbering the sites as in Figure 8.5.

The number of configurations is $\binom{5}{2}^2 = 100$. One must determine how many remain invariant or change sign under the operations of the Group. Under C_2 , the only contributions come from $(4, 2, 4, 2), (4, 2, 5, 3), (5, 3, 4, 2), (5, 3, 5, 3)$, which remain invariant. Under σ_x , one finds invariant configurations

$(2, 1, 2, 1), (2, 1, 4, 1), (2, 1, 4, 2), (4, 1, 2, 1), (4, 1, 4, 1), (4, 1, 4, 2), (4, 2, 2, 1), (4, 2, 4, 1), (4, 2, 4, 2), (5, 3, 5, 3)$ while the configuration that change sign are

$(2, 1, 5, 3), (4, 1, 5, 3), (4, 2, 5, 3), (5, 3, 2, 1), (5, 3, 4, 1), (5, 3, 4, 2)$. The configurations $(5, 2, 5, 2), (5, 2, 4, 3), (4, 3, 5, 2), (4, 3, 4, 3)$ remain invariant under one of the σ_d reflections. Proceeding in this way, one finds the characters of the reducible representation $\Gamma(4)$ for 4 particles:

C_{4v}	I	C_2	$2C_4$	$2\sigma_v$	$2\sigma_d$	$g = 8$
A_1	1	1	1	1	1	z
A_2	1	1	1	-1	-1	R_z
B_1	1	1	-1	1	-1	$x^2 - y^2$
B_2	1	1	-1	-1	1	xy
E	2	-2	0	0	0	(x, y)
$\Gamma(4)$	100	4	0	4	4	

Applying the LOT one finds $\Gamma(4) = 15A_1 \oplus 11A_2 \oplus 24E \oplus 13B_1 \oplus 13B_2$.

8.2 The characters of $\Gamma(4)$ are 1296, 16, 0, 64, 16; hence, $\Gamma(4) = 184A_1 \oplus 144A_2 \oplus 320E \oplus 176B_1 \oplus 152B_2$.

Problems of Chapter 9

9.1

In $E \otimes E = A_1 \oplus A_2 \oplus E$ all the irreps are contained. Using the set of matrices (7.44),

E	C_3	C_3^2	σ_a	σ_b	σ_c
$\begin{pmatrix} 1 & 0 \\ 0 & 1 \end{pmatrix}$	$\begin{pmatrix} -\frac{1}{2} & -\frac{\sqrt{3}}{2} \\ \frac{\sqrt{3}}{2} & -\frac{1}{2} \end{pmatrix}$	$\begin{pmatrix} -\frac{1}{2} & \frac{\sqrt{3}}{2} \\ -\frac{\sqrt{3}}{2} & -\frac{1}{2} \end{pmatrix}$	$\begin{pmatrix} -1 & 0 \\ 0 & 1 \end{pmatrix}$	$\begin{pmatrix} \frac{1}{2} & \frac{\sqrt{3}}{2} \\ \frac{\sqrt{3}}{2} & -\frac{1}{2} \end{pmatrix}$	$\begin{pmatrix} \frac{1}{2} & -\frac{\sqrt{3}}{2} \\ -\frac{\sqrt{3}}{2} & -\frac{1}{2} \end{pmatrix}$

from the one-electron basis (x, y) we form the direct-product basis

$$(x_1x_2, x_1y_2, y_1x_2, y_1y_2).$$

Using $C_3x = -\frac{x+y\sqrt{3}}{2}$, $C_3y = \frac{-y+x\sqrt{3}}{2}$, $C_3^2x = \frac{-x+y\sqrt{3}}{2}$, $C_3^2y = \frac{-y+x\sqrt{3}}{2}$, $\sigma_1x = -x$, $\sigma_1y = y$, $\sigma_2x = \frac{x+y\sqrt{3}}{2}$, $\sigma_2y = \frac{-y+x\sqrt{3}}{2}$, $\sigma_3x = \frac{x+y\sqrt{3}}{2}$, $\sigma_3y = \frac{-y+x\sqrt{3}}{2}$ and the projection operator $P^{(A_1)} = \sum_{R \in G} R$, one finds

$$\begin{aligned} P^{A_1}x_1x_2 &= x_1x_2 + \left(\frac{-x_1+y_1\sqrt{3}}{2}\right)\left(\frac{-x_2+y_2\sqrt{3}}{2}\right) + \left(\frac{-x_1+y_1\sqrt{3}}{2}\right)\left(\frac{-x_2+y_2\sqrt{3}}{2}\right) \\ &+ x_1x_2 + \left(\frac{-x_1+y_1\sqrt{3}}{2}\right)\left(\frac{-x_2+y_2\sqrt{3}}{2}\right) + \left(\frac{x_1-y_1\sqrt{3}}{2}\right)\left(\frac{x_2-y_2\sqrt{3}}{2}\right) \\ &= 3(x_1x_2 + y_1y_2). \end{aligned}$$

This is the wave function, which is even in the exchange on 1 and 2, so it is singlet. Normalizing,

$${}^1A_1 = \frac{x_1x_2 + y_1y_2}{\sqrt{2}}. \quad (21.19)$$

9.2

$$|{}^1A_2\rangle = \frac{|x_1y_2\rangle - |y_1x_2\rangle}{\sqrt{2}}, \quad (21.20)$$

to be multiplied for the singlet spin function. Therefore the non-vanishing coefficients are: $\langle {}^1A_1 | Ex_1Ey_1 \rangle = \langle {}^1A_1 | Ey_1Ey_1 \rangle = \frac{1}{\sqrt{2}}$.

9.3 Using the set of matrices (7.44),

E	C_3	C_3^2	σ_a	σ_b	σ_c
$\begin{pmatrix} 1 & 0 \\ 0 & 1 \end{pmatrix}$	$\begin{pmatrix} -\frac{1}{2} & -\frac{\sqrt{3}}{2} \\ \frac{\sqrt{3}}{2} & -\frac{1}{2} \end{pmatrix}$	$\begin{pmatrix} -\frac{1}{2} & \frac{\sqrt{3}}{2} \\ -\frac{\sqrt{3}}{2} & -\frac{1}{2} \end{pmatrix}$	$\begin{pmatrix} -1 & 0 \\ 0 & 1 \end{pmatrix}$	$\begin{pmatrix} \frac{1}{2} & \frac{\sqrt{3}}{2} \\ \frac{\sqrt{3}}{2} & -\frac{1}{2} \end{pmatrix}$	$\begin{pmatrix} \frac{1}{2} & -\frac{\sqrt{3}}{2} \\ -\frac{\sqrt{3}}{2} & -\frac{1}{2} \end{pmatrix}$

we find that the contribution of the reflections is the same as that of the rotations for $P^{(E,y)}$ and opposite for $P^{(E,x)}$. Consequently,

$$\begin{aligned} P^{(E,y)}x_1x_2 &= x_1x_2 - \frac{1}{2}\left(\frac{x_1+y_1\sqrt{3}}{2}\right)\left(\frac{x_2+y_2\sqrt{3}}{2}\right) \\ &- \frac{1}{2}\left(\frac{-x_1+y_1\sqrt{3}}{2}\right)\left(\frac{-x_2+y_2\sqrt{3}}{2}\right) \\ &+ x_1x_2 - \frac{1}{2}\left(\frac{x_1+y_1\sqrt{3}}{2}\right)\left(\frac{x_2+y_2\sqrt{3}}{2}\right) - \frac{1}{2}\left(\frac{x_1-y_1\sqrt{3}}{2}\right)\left(\frac{x_2-y_2\sqrt{3}}{2}\right) \\ &= \frac{3}{2}(x_1x_2 - y_1y_2); \end{aligned}$$

$P^{(E,x)}x_1x_2 = 0$. Hence,

$$|{}^1Y\rangle = \frac{|x_1x_2\rangle - |y_1y_2\rangle}{\sqrt{2}}.$$

Thus,

$$\langle {}^1X | E_1x_1E_2x_2 \rangle = -\langle {}^1X | E_1y_1E_2y_2 \rangle = \frac{1}{\sqrt{2}}.$$

9.4 One can check the results with Appendix II.

9.5 To find the characters of the $\Gamma^{3/2}$ and $\Gamma^{5/2}$ representations in $C'_{4\omega}$, or similarly in D'_4 , under rotations by an angle ω we choose to rotate around the z axis; then $|LSJM\rangle \rightarrow |LSJM\rangle e^{iM\omega}$. So, the D matrix is diagonal and the character is given by the formula

$$\chi^{(J)}(\phi) = \frac{\sin[(J + \frac{1}{2})\phi]}{\sin(\frac{\phi}{2})} \tag{21.21}$$

which which generalizes (9.20) above and results from using the identity

$$\sum_{m=-J}^J \cos(mx) = \csc(\frac{x}{2}) \sin[(J + \frac{1}{2})x].$$

One finds

$$\chi^{(3/2)}(\omega) = \frac{\sin(2\omega)}{\sin(\frac{\omega}{2})} = 4 \cos(\omega) \cos(\frac{\omega}{2}). \tag{21.22}$$

The reflections and all the improper rotations can be written like products $\hat{i}R_\omega$. Proceeding in this way,

D'_4	E	\bar{E}	C_4	C_4^3	C_2	$2C'_2$	$2C''_2$
	$C_4^3\bar{E}$	$C_4\bar{E}$	$C_2\bar{E}$	$2C'_2\bar{E}$	$2C''_2\bar{E}$		
A'_1	1	1	1	1	1	1	1
A'_2	1	1	1	1	1	-1	-1
B'_1	1	1	-1	-1	1	1	-1
B'_2	1	1	-1	-1	1	-1	1
E'_1	2	2	0	0	-2	0	0
E'_2	2	-2	$\sqrt{2}$	$-\sqrt{2}$	0	0	0
E'_3	2	-2	$-\sqrt{2}$	$\sqrt{2}$	0	0	0
$\Gamma^{3/2}$	4	-4	0	0	0	0	0
$\Gamma^{5/2}$	6	-6	-2	2	0	0	0

and $\Gamma^{3/2} = E'_2 \oplus E'_3$, $\Gamma^{5/2} = E'_2 \oplus 2E'_3$.

Problems of Chapter 10

10.1 This result is most easily obtained in the time representation, keeping in mind that for $t' > t$ $G(t, t') = \sum_m \psi_m^*(\mathbf{x}') \psi_m(\mathbf{x}) e^{-i\epsilon_m(t-t')}$, where $\psi_m(\mathbf{x})$ are the energy eigenfunctions. Thus, each term yields half of the answer.

10.3 One easily recovers the results of Sect. 4.3.1.

10.4 As outlined in Ref. [205], one finds:

$$\begin{aligned} \left[\frac{\partial}{\partial \tau} + i\epsilon_k\right]F_{kk'}(\tau, \tau', t, t') &= \delta_{kk'}\delta(\tau - \tau')g(t - t') \\ &- i \sum_q V_{kq} F_{qk'}(\tau, \tau', t, t')\chi(\tau; t, t'), \end{aligned} \quad (21.23)$$

were $\chi(\tau; t, t') = 1$ for $t' > \tau > t$ and vanishes otherwise.

Problems of Chapter 11

11.1

$$\begin{aligned} R^{(d)} &= \sum_{iklj} (-i)U(ilkj)(-i)U(kjil) \int_0^t dt_1 \int_0^{t_1} dt_2 \\ &\times ig_i(t_2 - t_1)ig_k(t_1 - t_2)ig_l(t_2 - t_1)ig_j(t_1 - t_2). \end{aligned} \quad (21.24)$$

The integral yields (dropping an exponential term which goes to zero as $t \rightarrow \infty(1 - i\eta)$) $R^{(d)}(t) = it \sum_{iklj} \frac{U(ilkj)^2}{\epsilon_k + \epsilon_j - \epsilon_i - \epsilon_l}$.

11.2 From $\Sigma^* = \Sigma + \Sigma G_0 \Sigma + \Sigma G_0 \Sigma G_0 \Sigma + \dots$ one finds

$$\Sigma^* = \frac{1}{1 - \Sigma G_0} \Sigma. \quad (21.25)$$

11.3 b) is the only skeleton.

11.4 Putting the Hartree potential and φ in the one-body term, $G^{(0)-1}(1, 2) = i\frac{\partial}{\partial t} - H_0 - V_{eff}(1)\delta(1, 2)$ and we may rewrite (11.81) as $G^{(0)-1} = G^{-1} + \Sigma$, that is,

$$G^{-1}(1, 2) = \left(i\frac{\partial}{\partial t} - H_0 - V_{eff}(1)\right)\delta(1, 2) - \Sigma(1, 2). \quad (21.26)$$

Problems of Chapter 12

12.1 One gets $\frac{\delta \bar{E}}{\delta n} = \frac{(3\pi^2)^{\frac{2}{3}}}{2} n^{\frac{2}{3}}$, and inserting into (12.95) one finds $n = \frac{2^{\frac{2}{3}}}{3\pi^2} (\mu - \phi(x))^{\frac{2}{3}}$, that is, one is left with the semi-classical Thomas-Fermi method.

12.2

$$\begin{aligned} &-\frac{(-iU)^4}{2^8} \int_0^t dt_1 \int_0^{t_1} dt_2 \int_0^{t_2} dt_3 \int_0^{t_3} dt_4 (e^{-2iV(t_1+t_2-t_3-t_4)})^2 \\ &= \frac{-1}{32} \left(\frac{U}{V}\right)^4 \left[\frac{5 - e^{-4iVt} - 4e^{-2iVt}}{512} - iVt \frac{1 + 2e^{-2iVt}}{128} \right]. \end{aligned} \quad (21.27)$$

Problems of Chapter 13

13.1 Symbolically, one writes Equation (13.135)

$$J = \Gamma^{(L)} f^{(L)} (g^r - g^a) + \gamma^{(L)} g^<$$

but for the other electrode one writes

$$J = -\gamma^{(R)} f^{(R)} (g^r - g^a) - \gamma^{(R)} g^<;$$

the solution arrives eliminating $g^<$ algebraically; this is legitimate for every infinitesimal energy interval $d\epsilon$.

Problems of Chapter 14

14.1 Defining the combinations

$$p = u_m + u_s, \bar{p} = u_m - u_s, r = u_m + iu_s, s = u_m - iu_s,$$

one obtains

$$G_{mn}(E) = \frac{G_{pp} - G_{qq} - i[G_{rr} - G_{ss}]}{4}.$$

probl

14.2 One gets the moments and finds $a_n = 0$ and

$$b_n^2 = W^2 \frac{n^2}{4n^2 - 1}. \tag{21.28}$$

14.3 One gets the moments and finds $a_n = 0$ and

$$b_n^2 = \frac{W^2}{4}. \tag{21.29}$$

14.4 From Equation (14.101),

$$\begin{aligned} x_1 &= \frac{A_1 b_1}{A} - \frac{a_{12} A_{12} b_2 + a_{13} A_{13} b_3}{A} + \frac{a_{12} a_{23} A_{123} b_3 + a_{13} a_{32} A_{123} b_2}{A} \\ &= \frac{b_1}{D_1} - \frac{a_{12} b_2 + a_{13} b_3}{D_{12}} + \frac{a_{12} a_{23} b_3 + a_{13} a_{32} b_2}{D_{123}} \end{aligned} \tag{21.30}$$

We may proceed by noting that $D_{123} = D_{12} D_3^{12}$, $D_3^{12} = a_{33} D_{12} = D_1 D_2^1$, $D_2^1 = a_{22} - a_{23} a_{32} / D_3^{12}$, and we have all the ingredients to apply 14.86 and carry on the calculation.

Problems of Chapter 16

16.1 Using (16.15),(16.16), the exponent transforms to

$$i\left[\left(k - \frac{mvx}{\hbar}\right)x + t\left(-\frac{\hbar k^2}{2m} + \frac{mv^2}{2\hbar}\right)\right]$$

but this must be written in terms of x' . Thus one obtains

$$\psi'(x', t) = e^{ik'x' - i\hbar\frac{(k')^2 t}{2m}}$$

with $\hbar k' = \hbar k - mv$. Thus the plane-wave becomes a plane-wave with Galilean transformation of the momentum.

Problems of Chapter 17

17.1 Table III shows how the irreps of \mathcal{G} split in C_{4v} .

\mathcal{G}	C_{4v}
A_1	A_1
\tilde{A}_1	A_1
B_2	B_2
\tilde{B}_2	B_2
Γ_1	$2B_2$
Γ_2	$2A_1$
Σ_1	$A_1 + 2B_1$
Σ_2	$A_1 + 2B_1$
Σ_3	$2A_2 + B_2$
Σ_4	$2A_2 + B_2$
Λ_1	$A_1 + B_1 + E$
Λ_2	$A_1 + B_1 + E$
Λ_3	$A_2 + B_2 + E$
Λ_4	$A_2 + B_2 + E$
Ω_1	$A_2 + B_1 + 2E$
Ω_2	$A_2 + B_1 + 2E$
Ω_3	$A_1 + B_2 + 2E$
Ω_4	$A_1 + B_2 + 2E$
Π_1	$2A_1 + 2B_1 + 2E$
Π_2	$2A_2 + 2B_2 + 2E$

Table III. Reduction of the irreps of Optimal Group \mathcal{G} of the 4×4 model in the point Group.

17.2 The $W = 0$ Theorem ensures that no double occupancy is possible for pairs in the irreps $\tilde{A}_1, B_2, \Gamma_1, \Gamma_2, \Sigma_1, \Sigma_2, \Sigma_3, \Sigma_4, \Lambda_2, \Lambda_3, \Omega_1, \Omega_2, \Omega_3, \Pi_1$ and Π_2 .

Problems of Chapter 18

18.1 In the repulsive case, the Hamiltonian (14.58) reads

$$H = \begin{pmatrix} U & t & t & 0 \\ t & 0 & 0 & t \\ t & 0 & 0 & t \\ 0 & t & t & U \end{pmatrix}. \tag{21.31}$$

on the basis $(a \uparrow a \downarrow, a \uparrow b \downarrow, b \uparrow a \downarrow, b \uparrow b \downarrow)$ where a and b are the two sites. For $U > 0$, the ground state eigenvalue is $\epsilon = \frac{1}{2}(U - \sqrt{16 + U^2})$ (we measure energies in t units);

$$L = Q \begin{pmatrix} 2 & q \\ q & 2 \end{pmatrix}$$

with $Q = \frac{1}{\sqrt{16+U^2+U\sqrt{16+U^2}}}$, $q = -(U + \sqrt{16 + U^2})$. For $U = 7$, $\epsilon = -0.531129$, $L = \begin{pmatrix} 0.181492 & -0.683418 \\ -0.683418 & 0.181492 \end{pmatrix}$.

In the attractive case (21.32)

$$\tilde{H} = H(t, -U) + U = \begin{pmatrix} 0 & t & t & 0 \\ t & U & 0 & t \\ t & 0 & U & t \\ 0 & t & t & 0 \end{pmatrix}, \quad U > 0 \tag{21.32}$$

on the basis $(\alpha \uparrow a \downarrow, \alpha \uparrow b \downarrow, \beta \uparrow a \downarrow, \beta \uparrow b \downarrow)$ where $\alpha = b$ and $\beta = a$ for the new Fermions. The transformed matrix is

$$\tilde{L} = \tilde{Q} \begin{pmatrix} 2 & \tilde{q} \\ \tilde{q} & 2 \end{pmatrix}$$

with $\tilde{Q} = \frac{1}{\sqrt{16+U^2-U\sqrt{16+U^2}}}$, $\tilde{q} = -(-U + \sqrt{16 + U^2})$. For $U = 7$, $\epsilon = -0.531129$, $\tilde{L} = \begin{pmatrix} 0.683418 & -0.181492 \\ -0.181492 & 0.683418 \end{pmatrix}$.

18.2 With 2 fermions, $Q = P = \{1, 2\}$, $Q' = P' = \{2, 1\}$, let $k_1 < k_2$ denote the momenta, and we may write

$$\begin{cases} f_Q(x_1, x_2) = [QP]e^{i(k_1x_1+k_2x_2)} + [QP']e^{i(k_2x_1+k_1x_2)} & x_1 \leq x_2 \\ f_{Q'}(x_1, x_2) = [Q'P]e^{i(k_1x_2+k_2x_1)} + [Q'P']e^{i(k_2x_2+k_1x_1)} & x_1 \geq x_2 \end{cases}$$

con

$$[QP] = \frac{-\frac{U}{2i}[QP'] + \{\sin(k_1) - \sin(k_2)\}[Q'P']}{\sin(k_1) - \sin(k_2) + \frac{U}{2i}}, \tag{21.33}$$

and so on. For parallel spins U cannot act, sectors Q and Q' are disjoint and the coefficients are all determined by $[QP] = [Q'P'] = -[Q'P] = -[QP']$ and normalization.

For antiparallel spins, the periodicity conditions are also needed. In sector Q , with $1 \leq x_1 \leq x_2 \leq N_s$ let the amplitude be $f_Q(x_1, x_2)$. Let the electron 1 sit at be site x_1 ; if we decide to relabel $x_1 + N_s$ that site, the amplitude does not change, but we are now in sector Q' . So,

$$f_Q(x_1, x_2) = f_{Q'}(x_1 + N_s, x_2). \quad (21.34)$$

Now,

$$\begin{aligned} & [QP]e^{i(k_1x_1+k_2x_2)} + [QP']e^{i(k_2x_1+k_1x_2)} \\ = & [Q'P]e^{i(k_1x_2+k_2(x_1+N_s))} + [Q'P']e^{i(k_2x_2+k_1(x_1+N_s))} \end{aligned} \quad (21.35)$$

implies

$$\begin{cases} [QP] = [Q'P']e^{ik_1N_s} \\ [QP'] = [Q'P]e^{ik_2N_s}. \end{cases} \quad (21.36)$$

We eliminate $[Q'P]$ by (18.78) and get

$$[QP'] = ([QP] + [QP'] - [Q'P'])e^{ik_2N_s},$$

which yields:

$$\begin{aligned} [QP'](1 - e^{ik_2N_s}) &= ([QP] - [Q'P'])e^{ik_2N_s} \\ &= ([Q'P']e^{ik_1N_s} - [Q'P'])e^{ik_2N_s}. \end{aligned} \quad (21.37)$$

Total momentum is conserved; hence

$$e^{i[k_1+k_2]N_s} = 1 \quad (21.38)$$

and so

$$[Q'P'] = [QP].$$

Introduce the phase

$$\theta \in (0, 2\pi),$$

and since $k_1 < k_2$, let

$$\begin{cases} e^{ik_1N_s} = e^{-i\theta}, & N_s k_1 = 2\pi\lambda_1 - \theta, \quad \lambda_1 \in Z \\ e^{ik_2N_s} = e^{i\theta}, & N_s k_2 = 2\pi\lambda_2 + \theta, \quad \lambda_2 \in Z. \end{cases} \quad (21.39)$$

Integers $\lambda_1\lambda_2$ are Bethe quantum numbers that label the state with

$$[QP] = [QP']e^{-i\theta}. \quad (21.40)$$

In sector Q' one finds:

$$\begin{aligned} & [Q'P]e^{i(k_1x_2+k_2x_1)} + [Q'P']e^{i(k_1x_1+k_2x_2)} \\ = & [Q'P]e^{i(k_1x_1+k_2x_2+k_2N_s)} + [Q'P']e^{i(k_1x_2+k_2x_1+k_1N_s)}. \end{aligned} \quad (21.41)$$

This yields

$$\begin{cases} [Q'P] = [Q'P']e^{-i\theta} \\ [Q'P'] = [Q'P]e^{i\theta}. \end{cases} \quad (21.42)$$

Using (21.40,21.42, 18.78) one gets

$$[QP] = [Q'P], \quad [QP'] = [Q'P'] = [QP]e^{i\theta}. \quad (21.43)$$

Then, (21.33) becomes

$$e^{i\theta} = \frac{\sin(k_2) - \sin(k_1) - \frac{U}{2i}}{\sin(k_2) - \sin(k_1) + \frac{U}{2i}} \quad (21.44)$$

and the (un-normalized) wave function reads

$$\begin{cases} f_Q(x_1, x_2) = e^{i(k_1x_1+k_2x_2)} + e^{i(k_2x_1+k_1x_2+\theta)} & x_1 \leq x_2 \\ f_{Q'}(x_1, x_2) = e^{i(k_1x_2+k_2x_1)} + e^{i(k_2x_2+k_1x_1+\theta)} & x_1 \geq x_2 \end{cases} .$$

This may be taken real if λ 's are opposite; then we may write

$$-k_1 = k_2 = k > 0;$$

besides,

$$e^{i\theta} = \frac{i \sin(k) - \frac{U}{4}}{i \sin(k) + \frac{U}{4}} \quad (21.45)$$

We can simplify by an algebraic transformation based on

$$\cot\left(\frac{\theta}{2}\right) = i \frac{e^{i\theta} + 1}{e^{i\theta} - 1}. \quad (21.46)$$

This leads to

$$U \cot\left(\frac{\theta}{2}\right) = 4 \sin(k). \quad (21.47)$$

For odd n we may also write

$$-\tan\left(\frac{\theta}{2} - n\frac{\pi}{2}\right) = \frac{4}{U} \sin(k). \quad (21.48)$$

Introducing

$$\vartheta_0(p) = -2 \arctan\left(\frac{2p}{U}\right), \quad (21.49)$$

we get

$$\theta = n\pi + \vartheta_0(2\sin(k)).$$

One can verify the above results for $N_s = 3$, in the singlet sector. Direct diagonalization yields the eigenvalues $\frac{1+U-\sqrt{9-2U+U^2}}{2}$ (2 times), $\frac{1+U+\sqrt{9-2U+U^2}}{2}$ (2 times), $\frac{-2+U+\sqrt{36+4U+U^2}}{2}$ and for the ground state $\frac{-2+U-\sqrt{36+4U+U^2}}{2}$.

These results are reproduced by the Bethe ansatz with Equation (18.77). From $\lambda = 0$, that is $k = \frac{\theta}{3}$ the solution of (21.47)

$$\theta = 6 \arccos \left[\sqrt{\frac{5}{8} - \frac{U}{16} + \frac{\sqrt{36 + 4U + U^2}}{16}} \right]$$

leads to the ground state and to the last but one. The other states arise from $\lambda = 1$ and $\lambda = 2$, and each choice yields both eigenvalues.

References

1. Charles P. Enz, *A Course on Many-Body Theory Applied to Solid-State Physics*, World Scientific (1992)
2. A.L. Fetter and J. D. Walecka, *Quantum theory of Many-particle systems*, McGraw Hill, New York (1971)
3. Evgenij M. Lifšits and Lev P. Pitaevskij, *Teoria dello Stato Condensato*, Ed. Mir, Moskow (1981)
4. L S Cederbaum 1975 J. Phys. B: At. Mol. Phys. 8 290-303
5. G. Grosso e G. Pastori Parravicini “Solid State Physics”, academic Press Cambridge (2000)
6. H.B.G. Casimir, Proc. Kon. Ned. Akad. Wetensch. B51, 793 (1948)
7. S. Lamoreaux, Phys Rev Lett, 78, p5 (1996)
8. J. Schwinger, U.S. Atomic Energy Commission Rept. NYO-3071 (1952)
9. P. W. Anderson, Phys. Rev. **124**, 41 (1961)
10. D.M. Newns, Phys. Rev. **179**, 1123 (1969)
11. P. Coleman, cond-mat/0206003
12. M.L. Knotek and P.J. feibelman, Phys. Rev.Lett. **40**, 964 (1978)
13. Michele Cini, Phys. Rev. **B32**,1945 (1985)
14. S. Pancharatnam, Proc. Indian Acad. Sci. A **44**, 247 (1956)
15. D. Jaksch, C. Bruder, J.I. Cirac, C. W. Gardiner and P. Zoller, Phys.Rev Letters **81**, 3108 (1998).
16. R.Resta, J. Phys.: Condens. Matter **12** R107 (2000)
17. J. Hubbard, Proc. R. Soc. Lond. **A276**, 238 (1963)
18. Michele Cini, Gianluca Stefanucci, Enrico Perfetto and Agnese Callegari, J. Phys.: Condens Matter **14**, L709 (2002).
19. P. Coleman, cond-mat/0206003
20. A.C. Hewson,*The Kondo problem to Heavy fermions* ,Cambridge University Press (1997)
21. C. Lacroix, J. Phys. F: Metal Phys. **11**(1981) 2389
22. O. Gunnarsson and K. Schönhammer, Phys. Rev. **B22**, 3710 (1980)
23. Brian L. Silver, Irreducible Tensor Methods, Academic Press New York (1976)
24. W. Borchardt-Ott, Crystallography, Springer -Verlag Berlin (1995)
25. Leonard I. Schiff, Quantum Mechanics, McGraw-Hill New York
26. O. Gunnarsson, K. Schönhammer, J.C. Fuggle and R. Lässer, Phys. Rev. **B23**, 4350 (1981)
27. O. Gunnarsson and K. Schönhammer, Phys. Rev. **B28** , 4315 (1983)
28. C. Zener, Phys. Rev. **81**, 440 (1951).
29. Ryogo Kubo, J. Phys. Soc. Japan **12**, 570 (1957).
30. L.C. Davis and L.A. Feldkamp, Phys. Rev. **B 15** 2961 (1977)

31. E.N. Lassetre, Suppl. Radiation Research 1, 530 (1959)
32. U. Fano, Phys. Rev. **124** 1866 (1961)
33. P.W. Anderson, Phys. Rev. **124** 41 (1961)
34. J. Kondo, *Prog. Theor. Phys.* **32**, 37 (1964).
35. J. Kondo, 'Theory of dilute Magnetic Alloys', in *Solid State Physics*, Ed. Seitz **23**, (1969).
36. C. Verdozzi, Y. Luo, and Nicholas Kioussis, Phys. Rev. **B 70**, 132404 (2004)
37. E. H. Lieb, Phys. Rev. Lett. **62**, 1201 (1989).
38. B. I. Lundqvist, Phys. Kondensierten Materie **9**, 236 (1969).
39. David C. Langreth, Phys. Rev. **B 1**, 471 (1970).
40. R. Brout and P. Carruthers, Lectures on the Many-Electron Problem (Wiley-Interscience, New York, 1963)
41. Gerald D. Mahan, Phys. rev. **B 11** 4814 (1975)
42. Gerald D. Mahan, Many-Particle Physics, Plenum Press, New York and London (1990)
43. H. Ehrenreich and M. H. Cohen, Phys. Rev. **115**, 786 (1959)
44. E. N. Economou : *Green's functions in Quantum Physics*, Springer - Verlag, 1979. Second edition 1983
45. Michele Cini and Andrea D'andrea, J. Phys. C **21**, 193 (1988)
46. M.Cini, A. D'Andrea and C. Verdozzi, International Journal of Modern Physics B9, 1185 (1995)
47. M.Cini, Il Nuovo Cimento 9D, 1515 (1987)
48. A. Blandin, A. Nourtier and D.W. Hone, J. Phys. (paris) **37**, 369 (1976)
49. Adolfo Avella, Ferdinando Mancini and Roland Münzner, Phys. Rev. **B63**, 645117 (2001)
50. Ferdinando Mancini and Adolfo Avella, cond-mat/0006377
51. Ferdinando Mancini and Adolfo Avella, *The Hubbard model within the equation of motion approach*, advances in Physics **53**, 537 (2004)
52. J. Lindhard, Kgl. Danske Videnskab. Selskab, Mat.-Fys. Medd., **28**, no.8 (1954)
53. Lars Hedin, Phys. Rev. **139**, A796 (1965).
54. G. Onida, L. Reining and A. Rubio, Rev. Modern Phys. **74**, 601 (2002)
55. J.M. Luttinger and J.C. Ward, Phys. Rev. **118**, 1417 (1960).
56. G. Baym and L. Kadanoff, Phys. Rev. **124**, 287 (1961);
57. G. Baym, Phys. Rev. **127**, 1391 (1962).
58. C. Lanczos, J. Res. Natl. Bur. Stand. **45**, 255 (1950).
59. R. Haydock, V. Heine and M.J. Kelly, J. Phys. C **5**, 2845 (1972), R. Haydock, *Solid State Physics* Ed. Ehrenreich, F. Seitz and D. Turnbull (London, Academic Press, 1980), R. Haydock and C.M.M. Nex, J. Phys. C **18**, 2235 (1985).
60. F. Cyrot-Lackmann, J. Phys. C: Solid State Phys. **5**, 300 (1972); F. Cyrot-Lackmann, M.C. Desjonqueres and J.P. Gaspard, J. Phys. C: Solid State Phys. **7**, 925 (1974)
61. R. Landauer, IBM J. Res. Dev. **1**, 233 (1957); Philosof. Mag. **B21**, 863 (1970)
62. C. Caroli, R. Combescot, P. Nozieres and D. Saint-James, J. Phys. C: Solid State Phys. **4**, 916 (1971); *ibidem* **5**, 21 (1972)
63. Michele Cini, Phys. Rev. **B22**, 5887 (1980)
64. Yigal Meir and Ned S. Wingreen, Phys. Rev. Letters **68**, 2512 (1992).
65. M.V. Berry, Proc. R. Soc. Lond. A392, 45 (1984)
66. C. Verdozzi and M. Cini, Phys. Rev. **51**, 7412 (1995).

67. J. Kanamori, Prog. Theor. Phys. **30**, 275 (1963).
68. H. Bethe, Z. Phys. **71**, 205 (1931), *Zur Theorie der Metalle. Eigenwerte und Eigenfunktionen der linearen Atomketten.*
69. C.W. Beenakker, Phys. Rev. **B44**, 1646 (1991)
70. E. Perfetto and Michele Cini, Phys. Rev. **B 71**, 014504 (2005)
71. Enrico Perfetto and Michele Cini, Phys. Rev. **B 69**, 092508 (2004)
72. Michael Karbach and Gerhard Müller, cond-mat/9809162; cond-mat/0008018
73. E.H. Lieb and F.Y. Wu, cond-mat/0207529
74. C.N. Yang, Phys. Rev. Letters **19**, 1312 (1967).
75. Michele Cini, Solid State Commun. **20**, 605 (1976);
76. Michele Cini, Solid State Commun. **24**, 681 (1977)
77. Michele Cini, Phys. Rev. **B17**, 2486 (1978)
78. M. Cini, A. D'Andrea and C. Verdozzi, International Journal of Modern Physics **B9**, 1185 (1995).
- 79.
80. Q Niu and D J Thouless, J. Phys. A: Math. Gen. **17** (1984) 2453
81. Walter Kohn, Phys. Rev. **133** (1964) A171
82. L.P. Kadanoff and G. Baym, Quantum Statistical Mechanics, W.A. Benjamin, Inc., New York (1962)
83. M. Gell-Mann and F. Low, Phys. Rev. **84**, 350 (1951)
84. L.V. Keldysh, J. Exptl. Theoret. Phys. (U.S.S.R.) **47**, 1515 (1964) [English translation Soviet Phys. JETP **20**, 1018 (1965)]
85. T.E. Feuchtwang, Phys. Rev. **B10**, 4121 (1974) and Phys. Rev. **B12**, 3979 (1975)
86. C.R. Natoli et al., Phys. Rev. **B 42**, 1944 (1990)
87. D.C. Langreth and J.W. Wilkins, Phys. Rev. **B6**, 3189 (1972); D.C. Langreth, 1975 N.A.T.O. Advanced Study Institute, Antwerp, Belgium, on *Linear and Nonlinear Electron Transport in Solids*;
88. Jhy-Jiun Chang and D.C. Langreth, Phys. Rev. **B8**, 4638 (1973)
89. L.D. Landau e E.M. Lifshitz, *Fisica Cinetica*, Editori Riuniti, Roma (1984)
90. R.D. King-Smith and D. Vanderbilt, Phys. Rev. **B 47**, 1651 (1993)
91. M. Cini, Surface Sci. **87**, 483 (1979)
92. M.J. Lighthill, An introduction to Fourier analysis and generalised functions, Cambridge University Press Cambridge 1958
93. Melvin Lax, Symmetry principles in Solid State and molecular Physics, ISBN: 0486420019 Dover Publications
94. K. Siegbahn et al. Esca applied to free molecules, North-Holland Publishing Company Amsterdam London (1969).
95. P. Weightman, J. Phys. **C** (1982)
96. Michele Cini, Corso di Fisica Atomica e Molecolare-Introduzione alla Fisica Teorica per Strutturisti, II Edizione, Edizioni Nuova Cultura, Roma (1998) (in Italian)
97. E. Feenberg, Phys. Rev. **74**, 206 (1948); Phys. Rev. **74**, 664 (1948)
98. S. Swain, *continued fraction methods in atomic physics*, in Advances in atomic and molecular Physics, **22**, 387 (1986)
99. Michele Cini, Il Nuovo Cimento **8D**, 333 (1986)
100. Hitoshi Sumi, J. Phys. Soc. Japan **36**, 770 (1974)
101. Matias Wagner, Phys. Rev. **B44**, 6104 (1991)
102. S. Kurth, G. Stefanucci, C.O. Ambladh, A. Rubio and E.K.U. Gross, Phys. Rev. **B72**, 035308 (2005)

103. G.Stefanuucci and C.O. Ambladh, Phys. Rev.**B 69**, 195318 (2004)
104. Michele Cini, Phys. Rev. **B43**,4792 (1991); Michele Cini,R. Del Sole, Jang Guo Ping and L. Reining, *Calculation of the linear and nonlinear optical properties of Si(111)1x1-As*, Proceedings of the Epioptic meeting, Berlin, June 1991.
105. Y.R. Shen, The principles of Nonlinear Optics, John Wiley and Sons, New York (1984).
106. Schuda, C R Stroud Jr and M Hercher, J. Phys. B: Atom. Molec. Phys. **7**, L198 (1974)
107. P.Auger, J. Physique Radium **6**, 205 (1925)
108. J.J.Lander, Phys. Rev. **91**, 1382 (1953)
109. Claudio Verdozzi, Michele Cini and Andrea Marini, Jnl. Electron Spectroscopy and Related Phen VOL.117-118, 41-55 (2001)
110. C.J.Powell,Phys. Rev. Letters **30**, 1179 (1973)
111. L.I. Yin, T.Tsang and I. Adler,Physics Letters 57A,193 (1976); Phys. Rev. **B 15**, 2974 (1977)
112. G.A. Sawatzky, Phys. Rev. Letters **39**, 504 (1977)
113. Knotek and Feibelman, Phys. Rev. 1978
114. J.E. Inglesfield, J. Phys. C:Solid State Phys. **14**, 3795 (1981)
115. S. Crampin, J. Phys.: Condens. Matter **16**, 8875 (2004)
116. Richard D. Mattuck, *A Guide to Feynman Diagrams in the Many-Body Problem*,Dover, New York
117. John Inkson, *Many-Body theory of Solids - An Introduction*,Plenum Press New York 1984
118. R. P. Feynman,*Statistical Mechanics - A set of lectures*, W.A. BENJAMIN, INC, Reading, Massachussetts (1972)
119. G. Vignale and Mark Rasolt, Phys. Rev. Letters **59**, 2360 (1987)
120. Robert van Leeuwen, Nils Erik Dahlen, Gianluca Stefanucci, Carl-Olof Almbladh and Ulf von Barth, Lectures Notes in Physics, Springer Verlag, 2005 (to appear); also cond-mat/0506130.
121. P. Hohenberg and W.Kohn, Phys. Rev. **136**, B864 (1964)
122. W. Kohn and L.J. Sham, Phys. Rev. **140**, A1133 (1965)
123. L.J. Sham and M. Schlüter, Phys. Rev. Letters **51**, 1888 (1983)
124. Michele Cini and A. D'Andrea, J. Phys. C **16**, 4469 (1983)
125. R.M. Dreizler and E.K.U. Gross, *Density Functional Theory*, Springer Verlag 1990
126. Ulf von Barth, Niels Erik Dahlen, Robert van Leeuwen, and Gianluca Stefanucci,Phys. Rev. **B72**, 235109-1 (2005)
127. Andrea Marini and Michele Cini, Phys. Rev. **B 60**, 11391 (1999)
128. M. Cini and V. Drchal, J. Phys.: Condens. Matter **6**, 8549 (1994);M. Cini and V. Drchal, J. Electron Spectrosc. Relat. Phen.**72**, 151 (1995)
129. M.J. Stott and E. Zaremba, Phys Rev **A 21**, 12 (1980)
130. A. Zangwill and P. Soven, Phys Rev **A 21**, 1561 (1980)
131. E. Runge and E.K.U. Gross, Phys. Rev. Letters **52**, 997 (1984).
132. J.R. Schrieffer and D. C. Mattis, Phys. Rev **140**, A1412 (1965);B. Kjöllersström, D.J. Scalapino and J.R. Schrieffer,Phys. Rev **18**, 665 (1966)
133. V. Galitzkii, Soviet Phys. JETP **7**, 104 (1958).
134. M. Cini and C. Verdozzi, Solid State Commun.**57**, 657 (1986);M. Cini and C. Verdozzi, Nuovo Cimento **9D**, 1 (1987).
135. A. Parnasclci and M. Cini, J. Electron Spectrosc. and Relat. Phen. **82**,79 (1996).

136. M. Hindgren, Ph.D. Thesis Lund University, 1997.
137. Niels Eric Dahlen and Ulf von Barth, Phys. Rev. **B 69**, 195102 (2004)
138. J.P. Perdew, K. Burke and M. Ernzerhof, Phys. Rev. Letters **77**, 3865 (1996)
139. L.G.Molinari, Phys. Rev. **B 71**, 113102 (2005)
140. M. Revzen, T. Toyoda, Y. Takahashi and F. C. Khanna, Phys. Rev. **B 40**, 769 (1989)
141. J.C. Ward, phys. Rev. **78**, 182 (1950); Y. Takahashi, Nuovo Cimento **6**, 371 (1957).
142. Andrei, Furuya and Lowenstein, Rev. Modern Phys. **55**, 331 (1983)
143. H.B. Thacker, Rev. Modern Phys. **53**, 253 (1981)
144. E.U. Condon and G.H. Shortley, *The theory of Atomic Spectra*, Cambridge University Press, Cambridge (1935)
145. John C. Slater, *Quantum theory of Atomic Structure*, Volume II, McGraw-Hill Book company, New York (1960)
146. J. F. Janak, Phys. Rev. **B 18**, 7165 (1978)
147. Mitchel Weissbluth, Atoms and Molecules, Academic Press San Diego (1978)
148. Nielsen C.W. and Koster G.F. Spectroscopic coefficients for p^n, d^n and f^n Configurations, MIT press, Cambridge, Massachusetts (1963)
149. Andrea Dal corso, Phys. Rev. **B 64** 235118-1 (2001).
150. M.Cini, R.Del Sole and L. Reining, Surface Sci. 287/288, 693 (1993)
151. M. Cini, Surface Review and Letters 1,4 , 443 (1994)
152. K.G. Dyall et al., Computer Physics Communications **B 55** 425 (1989).
153. C. Verdozzi, M. Cini, J.F. McGilp, G. Mondio, D. Norman, J.A. Evans, A.D. Laine, P.S. Fowles, L. Duo' and P. Weightman, Phys. Rev. **B 43** 9550 (1991)
154. S. aksela, M. Harkoma, M. Pohjola and H. Aksela, J. Phys. **B 17**, 2227 (1984)
155. R.J. Cole, C. Verdozzi, M. Cini and P. Weightman, Phys. Rev. **B 49** 13329 (1994)
156. Morton Hamermesh, *Group Theory and its application to physical problems*, Dover Publications, Inc., New York (1962).
157. G.A. Baker Jr and P. Graves-Morris, *Pade' approximants*, Encyclopaedia of Mathematics and its Applications Volume 14, Cambridge MA Addison-Wesley (1981).
158. K.G. Dyall et al., Computer Physics Communications **55**, 425 (1989)
159. DKG de Boer, C Haas and G A Sawatzky, J. Phys. F: Met.Phys. **14**, 2769 (1984)
160. P. Hedegpard and F Hillebrecht, Phys. Rev. B34 3045 (1986)
161. H.ksela and S. Aksela, J.Phys. **B 7**, 1262 (1974).
162. N.E. Bickers, D.J. Scalapino and S.R. White, Int.J. Mod. Phys. **1**, 687 (1987)
163. N.E. Bickers, D.J. Scalapino and S.R. White, Phys. Rev. Letters **62**, 961 (1989)
164. R. Shankar, rev. Mod. Phys. **66**, 129 (1994)
165. D. Zanchi and HJ Schulz, Phys. Rev. **B63**, 13609 (2000)
166. C.J. Halboth and W. Metzner Phys. Rev. Letters **61**, 7364 (2000)
167. C. Honerkamp and M. Salmhofer, Phys. Rev. Letters **64**, 184516 (2001)
168. P.W.Anderson, G. Baskaran, Z. Zou and T. Hsu, Phys. Rev. Letters **58**, 2790 (1987)
169. P.W.Anderson and Z. Zou, Phys. Rev. **B 60**, 132 (1988)
170. G. Su and M. Suzuki, Phys. Rev. **B58**, 117 (1998)
171. Michele Cini and Adalberto Balzarotti, Nuovo Cimento D **18**, 89 (1996)
172. Michele Cini and Adalberto Balzarotti, Phys. Reb **B56**, 14711 (1997)

173. Adalberto Balzarotti, Michele Cini, Enrico Perfetto and Gianluca Stefanucci, *J. of Phys.: Condens. Matter* **16** R1387 (2004)
174. W.Kohn and J.M. Luttinger, *Phys. Rev. Letters* **15**, 524 (1965)
175. J.G. Bednorz and K.A. Müller, *Z. Phys.* **B64**, 189 (1986)
176. RW Richardson, *Phys. Rev.* **141**, 949 (1966)
177. G. Fano, F. Ortolani and A. Parola, *Phys. Rev.* **B 42**, 6877 (1990); A. Parola, S. Sorella, M. Parrinello and E. Tosatti, *Phys. Rev.* **B 43**, 6190 (1991); G. Fano, F. Ortolani and A. Parola, *Phys. Rev.* **B 46**, 1048 (1992).
178. C. A. Balseiro, A. G. Rojo, E. R. Gagliano and B. Alascio, *Phys. Rev.* **B 38**, 9315 (1988).
179. J. E. Hirsch, S. Tang, E. Loh and D. J. Scalapino, *Phys. Rev. Lett.* **60**, 1668 (1988).
180. M. Ogata and H. Shiba, *J. Phys. Soc. Jpn.* **57**, 3074 (1988).
181. J. Bardeen, L.N. Cooper and J. R. Schrieffer, *Phys. Rev.* **108**, 1175 (1957); J.R. Schrieffer, *The theory of superconductivity*, Perseus Books, Reading, Massachusetts (1964)
182. E. Cappelluti, B. cerruti and L. Pietronero, *Phys. Rev.***B 69** , 161101 (2004)
183. M. S. Hybertsen, M. Schlüter and N. Christensen, *Phys. Rev.* **B 39**, 9028 (1988); M. Schlüter, in *Superconductivity and Applications*, edites by H. S. Kwok *et al.* (Plenum Press, New York, N. Y.) p. 1 (1990).
184. F. C. Zhang and T. M. Rice, *Phys. Rev.* **B 37**, 3759 (1988)
185. M. Cini, A. Balzarotti, R. Brunetti, M. Gimelli and G. Stefanucci, *Int. J. Mod. Phys.* **B 14**, 2994, (2000).
186. M. Cini and A. Balzarotti, *Solid State Comm.* **101**, 671 (1997); M. Cini, A. Balzarotti, J. Tinka Gammel and A. R. Bishop, *Il Nuovo Cimento* **D 19**, 1329 (1997).
187. M. Cini, A. Balzarotti and G. Stefanucci *Eur. Phys. J.* **B 14**, 269 (2000).
188. E. Perfetto, G. Stefanucci, and M. Cini, *Phys. Rev. B* **66**, 165434 (2002); E. Perfetto , G. Stefanucci , M. Cini *Eur. Phys. J.***B 30**, 139 (2001).
189. M. Cini, E. Perfetto and G. Stefanucci, *Eur. Phys. J.* **B 20**, 91 (2001).
190. Michele Cini, Adalberto Balzarotti, Raffaella Brunetti, Maria Gimelli and Gianluca Stefanucci, *International J. Modern Phys.* **14**, Nos. 25-27, pag. 2994 (2000)
191. C.P. Lund, S.M. Thurgate and A.B. Wedding, *Phys Rev.* **B55**, 5455 (1997)
192. Stefano Bellucci, Michele Cini, Pasquale Onorato and Enrico Perfetto, *J. Phys.: Condens. Matter* **18**,S2069 (2006)
193. G.W. Fernando, A.N. Kocharian, K. Palandage, Tun Wang and J.W. Davenport, *Cond-mat/0608579*
194. David J. Griffiths, *Introduction to Quantum Mechanics*, Prentice Hall , upper Sadle River, New Jersey 07458 (1994)
195. A. Callegari, M. Cini, E. Perfetto and G. Stefanucci, *Eur. Phys. J.* **B 34**, 455 (2003)
196. M. Cini, G. Stefanucci and A. Balzarotti, *Eur. Phys. J.* **B 10**, 293 (1999).
197. M. Kociak et al., *Phys. Rev. Lett.* **86**, 2416 (2001). A. Kasumov et al., *Phys. Rev. B* **68**, 214521 (2003)
198. F. Mancini and A. Avella, *Advances in Physics* **53**, 537 (2004)
199. Satoro Odashima, Adolfo Avella and Ferdinando Mancini, *Phys. Rev.* **B 72**, 205121 (2005)
200. G. Bressi, G. Carugno, R. Onofrio and G. Ruoso, *Phys. Rev. Lett.* **88** 041804 (2002)

201. M. Cini and C. Verdozzi, *J.Phys.(Condensed Matter)* **1**, 7457 (1989)
202. Bernd Thaller, *The Dirac Equation*, Springer-Verlag Berlin Heidelberg (1992)
203. W. Greiner, *Relativistic Quantum Mechanics- Wave Equations*, Springer-Verlag Berlin Heidelberg (1990)
204. D. Chattarji, *The theory of Auger Transitions*, Academic Press London (1976)
205. D.C. Langreth, *Phys. Rev.* **182**, 973 (1969)
206. L.D. Faddeev, *Sov. Phys. JETP* **12**, 1014 (1961)
207. Stefano Bellucci, Michele Cini, Pasquale Onorato and Enrico Perfetto, *Phys. Rev. B* **75**, 014523 (2007)
208. H. Mori, *Prog. Theor. Phys.* **33**, 423 (1965); **34**, 399 (1965)
209. M. Howard Lee, *Phys. Rev.E* **61**, 3571 (2000)
210. Umerto Balucani, M. Howard Lee and Valerio Tognetti, *Dynamical Correlations*, *Physics Reports* **373**, 409 (2003)

Index

- C_{3v} , 137
- C_{3v} , 137
- $GL(n)$, 133
- $O(n)$, 134
- $O^+(3)$, 201
- $SL(n)$, 134
- $SO(3)$, 145
- $SO(4)$, 145
- $SU(5)$, 201
- $U(1)$, 145
- Δ -SCF method, 33
- Δ^{++} , 81
- 1-2-3 theory, 270

- Abelian Group, 133
- Abrikosov-Suhl peak, 96
- accidental degeneracy, 371
- adiabatic electronic Hamiltonian, 188
- adiabatic ionization energy, 115
- adiabatic theorem, 359
- advanced Green's functions, 57, 288
- AES, 109
- ammonia, 158
- Anderson, 285
- anti-Stokes, 335, 340
- APECS, 109, 267, 270
- APEX, 121
- ARUPS, 109
- atomic levels, 42
- atomic terms, 41
- Auger, 210
- Auger effect, 48
- Auger Electron Spectroscopy, 109
- Auger matrix elements, 52
- Auger Photoelectron Coincidence Spectroscopy, 109
- Auger selection rules, 50
- Auger spectroscopy, 56

- Bare Ladder Approximation, 266
- Baym-Kadanoff theorem, 275
- Berry phase, 358
- Bethe ansatz, 391, 393, 406
- Bethe-Salpeter equation, 246
- Biedernharn-Johnson-Lippman operator, 147
- bipartite graph, 67
- bipartite lattice, 383
- Bloch, 136, 169
- Bohr-van Leeuwen theorem, 387
- Born-Oppenheimer approximation, 190
- boson propagator, 63
- Breit interaction, 52
- Brillouin zone, 66, 170
- Burnside theorem, 155

- Carbon Nanotubes, 369
- Casimir effect, 7
- Cayley theorem, 138
- central field, 38, 39
- characters, 143
- characters of angular momentum eigenstates, 160
- chemical shift, 50, 111
- chemisorption, 285
- Cini-Sawatzky theory, 118, 127, 264
- classical radius, 341
- Clebsh-Gordan, 42
- Clebsh-Gordan coefficients, 186
- Clebsh-Gordan coefficients, 186
- coherent light, 345
- coherent state, 116
- Compact Lie Group, 145
- Complex time, 287
- composite operators, 213
- configuration, 39
- configuration interaction, 34

- conjugate irreps, 200
- conserving approximation, 272
- continuity equation, 273
- correlation energy , 31
- coset, 138, 139
- Coster-Kronig, 121
- Covering Group, 145
- crystal field, 162
- current-voltage characteristics, 308

- Density Functional Theory, 73, 282
- desorption, 122, 210, 299
- diagram rules, 224
- dielectric function, 251, 259
- differential cross section, 339
- dipole approximation, 336, 344
- Dirac characters, 140
- Dirac equation, 73
- Dirac-Fock , 52
- direct product, 134
- double groups, 186
- dynamical Jahn-Teller effect, 190
- Dyson equation, 70, 239, 241, 292

- Einstein coefficient, 349
- electron affinity, 77
- embedding, 70, 71
- equal-times rule, 237, 291
- equation of motion, 61, 62, 74, 82, 83, 207, 211, 285, 307
- ESCA, 109
- Excitation Amplitudes, 326

- Faddeev, 269
- Fano, 81, 212, 241, 242, 285, 299, 326
- Feenberg, 329
- fermion annihilation operator, 9
- fermion creation operator, 9
- Feynman, 285
- field operators, 11
- final state effects, 111
- fluctuation-dissipation theorem, 79
- fluxon, 358
- fractional parentage coefficients, 42
- Franck-Condon , 116
- Friedel oscillations, 260, 367
- functional chain rule, 253
- functional derivative, 249

- Galilean covariance, 356
- Galitzkii, 264
- Gell-Mann and Low Theorem, 233
- generalized Bethe ansatz, 406
- glide plane, 175
- Goldstone diagrams, 221
- Green's functions hierarchy, 212
- ground state energy, 208, 277
- Group, 133
- Group property, 23
- Group of the wave vector, 176
- GW approximation, 255, 266, 275

- Hartree potential, 31
- Hartree-Fock, 29, 272
- Haydock, 313
- Hedin's equations, 255
- Heisenberg model, 387
- Heisenberg picture, 287
- Herglotz, 87, 266, 270, 272, 314, 323
- Hewson-Newns model, 326
- Hohenberg-Kohn theorem, 279
- Hubbard, 13, 212
- Hund, 42
- Hydrogen, 13

- infrared, 340
- Inglesfield, 71
- initial state effects, 111
- interaction picture, 287
- Intermediate Coupling, 46
- International notation, 175
- inversion symmetry, 171
- ionization potential, 77
- irreducible interaction, 246
- Irreducible Representations, 140, 141
- irreducible self-energy, 239
- irreducible tensors, 181
- irreducible tensors, 181
- irrep, 141

- Jahn-Teller Theorem, 189
- Janak theorem, 282
- Jellium, 35, 240, 281
- Josephson, 381
- Josephson effect, 308, 378
- junctions, 306

- Kadanoff-Baym method, 286

- Kanamori solution, 122, 127
 Keldysh, 210, 286, 294
 Klein-Gordon equation , 65
 Knotek-Feibelman mechanism, 121,
 122, 210, 212, 270
 Kohn-Sham equations, 281, 282
 Kondo, 95, 393
 Kondo Model, 99
 Kondo peak , 96
 Kondo temperature, 105
 Koopmans, 33
 Kramers, 340
 Kramers' Theorem, 172
 Kubo, 75, 285
 Kubo formulae, 73
- L-S multiplets, 40
 Lagrange theorem, 139
 Lanczos, 313, 325
 Landauer, 304
 Langreth, 288
 laser, 345
 LCAO, 93
 Lehmann, 76, 77
 lesser and greater Green's functions, 57
 Lie Group, 133, 144
 Lieb, 324, 383
 Ligand group orbitals, 161
 Linked Cluster Theorem, 225, 226, 231
 linked diagrams, 225
 Lippmann-Schwinger equation, 70
 little Group, 176
 Local Density Approximation, 281
 local density of states, 66, 86
 LOT, 152
 Low Density Approximation (LDA),
 264
- magnon, 388, 391
 many-body Hamiltonian, 12
 master equation, 305
 Matsubara, 60, 290
 mean field, 31
 Migdal theorem, 255
 mixed coupling scheme , 52
 mixed valence , 95
 molecular orbitals, 158
 moments, 322
- non-adiabatic operator, 194
 Normal divisor, 134
- O(4) Group, 147
 O(n), 134
 Open-path geometric phase, 360
 optical electron, 41
 orbitals of CH₄, 159
 orbitals of NH₃, 157
 Orthogonal polynomials, 318
 Orthohelium, 31
- Pade', 318, 323
 Pancharatnam phase, 357
 partition function, 224
 partition-free transport theory, 306
 Peierls, 358
 permanent, 9
 permutations, 1, 2
 photoemission, 106
 photon propagator , 65
 photon scattering, 337
 plasmon, 326
 plasmon satellites, 114
 Point Groups, 135
 Poisson statistics, 117
 polar form, 182
 Polarization bubble, 251
 polarization part, 238
 projection operators, 158
 propagator, 61
 pseudo-Jahn-Teller effect, 191
- Quadratic Response Formalism, 127
 quasi-particle, 241
 quotient Group, 139
- Raman, 335
 Raman effect, 185
 Rayleigh, 335
 rearrangement theorem, 138
 rectangular level, 120, 316, 328
 Regular representation, 155
 representation, 138
 resonances, 81
 resonant Raman scattering, 340
 Resta operator, 364
 restricted HF, 34
 retarded Green's functions, 57, 288

- Runge-Lenz Vector, 146, 147
 Russell-Saunders, 41, 46

 s-d model, 98
 scattering amplitude, 246
 Schönflies, 135
 Schrieffer-Wolff transformation., 98
 screw axis, 175
 second character orthogonality theorem,
 170
 selection rules, 184
 self-consistent field, 31
 self-energy, 89, 90, 94, 107, 127, 212,
 241–245, 247, 249, 258, 265,
 274–276, 283, 293, 300, 302
 self-energy part, 239
 semi-elliptic density of states, 94, 315
 semi-simple Group, 138
 semidirect product, 174
 seniority number, 35, 201, 203
 shake-off , 113
 shake-up, 113
 Sham - Schlüter equation, 283
 Shapiro, 381
 simple Group, 138
 sky, 340
 Slater integrals, 44
 Sommerfeld, 35
 spectral function, 77, 78
 spin eigenfunctions, 178
 spin-disentangled diagonalization, 323
 spin-orbit interaction, 39, 186
 spin-polarized HF, 34
 spontaneous emission, 349
 sputtering, 285, 299
 star of \overline{k} , 176
 Stokes, 335, 340
 SU(n), 134
 subgroup, 134
 superconducting flux quantization, 368,
 369, 378
 Symmetric Group, 199
 symmetry, 135
 symmorphic Group, 174

 t matrix, 70
 temperature Green's function, 59
 temperature Green's function , 62
 tensor, 340

 thermodynamic potential, 224
 Thomson, 341
 three-diagonal matrix, 331
 tight-binding Hamiltonian, 66
 Time Dependent Density Functional
 Theory, 308
 time reversal, 171
 Time-dependent Density Functional
 theory, 282
 time-dependent problems, 209
 time-ordered finite temperature
 propagator, 59
 time-ordered Green's function, 58
 Time-ordered propagator, 231
 Topologically equivalent diagrams, 236
 Tr, 23, 275
 transport, 210
 transpositions, 1, 2
 tunneling, 305
 two-hole resonances, 120, 121, 270

 U(n), 134
 U<0, 270
 Ultraviolet Photoemission Spec-
 troscopy, 109
 unrestricted HF, 34
 UPS, 109

 vacuum amplitude, 75
 vacuum level, 33
 Van Hove, 317
 variational principle, 279
 Variational principle, 16, 277
 Vector potential analogy, 361
 vertex, 252
 vertical ionization energy, 115
 vibration, 326
 vibrations of Ammonia, 167
 vibrations of Benzene, 168
 vibrations of Methane, 168
 vibrations of Water, 166
 vibronic couplings, 190
 Vibronic States, 193
 virtual orbitals, 34

 W=0 pairing, 369
 W=0 theorem, 373
 Ward identities, 278
 water, 137

Wick's theorem, 219

Wigner Eckart theorem, 45

Wigner matrices, 145

X-Ray Photoemission Spectroscopy,
109

XPS, 109

Young diagrams, 177

Young tables, 177, 178

Yukawa potential, 260

Zener model, 98